UNIVERSIDAD COMPLUTENSE DE MADRID
FACULTAD DE VETERINARIA

TESIS DOCTORAL

Interactions between high and low virulence isolates of Neospora caninum and target cells of the bovine innate immune response

MEMORIA PARA OPTAR AL GRADO DE DOCTOR

PRESENTADA POR

Marta García Sánchez

Supervisors

Luis Miguel Ortega Mora
Javier Regidor Cerrillo
Esther Collantes Fernández

Madrid

COMPLUTENSE UNIVERSITY OF MADRID

VETERINARY FACULTY

Animal Health Department

Interactions between high and low virulence isolates of *Neospora caninum* and target cells of the bovine innate immune response

Supervisors:

Luis Miguel Ortega Mora

Javier Regidor Cerrillo

Esther Collantes Fernández

DOCTORAL THESIS

Ms. Marta García Sánchez

Madrid, September 2019

UNIVERSIDAD COMPLUTENSE DE MADRID

FACULTAD DE VETERINARIA

Departamento de Sanidad Animal

Interacciones entre aislados de alta y baja viruencia de *Neospora caninum* y células diana de la respuesta inmunitaria innata bovina

Directores:

Luis Miguel Ortega Mora

Javier Regidor Cerrillo

Esther Collantes Fernández

TESIS DOCTORAL

Ms. Marta García Sánchez

Madrid, septiembre 2019

DECLARACIÓN DE AUTORÍA Y ORIGINALIDAD DE LA TESIS PRESENTADA PARA OBTENER EL TÍTULO DE DOCTOR

Dña. Marta García Sánchez, estudiante en el Programa de Doctorado de Veterinaria, de la Facultad de Veterinaria de la Universidad Complutense de Madrid, como autora de la tesis presentada para la obtención del título de Doctor y titulada: "Interacciones entre aislados de alta y baja virulencia de *Neospora caninum* y células diana de la respuesta inmunitaria innata bovina"

Y dirigida por: D. Luis Miguel Ortega Mora, D. Javier Regidor Cerrillo y Dña. Esther Collantes Fernández

DECLARO QUE:

La tesis es una obra original que no infringe los derechos de propiedad intelectual ni los derechos de propiedad industrial u otros, de acuerdo con el ordenamiento jurídico vigente, en particular, la Ley de Propiedad Intelectual (R. D. legislativo 1/1996, de 12 de abril, por el que se aprueba el texto refundido de la Ley de Propiedad Intelectual, modificado por la Ley 2/2019, de 1 de marzo, regularizando, aclarando y armonizando las disposiciones legales vigentes sobre la materia), en particular, las disposiciones referidas al derecho de cita.

Del mismo modo, asumo frente a la Universidad cualquier responsabilidad que pudiera derivarse de la autoría o falta de originalidad del contenido de la tesis presentada de conformidad con el ordenamiento jurídico vigente.

En Madrid, a 2 de septiembre de 2019

Fdo.: Marta García Sánchez

Memoria presentada por Dña. Marta García Sánchez para optar al grado de Doctor por la Universidad Complutense de Madrid

Madrid, 2 de septiembre de 2019

La realización de esta tesis doctoral ha sido posible gracias a la financiación del Ministerio de Economía y Competitividad, mediante un contrato predoctoral para la Formación de Personal Investigador (BES-2014-070723) del cual he sido beneficiaria.

La financiación de las investigaciones ha sido posible gracias a los siguientes proyectos:

- Ministerio de Economía y Competitividad (MINECO) del Gobierno de España (AGL2013-44694-R y AGL201675935-C2-1-R).

- Plataforma Tecnológica de Sanidad Animal de la Comunidad de Madrid (PLATESA) (S2013/ABI2906 y PLATESA2-CM P2018/BAA-4370).

D. Luis Miguel Ortega Mora, Doctor en Veterinaria y Catedrático de Universidad adscrito al Departamento de Sanidad Animal de la Facultad de Veterinaria de la Universidad Complutense de Madrid, **D. Javier Regidor Cerrillo**, Doctor en Farmacia e investigador contratado por la empresa Saluvet-innova, con base en el Departamento de Sanidad Animal de la Facultad de Veterinaria de la Universidad Complutense de Madrid y **Dña. Esther Collantes Fernández,** Doctora en Veterinaria y Profesora titular en el Departamento de Sanidad Animal de la Facultad de Veterinaria de la Universidad Complutense de Madrid

CERTIFICAN:

Que la tesis doctoral titulada "Interacciones entre aislados de alta y baja virulencia de *Neospora caninum* y células diana de la respuesta inmunitaria innata bovina" que presenta la Licenciada en Veterinaria Dña. Marta García Sánchez ha sido realizada en las dependencias del Departamento de Sanidad Animal de la Facultad de Veterinaria, de la Universidad Complutense de Madrid bajo su supervisión y cumple todas las condiciones exigidas para optar al grado de Doctor por la Universidad Complutense de Madrid con Mención Internacional.

De acuerdo con la normativa vigente, firmamos el presente certificado, autorizando su presentación como directores de la mencionada Tesis Doctoral.

En Madrid, a 2 de septiembre de 2019

Fdo. Prof. Dr. Luis Miguel Ortega Mora

Fdo. Dr. Javier Regidor Cerrillo

Fdo. Prof. Dra. Esther Collantes Fernández

DOCTORADO CON MENCIÓN INTERNACIONAL

La presente tesis doctoral cumple con los requisitos exigidos por la Universidad Complutense de Madrid para obtener la mención de Doctor Internacional:

1) Realización de una estancia mínima de tres meses en una institución de enseñanza superior o centro de investigación fuera de España:

- Centro receptor: Wenner-Gren Institute, Stockholm University, Stockholm, Sweden.
- Investigador principal: Prof. Dr. Antonio Barragan.
- Duración de la estancia: 3 meses (15/09/2017-14/12/2017).

2) Los apartados de resumen, introducción, resultados, discusión y conclusiones de la tesis doctoral han sido redactados en una de las lenguas habituales para la comunicación científica en su campo de conocimiento, distinta a cualquiera de las lenguas oficiales en España (inglés).

3) La tesis doctoral ha sido evaluada por dos expertos pertenecientes a alguna institución de educación superior o instituto de investigación no español.

4) El Tribunal evaluador de la tesis está compuesto por, al menos, un experto perteneciente a alguna institución de educación superior o centro de investigación no español.

"En lo alto está el Cielo, abajo está la Tierra, es muy difícil llegar con la piedrita al Cielo, casi siempre se calcula mal y la piedra sale del dibujo. Poco a poco, sin embargo, se va adquiriendo la habilidad necesaria para salvar las diferentes casillas".

Julio Cortázar, Rayuela

En estas páginas quiero mostrar mi agradecimiento a las personas que de una u otra forma me han ayudado a crecer como investigadora y como persona y han contribuido a hacer posible esta tesis doctoral.

Me gustaría dedicar las primeras líneas de agradecimiento a mis directores. A **Luis**, gracias por tus ideas y por orientar las mías con rigor. Por la confianza puesta en mi trabajo durante todos estos años, y por haberme facilitado siempre los medios suficientes para desarrollar todos los objetivos propuestos en esta tesis. A **Javier** y **Esther**, gracias por guiarme con paciencia en este proceso de aprendizaje, por estar siempre disponibles y por descubrirme, en vuestra persona, lo que es el trabajo bien hecho, la profesionalidad y la calidad personal. Extiendo mis agradecimientos a **Gema**, **Ignacio** y **Mercedes**. Gracias por vuestra cercanía, vuestro apoyo, y por lo mucho que me habéis enseñado.

A todos mis compañeros del grupo SALUVET, con los que he pasado grandes momentos. Nunca antes había tenido la suerte de encontrarme a tanta gente tan buena junta. Os habéis convertido en familia.

A mis compañeros de la *new generation*, que a pesar de llegar varios años después me acogieron como a una más desde el primer momento. A **Laura**, ejemplo a seguir. Inteligente, divertida, trabajadora, luchadora, con una fuerza de voluntad que mueve montañas y probablemente la persona más generosa que he conocido nunca. Gracias por ser el eje central de este grupo tan dispar, por proponer planazos que nos han unido aún más a todos, porque para paciencia la tuya (y ya sabes cómo continúa la frase) y porque cuando la pierdes ningún enfado te dura un minuto. Sin tu esfuerzo, dedicación, tu tremenda capacidad de organización y la infinidad de cualidades más que tienes que hacen de ti una investigadora increíble y la mejor de las compañeras esto no hubiera sido posible. Me quedo corta diciendo que la mitad de esta tesis es tuya. **Carlos**, (porque otra cosa no, pero) eres el mejor compañero de satélite que hubiese podido tener. Gracias por tu humor/amor inteligente y por el que no lo es tanto, por tu sabiduría en forma de refranes, por seguirme mis bromas y contar conmigo para las tuyas y por esas escapadas de las charlas aburridas que acaban en paseos por parques idílicos e intentos fallidos de captura de pavos reales. A **Álex**, que fuiste Gentilálex durante toda la tesis excepto el primer día. Te perdono porque sé que no era por mí (que es una película). Qué te voy a decir que no te haya dicho ya, pero en la lista de impedimentos que te hice hace tiempo ahora hay uno menos. No tengo ninguna duda de que vas a llegar lejos porque te lo mereces, pero antes pásate un tiempo por aquí, que se te echa de menos. A **Rober**, por ser naturalmente único. Porque no he decidido aún si me gustan más tus piropos, canciones y dibujos que los poemas de Vicente, pero el nivel anda cerca. Gracias por tus visitas al satélite y tus palabras de ánimo en los últimos tiempos. Tenemos que repetir esos pacharanes/cremas de orujo de Santander (a ser posible allí y con toboganes).

A la *new new generation*: **Merche**, no sé cómo consigues ser toda energía con todo lo que madrugas. Admiro tu valentía y tu fortaleza, que te hacen ser capaz de romper con todo y empezar de nuevo algo mejor con las mismas ganas. Sabes de sobra lo que vales y vas a hacer una tesis genial. A **María**, que va siguiendo mis pasos tan rápidamente que en nada va a adelantarme. Porque sabes combinar a la perfección el saber estar con la naturalidad, porque no hay nadie con tantas anécdotas como tú y porque no puedo parar de reír cuando las cuentas. Ha costado más de un ¡ay Dios mío!, pero tienes a los macrófagos dominados. A **Laurita**, con esa sonrisa tuya me conquistaste en una semana. Me voy tranquila sabiendo que te di un consejo de vida ya que los consejos de laboratorio no te hacen falta: si llegas tarde es porque sales tarde.

De nada. No te pongas en modo seminarista que no molas y yo también quiero una fiesta. A **Ali**, que nos trajo lo mejor de Perú en formato de bolsillo. Nunca he visto tanto aguante sin bajar de los tacones. No dudes de que todo tu esfuerzo tendrá su recompensa.

A **Pili**, **Rafa** y **David**, los post-doc del grupo. Gracias por tantísima ayuda, en especial a Pili por aportar tanto a este trabajo. Sois toda una inspiración personal y profesionalmente. Vais a llegar muy alto. Al resto de miembros de SALUVET. A las primas **Lola** y **Vane,** gracias por estar ahí dispuestas a echar siempre una mano. A **Cinta**, **Javier Lobo**, **Isabel** y **Chema** por compartir vuestra sabiduría y vuestro material. A Ángeles, **Laura** y en especial a **Jaime** y **Juanjo**, por vuestro buen carácter, por ayudarme siempre y por tantas risas. A **Gustavo** y **Javier**, que siempre han sabido responderme todas las dudas. **Abel** y **Alicia**, gracias en especial por los momentos geniales vividos en Buenos Aires. Guardo un millón de anécdotas.

A las chicas Innova: **Patri**, nuestra vasqui con pelazo y un gran cerebro debajo. Gracias por estar ahí cuidando de todos, devolviendo siempre el triple de lo que recibes. Y por rellenarme el cajón con chocolate para las emergencias. Por aportar tanto glamour al grupo, por tus frases únicas que hemos incorporado todos a nuestro vocabulario y porque a pesar de ser incapaz de salir a tu hora del trabajo no hay plan al que no te apuntes. **Ángela**, nadie da los buenos días como tú, gracias por alegrarme tantas mañanas. Porque aunque no me gusten los abrazos siempre has sabido cuándo necesitaba uno. Eres fuerte, luchadora y con un corazón enorme. No dudo que conseguirás todo lo que te propongas. A **Raquel**, insultantemente joven y guapa por dentro y por fuera. Gracias porque aunque no podemos verte a diario sigues estando. A las (ya no tanto) recién llegadas **Sheila** y **Sofía**, siento que llegarais cuando menos tiempo tenía. Me parecéis geniales y espero poder demostraros que no soy sólo una persona pegada a una silla refunfuñando todo el día. Gracias también a los que ya se fueron, **Luis Corpa**, **Jorge** y **Ana**.

La *old generation*: **Paula**, **David** e **Iván**, gracias por todos vuestros buenos consejos en el principio de esta tesis, y por demostrarme que con esfuerzo y dedicación hay un futuro después. A Dani, que ha sido *old*, *new*, y si le dais un poco de pie se apunta a la new *new generation*. Gracias por hablar tan bien de nosotras en León y por integrarnos en tu grupo. Porque nadie posa como tú, y por enseñarme que si algo no te gusta sólo hay que poner un buen filtro. A **Moreno**, gracias por todas las risas, por el poliestireno expandido (hay que recuperar el himno de SALUVET) y quizá (según vaya la defensa) por la fractura de tobillo de quien se excede con las preguntas.
A la gente estupenda que ha venido de estancia desde Argentina, Perú, Méjico, Italia y Brasil. **Müller**, que aunque te envié a ordenar la selva no sabes ya qué inventarte para volver. **Pomy**, eres de lo mejor sin duda que ha pasado por aquí. Totalmente inolvidable. **Marcelo**, la persona con más calma y paciencia del universo. **Yani**, gracias por los buenos momentos aquí y allí. Y por los alfajores. Gracias también a **Nacho**, **Lucy**, **Alexandra**, **Wagner**, **Larissa**, **Luca** y **Cristina**. Espero volveros a encontrar a todos en cualquier rincón del mundo.

A los grupos que me han acogido en mis distintas estancias: A **Antonio**, gracias por darme la oportunidad de pertenecer durante unos meses a tu fantástico grupo durante mi estacia en el Wenner-Gren Institute. Thanks to your team **Einar**, **Emily**, **Sachie**, **Arne**, and particularly to **Amol**, for all your pacience. Gracias **Carina** por ser la única allí que entiende que comer delante del ordenador no puede ser sano. **Sergi**, gracias por la compañía en el laboratorio a altas horas de la noche, cuando descubrí que si eres investigador predoctoral el estilo de vida sueco no es tan diferente del español. A todo el Área de Investigación en Sistemas de Producción Animal del SERIDA, en especial a **Koldo** y **Ali** (no sé cuántas veces me salvaste de imprevistos diferentes). Gracias también al Instituto de Ganadería de Montaña y especialmente a **Julio** por toda su ayuda prestada allí y en Asturias.

Para terminar quiero agradecer a mis amigos, en especial a los que más me han apoyado (y soportado) durante este tiempo: **Isa**, hermana gemela mayor y mejor compañía en la realización de sueños. Gracias por saber y hacerme ver lo que realmente importa y lo que no. Por reírte de los defectos compartidos, y por tantas risas en general. Gracias por Iquitos, por Kiruna, Río, Buenos Aires y la Patagonia. Y por disfrutar igual en Benidorm. Por los erizos. Por ser la más fiel seguidora de todos los capítulos pasados. La próxima temporada va a ser impresionante. Capítulo 1: El primer tango en París. A **Borja**, porque eres único escuchando, por tu sensibilidad y porque contigo todo es fácil. Gracias por colarte en mi vida cuando más lo necesitaba, has sido el mejor apoyo en los momentos difíciles del final de esta tesis. Espero poder compensarte los cafés en los que todo han sido dramas por mi parte con futuros vermuts que incluso superen nuestro primero. A mis chicos de Maldito Casanova **Yas**, **Ro**, **Sarita** y **Javi**. Y a **Martín**. Sé que os he tenido abandonados, pero prometo recuperar. Mañana mismo me veis en las milongas. Y hablando de milongas, gracias a **Luis**. Te debo la vida y un baile. Y el resto te deben estos agradecimientos, que menuda insistencia... A **Diego**, responsable en gran parte del inicio de todo esto, quien durante muchos años me apoyó en los momentos difíciles y bajo el pseudónimo de Damián disfrutó de los buenos como un saluvetiano más. Aquí hay gente que todavía te quiere más que a mí. A **Mario**, por sacar muchas horas nocturnas para hacer que esta tesis quedara más bonita. Eres un artista. Y a **Nuria**, aunque no te lo creas siempre has estado en el top. A ver si alguna vez consigo ahorrar para la isla.

Esta tesis tampoco habría sido posible sin en el apoyo de mi familia. Gracias a mi padre, por dármelo todo y por pensar desde que era pequeña que soy mucho más inteligente de lo que realmente soy. A mi madre, por apoyarme durante esta tesis y durante toda mi vida de todas formas posibles, y por saber cuál era mi vocación muchos años antes que yo. Gracias por transmitirme la pasión por la lectura y por los viajes, que ha marcado gran parte de lo que sé y de lo que soy. A **Sari**, por preocuparte siempre de todos y porque a pesar de la poca diferencia de edad siempre has ido muchos pasos por delante abriéndome camino. Sin ti no estaría donde estoy. A **Miky**, por tu inigualable buen carácter que tan nerviosa me ponía de pequeña y por hacerme reír hasta en los momentos más inoportunos. A **Bertis**, por ayudarme siempre con todo y por compartir momentos de ocio. Lo haces todo tan bien que me haces sentir que la hermana pequeña soy yo.

00

TABLE OF CONTENTS
ÍNDICE GENERAL

LIST OF TABLES

CHAPTER II INTRODUCTION / INTRODUCCIÓN

CHAPTER IV OBJECTIVE 1 / OBJETIVO 1

***In vitro* phenotypic characterization of bovine monocyte-derived macrophages infected with *Neospora caninum* isolates of high and low virulence.**

CHAPTER V OBJECTIVE 2 / OBJETIVO 2

Transcriptome modulation of bovine monocyte-derived macrophages by *Neospora caninum* isolates of different virulence.

LIST OF FIGURES

CHAPTER II INTRODUCTION / INTRODUCCIÓN

CHAPTER IV OBJECTIVE 1 / OBJETIVO 1

***In vitro* phenotypic characterization of bovine monocyte-derived macrophages infected with *Neospora caninum* isolates of high and low virulence.**

CHAPTER V OBJECTIVE 2 / OBJETIVO 2

Transcriptome modulation of bovine monocyte-derived macrophages by *Neospora caninum* isolates of different virulence.

Sub-objective 2.1:Gene expression profiling of bovine macrophages infected with high and low virulence *Neospora caninum* isolates.

Sub-objective 2.2: Gene expression profiling of high and low virulence *Neospora caninum* isolates in bovine macrophages.

LIST OF ABBREVIATIONS

2-DE	Two-dimensional gel electrophoresis	Electroforesis en gel bidimensional
ACTB	Beta actin	Beta actina
AKT	Protein kinase B	Proteína quinasa B
AMA	Apical membrane antigen	Antígeno apical de membrana
APC	Antigen presenting cell	Célula presentadora de antígeno
ARG	Arginase	Arginasa
BAG	Bradyzoite antigen	Antígeno de bradizoíto
BCEC-1	Bovine caruncular epithelial cell line 1	Línea celular del epitelio de la carúncula bovina
BeWo	Human placental trophoblast cell line	Línea celular humana del trofoblasto de la placenta
BKI	Bumped kinase inhibitors	Inhibidores de la proteína quinasa
BMDC	Bone marrow dendritic cell	Célula dendrítica de médula ósea
bo	Bovine	Bovino
BP	Biological process	Proceso biológico
bs	By-stander	Espectador
BSA	Bovine serum albumin	Albúmina sérica bovina
BVDV	Bovine viral diarrhea virus	Virus de la diarrea vírica bovina
CaCo2	Human epithelial colorectal adenocarcinoma cell line	Línea celular humana epitelial, aislada de carcinima de colon
CCL	Chemokine (C-C motif) ligand	Ligando de quimioquina (motivo C-C)
CCR	Chemokine (C-C motif) receptor	Receptor de quimioquina (motivo C-C)
CIITA	Major histocompatibility complex class II transactivator	Transactivador del complejo mayor de histocompatibilidad tipo II
CLR	C-type lectin receptors	Receptor de lectina tipo C
CM	Complete medium	Medio completo
CMI	Cell-mediated immunity	Immunidad de tipo celular
CNS	Central nervous system	Sistema nervioso central
CS	Chondroitin sulfate	Condroitin sulfato
CTL	Cytotoxic T lymphocyte	Linfocito T citotóxico
CXCL	Chemokine (C-x-C motif) ligand	Ligando de quimioquina (motivo C-X-C)
CyD	Cytochalasin D	Citocalasina D
DAVID	Database for annotation, visualization and integrated discovery	Base de datos para la anotación, visualización y descubrimiento integrado
DC	Dendritic cell	Célula dendrítica
DE	Diferentially expressed	Diferenciamente expresado
DEG	Diferentially expressed gene	Gen diferencialmente expresado
DH	Definitive host	Hospedador definitivo
DIGE	Difference gel electrophoresis	Electroforesis diferencial en gel
DNA	Deoxyribonucleic acid	Ácido desoxirribonucleico
dpi	Days post-infection	Días post-infección
e.g.	*Exempli gratia* (for instance)	*Exempli gratia* (por ejemplo)
EGF	Epidermal growth factor	Factor de crecimiento epidérmico

ELISA	Enzyme-linked immunosorbent assays	Ensayo inmunoenzimático
ERK	Extracellular signal-regulated kinase	Kinasa regulada por señales extracelulares
F3	Bovine placental trophoblast cell line	Línea celular del trofoblasto bovino
FAS	Fatty acid synthase	Ácido graso sintasa
FC	Fold change	Cambio en la proporción
FCS	Fetal calf serum	Suero fetal bovino
FDR	False discovery rate	Tasa de descubrimientos falsos
FOV	Field of view	Campo de visión
FOXO	Forkhead box O	Forkhead box O
G6PD	Glucose-6-phosphate dehydrogenase	Glucosa-6-fosfato deshidrogenasa
GA	Glutaraldehyde	Glutaraldehído
GAG	Glycosaminoglycan	Glicosaminoglicano
GAPDH	Glyceraldehyde 3-phosphate dehydrogenase	Griceraldehído 3-fosfato deshidrogenasa
GM-CSF	Granulocyte-macrophage colony-stimulating factor	Factor estimulante de colonias de granulocitos y macrófagos
GO	Gene ontology	Ontología génica
GPI	Glycosylphosphatidylinositol	Glicosilfosfatidilinositol
HeLa	Cell line derived from human cervical cancer cells	Línea celular humana derivada de células de cáncer cervical
HFF	Human foreskin fibroblasts	Línea celular humana de fibroblastos de piel de prepucio
HI	Heat-inactivated	Inactivado por calor
HK	Heat-killed	Muerto por calor
HS	Heparan sulfate	Heparán sulfato
i.e.	*Id est* (this is)	*Id est* (esto es)
IAP	Inhibitor of apoptosis	Inhibidor de la apoptosis
IBRV	Infectious bovine rhinotracheitis virus	Virus de la rinotraqueítis infecciosa bovina
IFAT	Indirect fluorescent antibody test	Test de inmunofluorescencia indirecta
IFN	Interferon	Interferón
Ig	Immunoglobulin	Immunoglobulina
IH	Intermediate host	Hospedador intermediario
IL	Interleukin	Interleuquina
IMC	Inner membrane complex	Complejo interno de membrana
iNOS	Inducible nitric oxide synthase	Óxido nítrico inducible sintasa
IR	Immune response	Respuesta inmunitaria
IRG	Immunity-related GTPase	Immunidad relacionada con GTPasas
IU	International units	Unidades internacionales
IV	Intravenous	Intravenoso
KEGG	Kyoto Encyclopedia of genes and genomes	Enciclopedia de genes y genomas de Kioto
LPS	Lipopolysaccharide	Lipopolisacárido
M1	Classically activated macrophage	Macrófago activado clásicamente
M2	Alternative activated macrophage	Macrófago activado alternativamente
MA-104	African Green monkey kidney cell line	Línea epitelial de riñón de mono verde africano
MEK	Mitogen-activated protein kinase	Proteína quinasa activada por mitógenos

MFI	Mean fluorescence intensity	Intensidad de fluorescencia media
MHC	Major histocompatibility complex	Complejo mayor de histocompatibilidad
MIC	Microneme protein	Proteína de micronemas
MIF	Macrophage migration inhibitory factor	Factor inhibidor de la migración de macrófagos
ml	Millilitre	Mililitro
MØ	Macrophage	Macrófago
MØ1H	Nc-Spain1H-inoculated macrophage	Macrófago inoculado con Nc-Spain1H
MØ7	Nc-Spain1H-inoculated macrophage	Macrófago inoculado con Nc-Spain7
MØC	Non-infected macrophage	Macrófago no infectado
MØHK	Nc-Spain1H-inoculated macrophage	Macrófago inoculado con taquizoítos muertos por calor
MOI	Multiplicity of infection	Multiplicidad de la infección
mpi	Months post-infection	Meses post-infección
MRC	Manose receptor	Receptor de manosa
mRNA	Messenger ribonucleic acid	Ácido ribonucleico mensajero
MS	Mass spectrometry	Espectrometría de masas
Nc	*Neospora caninum* (prefix)	*Neospora caninum* (prefijo)
NET	Neutrophil extracellular trap	Trampa extracelular de neutrófilos
NF-κB	Nuclear factor kappa-B	Factor nuclear kappa B
ng	Nanogram	Nanogramo
NK	Natural killer (cell)	(Célula) asesina natural
NKT	Natural killer T (cell)	(Célula) asesina natural T
NLR	Nucleotide-binding oligomerization domain-like receptors	Receptores similares al dominio de oligomerización de unión a nucleótidos
NOD	Nucleotide-binding and oligomerization domain	Dominio de oligomerización por unión de nucleótidos
NOS	Nitric oxyde synthase	Óxido nítrico sintasa
NS	Not stated	No indicado
OC	Ocular	Ocular
OG	Oregon green	Verde Oregón
P6	6-well culture plate	Placa de cultivo de 6 pocillos
padj	Adjusted p-value	Valor p ajustado
PAMP	Pathogen associated molecular patterns	Patrones moleculares asociados a patógenos
PBMC	Peripheral blood mononuclear cells	Células mononucleares de sangre periférica
PBS	Phosphate buffer saline	Tampón fosfato salino
PCR	Polymerase chain reaction	Reacción en cadena de la polimerasa
pDC	Plasmacytoid dendritic cell	Célula dendrítica plasmocitoide
PF	Paraformaldehyde	Paraformaldehído
pg	Picogram	Picogramo
PI3K	Phosphatidylinositol-3-kinase	Fosfatidilinositol-3-quinasa
pIR	Parasite invasion rate	Tasa de invasión del parásito
PKA	Protein kinase A	Proteína quinasa A
PLP	Patatin-like protein	Proteína proteolipídica
PMN	Polymorphonuclear neutrophil (cell)	Polimorfonuclear neutrófilo

PPG	Proteophosphoglycan	Proteofosfoglicano
PPRG	Peroxisome proliferator-activated receptor gamma	Receptor de peroxisoma proliferador activado gamma
PRR	Pattern recognition receptor	Receptor de reconocimiento de patrones
PV	Parasitophorous vacuole	Vacuola parasitófora
qPCR	Quantitative PCR	PCR cuantitativa
RAW 264.7	Murine macrophage cell line	Línea celular de macrófago murino
rbo	Bovine recombinant	Recombinante bovino
RIG-I	Retinoic acid inducible gene-I	Gen inducible por ácido retinoico
RLR	RIG-I-like receptor	Receptor de tipo RIG-I
RNA	Ribonucleic acid	Ácido ribonucleico
ROI	Route of administration	Vía de administración
RON	Rhoptry neck protein	Proteína del cuello de roptrias
ROP	Rhoptry protein	Proteína de roptrias
ROS	Reactive oxygen species	Especies reactivas de oxígeno
RPKM	Reads per kilo base per million mapped reads	Lecturas por kilo base por millón de lecturas mapeadas
RT	Room temperature	Temperatura ambiente
RT-qPCR	Real-time reverse transcription PCR	PCR a tiempo real con transcriptasa inversa
SAG	Surface antigen	Antígeno de superficie
SC	Subcutaneous	Subcutáneo
SD	Standard deviation	Desviación estándar
SEM	Standard error of the mean	Error estándar
SNP	Single nucleotide polymorphisms	Polimorfismo de nucleótido único
SRS	SAG-1 related sequence	Secuencia SAG-1 relacionada
SS	Serial sacrifice	Sacrificio seriado
Td	Doublinng time	Tiempo de duplicación
Tg	*Toxoplasma gondii* (prefix)	*Toxoplasma gondii* (prefijo)
TGF	Transforming growth factor	Factor transformante de crecimiento
Th	T helper (lymphocyte)	T colaborador (linfocito)
THP1	Human monocytic cell line	Línea celular monocítica humana
TLR	Toll-like receptor	Receptor tipo toll
TNF	Tumoral necrosis factor	Factor de necrosis tumoral
Treg	Regulatory T cell	Linfocito T regulador
TSP	Thrombospondin	Trombospondina
TY	Tachyzoite yield	Recolección de taquizoítos
WB	Western blotting	Western blot
wpi	Weeks post-infection	Semanas post-infección

I

SUMMARY

RESUMEN

Neospora caninum, the causal agent of neosporosis, is an apicomplexan obligate intracellular parasite closely phylogenetically related to *Toxoplasma gondii*. Bovine neosporosis causes severe economic losses in dairy and beef industries due to the abortion and stillbirth of calves. Currently, there are no effective vaccines or treatments against infection by *N. caninum*, and control options are based on diagnosis and management practices.

N*eospora caninum* infection underlies a complex immunological regulation that may lead to protection or contribute to the pathogenesis of abortion. Interactions of the parasite with cells of the host immune system during early infection (innate immune response), which represent the first line of defense against infections, should be critical in determining the character of the subsequent response. Macrophages play a key role in initiating early-immune responses against infections and establishing a link with the adaptive immune response. Despite the fact that these cells are essential for combating *N. caninum* infection, a limited number of studies have been conducted to investigate *N. caninum*-macrophages interaction, and most of them used murine and human cells. However, human and mouse are not natural hosts for *N. caninum* and it has been demonstrated that parasite virulence can be host-specific. In the present Doctoral Thesis, the interaction between *N. caninum* and bovine macrophages, as target cells of the host innate immune response, was investigated. Two isolates that have showed different virulence in cattle, the low virulence isolate Nc-Spain1H and the high virulence isolate Nc-Spain7, were used to reveal the main host and parasite mechanisms implicated in disease pathogenesis.

The first objective was the phenotypic characterization *in vitro* of bovine macrophages infected with *N. caninum* isolates of high and low virulence. The aim of this objective was to determine how *N. caninum* interacts with bovine macrophages and the influence of the isolate virulence in the cellular response to infection. The ability of *N. caninum* to invade, survive and proliferate in bovine macrophages was determined. Then, the cellular immune response to infection was investigated by studying reactive oxygen species (ROS) production, IL-12 and IL-10 cytokines expression, surface molecules expression and IFN-γ production by lymphocytes. Finally, the capacity of the parasite to induce a hypermigratory phenotype in the host cell was studied.

Both isolates actively invaded, survived and replicated in the macrophages. However, Nc-Spain7 showed a higher invasion rate and a faster replication, whereas Nc-Spain1H presented a delayed replication and a lower growth rate. *Neospora caninum* intracellular survival was achieved by a reduction in intracellular ROS levels and by the evasion of the lysosomal activity mediated by the infection.

Infected macrophages exhibited lower expression of surface molecules MHC Class II, CD86 and CD1b than uninfected cells, with no differences between isolates. A reduction in intracellular ROS levels was observed at early infection with both isolates. Later, Nc-Spain1H-infected macrophages showed an enhanced ROS production and IL-12p40 expression, which also resulted in an elevated IFN-γ release by lymphocytes in co-culture, compared to macrophages infected with Nc-Spain7. Furthermore, IL-10 was overexpressed in the macrophages infected with both isolates, but expression levels were higher for Nc-Spain1H-infected cells.

In addition, the results of the present Doctoral Thesis showed for the first time that *Neospora caninum* induces a hypermigratory phenotype in bovine macrophages upon infection. This phenotype, consistent with an ameboid migratory activation of the infected cell, was characterized by hypermotility, enhanced transmigration, abrogated extracellular matrix degradation and rapidly induced cytoskeletal changes. A significantly higher hypermotility was observed with the high virulence isolate Nc-Spain7.

The transcriptomic analysis of bovine monocyte-derived macrophages infected with Nc-Spain7 and Nc-Spain1H was studied with the aim of determining the molecular basis underlying the macrophage response to infection and the observed modulation of host cell functions by the parasite. The transcriptional profile of Nc-Spain7 and Nc-Spain1H was also investigated in order to correlate the differences in gene expression between isolates with their different behavior *in vitro*, and to determine the parasite effectors involved in the different immune response modulations.

Neospora caninum infection induced an upregulation of TLR (TLR2, TLR3 and TLR9) and NLR (NAIP, NOD2, NLRC4 y NLRP12) expression, and polarized the macrophage response toward a predominantly M1 (pro-inflammatory) phenotype, with the activation of NF-ƙB signaling pathway. Apoptosis and phagolysosome maturation were processes repressed by the parasite to ensure its intracellular survival. FoxO, Th1-Th2 differentiation and glycosaminoglycan degradation were signaling pathways enriched only for Nc-Spain1H infection. In addition, macrophage infection by this isolate induced a higher upregulation of genes involved in pathogen sensing, chemotaxis and inflammation, including NF-B signaling pathway and pro-inflammatory cytokines IL-12 and IL-8. As observed in the results of the first objective, the regulatory cytokine IL-10 showed higher expression levels in cells infected with the low virulence isolate than with the high virulence isolate.

The expression profile of Nc-Spain7 showed upregulation of genes involved in parasite growth and homeostasis redox, which correlates with the higher proliferation and survival in macrophages observed *in vitro* for this isolate. On the contrary, Nc-Spain1H showed an upregulation of genes related to the bradyzoite stage of the parasite. Furthermore, genes potentially involved in the induction of immune responses were highly expressed by the low virulence isolate, highlighting those coding for SRS proteins, highly immunogenic surface proteins. On the other hand, Nc-Spain7 showed an enhanced expression of proteophosphoglycans and genes related to the synthesis of glycosylphosphatidylinositol, both potentially involved in immune response evasion.

Altogether, these results suggest that Nc-Spain7 may limit the macrophage functions regarding pathogen killing and the induction of pro-inflammatory responses. This fact, together with the higher capabilities of the high virulence isolate to invade the host cells and proliferate, may explain the higher pathology induced by this isolate in pregnant bovine models. Nc-Spain1H induces a higher immune response. It would lead to the control of parasite proliferation and may explain the reduced parasite loads found in fetus and placental tissues in *in vivo* infections. Our results also suggest that the hijacking of macrophages may be a strategy used by *N. caninum* in order to disseminate and be transmitted to the offspring.

Neospora caninum, el agente causal de la neosporosis bovina, es un parásito apicomplejo intracelular obligado, relacionado filogenéticamente con *Toxoplasma gondii*. La neosporosis bovina causa importantes pérdidas económicas en la industria cárnica y lechera, como consecuencia del aborto o el nacimiento de terneros mortinatos. En la actualidad no existen tratamientos ni vacunas efectivas frente a *N. caninum*, y las opciones de control se basan en el diagnóstico y buenas prácticas de manejo.

Tras la infección por *N. caninum* subyace una compleja regulación inmunológica que puede conferir protección o contribuir a la patogenia del aborto. La interacción del parásito con células del sistema inmunitario en las primeras fases de la infección (respuesta innata del hospedador), que representan la primera línea de defensa, es crítica a la hora de determinar el carácter de la respuesta subsiguiente a la infección. Los macrófagos juegan un papel clave en el inicio de la respuesta inmunitaria temprana frente a infecciones y son nexo de unión con la respuesta adaptativa. A pesar de que estas células son esenciales para combatir la infección por *N. caninum*, se han llevado a cabo un número limitado de estudios para investigar la interacción entre este parásito y el macrófago, y la mayoría de ellas utilizaron células humanas y murinas. Sin embargo el ser humano y el ratón no son hospedadores naturales de *N. caninum* y se ha demostrado que la virulencia del parásito puede ser específica de hospedador. En la presente tesis doctoral se investigó la interacción entre *N. caninum* y el macrófago bovino, como célula diana de la respuesta inmunitaria innata del hospedador. Para la infección se utilizaron dos aislados de *N. caninum* que mostraron diferente virulencia en el ganado bovino, el aislado de baja virulencia Nc-Spain1H y el aislado de alta virulencia Nc-Spain7, con el fin de revelar los principales mecanismos del hospedador y del parásito implicados en la patogenia de la enfermedad.

El primer objetivo fue la caracterización fenotípica *in vitro* de macrófagos bovinos infectados con aislados de *N. caninum* de alta y baja virulencia. La finalidad fue determinar cómo *N. caninum* interacciona con el macrófago bovino y la influencia que tiene la virulencia del aislado en la respuesta de la célula a la infección. Se determinó la capacidad de *N. caninum* para invadir, sobrevivir y proliferar en macrófagos bovinos. También se estudió la respuesta inmunitaria celular a la infección mediante el estudio de la producción de especies reactivas de oxígeno (ROS), la expresión de citoquinasinas IL-12 e IL-10, la expresión de moléculas de superficie y la producción de IFN-γ por linfocitos. Finalmente se investigó la capacidad del parásito para inducir un fenotipo hipermigratorio en la célula hospedadora.

Ambos aislados invadieron activamente la célula, sobrevivieron y se replicaron en el interior de los macrófagos. Sin embargo, Nc-Spain7 mostró una tasa de invasión más alta y una replicación más rápida, mientras que Nc-Spain1H presentó un retraso en el inicio de la replicación y una tasa de crecimiento más baja. *Neospora caninum* logró sobrevivir en el interior del macrófago reduciendo los niveles de ROS intracelular y evadiendo la actividad de los lisosomas.
Los macrófagos infectados mostraron una menor expresión de las moléculas de superficie MHC II, CD86 y CD1b que las células no infectadas, sin diferencias entre aislados. Tras producirse una reducción en los niveles intracelulares de ROS en los primeros momentos tras la infección con ambos aislados, los macrófagos infectados con Nc-Spain1H mostraron una mayor producción de ROS y expresión de la citoquina IL-12p40, lo que también dio lugar a una elevada producción de IFN-γ por linfocitos en cocultivo. Además, IL-10 se sobreexpresó en macrófagos infectados con ambos aislados, pero los niveles de expresión fueron más altos para las células infectadas con Nc-Spain1H.

Además, los resultados de la presente tesis doctoral demostraron por primera vez que *N. caninum* es capaz de inducir un fenotipo hipermigratorio en macrófagos bovinos mediado por la infección. Este fenotipo, consistente con una activación migratoria ameboide de la célula infectada, se caracterizó por hipermotilidad, aumento de la transmigración, disminución de la degradación de la matriz extracelular y cambios citoesqueléticos inducidos en un breve periodo de tiempo tras la infeccion. Se observó una hipermotilidad significativamente mayor con el aislado de alta virulencia Nc-Spain7.

El análisis transcriptómico de macrófagos derivados de monocitos bovinos infectados con Nc-Spain7 y Nc-Spain1H se estudió con el objetivo de determinar las bases moleculares subyacentes a la respuesta de macrófagos a la infección y a la modulación observada de las funciones de la célula hospedadora por el parásito. También se investigó el perfil transcripcional de Nc-Spain7 y Nc-Spain1H, para correlacionar las diferencias en la expresión génica entre aislados con su diferente comportamiento *in vitro*, y para determinar posibles moléculas efectoras del parásito involucradas en la diferente modulación de la respuesta inmunitaria.

La infección por *N. caninum* indujo una regulación positiva de la expresión de Toll-like receptors (TLR2, TLR3 y TLR9) y NOD-like receptors (NAIP, NOD2, NLRC4 y NLRP12), y polarizó la respuesta de los macrófagos hacia un fenotipo predominantemente M1 (pro-inflamatorio), con activación de la ruta de señalización NF-ĸB. La apoptosis y la maduración del fagolisosoma fueron procesos inhibidos por el parásito para asegurar su supervivencia intracelular. Las rutas FoxO, de diferenciación Th1-Th2 y degradación de glucosaminoglicanos fueron rutas de señalización enriquecidas solo para la infección por Nc-Spain1H. Además, la infección de macrófagos por este aislado indujo una mayor sobreexpresión de genes implicados en la detección de patógenos, quimiotaxis e inflamación, incluida la ruta de señalización de NF-ĸB y las citoquinas proinflamatorias IL-12 e IL-8. En consonancia con los resultados del primer objetivo, la citoquina reguladora IL-10 mostró niveles de expresión más altos en células infectadas con el aislado de baja virulencia que con el aislado de alta virulencia.

El perfil de expresión de Nc-Spain7 mostró una sobreexpresión de genes implicados en el crecimiento del parásito y la homeostasis redox, lo que se correlaciona con la mayor proliferación y supervivencia en los macrófagos observada *in vitro* para este aislado. Por el contrario, Nc-Spain1H mostró una sobreexpresión de genes relacionados con la fase de bradizoíto del parásito. Además, se observó una mayor expresión de genes potencialmente implicados en la inducción de respuestas inmunitarias por el aislado de baja virulencia, destacando aquellos que codifican proteínas SRS, proteínas de superficie altamente inmunogénicas. Por otro lado, Nc-Spain7 mostró una mayor expresión de proteofosfoglicanos y de genes relacionados con la síntesis de glicosilfosfatidilinositol, ambos potencialmente involucrados en la evasión de la respuesta inmunitaria.

En conjunto, estos resultados sugieren que Nc-Spain7 puede limitar las funciones de los macrófagos con respecto a la eliminación de patógenos y la inducción de respuestas pro-inflamatorias. Este hecho, junto con la mayor capacidad de Nc-Spain7 para invadir las células del hospedador y proliferar, puede explicar la mayor virulencia de este aislado en el modelo bovino gestante. Nc-Spain1H parece estimular una mayor respuesta inmunitaria. Esta respuesta controlaría la multiplicación del parásito lo que explicaría la menor carga parasitaria encontrada en fetos y tejidos placentarios observada los animales infectados con este aislado. Nuestros resultados también sugieren que *N. caninum* podría utilizar al macrófago como caballo de Troya para su diseminación intraorgánica y su transmisión transplacentaria a la descendencia.

II

INTRODUCTION
INTRODUCCIÓN

1. *Neospora caninum* and bovine neosporosis

Neospora caninum, the etiologic agent of neosporosis, is an apicomplexan obligate intracellular parasite phylogenetically closely related to *Toxoplasma gondii* (Dubey et al., 2007, 2017). Misdiagnosed as toxoplasmosis until 1988, when *N. caninum* was first described as a new genus and species (Dubey et al., 1988), neosporosis is recognized today as a disease of worldwide concern. *Neospora caninum* infection causes nervous system dysfunctions in canids, definitive hosts for this parasite, and reproductive failure in cattle and other intermediate hosts including sheep, goats and deer (Dubey et al., 2017). Clinical disease in horses has been associated with *Neospora hughesi*, the second of the two species of the genus *Neospora* described to date (Marsh et al., 1996). Despite its wide host range, the greater importance lies in cattle, as bovine neosporosis causes severe economic losses in dairy and beef industries due to abortion and stillbirth of calves (Reichel et al., 2013). Currently, there are no effective vaccines or treatments against infection by *N. caninum* (Sánchez-Sánchez et al., 2018a) and control options are based on diagnosis and management practices (Dubey et al., 2007, 2017).

1.1. Parasite morphology and biology

Neospora caninum is a protozoan parasite of the subphylum Apicomplexa, family Sarcocystidae and subfamily Toxoplasmatinae, which includes other genera of cyst-forming parasites including *Toxoplasma*, *Besnoitia* and *Hammondia* (Tenter et al., 2002). To date, two species of the genus *Neospora* have been described, *N. caninum* and *N. hughesi*, which differ in pathogenicity and antigenicity traits (Marsh et al., 1996, 1998). The taxonomic classification of *N. caninum* is detailed in Figure 1.

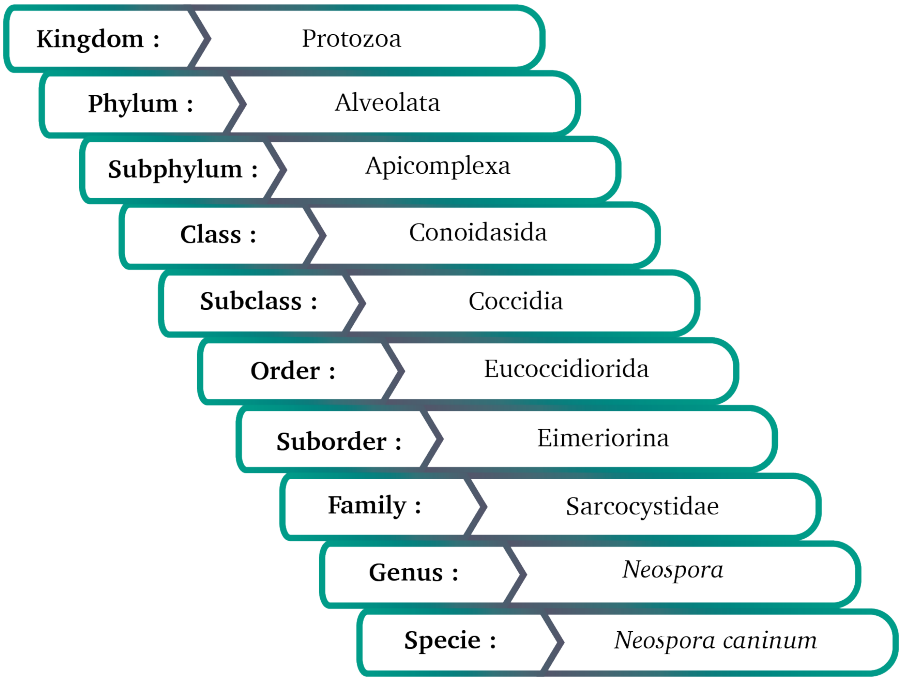

FIGURE 1 | Taxonomic classification of *N. caninum*.

There are three known infectious stages in the life cycle of *N. caninum*: tachyzoites and bradyzoites, invasive stages of the intermediate hosts, and sporozoites, contained within the oocysts which are excreted by the definitive hosts (Dubey et al., 2006). Gametocyte and merozoite stages, described in *T. gondii*, have not been characterized in *N. caninum* (Hehl et al., 2015).

Tachyzoites, lunate-shaped cells of approximately 2 × 6–7.5 µm, represent the fast replicative stage in the intermediate host (IH). They are capable of invading a large variety of nucleated cells, in whose interior the parasite multiplies asexually in cycles of endodyogeny within a parasitophorous vacuole. The tachyzoites egress by rupture of the cell when it can no longer support their growth, invading adjacent cells. The succession of cycles of invasion, proliferation and egress leads to the intra organic dissemination of the parasite and to tissue injury, this stage being responsible for the acute phase of infection (Dubey et al., 2006, 2017).

Bradyzoites are slowly replicating stages of the parasite, primarily found encysted in the central nervous system (CNS) of the IH and less frequently in skeletal muscle (Dubey et al., 2007; Peters et al., 2001). Tissue cysts are round or oval, up to 107 µm long, and are surrounded by an elastic cyst wall 0.5–4.0 µm-thick. Inside, bradyzoites of approximately 6.5 × 1.5 µm size are found in variable numbers, between 50 and 200 depending on the host, parasitized cell type and age of the cyst (Dubey et al., 2006, 2007, 2017). Bradyzoites divide asexually by endodyogeny and remain intracellular, in the cytoplasm of a single cell. They represent the quiescent life stage of the parasite, and can persist without causing clinical signs for the entire life of the IH (Goodswen et al., 2013).

Sporozoites are contained within the oocyst, the resistant stage of the parasite in the environment. Oocysts of 10–11 µm in diameter are shed unsporulated in the feces of the definitive host (DH). Under appropriate environmental conditions of temperature and humidity, sporulation occurs in approximately 24 h, becoming infective for the IH. Sporulated oocysts are bigger, 11.7 × 11.3 µm in diameter, and contain two sporocysts with four sporozoites each, 6.5 × 2 µm size (Lindsay et al., 1999; Dubey et al., 2017).

Ultrastructurally, besides the typical organelles of eukaryotic cells (nucleus, endoplasmic reticulum, Golgi complex, ribosomes and mitochondrion), tachyzoites present structures found uniquely in apicomplexan parasites (Goodswen et al., 2013; Dubey et al., 2017). Tachyzoites are surrounded by a pellicle composed of the outer plasma membrane and the inner membrane complex (IMC). The IMC is composed of flattened vesicles and interacts with the glideosome, actomyosin motor responsible for parasite motility, and with subpellicular microtubules that run the cell longitudinally (Ouologuem and Roos, 2014; Boucher and Bosch, 2015; Dubey et al., 2017). Subpellicular microtubules and the conoid, two apical rings and two polar rings, form the cytoskeleton of the parasite (Goodswen et al., 2013). The nucleus occupies the central part of the cell. Five characteristic organelles of apicomplexan parasites are located in the cytoplasm: micronemes, rhoptries, dense granules, amylopectin granules and the apicoplast. Rhoptries and micronemes are primarily located in the apical side of the cell, whereas dense granules are distributed throughout the tachyzoite, but mainly at the posterior end (Speer et al., 1999; Dubey et al., 2017) (Figure 2). The apicoplast is a non-photosynthetic plastid with importance as a therapeutic target, since it contains genetic material codifying for essential pathways of their metabolism, such as fatty acids biosynthesis (Sheinr et al., 2013).

Bradyzoites possess the same structures as tachyzoites, with differences regarding the number and location of the secretory organelles. These contain fewer rhoptries compared to tachyzoites,

located mainly anterior to the nucleus, but micronemes are found also posterior to the nucleus. Amylopectin granules are more abundant in bradyzoites than in tachyzoites. The bradyzoite nucleus is frequently found situated at the posterior end of the cell (Speer et al., 1999; Dubey et al., 2017) (Figure 2).

Although the ultrastructural features of sporozoites have not been described in detail, it is known that they have a nucleus situated centrally and possess amylopectin granules (Dubey et al., 2017).

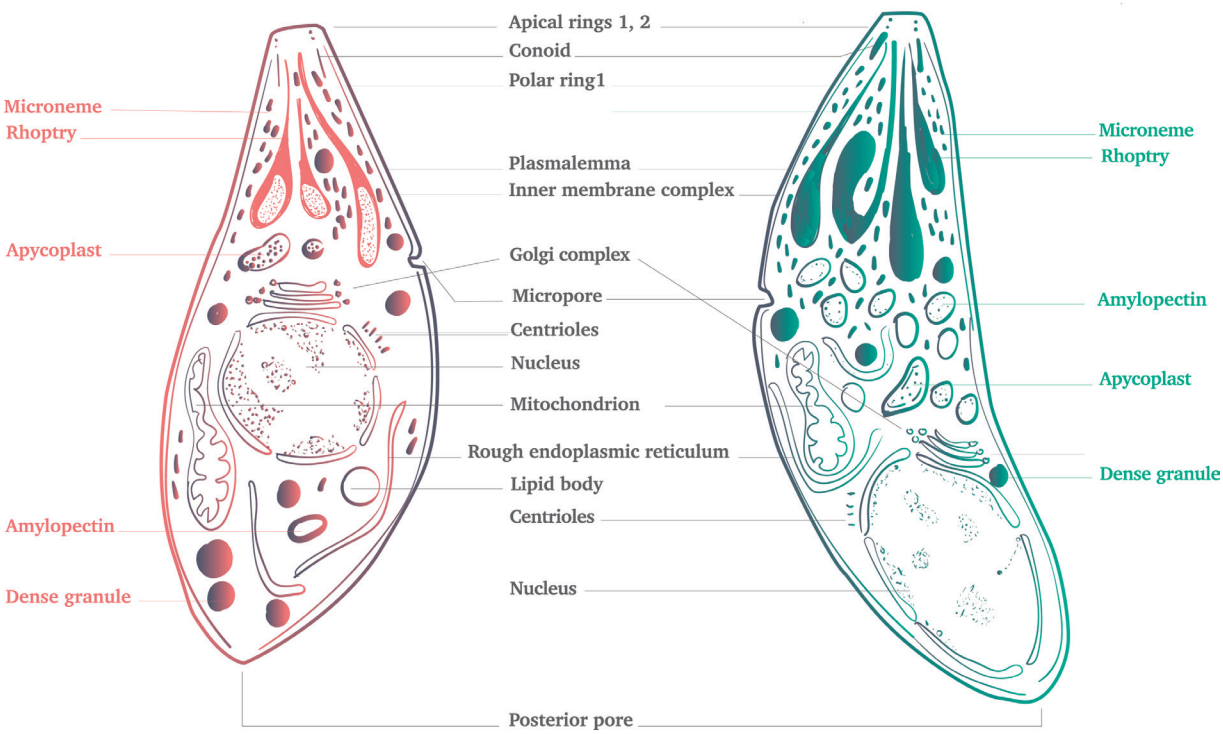

FIGURE 2 |Schematic drawings of the ultrastructure of *N. caninum* tachyzoites (left) and bradyzoites (right).

1.2. Life cycle and transmission of *Neospora caninum*

Neospora caninum has a complex facultative heteroxenous life cycle involving canids as DH and cattle and other ungulates as IH.. Dogs can act as DH as well as IH during *N. caninum* infections (Dubey et al., 2017). It is not considered to be zoonotic as, despite serological evidences of parasite exposure, presence of the parasite has not been detected in human tissues (Lobato et al., 2006; Calero-Bernal et al., 2019).

Dogs (*Canis lupus familiaris*), gray wolves (*C. lupus lupus*), coyotes (*C. latrans*) and dingoes (*C. lupus dingo*) are the confirmed DH to date. Parasite DNA and/or clinical disease have been detected in a wide range of domestic and wild animals, which constitute potential IH for *N. caninum*. Currently, viable tachyzoites have been isolated from cattle (*Bos taurus*), sheep (*Ovis aries*), water buffalo (*Bubalus bubalis*), axis deer (*Axis axis*), white tailed deer (*Odocoileus virginianus*), and European bison (*Bison bonasus*). Dogs and cattle are the most relevant hosts and maintain the domestic life cycle of the parasite (Donahoe et al., 2015; Dubey et al., 2017). In dogs and other DH, sexual replication of the parasite takes place, leading to the excretion of environmental resistant oocyst that become infective for the IH after sporulation occurs (Dubey et al., 2006).

Postnatal infection by ingestion of oocysts (horizontal transmission) and transplacental passage from the dam to the fetus (vertical transmission) are the only demonstrated transmission routes for cattle and other IH. After the ingestion of food or drinking water contaminated with sporulated oocysts, sporozoites are released and parasites invade the entero-epithelial cells, transforming into tachyzoites (Hemphill et al., 2006). These are spread by reaching the bloodstream due to their ability to infect a wide range of cells. Host immune responses lead to the switch from tachyzoites to bradyzoites, which can persist a lifetime in immunopriviledged tissues (Dubey et al., 2006, , 2017). Currently, there is no evidence that lactogenic of venereal infection occurs (Ferre et al., 2008; Osoro et al., 2009; Dubey and Schares, 2011).

Neospora caninum is one of the most efficiently transplacentally transmitted parasites. Two different forms of transplacental transmission have been described in bovine neosporosis. Reactivation of bradyzoites in persistently infected dams during gestation is responsible for endogenous transplacental transmission, considered the main route in cattle. Less frequently, exogenous transplacental transmission occurs when dams are primarily infected during gestation by ingestion of oocysts. Both exogenous and endogenous fetal infection may result in abortion or stillbirth associated with the asexual multiplication of tachyzoites, or in the majority of cases in the birth of clinically healthy calves, but congenitally infected. Up to 95% of calves born from infected cows can be infected, and in the future transmit the infection to their progeny intermittently or in several consecutive pregnancies (Dubey et al., 2017). A pattern of epidemic abortions is associated with exogenous transplacental transmission, whereas endemic outbreaks occur likely due to endogenous transmission (Dubey et al., 2007). The ingestion of bradyzoites contained in tissue cyst from infected tissues of the IH is the most likely source of infection for the DH (Dubey and Schares, 2011).

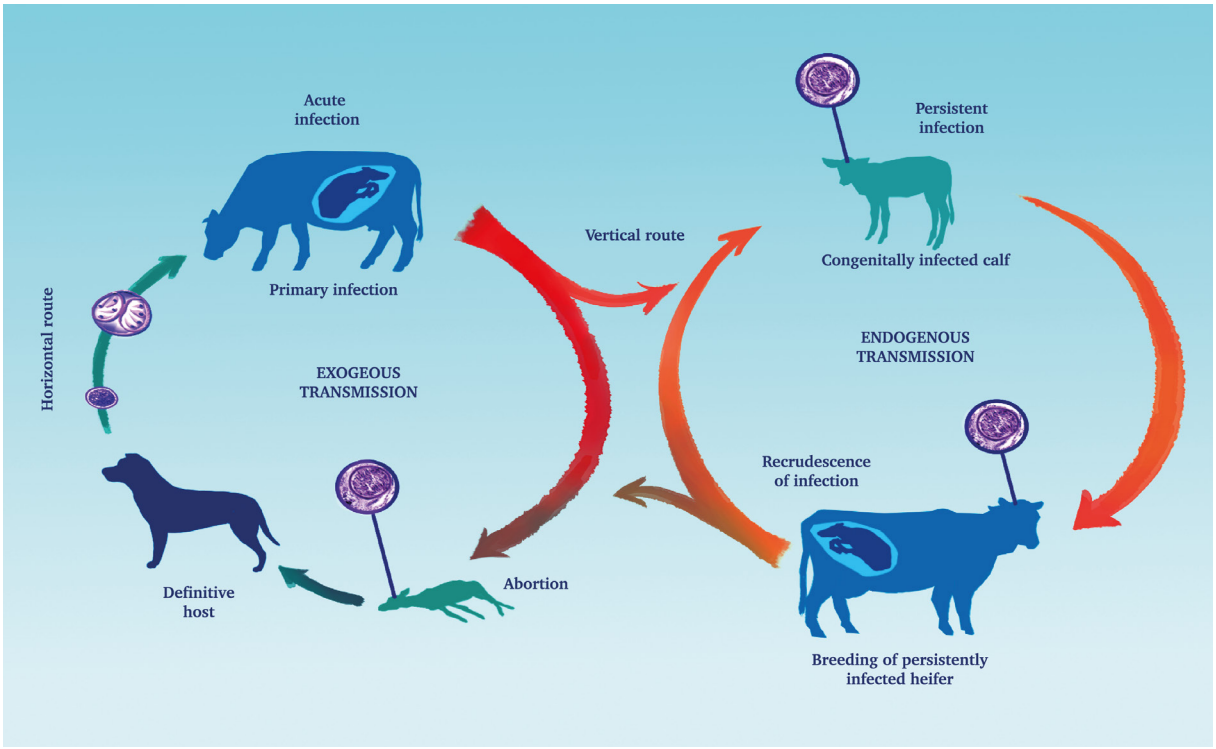

FIGURE 3 | *Neospora caninum* life cycle and transmission routes

1.3. Pathogenesis, clinical signs and lesions

It is not fully understood why abortion occurs. Tachyzoite invasion of placenta and fetal tissues followed by multiplication of the parasite may cause lesions incompatible with normal prenatal development. In addition, the presence of the parasite in the placenta and/or the parasite-induced placental damage may enhance the maternal immune response and induce the release of prostaglandins leading to luteolysis and fetal expulsion (Dubey et al., 2006).

Several factors are implied in the outcome of infection, among which the gestational period seems to be crucial. Reproductive losses are the main clinical manifestations of bovine neosporosis. Fetuses may die in utero or be reabsorbed, autolyzed, mummified, stillborn, born alive but with clinical signs, or more frequently born clinically healthy. Infection in non-pregnant cattle is generally asymptomatic (Dubey et al., 2007). Infections from three months of gestational age to term may lead to abortion, although most abortions occur at five-six months of gestation. Infections before three months of gestation likely lead to fetal reabsorption, and estrus repetition is observed. If the fetus dies between three and eight months, it is usually eliminated with the presence of moderate autolysis. Additionally, a fetus dying before five months of gestation may be retained in uterus and mummified. Finally, infections in late gestation are more likely to result in the birth of weak or healthy but congenitally infected calves, which will generally present precolostral antibodies (Dubey et al., 2006, 2017). These different effects derived from infection are probably related to variations in maternal immune responses, and the degree of development of the immunity and the placenta at different gestation periods (Dubey et al., 2017).

In aborted fetuses, lesions and presence of *N. caninum* have been detected in several tissues including brain, heart, liver, lung, kidney, skeletal muscle and placenta (Dubey et al., 2017). The severity of lesions is mainly dependent on the stage of pregnancy and the pattern of abortions, and seems to be more severe when abortion occurs after exogenous transplacental transmission. Lesions are more common in the gray matter of the brain. They begin with focal necrosis with or without inflammation. In fetuses before five months of gestational age (before immunocompetence develops) necrosis is more prominent, whereas inflammation is more prominent in older fetuses (Collantes-Fernández et al., 2006a; Dubey et al., 2017). This is evidenced by the presence of microglia, reactive astrocytes, and cell populations of the monocyte and lymphoid system, around the focus of central necrosis where mineralization may also occur (Dubey et al., 2017). Hepatic lesions are more severe in epidemic cases, and are characterized by periportal hepatitis and multifocal necrosis (Wouda et al., 1997; Collantes-Fernández et al., 2006b). The presence of inflammatory lesions with minimal necrosis is common in the heart, tongue and diaphragm (Dubey et al., 2017). Placental lesions consist of foci of necrosis and areas of intense inflammation nonsuppurative, with infiltration of mononuclear cells frequently observed. These can progress towards fibrosis and mineralization of the necrotic foci (Barr et al., 1994; Maley et al., 2003; Dubey et al., 2017).

Clinically affected calves may present low average weight, flexion or hyperextension of hind limbs or forelimbs, ataxia or complete paralysis, impaired patellar reflexes and loss of proprioception (Dubey and Schares 2011). In severe cases, exophthalmia, hydrocephalia, deviation of the vertebral column and a reduction in the diameter of the spinal cord have been described (Dubey et al., 2017). Lesions are predominantly confined in the brain and spinal cord, but arthrogryposis, myocarditis, nephritis and pneumonia have also been reported (Dubey et al., 2006, 2017; Donahoe et al., 2015).

1.4. Prevalence and economic impact of bovine neosporosis

Neospora caninum antibodies have been reported in cattle in most regions of the world, with serological prevalences varying across countries, regions, and depending on the age of the animals and breed. However, the use of different serological diagnosis methods, cutoff points and sample sizes makes the comparison between studies of prevalence difficult (Dubey and Schares, 2011). Data obtained from studies conducted in Germany, Netherlands, Sweden and Spain and carried out with the use of enzyme-linked immunosorbent assays (ELISA), previously standardized among laboratories (Von Blumroder et al., 2004; Bartels et al., 2006), enabled the comparison of seroprevalences in dairy and beef cattle. Moderate to high seroprevalences were found in Spain and Netherlands, whereas Sweden showed the lowest seroprevalences followed by Germany. In addition, prevalences in dairy cattle were higher than in beef cattle (Dubey et al., 2007). A value of 46% of seropositive herds for beef cattle and a 63 % for dairy cattle were reported in Spain (Bartels et al., 2006). In later studies carried out in the northwestern region of Spain, higher prevalences of 77% and 88% were shown in beef and dairy cattle respectively (González-Warleta et al., 2008; Eiras et al., 2011). It has not been fully elucidated if differences are caused by the different production system used for both breeds rather than the breed-related susceptibility to infection (Dubey et al., 2017). In addition, seroprevalence seems to have a direct relation to the age of the animals, probably due to the contact with the parasite associated to horizontal transmission (Eiras et al., 2011).

Major economic impact associated with bovine neosporosis is due to abortion. Epidemic abortions associated with primary infection of dams by horizontal transmission are more costly, since a large proportion of animals may abort over a short period of time. However, there are many other indirect losses to consider, derived from epidemic or endemic abortions, when evaluating the actual costs. These include expenses associated with professional help and diagnosis, loss of the genetic value of the animals, extended intervals for rebreeding and replacement of animals if aborted cows are culled. There is controversy regarding a possible impact on reduced weight gain and milk yield in infected animals (Dubey et al., 2017). It has been estimated that the global *N. caninum*-related losses represent an annual average exceeding 1.298 billion US $. In Spain, these seem to reach 9.8 and 19.8 million US $ in beef and dairy cattle, respectively (Reichel et al., 2013).

1.5. Diagnosis of bovine neosporosis

The best choices for *N. caninum* diagnosis in aborted fetuses are the detection of lesions by histological techniques and the PCR detection of the parasite in target tissues, mainly brain, heart and liver (Ortega-Mora et al., 2006; Dubey et al., 2017). Histological diagnosis may be facilitated by immunohistochemistry analysis with the use of specific *N. caninum* antibodies. However, infection cannot be discarded because of the obtaining of negative results, due to the low number of parasites in fetal tissues and the low sensitivity of this technique (Dubey et al., 2017). Also note that *N. caninum* congenital infections are frequent, therefore the presence of the parasite does not imply that it caused the abortion (Dubey et al., 2007). Abdominal and thoracic fluids from fetuses older than five months can also be used for the detection of *N. caninum* specific antibodies by ELISA, indirect immunofluorescence (IFAT), or Western blotting (WB), since maternal antibodies cannot cross the placental barrier (Dubey and Schares, 2006; Ortega-Mora et al., 2006).

In live animals, diagnosis of *N. caninum* infection is mainly carried out by serology, by detection of antibodies in serum or milk. Routinely, ELISA is the technique of choice for high

throughput screening at the herd level to support the control of neosporosis. Nevertheless, as commercial ELISAs are based on *N. caninum* tachyzoite antigens, these may not identify animals persistently infected if the parasite is quiescent. Bulk milk testing, due to its being cost-effective and non-invasive, is considered a good tool to determine a herd status, to be applied for *N. caninum* control and surveillance (Guido et al., 2016). Finally, the avidity ELISA permits the differentiation of herds with a primo-infection and high risk of exogenous transplacental transmission (low avidity in most animals) from herds with chronic infection and endogenous transplacental transmission (high avidity) (Ortega-Mora et al., 2019).

Individual serology is a good indicator of the risk of abortion, as a 2-26 fold higher abortion rate has been observed in serologically positive than in negative cows (López-Gatius et al., 2004; Weston et al., 2005). Timing of testing is important for the detection of positive animals. Because colostral antibodies may interfere with serological assays, animals should be tested when older than six months (Dubey et al., 2007). Most importantly, during the second half of gestation there is a higher chance of detecting infected animals, as the rise of antibody titers is higher at this period (Quintanilla-Gozalo et al., 2000; Pereira-Bueno et al., 2003; Nogareda et al., 2007). Due to the occurrence of false negative and positive results related to the limitations of diagnostic techniques and fluctuation of antibody titers, sampling repetition over subsequent pregnancies is recommended (Guido et al., 2016). If cows did not suffer abortion and purchase purposes are pursued, the preferential technique is WB since it is more specific and sensitive (Ortega-Mora et al., 2019).

In summary, establishing the cause-effect between abortion and *N. caninum* infection is complex. A positive result in the serologic test of maternal sera and fetal body fluids combined with the histological and PCR analysis are still not conclusive, although they may provide evidence for a *N. caninum*-associated abortion. When the observed lesions are severe and linked immunohistochemically to the parasite, it may be concluded that *N. caninum* was the cause of the abortion. A statistically significant association between seropositivity and abortion, by calculating the odds ratio between aborted and non-aborted cows, may help to confirm the diagnosis (Dubey et al., 2017) (Figure 3).

1.6. Prevention and control

The implementation of a control program against *N. caninum* in a herd should ideally be based on a combination of vaccination applied before mating and chemotherapy applied during gestation, in the fetal development period where most abortions occur (Hemphill et al., 2016). To date, the lack of effective vaccines or treatments reduces the control options to the diagnosis of the animals combined with appropriate management practices. However, considerable efforts have been made in vaccine and drug development, obtaining promising results in the last years (Horcajo et al., 2016; Sánchez-Sánchez et al., 2018a). The current status of research is described below.

1.6.1. Management control measures

The artificial insemination of seropositive cows with semen from beef bulls, replacement of seropositive animals having undergone two or more abortions, and embryo-transfer are some of the proposed measures to reduce *N. caninum* transmission in herds (Dubey et al., 2007; Dubey and Schares 2011; Almeria and López Gatius 2013). A mathematical modeling of the costs and benefit of the different measures showed that in farms with a high prevalence, replacements with seronegative cows may be the better option (Hasler et al., 2006).

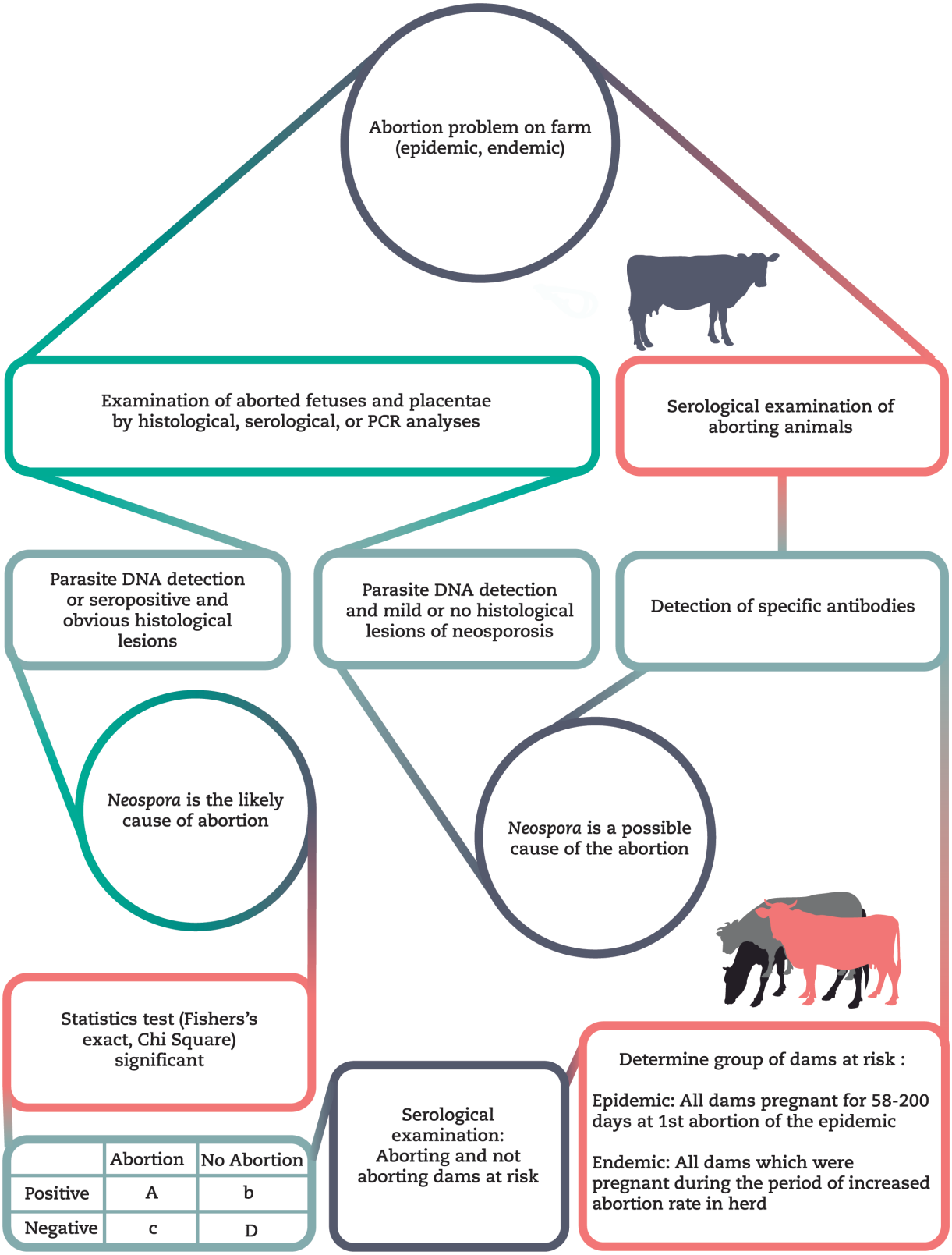

FIGURE 4 | Diagnosis of bovine neosporosis, based on Dubey et al., 2017.

Although it is well accepted that bovine neosporosis is mainly maintained within herds by vertical transmission, mathematical models indicate that certain levels of horizontal transmission are necessary for a lasting maintenance of infection (French et al., 1999). Thus, the control of horizontal transmission would be essential for *N. caninum* eradication. The access of dogs to potentially infected tissues should be avoided, as well as to the housing area, feed storage and drinking water of cows (Dubey et al., 2017).

1.6.2. Vaccination

Vaccination is considered the best control measure against *N. caninum* in the cost-benefit relation (Reichel and Ellis, 2009). Vaccine formulations employing *N. caninum* tachyzoite extracts have been assessed, and a vaccine based on tachyzoite lysate (Bovis Neoguard) was commercialized. However, later studies showed a variable efficacy of this vaccine in preventing abortion and no efficacy against transmission (Romero et al., 2004; Weston et al., 2012).

Studies carried out with the use of experimentally or naturally attenuated *N. caninum* strains delivered the most promising results regarding the development of a protective immune response against infection (Williams et al., 2007; Hecker et al., 2013; Rojo-Montejo et al., 2013; Weber et al., 2013). However, disadvantages associated to risk of virulence reversion, special needs of conservation and large-scale production complicate the commercialization of live attenuated vaccines (Reichel et al., 2015; Horcajo et al., 2016).

Vaccines based on recombinant subunit antigens may represent promising options. But to date, these have shown limited efficacy. A liposome-entrapped recombinant Nc-GRA7 has been assessed in a non-pregnant cattle infection model, inducing specific antibody and IFN-γ production. Immunization also resulted in a reduction of the parasite loads in the brain (Nishimura et al., 2013). However, in pregnant animals, formulations with recombinant antigens NcGRA7, NcSAG1 and Hsp20 combined with immune stimulating complexes failed to prevent fetal infection despite inducing high antibody responses before and after challenge (Hecker et al., 2014). The development of new subunit vaccines is hampered by the scarcity of parasite antigenic candidates, and also due to limitations in the current knowledge of the immune responses that should be induced to confer protection against *N. caninum* (Horcajo et al., 2016; Almería et al., 2017).

1.6.3. Chemotherapy and chemoprophylaxis

A great number of efficacy drug studies against *N. caninum* have been carried out in cell cultures and in murine models, but studies in bovine, and especially in pregnant models are scarce, showing a lack or moderate efficacy (Sánchez-Sánchez et al., 2018a).

Treatment with monensin in *N. caninum* non-pregnant cows was related to a lower specific immune response (Vanleeuwen et al., 2011), but its effectiveness in pregnant cattle remains to be assessed. Administration of decoquinate to naturally infected pregnant heifers reduced abortion rate and transplacental transmission (Journel et al., 2002). Ponazuril, tested in experimentally infected calves, allowed a complete abrogation of *N. caninum* DNA detection in the brain and other organs (Kritzner et al., 2002). In naturally infected herds, treatment of newborn calves and dogs with toltrazuril, along with the treatment of calves with sulphadiazine and trimethoprim drastically reduced *N. caninum*-associated abortions and seroprevalence (Cuteri et al., 2005).

More recent approaches have revealed new compounds with *in vitro* and *in vivo* activity in murine models against *N. caninum*. Most of them showed efficacy against the tachyzoite stage, but there is a lack of information with regard to their efficacy against the bradyzoite stage. Best results have been reported with the use of diamidines DB750 and DB745, miltefosine, buparvaquone, the quinolone ELQ-400 and bumped kinase inhibitors (BKI) 1517, 1294 and 1553 (Sánchez-Sánchez et al., 2018a). BKIs have been demonstrated to be promising compounds against neosporosis, as BKI 1553 conferred partial protection against abortion in a pregnant sheep model, also reducing parasite detection, parasite loads and lesion in the brain of the fetus (Sánchez-Sánchez et al., 2018b).

2. *Neospora caninum*-host cell interaction

Neospora caninum is able to actively invade a wide variety of cell types from its hosts. Because of its condition of obligate intracellular parasite, host-cell interactions are of crucial importance to ensure its development, reproduction, dissemination and transmission. Considerable efforts have been made to discern the processes which lead to *N. caninum* host-cell invasion and proliferation (Hemphill et al., 2006). On the other hand, due to the essential role that innate immunity plays as a primary effector at the interface between host and parasite until the establishment of adaptive immunity (Nishikawa et al., 2010), elucidating the mechanisms involved in the complex relationship between *N. caninum* and innate immune cells is key for the development of vaccines and other control measures (Hemphill et al., 2006).

2.1. *Neospora caninum* intracellular development and quiescence

2.1.1. *Lytic cycle*

The lytic cycle of *N. caninum* is a tightly regulated process which includes adhesion to the host cell, invasion, parasitophorous vacuole formation, multiplication and egress. The succession of cycles permits the parasite to proliferate and disseminate intra organically during the acute phase of infection (Pastor et al., 2016).

The adhesion process initiates with a parasite approach to the host cell through flexion-extension movements mediated by the actomyosin motor of the parasite cytoskeleton, also known as “gliding motility” (Jewett and Sibley, 2003). Later, adhesion takes place mediated by surface proteins of the parasite (mainly SAGs and SRS proteins) (Naguleswaran et al., 2005). Once attached, the tachyzoites are reoriented in a perpendicular position in respect to the host cell, establishing a stronger anchorage by the secretion of proteins of micronemes (MICs). A sequential secretion of MICs, proteins of rhoptries (ROPs) and proteins of dense granules (GRAs) allows the invasion of the host cell, supported physically by the conoid extrusion. The invasion is an active process in which the tachyzoites form the moving junction, an annular structure between the host cell and the parasite plasma membranes, which allows the progressive internalization of the tachyzoite into the cytoplasm of the host cell, pushed by the glideosome (Boucher and Bosch, 2015). The invagination of tachyzoite membrane together with the host cell membrane leads to the formation of the parasitophorous vacuole, which encompasses the tachyzoite. At the same time, ROPs and GRAs are secreted. These proteins participate in the formation and maturation of the parasitophorous vacuole as well as in the establishment of a tubulovesicular network inside the vacuole that communicates the parasite with the host cell (Hemphill et al., 2013). Finally, the host cell undergoes ultrastructural modifications, such as redistribution of intermediate filaments and microtubules of the cytoskeleton, as well as a reorganization of the

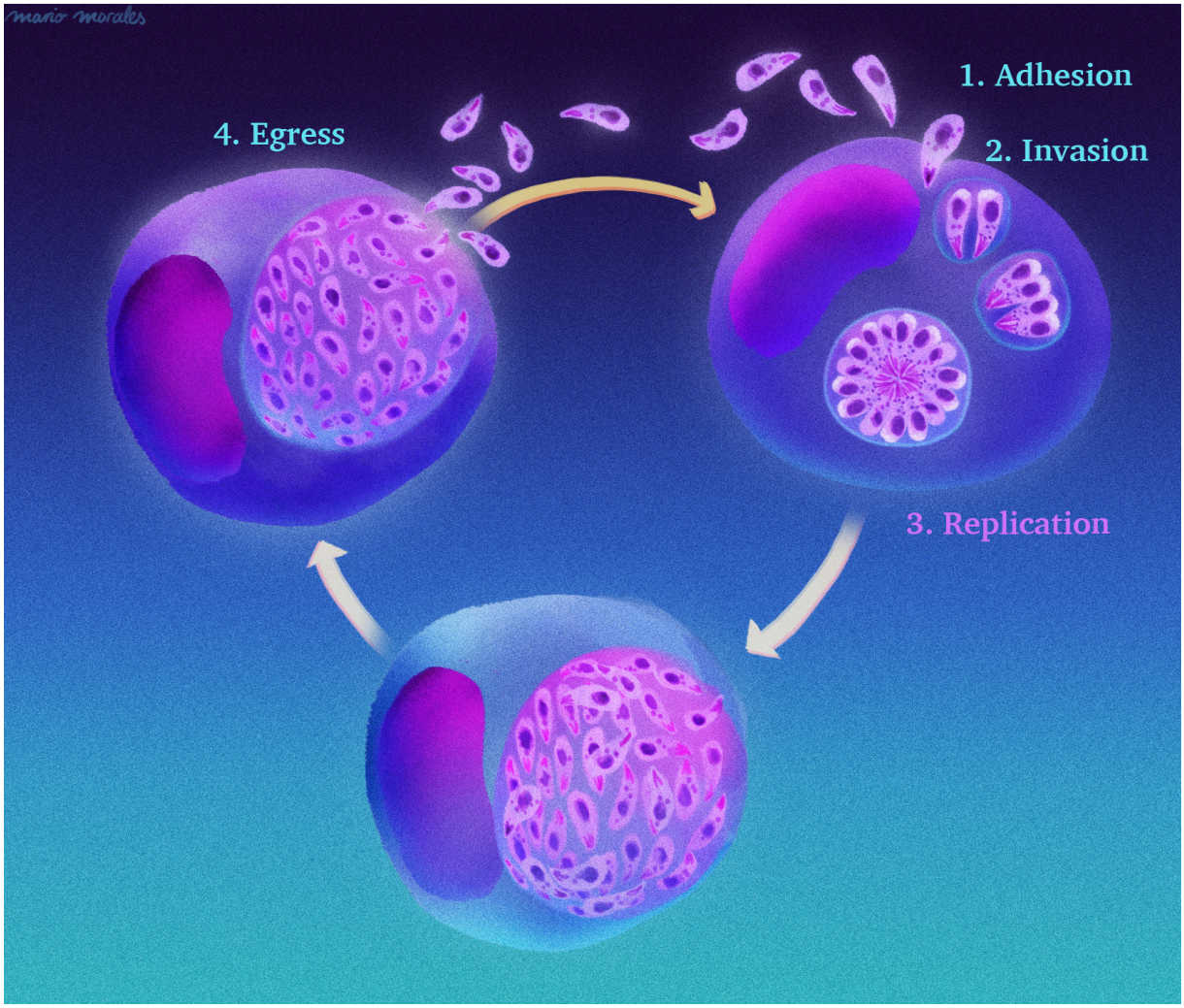

FIGURE 5 | ***Neospora caninum*** **lytic cycle.**

mitochondria and endoplasmic reticulum, enabling the nutrient transfer from cytosol to the parasite.

Tachyzoites replicate asexually by endodyogeny within the parasitophorous vacuole, producing up to 100 tachyzoites per vacuole in a few days. Egress is the final phase of the lytic cycle and involves the release of parasites into the inhospitable extracellular environment. This phenomenon is directly responsible for the lesions present in the host, which are a consequence of cell lysis and the immune reaction triggered locally. The process of egress seems to be closely regulated and coordinated with the process of the invasion of new cells. However, the mechanisms involved in the egress of *N. caninum* are not known yet. At a specific moment, some signals trigger the release of the tachyzoites, as occurs in *T. gondii* when intracellular calcium levels increase (Arrizabalaga and Boothroyd, 2004; Millholland et al., 2013). This calcium increment determines the activation of kinases and methyltransferases essential for the achievement of the process (Heaslip et al., 2010, 2011; Garrison et al., 2012; Lourido et al., 2012; McCoy et al., 2012). The egress also depends on the secretion of the PL1 protein (Perforin-like) of micronemes, which disorganizes the membrane and facilitates the exit of the parasites (Lavine and Arrizabalaga, 2008; Kafsack et al., 2009; Roiko and Carruthers, 2013),

and on a disturbance in the cytoskeleton of the host cell (Chandramohanadas et al., 2009). Whereas tachyzoites from other apicomplexan parasites, such as *T. gondii* or *B. besnoiti,* are able to remain infective in the *in vitro* extracellular environment for a long time (Hemphill et al., 1996; Frey et al., 2016), *N. caninum* tachyzoites must invade new cells over a short period of time (about four hours) in order to continue with the lytic cycle (Regidor-Cerrillo et al., 2011).

2.1.2. *Tachyzoite to bradyzoite interconversions*

Tachyzoite to bradyzoite conversion likely occurs due to the immune response generated by the host against the parasite which is able to eliminate most of the tachyzoites. Bradyzoites form intracellular cysts, which surrounded by a cyst wall, are protected from the immunological reaction of the host, which remains chronically infected (Weiss et al., 1999; Hemphill et al., 2006; Almería et al., 2017). Bradyzoite differentiation is a fast and asynchronous process (Risco-Castillo et al., 2004) during which, important changes in the protein expression profile take place. Of particular note are the expression of surface proteins specific to this stage (NcSRS9, NcSAG4 and NcBSR4) (Risco-Castillo et al., 2007, 2011; Aguado-Martínez et al., 2009), and proteins involved in anaerobic metabolism, stress response and DNA repair (Marugán-Hernández et al., 2010). Tissue cysts are mainly located in the CNS, although they have also been detected in the striated musculature (Dubey et al., 2017), and inside them bradyzoites can remain latent within an immunocompetent animal for many years without causing disease (Hemphill et al., 2006). The reactivation of bradyzoites has been associated with immunosuppression states. During pregnancy the efficient Th1 response, which keeps parasite proliferation in check, shifts to Th2 type, contributing to the reactivation of bradyzoites which reconvert to tachyzoites, proliferate and reach placental tissues and the fetus (Quinn et al., 2002; Innes et al., 2005).
Knowledge of *T. gondii* formation of tissue cysts *in vitro* has been used to study *in vitro* formation of *N. caninum* tissue cysts. However, many of the stress factors which stimulate conversion of *T. gondii* tachyzoites to bradyzoites, including higher incubation temperature, high pH, sodium arsenite treatment, and mitochondrial inhibitors were not suitable or had low efficacy for *N. caninum* conversion. Instead, the treatment of cell cultures for nine days with 70 µM sodium nitroprusside was most successful using a variety of *N. caninum* isolates and cell lines (Risco-Castillo et al., 2004).

2.2. Modulation of target cells of the innate immune system

Several *in vitro* and *in vivo* murine models studies have been carried out with the aim of discerning the role of the innate immune cells in the early response against *N. caninum* infection and the mechanisms involved in parasite immune evasion. Innate immune responses at the initial sites of infection are required for the control of *N. caninum*, and the early production of pro-inflammatory cytokines IL-12 and IFN-γ seems essential to restrict parasite growth and dissemination (Mineo et al., 2010; Almería et al., 2017). Innate immune cells that produce and respond to these cytokines include Natural killer (NK) cells, neutrophils, dendritic cells (DCs) and macrophages (Gurung et al., 2016), which may exert distinct roles in protective immunity.

2.2.1. Natural killer cells

The main source of IFN-γ during neosporosis has been traditionally attributed to $CD4^+$ T cells (Marks et al., 1998). However, several authors have demonstrated that NK, activated upon infection, contribute to IFN-γ production (Boysen, 2006).

The first description of an experimental infection of NK by *N. caninum* tachyzoites *in vitro* was provided by Boysen et al. (2006). These authors demonstrated that *N. caninum* was able to invade bovine NK isolated from peripheral blood, multiplying inside these cells. The parasite also triggered IFN-γ production from IL-2-activated NK. Although IFN-γ production did not require IL-12, it was enhanced in the presence of this cytokine. While mechanisms of NK activation by *N. caninum* have not been fully explored, it was suggested that they may occur among others, mediated by glycosylphosphatidylinositol (GPI) molecules of the parasites throughout toll-like receptors (TLR), as described for *Leishmania spp* (Becker et al., 2003). Additionally, the capacity of NK cells to kill infected target cells by incubating bovine fibroblast with *N. caninum* was assessed. Cytotoxic activity was observed in response to infection by a perforin-mediated mechanism (Boysen et al., 2006).

Noting that NK seem to act as early responders in *N. caninum* infections in bovine models (Klevar et al., 2007), the roles of NK and NKT (Natural killer T) cells in protective immunity were further investigated in a murine model. The depletion of NKT cell subset, but not of classical NK, resulted in increased parasite burdens in the brain and in the suppression of $CD4^+$ T cells activation. This suggests that NKT, but probably not NK cells, may play a crucial role in the early stage of *N. caninum* infection by activating $CD4^+$ T cells (Nishikawa et al., 2010).

2.2.2. Neutrophils

The role of neutrophils in combating *N. caninum* has been poorly investigated. Taubert et al. (2006) demonstrated that *N. caninum* infection induces the transcription of proinflammatory and adhesion molecules in bovine endothelial cells, thus stimulating polymorphonuclear neutrophil cells (PMN) adhesion. PMN early attraction and adhesion to the endothelium may lead to enhanced extravasation and the migration of these cells to the sites of infection (Taubert et al., 2006). In relation to this, following intraperitoneal *N. caninum* infection in mice, elevated numbers of monocytes/macrophages, but also neutrophils, are recruited at the initial site of infection (Wang et al., 2018). These mechanisms may be relevant in the subsequent reactions against the parasite, as both PMN and activated endothelial cells act by initiating innate and adaptive immune responses by recruiting other immune cells such as macrophages and T cells, by means of chemokine production. Additionally, because activated PMN are able to produce IFN-γ (Sohn et al., 2007), they may even participate in directing the bovine immune response towards a Th1-type (Taubert et al., 2006).

Besides the mechanisms previously shown, neutrophil extracellular trap (NET) generation has been recently described as an efficient mechanism of defense of PMN against diverse parasite infections including *N. caninum* (Villagra-Blanco et al., 2017). Interactions of *N. caninum* with bovine PMNs *in vitro* resulted in NET formation, entrapping the parasites and thus reducing their infectivity and thereby proliferation. Taken into account that *N. caninum* must infect bovine endothelial cells *in vivo* for intravascular dissemination, combined PMN adhesion to the endothelium and NET formation might represent efficient defense mechanisms to reduce parasitaemia during acute bovine neosporosis (Taubert et al., 2006; Villagra-Blanco et al., 2017).

2.2.3. Dendritic cells

DCs are innate immune cells specialized in antigen presentation to naive T cells, thus being the link with the adaptive response, directing Th1 or Th2 responses (Hume, 2008). Strobusch et al. (2009) demonstrated for the first time that *N. caninum* was able to infect and proliferate in

murine bone marrow DCs (BMDCs). Exposure of BMDCs to viable and inactivated tachyzoites resulted in cell RNA expression of pro-inflammatory cytokines IL-12p40 and TNF-α, and the regulatory IL-10, whereas IL-4 expression was not detected. In the light of the obtained results, the authors concluded that the intracellular presence of *N. caninum* tachyzoites does not seem to impair the early primary DC function.

The first *in vivo* evidence that plasmacytoid DCs (pDCs) and conventional DCs act in the early immune response against *N. caninum* was obtained with the use of murine models, demonstrating that these cell subsets are major producers of IL-12 when activated by parasite infection **(**Teixeira et al., 2009). Regarding plasmacytoid DCs, contrary to what was reported in *T. gondii* infections (Pepper et al., 2008), their splenic proliferation did not increase upon *N. caninum* mice infection, significant production of IFN-γ by these cells was not detected and depletion of these cells did not increase the susceptibility to *N. caninum*. These results suggest that pDCs do not play a major role in host immunity to *N. caninum* (Teixeira et al., 2009). Supporting these results, Mineo et al. (2009) showed that IFN-γ-mediated immunity against *N. caninum* in mice is dependent on MyD88 initial signaling, in a mechanism triggered by IL-12 release by DCs. MyD88 genetically deficient mice succumb to infection with low *N. caninum* infection dose due to uncontrolled tachyzoite replication related to a reduction in IFN-γ response by NKT, $CD4^+$ and $CD8^+$ T cells. Later, the participation of TLR2 in the initial recognition of *N. caninum* by BMDC was shown (Mineo et al., 2010).

The study of cytokine production by naïve murine BMDCs showed that live, freeze-killed and total whole-cell tachyzoite lysate of *N. caninum* tachyzoites stimulated the production of high levels of IL-12, IFN-γ and TNF-α cytokines. On the contrary, heat-killed tachyzoites or soluble antigens may not be able to elicit a strong enough pro-inflammatory immune response against the disease (Feng et al., 2010). Differences in murine BMDCs response induced by viable and nonviable *N. caninum* (heat-killed and antigenic extracts) was again shown by Dion et al (2011). In agreement with the previous work, live tachyzoites and antigenic extract but not heat-killed parasites altered the phenotype of immature DCs. Viable tachyzoites downregulated the expression of CD40 and MHC-II in DCs, whereas antigenic extract upregulated their expression. CD80 and CD86 were shown downregulated in DCs exposed to any of both stimulus. In addition, only viable tachyzoites and antigenic extract were able to induce IL-12 synthesis by DCs with the consequent IFN-γ secretion by T cells. These kind of studies facilitate the understanding of antigen priming, which is essential for the design of vaccines and adjuvants against neosporosis (Feng et al., 2010).

On the other hand, *N. caninum* exploit the migratory properties of DCs for shuttling into the organism by a Trojan horse mechanism like as *T. gondii* (Courret et al., 2006; Lambert et al., 2006)Ne*ospora caninum* induces a hypermigratory phenotype in human and murine DCs and adoptive transfer of tachyzoite-infected DCs in mice resulted in rapid dissemination of *N. caninum* and potentiated the transplacental passage to the offspring (Collantes-Fernández et al., 2012).

To date, no studies have shown the effects of *N. caninum* interaction with bovine DCs. However, the results derived from a recent work suggest that responses to *N. caninum* may vary depending on the host origin of antigen presenting cells (APCs) (Débare et al., 2019). Mouse DCs, mouse macrophages and bovine peripheral blood mononuclear cells (PBMCs) were exposed to parasite GPIs excreted in the supernatant of *N. caninum* culture. These glycolipids induced the production of IL-1β, TNF-α and IL-12p40 by murine DCs and macrophages, by signaling

cascades likely activated by TLR4, and reduced expression of MHC-I in murine DCs. In contrast to murine cells, bovine blood mononuclear cells produced increased levels of IFN-γ and IL-10, but reduced levels of IL-12p40 in response to GPIs. Furthermore, upregulation of MHC-I and downregulation of MHC-II was observed.

2.2.4. *Macrophages*

As well as DCs, macrophages are able to recognize pathogens by means of pattern recognition receptors including TLRs, C-type lectin receptors (CLRs), NOD-like receptors (NLRs) and retinoic acid inducible gene-I (RIG-I)-like receptors (RLRs). Signaling pathways are subsequently activated leading to phagocytosis, antigen presentation and release of cytokines and chemokines, which in turn recruit and activate other immune cells including circulating monocytes, thus enhancing the initial response. They also have an essential regulatory role, and by their conversion to an anti-inflammatory phenotype are able to terminate the inflammatory response and promote tissue repair (Hume et al., 2008; Zhang et al., 2014). Probably due to the fact that these cells mediate innate immune responses directly and make a crucial contribution to the effector phase of the adaptive immune response, macrophages are the innate immune cells which have received the greatest attention in studying *N. caninum*-host cell interaction. Since Abe et al. (2014) demonstrated that macrophage depletion prior to infection results in severe neosporosis in mice, increasing efforts have been carried out to unravel the role of these cells in fighting *N. caninum* and the mechanisms used by the parasite to avoid macrophage killing.

Several works have focused on the study of how *N. caninum* is recognized by macrophages as the first step to develop a protective response. Evaluation of TLR2 expression in mouse peritoneal macrophages showed upregulation of this receptor induced by *N. caninum* soluble antigens. The participation of TLR2 in the generation of effector immune responses against the parasite was also demonstrated, as diminished $CD4^+$ and $CD8^+$ T cell proliferation was observed in TLR2 deficient mice (Mineo et al., 2010). In support of this work, it has been recently described that TLR2 is involved in recognizing *N. caninum* cyclophilin by the murine macrophage cell line RAW 264.7, which correlates to the activation of the signal transduction of NF-κB and IL-12p40 production. TLR2 deficient mice succumb to *N. caninum* infection, suggesting the marked contribution of this receptor to the protective immunity *in vivo* against the parasite (Fereig et al., 2019). It has also been reported that extracellular vesicles secreted by *N. caninum* are recognized by murine bone marrow derived macrophages (BMDM) via TLR2, leading to modulation of cytokines TNF-α, IFN-γ and IL-12p40 production through the MAPK pathways (Li et al., 2018). On the contrary, Jin et al (2017) related the upregulation of IL-12p40 observed in mouse peritoneal macrophages challenged by *N. caninum* to MEK-ERK signaling via parasite recognition by TLR11. Finally, TLR3 has been shown to mediate type IL12p40, IFN-γ and IFN-β response to *Neospora* in BMDM by signaling through its adaptor protein TRIF, and TLR3-TRIF signaling enhances resistance against *N. caninum* in mice since it improves Th1 responses leading to reduced tissue inflammation and controlled parasitism (Beiting et al., 2014; Miranda et al., 2019).

Not only TLR but also NLR have been studied with the aim of determining their association with host innate immune responses developed during *N. caninum* infection. It has been suggested that the cytosolic receptor NOD2 may cooperate with TLRs to control parasite replication in *N. caninum* infected BMDMs, triggering an increment in the inflammatory profile which may induce pathogenesis in infected mice (Davoli-Ferreira et al., 2016) Additionally, the role of

inflammasome activation in restricting *N. caninum* intracellular proliferation in macrophages has been recently described (Wang et al., 2017, 2018). It was shown that *N. caninum* infection activates NLRP3 inflammasome in murine BMDM resulting in caspase-1 cleavage and the release of IL1β and IL-18. In addition, macrophages of NLRP3 deficient mice failed to limit *N. caninum* replication in the site of infection and reduced levels of IL-18 and IFN-γ were found in serum (Wang et al., 2017, 2018). C-type lectin receptors may also participate in *N. caninum* recognition in mice. Specifically, Dectin-1 seems to be involved in the parasite-induced downregulation of reactive oxygen species (ROS) and IL-12p40 (Da Silva et al., 2017).

The cell immune response triggered after parasite recognition has also been studied. Abe et al. (2014) described that murine peritoneal macrophages respond to *N. caninum* infection *in vitro* with increased expression levels of CD40, CD80 and CD86, and with the release of IL-6, IL-12 and IFN-γ. In addition, the intraperitoneal inoculation of mice with *N. caninum* induces macrophage migration to the site of infection. However, Dion et al. (2011) reported a downregulation of CD86 at the surface of these cells. An upregulation of MHC-II expression and IL-12 secretion was also observed upon *N. caninum* infection (Dion et al., 2011).

Several parasite effector molecules seem to be implicated in the induction of host immune responses during early infection in macrophages. One of them is GRA7, implicated in its pathogenesis by modulating the host cytokine and chemokine production. Murine peritoneal macrophages infected with GRA7 deficient tachyzoites showed a downregulation of RNA expression of genes involved in TNF signaling pathway, IL-17 signaling pathway and cytokine-cytokine receptor interaction pathway. In addition, IL12p40 and IL-6 cytokine production decreased in GRA7 deficient parasites in relation to wild type. GRA7-deficient parasites showed a reduced virulence in mice, as IFN-γ levels, parasite burdens and necrosis in the brain were higher for infection with the parental strain than with deficient tachyzoites (Nishikawa et al., 2018). Immune stimulating activity has also been demonstrated for *N. caninum* GRA6, which triggers IL-12p40 in mouse peritoneal macrophages. Protective cellular immune responses are also induced in murine models by this protein (Fereig et al., 2019). In addition, *N. caninum* 14-3-3 protein may be an infection-associated antigen involved in the host immune response by stimulating expression of pro-inflammatory cytokines such as IL-6, IL12p40 and TNF-α. This cytokine expression seems to be mediated by activation of MAPK, AKT and NF-κB signaling pathways by murine peritoneal macrophages (Li et al., 2019), independent of TLR2.

He et al. (2017) studied macrophage polarization dynamics during *N. caninum* infection in BALB/c mice and concluded that during the acute stage of infection, macrophages mainly polarize towards an M1 phenotype whereas they polarize towards an M2 type during the chronic stage. With the use of macrophage cell line J774A.1, derived from mouse ascites, they described that macrophage polarization towards M2 is mediated by peroxisome proliferator-activated receptor-γ (PPAR-γ) activation and NF-κB inhibition.

Neospora caninum has developed several mechanisms of immune evasion and dissemination. It has been suggested that during early infection, excreted/secreted antigens from *N. caninum* are capable of inducing monocyte and macrophage cell migration to the sites of infection. As it has been demonstrated that *N. caninum* is able to infect and replicate in these cells, this mechanism would enhance initial parasite invasion and proliferation. *In vitro* and *in vivo* assays support this hypothesis. Among the parasitic proteins involved in monocytes recruitment in infected mice, cyclophilins seem to present chemoattractant properties for monocytes and DCs, in a mechanism dependent of CCR5 receptor expression (Mineo et al., 2010). As a mechanism of evasion of

the host´s innate immune responses, *N. caninum* may manipulate p38 phosphorylation in its favor, inducing downregulation of IL12p40 production in BMDM isolated from mice. Although parasite effector proteins implicated are unknown, p38 activation is induced by a mechanism dependent on G-protein coupled receptor, PI3K and AKT signaling pathways (Mota et al., 2016). Despite the fact that *N. caninum* is not considered to be zoonotic (Calero-Bernal et al., 2019), *in vitro* studies using human macrophages have also been carried out. Invasion of the THP-1 human monocytic cell line by *N. caninum* induced an increased expression of proinflammatory cytokines IFN-γ, IL-1β, IL-8 and TNF-α and defense peptides (cathelicidins) mediated by MEK1/2 MAPK pathway. Furthermore, the secretion of these molecules restricted parasite infection and promoted the secretion of proinflammatory cytokines in naïve macrophages (Boucher et al., 2018).

Very few studies have been performed with the use of bovine macrophages. Similar to the reported results for neutrophils (Villagra-Blanco et al., 2017), it has been shown that *N. caninum* induces the formation of extracellular traps in bovine macrophages *in vitro* in an ERK 1/2- and p38 MAPK-dependent process. This mechanism may help reduce the initial infection rates in the acute phase of neosporosis in cattle, although *in vivo* studies in cattle are necessary to confirm this hypothesis (Wei et al., 2018). The restraining of *N. caninum* growth mediated by inflammasome activation was demonstrated in a bovine peritoneal macrophage cell line, also suggesting that the pyroptotic supernatant released from activated cells could impair *N. caninum* infection of new macrophages (Wang et al., 2018). Finally, the capacity of *N. caninum*-infected bovine macrophages to prime naïve T-cell responses has been studied. Macrophages primed with *N. caninum* antigen or with LPS limited parasite growth in relation to PBS-treated cells, related to IL-6 and IL-1β production and NF-κB activation. When in contact with infected macrophages, T-cells produced IL-17 and IFN-γ following a different pattern that is dependent on whether the macrophage was primed or not prior to infection. Unprimed macrophages induced a higher release of IFN-γ but lower IL-17A levels in T-cells than those primed. In the light of these results, the authors suggest that the dual pathological or protective role of IFN-γ during infection may be related to the simultaneous presence or not of a second major proinflammatory cytokine, IL-17 (Flynn and Marshall, 2011).

3. Immune response against *Neospora caninum*

A bigger question to understand neosporosis and yet to be answered is why only a low percentage of infected pregnant cows abort and why not all their progeny is born naturally infected. *Neospora caninum* infection underlies a complex immunological regulation that may lead to protection or contribute to the pathogenesis of abortion (Almeria et al., 2017). Interactions of the parasite with host cells of the innate immunity, first line of defense against infections, should be critical in determining the character of the subsequent response (Taubert et al., 2006). Studies *in vitro* with bovine cells and *in vivo* with murine models point toward a key role of macrophages (Flynn and Marshall, 2011; Abe et al., 2014; Wei et al., 2018), NK (Boysen et al., 2006) and neutrophils (Villagra-Blanco et al., 2017) in the early immune response against *N. caninum*. However, this has been poorly characterized *in vivo* in cattle, as studies have been mainly focused on cell-mediated immunity (CMI) and humoral adaptive immunity. In addition, the high degree of variability between studies in relation to the use of pregnant or non-pregnant animals, times of inoculation and culling, breeds, *N. caninum* isolates and routes of inoculation hampers the obtaining of relevant conclusions based on the comparison of findings (Benavides et al., 2014).

3.1. Non-pregnant bovine model

Most of the research carried out in non-pregnant cattle was focused on the study of the parasite cycle or the possibility of post-natal transmission of neosporosis (Benavides et al., 2014). However, several experimental studies aimed to characterize the immune responses generated against *N. caninum* infection and to assess the immunogenicity of vaccine candidates. The main results obtained in these studies using non-pregnant bovine models are summarized in Table 1.

3.1.1. Cell-mediated immune responses

The innate immune response against *N. caninum* may be especially important during the early life period of calves, which may compensate for the lack of a fully functional adaptive response. This hypothesis is supported by the fact that a higher proportion of monocytes was found in neonatal blood compared with adults, and these are more sensitive to infection following *in vitro* challenge, secreting higher amounts of proinflammatory cytokines and triggering enhanced NK activation. A greater inflammatory baseline in monocytes of neonates was also demonstrated by microarray analysis, followed by a higher activation of the JAK-STAT pathway (Sharma et al., 2018). CMI responses characterized by cell proliferation associated with the production of IFN-γ were recorded in calves before one week of *N. caninum* subcutaneous tachyzoite infection (Lunden et al., 1998) and from one week onward following oral infection with sporulated oocysts (de Marez et al., 1999).

Klevar et al, (2007) demonstrated that NK are early responders in *N. caninum* infection in calves, producing IFN-γ and promoting a stronger $CD8^+$ T cell response which also contribute to the IFN-γ pool, whereas the major source of this cytokine in later times are $CD4^+$ T cells (Marks et al., 1998; Klevar et al., 2007). *Neospora caninum* specific cytotoxic T lymphocytes CTL response was shown in experimentally infected non-pregnant cows, providing evidence that the killing of infected cells is mediated by $CD4^+$ CTL through a perforin/granzyme pathway (Staska et al., 2003).

In experimental infected bulls, a significant increase in serum IFN-γ was reported as soon as three days post-infection (dpi) (Serrano-Martínez et al., 2007; Ferre et al., 2008), suggesting that IFN-γ level seems to be a good indicator of a recent *N. caninum* infection (Ferre et al., 2008).

3.1.2. Humoral immune responses

A specific serological response can be detected from two weeks after infection of calves with *N. caninum* parasites. The antibody titers may not be influenced by the dose of infection, as animals inoculated with 106 tachyzoites showed similar specific humoral responses than those inoculated with 108 tachyzoites (Maley et al., 2001). Fluctuation of antibody levels throughout large periods of time after parasite inoculation has been shown to occur, which may indicate a recrudescence of infection with antigen stimulation (de Marez et al., 1999; Maley et al., 2001). Experimentally infected bulls developed specific serum IgG1, IgG2, and IgM responses to *N. caninum*. Specific anti-*N. caninum* IgG antibodies were also detected in seminal plasma (Serrano-Martínez et al., 2007) whose levels increased after re-infection (Ferre et al., 2008).

TABLE 1 | Experimental infections in non-pregnant cattle involving the study of cell-mediated and humoral immune responses against *N. caninum*

References	Breed	Age	Isolate	ROI	Dosage	Parasite stage	Aim of the study	Main findings
Marks et al., 1998	NS	6 months	Nc-1	SC	$2.5x10^8$	tachyzoite	Identification of *N. caninum* antigens that are important in humoral an CMI responses to the parasite	A group of tachyzoite antigens ≤ 30 Kda stimulated *in vitro* proliferation of $CD4^+$ T cells from infected calves, with high IFN-γ production levels. Several antigens were recognized by antibodies produced in these animals
Lunden et al., 1998	NS	2-4 months	Nc-1	SC	$2.5x10^8$	tachyzoite	To examine cell proliferative responses and induction of IFN-γ in *N.caninum* experimentally infected calves	Significant proliferative responses to *N. caninum* were recorded from 4–6 dpi, accompanied by production of high levels of IFN-γ.
De Marez et al., 1999	Holstein-Friesian	2.5 months	Nc-2	Oral	10^4–10^5	oocysts	To determine the potential of *N. caninum* oocysts to infect calves, and to investigate initial immune responses that arise after oral infection	CMI response was seen at 1 wpi; At 2-4 wpi specific IgG1 and IgG2 antibodies were detected. Presence of reactive cells in organs 2.5 mpi, and parasite DNA detected in nervous system, indicates systematically stimulation by parasite antigen.
Maley et al., 2001	Friesian, Hereford or Friesian-cross-Hereford	6 months	Nc-1	SC	$5x10^6$ & $5x10^8$	tachyzoite	To analyze the serological responses of calves to low or high dose of *N. caninum* tachyzoites infection during 1 year	IgG avidity increased 2 wpi, until week 12 when infection was well established. The two different doses produced a similar antibody response. Fluctuation in the levels of specific antibody throughout the yearlong study, may indicate periodic recrudescence of infection.
Staska et al., 2003	Holstein-Friesian	5–7 year	Nc 1	IM & IV	10^7 & 5×10^6	tachyzoite	To study parasite-specific responses of $CD4^+$ cytotoxic T lymphocytes	Cytotoxic T lymphocytes (CTL) are important mediators of protective immunity against *N. caninum*, killing infected cells through a perforin/granzyme pathway
Klevar et al., 2007	Norwegian Red	3 months	Nc-Liverpool	IV	10^7	tachyzoite	To investigate the role of NK cells and other CMI responses in an experimental *N. caninum* infection model.	$CD4^+$ T cells were the major IFN-γ producing cells, but in the early stages of the infection both NK cells and $CD8^+$ T cells contributed to IFN-γ production
Serrano-Martinez et al., 2007	Asturiana de los Valles	3.4-6.5 years	Nc-1	IV	10^8	tachyzoite	To investigate the presence of *N. caninum* in semen and blood of experimentally infected bulls, and the development of specific antibody and IFN-γ responses.	Presence of N. caninum DNA in the semen and blood of experimentally infected bulls was reported. Specific antibody and IFN-γ responses were developed. Anti-*N. caninum* IgG was detected in seminal plasma

Ferre et al., 2008	Asturiana de los Valles	3.9-12.6 years	Nc-1	IV	10^8	tachyzoite	To study the effects of *N. caninum* re-infection in bulls on parasite detection and immunological responses	Significant and persistent serum-specific IgM and IgG antibody responses after re-infection. Higher IgG levels in seminal plasma, and IFN-γ levels in serum in re-infected rather than in chronically infected bulls. Parasite load in semen very similar between both groups.
Rocchi et al., 2011	NS	2 months	Nc-1	SC	10^8	tachyzoite	To identify *N. caninum* antigens that are recognized by $CD4^+$ T cells derived from infected cattle	Identification of 6 *N. caninum* target proteins and 16 functional orthologues of *T. gondii*

NS: not stated; ROI: route of administration; IV: intravenous; SC: subcutaneous; dpi: days post-infection; wpi: weeks post-infection; mpi: months post-infection; IR: immune response.

3.2. Pregnant bovine model

Two main factors seem to be linked to the outcome of infection in pregnant cattle, virulence of the infecting strain and timing. More specifically, the period of gestation when infection occurs is important because the immune response generated will be highly dependent on the status of the immune system of the dam and the immunological maturity of the fetus (Goodswen et al., 2013; Dubey et al., 2006). In addition, the development of effective immunity to the parasite seems to vary depending on whether the infection occurs prior to or during gestation. It has been shown that animals naturally or experimentally infected prior to gestation can develop immunity which will protect them against abortion and may prevent, or not, vertical transmission when infected during a later gestation (Innes et al., 2001; Williams et al., 2000, 2003).

Many experimental infections have been carried out with the aim of unraveling the immunological regulation that takes place in the infected pregnant cattle, which is determinant for the outcome of the infection. These are summarized in Table 2.

3.2.1. *Cell-mediated immune responses*

As in *T. gondii*, CMI mechanisms likely play the most important role in reducing *N. caninum* proliferation within the host, diminishing parasitaemia (Almería et al., 2003). It has been demonstrated that following stimulation with *N. caninum* antigen, PBMCs and $CD4^+$ T cells obtained from experimentally infected pregnant cows proliferate and increase the production of IFN-γ and IL-4 from the end of the first week post infection (wpi) (Rosbottom et al., 2007; Regidor-Cerrillo et al., 2014). This early response, not transiently polarized towards Th1 or Th2, is likely to be associated with an innate immune response triggered by the interaction of parasite-associated molecular patterns and recognition receptors such as TLR on APC (Regidor-Cerrillo et al., 2014). Regarding TLR, studies have suggested the involvement of TLR3, TLR7 and TLR8 during early pregnancy (day 70) or TLR2 and TLR9 in late pregnancy (from day 210) in triggering maternal and fetal immune responses to *N. caninum* infection (Bartley et al., 2013; Marin et al., 2017).

The most important subsets of the CMI response during pregnancy are T helper (Th) cells, which polarize and regulate the strength of the response through cytokines, classified in pro-inflammatory, anti-inflammatory and regulatory. Pro-inflammatory cytokines, such as IFN-γ, IL-12 and TNF-α, are secreted by Th1 cells and induce CMI, critical for the control of intracellular parasites. Anti-inflammatory cytokines such as IL-4 are secreted by Th2 cells and promote humoral responses. Treg cells are essential to maintain the homeostasis of cells involved in the adaptive immune response, either by contact-dependent suppression or by releasing anti-inflammatory cytokines such as IL-10 and TGF-β (Almeria et al., 2017). A key role of Th1 cytokines IFN-γ and IL-12 in protective immunity against this parasite has been indicated in murine models (Baszler et al., 1999). However, during pregnancy Th1 responses may be potentially damaging and cause fetal rejection or the destruction of the placental tissues incompatible with fetal survival (Maley et al., 2006). Infected cows may abort from 3 months of gestation to term, but most of the *N. caninum* associated abortion in naturally infected animals occur at mid gestation (Dubey et al., 2007; Almería et al., 2017). Studies performed in pregnant cattle infected at this period reported a transient suppression of T-cell responsiveness from week 18 of gestation (Innes et al., 2001). This state of hyporesponsiveness to the parasite was accompanied by decreased lymphocyte subpopulations, reduced cell proliferation and downregulation of IFN-γ production, which may result in an uncontrolled *N. caninum* proliferation (Innes et al., 2001; Almería et al., 2003).

The knowledge obtained from experimental infections in pregnant cattle (Table 2) points toward the requirement of IFN-γ to limit *N. caninum* proliferation, but a critical threshold of IFN-γ levels and the counterbalance with other cytokines seems to be necessary to limit adverse effects on pregnancy (Almería et al., 2014, 2016a. Almería and López Gatius, 2015). In fact, several studies have shown the concomitant production of both Th1-, Th2- and Treg-cytokines during experimental *N. caninum* infection in both aborting and non-aborting cows at any point of the pregnancy. Almeria et al. (2003) demonstrated an increased expression of TNF-α, IL-12 and IL-4 in dams and IFN-γ, TNF-α and IL-10 in fetuses infected at 110 days of gestation. This response resulted protective against abortion but failed to prevent transplacental transmission. Accordingly, Rosbottom et al. (2007) showed high percentages of circulating $CD4^+$ cells that expressed both IFN-γ and IL-4 in infected dams at 70 and 210 of gestation, which suggests that the clear Th1/Th2 dichotomy observed in other species is rare in cattle (Hecker et al., 2013). Dams experimentally infected at 110 days of gestation with live fetuses showed higher IL-4 levels and lower IFN-γ/IL-4 ratios than cows with dead fetuses (Darwich et al., 2016). In addition, Almería et al., 2016a described the upregulated expression of Th1, Th2 and Treg-cytokines in infected dams at 110 days of gestation carrying live fetuses and in their fetuses. The downregulation of Th2 and Treg cytokines observed in infected dams which aborted, suggests an immunological recovery of cytokine gene expression levels in dams a few weeks after abortion (Almería et al., 2016a).

Finally, very few studies have analyzed Th17 cytokines in *N. caninum* infections. Darwich et al. (2016) studied IL-17A production in aborting and non-aborting dams infected at 110 days of gestation and in their fetuses, and found very low levels for this cytokine, despite the fact that *in vitro* studies with bovine macrophages suggested that the dual protective or pathogenic effect of IFN-γ may depend on the simultaneous production of IL-17 (Flynn and Marshall, 2011).

3.2.2. Humoral immune response

As described above, protective immunity to neosporosis rather than humoral is mainly cell-mediated. The presence of specific *N. caninum* antibodies indicates exposure to the parasite (Almeria et al., 2017).

Several studies have shown that seropositive cows are more likely to abort than seronegative ones, and elevated antibody titers have been related to a higher risk of abortion (Conrad et al., 1993; Quintanilla-Gozalo et al., 2000; López-Gatius et al., 2004; Guido et al., 2016). In addition, reactivation of chronic infections leading to transplacental infection has been associated with an acute increase of *N. caninum*-specific antibodies (Quintanilla-Gozalo et al., 2000; Guy et al., 2001; Andrianarivo et al., 2005).

TABLE 2 | Experimental infections in pregnant cattle involving the study of cell-mediated and humoral immune responses against *N. caninum*

References	Breed	Gestation period	Isolate[1]	ROI	Dosage	Fetal mortality[2]	Aim of the study	Main findings
Conrad et al., 1993	NS	Natural infection					Detection of humoral responses in cattle with *N. caninum* natural or experimental infection	High antibody titers at the time of abortion. High precolostral titers in congenitally infected calves
	NS	120	Nc-BPA1	IV&IM	$3x10^6$& $5x10^6$	0/2 (SS)		Seroconversion 9 dpi with peaks at 32 dpi. High titers in fetus
Williams et al., 2000	Holstein-Fresian	70	Nc-Liverpool	IV	10^7	5/6 (21)	To determine the association between the time of infection during gestation and fetal survival	High IFN-γ and lymphoproliferation in both groups. IgG2 biased response indicating a profound Th1 helper-like response. Infection at 70 days of gestation resulted in fetopathy and resorption, and at 210 days of gestation in the birth of asymptomatic, congenitally-infected calves
		210				0/6		
Andrianarivo et al., 2001	NS	159-169	Nc-BPA1	IV&IM	$3x10^7$& $5x10^7$	0/5 (SS)	To study immune responses in pregnant cattle and bovine fetuses following experimental infection	Variable predominant IgG1, IgG2 or mixed IgG1-IgG2 among animals. No correlation between IgG2 titers and IFN-γ levels. CD4-T cells were the main responsible for CMI responses. Strong specific humoral responses in fetuses, predominantly IgG1, and CMI responses highly variable among fetuses
Innes et al., 2001	Holstein-Fresian	140	Nc-1	SC	10^8	0/6	To determine if infection of cattle prior to pregnancy would protect the fetus if the dams were challenged with *Neospora caninum* at mid-gestation	Positive CMI and humoral responses to *N. caninum* were recorded after infection prior to pregnancy and at mid gestation. The immune response generated prior to pregnancy protected against vertical transmission of *N. caninum* following infection at mid-gestation
Almeria et al., 2003	Angus	110	Nc-Illinois	IV	10^7	0/6 (SS)	To study cytokine expression in dams and fetuses after experimental *N. caninum* infection at mid gestation	Infected dams showed compartmentalized changes in lymphocyte subpopulations. Increased levels of T lymphocytes were observed in the fetuses. Dams and fetuses showed increased Th1 and Th2 cytokines expression. Transplacental transmission but not abortion was recorded.
Williams et al 2003	Holstein-Freisian	70	Nc-Liverpool	IV	10^7	4/4 (21-35)	To investigate the nature of the immune response during gestation in naturally chronically infected cattle	Protective immunity occurs in neosporosis. Whilst immunity to a pre-existing infection will protect against abortion after an exogenous challenge, will not prevent transplacental transmission

De Yaniz et al., 2007	Aberdeen Angus, Hereford and their crossbreeds	150	Nc-1	IV/CO	10^8	0/19	To compare systemic humoral immune responses in pregnant heifers inoculated with *N. caninum* tachyzoites by conjunctival and IV routes	The conjunctival inoculation of *N. caninum* tachyzoites induces specific systemic antibodies in pregnant heifers
Rosbottom et al., 2007	Holstein-Freisian	70/210	Nc-Liverpool	IV	10^7	NA	To test if divergent outcomes of *N. caninum* infection of cattle in early and late gestation may be caused by temporal differences in the maternal immune response	Similar immune response to *N. caninum* based on IFN-γ and IL-4 expression by $CD4^+$ T-cells isolated from infected pregnant cattle, irrespective of the time of infection
Rojo-Montejo et al., 2009b	Holstein-Freisian	70	Nc-1	IV	10^7	3/5 (26-34)	To determine the ability of Nc-Spain1H, with low virulence in the murine model, to induce fetal death in a pregnant bovine model	The virulence of Nc-Spain1H was also reduced in cattle. The magnitude of the CMI and humoral response was significantly higher in the Nc-1- than in the Nc-Spain1H-inoculated group.
			Nc-Spain1H			0/5		
Caspe et al., 2012	Aberdeen Angus	65	Nc-Spain7	IV	10^8	7/7 (28-35)	To characterize the pathogenesis of infection of Nc-Spain7 isolate at day 65 of gestation	Higher mortality and total anti-*N. caninum* IgG earlier and higher in the Nc-Spain7 group . Immune response towards a Th2 profile is suggested. Similar IFN-γ production in both groups. The higher pathogenicity of Nc-Spain7 may be related with a higher rate of multiplication.
			Nc-1			2/4 (SS)		
Bartley et al., 2012	Holstein-Fresian	70	Nc-1	IV	$5x10^8$	6/6 (28-42)	To study maternal and fetal immune responses after experimental infected with *N. caninum* at day 70 of gestation	Higher priming of a CMI response in dams inoculated via SC carrying live fetuses, which inhibited vertical transmission. IV route resulted in greater fetal mortality and less efficient immune priming. Fetuses from day 84 of gestation were capable of producing CMI responses including IFN-γ, IL-4, IL-10, and IL-12 production, and humoral responses from day 98
				SC	$5x10^8$	3/6 (28-56; SS)		
Bartley et al., 2013	Aberdeen Angus cross or Belgian Blue cross cattle	210	Nc-1	SC	10^8	0/11 (SS)	To study maternal and fetal immune responses after experimental infected with *N. caninum* at day 210 of gestation	Dams and fetuses mounted specific CMI, humoral and innate responses. The increasing immunological maturity of the fetus limites the clinical severity of the infection compared to earlier infections. Fetuses mounted humoral and CMI responses by 14 dpi, involving anti-*Neospora* IgG, and the production of IFN–γ, IL-4 and IL-10. Overexpression of TLR-2 and TLR-9 in dams and TLR-9 in fetuses.

Bacigalupe et al., 2013	Aberdeen Angus	65	Nc-6 Argentina	IV	$5x10^7$	0/4 (SS)	To study the biological behavior of Nc-6 Argentina isolate by experimental inoculations into seronegative and seropositive pregnant cattle	In the seropositive group, the antibody titers raised earlier and higher. The CMI response was triggered by infection in both groups, but was not effective in preventing transplacental transmission and induce fetopathy. This could be due to the early age of gestation in which the inoculation was made.
Regidor-Cerrillo et al., 2014	Holstein Fresian	70	Nc-Spain7	IV	10^7	6/6 (24-49)	To study the influence of *Neospora caninum* intra-species diversity on abortion outcome, parasite dissemination and immune responses in pregnant cattle	Fetal mortality in all infected heifers but earlier in Nc-Spain7-infected, with parasites more frequently detected in placenta and fetus, and earlier and higher total IgG levels. Seropositive titers in fluids of dead fetuses. Specific stimulation of PBMCs triggered increase of IFN-γ and IL-4 levels from 6 dpi onwards for both infection groups. IFN-γ production peaked earlier for Nc-Spain8 and IL-4 for Nc-Spain7.
			Nc-Spain8			6/6 (30-44)		
Almeria et al., 2016b	Friesian	110	Nc-Spain7	IV	10^7	3/6 (14-28; SS)	To investigate the pathogenesis of bovine neosporosis during the second term of gestation	Specific humoral immune responses from 3-4 wpi. Higher antibody levels in dams with dead fetuses. Infected fetuses developed antibodies by 6 wpi. Higher levels in dead fetuses. Lower antibody levels in dams with live fetuses. One dam with an aborted fetus showed plasma IFN-γ production.
Almeria et al., 2016a	Friesian	110	Nc-Spain7	IV	10^7	3/6 (14-28; SS)	To determine the cytokine gene expression in aborting and non-aborting dams and in their fetuses after *N. caninum* infection at 110 days of gestation	Up-regulated expression of Th1, Th2 and Treg in infected dams with live fetuses and in their fetuses. Down-regulation of Th2 and Treg cytokines in infected dams which aborted, suggesting immunological recovery of cytokine expression levels in dams a few weeks after abortion.
Darwich et al., 2016	Friesian	110	Nc-Spain7	IV	10^7	3/6 (14-21; SS)	To determine cytokine production in dams and their fetuses naturally infected or after experimental infection at 110 days of gestation	Higher IFN-γ and IL-4 production in PBMCs from experimentally-infected animals compared to naturally-infected. No differences in IFN-γ regardless of the incidence of live or dead fetuses. IL-17A production very low. Infected dams with live fetuses showed higher IL-4 levels and lower IFN-γ/IL-4 ratios than cows with dead fetuses. The results highlight the important role of an inverse IFN-γ/IL-4 balance in conferring protection against abortion.

[1]Isolates were inoculated in the tachyzoite stage in all the experimental infections.
NS: not stated; ROI: route of administration; IV: intravenous; SC: subcutaneous; OC: ocular; SS: serial sacrifice. PBMC: peripheral blood mononuclear cell

3.3. Fetal immunity

The capability of the fetus to mount an immune response against infection increases as the gestation progresses, in relation to the degree of development of its immune system. The gestation period for cattle is about 280 days long. During the first third of pregnancy, the fetus is especially vulnerable, and is unlikely to survive if it is infected by *N. caninum* (Dubey et al., 2017). Fetuses aborted in early pregnancy show necrotic lesions without inflammatory reactions, and parasite dissemination with uncontrolled multiplication is detected (Macaldowie et al., 2004; Dubey et al., 2006; Gibney et al., 2008; Almería et al., 2017). From day 100 of gestation onward, fetuses are able to show a specific humoral and cellular response against this parasite (Bartley et al., 2012, 2013), coincident with the period when the thymus, spleen and peripheral lymph nodes have attained a stage of development which enable them to start to recognize and respond to pathogens. In fetuses of experimentally infected dams at 110 days of gestation, significant cytokine expression was observed as early as four months of gestational age (Almeria et al., 2003, 2010). This response may or may not be sufficient to resolve the infection and save the fetus. Infection in mid pregnancy results in a reduction of parasite dissemination, more restricted multiplication and fewer lesions. Small foci of necrosis can be observed surrounded by an inflammatory infiltrate (Dubey et al., 2006, 2017). In the third trimester, the increasingly competent defense reached by the fetus along with the maternal immune response leads to survival. Experimental infections at day 210 of pregnancy showed no abortion and an absence of lesions in the fetus (Williams et al., 2000; Benavides et al., 2012). The better control of the parasite by the immune response of both mother and fetus may explain the lower parasite loads in placental and fetal tissues reported at this period when compared to infections at 70 and 140 days of gestation (Benavides et al., 2012). At this period, a high rate of vertical transmission is usually observed (Almería et al., 2017).

4. *Neospora caninum* biological diversity

A major factor linked to the outcome of infection is the virulence of the infecting isolate (Dubey et al., 2006). However, little is known about how the biological diversity of *N. caninum* influences clinical presentation and immune responses in bovine neosporosis (Regidor-Cerrillo et al., 2014).

4.1. *Neospora caninum* population

More than 100 *N. caninum* isolates have been obtained to date, from infected domestic and wild hosts. Tachyzoites are elicited by cultivating a homogenate of the infected tissue in cell cultures, or by the inoculation of immunodeficient mice, whereas oocysts are recovered by feeding dogs with these tissues (Dubey et al., 2017; Ortega-Mora et al., 2019). A total of 10 isolates have been obtained by the SALUVET research group in Spain, mainly from clinically healthy, but congenitally infected calves (Table 3), with the purpose of characterizing their intra-specific variability (Regidor-Cerrillo et al., 2008; Rojo-Montejo et al., 2009a). To do so, they have used *in vitro* (cell cultures) and *in vivo* (murine and bovine) infection models, and more recently, -omics technologies have been incorporated to the comparative studies. These tools have helped advance the understanding of host-parasite interactions and the identification of potential *N. caninum* virulence factors, which could represent targets for chemotherapy and vaccine development (Horcajo et al., 2018).

TABLE 3 | Virulence classification of *N. caninum* isolates, according to their behavior *in vitro* and in murine pregnant models

Isolate	Origin	*In vitro* model		Pregnant mice model			Virulence consensus	References
		pIR4h	TY56h	Neonatal morbidity	Neonatal mortality	Vertical transmission		
Nc-Bahia	Brain, dog with neurological signs	High	High	High	High 100%	High 100%	High	Gondim et al., 2001
Nc-Liverpool	Brain, dog with neurological signs	High	High	High	High 100%	High 100%	High	Barber et al., 1995
Nc-1	Brain, dog with neurological signs	-	Moderate	High	High 76.8%	High 92.8%	High	Dubey et al., 1988
Nc-2	Muscle, dog	-	-	-	-	-	-	Hay et al., 1990
Nc-Ger2	Feces (oocysts), dogs	Low	Low	Low	Low 7.7%	Low 30.8%	Low	Schares et al., 2005
Nc-Ger3	Feces (oocysts), dogs	Moderate	High	Moderate	Moderate 19%	Low 9.1%	Moderate	Schares et al., 2005
Nc-Ger6	Feces (oocysts), dogs	Low	Low	Low	Low 4%	Low 23.1%	Low	Schares et al., 2005
Nc-6 Argentina	Feces (oocysts), dogs	Moderate	Moderate	Low	Low 0%	Moderate 53.8%	Low-Moderate	Basso et al., 2001
Nc-Nowra	Brain, asymptomatic congenitally infected calf	-	-	Moderate	Low	High 87%	Low-Moderate	Miller et al., 2002
Nc-Spain1H	Brain, asymptomatic congenitally infected calf	Low	Low	Low	Low 0.5%	Low 5%	Low	Rojo-Montejo et al., 2009a
Nc-Spain2H	Brain, asymptomatic congenitally infected calf	Moderate	Low	Moderate	Moderate 20%	Moderate 61.3%	Low-Moderate	Regidor-Cerrillo et al., 2008
Nc-Spain3H	Brain, asymptomatic congenitally infected calf	Low	Low	Low	Low 5%	High 89%	Low-Moderate	Regidor-Cerrillo et al., 2008
Nc-Spain4H	Brain, asymptomatic congenitally infected calf	High	High	High	High 100%	High 97.3%	High	Regidor-Cerrillo et al., 2008
Nc-Spain5H	Brain, asymptomatic congenitally infected calf	Moderate	High	High	High 95%	High 100%	High	Regidor-Cerrillo et al., 2008
Nc-Spain6	Brain, asymptomatic congenitally infected calf	Moderate	High	Moderate	Moderate 30%	Moderate 57.6%	Low-Moderate	Regidor-Cerrillo et al., 2008
Nc-Spain7	Brain, asymptomatic congenitally infected calf	Moderate	High	High	High 95%	High 79.1%	High	Regidor-Cerrillo et al., 2008
Nc-Spain8	Brain, asymptomatic congenitally infected calf	Moderate	Low	Low	Low 1.1%	Moderate 56.4%	Low-Moderate	Regidor-Cerrillo et al., 2008
Nc-Spain9	Brain, asymptomatic congenitally infected calf	Moderate	Moderate	Moderate	Moderate 30%	Moderate 52.6%	Low-Moderate	Regidor-Cerrillo et al., 2008
Nc-Spain10	Brain, symptomatic congenitally infected calf	Moderate	Moderate	Moderate	Moderate 18-20%	Moderate 65.5%	Moderate	Regidor-Cerrillo et al., 2008
Nc-S197	Brain, symptomatic congenitally infected calf	-	-	-	-	-	-	Weber et al., 2012
Nc-BPA-1	Brain, aborted calf	-	-	-	-	-	-	Conrad et al., 1993
Nc-Illinois	Brain, infected calf	-	-	-	-	-	-	Gondim et al., 2002
Nc-SweB1	Brain, aborted calf	-	Low	-	Low	-	Moderate	Atkinson et al., 1999

pIR4h: parasite invasion rate determined at 4 hpi; TY56h: Tachyzoite yield determined at 56 hpi.

4.2. *Neospora caninum* variability in *in vitro* models

Success in establishing *in vitro* cultures of parasites has greatly facilitated the description of their morphology, ultra-structural organization, behavior, physiology and metabolism (Ahmed et al., 2014). *In vitro* models provide an excellent way of studying host cell-parasite relationship in apicomplexan parasites, allowing the comparison of data generated by diverse researchers with the standardization of techniques, and the reduction of the use of experimental animals (Muller and Hemphill, 2012).

Neospora caninum tachyzoites are able to invade and grow in almost every cell type, and the culture of this parasite has been achieved in diverse primary cells and established cells lines. These include endothelial cells, human fibroblasts (HFF), cervical cancer (HeLa), colon cancer (CaCo2), bovine trophoblasts (F3) or epithelial cells of African green monkey kidney (MA-104 and Vero) amongst others, the last one being the most used (Hemphill et al., 2006, 2013; Regidor-Cerrillo et al., 2011; Jiménez-Pelayo et al., 2017). *Neospora caninum* cell culture has enabled the isolation, *in vitro* phenotypical characterization and genotyping of the isolates, being the basis for parasite antigens production used in diagnosis and research, and for the identification of targets for intervention. In addition, the most recent advances related to genetic manipulation and -omics studies have only been possible because of the use of *in vitro* culture models (Dubey et al., 2017). However, it is important to know that adaptation of the parasites to the cell cultures as a consequence of prolonged passages has been described, and related to modifications in their natural behavior and virulence (Pérez-Zaballos et al., 2005; Bartley et al., 2006). Thus, to allow their reproducibility, comparative studies should be carried out with the use of tachyzoites maintained at a low number of passages in cell culture (Regidor-Cerrillo et al., 2011).

The *in vitro* characterization of different *N. caninum* isolates has revealed the existence of an extensive heterogeneity in virulence-related traits such as tachyzoite invasion and proliferation, ability to disseminate and transmigrate trough biological barriers, and capability to evade immune responses (Regidor-Cerrillo et al., 2011; Collantes-Fernández et al., 2012; Dellarupe et al., 2014a; Jiménez-Pelayo et al., 2019a), which may underlie the range of pathologies observed upon infection in cattle.

4.2.1. *Tachyzoite invasion and growth rate*

One of the main applications of *in vitro* cultures of apicomplexan parasites has been the study of the processes involved in their lytic cycle. A marked variability has been shown between *N. caninum* isolates with regard to the tachyzoite growth. Schock et al. (2001) measured the growth rate of six *N. caninum* isolates obtained from cattle (BPA-1, Nc-SweB1, JPA-2 and Nc-LivB1) and dogs (Nc-1 an Nc-Liverpool). Nc-Liverpool showed the highest growth rates, Nc- SweB1 multiplied significantly more slowly, and intermediate rates were observed in all other isolates. Investigations carried out by the SALUVET group showed that the low virulent Nc-Spain1H displayed a lower tachyzoite yield than the Nc-1 isolate (Rojo-Montejo et al., 2009a), finding an association between the *in vitro* tachyzoite invasion and proliferation and the virulence phenotype of *N. caninum* in pregnant mice. Moreover, ten bovine isolates from asymptomatic calves (Nc-Spain 1H, 2H, 3H, 4H, 5H, 6, 7, 8, 9 and 10), four canine isolates obtained from oocysts (Nc-Ger2, Nc-Ger3, Nc-Ger6 and Nc-6Arg) and two canine isolates obtained from the brain of a clinically affected dog (Nc-Bahia and Nc-Liverpool) were compared (Regidor-Cerrillo et al., 2011; Dellarupe et. al., 2014a). Most of them showed a short-time for invasion (four

to six hpi). However, dramatic differences were found in invasion capacities, lag period for intracellular adaptation before exponential growth and duplication time during exponential growth that define tachyzoite yield in the lytic cycle. Furthermore, in a BALB/c mouse pregnant model for neosporosis, a significant correlation was reported between *N. caninum* tachyzoite yield and pup mortality (Regidor-Cerrillo et al., 2010; Dellarupe et al., 2014b). These findings support the hypothesis that isolates showing the highest growth capacities reach higher parasite burdens in placental and fetal tissues, contributing to pathogenesis of abortion.

Finally, recent work of the SALUVET group focused on the characterization of parasite interaction between high and low virulence isolates of *N. caninum* and bovine placental target cells *in vitro*. The aim of that study was to try to elucidate the mechanisms used by the parasite to cross the placenta and the factors that enable some isolates to be more effectively transmitted than others. To that end, tachyzoite adhesion, invasion, proliferation and egress of high (Nc-Spain7) and low (Nc-Spain1H) virulence *N. caninum* isolates were investigated in established cultures of bovine caruncular epithelial (BCEC-1) and trophoblast (F3) cells. The high virulence isolate Nc-Spain7 showed higher invasion and infection than the low virulent isolate Nc-Spain1H, mainly in trophoblast cells, as well as higher proliferation abilities, similar to what was observed in previous established cell cultures (Jiménez-Pelayo et al., 2017).

4.2.2. *Tachyzoite dissemination and transmigration through biological barriers*

The ability to modulate the migratory capacities of parasitized APCs is another putative virulence-related phenotypic trait of apicomplexan parasites. The induction of a hypermigratory phenotype in these cells upon infection, which may potentiate parasite dissemination and transmission, has been widely described for *T. gondii*. This phenotype is characterized by an amoeboid migratory activation of the host cell mediated by rapid morphological changes and an abrogated extracellular matrix degradation, which enhances their motility and increases their transmigration across cellular barriers (Lambert et al., 2006; Fuks et al., 2012; Weidner et al., 2013; Kanatani et al., 2015; Ólafsson et al., 2018). *T. gondii*-induced APC hypermigration has been related to enhanced dissemination in mice (Lambert et al., 2006). Curiously, this strategy known as the Trojan horse mechanism seems to be chiefly used by *T. gondii* clonal genotypes II and III (Lambert and Barragan, 2010; Lambert et al., 2011), whereas genotype I tachyzoites disseminate and cross restrictive barriers supported principally by their apparent superior gliding motility (Barragan and Sibley 2002; Taylor et al., 2006).

Strategies for parasite dissemination to immunoprivileged sites such as the brain and the placenta in order to reach the fetus and establish chronic infections, may be conserved throughout apicomplexan parasites. This hypothesis is supported by the results obtained by Collantes-Fernández et al. (2012) in an *in vitro* model based on the infection of a trophoblast-derived cell line (beWo cells) by *N. caninum*. In that work it was demonstrated that *N. caninum*, just like *T. gondii*, is able to use two complementary pathways to cross restrictive barriers, the DC-mediated transmigration and direct transmigration powered by their own gliding motility. In the same work, a comparative study indicated that the different isolates (Nc-Liverpool, Nc-SweB1, and the Spanish Nc-Spain 3H, 4H, 6, 7 and 9) preferentially rely on one or other mechanism of transmigration *in vitro*. The same authors described that the inoculation of mice with *N. caninum*-infected DCs resulted in higher parasite loads in several organs compared to the inoculation of free parasites. In addition, an increased transmission and neonatal mortality rate was obtained by the infection of pregnant mice with tachyzoite-infected DCs.

In line with these studies, it was reported that during early infection of mice, effector molecules secreted by *N. caninum* are able to potentiate the recruitment of monocytes and DCs to the sites of infection, enhancing parasite invasion and proliferation (Mineo et al., 2010). Combined, both works motivate future studies to address the impact of APCs infection on the pathogenesis of bovine neosporosis.

4.2.3. *Immune response modulation*

Several studies have described the ability of *T. gondii* to manipulate host immunity with the aim of surviving and being transmitted. In particular, *T. gondii* modulates immune responses through the secretion of parasite effector molecules, mainly from the apical secretory organelles, which impact on host cell transcription and signaling pathways. This results in the regulation of the microbicidal mechanisms of the cells, enabling the parasite to establish its replicative intracellular niche (Lima et al; 2019) Furthermore, the host immune modulation seems to differ among the three dominant *T. gondii* clonal lineages. In this connection, activation of STAT3 and STAT6 transcription factors mediated by ROP16 is achieved by type I and III, but not type II strains, with the consequent suppression of IL-12 cytokine release by infected macrophages (Saeij et al., 2006). Differences in IL-12 induction have also been related to the release of GRA15 exclusively by type II strains, inducing the activation of NF-κB, whereas type I inhibits this pathway through ROP18 release, resulting in the suppression of pro-inflammatory cytokines and consequently facilitating parasite survival (Rosowski et al., 2011; Du et al., 2014). Infected cells stimulated by IFN-γ respond by regulating effector molecules, such as immunity-related p47 GTPases (IRGs), which leads to the disruption of the parasitophorous vacuoles. Genotypes II and III are susceptible to IRGs action, whereas virulent strains resist this immunity mechanism by the secretion of ROP5, ROP17 and ROP18 which phosphorylate IRGs, preserving the parasitophorous vacuole integrity (Brasil et al., 2017). Finally, it has been suggested that the different survival ability in macrophages between *T. gondii* strains may be related to an induced blockade of ROS production by type I but not type III strains (Shrestha et al., 2006; Matta et al., 2018).

Studies of interaction of *N. caninum* with cells of the immune system besides being scarce, fail to take into consideration that isolates of different virulence may impact host cell signaling in different ways. In order to determine the relation of virulence and immune response modulation, the SALUVET group has characterized for the first time innate immune responses by bovine trophoblast (F3) and bovine caruncular placental cells (BCEC-1) after infection with high (Nc-Spain7) and low (Nc-Spain1H) virulence *N. caninum* isolatesN*eospora caninum* infection favored a pro-inflammatory response in placental target cells *in vitro* consisting of upregulation of pro-inflammatory TNF-α and IL-8 and downregulation of IL-6 and TGF-β1 in infected cultures. Higher expression levels of TLR-2 and TNF-α were found in trophoblasts infected with the low virulence isolate Nc-Spain1H, suggesting a different immunomodulation induced by both isolates, which would be related to the differences in virulence shown *in vivo* (Jiménez-Pelayo et al., 2019a).

4.3. *Neospora caninum* variability in the mouse model

Mouse models are an appropriate first step for the investigation of bovine neosporosis pathogenesis. Indeed, non-pregnant and congenital mouse models of *N. caninum* infections associated with exogenous transplacental transmission have been successfully developed. However, low rates of reactivation of *N. caninum* infection in infected mice do not make the mouse a suitable species for the induction of endogenous transplacental transmission, which

occurs frequently in naturally infected cattle (Benavides et al., 2014). The infection of mice represents a good approach for the study of the intra-specific variability of *N. caninum* isolates. In fact, the use of murine models permitted to demonstrate that the outcome of infection was highly dependent on the isolate used for the infection (Atkinson et al., 1999; Rojo-Montejo et al., 2009a; Regidor-Cerrillo et al., 2010; Dellarupe et al., 2014b). Parameters associated with virulence in the murine model include clinical signs, parasite tissue distribution and parasite load. In the pregnant murine model, transplacental transmission, neonatal morbidity and mortality are also determined (Rojo Montejo et al., 2009b).

Studies in non-pregnant or brain infection models have associated a higher virulence with Nc-1 and Nc-Liverpool isolates in relation to Nc-3, Nc-SweB1 and Nc-Nowra (Lindsay et al., 1995; Atkinson et al., 1999; Miller et al., 2002). Interestingly, the studies of parasites isolated from the brain of congenitally infected dog (Nc-1 and Nc-Liverpool) and from asymptomatic but congenitally infected calves (Nc-Spain2H, 3H, 4H, 5H, 6, 7, 8 and 9) showed marked differences in the dynamics of infection, immune response and pathogenicity in infected mice (Collantes-Fernández et al. 2002, Pereira García-Melo et al. 2009).

In the pregnant mouse model, infection with Nc-1 showed a high transplacental transmission rate (92.8% of pups) and a high neonatal mortality rate (76.8%). In contrast, offspring from Nc-Spain 1H-infected dams remained clinically normal, the survival rate was almost 100% and *N. caninum* DNA was only detected in one pup (Rojo-Montejo et al., 2009a). In further studies, Spanish isolates and Nc-Liverpool showed differences in their ability to produce pathology, in their vertical transmission and in their effects on the offspring. Only four isolates (Nc-Spain4H, Nc-Spain5H, Nc-Spain7 and Nc-Liverpool) were able to produce disease in dams, showing a higher frequency of parasite DNA detection in the brain and a higher humoral immune response than in dams infected with other isolates. In the same way, the highest vertical transmission rates were found in pups infected with these four virulent isolates (Regidor-Cerrillo et al., 2010).

New studies with isolates obtained from dogs also showed diverse virulence in the pregnant mouse model depending on their origin (Dellarrupe et al., 2014b), with a higher virulence associated with isolates obtained from animals with clinical signs (Nc-Bahia and Nc-Liv) than those obtained from oocysts (Nc-Ger2, Nc-Ger3, Nc-Ger6 and Nc-6 Argentina).

The relation between isolate virulence and specific antibody responses has also been investigated. Aguado-Martinez et al. (2009), reported higher levels of anti-rNcGRA7 antibodies in mice inoculated with the Nc-Liverpool isolate compared to mice inoculated with the Nc-1 isolate. Specific antibody responses against key parasite proteins involved in the lytic cycle (NcGRA7) and the tachyzoite-bradyzoite transition (NcSAG4, NcBSR4 and NcSRS9) was assessed by Jiménez-Ruiz et al. (2013), showing that antibodies against the NcGRA7 protein were significantly higher in mice inoculated with high virulence isolates. It could be explained by a higher parasite dissemination and growth rate in host tissues compared with low-to-moderate virulence isolates, because a correlation with the tachyzoite yield values at 56 hpi was detected. In this relation, high virulence isolates (e.g. Nc-Spain 5H, Nc-Spain7 and Nc-Liverpool) induced higher levels of anti-*N. caninum* IgG1 and IgG2 than low-to-moderate virulence isolates (e.g. Nc-Spain3H, Nc-Spain2H and Nc-Spain9) (Regidor-Cerrillo et al., 2010).

4.4. *Neospora caninum* variability in cattle

Bovine models represent powerful tools to study pathogenesis of neosporosis and host immune responses to *N. caninum* infection, to evaluate therapeutic candidates and to investigate the

biological diversity of *N. caninum*. In the numerous experimental studies that have been carried out based on *N. caninum* infection in pregnant and non-pregnant cattle, different isolates have been employed. Isolate virulence characterized in murine models have also been demonstrated in the bovine model. However, the lack of standardization of experimental conditions employed, such as breed, age of gestation, route, dose of inoculation parasite stage, hampers the comparison between studies (Benavides et al., 2014).

There are currently few published works comparing the pathogenicity of *N. caninum* isolates of different virulence in the bovine model. Infection of pregnant heifers at 70 days of gestation with Nc-1 and Nc-Spain1H tachyzoites was carried out by Rojo-Montejo et al. (2009b) to determine the capability of these isolates to induce fetal death. During the period studied, fetal mortality was detected in three out of five Nc-1-infected animals but not in those infected with Nc-Spain1H. Parasitaemia, placental lesions and parasite detection was lower for Nc-Spain1H infection. After parasite inoculation, both groups of infection showed *N. caninum* specific responses and similar IFN-γ levels. However, these declined in the Nc-Spain1H infected group whereas they remained high until the end of the experiment in Nc-1-infected cows. In that work it is indicated that further studies are necessary to determine if the observed decrease in IFN-γ is due to a reduction in parasite burden by the immune response developed, or if on the contrary Nc-Spain1H induces lower antigenic stimulus related to its lower proliferation capacity.

Pathogenicity of *N. caninum* Nc-1 and the Brazilian strain Nc-Bahia, both isolated from the brains of dogs with clinical signs, was compared in a pregnant model of cattle and buffaloes at 70 days of gestation (Chryssafidis et al., 2014). All the animals inoculated with Nc-1 but only one from the Nc-Bahia infection group did abort. Although vertical transmission rate was very high for both isolates, parasitaemia and severity of lesions were higher for Nc-1 infected animals. These results correlated with the faster multiplication of this isolate *in vitro* in relation to Nc-Bahia. In that work only humoral immune responses were assessed, with no differences found between both experimental groups.

Regidor-Cerrillo et al., 2014 studied the influence of the biological diversity of two isolates with marked differences in virulence demonstrated in the murine model (Nc-Spain7 of high virulence and Nc-Spain8 of low-to-moderate virulence) on abortion outcome and infection dynamics in pregnant cattle at 70 days of gestation. Fetal death occurred in all infected animals regardless of the isolate, but sooner for the heifers inoculated with Nc-Spain7 tachyzoites. Although similar lesions were found in placental and fetal tissues for both groups of infection, *N. caninum* was more frequently detected in Nc-Spain7-infected animals. Peripheral and local immune responses were studied, demonstrating the influence of the isolate in the immune profile induced by the parasite. Specific antibody responses were developed in both groups, remaining higher for animals inoculated with Nc-Spain7. Higher levels of IFN-γ and IL-4 were also achieved for this isolate in the first week of infection. A mixed Th1 and Th2 pattern was observed in *N. caninum*-infected caruncles, with higher IFN-γ mRNA levels in those infected with Nc-Spain7 compared to Nc-Spain8. The authors suggest that higher levels are likely caused by the faster multiplication of Nc-Spain7 and thus faster antigen production. An increase in IL-10 levels was instead observed in Nc-Spain8 infected-caruncles. Regardless of the isolate, the local immune response developed was not able to control *N. caninum* in the placenta. Interestingly, for the first time fetal immune responses induced between different isolates were compared. Nc-Spain7-infected fetuses mounted a humoral immune response against *N. caninum* earlier than those infected by Nc-Spain8, which was suggested again to be related with their different proliferative characteristics. However, the immune response mounted by infected fetuses of any of both groups did not protect against fetal death.

The most recent study comparing isolates of different virulence in the bovine model was carried out by the SALUVET group (Jiménez-Pelayo, 2019b). Inoculation of Nc-Spain7 and Nc-Spain1H isolates at mid-gestation and culling at two early stages of infection (10 and 20 dpi) showed earlier detection of Nc-Spain7 tachyzoites in placental tissues, whose proliferation led to lesion development, transmission to the fetus and fetal mortality (40%), whereas Nc-Spain1H was not detected in the placenta until 20 dpi and lesion development or transmission were not observed during early infection. A higher parasite burden, lesion development and fetal death were associated to a better ability to proliferate of Nc-Spain7 isolate. Innate and adaptive immune responses in placental tissues were also investigated in this experimental model, and surprising results showed that Nc-Spain7 may be able to evade placental immune responses at 10 dpi, avoiding activation of pattern recognition receptors (PRRs) traditionally involved in *N. caninum* sensing, and subsequently avoiding the development of pro-inflammatory responses. However, it was suggested that parasite replication and lesion development at 20 dpi led to PRRs activation and an exacerbated expression of cytokines and chemokines, with a Th1/Th2 balance displaced towards a predominant Th1 response that probably contributed to fetal death. Moreover, IL-8, TNF-α, and iNOS were upregulated and TGF-β1 downregulated in placental tissues from non-viable fetuses, suggesting that they may be directly related to *N. caninum* abortion. On the other hand, the low-virulent isolate Nc-Spain1H induced upregulation of PRRs, cytokines, chemoattractant genes and extracellular matrix modulators as early as 10 dpi, which was kept at 20 dpi at constant levels, maintaining Th1/Th2 responses balanced. Therefore, rapid immune responses together with minor replication ability could control parasite replication, which would explain the lower Nc-Spain1H burdens found in placental tissues. It is also suggested that Nc-Spain1H mechanism to cross the placental barrier may be based on an extracellular matrix modulation and hijacking of the immune cells in order to be transmitted avoiding placental damage (Jiménez Pelayo, 2019b).

These studies highlight the importance of the isolate in the outcome of infection which may be related, besides their invasion and proliferation capacities, with their interaction with the maternal and fetal immune system.

4.5. Molecular basis of the variability

A key question for apicomplexan parasites is to understand the molecular basis that govern virulence of these pathogens, which may help the development of control measures. The wide host range of *N. caninum* together with its global distribution suggest a high genetic diversity. However, this has been poorly explored (Beck et al., 2009). Several approaches frequently used to investigate the genetic diversity of *T. gondii* have been applied to *N. caninum* research: characterization of 18S locus or ITS-1 region showed a limited variation among isolates of diverse geographical and host species origin (Sreekumar et al., 2002; Gondim et al., 2004), and no nucleotide differences were found in the nuclear ssrRNA gene sequence of seven isolates obtained from cattle and dogs (Marsh et al., 1995). No variation was either observed in the sequences of surface and dense granule proteins, whose orthologous in *T. gondii* are known to be polymorphic (Beck et al., 2009). However, an extensive genetic diversity based on highly polymorphic microsatellite and minisatellite markers was demonstrated in *N. caninum* (Regidor-Cerrillo et al., 2006, 2008, 2013; Pedraza-Díaz et al., 2009; Basso et al., 2009, 2010), although the relation between certain microsatellite sequences variation and the virulence of *N. caninum* isolates has not been found.

Phylogenetic analysis and genetic distance indexes of 50 isolates collected worldwide using 19 genetic markers resolved a single genotype of *N. caninum*. Whole genome sequencing of 7

isolates with origin in two different continents identified a significant structural variation, but only limited polymorphism, with 5,766 biallelic single nucleotide polymorphisms (SNPs) total. More than half of these SNPs clustered into only six distinct haploblocks. Importantly, the alleles at each haploblock had independently segregated across the strains, suggesting that the clonal expansion of a single *N. caninum* lineage maintained by vertical transmission with asexual reproduction in the intermediate host originated the current *N. caninum* population. However, important differences found between mitochondrial and apicoplast DNA in relation to nuclear DNA evidence sexual recombination of the parasite in the definitive host that may explain the intra-specific variability of the isolates (Khan et al., 2015).

Despite the fact that genetic variation in repetitive elements has been confirmed, little is known about polymorphisms occurring in the coding regions of *N. caninum* genome. Differences in virulence traits between *N. caninum* isolates may be due to the existence of genetic diversity within, upstream or downstream of genes that are transcriptionally active in tachyzoites (Calarco et al., 2018). The expansion of the "-omics" disciplines has enabled significant progress in the knowledge of the genetics and biology of apicomplexan parasites (Suarez et al., 2017), revealing molecular mechanism involved in host cell-parasite interaction which may be related to their biological diversity and virulence.

4.5.1. Genomic studies

The Sanger Institute, in collaboration with the University of Liverpool sequenced the genome of the Nc-Liverpool isolate. To date, that is the only available genome sequence of *N. caninum*. It is estimated to have a size of 61 Mb divided into 14 chromosomes (Reid et al., 2012). The same research group sequenced the transcriptome of the tachyzoite stage of Nc-Liverpool and of *T. gondii* VEG strain with the aim of improving genome annotation and determining differences in gene expression between both species. A total of 7121 protein-coding genes were identified, the 74% expressed during tachyzoite stage. Excluding surface-antigen coding genes, 113 genes were found to be *N. caninum*-specific, with no orthologue or paralogue in *T. gondii*. Interestingly, the comparison of the predicted metabolic enzymes and pathways showed no differences between species despite differences in host range between *N. caninum* and *T. gondii*. The greatest divergences were found in surface antigen gene families, which were found to be expanded in *N. caninum*, although *T. gondii* expressed a higher repertory of SRS genes during tachyzoite stage. Important differences in ROP kinases, MIC and GRA proteins were also described. ROP18, is considered a virulence factor in *T.gondii,* which expressed in high levels by virulent strains enables parasite survival by the mechanisms described above. However, ROP18 is reduced to a pseudogene in *N. caninum*. Additionally, the locus encoding ROP2A, ROP2B and ROP8 is missing in *N. caninum.* Whereas MIC26 and MIC19 are unique to *N. caninum,* GRA11 and GRA12 are absent in the genome of this parasite (Reid et al., 2012).

Genes characterized by their high polymorphism in *T. gondii* have been sequenced and compared amongst *N. caninum* isolates of different geographical and hosts origin. These included genes encoding surface antigens NcSAG1 and NcSRS2 and the bradyzoite-specific SAG4, and dense granule proteins GRA6 and GRA7. However, no variation was shown in the sequences of these genes (Beck et al., 2009). Clonal expansion of genes with attributed roles in virulence may drive phenotypic variants by gene dosage between isolates (Jung et al., 2004; Adomako-Ankomah et al., 2014; Pastor-Fernández et al., 2016). However, the putative variation in the number of copies of these genes within *N. caninum* remains to be elucidated.

4.5.2. Transcriptomic studies

Very few comparative studies of the transcriptome of *N. caninum* have been carried out. In the last few years the SALUVET group has characterized the RNA expression profile of Nc-Spain7 and Nc-Spain1H, isolates with marked differences in virulence, during the tachyzoite stage (Horcajo et al., 2016, 2018). These works provided insights into mechanisms probably involved in *N. caninum* specific traits and host-cell modulation. Specifically, genes encoding SAG-related, MIC and ROP proteins were amongst the most differentially expressed between isolates. Important differences were also found in the levels of expression of genes implicated in metabolic pathways, cell cycle and stress response (Horcajo et al., 2016). In addition, genes previously characterized as bradyzoite stage-specific (BAG1, SAG4 and BSR4) were highly expressed in the Nc-Spain1H isolate (Horcajo et al., 2018). Despite the different expression profile shown between both isolates, these induced a very similar impact on bovine trophoblast cells. Cholesterol metabolism and extracellular matrix organization were the main networks modulated by *N. caninum* infection. Interestingly, a higher number of genes were regulated upon infection with the low virulence isolate Nc-Spain1H in relation to Nc-Spain7 infection (Horcajo et al., 2018). Higher differences in host-cell regulation amongst isolates may be obtained by the use of different target cells, as it has been described for *T. gondii* that parasite-host cell interaction is cell-type specific (Swierzy et al., 2017).

Another recent study compared the tachyzoite transcriptome profiles of Nc-Liverpool and Nc-Nowra (virulent and avirulent *N. caninum* strains respectively) (Calarco et al., 2018). In that work, 3130 SNPs and 6123 indels were identified between the strains. Sanger sequencing of nine markers for these two and eight additional strains permitted their classification into two major clades with no obvious geographical segregation. In addition, authors identified SNP hotspot regions mainly located in loci related to transcription, translation, protein binding and protein-protein interaction. Furthermore, 468 nonsynonymous SNPs identified within protein-coding genes were associated with protein kinase activity, protein binding, protein phosphorylation, and proteolysis. These processes and the specific proteins involved may represent effectors of *N. caninum* tachyzoite virulence, although the lack of annotation of *N. caninum* genome hindered further identification (Calarco et al., 2018).

4.5.3. Proteomic studies

Proteomics consist in the systematic analysis of gene expression at protein level. Analysis of protein profiles have been shown to be valuable tools for obtaining understanding of the aspects of biological proceedings of apicomplexan parasites. Different proteomic methods have been used to characterize the proteome of *N. caninum* isolates and for the comparison of *N. caninum* and *T. gondii* tachyzoite proteomes (Lee et al., 2005).

First approaches used two-dimensional gel electrophoresis (2-DE) to determine the protein composition of *N. caninum* in the tachyzoite stage (Lee et al., 2003, 2004) Afterwards, the same technique was used to compare the tachyzoite proteome between *N. caninum* isolates (Lee et al., 2005; Shin et al., 2005a), and also with *T. gondii* (Lee et al., 2005). The results of those works demonstrated a high degree of similarity between *N. caninum* isolates KBA-2, JPA1 and VMDL-1, and at the same time highlighted large differences with *T. gondii,* such as the specie specificity of *N. caninum* proteins NcSUB1, NcGRA2 and NcGRA7.
A proteomic study using Difference Gel Electrophoresis (DIGE) and mass spectrometry (MS) compared the differences in abundance of proteins of three *N. caninum* isolates in the tachyzoite

stage, two of them of high virulence (Nc-Liverpool and Nc-Spain7) and one of low virulence (Nc-Spain1H) (Regidor-Cerrillo et al., 2012). Differences between isolates were found in proteins involved in processes potentially associated with virulence, with a higher abundance and variation of proteins which act on invasion and vacuole parasitophorous formation (e.g., MIC1, ACT1, MLC1 and ROP40) and oxidative stress responses (e.g., G6PDH) for the virulent isolates.

Horcajo et al. (2018) investigated the proteomic differences between Nc-Spain7 and Nc-Spain1H isolates throughout the tachyzoite lytic cycle by Label free LC-MS/MS. The greater differences between isolates were found during invasion and egress events, whereas a similar abundance of proteins was shown during tachyzoite replication. Similar to the observations made in the DIGE study and in the transcriptome analysis of Nc-Spain7 and Nc-Spain1H in trophoblast cells (Horcajo et al., 2016), MIC proteins were more abundant in the low virulence isolate. Likewise, ROP and GRA proteins, and proteins involved in stress response and metabolism showed differential abundances between Nc-Spain7 and Nc-Spain1H isolates. Thus, these studies suggest that different modulation of proteins involved in the lytic cycle, metabolism and stress response between isolates may likely drive the biological diversity of *N. caninum*.
On the other hand, besides variations in proteins mediating parasite biological processes, different immunodominant antigens among isolates may explain the differences in parasite virulence (Regidor-Cerrillo et al., 2015). However, the study of the antigenic diversity by WB showed a low intraspecific variability (Schock et al., 2001; Miller et al., 2002; Lee et al., 2005; Shin et al., 2005a, 2005b), despite the fact that the comparison of Nc-Spain7, Nc-Liverpool and Nc-Spain1H immunomes revealed important differences among these biologically different isolates (Regidor-Cerrillo et al., 2015).

III

JUSTIFICATION AND OBJECTIVES
JUSTIFICACIÓN Y OBJETIVOS

Neospora caninum is an apicomplexan cyst-forming protozoan parasite considered one of the main causes of reproductive failure in cattle worldwide (Dubey et al., 2017). Important economic losses related to the disease have been reported, mainly as a consequence of abortion, extended intervals for rebreeding and the replacement of animals (Reichel et al., 2013). Currently, there is no treatment or vaccine available against *N. caninum* infection. However, it has been estimated that vaccination would be the best control measure against *N. caninum* regarding the cost-benefit relationship (Reichel and Ellis, 2006). The development of effective vaccines is mainly limited by safety risks and technological challenges of live vaccines, by the scarcity of parasite antigenic canadidates for subunit vaccines, and also due to gaps in the current knowledge of the immune responses that should be induced to efficiently combat *N. caninum* infection and to confer long-lasting protection (Hemphill et al., 2016; Horcajo et al., 2016).

Neospora caninum infection in cattle, notably during gestation, underlies a complex immunological regulation that may lead to protection or contribute to the pathogenesis of abortion (Almeria et al., 2017). Because of its condition of obligate intracellular parasite, immunity to neosporosis is mainly cell-mediated. A key role of Th1 cytokines, particularly IFN-γ and IL-12, in limiting *N. caninum* proliferation has been indicated. However, Th1 responses may be potentially detrimental to the maintenance of pregnancy, causing fetal rejection or destruction of the placental tissues (Almería et al., 2017). On the other hand, an imbalance toward Th2 cytokines seems to occur in the dam, associated with a successful implantation of the fetus and maintenance of gestation, which may result in the inability to control the parasite growth and dissemination (Almería et al., 2003). It has been suggested that, in order to be effective and safe for the dam and the fetus, the adequate immune response would require a critical threshold of pro-inflammatory IFN-γ levels and a counterbalance with other regulatory cytokines, such as IL-10 (Rosbottom et al., 2007; Bartley et al., 2012, 2013; Almeria et al., 2016a; Darwich et al., 2016).

Neospora caninum interaction with host cells of the innate immunity, first line of defense against infections, should be critical in determining the strength and character of the response, and consequently its efficacy (Boysen et al., 2006; Taubert et al., 2006; Flynn and Marshall, 2011; Abe et al., 2014; Villagra-Blanco et al., 2017; Wei et al., 2018). Macrophages play a key role in initiating early-immune responses against infection and priming the immune system for the development of adaptive immune responses (Werling and Jungi., 2003; Jensen et al., 2018). These cells seem essential for combating *N. caninum* infection, as macrophage depletion prior to infection results in severe neosporosis in mice (Abe et al., 2014). Studies in murine and macrophages have identified signaling pathways implicated in host resistance against *N. caninum* (Jin et al., 2017; Boucher et al., 2018; Li et al., 2019; Wang et al., 2018; Miranda et al., 2019), and mechanisms involved in *N. caninum* immune response evasion (Mota et al., 2016; He et al., 2017; Silva et al., 2017). However, it is worth noting that mice and humans are not natural hosts for *N. caninum* and very important differences exist with regard to the immune response in the cow (Jungi et al., 2011). Thus, the ability of *N. caninum* to modulate innate immune responses should be determined in target cells of the bovine host. In support of this affirmation, Sánchez-Sánchez et al. (2018b) demonstrated that *T. gondii* parasite virulence may be host-dependent, because TgShSp1 type II isolate obtained recently from an ovine aborted fetus did not cause disease in mice, although abortion was observed in pregnant sheep.

To date, scarce studies have been performed with the use of bovine macrophages, and all of them focus on the mechanisms used by the cell to restrain parasite infection. (Flynn and Marshall, 2011; Wei et al., 2018 Wang et al., 2019). Currently, the mechanisms used by *N. caninum* to evade immune mediated-killing triggered by bovine macrophages have not been

investigated. In addition, despite the fact that several studies have established a correlation between phenotypic traits linked to virulence *in vitro* and variation in the outcome of infection and immune responses in pregnant cattle (Rojo-Montejo et al., 2009b; Caspe et al., 2012; Jiménez-Pelayo et al., 2019b; Jiménez-Pelayo et al., submitted), the isolate-specific virulence determinants in cells of the bovine immune system that may mediate these differences remain unidentified.

In this scenario, the **general aim of the present Doctoral Thesis was to investigate the interaction between *N. caninum* and bovine macrophages, as target cells of the host immune system**. Two different isolates that have showed different virulence in cattle were used to reveal the main host and parasite mechanisms implicated in disease pathogenesis in the natural host. The study of the influence of the isolate virulence in innate immune responses mediated by bovine macrophages may contribute to the identification of parasite factors implicated in host cell regulation. This would allow opportunities to counteract the parasite survival strategies and shift the balance in favor of the host.

The high virulence *N. caninum* isolate Nc-Spain7 and the low virulence isolate Nc-Spain1H, which showed marked differences in their biological behavior in *in vitro* and *in vivo* models, were used in all the experiments. Specifically, higher invasion and proliferation rates *in vitro* have been demonstrated for Nc-Spain7 than for Nc-Spain1H (Regidor-Cerrillo et al., 2011; Dellarupe et al., 2014b; Jiménez-Pelayo et al., 2017). A higher parasite burden and more severe lesions, together with high rates of transplacental transmission and neonatal mortality were shown in pregnant mice infected with Nc-Spain7 (Regidor-Cerrillo et al., 2011; Dellarupe et al., 2014a), whereas very low vertical transmission and neonatal mortality were observed in mice infected with Nc-Spain1H (Rojo-Montejo et al., 2009a). In pregnant bovine models at early and mid-gestation, high transplacental transmission and fetal mortality rates were detected after Nc-Spain7 infection (Caspe et al., 2012; Regidor-Cerrillo et al., 2014; Almería et al., 2016a; Jiménez-Pelayo et al., submitted; Vázquez et al., submitted), whereas Nc-Spain1H infection spared the fetus (Rojo-Montejo et al., 2009a; Jiménez-Pelayo et al., submitted).

In vitro cultures of primary bovine monocyte-derived macrophages have been used in the present Doctoral Thesis in order to characterize the host-parasite crosstalk. With this purpose, monocytes were isolated from peripheral blood, differentiated *in vitro* into macrophages and morphologically and phenotypically characterized.

The following specific objectives were pursued:

Objective 1: *In vitro* phenotypic characterization of bovine monocyte-derived macrophages infected with *Neospora caninum* isolates of high and low virulence.

The aim of this objective was to determine how *N. caninum* interacts with bovine macrophages and the influence of the isolate virulence on the subsequent cellular response. The ability of *N. caninum* isolates of high (Nc-Spain7) and low (Nc-Spain1H) virulence Nc-Spain7 and Nc-Spain1H to invade, proliferate and survive in bovine macrophages was broadly investigated in order to establish differences in their lytic cycle. Then, immunological macrophage response to Nc-Spain7 and Nc-Spain1H infection was also characterized. Finally, the capacity of *N. caninum* to induce a hypermigratory phenotype in these cells upon infection, characterized by hypermotility and enhanced transmigration, and accompanied by rapid morphological changes and abrogation of extracellular matrix degradation, was studied.

The obtained results will allow us to define the parasite modulation of the innate immune target cells during the early phases of infection and find differences between isolates which may be related to the differences in pathogenesis observed *in vivo*.

Sub-objective 1.1: Characterization of the lytic cycle of high and low virulence isolates of *Neospora caninum* in bovine monocyte-derived macrophages *in vitro*.

In this sub-objective, we studied the capacity of *N. caninum* to actively invade, survive and grow in bovine macrophages. Then, lytic cycle dynamics of Nc-Spain7 and Nc-Spain1H tachyzoites were investigated to identify variations between isolates in invasion, proliferation and egress events which may be involved in their differences in pathogenesis.

Sub-objective 1.2: Comparison of the immunological macrophage response to infection with high and low virulence *Neospora caninum* isolates.

In this sub-objective, production of ROS, cytokine expression, changes in cell surface markers and induction of IFN-γ release by lymphocytes were determined to assess the cell immune response to *N. caninum* infection, and whether parasite virulence correlates with the induction of quantitative or qualitative different responses.

Sub-objective 1.3: Determination of the induction of a hypermigratory phenotype in bovine monocyte-derived macrophages upon *Neospora caninum* infection.

The impact of *N. caninum* infection on the migratory properties of bovine macrophages was determined by means of the study of four parameters related to the induction of a hypermigratory phenotype in DCs by *T. gondii*: cellular motility, transmigration across membranes, induction of cytoskeletal changes and impact on extracellular matrix degradation. The capacity to modulate cell migration may impact on parasite dissemination and transmission across restrictive biological barriers to establish in chronic infection.

Objective 2: Transcriptome modulation of bovine monocyte-derived macrophages by *Neospora caninum* isolates of different virulence

The aim of this objective was to determine the bovine macrophage response to *N. caninum* infection at the molecular level, and the influence of the isolate in cell modulation. The transcriptional profile of bovine monocyte-derived macrophages infected with Nc-Spain7 and Nc-Spain1H was investigated. Additionally, we studied the parasite transcriptome to reveal the molecular basis of macrophage modulation by *N. caninum*.

Sub-objective 2.1: Gene expression profiling of bovine macrophages infected with high and low virulence *Neospora caninum* isolates.

In this sub-objective, the transcriptome profile of bovine monocyte-derived macrophages infected with Nc-Spain7 and Nc-Spain1H isolates was investigated to reveal the main processes involved in parasite recognition and subsequent response by the macrophages against *N. caninum* infection. Those processes related to parasite manipulation of the host cell environment were further investigated by means of the comparison of macrophage responses infected with both isolates. The results from this study will show how *N. caninum* impacts on the host signaling pathways to escape cellular defenses, and the molecular basis implicated in the differences in host cell modulation between high and low virulence isolates.

Sub-objective 2.2: Gene expression profiling of high and low virulence *Neospora caninum* isolates in bovine macrophages.

In this sub-objective, the transcriptome profile of Nc-Spain7 and Nc-Spain1H was studied with the aim of investigating the parasite gene profile in bovine macrophages, correlating the different gene expression between isolates with the differences observed in their behavior, and determining potential parasite effectors implicated in the host-cell modulation. The results of this study will help identify potential parasite factors associated to virulence and thus, to disease traits, such as abortion and transmission.

IV

OBJECTIVE I

OBJETIVO I

OBJETIVO I | Caracterización fenotípica *in vitro* de macrófagos bovinos derivados de monocitos infectados con aislados de alta y baja virulencia de *Neospora caninum*.

La infección por *Neospora caninum*, parásito apicomplejo intracelular obligado, se considera una de las principales causas de aborto en el ganado bovino a nivel mundial. La respuesta inmunitaria innata es clave en la patogenia de la neosporosis bovina. Los macrófagos constituyen la primera línea de defensa frente a infecciones intracelulares y juegan un papel importante en el inicio de la respuesta inmunitaria innata e influyendo posteriormente en la respuesta adaptativa. Por ello, la interacción entre *N. caninum* y el macrófago puede ser determinante en el desarrollo de la infección. Hasta la fecha, la mayoría de estudios han utilizado macrófagos humanos o de ratón, pero estas especies no son hospedadores naturales para *N. caninum*.

En el presente estudio se utilizó un modelo de infección de macrófago bovino por *N. caninum* con el objetivo de determinar los mecanismos utilizados por el parásito para modular dichas células durante la fase temprana de la infección. Además, se estudió por primera vez la interacción entre macrófagos bovinos y dos aislados de distinta virulencia para identificar mecanismos de modulación específicos de cada aislado que pudieran explicar sus diferencias en patogenia observadas *in vivo.* Se estudió la habilidad de *N. caninum* para invadir activamente el macrófago, sobrevivir y proliferar en su interior. Asimismo se determinó la respuesta inmunitaria celular a la infección mediante el análisis de la producción de especies reactivas de oxígeno, expresión de citoquinas, inducción de la producción de IFN-γ por linfocitos en co-cultivo y cambios en la expresión de marcadores de superficie en el macrófago infectado. Finalmente se investigó la capacidad del parásito de inducir un fenotipo hipermigratorio en la célula hospedadora. Además se comparó la respuesta celular y los parámetros asociados al ciclo lítico del parásito entre el aislado de alta virulencia de *N. caninum* (Nc-Spain7) y el de baja virulencia (Nc-Spain1H).

Ambos aislados fueron capaces de invadir activamente el macrófago y completar en él su ciclo lítico, escapando de la degradación por los lisosomas y disminuyendo la concentración de ROS intracelulares. Sin embargo, el aislado de alta virulencia Nc-Spain7 mostró una mayor tasa de invasión junto con una mayor capacidad de supervivencia y proliferación.

Tras la disminución observada en los niveles intracelulares de ROS común a la infección por ambos aislados, los macrófagos infectados con el aislado de baja virulencia Nc-Spain1H mostraron un aumento dichos niveles y en la expresión de IL-12p40, lo que resultó en un incremento de la producción de IFN-γ por los linfocitos, comparado con las células infectadas por Nc-Spain7. Además, la expresión de IL-10 aumentó en macrófagos infectados con ambos aislados, pero fue mayor para la infección por Nc-Spain1H. Finalmente, los macrófagos infectados exhibieron una menor expresión de las moléculas CMH II y CD1b, relacionadas con la presentación de antígeno, y de CD86, molécula de superficie involucrada en la maduración y activación de linfocitos T.
La infección por *N. caninum* indujo un fenotipo hipermigratorio en el macrófago bovino caracterizado por un aumento en la motilidad y en la transmigración celular *in vitro*. Dicho fenotipo se acompaña de rápidos cambios en el citoesqueleto de la célula con desaparición de podosomas y de una disminución en la degradación de la matriz extracelular, que conducen a un movimiento ameboide rápido del macrófago. Una hipermotilidad significativamente mayor se observó con la infección por el aislado Nc-Spain7.

Los resultados obtenidos sugieren que el aislado de alta virulencia posee una mayor capacidad para evadir la respuesta inmunitaria innata del hospedador mediada por macrófagos. Dicha evasión, junto con su mayor capacidad de proliferación se correlaciona con la mayor virulencia observada *in vivo* por infecciones con Nc-Spain7. Por el contrario el aislado de baja virulencia Nc-Spain1H parece estimular una mayor respuesta proinflamatoria que reduciría la carga parasitaria en las células. Dicha respuesta está compensada por una mayor expresión de citoquinas reguladoras, lo que ayudaría a minimizar el posible daño causado por una respuesta excesiva. La menor proliferación de Nc-Spain1H, unida a la inducción por dicho aislado de una respuesta inmunitaria protectora, podría ser responsable de la limitada patogenia de la infección por este aislado observada en infecciones experimentales en vacuno gestante. Los resultados también sugieren que los macrófagos bovinos podrían servir como vehículos para la diseminación de *N. caninum* en el organismo.

OBJECTIVE I | *In vitro* phenotypic characterization of bovine monocyte-derived macrophages infected with *Neospora caninum* isolates of high and low virulence

SUMMARY |

Neospora caninum, a protozoan parasite closely related to *Toxoplasma gondii*, represents one of the main causes of abortion in cattle. Macrophages (MØs) are mediators of the innate immune response against infection and likely one of the first cells encountered by the parasite during the host infection process. In this study, we investigated *in vitro* how high or low virulent isolates of *N. caninum* (Nc-Spain7 and Nc-Spain1H, respectively) interact with bovine monocyte-derived MØs and the influence of the isolate virulence on the subsequent cellular response. Both isolates actively invaded, survived and replicated in the MØs. However, Nc-Spain7 showed a higher invasion rate and a replication significantly faster, following an exponential growth model, whereas Nc-Spain1H presented a delayed replication and a lower growth rate without an exponential pattern. *N. caninum* infection induced a hypermigratory phenotype in bovine MØs that was characterized by enhanced motility and transmigration *in vitro* and was accompanied by morphological changes and abrogated extracellular matrix degradation. A significantly higher hypermotility was observed with the highly virulent isolate Nc-Spain7. Nc-Spain1H-infected MØs showed elevated reactive oxygen species (ROS) production and IL12p40 expression, which also resulted in increased IFN-γ release by lymphocytes, compared to cells infected with Nc-Spain7. Furthermore, IL-10 was upregulated in MØs infected with both isolates. Infected MØs exhibited lower expression of MHC Class II, CD86, and CD1b molecules than uninfected MØs, with non-significant differences between isolates. This work characterizes for the first time *N. caninum* replication in bovine monocyte-derived MØs and details isolate-dependent differences in host cell responses to the parasite.

1. BACKGROUND

Neospora caninum, an apicomplexan cyst-forming protozoan, is considered one of the main causes of abortion in cattle worldwide (Dubey et al., 2007; Almería et al., 2017). The transmission of *N. caninum* in cattle may occur by ingestion of sporulated oocysts from the environment (horizontal transmission) or, most frequently, transplacental during pregnancy (vertical transmission) by dissemination of tachyzoites from the infected dam to the fetus (Dubey et al., 2007).

Innate defenses triggered by monocytes/macrophages (MØs) are key in the pathogenesis of neosporosis (Abe et al., 2014). These cells constitute the first line of defense against intracellular infections and play an important role in initiating early innate-immune responses and priming the immune system for the development of adaptive-immune responses (Mota et al., 2016). It has been demonstrated that *Toxoplasma gondii*, a phylogenetically closely related apicomplexan parasite, has developed strategies to survive, replicate and disseminate via MØs. Through polarizing the host immune response to its own benefit *T. gondii* is able to persist and establish chronic infections (Muraille et al., 2014). To date, knowledge about *Neospora*-MØ crosstalk is predominantly restricted to mice (Tanaka et al., 2010; Dion et al., 2011; Mota et al., 2016; He et al., 2017; Silva et al., 2017) or humans (Boucher et al., 2018), neither of which have been identified as natural hosts for *N. caninum*. Flynn and Marshall (2011) published the only *in vitro* study regarding infection of bovine MØ (boMØ) by *N. caninum*, which focused on the description of cytokine production by naïve $CD4^+$ T-cells primed by infected MØs.

Another key question in bovine neosporosis is the influence of the parasite isolate on the outcome of infection, an effect that is known for *T. gondii* (Melo et al., 2011). Several studies have established the rate of invasion and the yield of tachyzoites *in vitro* as phenotypic traits associated with the virulence of *N. caninum* (Regidor-Cerrillo et al., 2011). Indeed, there seems to be a clear correlation with the isolate virulence and its efficiency in being transmitted to the growing fetus in mice (Rojo-Montejo et al., 2009a; Regidor-Cerrillo et al., 2010). Furthermore, virulence differences were associated with variation in clinical outcome, infection dynamics and immune responses in pregnant cattle (Rojo-Montejo et al., 2009b; Regidor-Cerrillo et al., 2014). However, the isolate-specific virulence determinants in cattle and specific genetic markers for virulent traits remain unidentified.

Toxoplasma gondii clonal lines have demonstrated differences in virulence based on distinct methods of subverting MØs (Jensen et al., 2011). In the present study, we used a boMØ model of *N. caninum* infection to study the interactions between boMØs and *N. caninum* and identify isolate-specific virulence properties at the cellular level. For this purpose, cells were infected with two isolates of high (Nc-Spain7) or low virulence (Nc-Spain1H), previously characterized *in vitro*, that exhibit marked divergence in transmission and dissemination *in vivo*. Specifically, the highly virulent isolate Nc-Spain7 demonstrates greater infection and proliferation rates compared to the low-virulent isolate Nc-Spain1H *in vitro* and a higher percentage of abortion and vertical transmission (as high as 100%) in a pregnant bovine model (Caspe et al., 2012; Regidor-Cerrillo et al., 2014). In contrast no fetal death occurs in pregnant cattle experimentally infected with the Nc-Spain1H isolate (Rojo-Montejo et al., 2009b).

Thus, we studied initially the ability of both isolates to infect boMØs, to survive and to proliferate in these cells. Thereafter, we studied the impact of *N. caninum* infection on the migratory

properties of boMØs. In murine toxoplasmosis, infected dendritic cells (DCs) potentiate parasite dissemination to peripheral organs by a Trojan horse mechanism (Lambert et al., 2006; Fuks et al., 2012; Kanatani et al., 2017). Moreover, *T. gondii* infection shifts DCs into an amoeboid rapid migration mode encompassing cytoskeletal changes with podosome dissolution and reduction of proteolysis of extracellular matrix (Weidner et al., 2013; Ólafsson et al., 2018, 2019). On this basis morphological changes and impact on extracellular matrix degradation of MØs upon *N. caninum* infection were investigated, which were related with induced hypermotility and enhanced transmigration. Finally, the immunological cell response to infection was characterized by analysis of reactive oxygen species (ROS) production, cytokine expression, induction of IFN-γ release by lymphocytes and changes in cell surface markers.

Our results suggest that differences in *N. caninum* isolates virulence correlate with MØ function, and this represents an important step towards our understanding how this parasite is transmitted across restrictive barriers. In addition, our work shows a direct impact of differences in virulence on the innate and subsequent adaptive immune response generated.

2. MATERIALS AND METHODS

2.1. Ethics statement

Handling of cows and blood sampling were conducted in accordance with Spanish and EU legislation (Law 32/2007, concerning animals, their exploitation, transportation, experimentation and sacrifice; Royal Decree 53/2013 for the protection of animals employed in research and teaching; Directive 2010/63/UE, related to the protection of animals used for scientific goals). Protocols were approved by the Ethical Committee of the Council of Agriculture, Farming and Autoctonous Resources of the Principality of Asturias, Spain (permit number PROAE 25/2016) and the Animal Welfare Committee of the Community of Madrid, Spain (permit number PROEX 236/17).

2.2. *In vitro* generation of bovine monocyte-derived macrophages

BoMØs were generated as previously described (Werling et al., 2004; Souza, 2015) from monocytes isolated from peripheral blood collected from six adult dairy cows testing negative for *N. caninum*, infectious bovine rhinotracheitis virus (IBRV) and bovine viral diarrhea virus (BVDV), both of which are known to induce immunosuppression. Motility, transmigration, cytoskeletal morphology and gelatin degradation assays were performed using monocytes isolated from bovine peripheral blood purchased from a commercial supplier (Håtunalab AB, Bro, Sweden).

Independent of the source of blood, peripheral blood mononuclear cells (PBMCs) were separated by gradient density centrifugation on Histopaque 1077 (Sigma-Aldrich, USA), and monocytes were isolated by positive selection using mouse anti-human CD14-coupled microbeads (Miltenyi Biotec Ltd., USA) according to the manufacturer´s instructions. The identity and purity of monocytes (≥95%) was determined by flow cytometry using a mouse anti-bovine CD14 FITC-labeled antibody (clone CC-G33, Bio-rad Laboratories, USA). Monocytes ($CD14^+$ cells) were seeded in 6-well culture plates at a density of 10^6 cells ml^{-1} in 3 ml of RPMI 1640 medium (Invitrogen, Life Technologies, UK) supplemented with 10% heat-inactivated fetal calf serum (FCS), 100 IU ml^{-1} of penicillin, 100 μg ml^{-1} of streptomycin and 50 μM β-mercaptoethanol (Merck Millipore, USA), referred to as complete medium (CM). Cells were incubated at 37ºC in

the presence of 5% CO_2 with 100 ng ml^{-1} recombinant bovine (rbo) GM-CSF (Kingfisher Biotech, USA). At day 3, 1 ml of medium from each well was replaced with 1 ml of fresh CM with 100 ng ml^{-1} rboGM-CSF. After 5 days of culture, further evidence of *in vitro* generation of MØs was assessed by light microscopy and flow cytometry based on increased size, increased adherence, cytoplasmic granularity, presence of cell appendages and expression of surface antigens using antibodies specific for the bovine molecules CD14, MHC Class II, CD80, CD86, CD172a, CD11b and CD1b) (**Supplementary Figure 1**).

Prior to parasite infection, MØs were harvested using ice-cold PBS with 2 mM EDTA and soft scraping, reseeded in culture plates at the density of viable cells indicated for each assay and incubated for 24 h to minimize possible cellular stress due to the harvesting procedure. The viability of the cells was checked with a trypan blue exclusion test, and was normally above 95%.

2.3. Parasite cultures and macrophage infection

Neospora caninum isolates of high and low virulence (Nc-Spain7 and Nc-Spain1H, respectively) were obtained from healthy calves infected congenitally (Regidor-Cerrillo et al., 2008; Rojo-Montejo et al., 2009a) and characterized *in vitro* and *in vivo* using murine and bovine models. Virulence differences were based on infection and proliferation rates *in vitro* and percentage of abortion and vertical transmission *in vivo* (Rojo-Montejo et al., 2009a, 2009b; Regidor-Cerrillo et al., 2010, 2014). Tachyzoites were routinely maintained in a monolayer culture of the African green monkey cell line (MA-104 clone 8, provided by Hipra Laboratories, SA) as described previously (Regidor-Cerrillo et al., 2008). On each passage, the cultures were scraped, passed by 25 G needle, and inoculated onto a new monolayer cell culture. To reduce potential changes in virulence due to prolonged maintenance *in vitro* (Pérez-Zaballos et al., 2005), parasites were used at a passage lower than 15 for all the experiments. Tachyzoites used for boMØ infection were collected from 3-3.5 day-growth cultures, when the majority of the parasites (at least 80%) were still in parasitophorous vacuoles, and purified using PD-10 Desalting Columns (G.E. Healthcare, Buckinghamshire, UK) as previously described (Regidor-Cerrillo et al., 2011). Viable tachyzoites were counted in a Neubauer chamber via trypan blue exclusion and were inoculated within one hour of parasite collection.

For cell infection rate (cIR) determination, multiplicities of infection (MOI)s of 3 to 5 were chosen based on previous *in vitro* studies (Collantes-Fernández et al., 2012; Jiménez-Pelayo et al., 2017). A MOI of 3 was used in most of the assays to obtain an elevated cIR with a low percentage of multi-infection. For transmigration assay protocol, which requires an increased handling of the MØs, a MOI of 2 was used to ensure cell survival.

The *T. gondii* RFP-expressing Prugniaud line (PRU-RFP, type II) (Pepper et al., 2008) was used as reference line in motility, transmigration, morphology and matrix degradation assays. Tachyzoites were cultured as described for *N. caninum* and collected from 2.5-3 day-growth cultures. As a control of phagocytosis and cell response, MØs were inoculated with heat-inactivated (HI) *N. caninum* tachyzoites from Nc-Spain7 and Nc-Spain1H isolates mixed at a ratio 1:1. Purified tachyzoites were killed by incubation at 56 ºC for 30 min as described previously (Butcher and Denkers, 2002). Lack of viability of tachyzoites was confirmed by trypan blue exclusion and by real-time PCR that measured the expression of *NcTUBa* as previously described (Alaeddine et al., 2013) in cDNA samples of MA-104 cultures infected with HI tachyzoites for one week.

2.4. Cell infection rate and parasite survival

To study the differential ability of the *N. caninum* isolates to infect and survive in boMØs, cIR defined as the percentage of cells infected with one or multiple tachyzoites using different parasite doses, was determined and compared at 8 and 36 hours post-infection (hpi). MØs were cultured in 24-well plates at a density of 2.5×10^5 cells/well and inoculated with live Nc-Spain7 or Nc-Spain1H at a MOI of 3, 4 and 5. In addition, MØs were inoculated with HI tachyzoites at the same MOIs as a control for phagocytosis. Cultures were fixed with 0.05% glutaraldehyde (GA) and 3% paraformaldehyde (PF) and stained using double immunofluorescence staining as described previously (Jiménez-Pelayo et al., 2017). Overall number of cells, number of cells containing at least one tachyzoite and number of cells containing more than one tachyzoite (multi-infected cells) were counted in 10 arbitrarily selected fields using an inverted fluorescence microscope (Nikon Eclipse TE 200, Japan) at a magnification of 200×. Counting of events was carried out on images taken with different filters for visualization of nuclei and intracellular and extracellular tachyzoites using a Nikon DSL1 camera; the images were overlaid using Photoshop software (Adobe Systems Incorporated, USA). A mean value of 50 cells was counted in each field by a single operator in order to avoid possible differences due to subjectivity in individual appreciations, and only tachyzoites that retained an unaltered morphology were considered in the count.

To assess the ability of Nc-Spain7 and Nc-Spain 1H to actively invade the host cell, phagocytosis activity of MØs was inhibited by treatment with 10 μM Cytochalasin D (Sigma-Aldrich, Spain) for 30 minutes, following by washing cells three times with PBS. MØs were cultured, infected, fixed and stained as described above. A MOI of 3 was used for inoculation with Nc-Spain7, Nc-Spain1H and HI tachyzoites. Parasite invasion was determined in parallel in Cytochalasin D-treated and untreated MØs at 8 hpi.

2.5. Lysosomal activity of infected macrophages

To identify intracellular localization of tachyzoites and their ability to evade degradation, lysosomes were labelled by the addition of LysoTracker Red DND-99 (Thermo Fisher Scientific, USA) into the culture media at a concentration of 75nM 30 min prior the fixing. Cells were cultured and infected as indicated above using a MOI of 3. At 24 hpi cultures were fixed with 0.05% glutaraldehyde (GA) and 3% paraformaldehyde (PF). Immunofluorescence staining of the parasites is described below.

2.6. Proliferation assays

Proliferation kinetics of Nc-Spain7 and Nc-Spain1H isolates in MØs were determined by quantifying the number of tachyzoites at specific times (8, 24, 36, 48, 60 and 72 hpi) using quantitative real-time PCR (qPCR). Cells were cultured and infected as indicated above using an MOI of 3. Samples were collected by adding 200 µl of PBS, 180 µl of lysis buffer and 20 µl of proteinase K (Qiagen, Germany) to each well and were stored at -80 °C until DNA extraction. DNA extraction and qPCR were carried out as specified previously (Jiménez-Pelayo et al., 2017). Briefly, genomic DNA was extracted using a DNeasy Blood & Tissue Kit (Qiagen, Germany) according to the manufacturer's instructions. Quantification of *N. caninum* DNA was performed via qPCR using a 7300 Real-Time PCR System (Applied Biosystems, USA). A standard curve of 10^{-1} to 10^4 tachyzoites was used for the quantification (Collantes-Fernández et al., 2002). A bovine β-actin standard curve was constructed (from 64 to 0.2 ng DNA/µl) in

order to normalize the quantification of the parasites in each sample. The results are expressed as the relationship between the amounts of parasite DNA and cell DNA ($R^2 \geq 0.99$; slope values varied from -3.47 to -3.11).

The doubling time (Td), defined as the period of time required for a tachyzoite to duplicate during the exponential multiplication phase, was calculated as previously described (Regidor-Cerrillo et al., 2011) by applying non-linear regression analysis and an exponential growth equation using GraphPad Prism (GraphPad Software, USA). The Td for each isolate is presented as the average value obtained from all determinations that revealed a linear regression, $R^2 \geq 0.95$ (Regidor-Cerrillo et al., 2011). The tachyzoite yield (TY_{48h}) was defined as the average number of tachyzoites quantified by qPCR at 48 hpi for each isolate.

In parallel, cells were seeded on coverslips, infected and labeled using a double-immunostaining protocol as described previously (Jiménez-Pelayo et al., 2017) to study the proliferation kinetics of both isolates in MØs via microscopy, as a complementary technique to the quantification by qPCR. Three coverslips were photographed for each condition using an inverted fluorescence microscope (Nikon Eclipse TE 200).

2.7. Cytoskeletal morphology assay

MØs were seeded on poly-L-lysine (Sigma Aldrich, USA)-coated coverslips at a density of 4×10^4 cells/coverslip and inoculated with Nc-Spain7, Nc-Spain1H, HI tachyzoites or *T. gondii* (PRU-RFP) tachyzoites (MOI 2). Non-infected MØs were used as the negative control. At 8 hpi, cells were fixed with 0.05% GA and 3% PF and stained as indicated below. The morphology of MØs (100 cells/condition) was analyzed using a Leica DMRB epifluorescence microscope with a 100 × objective and scored on a 0-5 scale according to the following criteria (with non-infected MØs as the reference): *i)* Podosome structures: present (score 0) versus reduced (score 1) or absent (score 2); *ii)* Cell shape: elongated (score 0) versus rounded (score 1); *iii)* Filopodia-like extensions: present (score 0) versus absent (score 1); i*v)* Presence of membrane veils and/or ruffles: present (score 0) versus absent (score 1).

2.8. Gelatin degradation assay

The *in vitro* gelatinolytic activity of MØs, as a marker for their ability to degrade collagen extracellular matrix, was analyzed by gelatinolysis of Oregon green 488 (OG 488)-conjugated porcine gelatin (Molecular probes, Thermo Fisher Scientific, USA) as described previously (Ólafsson et al., 2018). Briefly, 2.5×10^4 MØs were inoculated with *N. caninum* Nc-Spain7, Nc-Spain1H tachyzoites or with *T. gondii* (PRU-RFP) tachyzoites (MOI as indicated), deposited on OG-488 gelatin-coated Lab-tek chambers (VWR) and incubated for 24 h in CM. Cells were subsequently fixed with 4% PF and stained with DAPI (Thermo Fisher Scientific, USA)N*eospora caninum* tachyzoites were stained as indicated below. After fixation and staining, images were generated (160 FOV/ condition, 1 FOV = 0.617 mm^2) using the 10× objective of the Zeiss Observer Z1. For each chamber, fluorescence (channels, Ex/Em: DAPI, 360/475; OG-488, 450/525; RFP, 555/585) and phase contrast images covering 0.98 cm^2/1.6 cm^2 (61.25% of the total well area) were recorded. Image analysis was automated with the open source software package Cellprofiler (v2.1.1, rev: 9969f42). All images were run through a pipeline designed to define gelatin degradation, non-infected cells and infected cells. Gelatin degradation was defined as loss of signal (gelatin, Oregon green-488). Cells were defined as the Euclidian center of a signal (nuclei) + 15 μm radius. Infected cells were defined as the presence of signal (*N.*

caninum: Alexa 594 or *T. gondii*: RFP) overlapping with a Euclidian center of signal (nuclei) + 15 μm radius. Degradation was then ascribed to each cell population by overlaying non-infected and infected cells with degradation. Co-ascribed degradation was omitted.

2.9. Motility assay

The motility assay was conducted as previously described (Weidner et al., 2013). Briefly, MØs were seeded in a 96-well plate at a density of 2×10^4 cells/well and inoculated with *N. caninum* Nc-Spain7, Nc-Spain1H or HI tachyzoites (MOI 3). In addition, MØs inoculated with *T. gondii* (PRU-RFP, MOI 3) tachyzoites were used for motility comparisons, and non-infected MØs served as the negative control. Prior to infection, *N. caninum* tachyzoites were incubated for 15 min with CMTMR dye (2.5 µM, Thermo Fisher Scientific, USA). Bovine collagen I (0.75 mg ml^{-1}, Thermo Fisher Scientific, USA) was added at 4 hpi, and cells were imaged every min for 60 min with a 10× objective (Zeiss Observer Z1, Zen 2 Blue v.4.0.3). The infection rate was determined, and the absence of differences between groups of inoculated MØs was confirmed (data not shown). Motility data were obtained from 50 cells/condition using ImageJ (Manual Tracking and Chemotaxis and Migration tool plugins).

2.10. Transmigration assay

Transmigration assays were performed as previously described (Lambert et al., 2006), with minimal modifications. Briefly, MØs were seeded at a density of 1×10^6 cells/well and inoculated with Nc-Spain7, Nc-Spain1H or HI tachyzoites at a MOI of 2. *Toxoplasma gondii*-infected MØs (PRU-RFP) were also included in the study as above, and non-infected MØs were used as the negative control. At 6 hpi, MØs were recovered by soft scraping, and 3×10^5 cells/condition were transferred to transwell filters (8 µm pore size; BD biosciences, San José, CA, USA) and incubated for 16 h at 37ºC with 5% CO_2. In addition, 2×10^4 cells/condition were seeded on coverslips, fixed and stained as indicated below, and the infection rate was determined, confirming the absence of differences between groups of inoculated MØs (data not shown). Migrated MØs were recovered by trypsinization and quantified using a Neubauer chamber.

2.11. Analysis of ROS generation

Analysis of intracellular ROS generation by infected MØs was performed via flow cytometry. MØs were seeded in 6-well plates at a final density of 1.5×10^6 cells/well and incubated in CM for 1 or 24 h post inoculation with Nc-Spain7, Nc-Spain1H or HI tachyzoites (MOI 3). MØs inoculated with H_2O_2 (2 μM) were used as the positive control and non-infected MØs as the negative control. Cells were then harvested and stained with 5 µM CellROX Green Reagent (Thermo Fisher Scientific, USA) for 30 min at 37 °C, and the fluorescence of viable cells, gated for propidium iodide (5 μg ml^{-1}) staining, was assessed in a FACS Calibur cell Analyzer (BD Bioscience, USA).

2.12. Analysis of bovine IL-10 and IL-12 cytokine expression

The mRNA expression levels of IL-10 and IL-12p40 were determined by quantitative reverse-transcription real-time PCR (RT-qPCR). MØs were seeded at a density of 10^6 cells ml^{-1} in 6-well culture plates and inoculated with Nc-Spain7, Nc-Spain1H, and HI tachyzoites at MOI 3 or with LPS (100 ng ml^{-1}) as the control for MØ activation for 8 h and then resuspended in 300

μl of RNAlater (Qiagen, Germany). Non-infected MØs were used as the negative control. Samples were recovered 8 h later by scraping and centrifugation at 1350 x g for 15 min at 4ºC. The obtained pellets were resuspended in 300 μl of RNAlater (Qiagen, Germany) and stored at -80ºC until RNA extraction. Analysis was performed on three replicates obtained from three independent experiments. RNA was extracted using the commercial Maxwell 16 LEV simply RNA Purification Kit (Promega, USA) following the manufacturer's recommendations. Integrity was checked by 1% agarose gel and and RNA concentrations were determined using a spectrophotometer (Nanophotomer, Implen GmbH, Germany). cDNA was obtained by reverse transcription using a master mix SuperScript VILO cDNA Synthesis Kit (Invitrogen, UK), and IL-10 and IL-12p40 mRNA expression was determined using the primers and conditions previously described (Regidor-Cerrillo et al., 2014). Genes were considered to be differentially expressed when they presented a fold change (FC) ≥ 2 and $p < 0.05$.

2.13. Surface marker expression analyses of immune cell subsets by flow cytometry

Surface expression of CD14, MHC Class II, CD80, CD86, CD172a, CD11b, and CD1b by boMØs after exposure to *N. caninum* was determined by flow cytometry. To do so, MØs were seeded in 24 well plates at a density of 3×10^5 cells/well and inoculated with Nc-Spain7, Nc-Spain1H and HI tachyzoites (MOI 3) or LPS (100 ng ml^{-1}) for 4 h as the control for MØ activation. After 4 hours, cells were detached from the culture plates by incubation with cold PBS with 2 mM EDTA at 4ºC for 10 min and soft scraping. Cultures were recovered in 30 ml centrifuge tubes and centrifuged at 1200 rpm for 5 min at 4ºC. After centrifugation, cells were resuspended in cold PBS at a density of 2×10^5 cell/100 μl. A volume of 100 μl of cells per well was pelleted in a V-bottom 96-well plate and centrifuged at 1300 rpm 4ºC for 3 min. PBS was discarded and cells were incubated with 50 μl of diluted antibody (1:100) or 50 μl of PBS for 30 min on ice and protected from light. After the incubation, samples were washed with PBS before adding the fixative BD Cellfix (BD Bioscience, USA).

The negative fraction ($CD14^-$ cells) obtained during positive selection of monocytes ($CD14^+$ cells) and used for determination of IFN-γ secretion assay was characterized following the protocol described for surface marker analysis of MØs. The percentage of CD4 T cells ($CD4^+$), CD8 T cells ($CD8^+$), Natural Killer (NKp46, $CD335^+$), gamma delta T cells ($WC1^+$) and B cells ($CD21^+$) in the population was determined (**Supplementary Figure 2**).

The percentage of positive cells and mean fluorescence intensity (MFI) was measured for each marker using a Becton Dickinson FACSCalibur cytometer (BD Bioscience, USA). The data were analyzed using FlowJo software (FlowJo, LLC, USA). The list of antibodies used to analyze subsets is given in **Supplementary Table 1**.

2.14. Determination of IFN-γ secretion by lymphocytes

IFN-γ secretion was measured in supernatants of lymphocytes incubated with MØs. Lymphocytes used in the assay ($CD14^-$ cells) were obtained as the flow through after magnetic isolation of $CD14^+$ cells. This cell population, characterized by flow cytometry as indicated below, contained $CD4^+$ T cells (26.53% ± 1.45), $CD8^+$ T cells (34.05% ± 1.07), B cells (18.06% ± 0.77) Natural Killer (8.46% ± 0.23) and γδ T cells (18.26% ± 1.14). MØs were seeded in 24-well plates at a density of 2.5×10^5 cells/well and inoculated with Nc-Spain7, Nc-Spain1H or HI tachyzoites at MOI 3 or with LPS (100 ng ml^{-1}). Twenty-four hours later, lymphocytes were added at a

density of 12.5 × 10^5 cells/well. To verify that IFN-γ was secreted in our samples exclusively by lymphocytes upon induction by infected MØs, MØs inoculated at the conditions previously described without lymphocyte addition and lymphocytes without MØs were included in the experiment as controls. Supernatants were recovered 48 and 72 hpi and bovine IFN-γ concentrations were determined using a bovine IFN-γ ELISA development kit (Mabtech AB, Sweden), following the manufacturer's recommendations. The color reaction was developed by the addition of 3,3',5,5'-tetramethylbenzidine substrate (TMB, Sigma-Aldrich, Spain) and incubated for 5-10 min in the dark. Reactions were stopped by adding 2N H_2SO_4. Then, plates were read at 450 nm. The cytokine concentrations were calculated by interpolation from a standard curve generated with recombinant cytokines provided by the kit.

2.15. Immunofluorescence staining of macrophages and *Neospora caninum* tachyzoites

For the gelatin degradation assay, a single immunofluorescence staining of tachyzoites was carried out as described previously (Jiménez-Pelayo et al., 2017). After permeabilization with Triton X-100 (Thermo Fisher Scientific, USA), parasites were stained using hyperimmune rabbit antiserum directed against *N. caninum* tachyzoites (1:1000) as the primary antibody (Álvarez-García et al., 2007) and goat anti-rabbit IgG conjugated to Alexa Fluor-594 (Thermo Fisher Scientific, USA) (1:1000) as the secondary antibody.

For cIR determination, intracellular proliferation and cytoskeletal morphology assays, a double immunofluorescence staining of tachyzoites was carried out as described previously (Jiménez-Pelayo et al., 2017). Parasites were stained using hyperimmune rabbit antiserum directed against *N. caninum* tachyzoites (1:1000) as the primary antibody. For the double immunostaining, when F-actin filaments were stained (intracellular proliferation assay) with Alexa Fluor-594 Phalloidin (Thermo Fisher Scientific, USA) or non-stained (cIR determination), a 1:1000 dilution of goat anti-rabbit IgG conjugated to Alexa Fluor-488 (Thermo Fisher Scientific, USA) was added before permeabilization with Triton X-100 to stain extracellular tachyzoites. After permeabilization, a 1:1000 dilution of goat anti-rabbit IgG conjugated to Alexa Fluor 594 was used to stain both extra- and intracellular tachyzoites. When Alexa Fluor-488 Phalloidin was used for the staining of F-actin filaments (morphology assay), donkey anti-rabbit Alexa Fluor 350 (Thermo Fisher Scientific, USA) was added to stain extracellular tachyzoites, and goat anti-rabbit IgG conjugated to Alexa Fluor 594 (Thermo Fisher Scientific, USA) was used to stain both extra- and intracellular tachyzoites. The nuclei were stained by washing the cells with a solution of 1:5000 DAPI (Thermo Fisher Scientific, USA) in PBS, and the coverslips were embedded in Fluoroprep (BioMerieux, France).

For the study of the lysosomal activity of infected MØs, cells were permeabilized with 0.5% saponin (Fluka BioChemika, Spain). Parasites were stained using hyperimmune rabbit antiserum directed against *N. caninum* tachyzoites (1:1000) as the primary antibody and goat anti-rabbit IgG conjugated to Alexa Fluor-488 (Thermo Fisher Scientific, USA) (1:1000) as the secondary antibody.

2.16. Statistical analysis

After testing the samples for normal distribution, differences in cIR, proliferation and cytokine expression were analyzed using a non-parametric Kruskal-Wallis test followed by Dunn's post hoc test for comparisons between groups. Mann–Whitney U test was used for pairwise comparisons.

ROS generation, IFN-γ secretion, surface marker detection, motility, transmigration, cytoskeletal morphology and gelatin degradation assay data were analyzed via parametric one-way ANOVA, followed by Tukey´s post hoc test for multiple comparisons and Student's t-test for pairwise comparisons. Dunnett's test was used to compare all the groups to the non-infected group. Statistical significance was established at $p < 0.05$.GraphPad Prism 7 v.7.04 (San Diego, CA, USA) software was used to perform all statistical analyses and graphical illustrations.

3. RESULTS

3.1. The highly virulent isolate Nc-Spain7 replicates significantly faster in bovine macrophages

In an initial experiment, we compared the ability of *N. caninum* isolates of different virulence to complete their life cycle in boMØs. First, we evaluated the capacity of the parasite to infect and survive in boMØs. At 8 hpi, MØs internalized tachyzoites with the same efficiency for all assayed conditions. The cIR and the percentage of multi-infected cells did not increase significantly with increasing the MOI, and non-significant differences were found between isolates or between live *versus* HI tachyzoites (**Figure 1A**, $p > 0.05$). To study the ability of both isolates to survive in MØs, cIR and the percentage of multi-infected cells was also evaluated at 36 hpi. The time point of 36 hpi was chosen to permit degradation of dead tachyzoites in order to count only live tachyzoites. Discerning between live and dead tachyzoites was also facilitated by the higher multiplication of the parasites at that time-point. Tachyzoites with unaltered morphology (regarding size, shape and keeping a smooth surface in the absence of visible defects on its membrane) were counted in MØs infected with Nc-Spain7 and Nc-Spain1H isolates. However, only degraded tachyzoites were observed in MØs inoculated with HI tachyzoites at 36 hpi. A statistically significant reduction in cIR (from 61.34 ± 12.4 to 34.94 ± 14.35; $p < 0.001$) and the percentage of multi-infected cells (from 35.91 ± 15.08 to 12.50 ± 8.74; $p < 0.001$) was shown for both isolates at 36 hpi compared with 8 hpi at all MOIs assayed (**Figure 1A**). Additionally, when comparing both isolates at 36 hpi, the highly virulent isolate Nc-Spain7 showed a higher multi-infected cell number ($p < 0.05$ for MOI 4 and 5) than the low virulence isolate Nc-Spain1H.

As the presence of intracellular tachyzoites can be either based on active invasion or actin-filament dependent phagocytosis, we next assessed these possibilities by disrupting the actin skeleton using Cytochalasin D. After inhibition of phagocytosis, Nc-Spain7 showed a higher cIR and percentage of multi-infected cells (34.96 ± 5.89 and 13.22 ± 4.89 respectively; $p < 0.001$) compared to Nc-Spain1H (25.45 ± 6.80 and 7.09 ± 3.33) at 8 hpi (MOI 3). Cytochalasin D-treated MØs inoculated with HI tachyzoites showed a cIR of 2.24 ± 2.68, with a percentage of multi-infected cells of 0.44 ± 0.75. No differences were observed between cIR in Cytochalasin D-treated MØs at 8 hpi (**Figure 1B)** *versus* cIR at 36 hpi (**Figure 1A**).

Having established that tachyzoites of both isolates are able to actively invade boMØs, we next assessed whether these would thus also evade lysosomal degradation at 24 hpi. As expected based on the results obtained with Cytochalasin D, MØs exposed to HI tachyzoites showed clear co-localization of LysoTracker and degraded tachyzoites. In contrast, this was absent for tachyzoites of both strains in replication, indicating no fusion of the parasitophorous vacuole with lysosomal compartments (**Figure 1C**). These results show that those tachyzoites internalized by phagocytosis suffer the macrophage driven degradation effects.

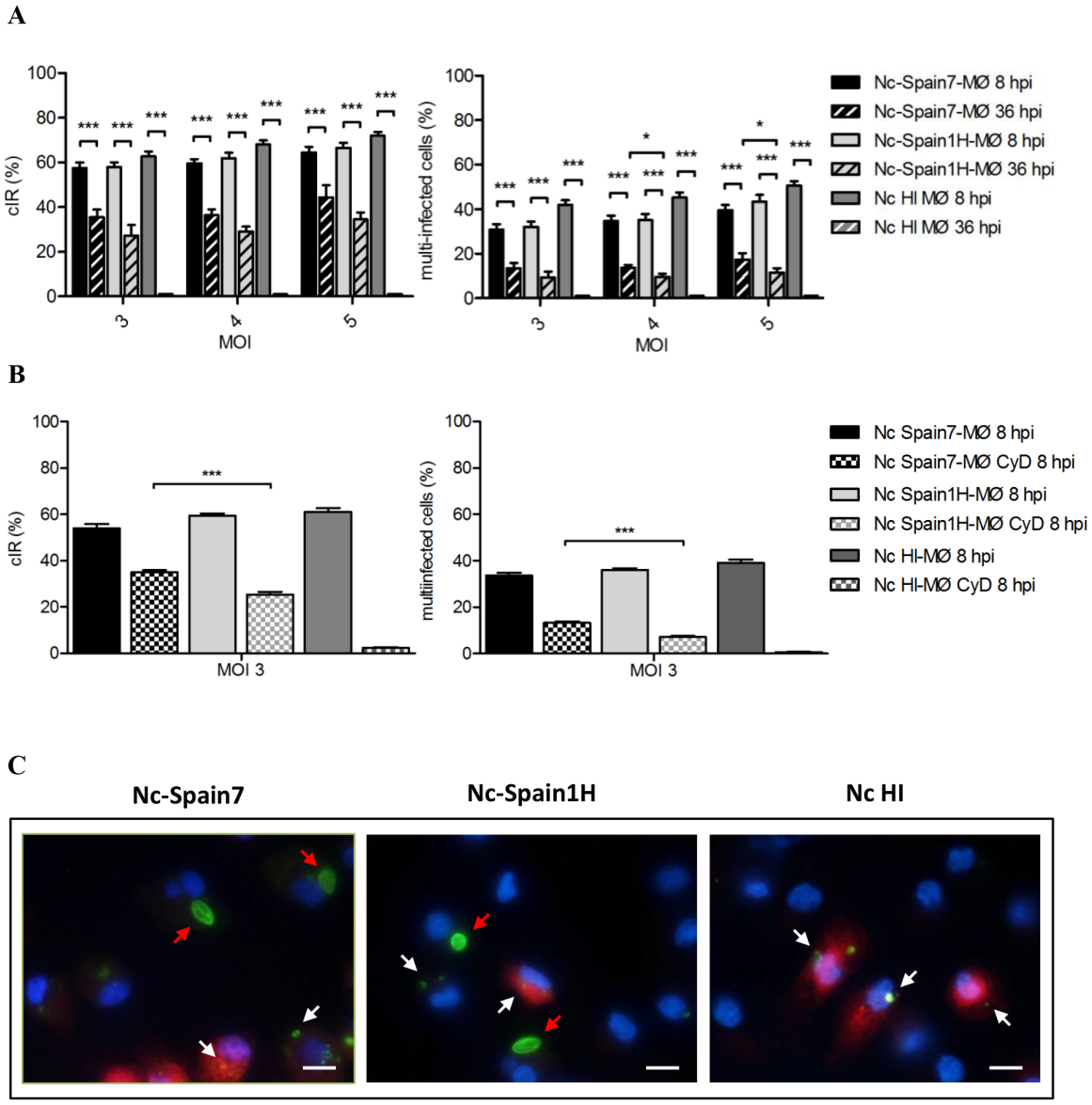

FIGURE 1 | Active invasion and parasite survival of Nc-Spain7 and Nc-Spain1H isolates in bovine MØs. (A) Graphs represent the cell infection rates at 8 and 36 hpi as the percentage of infected cells and multi-infected cells in bovine MØs for both isolates. Each column and error bar represents the mean value and SEM of three replicates from three independent experiments using MOIs of 3, 4, and 5. The total number of cells, the number of infected cells (with intact tachyzoites) and the number of cells with multi-infection were determined by double immunofluorescence staining followed by counting using an inverted fluorescence microscope. Degraded tachyzoites were found inside MØs inoculated with HI tachyzoites at 36 hpi. Significant differences are indicated (*$p < 0.05$; ***$p < 0.001$). (B) Graphs represent the cell infection rates at 8 hpi as the percentage of infected cells and multi-infected cells in untreated and Cytochalasin D treated MØs (MØ CyD) for both isolates. Each column and error bar represents the mean value and SEM of three replicates from three independent experiments using a MOI of 3. Significant differences are indicated (***$p < 0.001$). (C) Representative images (at 1,000×) show the proliferation of Nc-Spain7 and Nc-Spain1H isolates in bovine MØs (red arrows) and the degradation of phagocyted tachyzoites in phagolysosomes (white arrows). Lysosomes stained with LysoTracker Red DND-99 are presented in red, nuclei in blue and parasites in green. Scale bar is 10 μm.

As a second marker to identify potential differences, we assayed the ability of both *N. caninum* isolates to proliferate in boMØs *in vitro*. Microscopic examination of cultures infected at a MOI of 3 and fixed at different times post-infection showed that Nc-Spain7 and Nc-Spain1H tachyzoites had already begun to multiply at 24 hpi. Parasitophorous vacuoles of Nc-Spain7 were bigger than Nc-Spain1H vacuoles from 48 hpi onwards. For Nc-Spain7, rupture of the host cells and egression of the tachyzoites began to be visualized from 48 hpi and was complete before 72 hpi, at which time point, invasion of new cells by the egressed tachyzoites was observed. For Nc-Spain1H egression did not begin until 60 hpi. At 72 hpi egression is not completed, since intact vacuoles were still visualized (**Figure 2A**). Proliferation kinetics over time assessed by qPCR are presented in **Figure 2B**. From 24 hpi onwards, the average number of tachyzoites was higher for Nc-Spain7 for each time point assayed ($p < 0.001$). The Td value was analyzed to determine the length of the cell cycle for both isolates. Nc-Spain7 showed an exponential growth with an average Td value of 13.15 ± 3.64. Nc-Spain1H failed to produce an exponential pattern growth, and thus, their Td value could not be calculated. The TY_{48h} was also assessed to determine the number of tachyzoites produced during the same intracellular period after invasion, prior to complete tachyzoite egress from cell cultures (**Figure 2B**). The TY_{48h} value was 4-times higher in Nc-Spain7-infected cultures (1,663 ± 185) than in Nc-Spain1H-infected cultures (442 ± 99) ($p < 0.001$).

Altogether, these findings demonstrated that *N. caninum* was able to infect, survive and complete the parasite lytic cycle in boMØs. Remarkably, a higher active invasion rate and proliferation over time was observed for the highly virulent isolate Nc-Spain7. We therefore analyzed in the next steps whether this increased rate was due to a more severe impact of this isolate in immune function of MØs.

3.2. Active invasion by *Neospora caninum* tachyzoites leads to isolate-specific morphological changes in bovine macrophages

Upon infection of human or murine DCs, *T. gondii* rapidly induces cytoskeletal changes which have been linked to the migratory activation of the parasitized cell (Weidner et al., 2013; Kanatani et al., 2015). To analyze the cytoskeletal morphology of boMØs challenged with *N. caninum* and *T. gondii*, F-actin filaments were stained and MØs were scored according to set criteria, detailed under *Materials and methods*. A dramatic impact on cytoskeletal parameters was observed upon challenge with parasites (**Figure 3A**), with significant differences in total scores between *T. gondii*- or *N. caninum*-infected MØs (median score = 3) and unchallenged MØs (median score = 1) ($p < 0.001$). BoMØs challenged with HI tachyzoites and by-stander boMØs (non-infected cells in challenged cell cultures) exhibited a median score of 2 (**Figure 3B**). Significant score differences were observed between groups when the morphology parameters were studied separately (**Figure 3C**). Infection with *T. gondii* resulted in cytoskeletal remodeling characterized by an increase in the percentage of cells that exhibited a rounded shape ($p < 0.05$), total absence of podosomes ($p < 0.001$), maintenance of filopodia-like extensions and a higher presence of ruffles and/or veils ($p < 0.001$). For Nc-Spain7, the most frequently observed phenotype was partial loss of podosomes ($p < 0.001$), loss of filopodia-like extensions ($p < 0.01$) and a higher presence of ruffles and/or veils ($p < 0.001$). Significant differences were also observed in the percentage of cells that exhibited a rounded shape ($p < 0.01$). The morphology of Nc-Spain1H-infected MØs was chiefly characterized by total absence of podosomes ($p < 0.001$), an elongated or dysmorphic shape and a higher frequency of ruffles and/or veils ($p < 0.001$). HI and by-stander cells exhibited an elongated shape, a partial or null loss of podosomes, presence of filopodia and an increment of ruffles/veils ($p < 0.001$).

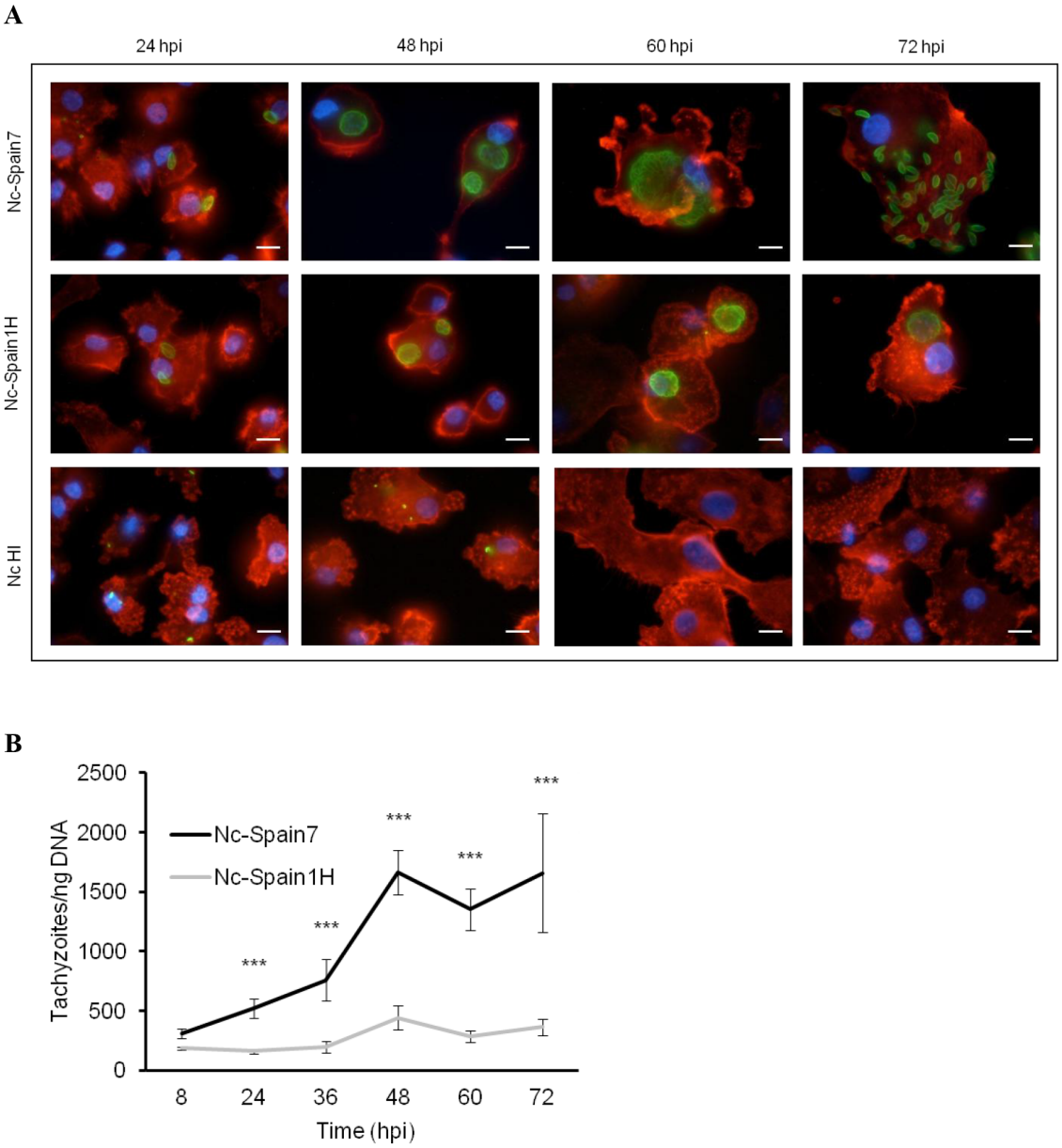

FIGURE 2 | Proliferation of Nc-Spain7 and Nc-Spain1H isolates in bovine MØs. (A) Representative images (at 1,000×) show the proliferation kinetics in MØs over time of Nc-Spain7 and Nc-Spain1H isolates and the degradation of HI tachyzoites in bovine MØs cultures. F-actin is presented in red, nuclei in blue and parasites in green. Scale bar is 10 μm. (B) The graph represents the average number of tachyzoites for each time point assayed. The growth of Nc-Spain1H in bovine MØs did not fit the exponential growth equation. Error bars indicate the SD. Significant differences are indicated (***$p < 0.001$).

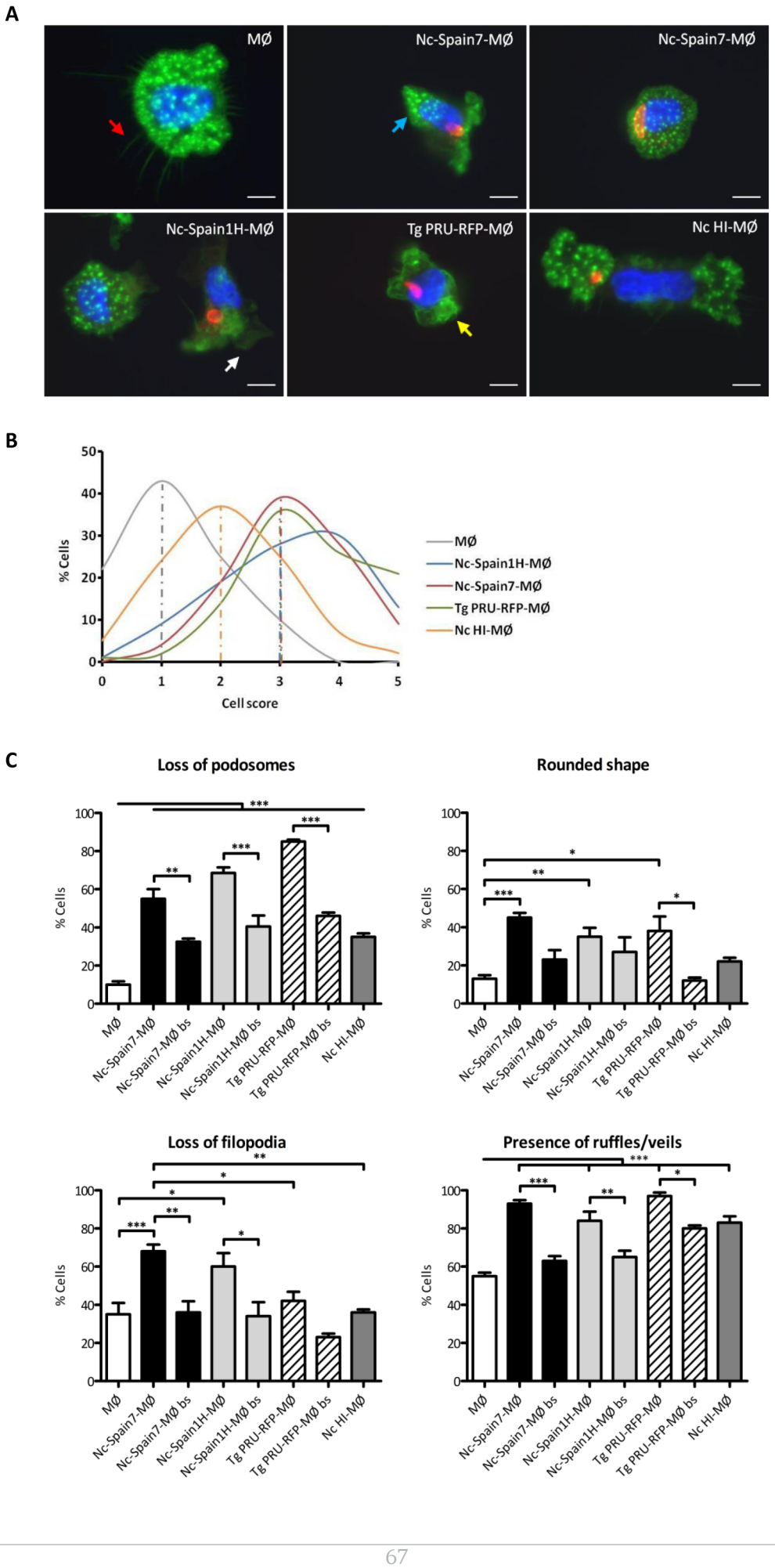
A
MØ
Nc-Spain7-MØ
Nc-Spain7-MØ
Nc-Spain1H-MØ
Tg PRU-RFP-MØ
Nc HI-MØ
B
% Cells
Cell score
MØ
Nc-Spain1H-MØ
Nc-Spain7-MØ
Tg PRU-RFP-MØ
Nc HI-MØ
C
Loss of podosomes
Rounded shape
Loss of filopodia
Presence of ruffles/veils
% Cells
MØ
Nc-Spain7-MØ
Nc-Spain7-MØ bs
Nc-Spain1H-MØ
Nc-Spain1H-MØ bs
Tg PRU-RFP-MØ
Tg PRU-RFP-MØ bs
Nc HI-MØ

FIGURE 3 | Morphological changes in bovine MØs induced by *N. caninum* and *T. gondii* active invasion. (A) Representative micrographs of non-infected MØs (MØ) and MØs challenged for 8 h with *N. caninum* Nc-Spain7 (Nc-Spain7-MØ), Nc-Spain1H (Nc-Spain1H-MØ), heat-inactivated tachyzoites (Nc HI-MØ), or *T. gondii* PRU-RFP (Tg PRU-RFP-MØ). F-actin is presented in green, nuclei in blue and parasites in red. Cell structures studied are pointed with arrows: podosomeS (blue), filopodia-like extensions (red), ruffles (yellow), and veils (white). Scale bar is 10 μm. (B) The distribution of the total scores obtained are presented as the percentage relative to the total population of MØs, Nc-Spain7-MØs, Nc-Spain1H-MØs, Tg PRU-RFP-MØs, and Nc HI-MØs. Cells were graded according to the following morphological criteria: (i) Podosome structures: present (score 0) vs. reduced (score 1) or absent (score 2); (ii) Cell shape: elongated (score 0) vs. rounded (score 1); (iii) Filopodia-like extensions: present (score 0) vs. absent (score 1); iv) Membrane veils and/or ruffles: present (score 0) vs. absent (score 1). (C) Bar graph indicates the percentage of cells that exhibited podosome loss, a rounded shape, filopodia-like extension loss and the presence of ruffles or veils, relative to the total cell population of unchallenged, infected and non-infected by-stander MØs (bs). A total of 100 cells were analyzed for each condition on four coverslips from two independent experiments. Significant differences are indicated (*$p < 0.05$; **$p < 0.01$; ***$p < 0.001$).

Overall, we conclude that the intracellular presence of live *N. caninum* induced cytoskeletal remodeling in boMØs consistent with cellular activation. The morphological impact was similar to that observed for *T. gondii* but significantly different from the morphological changes induced by HI *N. caninum* or those observed in by-stander boMØs.

3.3. *Neospora caninum* infection reduces pericellular proteolysis of extracellular matrix by bovine macrophages

Toxoplasma Gondii modulates the interaction of hypermigratory parasitized DCs with extracellular matrix (Ólafsson et al., 2018, 2019). To address if *N. caninum* infection had an impact on matrix degradation by boMØs, cells were challenged with *N. caninum* isolates, and the pericellular degradation of gelatin (denatured collagen) was assessed (**Figure 4A**). *T. gondii* PRU-RFP-challenged MØs were included in the assays as the positive control. The proteolytic activity of non-infected by-stander boMØs was also determined. A similar significant reduction in gelatin degradation was observed in boMØs infected with Nc-Spain7, Nc-Spain1H and *T. gondii* PRU-RFP compared with unchallenged boMØs ($p > 0.05$). A dose-dependent (MOI) reduction in pericellular proteolysis was observed in by-stander MØs. In contrast, abrogation of the matrix proteolysis in infected boMØs was MOI-independent (**Figures 4B-D**).

We conclude that live intracellular *N. caninum* reduces or abrogates the matrix degradation capability of infected boMØs.

3.4. Live *Neospora caninum* tachyzoites induce a hypermigratory phenotype in bovine macrophages

In murine *T. gondii* infections, induced hypermigration of parasitized DCs has been associated with enhanced parasite dissemination to peripheral organs (Lambert et al., 2006; Kanatani et al., 2017). To investigate whether *N. caninum* is able to exploit the migratory properties of boMØs, the motility and transmigration of boMØs challenged with Nc-Spain7 and Nc-Spain1H isolates were assessed. BoMØs challenged with the *T. gondii* PRU-RFP line were also included in the study. A significantly enhanced velocity was observed in boMØs challenged with both *N. caninum* and *T. gondii* parasites ($p < 0.001$). When comparing both *N. caninum* isolates, significantly higher elevated velocity values were recorded for the highly virulent isolate Nc-Spain7 ($p < 0.01$), which were similar to those for *T. gondii* ($p > 0.05$). In contrast, challenge of boMØs with *N. caninum* HI tachyzoites yielded velocities significantly lower than the baseline velocities of unchallenged boMØs ($p < 0.05$) (**Figures 5A and 5B**).

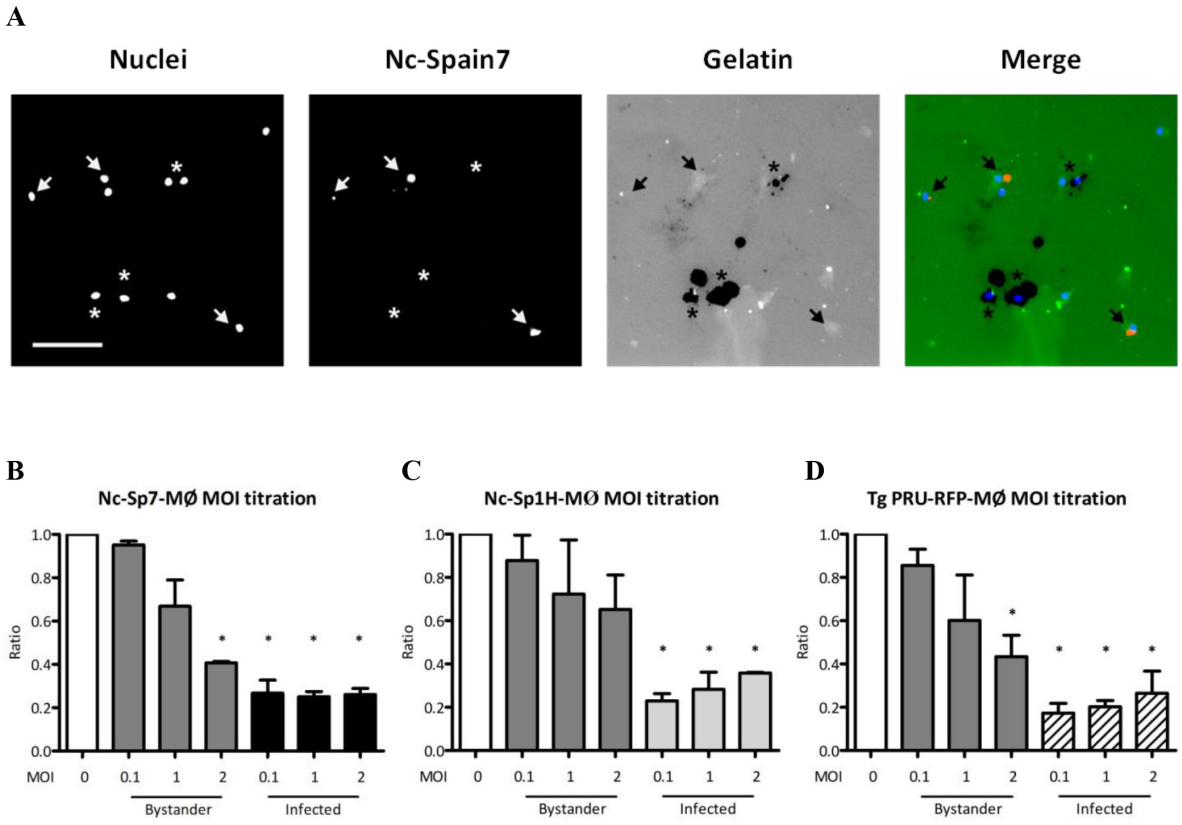

FIGURE 4 | Pericellular proteolysis of bovine MØs upon challenge with *N. caninum* and *T. gondii*. Gelatin degradation of MØs challenged with *N. caninum* Nc-Spain7 (Nc-Spain7-MØ), Nc-Spain1H (Nc-Spain1H-MØ), or *T. gondii* PRU-RFP (T. gondii PRU-RFP-MØ) at the indicated MOIs**. (A)** Representative micrographs show MØ nuclear staining (Nuclei), Alexa-594-stained tachyzoites (Nc-Spain7), and fluorescent gelatin (Gelatin) with areas of gelatin degradation (absence of fluorescence signal). Arrowheads exemplify Nc-Spain7-infected MØs with an absence of gelatin degradation. Asterisks exemplify non-infected by-stander MØs and co-localization with gelatin degradation. Scale bar represents 100 μm. (B–D) Bar graphs show the mean (±SEM) relative gelatin degradation of unchallenged cells in CM (set to 1.0, MOI 0), non-infected by-stander cells (Bystander) and *Neospora* Nc-Spain7- (B), Nc-Spain1H- (C) or *T. gondii*-infected (D) cells (Infected). The analysis comprised 160 FOVs and a total of 15.579 ± 1.087 (SEM) cells per condition from two independent experiments. Significant differences are indicated (*$p < 0.05$).

In transmigration assays, significantly higher transmigration frequencies were also recorded for boMØs infected with both *N. caninum* and *T. gondii* tachyzoites ($p < 0.001$) than for unchallenged boMØs. When comparing both *N. caninum* isolates, non-significant differences in transmigration frequency were found. *T. gondii* induced the highest enhanced transmigration, with statistically significant differences compared with Nc-Spain1H ($p < 0.001$) but not with Nc-Spain7 ($p > 0.05$). Challenge of boMØs with HI tachyzoites resulted in non-significantly altered transmigration frequency ($p > 0.05$) (**Figure 5C**).

Taken together, these results show for the first time that *N. caninum* induces a hypermigratory phenotype (hypermotility and enhanced transmigration) in boMØs. A significantly higher hypermotility was observed for the highly virulent isolate Nc-Spain7 compared with Nc-Spain1H.

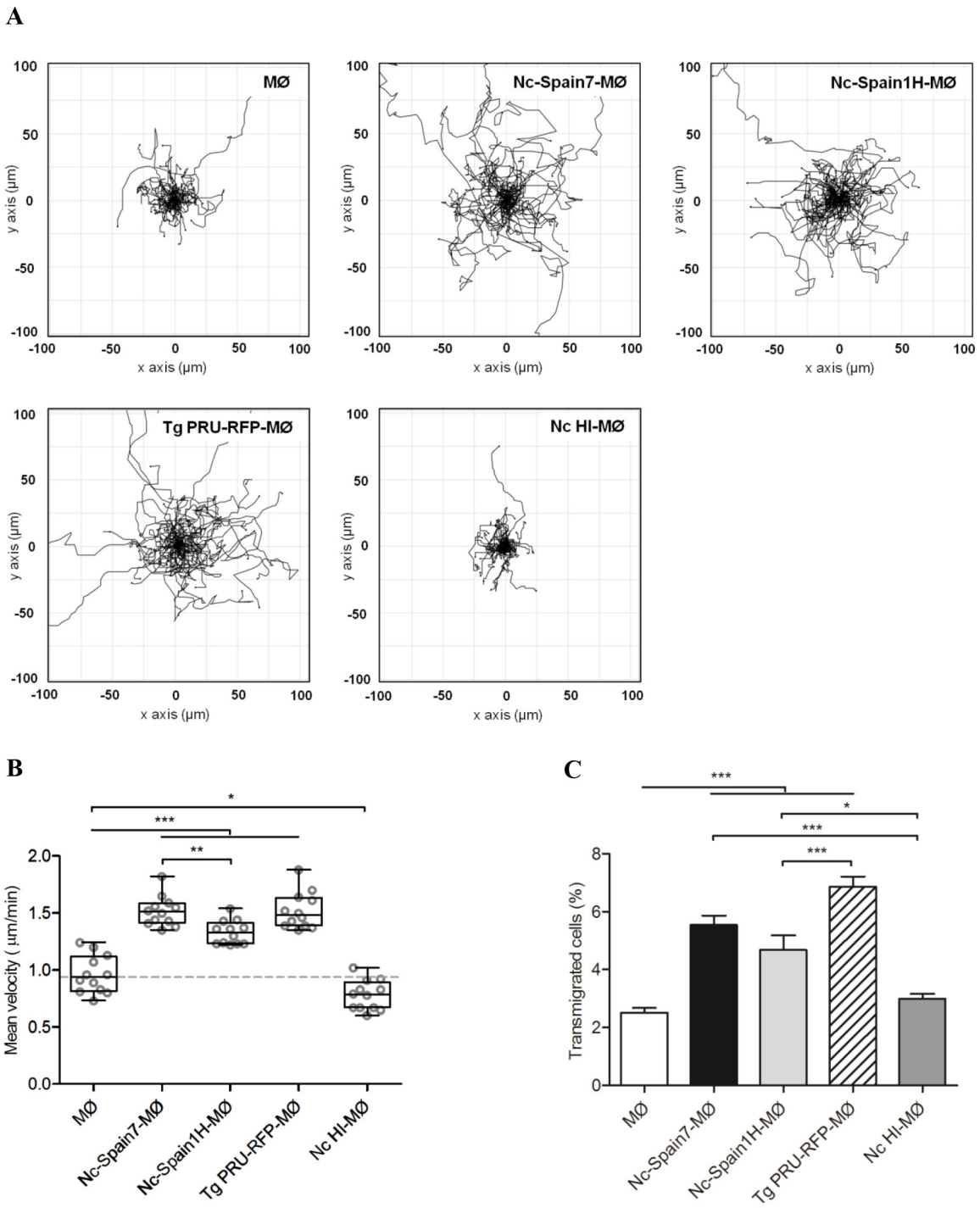

FIGURE 5 | Hypermotile phenotype and enhanced transmigration in bovine MØs induced by *N. caninum* infection. (A) Motility plot of unchallenged MØs (MØ) and MØs challenged for 4 h with *N. caninum* Nc-Spain7 (Nc-Spain7-MØ), Nc-Spain1H (Nc-Spain1H-MØ), heat-inactivated tachyzoites (Nc HI-MØ) or *T. gondi*i PRU-RFP tachyzoites (Tg PRU-RFP-MØ). (B) Graph represents the mean velocity and SEM of three independent experiments. Circles indicate the average velocity of 50 cells tracked in two different tiles and two different wells per experiment. Box plot shows upper and lower interquartile range with median. (C) The graph represents the percentage of transmigration 18 hpi of MØs, Nc-Spain7-MØs, Nc-Spain1H-MØs, Nc HI-MØs, and Tg PRU-RFP-MØs. The data represent the mean values and SD of three independent experiments; Significant differences are indicated (*$p < 0.05$; **$p < 0.01$; ***$p < 0.001$).

3.5. The highly virulent isolate Nc-Spain7 completely down-regulates ROS production in infected macrophages

Having established the impact of different *N. caninum* isolates on boMØ morphology and cytoskeletal functionality, we next evaluated whether the infection also impact on innate immune parameters in a virulence-specific manner. To assess the ability of boMØ to kill invading *N. caninum* by production of ROS, differential ROS production upon *N. caninum* inoculation with Nc-Spain7, Nc-Spain1H and HI tachyzoites was evaluated by flow cytometry at 1 and 24 hpi (**Figure 6**). At 1 hpi, a significant increase in ROS production was found in MØs inoculated with Nc-Spain1H ($p < 0.05$) and HI tachyzoites ($p < 0.001$) *versus* non-infected cells but not in MØs inoculated with Nc-Spain7 ($p > 0.05$). However, at this time-point no significant differences were found between isolates, which both induced lower ROS generation by MØs compared with HI tachyzoites ($p < 0.05$). At 24 hpi, the production of ROS by Nc-Spain1H-infected MØs was enhanced ($p < 0.001$) compared to that of non-infected MØs as well as MØs incubated with HI tachyzoites. Interestingly however, no ROS production above either control or MØs incubated with HI tachyzoites was seen in MØs inoculated with the highly virulent isolate Nc-Spain7.

We conclude that live intracellular *N. caninum* reduces the ROS response of infected MØs at early infection, but only the highly virulent isolate Nc-Spain7 maintains the abrogated ROS production over time.

3.6. *Neospora caninum* infection of macrophages induces a virulence-dependent IL-10 and IL-12 mRNA expression pattern

MØ have the ability to subsequently prime the adaptive immune response through secretion of cytokines, specifically the Th1-supporting IL-12 and the regulatory IL-10. Thus, in a next step, we investigated whether the differences in strain-specific ROS production would also be mirrored on the cytokine level. As expected, untreated MØ produced hardly any mRNA for either cytokine, whereas MØ incubated with LPS responded with a significantly enhanced mRNA expression for the pro-inflammatory cytokine IL-12 (148.7-fold; $p < 0.001$), and only mildly increased IL-10 mRNA production (3.6-fold; $p < 0.01$). Inoculation of MØ with HI tachyzoites did not increase IL-12p40 mRNA expression levels (0.99-fold; $p > 0.05$), and only marginally impacted on IL-10 mRNA expression (2.22-fold; $p < 0.01$) (**Figure 7**). In contrast, incubation of MØ with both types of live *N. caninum* tachyzoites induced a strain-specific increase in IL-12p40 mRNA and IL-10 mRNA expression compared to non-infected MØ, with the low virulent isolate Nc-Spain1H inducing more IL-12p40 (7.7-fold; $p < 0.001$) and IL-10 (19.6-fold; $p < 0.001$) than the highly virulent Nc-Spain7 isolate (4.8-fold; $p < 0.01$ and 14.5-fold; $p < 0.001$, respectively), although the differences between isolates were not statistically significant ($p > 0.05$).

In summary, live tachyzoites of both isolates induced IL-12p40 and IL-10 expression in boMØs. However, expression levels of both cytokines were higher for cells infected with the low virulent isolate Nc-Spain1H.

3.7. *Neospora caninum* infection results in changes in surface marker expression in bovine macrophages

As the production of cytokines can also impact on surface antigen expression levels, we next analysed the effects of the different *N. caninum* isolates on MØ activation by assessing surface

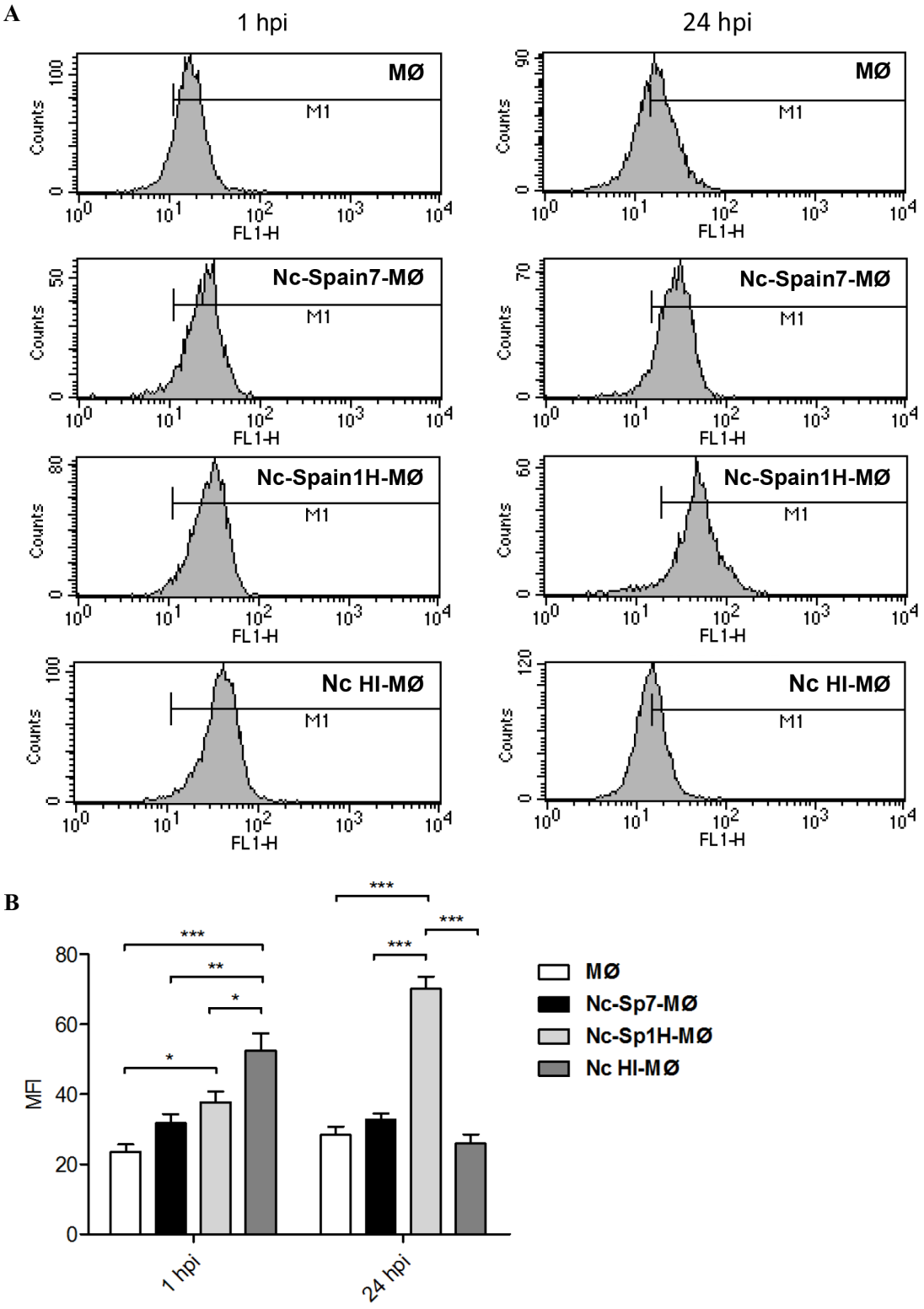

FIGURE 6 | ROS generation induced by *N. caninum* infection. (A) Representative histograms show the mean fluorescence intensity (MFI) determined by flow cytometry analysis of non-infected MØs (MØ), MØs challenged for 1 and 24 h with *N. caninum* Nc-Spain7 (Nc-Spain7-MØ), Nc-Spain1H (Nc-Spain1H-MØ), and heat-inactivated tachyzoites (Nc HI-MØ) stained with CellROX Green Reagent. (B) The bar graph show the comparison of the MFI between groups. Each column and error bar represents the mean and SD of three replicates from three independent experiments; Significant differences are indicated (*$p < 0.05$; **$p < 0.01$; ***$p < 0.001$).

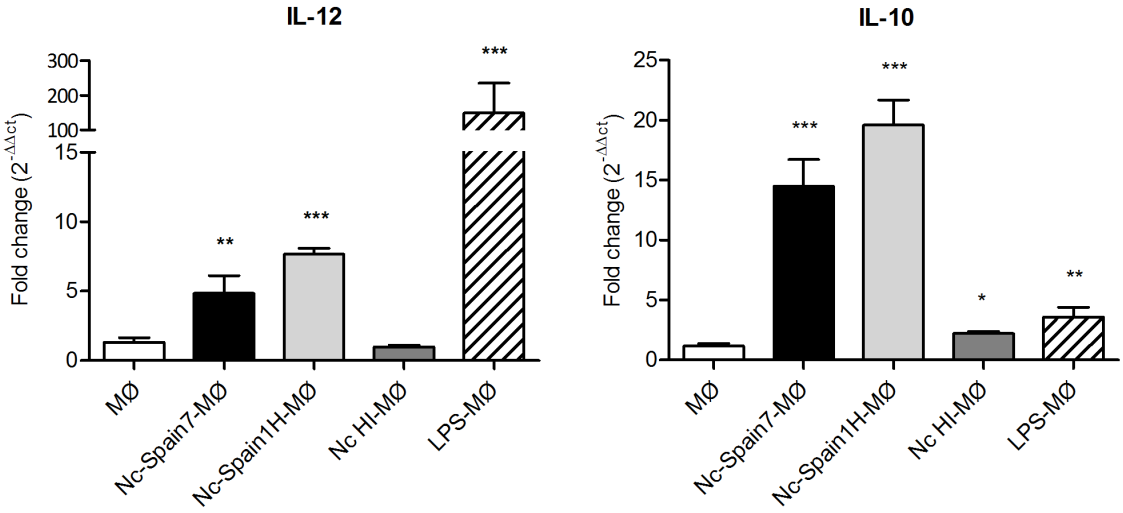

FIGURE 7 | Cytokine mRNA expression in bovine MØs infected with *N. caninum*. Graphs represent the relative quantification of IL-10 and IL-12p40 mRNA expression levels (x-fold change in expression) in MØs challenged for 8 h with *N. caninum* Nc-Spain7 (Nc-Spain7-MØ), Nc-Spain1H (Nc-Spain1H-MØ), heat-inactivated tachyzoites (Nc HI-MØ), and stimulated with 100 ng ml−1 LPS (LPS-MØ) in relation to non-infected MØs (MØ). Significant differences are indicated (*p < 0.05; **p < 0.01; ***p < 0.001).

antigen expression. Flow cytometry was used to quantify the expression of molecules involved in antigen presentation (CD1b, MHC Class II), T-cell activation and maturation (CD80, CD86), cell adhesion (CD11b) and phagocytosis (CD172a). As expected, MØ upregulated CD86 in response to LPS ($p < 0.05$). Infection of MØs with Nc-Spain7 or Nc-Spain1H resulted in a significant reduction in the percentage of MHC Class II ($p < 0.05$), CD86 ($p < 0.05$) and CD1b ($p < 0.0001$) expressing cells, whereas inoculation with HI tachyzoites resulted only in a significant reduction of MHC Class II ($p < 0.05$) and CD1b ($p < 0.0001$) (**Table 1**). The mean MFI of CD11b and CD1b diminished in MØs inoculated with Nc-Spain7, Nc-Spain1H and HI tachyzoites *versus* non-infected MØs ($P < 0.01$-0.001) (**Figure 8**). Significant differences between isolates were not found in the expression of any surface antigen studied.

3.8. Infection of bovine macrophages with the highly virulent isolate Nc-Spain7 resulted in diminished IFN-γ secretion by co-cultured autologous lymphocytes

As the previous data clearly indicated an isolate specific impact on the innate immune response created by boMØ to *N. caninum* isolates, we lastly assessed whether these differences would also affect the adaptive immune response. To do so, IFN-γ release by lymphocytes induced by *N. caninum*-infected MØs was assessed in the supernatant of co-cultures (**Figure 9**). As expected, the highest concentrations of IFN-γ were produced by lymphocytes when MØs were inoculated with LPS ($p < 0.0001$). MØs infected with Nc-Spain1H also stimulated IFN-γ production by lymphocytes, higher production than that by MØs infected with Nc-Spain7, at 48 hpi ($p < 0.05$) and 72 hpi ($p < 0.0001$). Exposure to Nc-Spain7 or HI tachyzoites did not result in significant IFN-γ variations compared with the negative control (co-culture of non-infected MØs and lymphocytes) at any time point. Samples of lymphocyte cultures reached average values of IFN-γ lower than 1000 pg ml^{-1}, and IFN-γ was not detected in MØ cultures without lymphocytes (MØs, MØs inoculated with Nc-Spain7, Nc-Spain1H, HI tachyzoites or LPS).

Altogether, our results showed that the IFN-γ response was impaired by Nc-Spain7 infection.

TABLE 1 | Immunophenotypic analysis by flow cytometry of bovine MØs exposed to *N. caninum*.

	CD14	MHC Class II	CD80	CD86	CD172a	CD11b	CD1b
Monocytes	95.95 ± 4.52	85.40 ± 12.86	85.05 ± 2.47	61.45 ± 8.38	98.55 ± 0.21	98.90 ± 0.42	90.95 ± 1.25
MØ	95.2 ± 2.14	27.02 ± 10.89	89.20 ± 1.60	59.48 ± 7.78	96.47 ± 2.91	94.58 ± 3.41	93.33 ± 4.39
Nc-Spain7-MØ	95.57 ± 3.14	11.66* ± 3.56	86.72 ± 5.13	47.40* ± 14.99	94.87 ± 4.22	96.47 ± 3.48	43.07* ± 13.44
Nc-Spain1H-MØ	95.17 ± 3.56	11.96* ± 2.61	85.32 ± 5.15	43.30* ± 13.60	94.05 ± 4.31	96.18 ± 3.60	31.42* ± 8.11
Nc HI-MØ	95.95 ± 2.48	13.35* ± 7.18	83.45 ± 3.41	54.46 ± 10.15	95.52 ± 3.19	97.07 ± 2.46	40.56* ± 6.32
LPS-MØ	95.18	21.01	90.05	70.81*	96.00	95.77	92.92

The results are expressed as the percentage of stained cells for each surface molecule in monocytes, non-infected MØs (MØ), and MØs challenged for 4 h with *N. caninum* Nc-Spain7 (Nc-Spain7-MØ) or Nc-Spain1H (Nc-Spain1H-MØ) isolates, heat-inactivated tachyzoites (Nc HI-MØ), and 100 ng ml-1 LPS (LPS-MØ). The data are presented as the mean values ± SD of three independent experiments. (*) Indicates significant differences in challenged MØs *vs.* non-infected cells ($p < 0.05$).

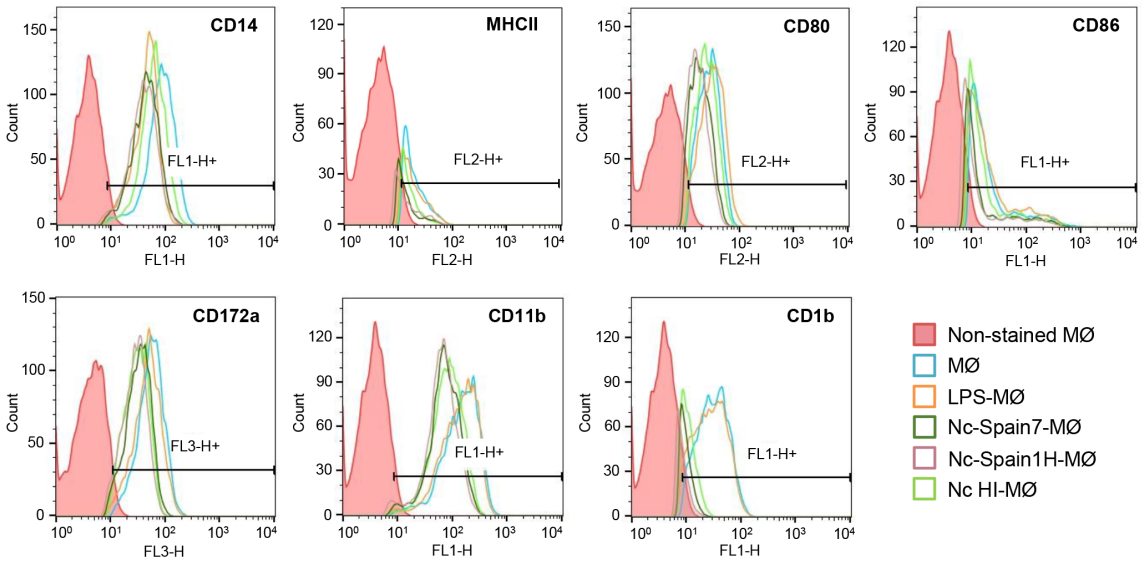

FIGURE 8 | Phenotypic characterization of bovine MØs inoculated with Nc-Spain7, Nc-Spain1H, and HI tachyzoites. Histograms represent the percentage of positive cells and mean fluorescence intensity (MFI) of CD14, MHC class II, CD80, CD86, CD172a, CD11b, and CD1b markers determined by flow cytometry in non-infected MØs (MØ) and MØs challenged for 4 h with *N. caninum* Nc-Spain7 (Nc-Spain7-MØ), Nc-Spain1H (Nc-Spain1H-MØ), heat-inactivated tachyzoites (Nc HI-MØ), and stimulated with 100 ng ml^{-1} LPS (LPS-MØ). Histograms are representative of three independent experiments.

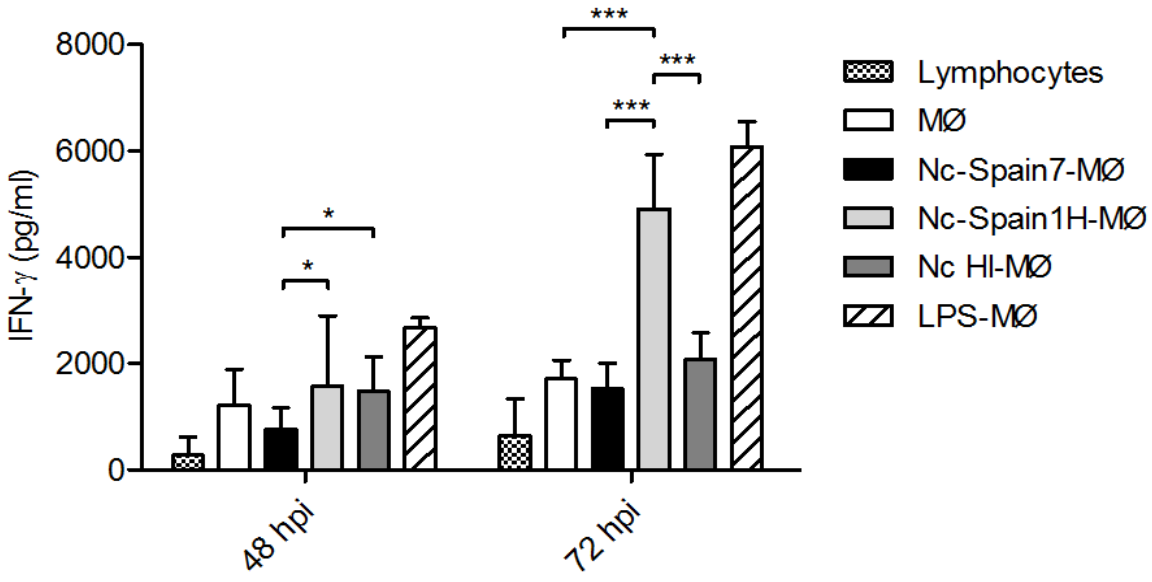

FIGURE 9 | IFN-gamma production by lymphocytes in co-culture with *N. caninum*-infected MØs. The graph represents the concentration of IFN-γ in supernatants obtained from lymphocytes in co-culture with non-infected MØs (MØ) or MØs challenged with *N. caninum* Nc-Spain7 (Nc-Spain7-MØ), Nc-Spain1H (Nc-Spain1H-MØ), heat-inactivated tachyzoites (Nc HI-MØ) or 100 ng ml^{-}1 LPS (LPS-MØ). Each column and error bar represents the mean and SD of three replicates from three independent experiments. Significant differences are indicated (*p < 0.05; ***p < 0.001). IFN-γ was not detected in samples without lymphocytes, and lymphocytes without macrophages (lymphocytes) reached average IFN-γ values lower than 1,000 pg ml^{-1}.

4. DISCUSSION

Neospora caninum virulence is likely determined by several factors, such as invasiveness, replication capability and the strength and characteristics of the induced immune response in the host. However, specific virulence factors for *N. caninum* in cattle have not yet been determined and the mechanisms used by the parasite to modulate bovine host cells during the early phase of infection are still poorly understood, supporting the need for new investigations. Recently, large-scale transcriptomic and proteomic studies carried out by our group in a bovine trophoblast cell model highlighted a very similar regulation pattern by Nc-Spain7 and Nc-Spain1H isolates, even though the low virulence isolate seems to exert a higher modulation of the host cell (Horcajo et al., 2017). Additionally, a different expression of genes involved in invasion, metabolic processes, cell cycle and stress response were described for Nc-Spain7 and Nc-Spain1H (Regidor-Cerrillo et al., 2012; Horcajo et al., 2017).

Studies in murine and human *in vitro* cellular models suggest that infection of antigen presenting cells (MØs and DCs) by *N. caninum* may have modulatory effects on cytokine secretion and lymphocyte activation (Dion et al., 2011; Strohbusch et al., 2012; Mota et al., 2016; Boucher et al., 2018). However, mice and humans are not natural hosts for *N. caninum*, so these models may not accurately reflect the dynamic of the host (bovine)–pathogen relationship. Thus, the ability of the parasite to initiate innate immune responses should be determined in the bovine host.

BoMØs can be used as an infection model for identification of strain-specific virulence properties or mechanisms to subvert immune response activation. Here, we studied for the first time the interaction between boMØs and two *N. caninum* isolates of different virulence (Regidor-Cerrillo et al., 2008; Rojo-Montejo et al., 2009a, 2009b).

The *N. caninum* lytic cycle in host cells comprises the processes of invasion, adaptation to intracellular conditions, proliferation, and egress from host cells. This sequence of events is required for parasite survival and propagation in the course of infection. The ability of *N. caninum* to infect, survive and replicate in boMØs was studied. A comparison of infection rates showed that both isolates were internalized into boMØs with a higher efficiency than described for other cell lines (Rojo-Montejo et al., 2009a; Regidor-Cerrillo et al., 2011; Jiménez-Pelayo et al., 2017). This fact can be due because MØs are phagocytic cells, which would enable tachyzoites to enter MØs by two complementary routes: uptake by MØs and active invasion by the parasite. In a recent study in human MØs, the internalization of *N. caninum* was found to likely occur via active invasion (Boucher et al., 2018). In our study both processes were involved in the internalization of *N. caninum* tachyzoites, with differences found between isolates in the percentages attributable to active invasion, similar to those determined in previous studies (Regidor-Cerrillo et al., 2011; Jiménez-Pelayo et al., 2017). Different receptors and signaling pathways could be implicated depending on how the parasite is internalized. These might facilitate replication of the parasite in the parasitophorous vacuoles when active invasion occurs or killing and degradation of the parasite if tachyzoites are internalized via endocytosis.

When parasite proliferation was monitored over time, *N. caninum* replication efficacy in boMØs was lower than in other types of cells previously assayed (Regidor-Cerrillo et al., 2011; Jiménez-Pelayo et al., 2017), suggesting the ability of MØs to limit the growth of the parasite. Furthermore, the efficient growth of Nc-Spain7 in boMØs, significantly higher than that of Nc-Spain1H, suggests the success of the highly virulent isolate in establishing an intracellular replicative niche in boMØs. The higher growth rate of Nc-Spain7 could be related to more efficient mechanisms to obtain energy and multiply intracellularly (Horcajo et al., 2017, 2018) and to the ability of the isolate to modulate the immune response, which would allow the parasite to survive and replicate more efficiently in MØs.

Another phenotypic trait putatively related to virulence is the capacity to modulate the migratory properties of parasitized immune cells, which may potentiate parasite dissemination in the host passage to immunoprivileged sites (i.e., brain, placenta) by crossing biological barriers, transmission or establishment of chronic infection. Previous studies have described the induction of a hypermigratory phenotype in *T. gondii*-infected murine and human MØs and DCs characterized by hypermotility (Fuks et al., 2012), enhanced transmigration across cellular barriers (Lambert et al., 2006; Kanatani et al., 2015) and extracellular matrix, and rapidly induced cytoskeletal changes post-invasion (Weidner et al., 2013). These processes are consistent with amoeboid migratory activation of the infected leukocyte (Ólafsson et al., 2018). In the present work, we report for the first time the induction of hypermigration by *N. caninum* in boMØs. Additionally, we describe the ability of *T. gondii* to induce hypermigration in boMØs, previously described in human and murine MØs (Lambert et al., 2011). Moreover, shortly after infection with *N. caninum*, boMØs exhibited dramatic morphological changes and abrogated pericellular proteolysis, all consistent with non-proteolytic amoeboid migratory activation in boMØs and in line with effects reported for *T. gondii* in murine and human DCs (Weidner et al., 2013; Ólafsson et al., 2018). In line with the above, podosome dissolution was observed in *Neospora*-infected boMØs. Podosomes are important cytoskeletetal structures linked to cell signaling, adhesion, matrix degradation, and therefore migration. The dissolution of podosomes upon infection by *N. caninum* implies fundamental mechanistic changes in how the parasitized cells interact with the surrounding microenvironment and migrate. Specifically, integrin-mediated adhesion and signaling and metalloproteinase activity is focalized and regulated in podosomes (Ólafsson et al., 2018, 2019). Because parasite-induced leukocyte hypermigration has been linked with

enhanced dissemination for *T. gondii* in mice (Lambert et al., 2006) and in a murine neosporosis infection model (Collantes-Fernández et al., 2012), this motivates further studies to address its putative impact in bovine *Neospora* infection. Additionally, how *N. caninum* molecularly orchestrates the migratory activation of parasitized boMØs and the identification of implicated parasite and host cell-mediated signaling, awaits further investigation. The elucidation of these processes may provide novel insights in how *N. caninum* evades immune responses while ensuring dissemination, and ought to be relevant for vaccination strategies in bovines.

Jointly, the data demonstrate that boMØs respond with a migratory phenotype upon infection with *N. caninum* and *T. gondii*. Contrary to *N. caninum*, *T. gondii* is not a prominent pathogen in bovines. However, the data are consistent with the existence of a conserved mechanism between *N. caninum* and *T. gondii* for migratory activation of infected leukocytes. Consequently, the utilization of a Trojan horse mechanism for systemic dissemination (Kanatani et al., 2017) may therefore be a conserved strategy for these two coccidian parasites (Collantes-Fernández et al., 2012). Despite that virulence traits are complex and can be host species-specific (Sánchez-Sánchez et al., 2018b), our findings also indicate that both virulent and non-virulent *N. caninum* isolates have the potential to use boMØs to disseminate and suggest that the virulent isolate Nc-Spain7 may have a superior capacity to induce migration of boMØs. However, further studies with a larger panel of isolates are necessary to determine if variations in the induction of hypermigration could be related to differences in transmission and dissemination found *in vivo* (Collantes-Fernández et al., 2012). Altogether, this highlights that (*i*) targeted survival in MØ/DCs constitute a replicative niche and that (*ii*) interference with migration of parasitized MØ/DCs are conserved features for the two coccidia, as shown with cells of bovine, murine and human origin. It also advocates for evolutionary conserved dissemination strategies by coccidia in vertebrates.

An efficient cell-mediated Th1 immune response is critical for restricting parasite replication (Innes and Mattson, 2007; Mineo et al., 2010). The expression of IL-12 by MØs stimulates lymphocytes to produce IFN-γ, which is important for restricting intracellular replication due to its role in activating MØ-mediated mechanisms that kill intracellular pathogens and T-cell proliferation (Hemphill et al., 2006). ROS generation is also an important mechanism in the control of *N. caninum* replication (Silva et al., 2017). Persistent intracellular parasites such as *T. gondii* or *Leishmania* are able to modulate mitochondrial and NADPH oxidase-induced ROS with the aim to maintain long-term carriage by avoiding their clearance (Shrestha et al., 2006; Spooner and Yilmaz, 2011; Moradin and Descoteaux, 2012). Mechanisms of modulation of intracellular ROS by infection of intracellular pathogens include interference of NADPH complex assembly; scavenging of ROS produced by NADPH oxidase and interference of mitochondrion-based ROS production during infection (Spooner and Yilmaz, 2011). In the present study, infection of boMØs with viable *N. caninum* tachyzoites repressed ROS and IFN-γ production at the early stages of infection, which would result in an inability to control the infection by the host. Moreover, our results also indicate that Nc-Spain7 shows a higher ability to evade the host immune response, since lower ROS and IFN-γ production, as well as lower IL-12p40 expression, was observed. In a previous work, we showed that the glucose-6-phosphate dehydrogenase (G6PD) was more abundantly expressed in Nc-Spain7 than Nc-Spain1H tachyzoites (Moradin and Descoteaux, 2012). This enzyme is indispensable to the maintenance of the cellular redox balance and detoxification of ROS by producing NADPH (Ho et al., 2007). The level of G6PD activity of the isolates may determine their sensitivity to oxidative stress and thus its ability to reduce ROS levels and facilitate the survival into MØs. Further studies are necessary to determine the role of *N. caninum* G6PD in bovine MØs.

In contrast, the less virulent isolate Nc-Spain1H elicits a stronger Th1 response initiated by boMØs, which would control parasite replication and dissemination in the host. In this sense, highly immunogenic cell surface proteins are differentially regulated between isolates, being more abundant on the Nc-Spain1H isolate (Horcajo et al., 2017, 2018), which may explain the stronger stimulation of the immune system. In previous studies we described that infection by the low virulence isolate Nc-Spain1H induced a higher expression of TLR-2, starting an inflammatory response in bovine trophoblast cells, which may be the cause of the lower proliferation of this isolate (Horcajo et al., 2017; Jiménez-Pelayo et al., 2017). TLR activation is crucial for initiating the innate immune responses responsible for the elimination of intracellular parasites such as *N. caninum*. The signaling pathway activated by TLR-2 leads to an increase in the transcription factors NF-κb and AP-1, which trigger the synthesis of pro-inflammatory cytokines (Liu et al., 2017). The implication of TLR-2 in *N. caninum* recognition has been also described in murine bone marrow derived MØs, activating proinflammatory signaling pathways which leads to production of Th-1 cytokines including IL-12 (Mineo et al., 2010; Li et al., 2018). In *T. gondii* infections, strain-specific differences in NF-κB signaling were observed in murine bone marrow-derived macrophages, with higher levels of NF-κB activation and IL-12 production induced by type II parasites (considered low virulent in mice) than type I strains (high virulent in mice) (Melo et al., 2011).

On the other hand, regulatory cytokines, such as IL-10, are required to limit the response against *N. caninum*, protecting the host from infection-associated immunopathology (Hemphill et al., 2006; Ma et al., 2015). High IL-10 expression levels by *N. caninum*-infected MØs were observed for both isolates (being higher for Nc-Spain1H) but not in MØs inoculated with HI tachyzoites, suggesting a modulatory role of live *Neospora* in the immune response generated during infection to guarantee host survival. As it has been suggested for *T. gondii*, succeeding in finding a balance between pro- and anti-inflammatory responses may be a possible strategy to establish a chronic infection, promoting survival of both parasite and host (Jensen et al., 2011). Thus, the higher levels of IL-12 induced by the low virulent isolate may justify its higher expression levels of IL-10 in an isolate that is able to transmit without causing pathology (Rojo-Montejo et al., 2009b).

Modulation of cell surface proteins was also induced by *N. caninum* infection. Diminished MHC Class II, CD1b and CD86 presentation was observed on the surface of infected MØs at 4 hpi, which could be related to parasite immune evasion strategies. The reduction in MHC Class II has also been observed in *T. gondii*-infected murine MØs (Luder et al., 1998; Leroux et al., 2015), where the interference with the antigen presentation pathway has been indicated as an important strategy for intracellular survival of the parasite. A similar strategy may be assumed for *N. caninum*, supported by the fact that up-regulation of MHC class II on *N. caninum* murine MØs has been associated with host survival (Nishikawa et al., 2001). In addition, lower CD1b expression has been correlated with a reduced induction of specific T-lymphocyte proliferation (Balboa et al., 2010). The decrease in CD86 observed in MØs inoculated with live but not HI tachyzoites could suggest a modulation induced by components secreted by actively replicating parasites. CD86 is a co-stimulatory signal for activation of lymphocytes (Subauste et al., 1998). A reduction in CD86 expression has also been observed in *Leishmania*-infected MØs (Denkers and Butcher, 2005) and in murine peritoneal MØs exposed to *N. caninum* (Dion et al., 2011). These data could indicate that *N. caninum* would interfere with intracellular signaling to selectively reduce antigen presentation and the expression of ligands related to T-cell activation, a mechanism to escape the host immune response. In the current study, no major differences in the expression of the different surface markers between isolates were observed at 4 hpi, being

necessary more studies at different time points. Moreover, the functional consequences of the infection by different parasite isolates in boMØs should be investigated in future studies.

In summary, the results of the present study indicate that the highly virulent isolate Nc-Spain7 shows a higher ability to evade the host immune response via a reduction in ROS and IFN-γ secretion, which could be attributable to a lower IL-12 expression. The consequence would be lower control of intracellular parasite survival, which in conjunction with its higher replication and transmigration capacity may be associated with the higher virulence and pathology found *in vivo*. On the other hand, Nc-Spain1H elicits a strong Th1 response (which would reduce the parasite load in host cells) and that would be counterbalanced by a higher expression of regulatory cytokines (IL-10), minimizing pathology. This strategy may suggest a better adaptation of the low virulence isolate Nc-Spain1H to be transmitted without causing clinical disease, maintaining a delicate balance between suppression and induction of the host immune response to ensure host survival and chronic infection. Our results also suggest that boMØs may serve as a vehicle for *N. caninum* dissemination throughout the organism to find the optimal host cells for replication (e.g., epithelial cells in the placenta) and as a niche for parasite long-term survival.

Understanding how *N. caninum* manipulates inhibitory signaling affords promising opportunities to counteract the parasite escape strategies and tip the balance in favor of the host. Further in-depth studies are needed to study the specific pathways modulated by *N. caninum* and to examine the differences between high and low virulence isolates that may explain the differences observed in their biological behavior. Proteomic approaches based on the study of differential protein determinants between Nc-Spain7 and Nc-Spain1H may help explain differences in the strength and character of the immune response induced by the isolates. In addition, experimental *in vivo* infections in cattle are necessary to determine if the results obtained in our *in vitro* study correspond with an expected enhanced early protective response to infection induced for the less virulent isolate Nc-Spain1H.

SUPPLEMENTARY FILES

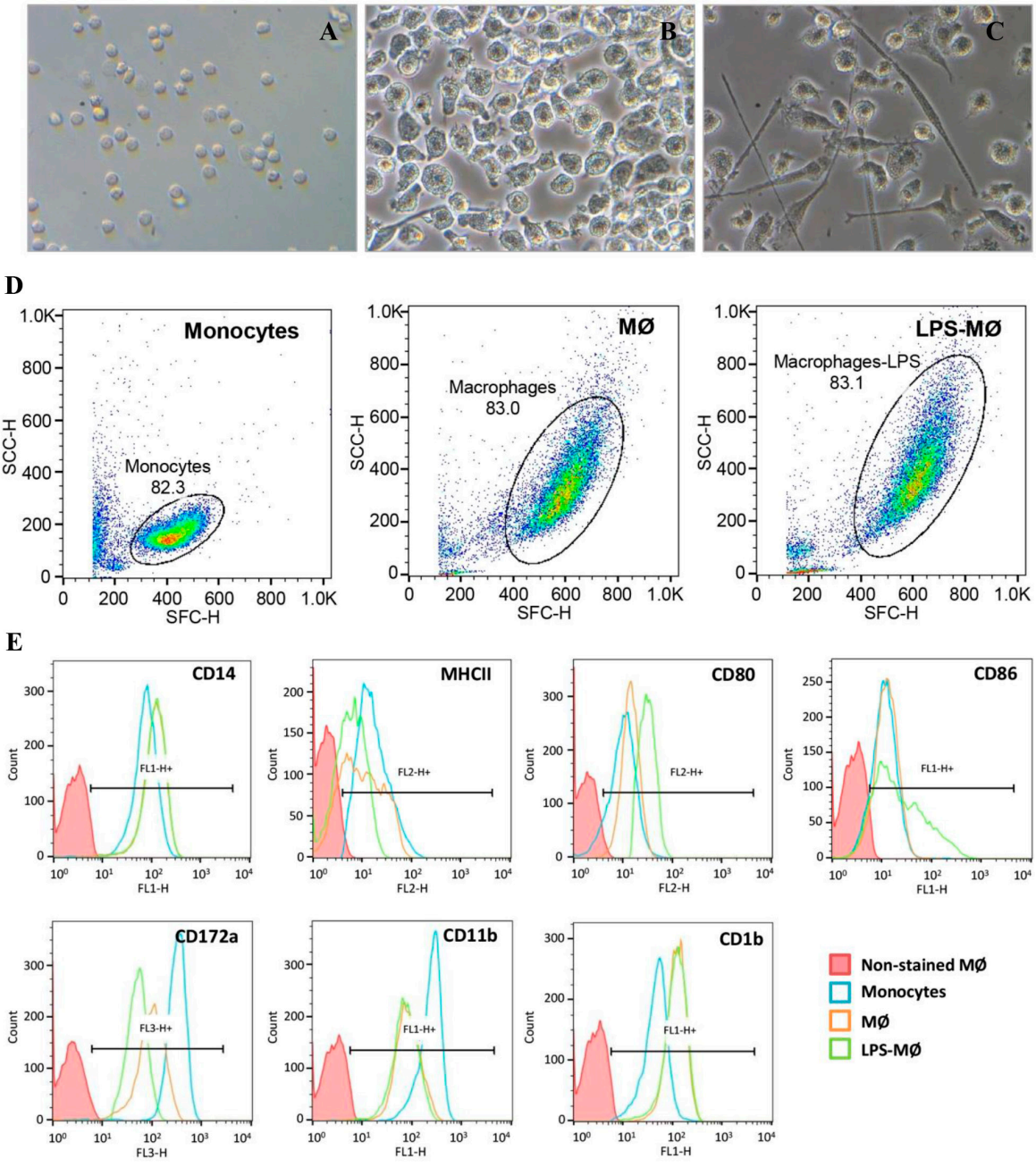

SUPPLEMENTARY FIGURE 1 | Characterization of bovine monocyte-derived macrophages. (A) Representative micrographs of monocytes (day 0 of culture), **(B)** macrophages (MØ, day 5 of culture with GM-CSF) and **(C)** MØ challenged for 4 hours with 100 ng/ml LPS (LPS-MØ). **(D)** Dot plots present the shape, size and internal complexity, determined by flow cytometry, of monocytes, MØ and LPS-MØ. **(E)** Histograms present the percentage of positive cells and the mean fluorescence intensity (MFI) of CD14, MHC class II, CD80, CD86, CD172a, CD11b and CD1b markers determined by flow cytometry in monocytes, MØ and LPS-MØ.

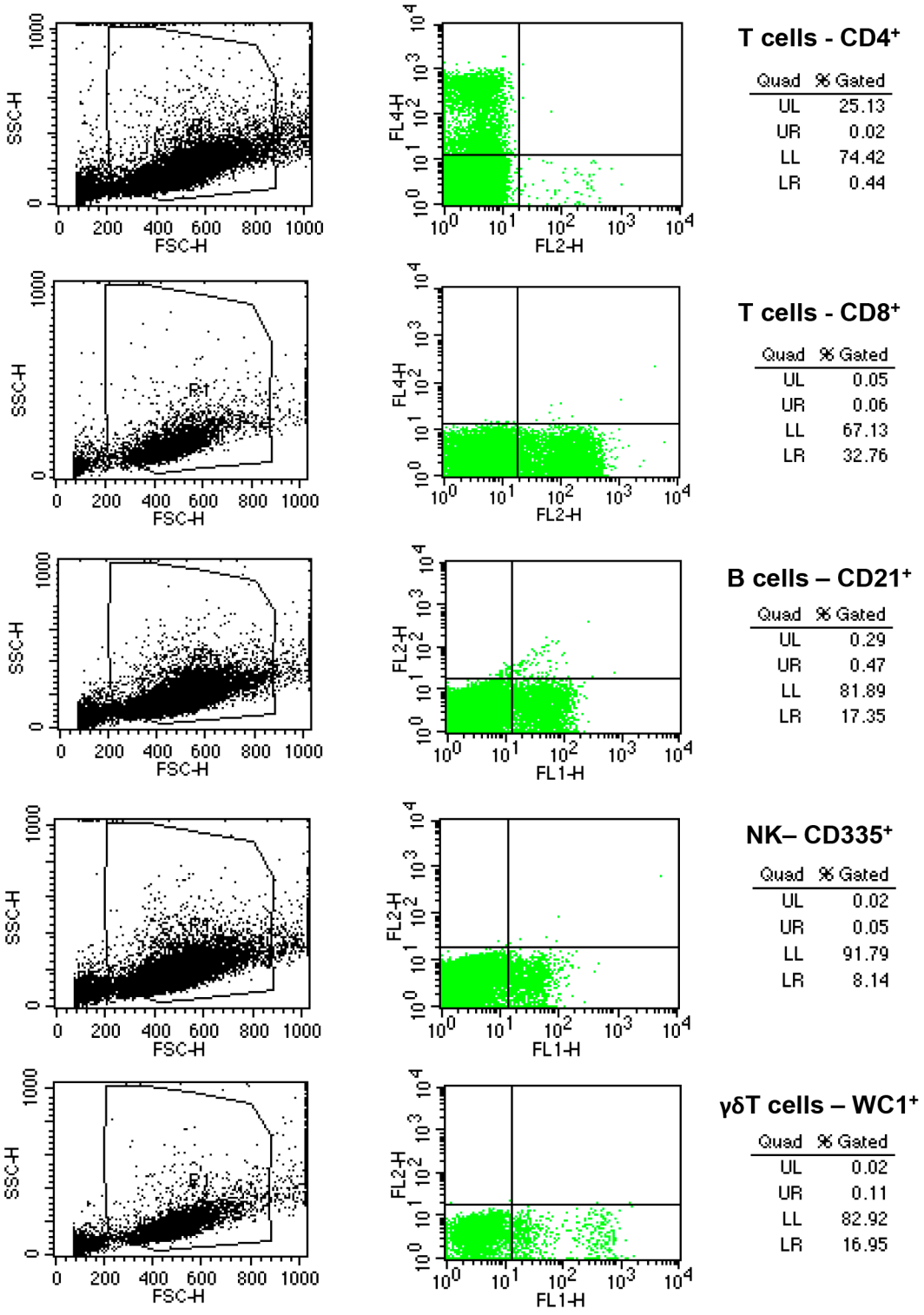

SUPPLEMENTARY FIGURE 2 | Characterization of bovine lymphocytes. The cytometry profile shows de percentage of CD4 T cells (CD4$^+$), CD8 T cells (CD8$^+$), B cells (CD21$^+$) Natural Killer (NK, CD335$^+$) and γδ T cells (WC1$^+$) in a cell population obtained from bovine peripheral blood mononuclear cells, after magnetic isolation of monocytes.

SUPPLEMENTARY TABLE 1 | List of antibodies used for immunophenotypic analysis of bovine monocyte-derived macrophages and characterization of lymphocytes.

Antibody	Conjugate	Supplier	Species	Type	Clone	Reference
CD14	FITC	Bio-Rad Laboratories (Pleasanton, USA)	Mouse anti-bovine	Monoclonal	CC-G33	MCA2678F
MHC Class II	RPE				CC108	MCA5656PE
CD80	RPE				IL-A159	MCA2436PE
CD86	FITC				IL-A190	MCA2437F
CD172a	RPE-Cy5				CC149	MCA2041C
CD11b	FITC				CC126	MCA1425F
CD1b	Alexa Fluor 488	Novus Biologicals (Littleton, USA)			CC20	NB100-65315AF488
CD4	Alexa Fluor 647	Bio-Rad Laboratories (Pleasanton, USA)			CC8	MCA1653A647
CD8	RPE				CC63	MCA837PE
CD335	Alexa Fluor 488				AKS1	MCA2365A488
WC1	FITC				CC15	MCA838F
CD21	FITC		Mouse anti-human		LB21	MCA1195F

V

OBJECTIVE II

OBJETIVO II

OBJETIVO II | Estudio transcriptómico de la modulación de macrófagos bovinos derivados de monocitos por aislados de *Neospora caninum* de distinta virulencia.

La capacidad de *N. caninum* para modular las células de la respuesta inmunitaria innata durante la infección temprana podría ser clave para el establecimiento de la infección en el bovino. En el objetivo 1 de la presente tesis doctoral se ha demostrado que *N. caninum* es capaz de sobrevivir multiplicarse en el interior de macrófagos bovinos, modular sus mecanismos microbicidas con el fin de evitar su eliminación y explotar su motilidad para diseminarse. Además, los mecanismos de modulación de la respuesta inmunitaria celular parecen ser dependientes de la virulencia de los aislados.

En el presente objetivo se investigó el perfil transcriptómico de macrófagos bovinos derivados de monocitos infectados con aislados de alta virulencia (Nc-Spain7) o baja virulencia (Nc-Spain1H) de *N. caninum* con el fin de determinar las bases moleculares del reconocimiento del parásito y la subsiguiente respuesta del macrófago frente a la infección. Posteriormente se investigó el perfil transcripcional de Nc-Spain7 y Nc-Spain1H en macrófagos bovinos, para correlacionar las diferencias de expresión génica entre aislados con su diferente comportamiento *in vitro* y determinar potenciales efectores del parásito implicados en la modulación de la célula hospedadora.

En relación a la respuesta celular a la infección, el enriquecimiento funcional reveló la sobreexpresión de genes implicados en señalización por quimioquinas, inflamación y supervivencia celular, así como la inhibición de genes relacionados con la maduración del fagolisosoma y el metabolismo. La activación del macrófago se caracterizó por la inducción de un fenotipo predominantemente M1 (proinflamatorio) con sobreexpresión de TLR (TLR2, TLR3 y TLR9) y NLR (NAIP, NOD2, NLRC4 y NLRP12) y activación de la ruta de señalización NF-ĸB. La inoculación de taquizoítos de *N. caninum* inactivados por calor no fue capaz de activar la ruta NF-ĸB y de inhibir la actividad de los lisosomas y la apoptosis celular, lo cual es indicativo de la existencia de una modulación activa por parte del parásito. Las rutas de señalización celular FoxO, diferenciación Th1-Th2, degradación de glicosaminoglicanos y apoptosis aparecieron enriquecidas exclusivamente por la infección por Nc-Spain1H. Además, la infección por dicho aislado indujo una sobreexpresión de citoquinas proinflamatorias IL12A e IL8, mientras que la expresión de IL23 se vio infraexpresada con la infección por Nc-Spain7.

Respecto al estudio transcriptómico de los aislados de *N. caninum* en macrófagos bovinos, los resultados obtenidos demostraron que las diferencias fenotípicas observadas *in vitro* y descritas en el objetivo 1 se correlacionan con perfiles específicos de expresión génica. Más concretamente, el aislado de baja virulencia Nc-Spain1H mostró un incremento en la expresión de genes que codifican antígenos de superficie y genes relacionados con la fase de bradizoíto. Entre los genes sobreexpresados en Nc-Spain7, aquellos involucrados en el crecimiento del parásito y la homeostasis redox son particularmente importantes, porque se podrían correlacionar con la mayor proliferación de Nc-Spain7 observada en macrófagos bovinos en relación con Nc-Spain1H. La sobreexpresión de genes que codifican antígenos de superficie altamente inmunógenos SRS en el aislado de baja virulencia podría estar involucrada en la su mayor inducción de respuestas proinflamatorias en el macrófago. Por el contrario el aislado de alta virulencia mostró un aumento en la expresión de proteofosfoglicanos y de genes relacionados con la síntesis de glicosilfosfatidilinositol, ambos potencialmente involucrados en la evasión de la respuesta inmunitaria.

En conjunto, estos resultados indican que Nc-Spain7 podría ser capaz de limitar la respuesta proinflamatoria del macrófago, lo que sumado a su mayor capacidad de proliferación podría explicar al menos en parte la mayor tasa de transmisión y aborto inducida *in vivo* por este aislado. Por el contrario Nc-Spain1H induce una respuesta proinflamatoria que limitaría la multiplicación del parásito, lo que explicaría la infección limitada de tejidos placentarios sin transmisión fetal durante la infección temprana observada en el modelo bovino gestante.

OBJECTIVE 2 | Transcriptome modulation of bovine monocyte-derived macrophages by *Neospora caninum* isolates of different virulence

SUB-OBJECTIVE 2.1 | Gene expression profiling of bovine macrophages infected with high and low virulence *Neospora caninum* isolates.

SUMMARY |

Neospora caninum is an obligate intracellular parasite, and its ability to survive inside host immune cells may be a key mechanism for the establishment of infection in cattle. *In vitro* studies carried out by our group have shown that *N. caninum* is able to replicate in bovine macrophages (MØs), alter their microbicidal mechanisms and exploit their motility. Furthermore, host-cell subversion seems to be isolate virulence-dependent. Herein, the transcriptome profile of bovine monocyte-derived MØs infected with high (Nc-Spain7) or low (Nc-Spain1H) virulence *N. caninum* isolates was investigated. Functional enrichment revealed up-regulation of genes involved in chemokine signalling, inflammation, cell survival, and inhibition of genes related with metabolism and lysosome. MØs activation was characterized by the induction of a predominantly M1 phenotype with expression of TLR2, TLR3 and TLR9 and activation of the NF-ĸB signalling pathway. Heat-killed *N. caninum* tachyzoites failed to activate NF-ĸB, and to inhibit lysosomal activity and apoptosis, which indicates active modulation by the parasite. The FoxO signalling pathway, Th1-Th2 differentiation, glycosaminoglycan degradation and apoptosis were pathways enriched only for Nc-Spain1H infection. In addition, Nc-Spain1H infection upregulated the IL12A and IL8 proinflammatory cytokines, whereas IL23 was downregulated by Nc-Spain7. These results indicate that Nc-Spain7 may be able to partially circumvent the pro-inflammatory response whereas Nc-Spain1H induces a protective response to infection, which may explain the more efficient transmission of the high virulence isolate observed *in vivo*.

1. BACKGROUND

Neospora caninum is an apicomplexan parasite that is phylogenetically related to *Toxoplasma gondii* and is responsible for major economic losses due to reproductive failure in cattle (Dubey et al., 2007). Macrophages (MØs) are key effectors in the innate immune system and play a major role in early host resistance to *N. caninum* infection (Abe et al., 2014). MØs are able to detect pathogens by means of pattern recognition receptors (PRR), resulting in phagocytosis and elimination of the pathogen by nitrogen intermediates, reactive oxygen species (ROS) and lysosomal enzymes. These cells also link the innate and the adaptive response by the release of cytokines and chemokines and by their ability to present antigens to naïve T-cells (Stafford et al., 2002; Hume, 2008).

Studies in murine MØs have identified the TLR2-MAPK, TLR3-TRIF, and TLR11-MEK/ERK pathways and NLRP3-inflammasome activation as signalling pathways implicated in host resistance against *N. caninum,* that trigger the production of pro-inflammatory cytokines (Jin et al., 2017; Li et al., 2018; Wang et al., 2018; Miranda et al., 2019). Several works have demonstrated that *N. caninum* has evolved mechanisms to evade the immune response mounted by murine MØs. Enhanced expression of C-type lectin receptor Dectin-1 has been related to the downregulation of ROS (Silva et al., 2017), p38 MAPK-dependent GPCR/PI3K/AKT pathway activation with the downregulation of IL-12 production (Mota et al., 2016), and upregulation of PPARG receptor and inhibition of NF-κB activation with the polarization of MØs from a M1 (pro-inflammatory) to a M2 (anti-inflammatory) phenotype (He et al., 2017). In human MØs, MEK 1/2-mediated expression of cathelicidins has been proposed as a mechanism of defence against *N. caninum* infection (Boucher et al., 2018). Although these studies provide important advancements towards the understanding of the *N. caninum*-MØ interaction, it is important to consider that mice and humans are not natural hosts for *N. caninum* and that essential differences exist regarding the immune response in cattle (its natural host). These include the lack of TLR11 and TLR12 in the genomes of cattle, which are by contrast present in mice, or the limited (65–77% in average) nucleotide homology to human TLR genes (Jungi et al., 2011). Thus, the ability of *N. caninum* to modulate innate immune responses should be determined in bovine MØs.

Recent *in vitro* studies carried out by our group have shown the capacity of *Neospora* to survive and grow in bovine monocyte-derived MØs by circumventing lysosomal degradation and, for the first time, have shown isolate-dependent differences regarding parasite behaviour in this host cell and the cellular response to infection. Nc-Spain7, a high virulence isolate in cattle, exhibited higher capacities to invade, survive and replicate in bovine MØs than the low virulence Nc-Spain1H. Moreover, Nc-Spain7 infection induced lower ROS production, IL10 and IL12B expression by MØs than Nc-Spain1H infection, which also resulted in decreased IFN-γ release by activated lymphocytes (García-Sánchez et al., 2019). These results suggest that *N. caninum* is able to modulate host defences in order to survive and be transmitted in a virulence-dependent manner, and differences in pathogenesis between isolates may be highly related to their ability to induce or subvert protective immune responses in the host.

Transcriptome analysis has been demonstrated to be a suitable approach for studying *N. caninum* host-parasite interactions in target cells (Horcajo et al., 2017). To investigate the molecular basis underlying the innate responses in MØs against *N. caninum* and the mechanisms of parasite manipulation of the host cell environment, we studied the transcriptional profile of bovine monocyte-derived MØs infected with high (Nc-Spain7) and low- (Nc-Spain1H) virulence *N. caninum* isolates, revealing the main processes involved in MØ activation and modulation.

2. MATERIAL AND METHODS

2.1. Ethical statements

Handling of cows and blood sampling were conducted in accordance with Spanish and EU legislation (Law 32/2007, concerning animals, their exploitation, transportation, experimentation and sacrifice; Royal Decree 53/2013 for the protection of animals employed in research and teaching; Directive 2010/63/UE, related to the protection of animals used for scientific goals). Protocols were approved by the Animal Welfare Committee of the Community of Madrid, Spain (permit number PROEX 236/17).

2.2. Bovine monocyte isolation and *in vitro* macrophage differentiation

Monocyte-derived MØs were obtained from peripheral blood from a healthy adult Holstein dairy cow that tested negative for infectious bovine rhinotracheitis virus (IBRV), bovine viral diarrhoea virus (BVDV) and *N. caninum*, following the protocol previously described by García-Sánchez et al. (2019). Briefly, peripheral blood mononuclear cells (PBMCs) were separated by density gradient with Histopaque 1077 (Sigma-Aldrich, USA) and monocytes were isolated using microbeads conjugated to mouse anti-human CD14 antibodies (Miltenyi Biotec Ltd., USA). Monocytes were seeded in six-well culture plates at a density of 3×10^6 cells/well and incubated with 100 ng/ml recombinant bovine GM-CSF (Kingfisher Biotech Inc, USA) at 37ºC and 5% CO2 for 5 days. After five days of culture, morphological and functional characteristics compatible with MØs (García-Sánchez et al., 2019) were checked. Cells were harvested, re-seeded at 3 x 106 cells/well in six-well culture plates, and incubated for 24 hours prior to infection.

2.3. Parasite culture and macrophage infection

N*eospora caninum* Nc-Spain7 and Nc-Spain1H isolates were routinely maintained in an MA-104 cell line culture as described previously (Regidor-Cerrillo et al., 2008), keeping in the parasites at a low number of culture passages (<15) to minimize potential changes in virulence (Pérez-Zaballos et al., 2005). Tachyzoites used for MØ infection were collected from three day-growth cultures, when at least 80% of the parasites were still intracellular, and purified with PD-10 Desalting Columns (G.E. Healthcare, UK) as described previously (Regidor-Cerrillo et al., 2011). Cells were inoculated before one hour of parasite harvest to minimize loss of viability. A multiplicity of infection (MOI) of three was selected for the inoculation of macrophages with each isolate, to obtain the highest number of infected cells (50-60%) while maintaining cell integrity as described previously (García-Sánchez et al., 2019). The absence of differences in the percentage of infected cells between groups was confirmed by infecting 3×10^5 cells seeded on coverslips in parallel and under the same conditions and determining the infection rate following the protocol described previously (García-Sánchez et al., 2019). MØs were also inoculated with the same MOI of three with heat-killed (HK) *N. caninum* parasites to study the cell response against *N. caninum* antigens *versus* live tachyzoite infection. Equal quantities of Nc-Spain7 and Nc-Spain1H tachyzoites were mixed and were killed by incubation at 56 ºC for 30 min. Loss of viability was checked by trypan blue exclusion prior to culture inoculation and by reverse transcription PCR at 1 week post-infection as previously described (García-Sánchez et al., 2019). Non-infected MØs were included as control samples.

At eight hours post infection (hpi), cells were recovered by cell scraping and centrifuged at 1,350 g for 10 min at 4º C. The resulting pellet was resuspended in 300 μl of RNA later (Thermo Fisher Scientific, Spain) and stored at -80ºC until RNA extraction. All analyses were performed with three biological replicates obtained from three independent experiments. Each replicate was obtained from three wells ($9x10^6$ MØs) inoculated for each condition (Nc-Spain7, Nc-Spain1H, HK and non-infected).

2.4. RNA extraction and RNA-seq

Total RNA was extracted using the Maxwell 16 LEV simply RNA Purification Kit (Promega, USA), following the manufacturer's instructions. RNA integrity was determined by electrophoresis on a 1% agarose gel stained with GelRed (Biotium, USA) and visualized under UV light. The quality and quantity of the total RNA obtained was determined in Bioanalyzer 2100 (Agilent, USA) and a Qubit 2.0 (Thermo Fisher Scientific, Spain).

Twelve samples were sequenced individually by RNA-seq, which consisted of three biological replicates from each of the following samples: MØs inoculated with Nc-Spain7 (MØ7), Nc-Spain1H (MØ1H), HK tachyzoites (MØHK) and non-infected MØs (MØC). The Poly(A) + mRNA fraction was isolated from total RNA, and cDNA libraries were obtained following Illumina´s recommendations. Briefly, poly(A)+ RNA was isolated on poly-T oligo-attached magnetic beads and chemically fragmented prior to reverse transcription and cDNA generation. The cDNA fragments were then subjected to a repair process, addition of a single 'A' base to the 3' end and ligation of the adapters. Products were purified and enriched by PCR to create the final indexed double stranded cDNA library. The quantity of the libraries was determined by real-time PCR in LightCycler 480 (Roche, Germany), and their quality was analysed in Bioanalyzer 2100, High Sensitivity assay. Prior to cluster generation in cBot (Illumina, USA), equimolar pooling of the libraries was performed. The cDNA library pool was sequenced by paired-end sequencing (100 × 2) in an Illumina HiSeq 2000 sequencer (Illumina, USA).

2.5. Computational analysis of RNA-seq data

Data quality assessment was performed using the FastQC tool (http://www.bioinformatics.babraham.ac.uk/projects/fastqc). The raw paired-end reads were mapped against the *Bos taurus* genome version UDM3.1 (NCBI:GCA_000003055.3) obtained by the ENSEMBL/NCBI database (http://www.ensembl.org/), using the TopHat2 v2.1.0 algorithm (Kim et al., 2013). Low-quality reads were eliminated by the use of Picard Tools (http://picard.sourceforge.net) and selected high quality reads were assembled and identified through the recommended algorithm in Cufflinks v2.2.1 (Trapnell et al., 2010). The gene quantification process was carried out by the htseq_count 0.6.1p1 tool (Anders et al., 2015). The Cufflinks method (Trapnell et al., 2010) was used for the quantification and determination of differential expression of the isoforms.

2.6. Differential expression determination, functional enrichment analysis and network analysis

The correlation between samples of the same condition was determined in the statistical software R (http://www.r-project.org) and the whole transcriptome normalized by the size of the library was considered to accept the samples as biological replicates.

The differential expression between sample groups was studied by the recommended DESeq2 algorithm Anders and Huber, 2010) using a binomial negative distribution for the determination of the statistical significance (Love et al., 2014). Genes and isoforms with a fold change (FC) ≥ 1.5 and an FDR-adjusted (Benjamini and Hochberg, 1995) p-value (p adj) ≤ 0.05 were considered differentially expressed (DE).

For functional enrichment, a hypergeometric test was employed using the human orthologue obtained from *B. taurus* annotation. Categories with a p adj ≤ 0.05 for each condition were selected. The lists of generated Gene Ontology (GO) terms were summarized in clusters by removing redundant GO terms using the REVIGO tool (Supek et al., 2011). The Database for Annotation, Visualization and Integrated Discovery (DAVID) (Huang et al., 2009) was used to investigate the functional annotation or biological meaning of specific genes of interest. KEGG maps were generated using the Pathview R package (Luo and Brouwer, 2013).

2.7. Transcriptomic validation by RT-qPCR

Three additional biological replicates for each condition obtained from three independent experiments were collected and prepared as described for RNA-seq analysis. cDNA was reverse transcribed from extracted RNA using the master mix SuperScript VILO cDNA Synthesis Kit (Invitrogen, UK). The expression of selected genes of interest was measured by quantitative real-time PCR (qPCR) using four serial dilutions of each sample (1:20, 1:80, 1:320 and 1:1280) and normalized to the housekeeping gene beta actin (ACTB, ENSBTAG00000026199) and Glyceraldehyde-3-phosphate dehydrogenase (GAPDH, ENSBTAG00000014731). Relative gene expression of MØ7, MØ1H and MØHK was calculated by comparing with the expression in MØC using the 2-ΔΔCt method (Livak and Schmittgen, 2001). Reactions were performed in a 7500 Fast Real-Time PCR System (Applied Biosystems, USA) using Power SYBR PCR Master Mix (Applied Biosystems). Primers are listed in **Supplementary Table 1**.

2.8. Immunofluorescence analysis of NF-ĸB p65 nuclear translocation

The induction of NF-ĸB activation by *N. caninum* infection was investigated by analysing the nuclear translocation of the NF-ĸB p65 transcription factor. MØs were seeded on poly-L-lysine-coated coverslips (Sigma Aldrich, USA) at a density of 3 × 105 cells/coverslip and inoculated with Nc-Spain7, Nc-Spain1H or HK tachyzoites at an MOI of three. Non-infected MØs were used as a negative control. Cultures were fixed at eight hpi with 0.05% glutaraldehyde and 3% paraformaldehyde, permeabilized with 0.25% Triton X-100 for 20 minutes at 37ºC, and blocked with 3% bovine serum albumin (BSA, Roche, Germany) for one hour at room temperature (RT). Cells were labeled with NF-kB p65 rabbit polyclonal antibody (Sigma Aldrich, USA) at 2 μg/ml in 1% BSA for three hours. Then, Alexa Fluor 488-conjugated goat anti-rabbit IgG (Thermo Fisher Scientific, USA) was used as a secondary antibody at a dilution of 1:400 for 30 minutes at RT. Parasites were stained using hyperimmune mouse antiserum directed against *N. caninum* tachyzoites (1:200) as the primary antibody (Álvarez-García et al., 2007) for one hour and goat anti-rabbit IgG conjugated to Alexa Fluor 594-conjugated goat anti-mouse IgG (Thermo Fisher Scientific, USA) as the secondary antibody for 30 minutes at RT. The nuclei were stained by washing the cells with DAPI (Thermo Fisher Scientific, USA) at 1:5000 in PBS, and the coverslips were embedded in Fluoroprep (BioMerieux, France). Images were taken using an inverted fluorescence microscope Nikon Eclipse TE 200 and a Nikon DSL1 camera (Nikon, Japan) and were overlaid using Photoshop software (Adobe Systems Incorporated, USA).

3. RESULTS AND DISCUSSION

3.1. Sequencing and mapping of RNA-seq data

Nearly 600 million reads were produced, and between 36 and 59 million were obtained from each sample. Between 80-100% of reads were mapped against the reference *B. taurus* genome. Data quality control analysis of duplication studies indicated the lack of degradation of the starting biological material as well as the absence of significant deviations in the sequencing process. In addition, distribution analysis of normalized data showed a correct distribution of biological replicates with no outlier samples. **Supplementary Table 2** shows the information obtained for each sample in the sequencing process, namely, the number of total reads, mapped reads and splice reads (related to the capability of the system to detect isoforms and splicing events). Normal high values (80-100%) were observed in the percentage of mapped reads, similar to those reported in transcriptomic analysis of bovine MØs infected with other pathogens of cattle (Jensen et al., 2018).

Quantitative real-time PCR was used to validate the RNA-Seq results. The expression of 15 selected genes was measured in three new biological replicates of each condition, and the FCs in inoculated MØs in relation to non-infected cells were calculated and compared with those obtained by RNA-Seq. All genes showed similar expression profiles for both techniques and similar FCs for the two housekeeping genes used for validation (**Supplementary Figure 1)**.

3.2. Differential expression analysis of *B. taurus* genes displays different interactions between live and heat-killed *Neospora caninum* with bovine macrophages

A differential expression analysis was performed between *N. caninum*-inoculated MØs (MØ1H, MØ7, MØHK) and MØC. A total of 3,127 DEGs were identified in the MØ1H-MØC comparison, of which 1,538 were upregulated and 1,589 were downregulated in MØ1H. A total of 2,565 DEGs were found in MØ7-MØC comparison, with 1292 upregulated and 1273 downregulated in MØ7**.** Finally, 1496 DEGs were found in MØHK-MØC comparison, with 720 upregulated and 776 downregulated in MØHK.

A Venn diagram was generated to illustrate similarities and differences in the DEGs between the three groups of inoculated MØs and MØC. A common repertoire of genes was regulated under the three conditions, although a bigger number of DEGs was observed with live infection (MØ1H and MØ7), and especially with the MØ1H (**Figure 1**). These variances provide clues for differences in MØ modulation by live and dead parasites and, moreover, by isolates implicated on infection that may help to explain the differences in the virulence observed in cattle (Jiménez-Pelayo et al., 2019b).

To investigate the differential transcriptional response in bovine MØ1H, MØ7 and MØHK, the Gene Ontology (GO) analysis related the Biological Process (BP) domain was carried out for each condition (**Supplementary Table 3**). Enrichment analysis of the DEGs resulted in 54 GO terms grouped in 23 clusters for the MØ1H-MØC comparison, 52 GO terms in 25 clusters for the MØ7-MØC comparison, and 42 GO terms in 18 clusters for the MØHK-MØC comparison (**Supplementary Table 4**). The most representative clusters with GO terms related to the immune response, cell adhesion, cell survival and metabolism are shown in **Figure 2**. As expected, a higher representation was observed in inoculations with live tachyzoites than with

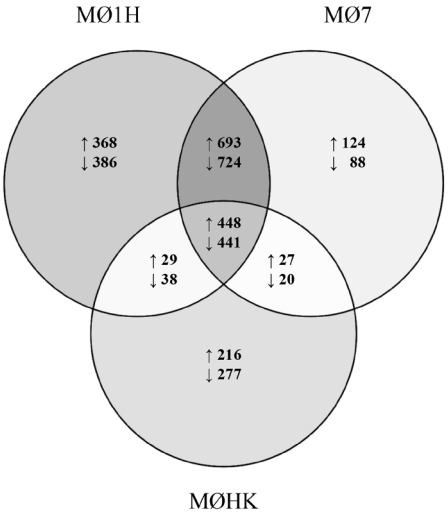

FIGURE 1 | Venn diagram representing DEG between the three groups of *N. caninum* inoculated macrophages versus non-infected cells. The diagram shows the number of unique and shared DEG (up- and downregulated) in bovine macrophages infected for 8 h with live tachyzoites of *N. caninum* Nc-Spain7 (MØ7) and Nc-Spain1H (MØ1H), and inoculated with heat-killed tachyzoites (MØHK) in relation to non-infected cells. Genes were considered as differentially expressed when presented a FC ≥1.5 and with a P adj ≤0.05

HK parasites, and interestingly, in infection with the low virulence isolate Nc-Spain1H than with the Nc-Spain7 isolate. MØ1H-MØC, MØ7-MØC and MØHK-MØC comparisons were also mapped on Kyoto Encyclopedia of Genes and Genomes (KEGG) pathways (**Supplementary Table 5**). KEGG pathway analysis of the DEGs reveald 36 pathways for MØ1H-MØC, 35 for MØ7-MØC and 12 for MØHK-MØC **(Figure 3**). Important pathways enriched exclusively in live infections (MØ7 and MØ1H) were those related to pathogen recognition (NLR and RIG-I-like signalling pathways), signal transduction and cell interaction (IL17 signalling pathway, NF-ĸB signalling pathway, Th17 cell differentiation). In addition, those involved in cell growth and survival (ferroptosis, p53 signalling pathway), metabolism (tryptophan metabolism, pentose and glucuronate interconversions, fatty acid metabolism) and transport and catabolism involving "lysosome" were also modulated only by live parasites. Among these, remarkably metabolism and lysosome-related pathways appeared to be downregulated. The unique DEGs for MØ7 and MØ1H were also studied, but no significant results were obtained in any of the enrichment analyses. **Figure 4** shows differences in the expression of a selection of genes grouped into functional categories of interest.

In summary, different host cell modulation was induced by live than by HK parasites, with a higher impact observed for MØ1H. GO and KEGG pathway analyses in infected cells showed a specific gene expression profile for antigen-presenting cells (APCs) triggering innate immune mechanisms and their interactions in defence against *N. caninum* infection. Regulation was also observed in metabolism pathways that could be associated with immune response and the host modulation by intracellular *N. caninum* multiplication.

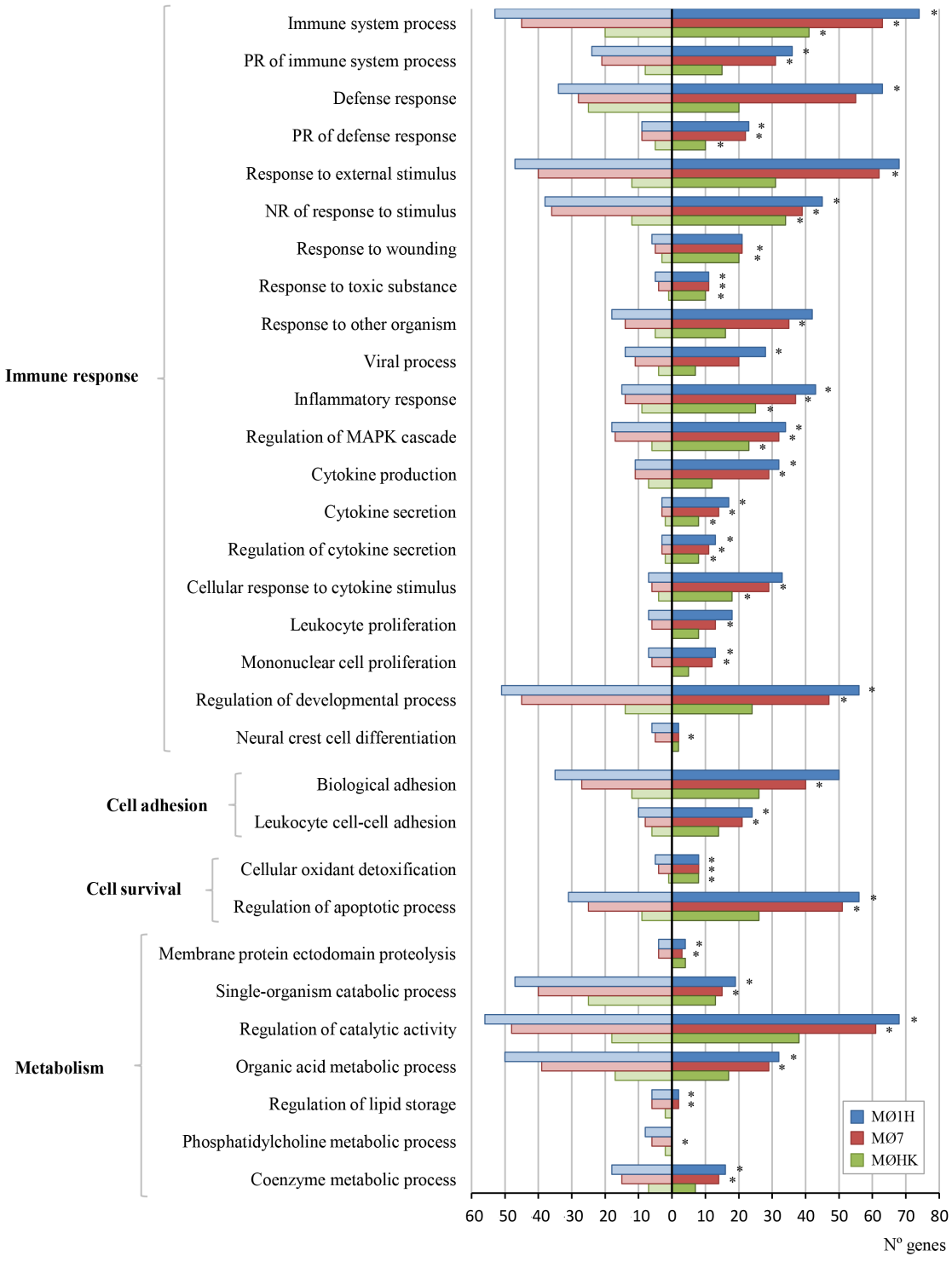

FIGURE 2 | GO terms enriched from DEG in macrophages inoculated with *N. caninum versus* non-infected cells. The graph shows the GO terms enriched from DEG of bovine macrophages infected for 8 h with *N. caninum* Nc-Spain7 (MØ7), Nc-Spain1H (MØ1H), and inoculated with heat-killed tachyzoites (MØHK) in relation to non-infected cells. The x-axe represents the number of DEG mapped for each GO term. Dark bars indicate upregulated genes and light bars downregulated genes. Asterisks indicate GO terms enriched with a p adj ≤ 0.05, considered statistically significant.

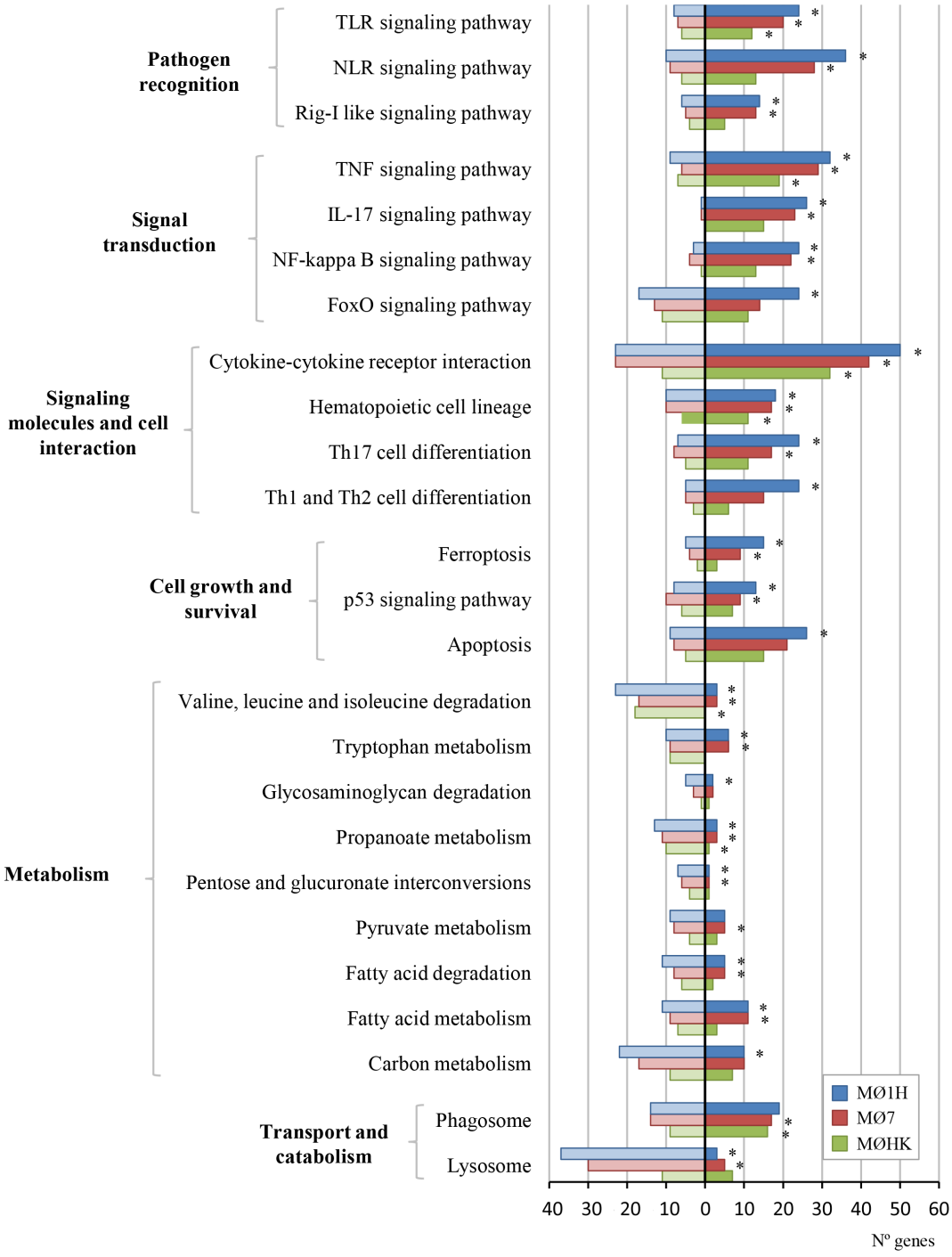

FIGURE 3 | KEGG pathways enriched from DEG in macrophages inoculated with *N. caninum* versus non-infected cells. The graph shows the pathways enriched from DEG of bovine macrophages infected for 8 h with *N. caninum* Nc-Spain7 (MØ7), Nc-Spain1H (MØ1H), and inoculated with heat-killed tachyzoites (MØHK) in relation to non-infected cells. The x-axe represents the number of DEG mapped in each pathway. Dark bars indicate upregulated genes and light bars downregulated genes. Asterisks indicate pathways enriched with a p adj ≤ 0.05, considered statistically significant.

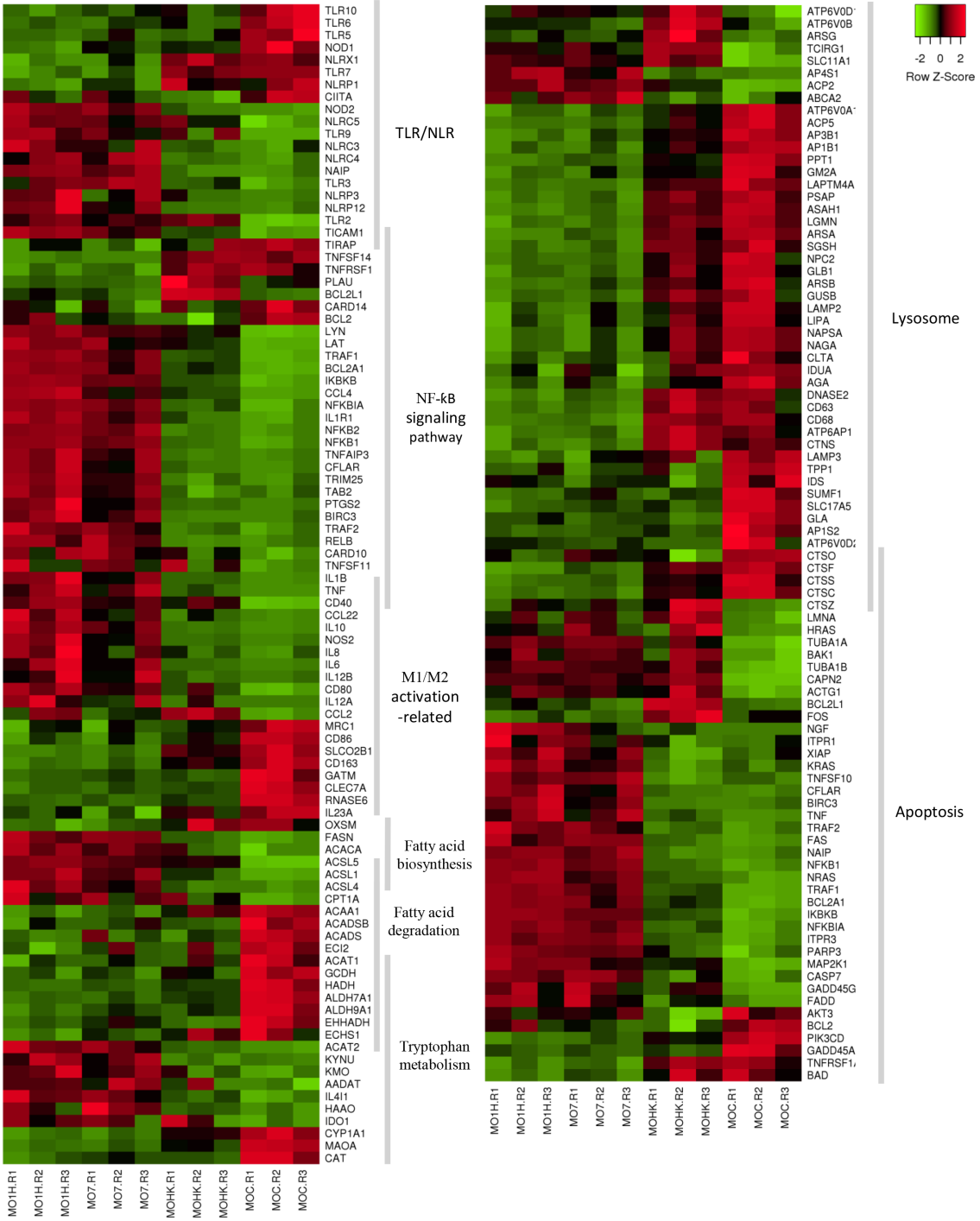

FIGURE 4 | Clustering of DEG in *N. caninum* infected macrophages. Heatmap of a selection of DEG showing row Z-scores based on expression data of three replicates (R1-R3) of MØs challenged for 8 h with Nc-Spain1H (MØ1H), Nc-Spain7 (MØ7), HK tachyzoites (MØHK) and non-infected MØs (MØC). Heatmap was generated by the use of Heatmapper (http://www2.heatmapper.ca). Genes are grouped according to functional categories and clustered into each category by Pearson computing distance method.

3.3. Pattern recognition receptor expression is differentially regulated by live *Neospora caninum*

A key element in the initiation of the innate immune response is the recognition of the pathogen by APCs by means of pattern recognition receptors (PRRs). Pathogen recognition by Toll-like receptors (TLRs) and nucleotide-binding and oligomerization domain (NOD)-like receptors (NLRs) leads to the activation of signalling cascades that stimulate host defences (Jungi et al., 2011; Kim et al., 2016).

Toll-like receptors TLR2 and TLR9 were upregulated, whereas TLR5, TLR6 and TLR10 were downregulated in MØ7, MØ1H and MØHK. Interestingly, there was upregulation of TLR3 and inhibition of TLR7 expression exclusively in those MØs infected with live parasites (MØ7 and MØ1H) (**Figure 4**). The importance of TLR2 and TLR3 in *N. caninum* recognition has been previously described in murine MØs, whereby TLR2 and TLR3 trigger the production of pro-inflammatory cytokines upon ligand binding (Mineo et al., 2010; Beiting et al., 2014; Miranda et al., 2019). TLR2 expression is also regulated by *N. caninum* infection in bovine trophoblast cells (Horcajo et al., 2017). Our results suggest a role of TLR2 and TLR3 in *N. caninum* infection in bovine MØ response and TLR9, whose expression by APCs has been demonstrated to be essential for initiating and developing an effective Th1-type immune response to *T. gondii* infection (Minns et al., 2006).

Conversely, thus far the role of NLRs in neosporosis is unclear, and only two members of these cytoplasmic receptors, NOD2 and NLRP3, have been related to murine MØ responsiveness in previous studies (Davoli-Ferreira et al., 2016; Wang et al., 2018). Here, the expression of the 22 NLR members grouped in the four subfamilies of NLRs was examined in bovine MØs inoculated with live or HK *N. caninum* tachyzoites. Ten NLRs were DE in MØ1H, eight in MØ7 and only three in MØHK, suggesting different recognition and thus subsequent responses induced by live and HK tachyzoites (**Figure 4**), likely because NLRs act as intracellular surveillance molecules. NLRs related to inflammasome formation (Kim et al., 2016) such as NAIP, NOD2, NLRC4 and NLRP12 were only over-expressed in cells infected with live tachyzoites of both isolates. The involvement of all these receptors in *T. gondii* sensing has been reported previously. NOD2 seems to be necessary for a Th1 immune response during murine toxoplasmosis (Clay et al., 2014). Additionally, *T. gondii* significantly upregulates NAIP and NLRC4 mRNA levels in human MØs (Chu et al., 2016), and a higher expression of NLRP12 has been detected in murine spleen after *T. gondii* infection (Znalesniak et al., 2017). In relation to *N. caninum*, NOD2 activation in mice has been related to an exacerbation of the inflammatory response, contributing to initial parasite control, but causing tissue damage during acute neosporosis (Davoli-Ferreira et al., 2016). Here, we suggest for the first time that NOD2, NLRP12, NAIP and NLRC4 may be involved in the bovine MØ inflammatory response against neosporosis.

Not only inflammasome formation but also signalling transduction and transcription activation are functions attributed to NLRs (Kim et al., 2016). Enhanced expression of NLRs related not only to NF-κB signalling pathway activation (NOD2), but also to NF-κB negative regulation (NLRC3 and NLRP12) (Cui et al., 2010; Tuncer et al., 2014; Kim et al., 2016), was observed in MØs infected with live tachyzoites, which points towards a modulation of the inflammatory response by *N. caninum* with the aim of avoiding pathologic consequences due to a persistent activation of NF-κB (Jha and Pan-Yun, 2015). The involvement of NLRP12 in the development of an adaptive response has been suggested to be mediated by inducing neutrophil and dendritic cell migration and MHC class I gene expression (Tuncer et al., 2014). However, this role has not yet been demonstrated in *N. caninum* or *T. gondii* infections.

The major histocompatibility complex (MHC) class II transactivator CIITA was over-expressed in MØHK, likely because of the exclusive antigen presentation via phagocytosis of inactivated parasites (García-Sánchez et al., 2019). However, a reduction of MHC II has also been detected in bovine MØs infected with live *N. caninum* internalized in MØs via active parasite invasion and phagocytosis (García-Sánchez et al., 2019), which suggests a downregulation of its expression by live parasites. Inhibition of CIITA expression seems to be a mechanism used by *T. gondii* to limit MHC II expression in neural APCs to evade $CD4^+$-mediated intracerebral immune responses (Lüder et al., 2003).

Autophagy has been associated with the control of infections by directing intracellular or phagocytosed pathogens to lysosomes for degradation (Bortoluci and Medzhitov, 2010). NLRX1 and NOD1 are related to autophagy, the latter located in the mitochondria and involved in ROS production (Tattoli et al., 2008), and were downregulated in MØ7 and MØ1H but not in MØHK. Thus, *N. caninum* may inhibit their expression in order to survive in the cell. In fact, a reduction in ROS response has been demonstrated for early *N. caninum* infection (García-Sánchez et al., 2019).

3.4. Activation of the NF-ĸB signalling pathway is induced in bovine macrophages during *Neospora caninum* infection

Activation of the NF-ĸB signalling pathway results in the induced transcription of pro-inflammatory cytokines and chemokines. In addition, the NF-ĸB pathway participates in inflammasome regulation and induces $CD4^+$ T-cell activation and differentiation, serving as a pivotal mediator of innate and adaptive immunity (Liu et al., 2017). The NF-ĸB signalling pathway was observed to be upregulated exclusively in MØs infected with live tachyzoites (MØ1H and MØ7) (**Figure 4)**. NF-ĸB activation by *N. caninum* infection was also functionally demonstrated in this study by examining the translocation of NF-ĸB p65 from the cytoplasm to the nucleus in MØ1H and MØ7 but not in MØHK and MØC (**Figure 5**). Activation of NF-κB signalling pathway upon *N. caninum* infection has been previously reported in murine MØs, and it has been related to the expression of *N. caninum* 14-3-3 protein (Li et al., 2019) and dense granule proteins NcGRA6, NcGRA7, and NcGRA14 (Nishikawa et al., 2018). Although a very similar response was observed regarding the DEGs implicated in this pathway for MØ1H and MØ7, for nearly all of them, the levels of mRNA regulation were higher for MØ1H, and expression was significantly higher for the adaptor TRAF2, which results in a higher expression of pro-inflammatory cytokines (**Figure 6**). In *T. gondii*, differences in the activation of this pathway have been related to parasite type since type II strains induce a higher NF-κB activation than type I and III strains, which affects cytokine expression and virulence (Rosowski et al., 2011).

Pro-inflammatory cytokine production induced by the activation of MAPK pathways ERK, JNK and p38 in MØs has been related to murine resistance against *N. caninum* (Jin et al., 2017; Li et al., 2019). In our study, the ERK and JNK pathways were not upregulated in MØs inoculated with either live or HK tachyzoites, suggesting that they are probably not involved in the bovine host immune response against *N. caninum.* Although the p38 pathway was not enriched in the KEGG analysis, the p38 genes MAPK11 and MAPK12 (encoding p38-β and p38-γ MAPK, respectively) appeared upregulated in MØ7, MØ1H and MØHK. Mota et al. (2016) proposed p38 MAPK activation as a mechanism used by *N. caninum* to evade murine innate immunity. In that study, p38-α phosphorylation, induced by live tachyzoites and antigen extracts was associated with a pronounced decrease in IL-12p40 production. Curiously, MAPK14 (encoding p38-α MAPK) mRNA levels were not altered in MØ7 and MØHK, whereas they were downregulated in MØ1H, which showed higher levels of IL12B (IL-12p40) expression.

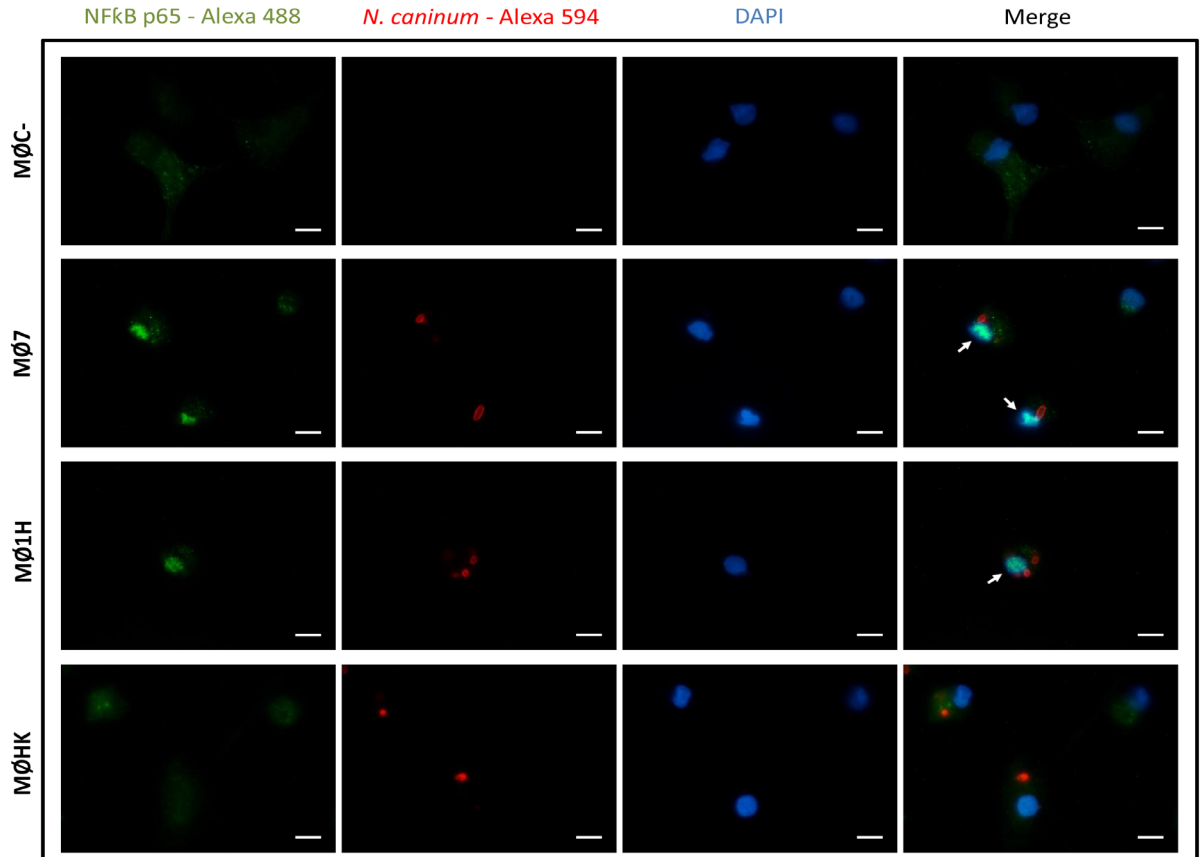

FIGURE 5 |Nuclear translocation of NF-κB p65 upon *N. caninum* active invasion. Representative micrographs of non-infected MØs (MØC) and MØs challenged for 8 h with Nc-Spain7 (MØ7), Nc-Spain1H (MØ1H) or HK tachyzoites (MØHK). NF-κB p65 is presented in green, parasites in red and nuclei in blue. Scale bar is 10 μm. Arrows exemplify co-location of NF-κB p65 and nuclei in *N. caninum* infected cells.

Altogether, these results indicate that NF-κB is the main signalling pathway implicated in the pro-inflammatory immune response against *N. caninum* in bovine MØs. However, new studies are necessary to establish the mechanisms involved in NF-κB activation and the participation of additional routes of MØ activation.

3.5. *Neospora caninum* infection induces macrophage polarization towards the M1 phenotype.

MØs exhibit a high degree of plasticity and are able to respond to stimuli and polarize to an M1 (classical activation) phenotype that promotes Th1 responses or an M2 (alternative activation) phenotype that promotes Th2 responses (Muraille et al., 2014). M1 macrophages respond to stimulation with enhanced expression of pro-inflammatory cytokines (IL12, IL23, TNF, IL6, IL1B), nitric oxide synthase (NOS2), chemokines (e.g., CCL2, IL8) and costimulatory factors (e.g., CD80, CD86, CD40). The alternative activation (M2) is mainly characterized by the expression of anti-inflammatory and regulatory cytokines (e.g., IL10) and arginase-1 (ARG1), although many other M2 phenotype-associated molecules have been proposed such as certain chemokines (e.g., CCL22), scavenger receptors (e.g., CD163), and a mannose

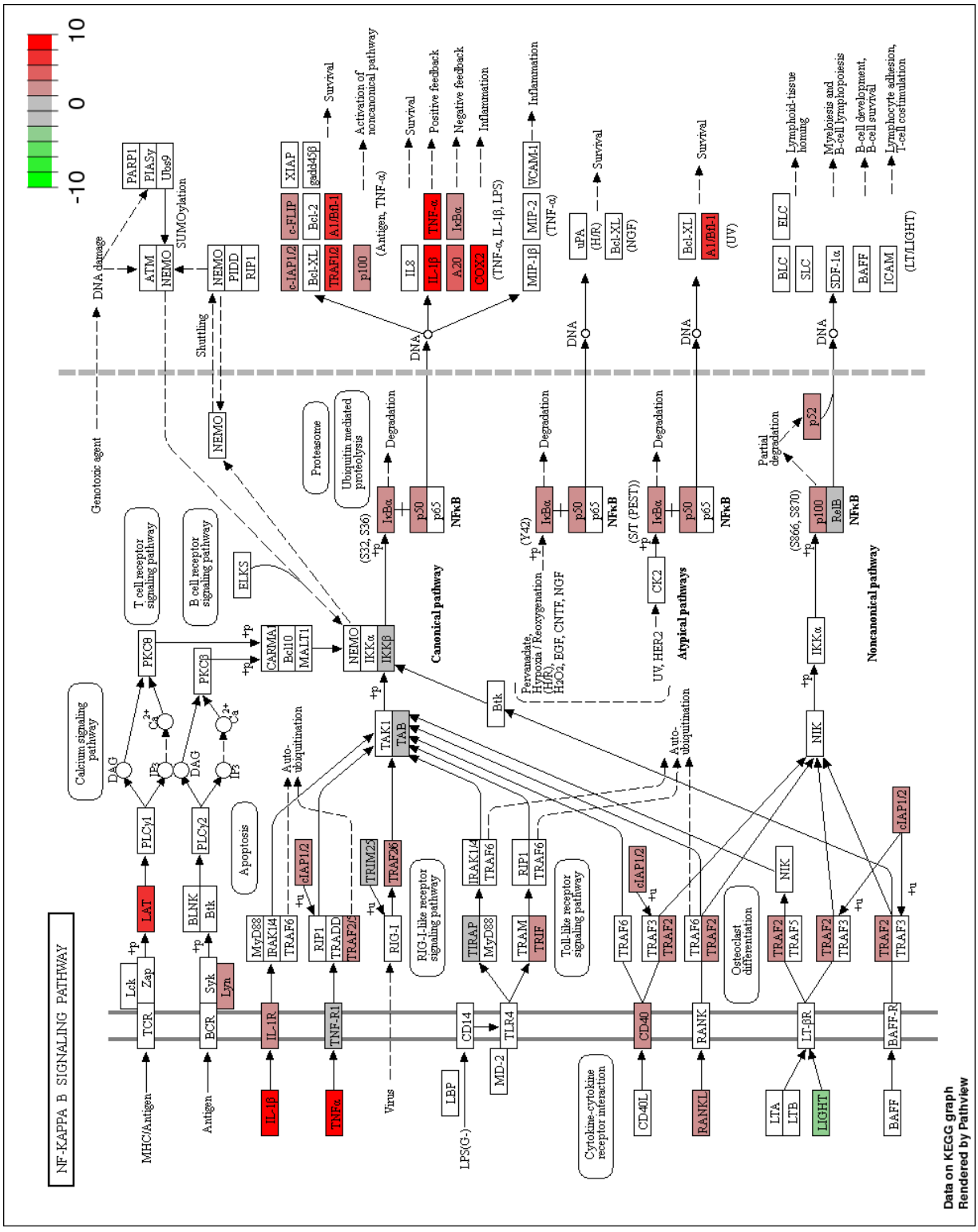
NF-KAPPA B SIGNALING PATHWAY
-10
0
10
Data on KEGG graph
Rendered by Pathview

A

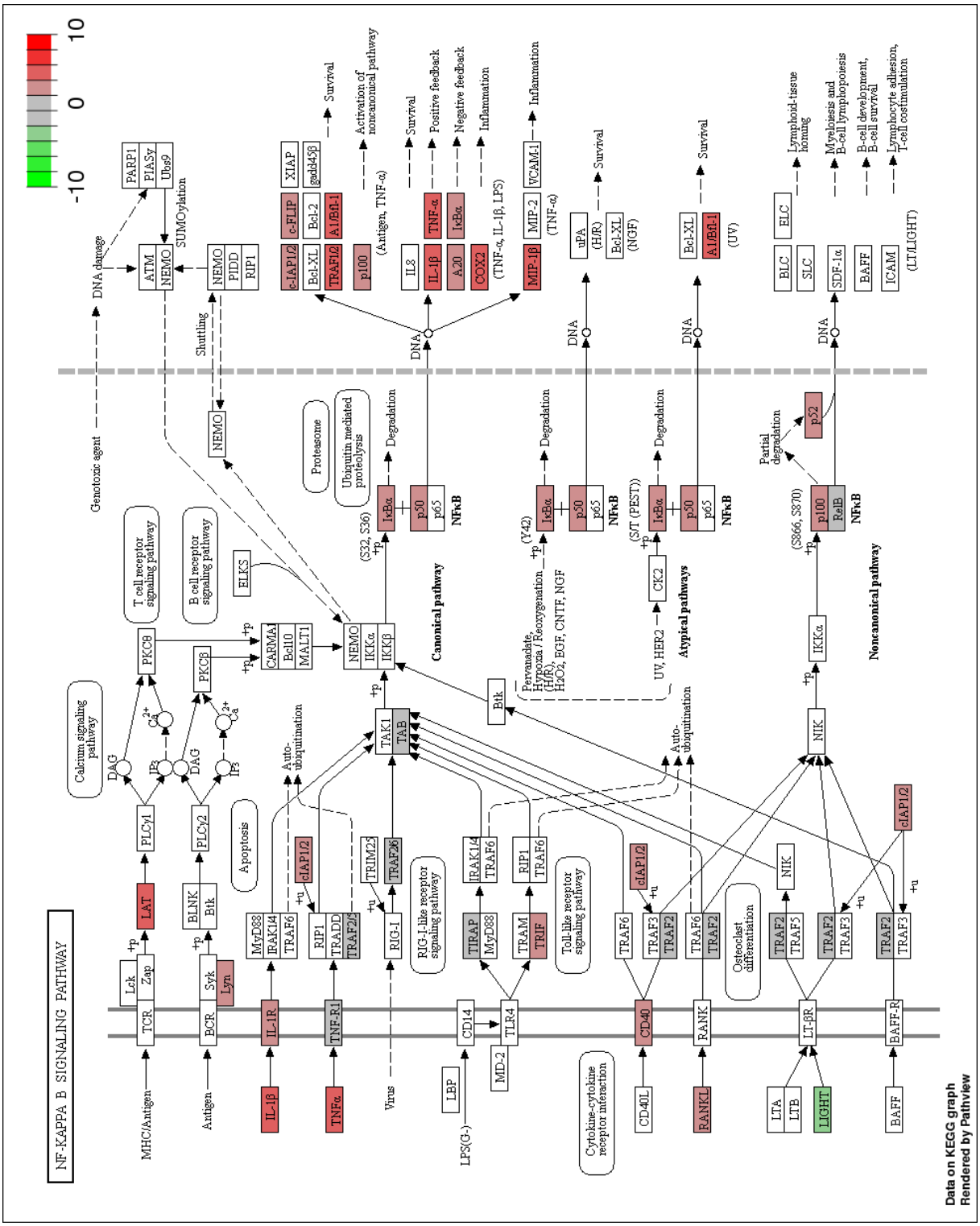

B

FIGURE 6 | NF-kB signalling pathway in macrophages infected with Nc-Spain1H and Nc-Spain7 *versus* non-infected cells. The pathway maps represents the NF-kB signalling pathway in which DEG in bovine macrophages infected with (A) Nc-Spain1H and (B) Nc-Spain7 *versus* non-infected macrophages are highlighted. Upregulated genes are represented in red and downregulated genes are represented in green. The color intensity corresponds to the level of up- or down-regulation.

receptor (MRC1) (Martínez and Gordon, 2014; Muraille et al., 2014; Kapellos and Iqbal, 2016). Moreover, virulence and evasion mechanisms of the pathogens may affect MØ polarization, with consequences for parasite burden and inflammation-related pathologies (Jensen et al., 2011; Martínez and Gordon, 2014). It has been demonstrated that diverse *T. gondii* strains can induce a different phenotype in MØs, where high virulence has been associated with M2 induction (Jensen et al., 2011).

Here, *N. caninum*-inoculated MØs (MØ7, MØ1H and MØHK) showed a predominantly M1 phenotype, characterized by an enhanced expression of pro-inflammatory cytokines TNF, IL6, IL1B, and other M1 markers (CCL2, CD80 and CD40) and downregulation of the M2 markers CLEC2A, MRC1, CD163, RNASE6, GATM, and SLCO2B1 (**Figure 4**). However, the M2-associated cytokine IL10 and chemokine CCL22 were also upregulated. In addition, the M1 costimulatory factor CD86 was downregulated in the three conditions MØ7, MØ1H and MØHK, although the FC for MØHK (-1.52) was very close to the cut-off point. Live tachyzoites infection (MØ7 and MØ1H) also induced upregulation of NOS2 and proinflammatory IL12B (that encodes IL12p40). Interestingly, mRNA levels of the pro-inflammatory cytokines IL12A (IL12p35) and IL8 were upregulated in MØ1H, and the pro-inflammatory cytokine IL23A was downregulated in MØ7. We have previously reported similar results, with enhanced expression of IL12p40 observed in bovine MØs infected only with live tachyzoites and of IL10 in MØs inoculated with live and HK tachyzoites, and with higher expression levels in MØ1H. In addition, surface expression of CD86 measured by flow cytometry significantly decreased in live parasite infection (García-Sánchez et al., 2019). In that work, we suggested that both *N. caninum* isolates modulate expression of cytokines and ligands related to T-cell activation, as a mechanism to escape the host immune response.

In this study, live tachyzoites showed different induction of pro-inflammatory cytokine expression that could influence innate and adaptive response efficacy against infection.

3.6. *Neospora caninum* circumvents phagolysosome activity

In the present study, the expression profiles indicated lysosome pathway inhibition in MØ7 and MØ1H but not MØHK. These results are in agreement with the phenotype previously described for *N. caninum*-infected bovine MØs, where the absence of lysosome activity was demonstrated in parasitophorous vacuoles and was limited to tachyzoites internalized by phagocytosis (García-Sánchez et al., 2019). Both isolates induced the downregulation of genes related to the maturation of the phagosome to a phagolysosome containing a robust antimicrobial environment (Uribe-Querol and Rosales, 2017) (**Figure 7**). Among the downregulated genes were genes encoding V-ATPase, which translocates protons (H+) into the lumen of the phagosome for its acidification and lysosomal-associated membrane proteins, essential for fusion of lysosomes with phagosomes; genes encoding proteins involved in the transport and activation of lysosomal enzymes; and a great number of genes encoding enzymes and peptides with microbicidal effects (proteases, glycosidases, lipases, nucleases, sulfatases and phosphatases), which destroy diverse components of the invading pathogen (Nalpas et al., 2015; Uribe-Querol and Rosales, 2017). Combined, the results of both studies suggest that impairing phagolysosome maturation is a mechanism used by *N. caninum* to survive and proliferate into phagocytic cells.

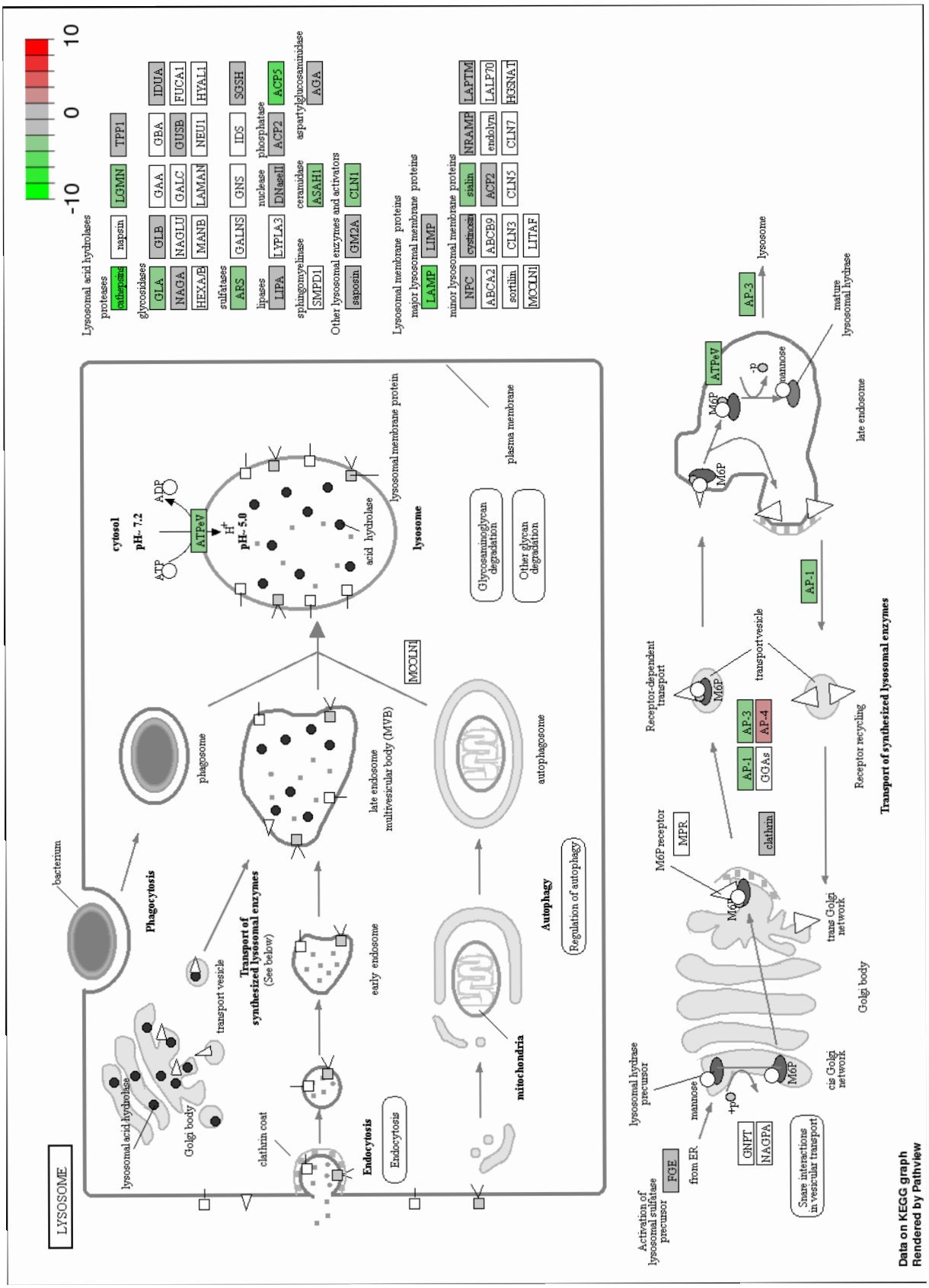

FIGURE 7 | Lysosome pathway in macrophages infected with Nc-Spain1H versus non-infected cells. The pathway map represents the molecular network "Lysosome" in which DEG in bovine macrophages infected with Nc-Spain1H versus non-infected macrophages are highlighted. Upregulated genes are represented in red and downregulated genes are represented in green. The color intensity corresponds to the level of up- or down-regulation.

3.7. *Neospora caninum* infection modulates macrophage apoptosis.

Programmed cell death, called apoptosis, is one of the main defence mechanisms that hosts possess against intracellular pathogens (Schaumburg et al., 2006; Besteiro, 2015). "Apoptosis" and "regulation of apoptosis" were KEGG pathways and GO terms associated with *N. caninum* infection in this study. Again, regulation of apoptosis was observed only in MØs inoculated with live parasites (MØ7 and MØ1H). Genes annotated as anti-apoptotic and as pro-apoptotic were both upregulated and downregulated (**Figure 4**). According to these results, *N. caninum* infection may regulate apoptosis in MØs. This behaviour has been largely described in many other protozoan parasites, including *T. gondii* (Schaumburg et al., 2006). On the one hand, stress signals provided by the parasite during infection may induce a pro-apoptotic response by the host cell as an innate defense mechanism. Obligate intracellular parasites need to hijack apoptosis-regulating cascades in order to suppress or delay cell death to favour parasite replication (Schaumburg et al., 2006). Our results indicate that Nc-Spain7 and Nc-Spain1H counteract stress-induced cell death by promoting the expression of certain anti-apoptotic BCL-2 genes, inhibitors of apoptosis (IAPs) and FLIP (also named CFLAR) among others. This would lead to a decreased release of cytochrome c from mitochondria into the cytosol and to a direct interference with caspase processing and function, as has been described for *T. gondii* and other protozoan parasites (Schaumburg et al., 2006; Besteiro et al., 2015).

3.8. *Neospora caninum* infection markedly impacts host metabolic pathways

Enrichment analysis showed an impact of *N. caninum* on the host cell metabolism. During adaptation to parasitism, apicomplexan parasites reduced metabolic pathways to make their metabolism more efficient. Manipulation of the host metabolism is achieved to obtain the energy and nutrients that the parasites need to survive and proliferate (Xu et al., 2010). Besides, there are provided evidences of a role for metabolic reactions and processes in controlling immunological effector functions such as cytokine production in response to pathogens (Diskin and Palsson-McDermott, 2018). Of particular interest, live parasites (MØ7 and MØ1H) infection regulated the KEGG pathways "Fatty acid metabolism", "Fatty acid degradation", "Pentose and gluconorate interconversions" and "Tryptophan metabolism"; and amongst GO terms "Regulation of catalytic activity", "Organic acid metabolic process" and "Regulation of lipid storage" (**Figures 2** and **3**).

Interestingly, fatty acid synthesis that occur in cytoplasm and fatty acid degradation in mitochondria have been related with MØ polarization. Inflammatory signals including LPS and IFN-γ, required to generate M1 MØs, have been shown to drive fatty acid synthesis, whereas the inhibition of inflammatory signals required for the differentiation of M2 MØs involves fatty acid degradation (Remmerie and Scott, 2018). In this study we observed a clear downregulation of fatty acid degradation together with upregulation of fatty acid synthesis (**Figures 4** and **8**) that may reflect M1 polarization of *N. caninum*-infected MØs.

"Tryptophan metabolism" is also modulated in *N. caninum* infected MØs (**Figure 4**). The majority of tryptophan is metabolized by the Kyneurine pathway by two different enzymes, indoleamine-2,3-dioxygenase 1 (IDO1) and tryptophan-2,3-dioxygenase (TDO) giving place to different catabolites collectively called kynurenines that can act as immunoregulatory factors (Grohmann et al., 2017). Enzymes involved in Tryptophan degradation were upregulated in *N. caninum* infected MØs. Activation of Indoleamine 2,3-dioxygenase (IDO) upon *T. gondii* infection has been described as a potent antiparasitic mechanism for its role in catabolizing

tryptophan, and the restriction of *N. caninum* proliferation induced by IDO activity has been demonstrated *in vitro* (Jesus et al., 2019). Remarkably, IDO was shown to be upregulated only in MØ1H, which may be related to the lower proliferation of Nc-Spain1H in bovine MØs (García-Sánchez et al., 2019).

3.9. Differences between *Neospora caninum* isolates define a mechanism for evasion of the immune response of the highly virulent isolate Nc-Spain7

A differential expression analysis between MØ1H and MØ7 resulted in four DEGs: C-C motif chemokine 4 (CCL4), C-X-C motif chemokine 6 (CXCL6) and metallothionein-2 (MT2) were upregulated in MØ1H, and coenzyme Q8A (ADCK3) was upregulated in MØ7. CXCL6 (or granulocyte chemotactic protein 2-GCP-2) and CCL4 (or macrophage inflammatory protein-1β, -MIP-1β) are chemokines for neutrophils and monocytes, and natural killer cells and regulatory T cells, respectively. In addition to their pro-inflammatory effects, CCL4 can also promote homeostasis by interacting with CCR5 receptors (Bystry et al., 2001; Linge et al., 2008). Activation and migration of immune cells via CCR5 seems to be essential for host survival following *T. gondii* infection and for controlling *N. caninum* during the acute phase of the disease (Abe et al., 2015; Khan et al., 2006). The MT2 gene encodes metallothionein, whose upregulation during infection may serve as a strategy to prevent host tissue damage because of its capability to neutralize ROS (Ruttkay-Nedecky et al., 2013). The observed enhanced expression of MT2 in MØ1H compared to MØ7 may be a response to the higher intracellular ROS levels induced in MØs infected by Nc-Spain1H as previously described. In contrast to Nc-Spain1H, Nc-Spain7 maintains downregulated intracellular ROS levels in MØs over time (García-Sánchez et al., 2019). MT2 may also be involved in the regulation of immune response signalling and inflammation by modulating the activation of NF-ƙB, pathogen clearance in MØs and inhibition of apoptosis through mediation of p53 activity (Ruttkay-Nedecky et al., 2013). ADCK3 encodes the atypical kinase COQ8a, which it is thought to be involved in ubiquinone (Coenzyme Q) biosynthesis, an essential lipid-soluble electron transporter for aerobic cellular respiration (source: UniProtKB).

Although only these 4 genes showed significant differences between the isolates, a higher number of differentially regulated genes were found for the Nc-Spain1H isolate in the comparison of MØ1H-MØC *versus* MØ7-MØC. Among the DEGs unique for MØ1H that belong to common pathways shared by MØ1H and MØ7, the following can be highlighted: genes associated with the "NLR signalling pathway" (NLRP1, NLRP3), "Chemokine signalling pathway" (e.g., BCAR1, GNAI3, GNG4, JAK2, ROCK2, CXCL5, IKBKB, MAP2K1, NRAS, and PIK3CG) and "Cytokine-cytokine receptor interaction" (e.g. IL8, TNFRSF8, IFNAR2, IL12A, IL17RA, TNFSF15 and TNFSF8). In addition, the pathways "FoxO signalling pathway", "Th1 and Th2 cell differentiation" "Glycosaminoglycan (GAG) degradation" and "Apoptosis" appeared to be statistically significant only for MØ1H. A stronger cellular stimulation induced by Nc-Spain1H has been previously described *in vitro* in bovine MØs and trophoblast cells, which could be related to a higher abundance of highly immunogenic cell surface proteins in this isolate, activating a more efficient immune response that leads to the control of Nc-Spain1H infection (Horcajo et al., 2018; García-Sánchez et al., 2019).

NLRP3 has been implicated in limiting parasite burden and host mortality in *T. gondii* infections (Clay et al., 2014). In addition, involvement of this receptor in the acute host immune response to *N. caninum* has been suggested to limit parasite growth via the Th1 response and IFN-γ induction in infected mice (Wang et al., 2018). The upregulation of NLRP3 in MØ1H is consistent with

A

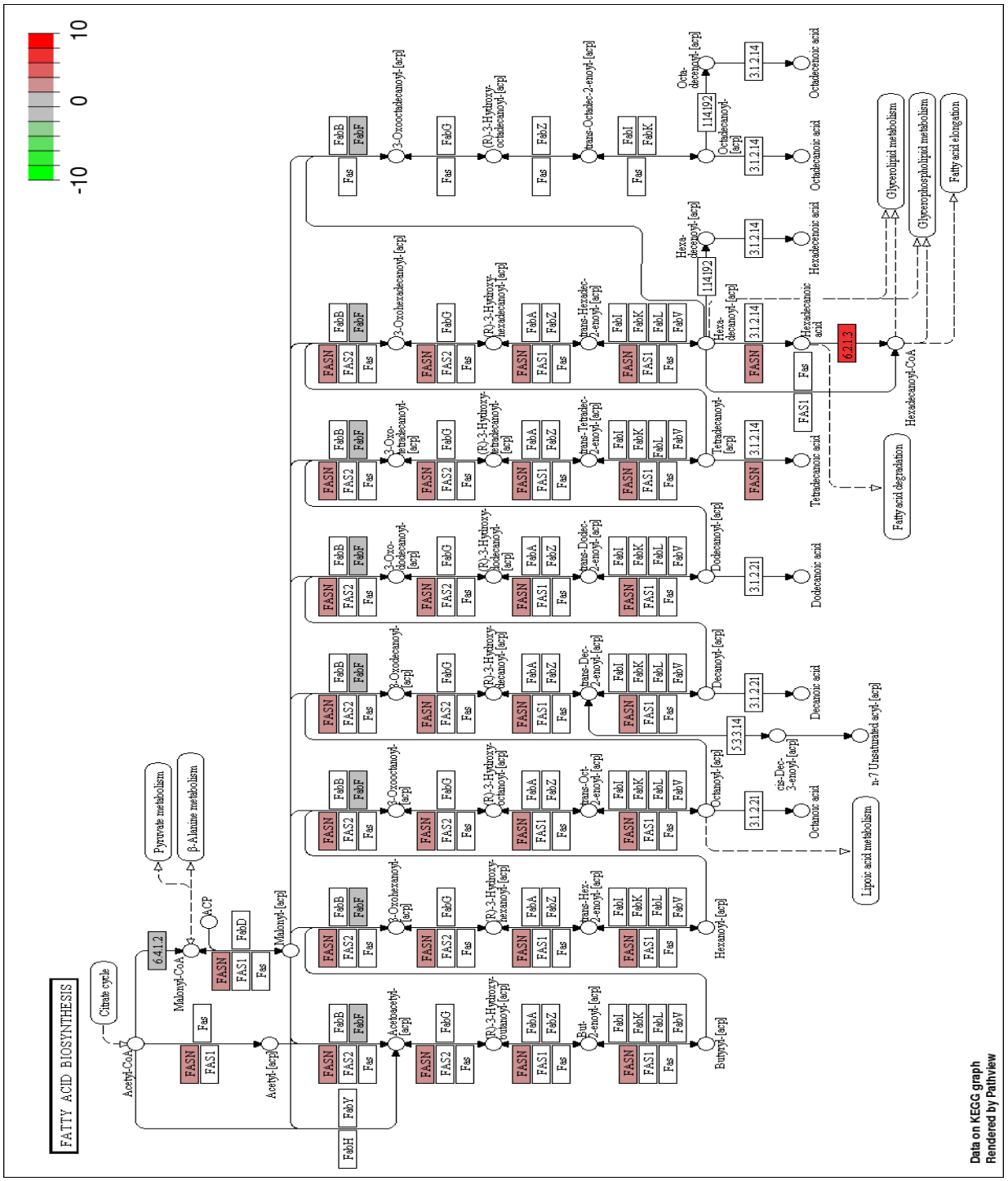
FATTY ACID BIOSYNTHESIS
-10
0
10
Citrate cycle
Acetyl-CoA
Malonyl-CoA
6.4.1.2
ACP
FabD
Malonyl-[acp]
Pyruvate metabolism
β-Alanine metabolism
Acetyl-[acp]
FabH
FabY
Acetoacetyl-[acp]
Butyryl-[acp]
Hexanoyl-[acp]
Octanoyl-[acp]
Decanoyl-[acp]
Dodecanoyl-[acp]
Tetradecanoyl-[acp]
Hexadecanoyl-[acp]
Octadecanoyl-[acp]
Octadecenoyl-[acp]
5.3.3.14
3.1.2.21
3.1.2.14
6.2.1.3
Octanoic acid
Decanoic acid
Dodecanoic acid
Tetradecanoic acid
Hexadecanoic acid
Octadecenoic acid
cis-Dec-3-enoyl-[acp]
n-7 Unsaturated acyl-[acp]
Lipoic acid metabolism
Fatty acid degradation
Hexadecanoyl-CoA
Glycerolipid metabolism
Glycerophospholipid metabolism
Fatty acid elongation
Data on KEGG graph
Rendered by Pathview

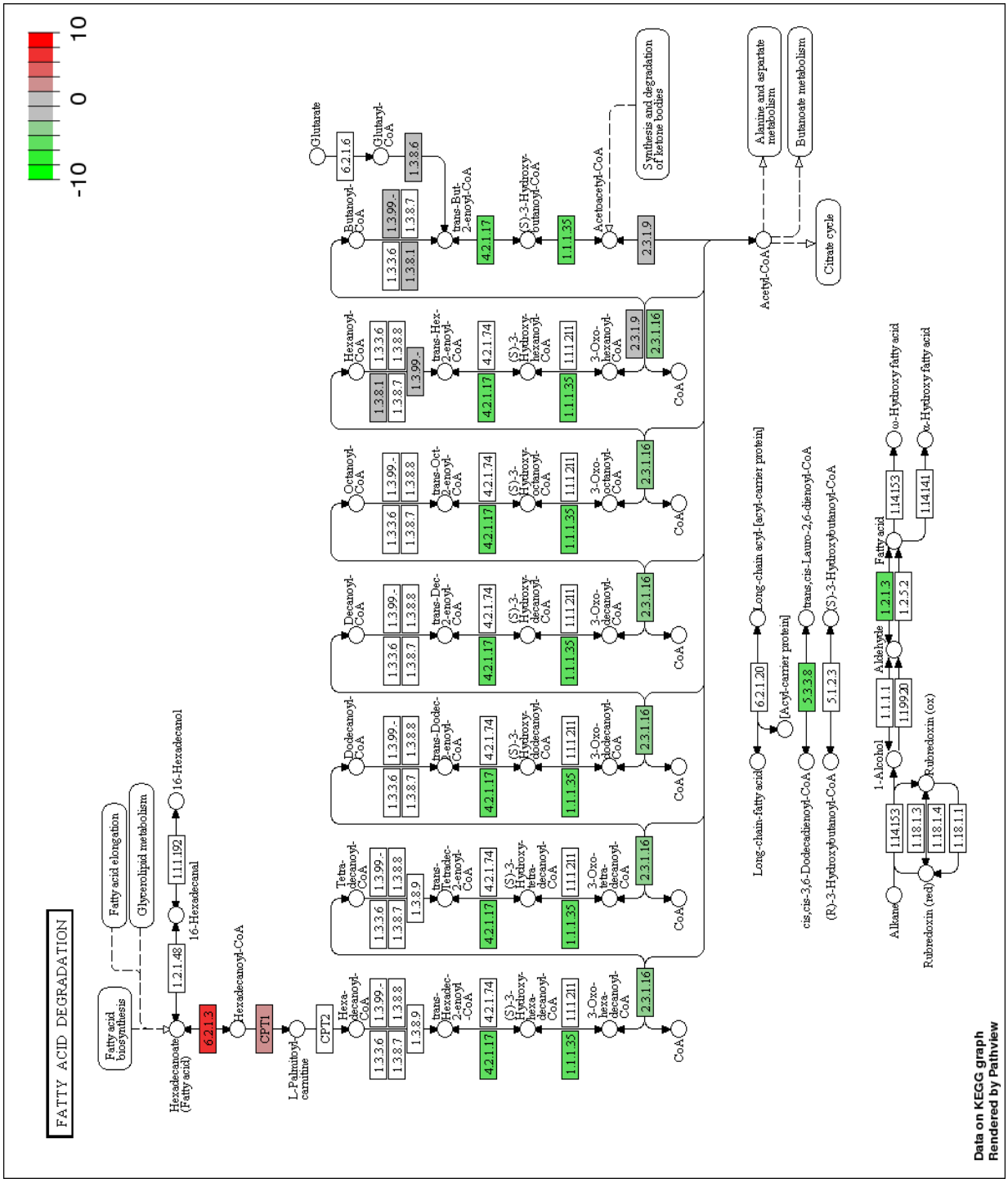

B

FIGURE 8 | Fatty acid metabolic pathways in macrophages infected with Nc-Spain1H *versus* non-infected cells. The pathway maps represent the molecular networks (A) Fatty acid biosynthesis and (B) Fatty acid degradation in which DEG in bovine macrophages infected with Nc-Spain1H versus non-infected macrophages are highlighted. Upregulated genes are represented in red and downregulated genes are represented in green. The color intensity corresponds to the level of up- or down-regulation. Similar regulation was observed for Nc-Spain7 infection.

the lower parasite survival of this isolate in MØs infected *in vitro* (García-Sánchez et al., 2019). Additionally, an apparent higher activation of the NF-ĸB signalling pathway by Nc-Spain1H may be related to variations in the expression of pro-inflammatory cytokines such as TNF, IL1B, IL6 and IL12B. TNF could enhance TRAF2 and NF-ĸB activation as is observed in MØ1H. Nc-Spain1H also induced enhanced expression of proinflammatory IL8 and IL12A, and IL27 that was not observed for Nc-Spain7. IL12A (IL12p35) and IL12B (IL12p40) need to be coordinately expressed to produce active IL12 (IL12p70) (Ma et al., 2015); therefore, reduced expression of IL12A would limit IL12 production in MØ7. This cytokine induces IFN-γ release by natural killer (NK) cells and $CD4^+$ T lymphocytes, and both IL12 and IFN-γ are essential for restricting *N. caninum* intracellular growth (Ma et al., 2015; Almería et al., 2017). A reduced secretion of IFN-γ was also detected in lymphocytes stimulated with MØs infected with Nc-Spain7 (García-Sánchez et al., 2019). IL-27 has both pro-inflammatory and anti-inflammatory properties. It induces the release of pro-inflammatory cytokines by MØs, enhances *ROS generation* and synergizes with IL12 to promote IFN-γ production by T-cells. On the other hand, IL-27 markedly suppresses the Th17 response during inflammation (Carl and Bai, 2008; Sowrirajan et al., 2017). In addition, IL23 was downregulated in MØ7. IL-23 is a pro-inflammatory cytokine important for controlling *T. gondii* infection (Matsuzaki and Umemura, 2007) by inducing the production of IL-17 by activated T-cells. Furthermore, high levels of IL10 expression, essential cytokine to limit the inflammation associated with infection (Almería et al., 2017), were induced by both isolates, although again, they were higher for MØ1H. This. This differential cytokine expression between the isolates suggests a higher induction of pro-inflammatory responses by the low virulence isolate Nc-Spain1H but highly regulated, whereas Nc-Spain7 seems to partially inhibit the pro-inflammatory response allowing its replication more efficiently (García-Sánchez et al., 2019). Altogether, our results may explain the lower induction of IFN-γ release by lymphocytes by MØ7 and the higher ability of Nc-Spain7 to survive in MØs observed in vitro (García-Sánchez et al., 2019) and may be related to the higher parasite burdens and the induction of placental lesions and abortions found *in vivo* (Jiménez-Pelayo et al., submitted).

Although it is widely accepted that a protective immunity against neosporosis requires a mixed Th1/Th2 response (Almería et al., 2017), the adequate balance between both has not been defined yet. Thus, this study may help to shed light on the factors implicated in neosporosis pathogenesis. Related to the Th1 and Th2 differentiation pathway, 10 genes were DE exclusively for MØ1H (CD247, GATA3, IKBKB, IL12A, JAK2, TIK2 and RBPJL were upregulated; DLL4, MAML3 and MAPK14 were downregulated). Of particular interest among these beyond IL12A and MAPK14, are GATA3, a transcriptional factor that plays an important role in MØ polarization towards an M2 phenotype and in the differentiation of Th2 cells (Zhong and Yi, 2016) and DLL4, involved in the induction of Th1 differentiation (Tindemans et al., 2017).

GAG degradation pathway was enriched for MØ1H, which showed downregulation of the ARSB, IDUA and SGSH genes, involved in the degradation of chondroitin sulfate (CS) and heparan sulfate (HS), the major GAG expressed on the cell surface membrane (Martínez et al., 2015). CS and HS mediate the initial interaction of several pathogens including *T. gondii* and *N. caninum* with the host cell (Sohn et al., 2011). In addition, inflammatory and immuno-regulatory mediators including many chemokines, cytokines, and growth factors interact with these cell-surface GAGs (Martínez et al., 2015), and the ability of pathogens to subvert GAG functions is considered an important virulence mechanism (Jinno and Park, 2015). On this basis, inhibition of HS and CS degradation in MØ1H may be related with a higher abundance of these GAGs in the cell surface, which may partially explain the different induction of pro-inflammatory responses between both isolates.

Finally, the Forkhead box O (FOXO) signalling pathway, which regulates the expression of genes involved in apoptosis, cell-cycle control, metabolism and oxidative stress resistance (Zhang et al., 2011) was enriched exclusively for MØ1H. The Nc-Spain1H isolate, despite showing a lower proliferation rate, induces a higher expression of Th1 cytokines and ROS production (García-Sánchez et al., 2019), which may be associated with a higher activation of stress signals in the cell and therefore expression of genes related to this pathway.

4. CONCLUDING REMARKS

The study of gene expression profiles in this work has revealed mechanisms implicated in the recognition of *N. caninum* by bovine MØs and in the subsequent immune response. NF-ĸB seems to be an essential signalling pathway implicated in the response against this pathogen of its natural host. Gene expression profile after MØs activation by *N. cannum* showed a metabolic and immune M1 inflammatory phenotype needed for the control of infection. Apoptosis and degradation by lysosomes are processes repressed by *N. caninum* infection, which may guarantee its survival in this cell type. Gene expression modulation by *N. caninum* infection resemble with phenotypic traits previously studied. This work shows that *N. caninum* is able to modulate MØ host signalling pathways to escape cellular defences and opens up a new avenue for further studies on parasite virulence.

The sum of the variations found between the high and the low virulence isolates in the expression of genes involved in pathogen sensing, microbial killing, cell survival, chemotaxis or cytokine release may result in important differences regarding the immune responses generated against these two isolates. An expected enhanced but highly regulated early protective response to infection induced by Nc-Spain1H would explain why Nc-Spain1H shows limited infection of placental tissues with no transmission during early infection in a bovine model. In contrast, mechanisms of evasion by Nc-Spain7 support the efficient transmission of this isolate to the foetus causing abortion (Jiménez-Pelayo et al., submitted). Further studies are necessary to determine the parasite factors implicated in virulence-related cell modulation.

DATA AVAILABILITY

Raw data are deposited in NCBI and are available for the review in the following address:

https://dataview.ncbi.nlm.nih.gov/_526?reviewer=kt4dnoctuuqej3rc24mfhe4vqq

SUPPLEMENTARY FILES

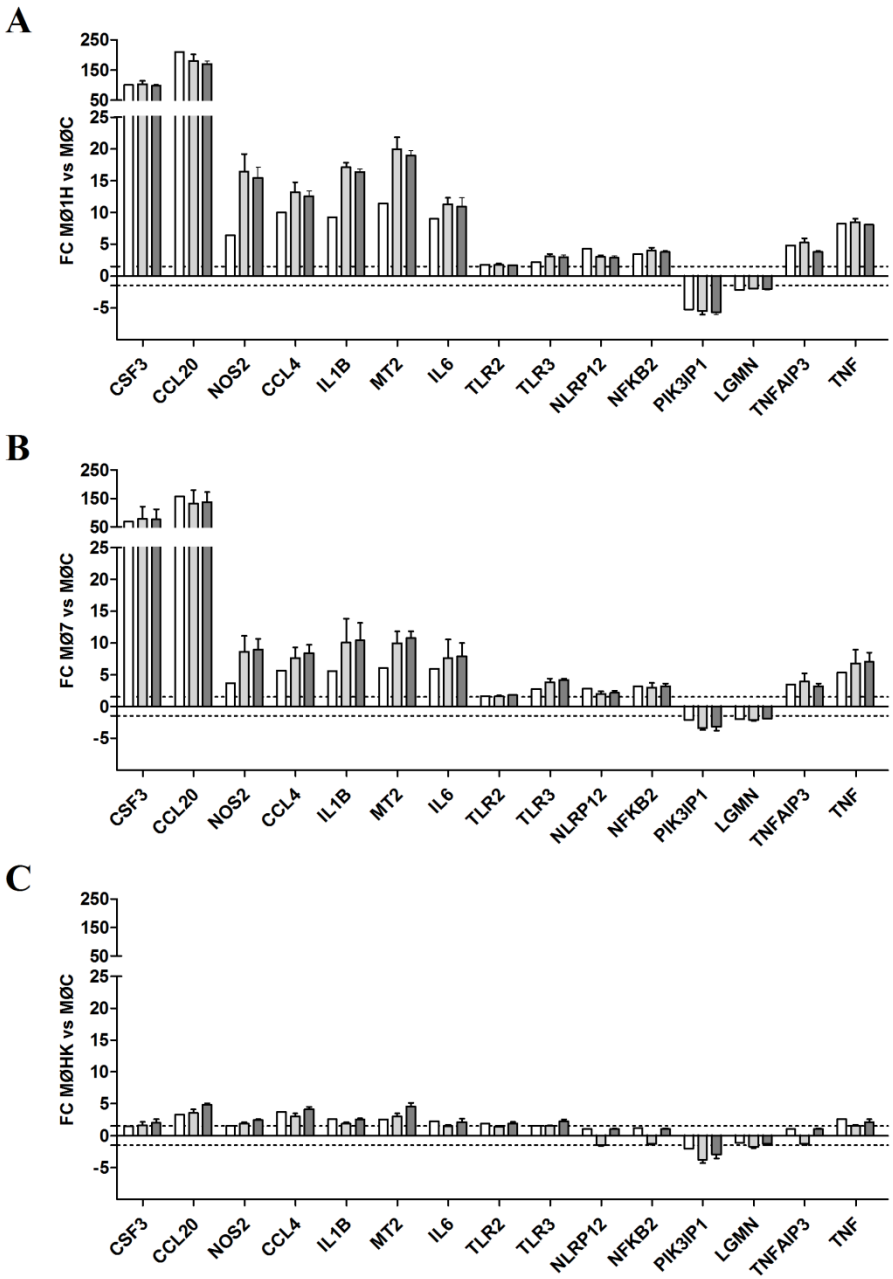

SUPPLEMENTARY FIGURE S1 | Transcriptomic validation of RNA-seq analysis by RT-qPCR. Fold changes (FC) in gene expression of *B. taurus* genes in the comparisons between (A) Nc-Spain1H-infected macrophages (MØ1H) *versus* non-infected macrophages (MØC), (B) Nc-Spain7-infected macrophages (MØ7) *versus* MØC, and (C) macrophages inoculated with heat-killed *N. caninum* tachyzoites (MØHK) *versus* MØC. Gene expression was measured by quantitative real-time PCR (RT-qPCR) and normalized with housekeeping Actin beta (ACTB) and Glyceralde-3-phosphate dehydrogenase (GAPDH). All the differentially expressed genes (FC ≥ 1.5, delimited by a discontinuous line) showed similar expression profile for both techniques and similar FC for the two housekeepings. Lack of correlation was only observed for three genes expressed by MØHK with FC < 1.5 and normalized with ACTB.

SUPPLEMENTARY TABLE 1 | Sequences of primers used for transcriptomic validation by RT-qPCR.

Ensembl id	Gene name	Gene symbol	Sequences (5' to 3')	Product size (bp)
ENSBTAG00000025257	C-C motif chemokine ligand 4	CCL4	AGCTGTGGTATTCCAGACCAA TCAAGGTCATCCACGTACTCC[1]	87
ENSBTAG00000023659	Metallothionein-2	MT2	GGCTCCTGCAAATGCAAAGAT CCGAAGCCCCTTTGCAGAC[2]	75
ENSBTAG00000021326	C-C motif chemokine ligand 20	CCL20	AATTAGCTGTGTGTGCAGATCC CATCCTTTTGACTCTTTGACTGA[1]	80
ENSBTAG00000006894	Nitric oxide synthase, inducible	NOS2	GCAGCAGCGGCTCCATGAGG CTTGGGCTGGTCAGGCAGGC[3]	141
ENSBTAG00000000436	TNF alpha induced protein 3	TNFAIP3	TGCTAAGCTGGCTGCAAGG TTGCTGTGTTGATGCTGCG[4]	59
ENSBTAG00000021462	Colony stimulating factor 3	CSF3	CTTGGCCCTGCCCGA TTCCTCACTTGCTCTAAGCACTTG[4]	62
ENSBTAG00000001321	Interleukin 1 beta	IL1B	ACCTGAACCCATCAACGAAATG TAGGGTCATCAGCCTCAAATAACA[1]	74
ENSBTAG00000006017	Nuclear factor kappa B subunit 2	NFKB2	CCTGCTGAATGCTCTGTCTG TCCTCCTTCACCTCTGTGCT[1]	102
ENSBTAG00000010667	Phosphoinositide-3-kinase interacting protein 1	PIK3IP1	GGAGCTGGAATTGTCCTTGG GCACACTTTCTGCTCGTGCT[1]	75
ENSBTAG00000046979	Legumain	LGMN	TGGAGGACCCTGAGGACG TACCAGCCGTTTGATCCTGC[4]	64
ENSBTAG00000008008	Toll like receptor 2	TLR2	ACGACGCCTTTGTGTCCTAC CCGAAAGCACAAAGATGGTT[5]	192
ENSBTAG00000008682	Toll like receptor 3	TLR3	GAGGCAGGTGTCCTTGAACT GCTGAATTTCTGGACCCAAG[5]	329
ENSBTAG00000038149	NLR family pyrin domain containing 12	NLRP12	GCGGATTTTGTGGTTGAAGAT CCTTCACACAGCAGCAGCAC[6]	106
ENSBTAG00000014921	Interleukin 6	IL6	CTGGGTTCAATCAGGCGATT GGATCTGGATCAGTGTTCTGA[7]	150
ENSBTAG00000025471	Tumor necrosis factor	TNF	CCAGAGGGAAGAGCAGTCC GGAGAGTTGATGTCGGCTAC[8]	126
ENSBTAG00000026199	Actin beta	ACTB	ACACCGCAACCAGTTCGCCAT GTCAGGATGCCTCTCTTGCT[8]	216
ENSBTAG00000014731	Glyceraldehyde-3-phosphate dehydrogenase	GAPDH	ATCTCGCTCCTGGAAGATG TCGGAGTGAACGGATTCG[9]	227

[1]Magee et al., 2012; [2]Fujie et al., 2016; [3]Li et al., 2011; [4]Chitko-McKown et al., 2004; [5]Menzies and Ingham., 2006; [6]this study; [7]Arranz-Solís et al., 2016; [8]Regidor-Cerrillo et al., 2014; [9]Puech et al., 2015.

SUPPLEMENTARY TABLE 2 | Mapped and paired reads by sample against *B. taurus* genome

Sample	Total reads	Mapped reads	% mapped reads	High quality reads	% high quality reads	Splice reads	% splice reads
MØC R1	57978010	57066703	98.43	39294793	67.78	12982893	22.39
MØC R2	48884602	48177970	98.55	33370638	68.26	10548504	21.58
MØC R3	49634030	48097516	96.90	32464469	65.41	9432877	19.00
MØ1H R1	45726510	38902639	85.08	26406712	57.75	7926380	17.33
MØ1H R2	49810014	45221494	90.79	29675634	59.58	9187373	18.44
MØ1H R3	46709092	42000811	89.92	30077799	64.39	9428874	20.19
MØ7 R1	50818888	42614504	83.86	26894321	52.92	8298603	16.33
MØ7 R2	59129224	51174478	86.55	32684186	55.28	10153185	17.17
MØ7 R3	48795612	39459440	80.87	28423812	58.25	8812206	18.06
MØHK R1	45889532	45436847	99.01	31928506	69.58	10123030	22.06
MØHK R2	36301526	36482426	100.00	16726768	46.08	5510135	15.18
MØHK R3	51781248	48520326	93.70	32549263	62.86	10305755	19.90

MØC: Non-infected macrophages; MØ1H: Nc-Spain1H infected macrophages; MØ7: Nc-Spain1H infected macrophages; MØHK: macrophages inoculated with *N. caninum* heat-killed tachyzoites; R1-R3: Biological replicates 1-3 collected from three independent experiments.

SUPPLEMENTARY TABLE 3. Gene ontology analysis (Biological process) of differentially expressed genes in bovine macrophages inoculated with *Neospora caninum versus* non-infected macrophages

ID	Description	P. adj	geneID
			MØ1H vs MØC
GO:0006955	immune response	2,39E-05	A2M / ADM / AIF1 / ALCAM / ANXA1 / BATF / BPI / C1QA / C1S / C3 / CACNB3 / CASP4 / CCL2 / CCL20 / CCL4 / CCL5 / CCR7 / CD40 / CLEC7A / CNPY3 / COLEC12 / CSF2 / CSF3 / CTSS / ECSIT / EDA / ENPP2 / EZR / F2RL1 / FADD / FAS / FYN / GATA3 / GPR183 / HLX / HMGB2 / IFNAR2 / IL10 / IL12A / IL12B / IL15 / IL1A / IL1B / IL2RA7 / IL6 / IL7 / IRAK2 / IRF1 / LIF / LPO / LYST / MEF2C / MR1 / MX2 / NFIL3 / NLRC4 / NLRP3 / NMI / NOD2 / PHPT1 / POLR3D / PPARG / PRDX1 / PSEN1 / RIPK2 / RSAD2 / S100A12 / S100A8 / S100A9 / SAMHD1 / SBNO2 / SEMA4A / SERINC3 / TICAM1 / TKFC / TLR10 / TLR2 / TLR3 / TLR6 / TMEM173 / TNF / TNFAIP8L2 / TNFRSF1A / TRAFD1 / TRIM38 / UBE2N / VAMP8
GO:0006952	defense response	5,74E-05	A2M / ADM / AIF1 / ALOX5AP / ANXA1 / BATF / BPI / C1QA / C1S / C3 / CASP4 / CCL2 / CCL20 / CCL4 / CCL5 / CCR7 / CCRL2 / CD163 / CD40 / CLEC7A / CNPY3 / COLEC12 / CTNNBIP1 / DDIT4 / DEFB7 / ECSIT / F2R / F2RL1 / F3 / FABP4 / FADD / FAS / FYN / GATA3 / HMGB2 / HYAL2 / IFNAR2 / IL10 / IL12A / IL12B / IL15 / IL1A / IL1B / IL2RA / IL6 / IRAK2 / IRF1 / ITGB6 / ITIH4 / LPO / LYST / LYZ / MEF2C / MR1 / MX2 / NLRC4 / NLRP3 / NMI / NOD2 / NOS2 / NTHL1 / OLR1 / PDE2A / PLAC8 / POLR3D / PPARG / PRDX1 / PTGFR / PTGIR / PTGS2 / RIPK2 / RSAD2 / S100A12 / S100A8 / S100A9 / SAMHD1 / SBNO2 / SERINC3 / SERPINB10 / SERPINE1 / SLC25A19 / STAT5A / TICAM1 / TKFC / TLR10 / TLR2 / TLR3 / TLR6 / TMEM173 / TMEM39B / TNF / TNFAIP8L2 / TNFRSF1A / TRAFD1 / TRIM38 / VAMP8 / ZC3H12A
GO:0050729	positive regulation of inflammatory response	5,74E-05	CCL2 / CCL4 / CCL5 / FABP4 / HYAL2 / IL6 / NOD2 / PDE2A / S100A8 / S100A9 / SERPINE1 / STAT5A / TLR10 / TLR2 / TLR3 / TNF / TNFRSF1A / VAMP8
GO:0006954	inflammatory response	5,74E-05	A2M / AIF1 / ALOX5AP / ANXA1 / C3 / CASP4 / CCL2 / CCL20 / CCL4 / CCL5 / CCR7 / CCRL2 / CD163 / CD40 / CLEC7A / CTNNBIP1 / F2R / F2RL1 / F3 / FABP4 / FAS / GATA3 / HMGB2 / HYAL2 / IL10 / IL12B / IL1A / IL1B / IL2RA / IL6 / IRAK2 / ITGB6 / ITIH4 / NLRC4 / NLRP3 / NOD2 / NOS2 / OLR1 / PDE2A / PTGFR / PTGIR / PTGS2 / S100A12 / S100A8 / S100A9 / SBNO2 / SERPINE1 / STAT5A / TICAM1 / TLR10 / TLR2 / TLR3 / TLR6 / TNF / TNFAIP8L2 / TNFRSF1A / VAMP8 / ZC3H12A
GO:0031349	positive regulation of defense response	1,35E-04	CCL2 / CCL4 / CCL5 / COLEC12 / FABP4 / FADD / HYAL2 / IL12A / IL12B / IL6 / IRAK2 / IRF1 / MEF2C / NLRC4 / NOD2 / PDE2A / POLR3D / RIPK2 / RSAD2 / S100A8 / S100A9 / SERPINE1 / STAT5A / TKFC / TLR10 / TLR2 / TLR3 / TLR6 / TMEM173 / TNF / TNFRSF1A / VAMP8
GO:1902531	regulation of intracellular signal transduction	2,20E-04	ALS2CL / ARHGDIB / ARHGEF10L / ARL6IP5 / ATF3 / ATP6AP1 / BCL2L2 / CAPN3 / CAT / CAV2 / CCDC22 / CCL2 / CCL20 / CCL4 / CCL5 / CD40 / CDK12 / CDK5 / CDKN2D / CMKLR1 / CSF2 / CSF3 / CTGF / CTH / CYTH2 / DDIT4 / DSTYK / DUSP18 / DUSP26 / EDA / EDN1 / ELL3 / ERP29 / EZR / F2R / F2RL1 / F3 / FADD / FAS / FBXL2 / FGF1 / FIS1 / FYN / GAB1 / GADD45A / GADD45G / GATA3 / GNAI1 / GPR183 / HCRTR1 / HEXIM1 / HYAL2 / IGF1R / IGFBP4 / IKBKB / IL10 / IL12A / IL12B / IL1A / IL1B / IL6 / IL6 / INHBA / LAMTOR2 / LIF / LIMD1 / LPAR1 / MAPK7 / NENF / NLRP3 / NOD2 / PIK3IP1 / PKD2 / PLAUR / PPIF / PRDX1 / PRKCDBP / PROK2 / PSEN1 / RASA3 / RASAL3 / RCAN1 / RNF34 / S100A8 / S100A9 / SERINC3 / SLC44A2 / SLC9A3R1 / SOCS2 / SPRY1 / SPRY4 / TBC1D7 / TGFBR1 / TKFC / TNF / TRIB2 / TRIB3 / TRIM38 / TXNDC12 / UACA / UBE2N / UCHL1 / VDAC2 / ZC3H12A
GO:0002376	immune system process	5,16E-04	A2M / ACP6 / ACTN1 / ADA / ADM / AIF1 / ALCAM / ANXA1 / ANXA2 / AP3B1 / ATP6AP1 / AZI2 / BATF / BPI / C1QA / C1S / C3 / CACNB3 / CASP4 / CCL2 / CCL20 / CCL4 / CCL5 / CCR7 / CD40 / CITED2 / CLEC7A / CMKLR1 / CNPY3 / COLEC12 / CSF2 / CSF3 / CTNNBIP1 / CTSS / DDIT4 / ECSIT / EDA / EDNRB / ENPP2 / EZR / F2RL1 / FADD / FAS / FYN / GATA3 / GCNT1 / GPATCH4 / GPR183 / HLX / HMGB2 / HYAL2 / IFI30 / IFNAR2 / IKZF3 / IL10 / IL12A / IL12B / IL15 / IL1A / IL1B / IL2RA / IL6 / IL6 / IL7 / INHBA / IRAK2 / IRF1 / JUNB / LIF / LPO / LYST / MEF2C / MR1 / MX2 / MZB1 / NDRG1 / NFIL3 / NLRC4 / NLRP3 / NMI / NOD2 / NTHL1 / OLR1 / PHPT1 / POLR3D / PPARG / PRDX1 / PSEN1 / PSMB10 / PTMS / RASAL3 / RIPK2 / RSAD2 / S100A12 / S100A8 / S100A9 / S1PR1 / SAMHD1 / SBNO2 / SCIN / SEMA4A / SERINC3 / SERPINB10 / SERPINE1 / SFXN1 / SLC25A19 / SNX10 / STAT5A / STK10 / TGFBR1 / TICAM1 / TKFC / TLR10 / TLR2 / TLR3 / TLR6 / TMEM173 / TMEM39B / TNF / TNFAIP8L2 / TNFRSF1A / TRAFD1 / TRIM38 / UBE2N / VAMP8 / VEGFA / VEGFB / ZC3H12A
GO:0002684	positive regulation of immune system process	1,12E-03	A2M / AIF1 / ANXA1 / AP3B1 / ATP6AP1 / C1QA / C1S / C3 / CACNB3 / CCL2 / CCL20 / CCL4 / CCL5 / CMKLR1 / COLEC12 / CSF3 / CTNNBIP1 / EZR / F2RL1 / FADD / FYN / GATA3 / GPR183 / HLX / HMGB2 / IL12A / IL12B / IL15 / IL1A / IL6 / IL7 / INHBA / IRAK2 / IRF1 / LIF / MEF2C / MZB1 / NLRC4 / NLRP3 / NOD2 / PHPT1 / POLR3D / PSEN1 / RASAL3 / RIPK2 / RSAD2 / SCIN / SERPINE1 / STAT5A / TKFC / TLR10 / TLR2 / TLR3 / TLR6 / TMEM173 / TNF / UBE2N / VAMP8 / VEGFA / VEGFB
GO:0043067	regulation of programmed cell death	1,19E-03	AAMDC / ARL6IP5 / ASNS / ATF3 / BCL2A1 / BCL2L14 / BCL2L2 / BNIP3 / CAPN3 / CASP4 / CAT / CCL2 / CCL5 / CD40 / CDK5 / CDKN2D / CFDP1 / CITED2 / CSF2 / CTH / DCPS / DDB1 / EEF1A2 / ELL3 / ERCC3 / ERP29 / F2R / F3 / FADD / FAS / FIS1 / FXN / FYN / GADD45A / GADD45G / GATA3 / GCLM / GRK5 / HYAL2 / IFI6 / IGF1R / IKZF3 / IL10 / IL12A / IL12B / IL6 / IL7 / ING4 / INHBA / KANK2 / MAPK7 / MDM4 / MEF2C / NGF / NLE1 / NLRC4 / NLRP3 / NOD2 / PDIA3 / PLAC8 / PLAUR / PPARG / PPIF / PPT1 / PROK2 / PSEN1 / PSEN2 / RHOB / RIPK2 / RNF34 / RSL1D1 / S100A8 / S100A9 / SCIN / SERINC3 / SERPINE1 / SGK1 / SLC9A3R1 / STAT5A / TGFBR1 / TNF / TNFRSF1A / TRIM2 / TXNDC12 / VDAC2 / VIL1 / ZC3H12A
GO:0050663	cytokine secretion	1,23E-03	CASP4 / EZR / F2R / F2RL1 / GATA3 / HYAL2 / IL10 / IL12A / IL12B / IL1A / LPL / NLRC4 / NLRP3 / NOD2 / NOS2 / TLR10 / TLR2 / TLR6 / TNF / ZC3H12A
GO:0043207	response to external biotic stimulus	1,23E-03	ADM / BAIAP2 / BATF / BPI / CCL2 / CCL5 / CD40 / DDIT4 / DEFB7 / F2R / F2RL1 / FADD / FAS / GATA3 / HMGB2 / HYAL2 / IFNAR2 / IL10 / IL12A / IL12B / IL15 / IL6 / IL6 / IRAK2 / IRF1 / JUNB / LPO / LYZ / MEF2C / MR1 / MX2 / NLRC4 / NLRP3 / NOD2 / NOS2 / NPC2 / NTHL1 / PLAC8 / POLR3D / RSAD2 / SAMHD1 / SBNO2 / SCARB1 / SERINC3 / SERPINB10 / SERPINE1 / SLC25A19 / SNX3 / SRR / TICAM1 / TKFC / TLR2 / TLR3 / TLR6 / TMEM173 / TMEM39B / TNF / TNFRSF1A / TRIM38 / VIL1 / ZC3H12A

GO:0051707	response to other organism	1,23E-03	ADM / BAIAP2 / BATF / BPI / CCL2 / CCL5 / CD40 / DDIT4 / DEFB7 / F2R / F2RL1 / FADD / FAS / GATA3 / HMGB2 / HYAL2 / IFNAR2 / IL10 / IL12A / IL12B / IL15 / IL6 / IL6 / IRAK2 / IRF1 / JUNB / LPO / LYZ / MEF2C / MR1 / MX2 / NLRC4 / NLRP3 / NOD2 / NOS2 / NPC2 / NTHL1 / PLAC8 / POLR3D / RSAD2 / SAMHD1 / SBNO2 / SCARB1 / SERINC3 / SERPINB10 / SERPINE1 / SLC25A19 / SNX3 / SRR / TICAM1 / TKFC / TLR2 / TLR3 / TLR6 / TMEM173 / TMEM39B / TNF / TNFRSF1A / TRIM38 / VIL1 / ZC3H12A
GO:0007159	leukocyte cell-cell adhesion	1,23E-03	ADA / AIF1 / ANXA1 / AP3B1 / AZI2 / BATF / CCL2 / CCL5 / EZR / F2RL1 / FADD / FAS / FYN / GATA3 / GCNT1 / GPR183 / HLX / IL12A / IL12B / IL15 / IL6 / IL6 / IL7 / IRF1 / NLRP3 / NOD2 / PSEN1 / PSMB10 / RASAL3 / RSAD2 / S100A8 / S100A9 / STAT5A / TNF / TNFAIP8L2
GO:0002286	T cell activation involved in immune response	1,36E-03	ANXA1 / BATF / F2RL1 / GATA3 / GPR183 / HLX / IL12A / IL12B / IL6 / IL6 / NLRP3 / PSEN1
GO:0043408	regulation of MAPK cascade	1,80E-03	ARL6IP5 / ATF3 / ATP6AP1 / CAV2 / CCL2 / CCL20 / CCL4 / CCL5 / CD40 / CDK12 / CTGF / DSTYK / DUSP18 / DUSP26 / EDN1 / ERP29 / EZR / F2R / F2RL1 / FAS / FGF1 / GAB1 / GADD45A / GADD45G / GPR183 / HCRTR1 / HYAL2 / IGF1R / IGFBP4 / IL1A / IL1B / IL6 / INHBA / LAMTOR2 / LIF / LPAR1 / MAPK7 / NENF / NOD2 / PRDX1 / PRKCDBP / PROK2 / PSEN1 / SLC9A3R1 / SPRY1 / SPRY4 / TGFBR1 / TNF / TRIB2 / TRIB3 / UCHL1 / ZC3H12A
GO:0050707	regulation of cytokine secretion	2,87E-03	CASP4 / EZR / F2R / F2RL1 / GATA3 / HYAL2 / IL10 / IL1A / LPL / NLRP3 / NOD2 / TLR10 / TLR2 / TLR6 / TNF / ZC3H12A
GO:1903708	positive regulation of hemopoiesis	2,88E-03	ANXA1 / AP3B1 / ATP6AP1 / CSF3 / CTNNBIP1 / FADD / GATA3 / HLX / HMGB2 / IL12A / IL12B / IL15 / IL6 / IL7 / INHBA / LIF / NLRP3 / SCIN / STAT5A / TNF
GO:0006082	organic acid metabolic process	3,74E-03	AADAT / AASS / ABAT / ACACA / ACADS / ACADSB / ACAT1 / ACO1 / ACSF2 / AHCY / AHCYL2 / ALDH6A1 / ALKBH7 / ALOX5AP / APOA4 / ARG2 / ASNS / BCKDK / C3 / CROT / CRYL1 / CTH / DARS / DARS2 / DDAH2 / DDIT4 / DPYD / ECHS1 / EDN1 / ELOVL5 / ENO3 / ERO1A / ETFB / FABP4 / FADS2 / FADS3 / FADS6 / FAM213B / FASN / GAMT / GCDH / GCLM / GFPT2 / GGH / HACD4 / HIBADH / HK1 / IDH2 / IVD / LDHA / LPL / LPO / LTA4H / MARS2 / MECR / MPC1 / NAGK / NPL / OAT / OXSM / PC / PDHB / PFKFB2 / PFKL / PFKM / PGK1 / PHGDH / PNKD / PRDX4 / PRKAB1 / PSPH / PTGS2 / RARS2 / SDHB / SDS / SHMT1 / SRR / TECR / TNFRSF1A / TPI1 / TRIB3 / VNN1
GO:0048585	negative regulation of response to stimulus	3,80E-03	A2M / ADA / ADM / AIF1 / ANXA1 / ANXA2 / ARRB2 / ATF3 / BCL2L2 / CAV2 / CCDC22 / CCL2 / CCL5 / CCND1 / CDKN2D / CSF2 / CTNNBIP1 / DDIT4 / DLK2 / DUSP18 / DUSP26 / EID2 / ELL3 / EZR / FXN / GATA3 / GCLM / GPC1 / HLX / HTRA1 / HYAL2 / IFI6 / IGF1R / IL10 / IL12B / IL1RN / IL7 / KANK2 / LGMN / LIF / LIMD1 / MAPK7 / MZB1 / NENF / NLE1 / NLRP3 / PHACTR4 / PHPT1 / PIK3IP1 / PKD2 / PLAUR / PPARG / PPIF / PRKACA / PRKCDBP / PRR5L / PSEN1 / RASA3 / RASAL3 / RGS16 / RGS2 / RGS9 / RNF34 / SEMA3C / SEMA4A / SERPINE1 / SLC9A3R1 / SOCS2 / SPRY1 / SPRY4 / SPX / TBC1D7 / TGFBR1 / TKFC / TMEM88 / TNF / TNFAIP8L2 / TRAFD1 / TRIM38 / TXNDC12 / UCHL1 / VDAC2 / ZC3H12A
GO:0071345	cellular response to cytokine stimulus	3,80E-03	AIF1 / CCL2 / CCL20 / CCL4 / CCL5 / CCR7 / CCRL2 / CD40 / CSF3 / EDA / F3 / FADD / FAS / GAB1 / GATA3 / HYAL2 / IFNAR2 / IKBKB / IL12B / IL12RB2 / IL1A / IL1B / IL1RN / IL2RA / IL6 / IL6 / IRAK2 / IRF1 / NFIL3 / NMI / PDE2A / PPARG / PTGS2 / SBNO2 / SOCS2 / STAT5A / TMEM173 / TNF / TNFRSF1A / TUBA1A / ZC3H12A
GO:0002521	leukocyte differentiation	4,16E-03	ANXA1 / ANXA2 / AP3B1 / ATP6AP1 / AZI2 / BATF / CITED2 / CSF2 / CTNNBIP1 / F2RL1 / FADD / FAS / GATA3 / GPR183 / HLX / IKZF3 / IL12A / IL12B / IL15 / IL6 / IL6 / IL7 / IRF1 / JUNB / LIF / NLRP3 / PPARG / PSEN1 / RSAD2 / SBNO2 / SNX10 / STAT5A / TNF
GO:0051046	regulation of secretion	4,45E-03	ACTN1 / ANXA1 / ATP6AP1 / CASP4 / CCL5 / CDK5 / DNM1 / DTNBP1 / EDN1 / ERP29 / EZR / F2R / F2RL1 / GATA3 / GOLPH3L / HMGN3 / HYAL2 / IL10 / IL1A / IL6 / INHBA / IP6K3 / LIF / LPL / NLRP3 / NOD2 / PFKL / PFKM / PNKD / RAB26 / RHBDF1 / RSAD2 / S100A8 / SCIN / SDC1 / SERGEF / SERP1 / SLC9A3R1 / SPX / SYP / TLR10 / TLR2 / TLR6 / TNF / VAMP8 / ZC3H12A
GO:0042325	regulation of phosphorylation	6,28E-03	ARL6IP5 / ATF3 / ATP6AP1 / BCCIP / C3 / CAV2 / CCL2 / CCL20 / CCL4 / CCL5 / CCND1 / CCNT1 / CD40 / CDK12 / CDK5 / CDKN2D / CSF2 / CSF3 / CTGF / DDIT4 / DSTYK / DUSP18 / DUSP26 / EDN1 / EEF1A2 / ENPP2 / ERP29 / EZR / F2R / F2RL1 / FABP4 / FAS / FGF1 / FYN / GAB1 / GADD45A / GADD45G / GPR183 / HCRTR1 / HEXIM1 / HYAL2 / IGF1R / IGFBP4 / IKBKB / IL12A / IL12B / IL1A / IL1B / IL6 / IL6 / INHBA / IP6K3 / LAMTOR2 / LIF / LPAR1 / MAD2L2 / MAPK7 / NENF / NOD2 / PIK3IP1 / PIK3R3 / PKD2 / PKIG / PLAUR / PPIF / PRDX1 / PRKAB1 / PRKAR2B / PRKCDBP / PROK2 / PRR5L / PSEN1 / PTGS2 / RIPK2 / SLC9A3R1 / SOCS2 / SPRY1 / SPRY4 / TADA3 / TGFBR1 / TNF / TRIB2 / TRIB3 / TWF1 / UCHL1 / VEGFA / ZC3H12A
GO:0046634	regulation of alpha-beta T cell activation	9,40E-03	ANXA1 / AP3B1 / GATA3 / HLX / IL12A / IL12B / IL6 / IRF1 / NLRP3 / RASAL3
GO:0010648	negative regulation of cell communication	9,40E-03	ADA / ADM / ARRB2 / ATF3 / BCL2L2 / CAV2 / CCDC22 / CCL5 / CCND1 / CDKN2D / CSF2 / CTNNBIP1 / DDIT4 / DLK2 / DUSP18 / DUSP26 / EID2 / ELL3 / EZR / FXN / GATA3 / GCLM / GPC1 / HTRA1 / HYAL2 / IFI6 / IGF1R / IL1RN / IL6 / IL7 / KANK2 / LGMN / LIF / LIMD1 / MAPK7 / NLE1 / NLRP3 / PFKL / PHACTR4 / PHPT1 / PIK3IP1 / PKD2 / PLAUR / PNKD / PPARG / PPIF / PRKACA / PRKCDBP / PRR5L / PSEN1 / RASA3 / RASAL3 / RGS16 / RGS2 / RGS9 / RNF34 / SERPINE1 / SLC9A3R1 / SOCS2 / SPRY1 / SPRY4 / TBC1D7 / TGFBR1 / TKFC / TMEM88 / TNF / TXNDC12 / UCHL1 / VDAC2 / ZC3H12A
GO:0023057	negative regulation of signaling	9,40E-03	ADA / ADM / ARRB2 / ATF3 / BCL2L2 / CAV2 / CCDC22 / CCL5 / CCND1 / CDKN2D / CSF2 / CTNNBIP1 / DDIT4 / DLK2 / DUSP18 / DUSP26 / EID2 / ELL3 / EZR / FXN / GATA3 / GCLM / GPC1 / HTRA1 / HYAL2 / IFI6 / IGF1R / IL1RN / IL6 / IL7 / KANK2 / LGMN / LIF / LIMD1 / MAPK7 / NLE1 / NLRP3 / PFKL / PHACTR4 / PHPT1 / PIK3IP1 / PKD2 / PLAUR / PNKD / PPARG / PPIF / PRKACA / PRKCDBP / PRR5L / PSEN1 / RASA3 / RASAL3 / RGS16 / RGS2 / RGS9 / RNF34 / SERPINE1 / SLC9A3R1 / SOCS2 / SPRY1 / SPRY4 / TBC1D7 / TGFBR1 / TKFC / TMEM88 / TNF / TXNDC12 / UCHL1 / VDAC2 / ZC3H12A
GO:1903039	positive regulation of leukocyte cell-cell adhesion	1,02E-02	AIF1 / ANXA1 / AP3B1 / CCL2 / CCL5 / FADD / GATA3 / HLX / IL12A / IL12B / IL15 / IL6 / IL7 / NLRP3 / NOD2 / RASAL3 / STAT5A / TNF
GO:0034097	response to cytokine	1,11E-02	AIF1 / CCL2 / CCL20 / CCL4 / CCL5 / CCR7 / CCRL2 / CD40 / CSF3 / EDA / F3 / FADD / FAS / GAB1 / GATA3 / HYAL2 / IFNAR2 / IKBKB / IL12B / IL12RB2 / IL1A / IL1B / IL1RN / IL2RA / IL6 / IL6 / IRAK2 / IRF1 / JUNB / MAPK7 / NFIL3 / NMI / PDE2A / PPARG / PTGS2 / SBNO2 / SOCS2 / STAT5A / TIMP2 / TMEM173 / TNF / TNFRSF1A / TUBA1A / ZC3H12A
GO:0001817	regulation of cytokine production	1,12E-02	ANXA1 / CASP4 / CCL2 / CMKLR1 / CSF2 / EZR / F2R / F2RL1 / FADD / GATA3 / HIF1A / HYAL2 / IL10 / IL12A / IL12B / IL15 / IL1A / IL6 / IRF1 / LPL / NLRP3 / NOD2 / NOS2 / POLR3D / RIPK2 / RSAD2 / SERPINE1 / STAT5A / TKFC / TLR10 / TLR2 / TLR3 / TLR6 / TMEM173 / TNF / TRIB2 / TRIM38 / ZC3H12A

GO:0016310	phosphorylation	1,22E-02	ACVR2B / AK4 / ARL6IP5 / ATF3 / ATP6AP1 / BCCIP / BCKDK / C3 / CAV2 / CCL2 / CCL20 / CCL4 / CCL5 / CCND1 / CCNT1 / CD40 / CDK12 / CDK5 / CDKN2D / CSF2 / CSF3 / CSNK1G1 / CTGF / DCAKD / DDIT4 / DSTYK / DUSP18 / DUSP26 / EDN1 / EEF1A2 / ENO3 / ENPP2 / ERCC3 / ERP29 / EZR / F2R / F2RL1 / FABP4 / FAS / FASTKD3 / FGF1 / FXN / FYN / GAB1 / GADD45A / GADD45G / GALK1 / GK5 / GPR183 / GRK5 / HCRTR1 / HEXIM1 / HK1 / HYAL2 / HYKK / IGF1R / IGFBP4 / IKBKB / IL12A / IL12B / IL15 / IL1A / IL1B / IL6 / IL6 / INHBA / IP6K3 / IRAK2 / LAMTOR2 / LIF / LIMD1 / LPAR1 / MAD2L2 / MAPK7 / MEF2C / MVK / MYLK / NAGK / NENF / NLK / NOD2 / NOL9 / PDXK / PFKFB2 / PFKL / PFKM / PGK1 / PIK3IP1 / PIK3R3 / PIP4K2C / PKD2 / PKIG / PLAUR / PPIF / PPM1L / PRDX1 / PRKAB1 / PRKACA / PRKAR2B / PRKCDBP / PROK2 / PRR5L / PSEN1 / PTGS2 / RIPK2 / ROCK2 / RSRC1 / SGK1 / SLC9A3R1 / SOCS2 / SPRY1 / SPRY4 / STK10 / TADA3 / TBRG4 / TGFBR1 / TKFC / TNF / TPI1 / TRIB2 / TRIB3 / TWF1 / UCHL1 / UQCC3 / USP15 / VEGFA / XYLB / ZC3H12A
GO:0001816	cytokine production	1,23E-02	ANXA1 / AZI2 / BATF / CASP4 / CCL2 / CMKLR1 / CSF2 / EZR / F2R / F2RL1 / FABP4 / FADD / GATA3 / HIF1A / HYAL2 / IL10 / IL12A / IL12B / IL15 / IL1A / IL6 / IRF1 / LPL / MR1 / NLRC4 / NLRP3 / NOD2 / NOS2 / POLR3D / RIPK2 / RSAD2 / SERPINE1 / STAT5A / TKFC / TLR10 / TLR2 / TLR3 / TLR6 / TMEM173 / TNF / TRIB2 / TRIM38 / ZC3H12A
GO:0045321	leukocyte activation	1,36E-02	ADA / AIF1 / ANXA1 / AP3B1 / AZI2 / BATF / CCL2 / CCL5 / CD40 / CSF2 / F2RL1 / FADD / FAS / FYN / GATA3 / GPR183 / HLX / HYAL2 / IKZF3 / IL10 / IL12A / IL12B / IL15 / IL6 / IL6 / IL7 / IRF1 / MEF2C / MZB1 / NDRG1 / NLRP3 / NOD2 / PSEN1 / PSMB10 / RASAL3 / RSAD2 / S100A12 / SBNO2 / STAT5A / TNFAIP8L2 / VAMP8
GO:0042990	regulation of transcription factor import into nucleus	1,40E-02	CCDC22 / CSF3 / EDA / MAPK7 / NLRP3 / PKD2 / PRDX1 / TMEM173 / TNF / ZC3H12A
GO:0042991	transcription factor import into nucleus	1,40E-02	CCDC22 / CSF3 / EDA / MAPK7 / NLRP3 / PKD2 / PRDX1 / TMEM173 / TNF / ZC3H12A
GO:0070201	regulation of establishment of protein localization	1,40E-02	ATG13 / CABP1 / CASP4 / CCDC22 / CCL5 / CDK5 / CSF3 / EDA / ERP29 / EZR / F2R / F2RL1 / FIS1 / GATA3 / GOLPH3L / HMGN3 / HNMT / HYAL2 / IL10 / IL1A / IL6 / IP6K3 / LPL / MAPK7 / MYO1C / NLRP3 / NOD2 / PDE2A / PFKL / PFKM / PKD2 / PRDX1 / PRKACA / PRR5L / RHBDF1 / RSAD2 / SERGEF / SERP1 / SLC9A3R1 / SNAP25 / SNX3 / TGFBR1 / TLR10 / TLR2 / TLR6 / TMEM173 / TMEM30A / TMEM59 / TNF / ZC3H12A
GO:0006509	membrane protein ectodomain proteolysis	1,55E-02	BACE1 / IL10 / PSEN1 / PSEN2 / TIMP2 / TIMP3 / TIMP4 / TNF
GO:0006732	coenzyme metabolic process	1,67E-02	AADAT / AASS / ACACA / AHCY / AHCYL2 / CROT / DCAKD / DCXR / DDIT4 / ELOVL5 / ENO3 / FAR2 / GAMT / GGH / HK1 / MAT2B / MOCOS / MPC1 / MTHFD1L / MTHFD2 / MVK / NADSYN1 / NAPRT / NNT / PDHB / PDXK / PFKFB2 / PFKL / PFKM / PGK1 / SHMT1 / TPI1 / VNN1
GO:0032943	mononuclear cell proliferation	1,92E-02	AIF1 / ANXA1 / AZI2 / CCL5 / FADD / FYN / GPR183 / IKZF3 / IL10 / IL12A / IL12B / IL15 / IL6 / IL6 / IL7 / IRF1 / MEF2C / MZB1 / PSMB10 / RASAL3 / STAT5A
GO:0006468	protein phosphorylation	2,00E-02	ACVR2B / ARL6IP5 / ATF3 / ATP6AP1 / BCCIP / BCKDK / C3 / CAV2 / CCL2 / CCL20 / CCL4 / CCL5 / CCND1 / CCNT1 / CD40 / CDK12 / CDK5 / CDKN2D / CSF2 / CSF3 / CSNK1G1 / CTGF / DDIT4 / DSTYK / DUSP18 / DUSP26 / EDN1 / ENPP2 / ERCC3 / ERP29 / EZR / F2R / F2RL1 / FABP4 / FAS / FASTKD3 / FGF1 / FYN / GAB1 / GADD45A / GADD45G / GPR183 / GRK5 / HCRTR1 / HEXIM1 / HYAL2 / IGF1R / IGFBP4 / IKBKB / IL12A / IL12B / IL15 / IL1A / IL1B / IL6 / IL6 / INHBA / IRAK2 / LAMTOR2 / LIF / LPAR1 / MAD2L2 / MAPK7 / MEF2C / MYLK / NENF / NLK / NOD2 / PKD2 / PKIG / PLAUR / PPM1L / PRDX1 / PRKAB1 / PRKACA / PRKAR2B / PRKCDBP / PROK2 / PRR5L / PSEN1 / PTGS2 / RIPK2 / ROCK2 / RSRC1 / SGK1 / SLC9A3R1 / SOCS2 / SPRY1 / SPRY4 / STK10 / TADA3 / TBRG4 / TGFBR1 / TNF / TRIB2 / TRIB3 / TWF1 / UCHL1 / USP15 / VEGFA / ZC3H12A
GO:0051249	regulation of lymphocyte activation	2,07E-02	AIF1 / ANXA1 / AP3B1 / CCL2 / CCL5 / FADD / FAS / GATA3 / GPR183 / HLX / IKZF3 / IL10 / IL12A / IL12B / IL15 / IL6 / IL7 / IRF1 / MEF2C / MZB1 / NLRP3 / NOD2 / RASAL3 / STAT5A / TNFAIP8L2
GO:1901575	organic substance catabolic process	2,20E-02	AADAT / AASS / ABAT / ABHD12 / ABHD2 / ACADS / ACADSB / ACAT1 / ADA / AGO3 / ANXA2 / APOA4 / BACE1 / BCKDK / BNIP3 / CAPN2 / CCDC22 / CDK5 / CNDP2 / CROT / CTSC / CTSS / DCPS / DDAH2 / DDB1 / DDIT4 / DERA / DERL3 / DHDH / DNASE2 / DPYD / ECHS1 / ENO3 / ENPP2 / ERCC8 / ETF1 / ETFB / EZR / FBXL2 / FUCA1 / FYN / GALM / GCDH / GK5 / GPC1 / GPD2 / HIBADH / HK1 / HNMT / HPSE / HSD17B14 / HYAL2 / IAH1 / IL10 / IP6K3 / IVD / LGMN / LPL / LTA4H / LYVE1 / MAD2L2 / MAOA / NAGA / NAGK / NEU3 / NPL / NUB1 / NUDT16 / OAT / OS9 / PAFAH2 / PAG1 / PDE2A / PDXP / PFKFB2 / PFKL / PFKM / PGK1 / PLA2G7 / PLBD1 / PLD3 / PNKD / PNPLA2 / PNRC2 / PPP1R3B / PPT1 / PRKACA / PRR5L / PSEN1 / PSMB10 / RETN / RHBDF1 / RNASEH2C / RNF144B / RNF34 / SAMHD1 / SAT2 / SCARB1 / SDF2L1 / SDS / SMG9 / SMPDL3A / SND1 / SNX3 / SORD / SPOP / TIMP2 / TIMP3 / TIMP4 / TMUB1 / TNF / TPI1 / TPP1 / TRIB2 / TRIB3 / TRIM38 / UBE2H / UBE2N / UBXN8 / UCHL1 / USP12 / USP14 / USP15 / USP20 / USP37 / VPS28 / ZC3H12A
GO:0050790	regulation of catalytic activity	2,27E-02	A2M / ACTN1 / ALOX5AP / ALS2CL / ANXA1 / ANXA2 / APOA4 / ARHGAP15 / ARHGDIB / ARHGEF10L / ARL6IP5 / ARRDC3 / BCAR3 / BCCIP / C3 / CAPN3 / CAST / CAV2 / CCL2 / CCL20 / CCL4 / CCL5 / CCND1 / CCNT1 / CDC42EP1 / CDC42EP2 / CDK12 / CDK5 / CDKN2D / CHN1 / CYTH2 / DSTYK / DUSP18 / DUSP26 / ECSIT / EDN1 / EEF1A2 / EIF2B3 / ERP29 / F2R / F3 / FABP4 / FADD / FAS / FGF1 / FGL2 / FIS1 / FXN / GAB1 / GABARAPL2 / GADD45A / GADD45G / GCLM / HEXIM1 / HMGB2 / HYAL2 / IFI6 / IGF1R / IKBKB / IL12B / IL7 / ITIH4 / LAMTOR2 / LPAR1 / MAD2L2 / MAPK7 / MAT2B / MEF2C / NGF / NIFK / NLE1 / NLRC4 / NLRP3 / NOS2 / PHACTR4 / PHPT1 / PIK3IP1 / PIK3R3 / PKD2 / PKIG / PLAUR / PPARG / PPIF / PPP1R3C / PRKAB1 / PRKAR2B / PROK2 / PSAP / PSEN1 / PSEN2 / RANGRF / RASA3 / RASAL3 / RASGEF1B / RCAN1 / RGS16 / RGS2 / RGS9 / RNF34 / S100A8 / S100A9 / SCARB1 / SERGEF / SERPINB1 / SERPINB10 / SERPINB6 / SERPINE1 / SLC9A3R1 / SOCS2 / SPRY4 / TBC1D1 / TBC1D7 / TFPI2 / TGFBR1 / TIMP2 / TIMP3 / TIMP4 / TNF / TRAPPC4 / TRIB2 / TRIB3 / UBE2N / UCHL1 / VIL1
GO:0044712	single-organism catabolic process	2,78E-02	AADAT / AASS / ABAT / ABHD12 / ABHD2 / ACADS / ACADSB / ACAT1 / ADA / APOA4 / BCKDK / CROT / CTSS / DDAH2 / DDIT4 / DERA / DERL3 / DHDH / DPYD / ECHS1 / ENO3 / ENPP2 / ETFB / FUCA1 / GALM / GCDH / GK5 / GPD2 / HIBADH / HK1 / HSD17B14 / IAH1 / IVD / LPL / MMP2 / NAGA / NAGK / NEU3 / NPL / NUDT16 / OAT / OS9 / PAFAH2 / PDE2A / PFKFB2 / PFKL / PFKM / PGK1 / PLA2G7 / PLBD1 / PLD3 / PNKD / PNPLA2 / PPP1R3B / PPT1 / RETN / SAMHD1 / SCARB1 / SDF2L1 / SDS / SMPDL3A / SORD / TMUB1 / TNF / TPI1 / UBXN8
GO:0009636	response to toxic substance	2,81E-02	CAT / CCL4 / CCL5 / CSN1S1 / FAS / GPX3 / GPX7 / LPO / PRDX1 / PRDX4 / PTGS2 / S100A8 / S100A9 / TNF / TXNRD1 / TXNRD2

GO:0044093	positive regulation of molecular function	2,81E-02	ALOX5AP / ALS2CL / ANXA2 / APOA4 / ARHGAP15 / ARHGDIB / ARHGEF10L / ARL6IP5 / ARRDC3 / BCAR3 / CAPN3 / CAT / CAV2 / CCL2 / CCL20 / CCL4 / CCL5 / CCND1 / CCNT1 / CDC42EP1 / CDC42EP2 / CDK5 / CHN1 / CSF3 / CTH / CTSS / CYTH2 / DSTYK / EDA / EDN1 / EEF1A2 / EIF2B3 / ERP29 / F2R / F3 / FADD / FGF1 / FGL2 / FIS1 / FXN / GAB1 / GABARAPL2 / GADD45A / GADD45G / GATA3 / GCLM / HMGB2 / HMGN3 / IKBKB / IL10 / IL12B / IL6 / IRAK2 / LAMTOR2 / LPAR1 / MEF2C / NDP / NLRP3 / NOD2 / NOS2 / PHACTR4 / PKD2 / PLAUR / PPARG / PROK2 / PSAP / PSEN1 / PSEN2 / RANGRF / RASA3 / RASAL3 / RASGEF1B / RGS16 / RGS2 / RGS9 / RIPK2 / S100A8 / S100A9 / SCARB1 / SERGEF / SGK1 / TBC1D1 / TBC1D7 / TGFBR1 / TMEM173 / TNF / TRAPPC4 / TRIB3 / TRIM38 / UBE2N
GO:0016032	viral process	3,20E-02	CAV2 / CCL4 / CCL5 / CCNT1 / DDB1 / DDIT4 / F2RL1 / FADD / GATA3 / HYAL2 / IFNAR2 / IL12A / IL12B / IL15 / IL6 / IL6 / IRF1 / ITGAV / ITGB6 / MVB12A / MX2 / NLRP3 / NPC2 / NTHL1 / PC / POLR3D / PPIB / PTBP1 / RSAD2 / SAMHD1 / SERINC3 / SERPINB10 / SLC25A19 / SNX3 / TICAM1 / TKFC / TLR3 / TMEM173 / TMEM39B / TNF / TRIM38 / VAMP8 / ZC3H12A
GO:0050793	regulation of developmental process	3,92E-02	AAMDC / ADM / ANXA1 / AP3B1 / ARHGAP15 / ARHGDIB / ATP6AP1 / BAIAP2 / BRINP1 / CAPN3 / CCDC151 / CCL2 / CCND1 / CDC42EP1 / CDC42EP2 / CDK5 / CFDP1 / CHN1 / CITED2 / CMKLR1 / CREB1 / CSF2 / CSF3 / CSNK1G1 / CTGF / CTNNBIP1 / DLK2 / EDN1 / EDNRB / ELL3 / ENPP2 / EZR / F3 / FADD / FAS / FGF1 / FIS1 / FXN / FYN / GAMT / GATA3 / GPC1 / GPR183 / HLX / HMGB2 / ID3 / IKBKB / IKZF3 / IL12A / IL12B / IL15 / IL1A / IL1RN / IL6 / IL7 / INHBA / IP6K3 / IRF1 / JUNB / LIF / LIMD1 / LPAR1 / LPL / MAFF / MAFG / MAPK7 / MEDAG / MEF2C / MSR1 / MYH10 / NGF / NLRP3 / PLAC8 / PPARG / PPIB / PRKACA / PROK2 / PSEN1 / PTBP1 / PTGS2 / RHOB / RSL1D1 / S1PR1 / SCIN / SDC2 / SEMA3C / SEMA4A / SERP1 / SERPINE1 / SLC9A3R1 / SNAP25 / SNX3 / SPRY1 / STAT5A / TAF8 / TBC1D7 / TGFBR1 / TMEM30A / TNF / TRIB2 / TRIB3 / TSPAN12 / VEGFA / VEGFB / VIL1 / YWHAG / ZC3H12A
GO:0044403	symbiosis, encompassing mutualism through parasitism	3,92E-02	CAV2 / CCL4 / CCL5 / CCNT1 / DDB1 / DDIT4 / F2RL1 / FADD / GATA3 / HYAL2 / IFNAR2 / IL12A / IL12B / IL15 / IL6 / IL6 / IRF1 / ITGAV / ITGB6 / MVB12A / MX2 / NLRP3 / NPC2 / NTHL1 / PC / POLR3D / PPIB / PTBP1 / RSAD2 / SAMHD1 / SCARB1 / SERINC3 / SERPINB10 / SLC25A19 / SNX3 / TICAM1 / TKFC / TLR3 / TMEM173 / TMEM39B / TNF / TRIM38 / VAMP8 / ZC3H12A
GO:0044419	interspecies interaction between organisms	3,92E-02	CAV2 / CCL4 / CCL5 / CCNT1 / DDB1 / DDIT4 / F2RL1 / FADD / GATA3 / HYAL2 / IFNAR2 / IL12A / IL12B / IL15 / IL6 / IL6 / IRF1 / ITGAV / ITGB6 / MVB12A / MX2 / NLRP3 / NPC2 / NTHL1 / PC / POLR3D / PPIB / PTBP1 / RSAD2 / SAMHD1 / SCARB1 / SERINC3 / SERPINB10 / SLC25A19 / SNX3 / TICAM1 / TKFC / TLR3 / TMEM173 / TMEM39B / TNF / TRIM38 / VAMP8 / ZC3H12A
GO:0010883	regulation of lipid storage	3,92E-02	ALKBH7 / C3 / LPL / MSR1 / PNPLA2 / PPARG / SCARB1 / ZC3H12A
GO:0046822	regulation of nucleocytoplasmic transport	3,93E-02	CABP1 / CCDC22 / CDK5 / CSF3 / EDA / HYAL2 / MAPK7 / NLRP3 / PDE2A / PKD2 / PRDX1 / PRKACA / SLC9A3R1 / TGFBR1 / TMEM173 / TNF / ZC3H12A
GO:0098869	cellular oxidant detoxification	4,46E-02	CAT / CSN1S1 / GPX3 / GPX7 / LPO / PRDX1 / PRDX4 / PTGS2 / S100A8 / S100A9 / TNF / TXNRD1 / TXNRD2
GO:0032944	regulation of mononuclear cell proliferation	4,59E-02	AIF1 / ANXA1 / CCL5 / FADD / GPR183 / IKZF3 / IL10 / IL12A / IL12B / IL15 / IL6 / IL7 / IRF1 / MEF2C / MZB1 / RASAL3 / STAT5A
GO:0010647	positive regulation of cell communication	4,94E-02	ACPP / ARL6IP5 / ARRDC3 / ATF3 / ATP6AP1 / C3 / CAT / CAV2 / CCDC22 / CCL2 / CCL20 / CCL4 / CCL5 / CD40 / CD63 / CITED2 / CSF2 / CSF3 / CTGF / CTH / DSTYK / DTNBP1 / EDA / EDN1 / ERP29 / F2R / F2RL1 / F3 / FADD / FAS / FGF1 / FIS1 / FYN / GAB1 / GADD45A / GADD45G / GATA3 / GPR183 / HCRTR1 / HEXIM1 / HYAL2 / IGFBP4 / IL10 / IL12A / IL12B / IL1A / IL1B / IL6 / INHBA / LAMTOR2 / LIF / LPAR1 / MYO1C / NENF / NLE1 / NOD2 / NUCKS1 / PAIP2 / PFKM / PKD2 / PLAUR / PPIF / PRKCDBP / PROK2 / PSEN1 / RSAD2 / S100A8 / S100A9 / SERINC3 / SERP1 / SLC44A2 / SLC9A3R1 / SNAP25 / TGFBR1 / TNF / TRIM38 / TSPAN17 / UBE2N / VAMP8 / ZC3H12A

MØ7 *vs* MØC			
GO:0050729	positive regulation of inflammatory response	5,69E-06	CCL2 / CCL4 / CCL5 / FABP4 / HYAL2 / IL6 / NOD2 / PDE2A / S100A8 / S100A9 / SERPINE1 / STAT5A / TLR10 / TLR2 / TLR3 / TNF / TNFRSF1A / VAMP8
GO:0006955	immune response	5,69E-06	A2M / ADM / ALCAM / ANXA1 / BATF / BPI / C1QA / C1QB / C1S / C3 / CASP4 / CCL2 / CCL20 / CCL4 / CCL5 / CCR7 / CD40 / CLEC7A / CNPY3 / COLEC12 / CSF2 / CSF3 / CTSS / EDA / ENPP2 / EZR / F2RL1 / FADD / FAS / FYN / GPR183 / HLX / IL10 / IL12B / IL15 / IL1A / IL1B / IL2RA / IL6 / IL6 / IL7 / IRAK2 / IRF1 / LIF / LPO / LYST / MEF2C / MR1 / MX2 / NFIL3 / NLRC4 / NMI / NOD2 / POLR3D / PPARG / PRDX1 / PSEN1 / RIPK2 / RSAD2 / S100A12 / S100A8 / S100A9 / SAMHD1 / SEMA4A / SERINC3 / TICAM1 / TKFC / TLR10 / TLR2 / TLR3 / TLR6 / TMEM173 / TNF / TNFAIP8L2 / TNFRSF1A / TRAFD1 / TRIM38 / VAMP8
GO:0031349	positive regulation of defense response	9,10E-06	CCL2 / CCL4 / CCL5 / COLEC12 / FABP4 / FADD / HYAL2 / IL12B / IL6 / IRAK2 / IRF1 / MEF2C / NLRC4 / NOD2 / PDE2A / POLR3D / RIPK2 / RSAD2 / S100A8 / S100A9 / SERPINE1 / STAT5A / TKFC / TLR10 / TLR2 / TLR3 / TLR6 / TMEM173 / TNF / TNFRSF1A / VAMP8
GO:0006954	inflammatory response	7,59E-05	A2M / ANXA1 / C3 / CASP4 / CCL2 / CCL20 / CCL4 / CCL5 / CCR7 / CCRL2 / CD163 / CD40 / CLEC7A / CTNNBIP1 / F2R / F2RL1 / F3 / FABP4 / FAS / HRH1 / HYAL2 / IL10 / IL12B / IL1A / IL1B / IL2RA / IL6 / IRAK2 / ITGB6 / ITIH4 / NLRC4 / NOD2 / NOS2 / PDE2A / PTGIR / PTGS2 / S100A12 / S100A8 / S100A9 / SERPINE1 / STAT5A / TICAM1 / TLR10 / TLR2 / TLR3 / TLR6 / TNF / TNFAIP8L2 / TNFRSF1A / VAMP8 / ZC3H12A
GO:1902531	regulation of intracellular signal transduction	2,37E-04	ALS2CL / ARHGEF10L / ARL6IP5 / ATF3 / BCL2L2 / CAPN3 / CAT / CAV2 / CCDC22 / CCL2 / CCL20 / CCL4 / CCL5 / CD40 / CDK12 / CDKN2D / CHP1 / CMKLR1 / CSF2 / CSF3 / CTGF / CYTH2 / DUSP18 / DUSP26 / EDA / EDN1 / ELL3 / ERP29 / EZR / F2R / F2RL1 / F3 / FADD / FAS / FBXL2 / FGF1 / FYN / GAB1 / GADD45A / GADD45G / GNAI1 / GPR183 / HCRTR1 / HEXIM1 / HYAL2 / IGF1R / IGFBP4 / IL10 / IL12B / IL1A / IL1B / IL6 / IL6 / LAMTOR2 / LIF / LIMD1 / MAPK7 / MEN1 / NENF / NOD2 / PIK3IP1 / PKD2 / PPIF / PRDX1 / PRKCDBP / PSEN1 / RASA3 / RASAL3 / RCAN1 / RNF34 / S100A8 / S100A9 / SERINC3 / SLC9A3R1 / SOCS2 / SPRY1 / SPRY2 / SPRY4 / TBC1D7 / TGFBR1 / TKFC / TNF / TRIB2 / TRIB3 / TRIM38 / TXNDC12 / UACA / UCHL1 / VDAC2 / ZC3H12A
GO:0043408	regulation of MAPK cascade	2,37E-04	ARL6IP5 / ATF3 / CAV2 / CCL2 / CCL20 / CCL4 / CCL5 / CD40 / CDK12 / CTGF / DUSP18 / DUSP26 / EDN1 / ERP29 / EZR / F2R / F2RL1 / FAS / FGF1 / GAB1 / GADD45A / GADD45G / GPR183 / HCRTR1 / HYAL2 / IGF1R / IGFBP4 / IL1A / IL1B / IL6 / LAMTOR2 / LIF / MAPK7 / MEN1 / NENF / NOD2 / PRDX1 / PRKCDBP / PSEN1 / SLC9A3R1 / SPRY1 / SPRY2 / SPRY4 / TGFBR1 / TNF / TRIB2 / TRIB3 / UCHL1 / ZC3H12A
GO:0042981	regulation of apoptotic process	4,70E-04	AAMDC / AIFM2 / ARL6IP5 / ASNS / ATF3 / BCL2A1 / BCL2L14 / BCL2L2 / BNIP3 / CAPN3 / CASP4 / CAT / CCL2 / CCL5 / CD40 / CDKN2D / CFDP1 / CITED2 / CSF2 / DDB1 / ELL3 / ERCC3 / ERP29 / F2R / F3 / FADD / FAM162A / FAS / FYN / GADD45A / GADD45G / GCLM / GRK5 / HYAL2 / IFI6 / IGF1R / IKZF3 / IL10 / IL12B / IL6 / IL7 / MAPK7 / MDM4 / MEF2C / NLE1 / NLRC4 / NOD2 / NR4A1 / PDIA3 / PLAC8 / PPARG / PPIF / PPT1 / PSEN1 / PSEN2 / RHOB / RIPK2 / RNF34 / RSL1D1 / S100A8 / S100A9 / SCIN / SERINC3 / SERPINE1 / SGK1 / SLC9A3R1 / SPRY2 / STAT5A / TGFBR1 / TNF / TNFRSF1A / TRIM2 / TXNDC12 / VDAC2 / VIL1 / ZC3H12A
GO:0002376	immune system process	6,98E-04	A2M / ACP6 / ACTN1 / ADM / ALCAM / ANXA1 / AP3B1 / AZI2 / BATF / BPI / C1QA / C1QB / C1S / C3 / CASP4 / CCL2 / CCL20 / CCL4 / CCL5 / CCR7 / CD40 / CITED2 / CLEC7A / CMKLR1 / CNPY3 / COLEC12 / CSF2 / CSF3 / CTNNBIP1 / CTSS / EDA / EDNRB / ENPP2 / EZR / F2RL1 / FADD / FAS / FOS / FYN / GCNT1 / GPATCH4 / GPR183 / HLX / HRH1 / HYAL2 / IKZF3 / IL10 / IL12B / IL15 / IL1A / IL1B / IL2RA / IL6 / IL6 / IL7 / IRAK2 / IRF1 / JUNB / LIF / LPO / LYST / MEF2C / MR1 / MX2 / MZB1 / NDRG1 / NFIL3 / NLRC4 / NMI / NOD2 / POLR3D / PPARG / PRDX1 / PSEN1 / PSMB10 / PTMS / RASAL3 / RIPK2 / RSAD2 / S100A12 / S100A8 / S100A9 / S1PR1 / SAMHD1 / SCIN / SEMA4A / SERINC3 / SERPINE1 / SFXN1 / SLC25A19 / SNX10 / STAT5A / TGFBR1 / TICAM1 / TKFC / TLR10 / TLR2 / TLR3 / TLR6 / TMEM173 / TNF / TNFAIP8L2 / TNFRSF1A / TRAFD1 / TRIM38 / VAMP8 / VEGFA / VEGFB / ZC3H12A
GO:0048585	negative regulation of response to stimulus	9,28E-04	A2M / ADM / ANXA1 / ARRB2 / ATF3 / BCL2L2 / CAV2 / CCDC22 / CCL2 / CCL5 / CCND1 / CDKN2D / CHP1 / CSF2 / CTNNBIP1 / DLK2 / DUSP18 / DUSP26 / ELL3 / EZR / F12 / GCLM / GPC1 / HLX / HTRA1 / HYAL2 / IFI6 / IGF1R / IL10 / IL12B / IL1RN / IL7 / LGMN / LIF / LIMD1 / MAPK7 / MEN1 / MZB1 / NENF / NLE1 / PHACTR4 / PIK3IP1 / PKD2 / PPARG / PPIF / PRKACA / PRKCDBP / PRR5L / PSEN1 / RASA3 / RASAL3 / RGS19 / RGS2 / RGS9 / RNF34 / SEMA3C / SEMA4A / SERPINE1 / SLC9A3R1 / SOCS2 / SPRY1 / SPRY2 / SPRY4 / SPX / TBC1D7 / TGFBR1 / TKFC / TNF / TNFAIP8L2 / TRAFD1 / TRIM38 / TXNDC12 / UCHL1 / VDAC2 / ZC3H12A
GO:0002684	positive regulation of immune system process	1,01E-03	A2M / ANXA1 / AP3B1 / C1QA / C1QB / C1S / C3 / CCL2 / CCL20 / CCL4 / CCL5 / CMKLR1 / COLEC12 / CSF3 / CTNNBIP1 / EZR / F2RL1 / FADD / FOS / FYN / GPR183 / HLX / IL12B / IL15 / IL1A / IL6 / IL7 / IRAK2 / IRF1 / LIF / MEF2C / MZB1 / NLRC4 / NOD2 / POLR3D / PSEN1 / RASAL3 / RIPK2 / RSAD2 / SCIN / SERPINE1 / STAT5A / TKFC / TLR10 / TLR2 / TLR3 / TLR6 / TMEM173 / TNF / VAMP8 / VEGFA / VEGFB
GO:0009605	response to external stimulus	1,13E-03	A2M / ABHD12 / ADM / ALCAM / ANXA1 / ASNS / ATF3 / BAIAP2 / BATF / BHLHE40 / BPI / CAPN3 / CASP4 / CCL2 / CCL20 / CCL4 / CCL5 / CCR7 / CCRL2 / CD40 / CD63 / CDKN2D / CHN1 / CMKLR1 / EDNRB / ENPP2 / EXT1 / F12 / F2R / F2RL1 / FABP4 / FADD / FAS / FGF1 / FOS / FYN / GABARAPL1 / GABARAPL2 / GADD45A / GPR183 / HOPX / HRH1 / HYAL2 / IL10 / IL12B / IL15 / IL6 / IL6 / IRAK2 / IRF1 / JUNB / LBH / LPO / MAP1LC3A / MEF2C / MR1 / MX2 / MYH10 / NENF / NLRC4 / NOD2 / NOS2 / NPC2 / PDE2A / PKD2 / PLAC8 / POLR3D / PTPRF / RGS9 / RSAD2 / S100A8 / S100A9 / S1PR1 / SAMHD1 / SCARB1 / SEMA3C / SEMA4A / SERINC3 / SERPINE1 / SLC25A19 / SLC2A1 / SNX3 / SPX / SRR / STAT5A / TICAM1 / TKFC / TLR10 / TLR2 / TLR3 / TLR6 / TMEM173 / TNF / TNFAIP8L2 / TNFRSF1A / TRIM38 / TUBB3 / VAMP8 / VDR / VEGFA / VEGFB / VIL1 / ZC3H12A
GO:0007159	leukocyte cell-cell adhesion	2,54E-03	ANXA1 / AP3B1 / AZI2 / BATF / CCL2 / CCL5 / EZR / F2RL1 / FADD / FAS / FYN / GCNT1 / GPR183 / HLX / IL12B / IL15 / IL6 / IL6 / IL7 / IRF1 / NOD2 / PSEN1 / PSMB10 / RASAL3 / RSAD2 / S100A8 / S100A9 / STAT5A / TNF / TNFAIP8L2
GO:0050663	cytokine secretion	3,63E-03	CASP4 / EZR / F2R / F2RL1 / HYAL2 / IL10 / IL12B / IL1A / LPL / NLRC4 / NOD2 / NOS2 / TLR10 / TLR2 / TLR6 / TNF / ZC3H12A
GO:0010648	negative regulation of cell communication	4,05E-03	ADM / ARRB2 / ATF3 / BCL2L2 / CAV2 / CCDC22 / CCL5 / CCND1 / CDKN2D / CHP1 / CSF2 / CTNNBIP1 / DLK2 / DUSP18 / DUSP26 / ELL3 / EZR / GCLM / GPC1 / HTRA1 / HYAL2 / IFI6 / IGF1R / IL1RN / IL6 / IL7 / LGMN / LIF / LIMD1 / MAPK7 / MEN1 / NLE1 / PFKL / PHACTR4 / PIK3IP1 / PKD2 / PNKD / PPARG / PPIF / PRKACA / PRKCDBP / PRR5L / PSEN1 / RASA3 / RASAL3 / RGS19 / RGS2 / RGS9 / RNF34 / SERPINE1 / SLC9A3R1 / SOCS2 / SPRY1 / SPRY2 / SPRY4 / TBC1D7 / TGFBR1 / TKFC / TNF / TXNDC12 / UCHL1 / VDAC2 / ZC3H12A

GO:0023057	negative regulation of signaling	4,05E-03	ADM / ARRB2 / ATF3 / BCL2L2 / CAV2 / CCDC22 / CCL5 / CCND1 / CDKN2D / CHP1 / CSF2 / CTNNBIP1 / DLK2 / DUSP18 / DUSP26 / ELL3 / EZR / GCLM / GPC1 / HTRA1 / HYAL2 / IFI6 / IGF1R / IL1RN / IL6 / IL7 / LGMN / LIF / LIMD1 / MAPK7 / MEN1 / NLE1 / PFKL / PHACTR4 / PIK3IP1 / PKD2 / PNKD / PPARG / PPIF / PRKACA / PRKCDBP / PRR5L / PSEN1 / RASA3 / RASAL3 / RGS19 / RGS2 / RGS9 / RNF34 / SERPINE1 / SLC9A3R1 / SOCS2 / SPRY1 / SPRY2 / SPRY4 / TBC1D7 / TGFBR1 / TKFC / TNF / TXNDC12 / UCHL1 / VDAC2 / ZC3H12A
GO:0001816	cytokine production	4,20E-03	ANXA1 / AZI2 / BATF / CASP4 / CCL2 / CMKLR1 / CSF2 / EZR / F2R / F2RL1 / FABP4 / FADD / HIF1A / HYAL2 / IL10 / IL12B / IL15 / IL1A / IL6 / IRF1 / LPL / MR1 / NLRC4 / NOD2 / NOS2 / POLR3D / RIPK2 / RSAD2 / SERPINE1 / STAT5A / TKFC / TLR10 / TLR2 / TLR3 / TLR6 / TMEM173 / TNF / TRIB2 / TRIM38 / ZC3H12A
GO:0071345	cellular response to cytokine stimulus	4,52E-03	CCL2 / CCL20 / CCL4 / CCL5 / CCR7 / CCRL2 / CD40 / CSF3 / EDA / F3 / FADD / FAS / GAB1 / HYAL2 / IL12B / IL12RB2 / IL1A / IL1B / IL1RN / IL2RA / IL6 / IL6 / IRAK2 / IRF1 / NFIL3 / NMI / PDE2A / PPARG / PTGS2 / SOCS2 / STAT5A / TMEM173 / TNF / TNFRSF1A / TUBA1A / ZC3H12A
GO:0050707	regulation of cytokine secretion	5,03E-03	CASP4 / EZR / F2R / F2RL1 / HYAL2 / IL10 / IL1A / LPL / NOD2 / TLR10 / TLR2 / TLR6 / TNF / ZC3H12A
GO:0042306	regulation of protein import into nucleus	5,17E-03	CABP1 / CCDC22 / CHP1 / CSF3 / EDA / HYAL2 / MAPK7 / PDE2A / PKD2 / PRDX1 / RGS19 / SLC9A3R1 / TGFBR1 / TMEM173 / TNF / ZC3H12A
GO:0001817	regulation of cytokine production	5,17E-03	ANXA1 / CASP4 / CCL2 / CMKLR1 / CSF2 / EZR / F2R / F2RL1 / FADD / HIF1A / HYAL2 / IL10 / IL12B / IL15 / IL1A / IL6 / IRF1 / LPL / NOD2 / NOS2 / POLR3D / RIPK2 / RSAD2 / SERPINE1 / STAT5A / TKFC / TLR10 / TLR2 / TLR3 / TLR6 / TMEM173 / TNF / TRIB2 / TRIM38 / ZC3H12A
GO:1903531	negative regulation of secretion by cell	5,64E-03	ANXA1 / DNM1 / ERP29 / EZR / F2R / IL10 / IL6 / LIF / PFKL / PNKD / RHBDF1 / RSAD2 / SERGEF / SYP / TNF / VAMP8 / ZC3H12A
GO:1904589	regulation of protein import	6,64E-03	CABP1 / CCDC22 / CHP1 / CSF3 / EDA / HYAL2 / MAPK7 / PDE2A / PKD2 / PRDX1 / RGS19 / SLC9A3R1 / TGFBR1 / TMEM173 / TNF / ZC3H12A
GO:0034097	response to cytokine	1,00E-02	CCL2 / CCL20 / CCL4 / CCL5 / CCR7 / CCRL2 / CD40 / CSF3 / EDA / F3 / FADD / FAS / GAB1 / HYAL2 / IL12B / IL12RB2 / IL1A / IL1B / IL1RN / IL2RA / IL6 / IL6 / IRAK2 / IRF1 / JUNB / MAPK7 / NFIL3 / NMI / PDE2A / PPARG / PTGS2 / SOCS2 / STAT5A / TIMP2 / TMEM173 / TNF / TNFRSF1A / TUBA1A / ZC3H12A
GO:0002521	leukocyte differentiation	1,04E-02	ANXA1 / AP3B1 / AZI2 / BATF / CITED2 / CSF2 / CTNNBIP1 / F2RL1 / FADD / FAS / FOS / GPR183 / HLX / IKZF3 / IL12B / IL15 / IL6 / IL6 / IL7 / IRF1 / JUNB / LIF / PPARG / PSEN1 / RSAD2 / SNX10 / STAT5A / TNF
GO:0050790	regulation of catalytic activity	1,12E-02	A2M / ACTN1 / ALS2CL / ANXA1 / ANXA3 / APOA4 / ARHGAP15 / ARHGEF10L / ARL6IP5 / ARRDC3 / BCAR3 / BCCIP / C3 / CAMK2N1 / CAPN3 / CAST / CAV2 / CCL2 / CCL20 / CCL4 / CCL5 / CCND1 / CDC42EP1 / CDC42EP2 / CDK12 / CDKN2D / CHN1 / CHP1 / CYTH2 / DUSP18 / DUSP26 / EDN1 / EIF2B3 / ERP29 / F2R / F3 / FABP4 / FADD / FAM162A / FAS / FGF1 / FGL2 / GAB1 / GABARAPL2 / GADD45A / GADD45G / GCLM / HEXIM1 / HYAL2 / IFI6 / IGF1R / IL12B / IL7 / ITIH4 / LAMTOR2 / MAD2L2 / MAPK7 / MAT2B / MEF2C / MEN1 / NIFK / NLE1 / NLRC4 / NOS2 / NR4A1 / PCNA / PHACTR4 / PIK3IP1 / PKD2 / PKIG / PPARG / PPIF / PPP1R3C / PSAP / PSEN1 / PSEN2 / RANGRF / RASA3 / RASAL3 / RASGEF1B / RASGRP2 / RCAN1 / RGS19 / RGS2 / RGS9 / RNF34 / S100A8 / S100A9 / SCARB1 / SERGEF / SERPINB1 / SERPINB6 / SERPINE1 / SLC9A3R1 / SOCS2 / SPRY2 / SPRY4 / TBC1D1 / TBC1D7 / TFPI2 / TGFBR1 / TIMP2 / TIMP3 / TIMP4 / TNF / TRIB2 / TRIB3 / UCHL1 / VIL1
GO:0046822	regulation of nucleocytoplasmic transport	1,14E-02	CABP1 / CCDC22 / CHP1 / CSF3 / EDA / HYAL2 / MAPK7 / PDE2A / PKD2 / PRDX1 / PRKACA / RGS19 / SLC9A3R1 / TGFBR1 / TMEM173 / TNF / ZC3H12A
GO:0006082	organic acid metabolic process	1,14E-02	AADAT / AASS / ABAT / ACACA / ACADSB / ACAT1 / ACO1 / ACSF2 / AHCY / AHCYL2 / ALDH6A1 / ALKBH7 / APOA4 / ARG2 / ASNS / BCKDK / C3 / CROT / CRYL1 / DARS / DDAH2 / DHRS9 / DPYD / EDN1 / ELOVL5 / ENO3 / ERO1A / FABP4 / FADS2 / FADS3 / FASN / GAMT / GCDH / GCLM / HAAO / HACD4 / HIBADH / HK1 / IVD / LDHA / LPL / LPO / LTA4H / MARS2 / MECR / MPC1 / NPL / OAT / OXSM / PC / PDHB / PFKFB2 / PFKL / PGK1 / PHGDH / PNKD / PRDX4 / PSPH / PTGS2 / SDHB / SDS / SHMT1 / SRR / TECR / TNFRSF1A / TPI1 / TRIB3 / VNN1
GO:1900180	regulation of protein localization to nucleus	1,18E-02	CABP1 / CCDC22 / CHP1 / CSF3 / EDA / FYN / HYAL2 / LIF / MAPK7 / PDE2A / PKD2 / PRDX1 / RGS19 / SLC9A3R1 / TGFBR1 / TMEM173 / TNF / ZC3H12A
GO:0042325	regulation of phosphorylation	1,49E-02	ARL6IP5 / ATF3 / BCCIP / C3 / CAMK2N1 / CAV2 / CCL2 / CCL20 / CCL4 / CCL5 / CCND1 / CD40 / CDK12 / CDKN2D / CHP1 / CSF2 / CSF3 / CTGF / DUSP18 / DUSP26 / EDN1 / ENPP2 / ERP29 / EZR / F2R / F2RL1 / FABP4 / FAS / FGF1 / FYN / GAB1 / GADD45A / GADD45G / GPR183 / HCRTR1 / HEXIM1 / HYAL2 / IGF1R / IGFBP4 / IL12B / IL1A / IL1B / IL6 / IL6 / LAMTOR2 / LIF / MAD2L2 / MAPK7 / MEN1 / NENF / NOD2 / PIK3IP1 / PKD2 / PKIG / PPIF / PRDX1 / PRKCDBP / PRR5L / PSEN1 / PTGS2 / RIPK2 / SLC9A3R1 / SOCS2 / SPRY1 / SPRY2 / SPRY4 / TGFBR1 / TNF / TRIB2 / TRIB3 / UCHL1 / VEGFA / ZC3H12A
GO:0042110	T cell activation	1,49E-02	ANXA1 / AP3B1 / AZI2 / BATF / CCL2 / CCL5 / F2RL1 / FADD / FAS / FYN / GPR183 / HLX / IL12B / IL15 / IL6 / IL6 / IL7 / IRF1 / NOD2 / PSEN1 / PSMB10 / RASAL3 / RSAD2 / STAT5A / TNFAIP8L2
GO:0070661	leukocyte proliferation	1,52E-02	ANXA1 / AZI2 / CCL5 / F2RL1 / FADD / FYN / GPR183 / IKZF3 / IL10 / IL12B / IL15 / IL6 / IL6 / IL7 / IRF1 / MEF2C / MZB1 / PSMB10 / RASAL3 / STAT5A
GO:0032943	mononuclear cell proliferation	1,52E-02	ANXA1 / AZI2 / CCL5 / FADD / FYN / GPR183 / IKZF3 / IL10 / IL12B / IL15 / IL6 / IL6 / IL7 / IRF1 / MEF2C / MZB1 / PSMB10 / RASAL3 / STAT5A
GO:0046651	lymphocyte proliferation	1,52E-02	ANXA1 / AZI2 / CCL5 / FADD / FYN / GPR183 / IKZF3 / IL10 / IL12B / IL15 / IL6 / IL6 / IL7 / IRF1 / MEF2C / MZB1 / PSMB10 / RASAL3 / STAT5A
GO:0022610	biological adhesion	1,67E-02	ACTG1 / ACTN1 / ADGRE5 / ALCAM / ANXA1 / AP3B1 / AZI2 / BATF / CCL2 / CCL5 / CD44 / CD63 / CFDP1 / CITED2 / CLDN1 / CTGF / DUSP26 / EDA / EZR / F2RL1 / FADD / FAS / FYN / GCNT1 / GPR183 / HAS2 / HLX / HPSE / ICAM3 / IL12B / IL15 / IL1RN / IL6 / IL6 / IL7 / IRF1 / ITGA5 / ITGAV / ITGB5 / ITGB6 / LRFN3 / LYVE1 / MAPK7 / MYH10 / NOD2 / PECAM1 / PSEN1 / PSMB10 / PTPRF / RASAL3 / RHOB / RND1 / ROM1 / RSAD2 / S100A8 / S100A9 / S1PR1 / SCARB1 / SELL / SELP / SERPINE1 / STAT5A / TGFBI / TNF / TNFAIP8L2 / TTYH1 / VCAN / VEGFA
GO:0006732	coenzyme metabolic process	1,69E-02	AADAT / AASS / ACACA / AHCY / AHCYL2 / CROT / DCAKD / DCXR / ELOVL5 / ENO3 / FAR2 / GAMT / HAAO / HK1 / MAT2B / MOCOS / MPC1 / MTHFD1L / NADSYN1 / NAPRT / NNT / PDHB / PDXK / PFKFB2 / PFKL / PGK1 / SHMT1 / TPI1 / VNN1
GO:0009636	response to toxic substance	1,69E-02	CAT / CCL4 / CCL5 / CSN1S1 / FAS / GPX3 / GPX7 / LPO / PRDX1 / PRDX4 / PTGS2 / S100A8 / S100A9 / TNF / TXNRD1
GO:0010883	regulation of lipid storage	1,74E-02	ALKBH7 / C3 / LPL / MSR1 / PNPLA2 / PPARG / SCARB1 / ZC3H12A

GO:1902107	positive regulation of leukocyte differentiation	1,89E-02	ANXA1 / AP3B1 / CTNNBIP1 / FADD / FOS / HLX / IL12B / IL15 / IL6 / IL7 / LIF / STAT5A / TNF
GO:0051248	negative regulation of protein metabolic process	2,19E-02	A2M / ATF3 / C3 / CAMK2N1 / CAPN3 / CAST / CDKN2D / CHP1 / DUSP18 / DUSP26 / EDN1 / EDNRB / EZR / FABP4 / FYN / GADD45A / HEXIM1 / HYAL2 / IFI6 / IGF1R / IL10 / IL6 / ITIH4 / ITM2B / LIF / LIMD1 / MAD2L2 / MAPK7 / MEN1 / MOV10 / NLE1 / NLRC4 / NR4A1 / PAIP2 / PKIG / PRR5L / PSEN1 / RNF34 / SERPINB1 / SERPINB6 / SERPINE1 / SLC9A3R1 / SNX3 / SOCS2 / SPRY1 / SPRY2 / SPRY4 / TFPI2 / TIMP2 / TIMP3 / TIMP4 / TMEM59 / TNF / TRIB2 / TRIB3 / UCHL1 / VIL1 / ZC3H12A
GO:0006509	membrane protein ectodomain proteolysis	2,57E-02	IL10 / PSEN1 / PSEN2 / TIMP2 / TIMP3 / TIMP4 / TNF
GO:0006468	protein phosphorylation	2,95E-02	ACVR2B / ARL6IP5 / ATF3 / BCCIP / BCKDK / C3 / CAMK2N1 / CAV2 / CCL2 / CCL20 / CCL4 / CCL5 / CCND1 / CD40 / CDK12 / CDKN2D / CHP1 / CSF2 / CSF3 / CTGF / DUSP18 / DUSP26 / EDN1 / ENPP2 / ERCC3 / ERP29 / EZR / F2R / F2RL1 / FABP4 / FAS / FASTKD3 / FGF1 / FYN / GAB1 / GADD45A / GADD45G / GPR183 / GRK5 / HCRTR1 / HEXIM1 / HYAL2 / IGF1R / IGFBP4 / IL12B / IL15 / IL1A / IL1B / IL6 / IL6 / IRAK2 / LAMTOR2 / LIF / MAD2L2 / MAPK7 / MEF2C / MEN1 / MYLK / NENF / NLK / NOD2 / PKD2 / PKIG / PPM1L / PRDX1 / PRKACA / PRKCDBP / PRR5L / PSEN1 / PTGS2 / RIPK2 / RSRC1 / SGK1 / SLC9A3R1 / SOCS2 / SPRY1 / SPRY2 / SPRY4 / TGFBR1 / TNF / TRIB2 / TRIB3 / UCHL1 / VEGFA / ZC3H12A
GO:0050793	regulation of developmental process	3,07E-02	AAMDC / ADM / ANXA1 / AP3B1 / ARHGAP15 / ASCL2 / BAIAP2 / BRINP1 / CAPN3 / CCL2 / CCND1 / CDC42EP1 / CDC42EP2 / CFDP1 / CHN1 / CITED2 / CMKLR1 / CSF2 / CSF3 / CTGF / CTNNBIP1 / DLK2 / EDN1 / EDNRB / ELL3 / ENPP2 / EZR / F3 / FADD / FAS / FGF1 / FOS / FYN / GAMT / GPC1 / GPR183 / HLX / HOPX / IKZF3 / IL12B / IL15 / IL1A / IL1RN / IL6 / IL7 / IRF1 / JUNB / LIF / LIMD1 / LPL / MAFF / MAFG / MAPK7 / MEDAG / MEF2C / MEN1 / MSR1 / MYH10 / PLAC8 / PPARG / PPIB / PRKACA / PSEN1 / PTGS2 / PTPRF / RHOB / RSL1D1 / S1PR1 / SCIN / SDC2 / SEMA3C / SEMA4A / SERP1 / SERPINE1 / SLC9A3R1 / SNAP25 / SNX3 / SPRY1 / SPRY2 / STAT5A / TBC1D7 / TGFBR1 / TMEM30A / TNF / TRIB2 / TRIB3 / TSPAN12 / VEGFA / VEGFB / VIL1 / YWHAG / ZC3H12A
GO:0098869	cellular oxidant detoxification	3,26E-02	CAT / CSN1S1 / GPX3 / GPX7 / LPO / PRDX1 / PRDX4 / PTGS2 / S100A8 / S100A9 / TNF / TXNRD1
GO:0014033	neural crest cell differentiation	3,74E-02	CITED2 / EDN1 / EDNRB / MEF2C / PHACTR4 / SEMA3C / SEMA4A
GO:0044093	positive regulation of molecular function	3,75E-02	ALS2CL / APOA4 / ARHGAP15 / ARHGEF10L / ARL6IP5 / ARRDC3 / BCAR3 / CAPN3 / CAT / CAV2 / CCL2 / CCL20 / CCL4 / CCL5 / CCND1 / CDC42EP1 / CDC42EP2 / CHN1 / CHP1 / CSF3 / CTSS / CYTH2 / EDA / EDN1 / EIF2B3 / ERP29 / F2R / F3 / FADD / FAM162A / FGF1 / FGL2 / GAB1 / GABARAPL2 / GADD45A / GADD45G / GCLM / IL10 / IL12B / IL6 / IRAK2 / LAMTOR2 / MEF2C / MEN1 / NDP / NOD2 / NOS2 / PCNA / PHACTR4 / PKD2 / PPARG / PSAP / PSEN1 / PSEN2 / RANGRF / RASA3 / RASAL3 / RASGEF1B / RASGRP2 / RGS19 / RGS2 / RGS9 / RIPK2 / S100A8 / S100A9 / SCARB1 / SERGEF / SGK1 / SPRY2 / TBC1D1 / TBC1D7 / TGFBR1 / TMEM173 / TNF / TRIB3 / TRIM38
GO:0046470	phosphatidylcholine metabolic process	3,75E-02	ABHD3 / APOA4 / CHPT1 / ENPP2 / PEMT / SCARB1
GO:0051249	regulation of lymphocyte activation	3,83E-02	ANXA1 / AP3B1 / CCL2 / CCL5 / FADD / FAS / GPR183 / HLX / IKZF3 / IL10 / IL12B / IL15 / IL6 / IL7 / IRF1 / MEF2C / MZB1 / NOD2 / RASAL3 / STAT5A / TNFAIP8L2
GO:0044092	negative regulation of molecular function	4,51E-02	A2M / ANXA1 / ANXA3 / BHLHE40 / C3 / CAMK2N1 / CAST / CAT / CDKN2D / CHP1 / CMKLR1 / CTNNBIP1 / DUSP18 / DUSP26 / FABP4 / GADD45A / HEXIM1 / HYAL2 / IFI6 / IGF1R / IL7 / IRAK2 / ITIH4 / MAD2L2 / MAPK7 / MEN1 / NIFK / NLE1 / NLRC4 / NR4A1 / PIK3IP1 / PKD2 / PKIG / PPIF / PSEN1 / PTPRF / RNF34 / SERPINB1 / SERPINB6 / SERPINE1 / SLC9A3R1 / SOCS2 / SPRY2 / SPRY4 / TFPI2 / TIMP2 / TIMP3 / TIMP4 / TNF / TRIB2 / TRIB3 / UCHL1 / VIL1 / ZC3H12A
GO:0032944	regulation of mononuclear cell proliferation	4,68E-02	ANXA1 / CCL5 / FADD / GPR183 / IKZF3 / IL10 / IL12B / IL15 / IL6 / IL7 / IRF1 / MEF2C / MZB1 / RASAL3 / STAT5A
GO:1903039	positive regulation of leukocyte cell-cell adhesion	4,79E-02	ANXA1 / AP3B1 / CCL2 / CCL5 / FADD / HLX / IL12B / IL15 / IL6 / IL7 / NOD2 / RASAL3 / STAT5A / TNF
GO:0044712	single-organism catabolic process	4,80E-02	AADAT / AASS / ABAT / ABHD12 / ACADSB / ACAT1 / APOA4 / BCKDK / CROT / CTSS / DDAH2 / DERL3 / DHDH / DPYD / ENO3 / ENPP2 / FUCA1 / GALM / GCDH / GPD2 / HAAO / HIBADH / HK1 / HSD17B14 / IAH1 / IVD / LIPE / LPL / NAGA / NEU3 / NPL / OAT / OS9 / PAFAH2 / PDE2A / PFKFB2 / PFKL / PGK1 / PLA2G7 / PLBD1 / PLD3 / PNKD / PNPLA2 / PPT1 / RETN / SAMHD1 / SCARB1 / SDF2L1 / SDS / SMPDL3A / SORD / TMUB1 / TNF / TPI1 / UBXN8
GO:0009611	response to wounding	4,94E-02	ACTG1 / ANXA1 / AP3B1 / CAPN3 / CCL2 / F11 / F12 / F13A1 / F2R / F2RL1 / F2RL2 / F3 / HOPX / HPSE / IL1A / IL6 / LBH / MYH10 / PRCP / PROCR / PTPRF / SDC1 / SERPINE1 / TFPI2 / THBD / VIL1

MØHK *vs* MØC			
GO:0006954	inflammatory response	8,37E-04	A2M / ABR / CCL2 / CCL20 / CCL4 / CCL5 / CD163 / CD40 / CLEC7A / CTNNBIP1 / F2R / F2RL1 / FABP4 / HMOX1 / HYAL2 / IL10 / IL1B / IL6 / ITGB6 / LTB4R / PTGER4 / PTGIR / PTGS2 / S100A12 / S100A8 / S100A9 / S100B / SERPINE1 / SOCS3 / TICAM1 / TLR10 / TLR2 / TLR6 / TNF
GO:0050729	positive regulation of inflammatory response	9,35E-04	CCL2 / CCL4 / CCL5 / FABP4 / HYAL2 / IL6 / S100A8 / S100A9 / SERPINE1 / TLR10 / TLR2 / TNF
GO:1902531	regulation of intracellular signal transduction	1,09E-03	ABR / AVPI1 / BCL2 / BGN / CAT / CCL2 / CCL20 / CCL4 / CCL5 / CD40 / CDKN2D / CISH / CLEC6A / CSF2 / DLC1 / DUSP18 / DUSP26 / DUSP6 / EDA / EDN1 / ELL3 / EZR / F2R / F2RL1 / GADD45A / GADD45G / HES1 / HMOX1 / HYAL2 / IGFBP4 / IL10 / IL1B / IL6 / IL6 / JSRP1 / LIMD1 / MAP2K6 / PAK1 / PDGFA / PIK3IP1 / PLAUR / PRDX1 / PRKCDBP / RASA3 / RASAL3 / RASGRP4 / S100A8 / S100A9 / S100B / SOCS2 / SOCS3 / SPRY4 / TGFBR1 / TNF / TRIB3 / UACA / UCHL1
GO:0009611	response to wounding	3,28E-03	ACTG1 / ANXA2 / CCL2 / CLIC1 / F13A1 / F2R / F2RL1 / F2RL2 / HMOX1 / HOPX / IL6 / LBH / PAK1 / PDGFA / PLAU / PRCP / PROCR / SDC1 / SERPINE1 / TFPI2 / THBD / VWF / ZFP36
GO:0050878	regulation of body fluid levels	5,15E-03	ACTG1 / ANXA2 / CLDN1 / CLIC1 / EDN1 / F13A1 / F2R / F2RL1 / F2RL2 / HAS2 / HYAL2 / LBH / P2RY2 / PDGFA / PLAU / PROCR / SERPINE1 / SFN / TFPI2 / THBD / TNF / VWF
GO:0008283	cell proliferation	5,66E-03	ADAM10 / BCL2 / BYSL / CCL5 / CD40 / CDK1 / CDKN2D / COL4A3BP / CSF2 / CTNNBIP1 / DNMT1 / EDN1 / EGR1 / ELL3 / F2R / F2RL1 / FABP4 / GLUL / GRK5 / HES1 / HGF / HMOX1 / IGFBP4 / IL10 / IL6 / IL6 / JUNB / KANK2 / LIMS2 / NDRG1 / NUDT16 / OSM / PAK1 / PDGFA / PDXK / PLA2G4A / PLAU / PPARG / PRDX1 / PSMB10 / RASAL3 / RASGRP4 / RHBDF1 / S1PR1 / SFN / TES / TGFBI / TGFBR1 / TIMP1 / TNF / TNK2 / UCHL1 / VEGFB / ZFP36
GO:0048585	negative regulation of response to stimulus	9,62E-03	A2M / ABR / ANXA2 / BCL2 / BGN / CCL2 / CCL5 / CDKN2D / CISH / CSF2 / CTNNBIP1 / DUSP18 / DUSP26 / DUSP6 / ELL3 / EZR / GPC1 / HMOX1 / HYAL2 / IFI6 / IL10 / IL1RN / KANK2 / LFNG / LIMD1 / PDGFA / PIK3IP1 / PLAU / PLAUR / PPARG / PRKCDBP / PRR5L / PTGER4 / RASA3 / RASAL3 / RGS16 / RGS19 / SEMA3C / SERPINE1 / SOCS2 / SOCS3 / SPRY4 / SPX / TGFBR1 / TNF / UCHL1
GO:0007596	blood coagulation	9,62E-03	ACTG1 / ANXA2 / CLIC1 / F13A1 / F2R / F2RL1 / F2RL2 / LBH / PDGFA / PLAU / PROCR / SERPINE1 / TFPI2 / THBD / VWF
GO:0050817	coagulation	9,93E-03	ACTG1 / ANXA2 / CLIC1 / F13A1 / F2R / F2RL1 / F2RL2 / LBH / PDGFA / PLAU / PROCR / SERPINE1 / TFPI2 / THBD / VWF
GO:0043408	regulation of MAPK cascade	9,93E-03	AVPI1 / CCL2 / CCL20 / CCL4 / CCL5 / CD40 / DUSP18 / DUSP26 / DUSP6 / EDN1 / EZR / F2R / F2RL1 / GADD45A / GADD45G / HYAL2 / IGFBP4 / IL1B / IL6 / MAP2K6 / PAK1 / PDGFA / PRDX1 / PRKCDBP / SPRY4 / TGFBR1 / TNF / TRIB3 / UCHL1
GO:0050707	regulation of cytokine secretion	1,69E-02	CLEC6A / EZR / F2R / F2RL1 / HYAL2 / IL10 / TLR10 / TLR2 / TLR6 / TNF
GO:0051348	negative regulation of transferase activity	1,69E-02	BGN / CDKN2D / CISH / DUSP18 / DUSP26 / DUSP6 / FABP4 / GADD45A / HYAL2 / PIK3IP1 / PKIG / SOCS2 / SOCS3 / SPRY4 / TRIB3 / UCHL1 / ZFP36
GO:0034097	response to cytokine	1,69E-02	ADAM10 / BGN / CCL2 / CCL20 / CCL4 / CCL5 / CD40 / CISH / EDA / EGR1 / HYAL2 / IL1B / IL1RN / IL6 / IL6 / JUNB / NFIL3 / PPARG / PTGS2 / SOCS2 / SOCS3 / TIMP1 / TMEM173 / TNF / TUBA1A / ZFP36
GO:0033673	negative regulation of kinase activity	1,69E-02	BGN / CDKN2D / CISH / DUSP18 / DUSP26 / DUSP6 / FABP4 / GADD45A / HYAL2 / PIK3IP1 / PKIG / SOCS2 / SOCS3 / SPRY4 / TRIB3 / UCHL1
GO:0034612	response to tumor necrosis factor	1,69E-02	ADAM10 / CCL2 / CCL20 / CCL4 / CCL5 / CD40 / HYAL2 / IL6 / TNF / ZFP36
GO:0010563	negative regulation of phosphorus metabolic process	1,69E-02	BGN / CDKN2D / CISH / DUSP18 / DUSP26 / DUSP6 / EDN1 / EZR / FABP4 / GADD45A / HYAL2 / KIAA0430 / MICAL1 / PDGFA / PIK3IP1 / PKIG / PRR5L / S100B / SOCS2 / SOCS3 / SPRY4 / TNF / TRIB3 / UCHL1
GO:0045936	negative regulation of phosphate metabolic process	1,69E-02	BGN / CDKN2D / CISH / DUSP18 / DUSP26 / DUSP6 / EDN1 / EZR / FABP4 / GADD45A / HYAL2 / KIAA0430 / MICAL1 / PDGFA / PIK3IP1 / PKIG / PRR5L / S100B / SOCS2 / SOCS3 / SPRY4 / TNF / TRIB3 / UCHL1
GO:0071345	cellular response to cytokine stimulus	1,70E-02	BGN / CCL2 / CCL20 / CCL4 / CCL5 / CD40 / CISH / EDA / EGR1 / HYAL2 / IL1B / IL1RN / IL6 / IL6 / NFIL3 / PPARG / PTGS2 / SOCS2 / SOCS3 / TMEM173 / TNF / TUBA1A / ZFP36
GO:0002376	immune system process	2,01E-02	A2M / ABR / ACP6 / ACTN1 / ADAM10 / ALCAM / ANXA2 / CCL2 / CCL20 / CCL4 / CCL5 / CD40 / CLEC6A / CLEC7A / COLEC12 / CSF2 / CTNNBIP1 / EDA / EZR / F2RL1 / FOS / GCNT1 / GPI / HES1 / HMOX1 / HYAL2 / IL10 / IL1B / IL6 / IL6 / JUNB / LFNG / LYST / MMP9 / MR1 / NDRG1 / NFIL3 / OAS2 / OSM / PPARG / PRDX1 / PSMB10 / PTGER4 / RASAL3 / S100A12 / S100A8 / S100A9 / S100B / S1PR1 / SAMHD1 / SERPINE1 / SNX10 / TGFBR1 / TICAM1 / TLR10 / TLR2 / TLR6 / TMEM173 / TNF / TNK2 / VEGFB / ZFP36
GO:0032103	positive regulation of response to external stimulus	2,03E-02	ADAM10 / CCL2 / CCL4 / CCL5 / F2RL1 / FABP4 / HYAL2 / IL6 / S100A8 / S100A9 / SERPINE1 / TLR10 / TLR2 / TNF / VEGFB
GO:0009636	response to toxic substance	2,22E-02	CAT / CCL4 / CCL5 / GPX3 / PRDX1 / PRDX5 / PTGS2 / S100A8 / S100A9 / TNF / TXNRD1
GO:0050900	leukocyte migration	2,25E-02	ABR / ADAM10 / CCL2 / CCL20 / CCL4 / CCL5 / F2RL1 / GCNT1 / MMP9 / PTGER4 / S100A8 / S100A9 / S1PR1 / SERPINE1 / TNF / VEGFB
GO:0006955	immune response	2,77E-02	A2M / ABR / ALCAM / CCL2 / CCL20 / CCL4 / CCL5 / CD40 / CLEC6A / CLEC7A / COLEC12 / CSF2 / EDA / EZR / F2RL1 / IL10 / IL1B / IL6 / IL6 / LFNG / LYST / MR1 / NFIL3 / OAS2 / OSM / PPARG / PRDX1 / S100A12 / S100A8 / S100A9 / S100B / SAMHD1 / TICAM1 / TLR10 / TLR2 / TLR6 / TMEM173 / TNF / TNK2
GO:0048659	smooth muscle cell proliferation	2,91E-02	CCL5 / CTNNBIP1 / EDN1 / HMOX1 / IL6 / PPARG / TNF
GO:0048660	regulation of smooth muscle cell proliferation	2,91E-02	CCL5 / CTNNBIP1 / EDN1 / HMOX1 / IL6 / PPARG / TNF
GO:0051248	negative regulation of protein metabolic process	2,91E-02	A2M / ANXA2 / BGN / CDKN2D / CISH / DNMT1 / DUSP18 / DUSP26 / DUSP6 / EDN1 / EZR / FABP4 / GADD45A / HYAL2 / IFI6 / IL10 / IL6 / LIMD1 / MICAL1 / MOV10 / PKIG / PLAUR / PRDX5 / PRR5L / SERPINB1 / SERPINE1 / SFN / SOCS2 / SOCS3 / SPRY4 / TFPI2 / TIMP1 / TIMP3 / TNF / TRIB3 / UCHL1 / ZFP36

GO:0007155	cell adhesion	2,91E-02	ACTG1 / ACTN1 / ADAM10 / ADGRE5 / ALCAM / ASS1 / CCL2 / CCL5 / CD44 / CLDN1 / CLIC1 / DUSP26 / EDA / EZR / F2RL1 / GCNT1 / HAS2 / IL1RN / IL6 / IL6 / ITGA5 / ITGB5 / ITGB6 / LFNG / LIMS2 / LYVE1 / PECAM1 / PLAU / PSMB10 / RASAL3 / RHOB / RND1 / S100A8 / S100A9 / S1PR1 / SELL / SERPINE1 / TGFBI / TNF / TTYH1 / VCAN / VWF
GO:0010648	negative regulation of cell communication	2,94E-02	BCL2 / BGN / CCL5 / CDKN2D / CISH / CSF2 / CTNNBIP1 / DUSP18 / DUSP26 / DUSP6 / ELL3 / EZR / GPC1 / HMOX1 / HYAL2 / IFI6 / IL1RN / IL6 / KANK2 / LFNG / LIMD1 / PIK3IP1 / PLAUR / PPARG / PRKCDBP / PRR5L / RASA3 / RASAL3 / RGS16 / RGS19 / SERPINE1 / SOCS2 / SOCS3 / SPRY4 / TGFBR1 / TNF / UCHL1
GO:0023057	negative regulation of signaling	2,94E-02	BCL2 / BGN / CCL5 / CDKN2D / CISH / CSF2 / CTNNBIP1 / DUSP18 / DUSP26 / DUSP6 / ELL3 / EZR / GPC1 / HMOX1 / HYAL2 / IFI6 / IL1RN / IL6 / KANK2 / LFNG / LIMD1 / PIK3IP1 / PLAUR / PPARG / PRKCDBP / PRR5L / RASA3 / RASAL3 / RGS16 / RGS19 / SERPINE1 / SOCS2 / SOCS3 / SPRY4 / TGFBR1 / TNF / UCHL1
GO:0031349	positive regulation of defense response	3,17E-02	CCL2 / CCL4 / CCL5 / COLEC12 / FABP4 / HYAL2 / IL6 / S100A8 / S100A9 / SERPINE1 / TLR10 / TLR2 / TLR6 / TMEM173 / TNF
GO:0040011	locomotion	3,22E-02	ABR / ADAM10 / ALCAM / ARRDC3 / CCL2 / CCL20 / CCL4 / CCL5 / EDN1 / EXT1 / F2R / F2RL1 / GCNT1 / HYAL2 / LIMD1 / MMP9 / MYO1C / PAK1 / PDGFA / PLAU / PRCP / PRR5L / PTGER4 / PTP4A2 / RHBDF1 / RHOB / S100A2 / S100A8 / S100A9 / S1PR1 / SDC1 / SDC2 / SEMA3C / SERPINE1 / SORD / SPNS1 / TGFBR1 / TIMP1 / TNF / TNK2 / VASP / VEGFB
GO:0016310	phosphorylation	3,36E-02	ADAM10 / AK4 / AVPI1 / BGN / CCL2 / CCL20 / CCL4 / CCL5 / CD40 / CDK1 / CDKN2D / CISH / CKB / COL4A3BP / CSF2 / DUSP18 / DUSP26 / DUSP6 / EDN1 / ENO3 / EZR / F2R / F2RL1 / FABP4 / GADD45A / GADD45G / GPI / GRK5 / GUCY2D / HES1 / HK1 / HYAL2 / HYKK / IGFBP4 / IL1B / IL6 / IL6 / LIMD1 / LIMK2 / MAP2K6 / MICAL1 / PAK1 / PDGFA / PDXK / PGK1 / PIK3IP1 / PKIG / PLAUR / PRDX1 / PRKCDBP / PRR5L / PTGS2 / RSRC1 / S100B / SFN / SOCS2 / SOCS3 / SPRY4 / TGFBR1 / TNF / TNK2 / TRIB3 / UCHL1 / XYLB / ZFP36
GO:0051049	regulation of transport	3,36E-02	ABR / ACTN1 / ANXA2 / APOE / ATP1A1 / CA2 / CCL2 / CCL4 / CCL5 / CLEC6A / CLIC1 / DNM1 / EDA / EDN1 / EZR / F2R / F2RL1 / HYAL2 / IL10 / IL6 / INSIG1 / JSRP1 / MYO1C / P2RY2 / PPT1 / PRDX1 / PRR5L / RAB26 / RGS19 / RHBDF1 / S100A8 / SCN4B / SDC1 / SEPT5 / SERPINE1 / SFN / SPX / SYP / TBC1D1 / TBC1D2 / TGFBR1 / TLR10 / TLR2 / TLR6 / TMEM173 / TMEM30A / TNF / TRIB3 / TSPAN13 / TXN
GO:0098869	cellular oxidant detoxification	3,46E-02	CAT / GPX3 / PRDX1 / PRDX5 / PTGS2 / S100A8 / S100A9 / TNF / TXNRD1
GO:0030335	positive regulation of cell migration	3,59E-02	ADAM10 / CCL2 / CCL20 / CCL4 / CCL5 / EDN1 / F2R / F2RL1 / MYO1C / PAK1 / PDGFA / PLAU / RHOB / SEMA3C / SERPINE1 / TGFBR1 / VEGFB
GO:0043547	positive regulation of GTPase activity	3,62E-02	ABR / ARHGAP15 / BCAR3 / CCL2 / CCL20 / CCL4 / CCL5 / CDC42EP2 / DLC1 / EIF2B3 / RAB3IL1 / RANGRF / RASA3 / RASAL3 / RASGRP4 / RGS16 / RGS19 / TBC1D1 / TBC1D2
GO:0006928	movement of cell or subcellular component	3,68E-02	ABR / ACTN1 / ADAM10 / ALCAM / CCL2 / CCL20 / CCL4 / CCL5 / DYNLRB2 / EDN1 / EXT1 / F2R / F2RL1 / GCNT1 / HYAL2 / LIMD1 / MMP9 / MYO1C / PAK1 / PDGFA / PLAU / PRCP / PRR5L / PTGER4 / PTP4A2 / RHBDF1 / RHOB / S100A2 / S100A8 / S100A9 / S1PR1 / SCN4B / SDC1 / SDC2 / SEMA3C / SERPINE1 / SORD / TGFBR1 / TIMP1 / TNF / TNK2 / TTLL1 / UCHL1 / VASP / VEGFB
GO:0006694	steroid biosynthetic process	3,95E-02	APOE / CYP51A1 / DHCR7 / EGR1 / FDFT1 / IDI1 / INSIG1 / LSS / STAR / TNF
GO:0044283	small molecule biosynthetic process	4,31E-02	APOE / ASS1 / CYP51A1 / DHCR7 / DPYD / EDN1 / EGR1 / ELOVL5 / FADS2 / FADS3 / FDFT1 / GLUL / GPI / IDI1 / INSIG1 / MMAB / OAT / PC / PHGDH / PLA2G4A / PTGS2 / SDS / SORD / SRR / TNF / TRIB3
GO:0080134	regulation of response to stress	4,31E-02	A2M / ABR / ANXA2 / CCL2 / CCL4 / CCL5 / CDKN2D / COLEC12 / EDN1 / ELL3 / EZR / F2R / FABP4 / GADD45A / GADD45G / HOPX / HYAL2 / IL1B / IL6 / LBH / NUDT16 / PAK1 / PDGFA / PLAU / PPARG / PRDX1 / PTGER4 / S100A8 / S100A9 / S100B / SAMHD1 / SERPINE1 / SOCS3 / TLR10 / TLR2 / TLR6 / TMEM173 / TNF
GO:0002237	response to molecule of bacterial origin	4,31E-02	ABR / CCL2 / CCL5 / CD40 / F2R / IL10 / IL6 / JUNB / SERPINE1 / SRR / TLR2 / TLR6 / TNF / ZFP36
GO:0006468	protein phosphorylation	4,31E-02	ADAM10 / AVPI1 / BGN / CCL2 / CCL20 / CCL4 / CCL5 / CD40 / CDK1 / CDKN2D / CISH / CSF2 / DUSP18 / DUSP26 / DUSP6 / EDN1 / EZR / F2R / F2RL1 / FABP4 / GADD45A / GADD45G / GRK5 / GUCY2D / HES1 / HYAL2 / IGFBP4 / IL1B / IL6 / IL6 / LIMK2 / MAP2K6 / MICAL1 / PAK1 / PDGFA / PKIG / PLAUR / PRDX1 / PRKCDBP / PRR5L / PTGS2 / RSRC1 / SFN / SOCS2 / SOCS3 / SPRY4 / TGFBR1 / TNF / TNK2 / TRIB3 / UCHL1 / ZFP36
GO:0050663	cytokine secretion	4,62E-02	CLEC6A / EZR / F2R / F2RL1 / HYAL2 / IL10 / TLR10 / TLR2 / TLR6 / TNF

MØ1H: Nc-Spain1H-infected macrophages; MØ7: Nc-Spain7-infected macrophages; MØHK: macrophages inoculated with heat-killed tachyzoites; MØC: non-infected macrophages.

SUPPLEMENTARY TABLE 4 | Gene Ontology analysis of DEG in MØ1H-MØC, MØ7-MØC, and MØHK-MØC comparisons

Biological processes enriched from DEG in MØ1H- MØC comparison						
GO term ID	Description	padj	Count	Frequency[a]	Uniqueness[b]	Dispensability[c]
GO:0002376	**Immune system process**	5.16E-04	128	10.27 %	0.97	0.00
GO:0002684	**PR of immune system process**	3.01E-02	60	3.65 %	0.72	0.00
GO:0051249	*Regulation of lymphocyte activation*	2.07E-02	25	1.77 %	0.73	0.83
GO:0006955	*Immune response*	2.39E-05	88	6.05 %	0.75	0.67
[d]GO:0045321	*Leukocyte activation*	1.36E-02	41	3.51 %	0.77	0.61
GO:0002521	*Leukocyte differentiation*	4.16E-03	33	2.47 %	0.76	0.74
[d]GO:1903708	*PR of hemopoiesis*	2.88E-03	41	0.80 %	0.70	0.69
GO:0006732	**Coenzime metabolic process**	1.67E-02	33	1.38 %	0.94	0.00
GO:0006954	**Inflammatory response**	5.74E-05	58	2.67 %	0.87	0.00
GO:0050729	*PR of inflammatory response*	5.74E-05	18	0.41 %	0.76	0.76
GO:0031349	*PR of defense response*	1.35E-04	32	1.29 %	0.77	0.66
GO:0007159	**Leukocyte cell-cell adhesion**	1.23E-03	35	2.37 %	0.88	0.00
[d]GO:0046634	*Regulation of alfa-beta T cell-activation*	9.40E-03	10	0.33 %	0.72	0.69
GO:1903039	*PR of leukocyte cell-cell adhesion*	1.02E-02	18	0.82 %	0.81	0.82
[d]GO:0002286	*T cell activation involved in immune response*	1.36E-03	12	0.57 %	0.72	0.73
[d]GO:0016032	**Viral process**	3.20E-02	43	1.24 %	0.91	0.00
[d]GO:0044419	*Interspecies interaction between organisms*	3.92E-02	44	1.46 %	0.92	0.65
[d]GO:0044403	*Symbiosis, mutualism through parasitism*	3.92E-02	44	1.44 %	0.91	0.96
GO:0050663	**Cytokine secretion**	1.23E-03	20	0.85 %	0.78	0.02
[d]GO:0042990	*Regulation of TF import into nucleus*	1.40E-02	10	0.40 %	0.78	0.68
[d]GO:0042991	*TF import into nucleus*	1.40E-02	10	0.41 %	0.83	0.78
GO:0001817	*Regulation of cytokine production*	1.12E-02	38	3.51 %	0.83	0.81
[d]GO:0070201	*Regulation of protein localization*	1.40E-02	50	3.44 %	0.78	0.55
GO:0046822	*Regulation of nucleocytoplasmic transport*	3.93E-02	17	0.98 %	0.80	0.75
[d]GO:0051046	*Regulation of secretion*	4.45E-03	46	2.86 %	0.78	0.72
GO:0050707	*Regulation of cytokine secretion*	2.87E-03	16	0.72 %	0.73	0.79
GO:0032943	**Mononuclear cell proliferation**	1.92E-02	21	1.42 %	0.89	0.02
GO:0032944	*Regulation of mononuclear cell proliferation*	4.59E-02	17	0.93 %	0.85	0.93
GO:0043067	**Regulation of programmed cell death**	1.19E-03	87	6.47 %	0.88	0.09
GO:0050793	**Regulation of developmental process**	3.92E-02	107	10.36 %	0.89	0.09
[d]GO:0051707	**Response to other organism**	1.23E-03	61	3.57 %	0.87	0.14
[d]GO:0043207	*Response to external biotic stimulus*	1.23E-03	61	3.58 %	0.87	0.95
GO:0043408	**Regulation of MAPK cascade**	1.80E-03	52	2.97 %	0.65	0.14
GO:1902531	*Regulation of intracellular signal transduction*	2.20E-04	104	7.58 %	0.74	0.62
GO:0023057	*NR of signaling*	9.40E-03	70	5.32 %	0.85	0.62
GO:0042325	*Regulation of phosphorylation*	6.28E-03	87	6.87 %	0.82	0.75
GO:0016310	*Phosphorylation*	1.22E-02	128	11.27 %	0.89	0.55
GO:0010648	*NR of cell communication*	9.40E-03	70	5.30 %	0.84	0.63
GO:0006468	*Protein phosphorylation*	2.00E-02	101	9.30 %	0.87	0.77
[d]GO:0010647	*PR of cell communication*	4.94E-02	80	6.61 %	0.81	0.65
GO:0071345	**Cellular response to cytokine stimulus**	3.80E-03	41	2.93 %	0.88	0.18
GO:0034097	*Response to cytokine*	1.11E-02	44	3.27 %	0.88	0.55
GO:0006509	**Membrane protein ectodomain proteolysis**	1.55E-02	8	0.25 %	0.94	0.18
GO:0001816	**Cytokine production**	1.23E-02	43	3.03 %	0.91	0.23
GO:0098869	**Cellular oxidant detoxification**	4.46E-02	13	0.46 %	0.90	0.28
GO:0009636	**Response to toxic substance**	2.81E-02	16	0.73 %	0.90	0.30
GO:0010883	**Regulation of lipid storage**	3.92E-02	8	0.20 %	0.84	0.33
GO:0006082	**Organic acid metabolic process**	3.74E-03	82	4.72 %	0.86	0.38
GO:0044712	**Single-organism catabolic process**	2.81E-02	66	3.68 %	0.87	0.39
[d]GO:1901575	*Organic substance catabolic process*	2.20E-02	127	8.73 %	0.92	0.76
GO:0050790	**Regulation of catalytic activity**	2.27E-02	124	10.94 %	0.88	0.46
GO:0044093	*PR of molecular function*	2.81E-02	90	7.90 %	0.89	0.72
GO:0048585	**NR of response to stimulus**	3.80E-03	83	6.25 %	0.79	0.49
[d]GO:0006952	**Defense response**	5.74E-05	98	5.99 %	0.87	0.50

Biological processes enriched from DEG in MØ7- MØC comparison						
GO term ID	Description	padj	Count	Frequency[a]	Uniqueness[b]	Dispensability[c]
GO:0002376	**Immune system process**	6.98E-04	109	10.27 %	0.97	0.00
GO:0007159	**Leukocyte cell-cell adhesion**	2.54E-03	30	2.37 %	0.89	0.00
[e]GO:0042110	*T cell activation*	1.49E-02	25	2.18 %	0.73	0.86
GO:1903039	*PR of leukocyte cell-cell adhesion*	4.79E-02	14	0.82 %	0.82	0.76
[e]GO:0022610	**Biological adhesion**	1.67E-02	68	6.66 %	0.97	0.00
GO:0031349	**PR of defense response**	9.10E-06	31	1.29 %	0.77	0.00
GO:0050729	*PR of inflammatory response*	5.69E-06	18	0.41 %	0.79	0.76
GO:0006954	*Inflammatory response*	7.59E-05	51	2.67 %	0.86	0.66
[e]GO:0070661	**Leukocyte proliferation**	1.52E-02	20	1.48 %	0.89	0.02
GO:0001816	**Cytokine production**	4.20E-03	40	3.03 %	0.90	0.02
GO:0006082	**Organic acid metabolic process**	1.14E-02	68	7.72 %	0.86	0.03
GO:0050790	**Regulation of catalytic activity**	1.12E-02	109	10.94 %	0.87	0.05
[e]GO:0044092	*NR of molecular function*	4.51E-02	54	5.20 %	0.87	0.66
GO:0044093	*PR of molecular function*	3.75E-02	76	7.90 %	0.87	0.72
GO:0006509	**Membrane protein ectodomain proteolysis**	2.57E-02	7	0.25 %	0.93	0.05
GO:0006732	**Coenzyme metabolic process**	1.69E-02	29	1.38 %	0.94	0.08
GO:0042981	**Regulation of apoptotic process**	4.70E-04	76	6.08 %	0.86	0.11
GO:0071345	**Cellular response to cytokine stimulus**	4.52E-03	36	2.93 %	0.87	0.12
GO:0034097	*Response to cytokine*	1.00E-02	39	3.27 %	0.88	0.55
[e]GO:0009605	**Response to external stimulus**	1.13E-03	103	8.74 %	0.90	0.16
[e]GO:0014033	**Neural crest cell differentiation**	3.74E-02	7	0.34 %	0.86	0.21
GO:0050707	**Regulation of cytokine secretion**	5.03E-03	14	0.72 %	0.70	0.23
GO:0050663	*Cytokine secretion*	3.63E-03	17	0.85 %	0.76	0.97
[e]GO:1903531	*NR of secretion by cell*	5.64E-03	17	0.69 %	0.74	0.71
GO:0001817	*Regulation of cytokine production*	5.17E-03	35	2.72 %	0.81	0.81
[e]GO:1904589	*Regulation of protein import*	6.64E-03	16	0.81 %	0.78	0.85
[e]GO:1900180	*Regulation of protein localization to nucleus*	1.18E-02	18	1.04 %	0.78	0.85
GO:0046822	*Regulation of nucleocytoplasmic transport*	1.14E-02	17	0.98 %	0.80	0.81
[e]GO:0042306	*Regulation of protein import into nucleus*	5.17E-03	16	0.80 %	0.76	0.69
GO:0050793	**Regulation of developmental process**	3.07E-02	92	10.36 %	0.86	0.25
[e]GO:0046470	**Phosphatidylcholine metabolic process**	3.75E-02	6	0.18 %	0.86	0.27
GO:0002684	**PR of immune system process**	1.01E-03	52	3.65 %	0.74	0.27
[e]GO:1902107	*PR of leukocyte differentiation*	1.89E-02	13	0.64 %	0.69	0.72
GO:0032943	*Mononuclear cell proliferation*	1.52E-02	19	1.42 %	0.66	0.97
GO:0032944	*Regulation of mononuclear cell proliferation*	4.68E-02	15	0.93 %	0.82	0.94
GO:0051249	*Regulation of lymphocyte activation*	3.83E-02	21	1.77 %	0.74	0.81
GO:0006955	*Immune response*	5.69E-06	78	6.05 %	0.77	0.67
[e]GO:0046651	*Lymphocyte proliferation*	1.52E-02	19	1.41 %	0.71	0.54
GO:0002521	*Leukocyte differentiation*	1.04E-02	28	2.47 %	0.74	0.58
GO:0098869	**Cellular oxidant detoxification**	3.26E-02	12	0.46 %	0.90	0.28
GO:0009636	**Response to toxic substance**	1.69E-02	15	0.73 %	0.90	0.30
GO:0010883	**Regulation of lipid storage**	1.74E-02	8	0.20 %	0.84	0.34
GO:0009611	**Response to wounding**	4.94E-02	26	1.96 %	0.88	0.38
GO:0044712	**Single-organism catabolic process**	4.80E-02	55	3.68 %	0.90	0.39
GO:0043408	**Regulation of MAPK cascade**	2.37E-04	49	2.97 %	0.63	0.40
GO:1902531	*Regulation of intracellular signal transduction*	2.37E-04	90	7.58 %	0.73	0.62
GO:0023057	*NR of signaling*	4.05E-03	63	5.32 %	0.81	0.62
GO:0051248	*NR of protein metabolic process*	2.19E-02	58	5.29 %	0.81	0.56
GO:0042325	*Regulation of phosphorylation*	1.49E-02	73	6.87 %	0.80	0.75
GO:0010648	*NR of cell communication*	4.05E-03	63	5.30 %	0.80	0.63
GO:0006468	*Protein phosphorylation*	2.95E-02	85	9.30 %	0.85	0.77
GO:0048585	**NR of response to stimulus**	9.28E-04	75	6.25 %	0.76	0.49

Biological processes enriched from DEG in MØHK- MØC comparison						
GO term ID	Description	padj	Count	Frequency[a]	Uniqueness[b]	Dispensability[c]
GO:0002376	**Immune system process**	2.01E-02	62	10.27 %	0.96	0.00
GO:0006954	**Inflammatory response**	8.37E-04	34	2.67 %	0.78	0.00
GO:0050729	*PR of inflammatory response*	9.35E-04	12	0.41 %	0.69	0.58
GO:0031349	*PR of defense response*	3.17E-02	15	1.29 %	0.70	0.76
[f]GO:0032103	*PR of response to external stimulus*	2.03E-02	15	1.15 %	0.72	0.68
GO:0009611	*Response to wounding*	3.28E-03	23	1.96 %	0.81	0.42
[f]GO:0007155	**Cell adhesion**	2.91E-02	42	6.62 %	0.96	0.00
[f]GO:0040011	**Locomotion**	3.22E-02	42	7.12 %	0.96	0.00
[f]GO:0050817	**Coagulation**	9.93E-03	15	0.92 %	0.92	0.00
[f]GO:0050878	**Regulation of body fluid levels**	5.15E-03	22	1.52 %	0.90	0.00
GO:0050900	**Leukocyte migration**	2.25E-02	16	1.42 %	0.82	0.02
GO:0006955	*Immune response*	2.77E-02	39	6.05 %	0.81	0.58
[f]GO:0030335	*PR of cell migration*	3.59E-02	17	1.82 %	0.76	0.66
[f]GO:0008283	**Cell proliferation**	5.66E-03	54	8.54 %	0.94	0.02
GO:0048660	**Regulation of muscle cell proliferation**	2.91E-02	7	0.33%	0.87	0.04
GO:0048659	*Smooth muscle cell proliferation*	2.91E-02	7	0.34 %	0.91	0.90
[f]GO:0051348	**NR of transferase activity**	1.69E-02	17	1.40 %	0.87	0.04
[f]GO:0043547	*PR of GTPase activity*	3.62E-02	19	2.67 %	0.88	0.50
[f]GO:0006928	**Movement of cell or subcellular component**	3.68E-02	45	7.97 %	0.92	0.10
GO:0043408	**Regulation of MAPK cascade**	9.93E-03	29	2.97 %	0.55	0.14
GO:0016310	*Phosphorylation*	3.36E-02	65	11.27 %	0.83	0.68
GO:0048585	*NR of response to stimulus*	9.62E-03	46	6.26 %	0.67	0.49
[f]GO:0080134	**Regulation of response to stress**	4.31E-02	38	5.11 %	0.71	0.54
GO:1902531	*Regulation of intracellular signal transduction*	1.09E-03	57	7.58 %	0.67	0.62
[f]GO:0033673	*NR of kinase activity*	1.69E-02	16	1.29 %	0.68	0.88
GO:0006468	*Protein phosphorylation*	4.31E-02	52	9.30 %	0.81	0.66
GO:0023057	*NR of signaling*	2.94E-02	37	5.32 %	0.77	0.62
GO:0010648	*NR of cell communication*	2.94E-02	37	5.30 %	0.78	0.63
[f]GO:0045936	*NR of phosphate metabolic process*	1.69E-02	24	2.70 %	0.72	0.65
GO:0051248	*NR of protein metabolic process*	2.91E-02	37	5.29 %	0.76	0.56
[f]GO:0010563	*NR of phosphorus metabolic process*	1.69E-02	24	2.70 %	0.73	0.65
GO:0034097	**Response to cytokine**	1.69E-02	26	3.27 %	0.79	0.14
[f]GO:0002237	*Response to molecule of bacterial origin*	4.31E-02	14	1.30 %	0.77	0.49
[f]GO:0034612	*Response to tumor necrosis factor*	1.69E-02	10	0.81 %	0.80	0.47
GO:0071345	*Cellular response to cytokine stimulus*	1.70E-02	23	2.93 %	0.77	0.79
GO:0050707	**Regulation of cytokine secretion**	1.69E-02	10	0.72 %	0.79	0.20
GO:0050663	*Cytokine secretion*	4.62E-02	10	0.852%	0.84	0.79
[f]GO:0051049	*Regulation of transport*	3.36E-02	50	7.79 %	0.81	0.51
GO:0098869	**Cellular oxidant detoxification**	3.46E-02	9	0.46 %	0.84	0.28
[f]GO:0006694	**Steroid biosynthetic process**	3.95E-02	10	0.66 %	0.89	0.29
[f]GO:0044283	*Small molecule biosynthetic process*	4.31E-02	26	2.35 %	0.89	0.59
GO:0009636	**Response to toxic substance**	2.22E-02	11	0.73 %	0.83	0.30

[a]Proportion of the GO term in the underlying protein annotation database (UniProt). Higher frequency implies more general terms and lower frequency more specific ones.
[b]Measures whether the term is an outlier when compared semantically to the whole list. Calculated as 1- (average semantic similarity of a term to all other terms). More unique terms tend to be less dispensable.
[c]Semantic similarity threshold at which the term was removed from the list and assigned to a cluster.
[d]GO terms not enriched from DEG in MØ7-MØC or MØHK-MØC comparisons.
[e]GO terms not enriched from DEG in MØ1H-MØC or MØHK-MØC comparisons.
[f]GO terms not enriched from DEG in MØ7-MØC or MØ1H-MØC comparisons.
PR, positive regulation; NR negative regulation; TF transcription factor. Representative GO terms for each of the clusters are shown in bold and GO terms included within the clusters are italicized.

SUPPLEMENTARY TABLE 5 | KEGG pathway analysis of differentially expressed genes in bovine macrophages inoculated with *Neospora caninum versus* non-infected macrophages

ID	Description	P. adj	geneID
			MØ1H vs MØC
bta04060	Cytokine-cytokine receptor interaction	1,39E-05	ACKR3 / ACVR1B / ACVR2B / CCL14 / CCL2 / CCL20 / CCL22 / CCL4 / CCL5 / CCR10 / CCR6 / CCR7 / CD40 / CLCF1 / CNTFR / CSF1 / CSF1R / CSF2 / CSF3 / CX3CL1 / CXCL13 / CXCR5 / EDA / EPOR / FAS / FLT1 / FLT4 / HGF / IFNAR2 / IFNGR1 / IL10 / IL11RA / IL12A / IL12B / IL12RB2 / IL15 / IL17RA / IL17RC / IL1A / IL1B / IL1R1 / IL1R2 / IL1RAP / IL23R / IL2RA / IL2RB / IL4R / IL6 / IL6 / IL6R / IL7 / IL7R / KDR / LIF / OSMR / TGFBR1 / TGFBR2 / TNF / TNFRSF18 / TNFRSF1A / TNFRSF1B / TNFRSF6B / TNFRSF8 / TNFSF10 / TNFSF11 / TNFSF12 / TNFSF12 / TNFSF13 / TNFSF14 / TNFSF15 / TNFSF18 / TNFSF8 / TNFSF9 / VEGFA / VEGFB
bta04668	TNF signaling pathway	2,98E-05	BIRC3 / CASP7 / CCL2 / CCL20 / CCL5 / CFLAR / CREB1 / CREB3L3 / CSF1 / CSF2 / CX3CL1 / EDN1 / FADD / FAS / IKBKB / IL15 / IL1B / IL6 / JUNB / LIF / MAP2K1 / MAP3K8 / MAPK11 / MAPK12 / MAPK14 / MLKL / NFKB1 / NFKBIA / NOD2 / PIK3CD / PIK3R3 / PTGS2 / RPS6KA5 / SELE / TAB2 / TNF / TNFAIP3 / TNFRSF1A / TNFRSF1B / TRAF1 / TRAF2
bta04621	NOD-like receptor signaling pathway	2,33E-04	ANTXR1 / BIRC3 / CARD9 / CASP4 / CCL2 / CCL5 / FADD / GABARAPL1 / GABARAPL2 / GBP5 / IFNAR2 / IKBKB / IKBKE / IL1B / IL6 / IL6 / ITPR1 / ITPR3 / MAPK11 / MAPK12 / MAPK14 / MEFV / NAIP / NEK7 / NFKB1 / NFKBIA / NLRC4 / NLRP1 / NLRP12 / NLRP3 / NLRX1 / NOD1 / NOD2 / PANX1 / RIPK2 / RNASEL / TAB2 / TBK1 / TICAM1 / TMEM173 / TNF / TNFAIP3 / TRAF2 / TRPM2 / TXNIP / TYK2 / VDAC2
bta00280	Valine, leucine and isoleucine degradation	5,47E-04	AACS / ABAT / ACAA1 / ACADS / ACADSB / ACAT1 / ACAT2 / ALDH6A1 / ALDH7A1 / ALDH9A1 / BCKDHA / BCKDHB / DBT / ECHS1 / EHHADH / HADH / HIBADH / IL4I1 / IVD / MCCC1 / MUT / PCCA / PCCB
bta04620	Toll-like receptor signaling pathway	5,47E-04	CCL4 / CCL5 / CD40 / CD80 / CD86 / FADD / IFNAR2 / IKBKB / IKBKE / IL12A / IL12B / IL1B / IL6 / IL6 / MAP2K1 / MAP3K8 / MAPK11 / MAPK12 / MAPK14 / NFKB1 / NFKBIA / PIK3CD / PIK3R3 / TAB2 / TBK1 / TICAM1 / TIRAP / TLR2 / TLR3 / TLR5 / TLR6 / TLR7 / TNF
bta01212	Fatty acid metabolism	8,31E-04	ACAA1 / ACACA / ACADS / ACADSB / ACAT1 / ACAT2 / ACSL1 / ACSL4 / ACSL5 / CPT1A / ECHS1 / EHHADH / ELOVL5 / FADS1 / FADS2 / FASN / HACD4 / HADH / MECR / OXSM / PPT1 / TECR
bta05142	Chagas disease (American trypanosomiasis)	8,31E-04	C1QA / C1QC / C3 / CCL2 / CCL5 / CD247 / CFLAR / FADD / FAS / GNAI1 / GNAI3 / GNAL / IFNGR1 / IKBKB / IL10 / IL12A / IL12B / IL1B / IL6 / IL6 / MAPK11 / MAPK12 / MAPK14 / NFKB1 / NFKBIA / NOS2 / PIK3CD / PIK3R3 / PPP2R2C / SERPINE1 / TGFBR1 / TGFBR2 / TICAM1 / TLR2 / TLR6 / TNF / TNFRSF1A
bta04142	Lysosome	1,32E-03	ACP2 / ACP5 / AGA / AP1B1 / AP1S2 / AP3B1 / AP4S1 / ARSA / ARSB / ASAH1 / ATP6AP1 / ATP6V0A1 / CD63 / CD68 / CLTA / CTNS / CTSC / CTSF / CTSO / CTSS / DNASE2 / GLA / GLB1 / GM2A / GUSB / IDUA / LAMP2 / LAMP3 / LAPTM4A / LGMN / LIPA / NAGA / NPC2 / PPT1 / PSAP / SGSH / SLC11A1 / SLC17A5 / SUMF1 / TPP1
bta00640	Propanoate metabolism	1,32E-03	ABAT / ACACA / ACAT1 / ACAT2 / ACSS2 / ACSS3 / ALDH6A1 / BCKDHA / BCKDHB / DBT / ECHS1 / EHHADH / LDHA / MUT / PCCA / PCCB
bta04380	Osteoclast differentiation	1,70E-03	ACP5 / CREB1 / CSF1 / CSF1R / FOSL1 / FYN / IFNAR2 / IFNGR1 / IKBKB / IL1A / IL1B / IL1R1 / IL6 / JUNB / MAP2K1 / MAPK11 / MAPK12 / MAPK14 / NCF4 / NFKB1 / NFKB2 / NFKBIA / PIK3CD / PIK3R3 / PPARG / RELB / SOCS1 / TAB2 / TGFBR1 / TGFBR2 / TNF / TNFRSF1A / TNFSF11 / TRAF2 / TREM2 / TYK2 / TYROBP
bta05164	Influenza A	1,98E-03	ACTG1 / BOLA-DRB3 / CCL2 / CCL5 / FAS / FURIN / IFIH1 / IFNAR2 / IFNGR1 / IKBKB / IKBKE / IL12A / IL12B / IL1A / IL1B / IL6 / IL6 / JAK2 / MAP2K1 / MAPK11 / MAPK12 / MAPK14 / NFKB1 / NFKBIA / NLRP3 / NLRX1 / NXF1 / NXT2 / PIK3CD / PIK3R3 / RNASEL / RSAD2 / TBK1 / TICAM1 / TLR3 / TLR7 / TNF / TNFRSF10D / TNFRSF1A / TNFSF10 / TRIM25 / TYK2
bta04068	FoxO signaling pathway	3,28E-03	BCL6 / BNIP3 / CAT / CCNB2 / CCND1 / CCNG2 / CDKN1A / CDKN2D / FOXO4 / GABARAPL1 / GABARAPL2 / GADD45A / GADD45G / IGF1R / IKBKB / IL10 / IL6 / IL7R / IRS2 / KRAS / MAP2K1 / MAPK11 / MAPK12 / MAPK14 / MDM2 / NLK / NRAS / PCK2 / PIK3CD / PIK3R3 / PLK2 / PLK3 / PRKAB1 / PRKAB2 / RBL2 / S1PR1 / SETD7 / SGK1 / TGFBR1 / TGFBR2 / TNFSF10
bta04658	Th1 and Th2 cell differentiation	3,76E-03	BOLA-DRB3 / CD247 / CD4 / DLL4 / GATA3 / IFNGR1 / IKBKB / IL12A / IL12B / IL12RB2 / IL2RA / IL2RB / IL4R / JAG1 / JAK2 / JAK3 / LAT / MAF / MAML3 / MAPK11 / MAPK12 / MAPK14 / NFKB1 / NFKBIA / NFKBIE / RBPJL / STAT5A / STAT6 / TYK2
bta04216	Ferroptosis	3,76E-03	ACSL1 / ACSL4 / ACSL5 / ATG7 / GCLC / GCLM / MAP1LC3A / NCOA4 / SAT2 / SLC39A14 / SLC39A8 / SLC40A1 / SLC7A11 / STEAP3 / TFRC / VDAC2
bta04640	Hematopoietic cell lineage	3,76E-03	BOLA-DRB3 / CD19 / CD38 / CD4 / CD44 / CD55 / CD59 / CSF1 / CSF1R / CSF2 / CSF3 / EPOR / IL11RA / IL1A / IL1B / IL1R1 / IL1R2 / IL2RA / IL4R / IL6 / IL6R / IL7 / IL7R / ITGA4 / ITGA5 / ITGA6 / TFRC / TNF
bta05152	Tuberculosis	5,13E-03	ATP6AP1 / ATP6V0A1 / BAD / BOLA-DRB3 / C3 / CARD9 / CD74 / CLEC7A / CREB1 / CTSS / CYP27B1 / EEA1 / FADD / IFNGR1 / IL10 / IL12A / IL12B / IL1A / IL1B / IL6 / IL6 / IRAK2 / JAK2 / LAMP2 / MAPK11 / MAPK12 / MAPK14 / MRC1 / MRC2 / NFKB1 / NOD2 / NOS2 / PLK3 / RIPK2 / SPHK1 / SPHK2 / SRC / TIRAP / TLR2 / TLR6 / TNF / TNFRSF1A / VDR
bta05133	Pertussis	7,51E-03	C1QA / C1QC / C1S / C3 / CASP7 / GNAI1 / GNAI3 / IL10 / IL12A / IL12B / IL1A / IL1B / IL6 / IRF1 / IRF8 / ITGA5 / MAPK11 / MAPK12 / MAPK14 / NFKB1 / NLRP3 / NOD1 / NOS2 / TICAM1 / TIRAP / TNF
bta04622	RIG-I-like receptor signaling pathway	8,34E-03	AZI2 / FADD / IFIH1 / IKBKB / IKBKE / IL12A / IL12B / IL6 / MAPK11 / MAPK12 / MAPK14 / NFKB1 / NFKBIA / NLRX1 / RNF125 / TBK1 / TBKBP1 / TKFC / TMEM173 / TNF / TRAF2 / TRIM25
bta05140	Leishmaniasis	8,34E-03	BOLA-DRB3 / C3 / IFNGR1 / IL10 / IL12A / IL12B / IL1A / IL1B / ITGA4 / JAK2 / MAPK11 / MAPK12 / MAPK14 / MARCKSL1 / NCF4 / NFKB1 / NFKBIA / NOS2 / PTGS2 / TAB2 / TLR2 / TNF
bta05145	Toxoplasmosis	9,27E-03	ALOX5 / BAD / BIRC3 / BOLA-DRB3 / CD40 / GNAI1 / GNAI3 / IFNGR1 / IKBKB / IL10 / IL12A / IL12B / ITGA6 / JAK2 / LAMB3 / LDLR / MAPK11 / MAPK12 / MAPK14 / NFKB1 / NFKBIA / NOS2 / PIK3CG / PIK3R5 / PIK3R6 / PPIF / SOCS1 / TAB2 / TLR2 / TNF / TNFRSF1A / TYK2

bta00040	Pentose and glucuronate interconversions	9,70E-03	CRYL1 / DCXR / DHDH / GUSB / SORD / UGDH / UGT1A1 / XYLB
bta04657	IL-17 signaling pathway	1,10E-02	CCL2 / CCL20 / CSF2 / CSF3 / FADD / FOSL1 / IKBKB / IKBKE / IL17RA / IL17RC / IL1B / IL6 / MAPK11 / MAPK12 / MAPK14 / MAPK7 / NFKB1 / NFKBIA / PTGS2 / S100A8 / S100A9 / TAB2 / TBK1 / TNF / TNFAIP3 / TRAF2 / TRAF4
bta04659	Th17 cell differentiation	1,17E-02	BOLA-DRB3 / CD247 / CD4 / GATA3 / HIF1A / IFNGR1 / IKBKB / IL1B / IL1R1 / IL1RAP / IL23R / IL2RA / IL2RB / IL4R / IL6 / IL6R / JAK2 / JAK3 / LAT / MAPK11 / MAPK12 / MAPK14 / NFKB1 / NFKBIA / NFKBIE / RORA / STAT5A / STAT6 / TGFBR1 / TGFBR2 / TYK2
bta05162	Measles	1,33E-02	CCND1 / CCND3 / CDK6 / FAS / FYN / IFIH1 / IFNAR2 / IFNGR1 / IKBKE / IL12A / IL12B / IL1A / IL1B / IL2RA / IL2RB / IL6 / IL6 / JAK2 / JAK3 / NFKB1 / NFKBIA / PIK3CD / PIK3R3 / SLAMF1 / STAT5A / TAB2 / TBK1 / TLR2 / TLR7 / TNFAIP3 / TNFRSF10D / TNFSF10 / TP73 / TYK2
bta00071	Fatty acid degradation	1,62E-02	ACAA1 / ACADS / ACADSB / ACAT1 / ACAT2 / ACSL1 / ACSL4 / ACSL5 / ALDH7A1 / ALDH9A1 / CPT1A / ECHS1 / ECI2 / EHHADH / GCDH / HADH
bta00380	Tryptophan metabolism	1,62E-02	AADAT / ACAT1 / ACAT2 / ALDH7A1 / ALDH9A1 / CAT / CYP1A1 / ECHS1 / EHHADH / GCDH / HADH / IDO1 / IL4I1 / KMO / KYNU / MAOA
bta05321	Inflammatory bowel disease (IBD)	2,75E-02	BOLA-DRB3 / IFNGR1 / IL10 / IL12A / IL12B / IL12RB2 / IL1A / IL1B / IL23R / IL4R / IL6 / MAF / NFKB1 / NOD2 / RORA / STAT6 / TLR2 / TLR5 / TNF
bta05144	Malaria	2,92E-02	CCL2 / CD40 / CSF3 / GYPC / HGF / IL10 / IL12A / IL1B / IL6 / PECAM1 / SDC1 / SDC2 / SELE / SELP / TLR2 / TNF
bta04115	p53 signaling pathway	4,11E-02	CCNB2 / CCND1 / CCND3 / CCNG1 / CCNG2 / CD82 / CDK6 / CDKN1A / CHEK2 / FAS / GADD45A / GADD45G / MDM2 / MDM4 / RFWD2 / SERPINE1 / SESN1 / SESN3 / STEAP3 / TP73 / ZMAT3
bta00531	Glycosaminoglycan degradation	4,27E-02	ARSB / GLB1 / GUSB / HPSE / HYAL2 / IDUA / SGSH
bta04210	Apoptosis	4,27E-02	ACTG1 / BAD / BCL2A1 / BIRC3 / CAPN2 / CASP7 / CFLAR / CTSC / CTSF / CTSO / CTSS / FADD / FAS / GADD45A / GADD45G / IKBKB / ITPR1 / ITPR3 / KRAS / MAP2K1 / NFKB1 / NFKBIA / NGF / NRAS / PARP3 / PIK3CD / PIK3R3 / TNF / TNFRSF10D / TNFRSF1A / TNFSF10 / TRAF1 / TRAF2 / TUBA1A / TUBA1B
bta04064	NF-kappa B signaling pathway	4,27E-02	BCL2A1 / BIRC3 / CARD10 / CCL4 / CD40 / CFLAR / IKBKB / IL1B / IL1R1 / LAT / LYN / NFKB1 / NFKB2 / NFKBIA / PTGS2 / RELB / TAB2 / TICAM1 / TIRAP / TNF / TNFAIP3 / TNFRSF1A / TNFSF11 / TNFSF14 / TRAF1 / TRAF2 / TRIM25
bta05205	Proteoglycans in cancer	4,27E-02	ACTG1 / ARHGEF1 / CAV2 / CCND1 / CD44 / CD63 / CDKN1A / CTTN / EZR / FAS / FLNA / FLNB / GAB1 / GPC1 / HGF / HIF1A / HPSE / HSPG2 / IGF1R / IL12B / ITGA5 / ITGAV / ITGB5 / ITPR1 / ITPR3 / KDR / KRAS / MAP2K1 / MAPK11 / MAPK12 / MAPK14 / MDM2 / MMP2 / NRAS / PDCD4 / PIK3CD / PIK3R3 / PLAUR / PRKACA / PTPN11 / PXN / ROCK2 / SDC1 / SDC2 / SDC4 / SRC / TIAM1 / TIMP3 / TLR2 / TNF / VEGFA / WNT5A
bta05134	Legionellosis	4,34E-02	BNIP3 / C3 / CASP7 / EEF1A2 / IL12A / IL12B / IL1B / IL6 / NAIP / NFKB1 / NFKB2 / NFKBIA / NLRC4 / TLR2 / TLR5 / TNF
bta01200	Carbon metabolism	4,41E-02	ACADS / ACAT1 / ACAT2 / ACO1 / ACSS2 / ALDH6A1 / CAT / ECHS1 / EHHADH / ENO3 / G6PD / GPT2 / HK1 / HK2 / IDH2 / ME2 / MUT / PC / PCCA / PCCB / PDHB / PFKL / PFKM / PGK1 / PHGDH / PSAT1 / PSPH / SDHB / SDS / SHMT1 / TKFC / TPI1
bta05323	Rheumatoid arthritis	4,46E-02	ACP5 / ATP6AP1 / ATP6V0A1 / BOLA-DRB3 / CCL2 / CCL20 / CCL5 / CD80 / CD86 / CSF1 / CSF2 / CTLA4 / FLT1 / IL15 / IL1A / IL1B / IL6 / TLR2 / TNF / TNFSF11 / TNFSF13 / VEGFA

MØ7 *vs* MØC			
bta04060	Cytokine-cytokine receptor interaction	2,92E-06	ACKR3 / ACVR1B / ACVR2B / CCL14 / CCL2 / CCL20 / CCL22 / CCL4 / CCL5 / CCR6 / CCR7 / CD40 / CLCF1 / CNTFR / CSF1 / CSF1R / CSF2 / CSF3 / CX3CL1 / CXCL13 / CXCR5 / EDA / EPOR / FAS / FLT1 / FLT4 / HGF / IFNGR1 / IL10 / IL10RA / IL11RA / IL12B / IL12RB2 / IL15 / IL17RC / IL1A / IL1B / IL1R1 / IL1R2 / IL23A / IL23R / IL2RA / IL2RB / IL4R / IL6 / IL6 / IL6R / IL7 / IL7R / LIF / TGFBR1 / TGFBR2 / TNF / TNFRSF18 / TNFRSF1A / TNFRSF6B / TNFSF10 / TNFSF11 / TNFSF12 / TNFSF12 / TNFSF13 / TNFSF14 / TNFSF18 / TNFSF9 / VEGFA / VEGFB / VEGFC
bta04668	TNF signaling pathway	1,39E-04	BIRC3 / CASP7 / CCL2 / CCL20 / CCL5 / CFLAR / CREB3L3 / CSF1 / CSF2 / CX3CL1 / EDN1 / FADD / FAS / FOS / IL15 / IL1B / IL6 / JUNB / LIF / MAP3K8 / MAPK11 / MAPK12 / MLKL / NFKB1 / NFKBIA / NOD2 / PIK3CD / PTGS2 / RPS6KA5 / TAB2 / TNF / TNFAIP3 / TNFRSF1A / TRAF1 / TRAF2
bta01212	Fatty acid metabolism	9,72E-04	ACAA1 / ACACA / ACADSB / ACAT1 / ACAT2 / ACSL1 / ACSL4 / ACSL5 / CPT1A / EHHADH / ELOVL5 / FADS1 / FADS2 / FASN / HACD4 / HADH / MECR / OXSM / PPT1 / TECR
bta04640	Hematopoietic cell lineage	9,72E-04	BOLA-DRB3 / CD19 / CD38 / CD4 / CD44 / CD59 / CSF1 / CSF1R / CSF2 / CSF3 / EPOR / IL11RA / IL1A / IL1B / IL1R1 / IL1R2 / IL2RA / IL4R / IL6 / IL6R / IL7 / IL7R / ITGA4 / ITGA5 / MS4A1 / TFRC / TNF
bta00280	Valine, leucine and isoleucine degradation	1,04E-03	AACS / ABAT / ACAA1 / ACADSB / ACAT1 / ACAT2 / ALDH6A1 / ALDH7A1 / ALDH9A1 / BCKDHB / DBT / EHHADH / HADH / HIBADH / IL4I1 / IVD / MCCC1 / MUT / PCCA / PCCB
bta05142	Chagas disease (American trypanosomiasis)	1,18E-03	C1QA / C1QB / C1QC / C3 / CCL2 / CCL5 / CFLAR / FADD / FAS / FOS / GNAI1 / IFNGR1 / IL10 / IL12B / IL1B / IL6 / IL6 / MAPK11 / MAPK12 / NFKB1 / NFKBIA / NOS2 / PIK3CD / PPP2R2C / SERPINE1 / TGFBR1 / TGFBR2 / TICAM1 / TLR2 / TLR6 / TNF / TNFRSF1A
bta04620	Toll-like receptor signaling pathway	1,18E-03	CCL4 / CCL5 / CD40 / CD80 / CD86 / FADD / FOS / IKBKE / IL12B / IL1B / IL6 / IL6 / MAP3K8 / MAPK11 / MAPK12 / NFKB1 / NFKBIA / PIK3CD / TAB2 / TBK1 / TICAM1 / TIRAP / TLR2 / TLR3 / TLR5 / TLR6 / TLR7 / TNF
bta04142	Lysosome	1,18E-03	ABCA2 / ACP2 / ACP5 / AGA / AP1B1 / AP1S2 / AP3B1 / AP4S1 / ARSA / ASAH1 / ATP6V0A1 / ATP6V0D2 / CD63 / CD68 / CTNS / CTSC / CTSF / CTSS / GLA / GLB1 / GM2A / GUSB / IDS / LAPTM4A / LGMN / LIPA / NAGA / NAPSA / NPC2 / PPT1 / PSAP / SLC11A1 / SLC17A5 / SUMF1 / TPP1
bta05323	Rheumatoid arthritis	1,18E-03	ACP5 / ATP6V0A1 / ATP6V0D2 / ATP6V1B2 / BOLA-DRB3 / CCL2 / CCL20 / CCL5 / CD80 / CD86 / CSF1 / CSF2 / FLT1 / FOS / IL15 / IL1A / IL1B / IL23A / IL6 / TLR2 / TNF / TNFSF11 / TNFSF13 / VEGFA
bta05133	Pertussis	1,18E-03	C1QA / C1QB / C1QC / C1S / C3 / CASP7 / FOS / GNAI1 / IL10 / IL12B / IL1A / IL1B / IL23A / IL6 / IRF1 / IRF8 / ITGA5 / MAPK11 / MAPK12 / NFKB1 / NOD1 / NOS2 / TICAM1 / TIRAP / TNF
bta04621	NOD-like receptor signaling pathway	1,21E-03	ANTXR2 / BIRC3 / CASP4 / CCL2 / CCL5 / FADD / GABARAPL1 / GABARAPL2 / GBP5 / IKBKE / IL1B / IL6 / IL6 / ITPR3 / MAPK11 / MAPK12 / MEFV / NAIP / NEK7 / NFKB1 / NFKBIA / NLRC4 / NLRP12 / NLRX1 / NOD1 / NOD2 / RIPK2 / RNASEL / TAB2 / TBK1 / TICAM1 / TMEM173 / TNF / TNFAIP3 / TRAF2 / TRPM2 / TXNIP / VDAC2
bta00640	Propanoate metabolism	1,99E-03	ABAT / ACACA / ACAT1 / ACAT2 / ACSS2 / ACSS3 / ALDH6A1 / BCKDHB / DBT / EHHADH / LDHA / MUT / PCCA / PCCB
bta05140	Leishmaniasis	5,94E-03	BOLA-DRB3 / C3 / FOS / IFNGR1 / IL10 / IL12B / IL1A / IL1B / ITGA4 / MAPK11 / MAPK12 / MARCKSL1 / NCF4 / NFKB1 / NFKBIA / NOS2 / PTGS2 / TAB2 / TLR2 / TNF
bta05152	Tuberculosis	6,67E-03	ATP6V0A1 / ATP6V0D2 / BAD / BOLA-DRB3 / C3 / CD74 / CLEC7A / CTSS / CYP27B1 / FADD / IFNGR1 / IL10 / IL10RA / IL12B / IL1A / IL1B / IL23A / IL6 / IL6 / IRAK2 / MAPK11 / MAPK12 / MRC1 / MRC2 / NFKB1 / NOD2 / NOS2 / RIPK2 / SPHK1 / SPHK2 / SRC / TIRAP / TLR2 / TLR6 / TNF / TNFRSF1A / VDR
bta05168	Herpes simplex infection	8,17E-03	ARNTL / BOLA-DRB3 / C3 / CCL2 / CCL5 / CD74 / CFP / FADD / FAS / FOS / IFIH1 / IFNGR1 / IKBKE / IL12B / IL15 / IL1B / IL6 / IL6 / NFKB1 / NFKBIA / NXF1 / PTPN11 / PVRL1 / RNASEL / TAB2 / TAF4B / TAF6L / TBK1 / TICAM1 / TLR2 / TLR3 / TNF / TNFRSF1A / TNFSF14 / TRAF1 / TRAF2 / UBE2R2
bta04380	Osteoclast differentiation	8,17E-03	ACP5 / CSF1 / CSF1R / FOS / FOSL1 / FYN / IFNGR1 / IL1A / IL1B / IL1R1 / IL6 / JUNB / MAPK11 / MAPK12 / NCF4 / NFKB1 / NFKB2 / NFKBIA / PIK3CD / PPARG / RELB / SOCS1 / TAB2 / TGFBR1 / TGFBR2 / TNF / TNFRSF1A / TNFSF11 / TRAF2 / TREM2
bta04064	NF-kappa B signaling pathway	8,17E-03	BCL2A1 / BIRC3 / CARD10 / CARD14 / CCL4 / CD40 / CFLAR / IL1B / IL1R1 / LAT / LYN / NFKB1 / NFKB2 / NFKBIA / PTGS2 / RELB / TAB2 / TICAM1 / TIRAP / TNF / TNFAIP3 / TNFRSF1A / TNFSF11 / TNFSF14 / TRAF1 / TRAF2
bta00380	Tryptophan metabolism	8,17E-03	AADAT / ACAT1 / ACAT2 / ALDH7A1 / ALDH9A1 / CAT / CYP1A1 / EHHADH / GCDH / HAAO / HADH / IL4I1 / KMO / KYNU / MAOA
bta04657	IL-17 signaling pathway	8,24E-03	CCL2 / CCL20 / CSF2 / CSF3 / FADD / FOS / FOSL1 / IKBKE / IL17RC / IL1B / IL6 / MAPK11 / MAPK12 / MAPK7 / NFKB1 / NFKBIA / PTGS2 / S100A8 / S100A9 / TAB2 / TBK1 / TNF / TNFAIP3 / TRAF2
bta05321	Inflammatory bowel disease (IBD)	8,70E-03	BOLA-DRB3 / IFNGR1 / IL10 / IL12B / IL12RB2 / IL1A / IL1B / IL23A / IL23R / IL4R / IL6 / MAF / NFKB1 / NOD2 / STAT6 / TLR2 / TLR5 / TNF
bta04216	Ferroptosis	1,61E-02	ACSL1 / ACSL4 / ACSL5 / GCLM / MAP1LC3A / NCOA4 / SAT2 / SLC39A14 / SLC39A8 / SLC40A1 / STEAP3 / TFRC / VDAC2
bta00040	Pentose and glucuronate interconversions	1,76E-02	CRYL1 / DCXR / DHDH / GUSB / SORD / UGDH / XYLB
bta04145	Phagosome	2,53E-02	ACTG1 / ATP6V0A1 / ATP6V0D2 / ATP6V1B2 / BOLA-DRB3 / C3 / CLEC7A / COLEC12 / CTSS / DYNC1H1 / ITGA5 / ITGAV / ITGB5 / MRC1 / MRC2 / MSR1 / NCF4 / SCARB1 / STX12 / TFRC / TLR2 / TLR6 / TUBA1A / TUBA1B / TUBB1 / TUBB2A / TUBB2B / TUBB3 / TUBB4A / TUBB4B / TUBB6
bta04115	p53 signaling pathway	2,53E-02	CCND1 / CCND3 / CCNG1 / CCNG2 / CD82 / CDK6 / CHEK2 / FAS / GADD45A / GADD45G / MDM4 / PPM1D / RFWD2 / RRM2 / SERPINE1 / SESN1 / SESN3 / STEAP3 / TP73
bta04622	RIG-I-like receptor signaling pathway	2,54E-02	AZI2 / FADD / IFIH1 / IKBKE / IL12B / IL6 / MAPK11 / MAPK12 / NFKB1 / NFKBIA / NLRX1 / RNF125 / TBK1 / TBKBP1 / TKFC / TMEM173 / TNF / TRAF2
bta05164	Influenza A	2,81E-02	ACTG1 / BOLA-DRB3 / CCL2 / CCL5 / FAS / FURIN / IFIH1 / IFNGR1 / IKBKE / IL12B / IL1A / IL1B / IL6 / IL6 / IVNS1ABP / MAPK11 / MAPK12 / NFKB1 / NFKBIA / NLRX1 / NXF1 / NXT2 / PIK3CD / RNASEL / RSAD2 / TBK1 / TICAM1 / TLR3 / TLR7 / TNF / TNFRSF1A / TNFSF10
bta00620	Pyruvate metabolism	3,17E-02	ACACA / ACAT1 / ACAT2 / ACSS2 / ACYP1 / ACYP2 / ALDH7A1 / ALDH9A1 / GRHPR / LDHA / PC / PCK2 / PDHB

bta05144	Malaria	3,17E-02	CCL2 / CD40 / CSF3 / GYPC / HGF / IL10 / IL1B / IL6 / PECAM1 / SDC1 / SDC2 / SELP / TLR2 / TNF
bta05162	Measles	3,17E-02	CCND1 / CCND3 / CDK6 / FAS / FYN / IFIH1 / IFNGR1 / IKBKE / IL12B / IL1A / IL1B / IL2RA / IL2RB / IL6 / IL6 / JAK3 / NFKB1 / NFKBIA / PIK3CD / SLAMF1 / STAT5A / TAB2 / TBK1 / TLR2 / TLR7 / TNFAIP3 / TNFSF10 / TP73
bta05332	Graft-versus-host disease	3,47E-02	BOLA-DRB3 / CD80 / CD86 / FAS / IL1A / IL1B / IL6 / TNF
bta05150	Staphylococcus aureus infection	3,55E-02	BOLA-DRB3 / C1QA / C1QB / C1QC / C1S / C3 / C3AR1 / C5AR1 / IL10 / SELP / SELPLG
bta04659	Th17 cell differentiation	3,74E-02	BOLA-DRB3 / CD4 / FOS / HIF1A / IFNGR1 / IL1B / IL1R1 / IL23A / IL23R / IL2RA / IL2RB / IL4R / IL6 / IL6R / JAK3 / LAT / MAPK11 / MAPK12 / NFKB1 / NFKBIA / NFKBIE / STAT5A / STAT6 / TGFBR1 / TGFBR2
bta05322	Systemic lupus erythematosus	3,74E-02	ACTN1 / BOLA-DRB3 / C1QA / C1QB / C1QC / C1S / C3 / CD40 / CD80 / CD86 / H2AFJ / H2AFV / HIST1H2BD / HIST1H2BN / HIST2H2AC / HIST2H2BE / IL10 / TNF
bta05134	Legionellosis	4,38E-02	BNIP3 / C3 / CASP7 / IL12B / IL1B / IL6 / NAIP / NFKB1 / NFKB2 / NFKBIA / NLRC4 / TLR2 / TLR5 / TNF
bta00071	Fatty acid degradation	4,38E-02	ACAA1 / ACADSB / ACAT1 / ACAT2 / ACSL1 / ACSL4 / ACSL5 / ALDH7A1 / ALDH9A1 / CPT1A / EHHADH / GCDH / HADH

MØHK *vs* MØC			
bta00280	Valine, leucine and isoleucine degradation	1,01E-04	ABAT / ACADSB / ACAT1 / ALDH6A1 / ALDH7A1 / ALDH9A1 / BCKDHB / DBT / EHHADH / HADH / HMGCS1 / IVD / MCCC1 / MCCC2 / MUT / OXCT1 / PCCA / PCCB
bta04668	TNF signaling pathway	2,52E-04	AKT3 / ATF2 / BCL3 / CCL2 / CCL20 / CCL5 / CREB3L3 / CSF1 / CSF2 / CX3CL1 / EDN1 / FOS / IL1B / IL6 / JUNB / MAP2K6 / MAPK11 / MAPK12 / MMP9 / PIK3CD / PTGS2 / RPS6KA5 / SOCS3 / TNF / TNFRSF1B / TRAF1
bta04060	Cytokine-cytokine receptor interaction	2,52E-04	CCL14 / CCL2 / CCL20 / CCL22 / CCL4 / CCL5 / CD40 / CLCF1 / CNTFR / CSF1 / CSF2 / CX3CL1 / CXCR5 / EDA / EPOR / FLT1 / FLT3LG / HGF / IFNGR1 / IL10 / IL17RC / IL1B / IL1RAP / IL21R / IL2RB / IL4R / IL6 / IL6 / IL6R / IL7R / OSM / OSMR / PDGFA / RELT / TGFBR1 / TGFBR2 / TNF / TNFRSF18 / TNFRSF1B / TNFRSF21 / TNFSF11 / TNFSF9 / VEGFB / VEGFC
bta05323	Rheumatoid arthritis	2,73E-04	ACP5 / ATP6V0A1 / ATP6V0B / ATP6V0D1 / ATP6V0D2 / CCL2 / CCL20 / CCL5 / CD80 / CD86 / CSF1 / CSF2 / FLT1 / FOS / IL1B / IL6 / TCIRG1 / TLR2 / TNF / TNFSF11
bta05205	Proteoglycans in cancer	5,13E-04	ACTG1 / AKT3 / ARHGEF1 / ARHGEF12 / CBL / CD44 / CDKN1A / CTTN / EZR / FLNA / FLNB / FRS2 / GPC1 / HGF / HRAS / HSPG2 / ITGA5 / ITGB5 / ITPR3 / MAPK11 / MAPK12 / MMP2 / MMP9 / PAK1 / PDCD4 / PIK3CD / PLAU / PLAUR / PPP1R12A / RRAS / SDC1 / SDC2 / SDC4 / SRC / TIMP3 / TLR2 / TNF / WNT10B / WNT5A
bta05418	Fluid shear stress and atherosclerosis	5,32E-04	ACTG1 / AKT3 / ASS1 / BCL2 / CALM2 / CCL2 / DUSP1 / EDN1 / FOS / GPC1 / HMOX1 / IL1B / MAP2K6 / MAPK11 / MAPK12 / MGST1 / MMP2 / MMP9 / NCF2 / PDGFA / PECAM1 / PIK3CD / SDC1 / SDC2 / SDC4 / SRC / THBD / TNF / TXN
bta00640	Propanoate metabolism	3,89E-03	ABAT / ACAT1 / ACSS3 / ALDH6A1 / BCKDHB / DBT / EHHADH / LDHA / MUT / PCCA / PCCB
bta05152	Tuberculosis	3,89E-03	AKT3 / ARHGEF12 / ATP6V0A1 / ATP6V0B / ATP6V0D1 / ATP6V0D2 / BCL2 / CALM2 / CARD9 / CIITA / CLEC7A / CYP27B1 / IFNGR1 / IL10 / IL1B / IL6 / IL6 / MAPK11 / MAPK12 / MRC1 / MRC2 / PLK3 / SPHK1 / SRC / TCIRG1 / TLR2 / TLR6 / TNF
bta04380	Osteoclast differentiation	5,04E-03	ACP5 / AKT3 / CSF1 / FOS / FOSL1 / IFNGR1 / IL1B / IL6 / JUNB / MAP2K6 / MAPK11 / MAPK12 / MITF / NCF2 / NCF4 / PIK3CD / PPARG / SOCS1 / SOCS3 / TGFBR1 / TGFBR2 / TNF / TNFSF11
bta04145	Phagosome	5,04E-03	ACTG1 / ATP6V0A1 / ATP6V0B / ATP6V0D1 / ATP6V0D2 / CLEC7A / COLEC12 / FCAR / ITGA5 / ITGB5 / MPO / MRC1 / MRC2 / MSR1 / NCF2 / NCF4 / TCIRG1 / TLR2 / TLR6 / TUBA1A / TUBA1B / TUBB1 / TUBB2A / TUBB4A / TUBB4B
bta05142	Chagas disease (American trypanosomiasis)	6,20E-03	AKT3 / CCL2 / CCL5 / FOS / GNA15 / GNAQ / IFNGR1 / IL10 / IL1B / IL6 / IL6 / MAPK11 / MAPK12 / PIK3CD / PPP2R2C / SERPINE1 / TGFBR1 / TGFBR2 / TICAM1 / TLR2 / TLR6 / TNF
bta04620	Toll-like receptor signaling pathway	8,54E-03	AKT3 / CCL4 / CCL5 / CD40 / CD80 / CD86 / FOS / IL1B / IL6 / IL6 / MAP2K6 / MAPK11 / MAPK12 / PIK3CD / TICAM1 / TLR2 / TLR5 / TLR6 / TNF
bta00100	Steroid biosynthesis	8,54E-03	CYP27B1 / CYP51A1 / DHCR24 / DHCR7 / FDFT1 / LSS / MSMO1 / SQLE
bta04640	Hematopoietic cell lineage	1,84E-02	CD37 / CD38 / CD4 / CD44 / CD59 / CSF1 / CSF2 / EPOR / FLT3LG / IL1B / IL4R / IL6 / IL6R / IL7R / ITGA4 / ITGA5 / TNF
bta04630	Jak-STAT signaling pathway	2,22E-02	AKT3 / BCL2 / BCL2L1 / CCND3 / CDKN1A / CISH / CNTFR / CSF2 / EPOR / HRAS / IFNGR1 / IL10 / IL21R / IL2RB / IL4R / IL6 / IL6 / IL6R / IL7R / OSM / OSMR / PIK3CD / SOCS1 / SOCS2 / SOCS3
bta04933	AGE-RAGE signaling pathway in diabetic complications	2,78E-02	AKT3 / BCL2 / CCL2 / EDN1 / EGR1 / HRAS / IL1B / IL6 / MAPK11 / MAPK12 / MMP2 / PIK3CD / PRKCE / SERPINE1 / TGFBR1 / TGFBR2 / THBD / TNF / VEGFB / VEGFC
bta05202	Transcriptional misregulation in cancer	2,78E-02	BCL2A1 / BCL2L1 / CD40 / CD86 / CDKN1A / CEBPE / CSF2 / ELK4 / ERG / FLT1 / IL2RB / IL6 / KLF3 / LMO2 / MAF / MLLT3 / MMP9 / MPO / PDGFA / PLAU / PPARG / RARA / REL / TGFBR2 / TRAF1
bta05144	Malaria	2,81E-02	CCL2 / CD40 / HGF / IL10 / IL1B / IL6 / PECAM1 / SDC1 / SDC2 / TLR2 / TNF
bta04750	Inflammatory mediator regulation of TRP channels	4,32E-02	CALM2 / F2RL1 / GNAQ / IL1B / IL1RAP / ITPR3 / MAP2K6 / MAPK11 / MAPK12 / P2RY2 / PIK3CD / PLA2G4A / PLA2G4F / PRKCE / PTGER2 / PTGER4 / SRC / TRPV1
bta05140	Leishmaniasis	4,58E-02	FOS / IFNGR1 / IL10 / IL1B / ITGA4 / MAPK11 / MAPK12 / MARCKSL1 / NCF2 / NCF4 / PTGS2 / TLR2 / TNF

MØ1H: Nc-Spain1H-infected macrophages; MØ7: Nc-Spain7-infected macrophages; MØHK: macrophages inoculated with heat-killed tachyzoites; MØC: non-infected macrophages.

SUB-OBJECTIVE 2.2 | Gene expression profiling of high and low virulence *Neospora caninum* isolates in bovine macrophages

SUMMARY |

Intraspecific differences in biological traits between *N. caninum* isolates have been widely described and associated with variations in virulence. However, the molecular basis underlying these differences has been poorly studied. We demonstrated previously that Nc-Spain7 and Nc-Spain1H, high and low virulence isolates, respectively, show different invasion, proliferation and survival capabilities in bovine macrophages, a key cell in the immune response against *Neospora*, and modulate the cell immune response in different ways. Here, we demonstrate that these differences are related to specific tachyzoite gene expression profiles. Specifically, the low virulence Nc-Spain1H isolate showed enhanced expression of genes encoding for surface antigens and genes related to the bradyzoite stage. Among the primary up-regulated genes in Nc-Spain7, genes involved in parasite growth and redox homeostasis are particularly noteworthy because of their correlation with the enhanced proliferation and survival rates of Nc-Spain7 in bovine macrophages relative to Nc-Spain1H. Genes potentially implicated in induction of proinflammatory immune responses were found to be up-regulated in the low virulence isolate, whereas the high virulence isolate showed enhanced expression of genes that may be involved in immune evasion. These results represent a further step in understanding the parasite effector molecules that may be associated to virulence and thus to disease traits as abortion and transmission.

1. BACKGROUND

Neospora caninum is an apicomplexan parasite that is one of the primary infectious causes of bovine abortion worldwide (Dubey et al., 2007). To survive, proliferate and transmit, this parasite has evolved mechanisms that modulate host cells according to parasite requirements, ensuring long-term survival not only of the parasite but also of the host cell (Hemphill et al., 2006). Because the immune response generated by the infection is highly associated with the control and pathogenesis of neosporosis (Almería et al., 2017), modulation of immune cell functions may be essential for parasite survival, tissue dissemination and transplacental transmission in the host.

Recent *in vitro* studies carried out by our group have shown the ability of *N. caninum* to grow into bovine monocyte-derived macrophages (boMØs) and shown isolate-dependent differences regarding parasite cell cycle and the cellular response to infection. Specifically, the highly virulent isolate Nc-Spain7 showed higher invasion, proliferation and capacity to survive in boMØs than the low virulence isolate Nc-Spain1H. In addition, Nc-Spain1H-infected boMØs exhibited a higher proinflammatory response (García-Sánchez et al., 2019). The boMØ transcriptome was found to be drastically regulated by *N. caninum*, which increased the expression of genes involved in pathogen recognition (e.g., TLR2, TLR3 and TLR9), NF-ƙB signaling pathway and proinflammatory cytokine and chemokine genes that elicit a Th1 response. *Neospora caninum* infection also restrained lysosome activity and apoptosis and modified cell metabolism. The results of the study also suggested that the high virulence isolate Nc-Spain7 is able to evade early innate immune responses, which could explain its high virulence *in vivo* (García-Sánchez et al., submitted).

Little is known about the parasite effectors implicated in modulation of the host immune response against *N. caninum*. ROP5, ROP16, GRA6 and GRA7 have been postulated as *N. caninum* virulence factors based on a mouse bioassay (Ma et al., 2017a; Ma et al., 2017b; Nishikawa et al., 2018; Fereig et al., 2019). However, their potential in modulating host cell functions has not been demonstrated in the natural bovine host of *N. caninum*.

Although *N. caninum* seems to be highly conserved genetically, an important biological diversity has been demonstrated between isolates (Beck et al., 2009). Proteomic and transcriptomic analyses have emerged as very useful tools for study of the molecular mechanisms governing differences in virulence (Horcajo et al., 2018). However, to date, the only comparative study of *N. caninum* gene expression between isolates with different virulence in bovine target cells was carried out using trophoblast cells infected with Nc-Spain7 and Nc-Spain1H. The study reported different expression levels of genes involved in cell cycle, stress response and metabolic processes between the isolates, which could explain their biological differences (Horcajo et al., 2017). In the present work, the transcriptional profile of Nc-Spain7 and Nc-Spain1H isolates in boMØs was investigated to identify parasite effectors implicated in the differential ability of the isolates to modulate cellular processes related to the host cell immune response, which may suggest potential targets for control of this parasite.

2. MATERIALS AND METHODS

2.1. Ethical statements

Blood sampling and cow handling were conducted according to Spanish and EU legislation (Law 32/2007, concerning animals, their exploitation, transportation, experimentation and sacrifice; Royal Decree 53/2013 for the protection of animals employed in research and

teaching; Directive 2010/63/UE, related to the protection of animals used for scientific goals). All procedures were approved by the Animal Welfare Committee of the Community of Madrid, Spain (permit number PROEX 236/17).

2.2. Generation of bovine monocyte-derived macrophages

BoMØs were generated following the protocol described by García-Sánchez et al. (2019). Briefly, 900 ml of peripheral blood was collected from a healthy adult Holstein dairy cow that tested negative for infectious bovine rhinotracheitis virus (IBRV), bovine viral diarrhea virus (BVDV) and *N. caninum*. Histopaque 1077 (Sigma-Aldrich, USA) was used to separate peripheral blood mononuclear cells by density gradient, and isolation of monocytes was carried out by positive selection using anti-human CD14 antibody-conjugated microbeads (Miltenyi Biotec Ltd., USA). Monocytes were incubated at 37ºC in a 5% CO2 atmosphere in medium containing 100 ng/ml recombinant bovine GM-CSF (Kingfisher Biotech Inc, USA). At day 5, boMØs were harvested, reseeded at 3 x 10^6 cells/well in 6-well culture plates (P6) and incubated for 24 h prior to infection to minimize cellular stress due to the harvest procedure.

2.3. Parasite culture and macrophage infection

The *N. caninum* isolates Nc-Spain7 and Nc-Spain1H were routinely maintained in an MA-104 cell line culture as described previously (Regidor-Cerrillo et al., 2011), with the number of culture passages limited to fewer than 15 to reduce potential changes in virulence (Pérez-Zaballos et al., 2005). For boMØ infection, tachyzoites were harvested from 3 day-growth cultures, when at least 80% of the parasites were still in parasitophorous vacuoles, and purified with PD-10 Desalting Columns (G.E. Healthcare, UK) as described previously (Regidor-Cerrillo et al., 2011). To preserve the viability and invasion capacity of the tachyzoites, boMØs were inoculated with each isolate at a multiplicity of infection (MOI) of 3 within one hour of parasite collection. At 8 hours post infection (hpi), samples were recovered by scraping of cells in three P6 wells/condition (Nc-Spain7- and Nc-Spain1H-infected boMØs) followed by centrifugation for 10 min at 1,350 g. The obtained pellet containing 9 x 10^5 cells was resuspended in 300 μl of RNA later (Thermo Fisher Scientific, Spain) and stored at -80ºC. Three biological replicates were assessed, obtained in three independent experiments.

2.4. RNA extraction, RNA-seq and data computational analysis

A Maxwell® 16 LEV simply RNA Purification Kit (Promega, USA) was used for total RNA extraction. RNA purity and concentration were determined at 260/280 nm using a NanoPhotometer Classic spectrophotometer (Implen, Germany). RNA integrity was assessed via electrophoresis on a 1% agarose gel stained with GelRed (Biotium, USA).
RNA-seq and computational analysis of the obtained data were performed as previously described (García-Sánchez et al. submitted) with minimal modification. The quality and quantity of total RNA were assessed with a Bioanalyzer 2100 (Agilent, USA) and Qubit 2.0 (Thermo Fisher Scientific, Spain). The poly (A) + mRNA fraction was isolated from total RNA, and cDNA libraries were obtained according to Illumina´s recommendations. The quantity of the libraries was determined via real-time PCR with a LightCycler 480 system (Roche, Germany) and the Bioanalyzer 2100. A High Sensitivity assay was used to assess their quality. Equimolar pooling of the libraries was performed prior to cluster generation in cBot (Illumina, USA). The pool of libraries was sequenced in an Illumina HiSeq 2000 sequencer (Illumina).

Data quality was assessed with the FastQC tool (http://www.bioinformatics.babraham.ac.uk/projects/fastqc). The raw paired-end reads were mapped against the *N. caninum* Liverpool strain genome provided by ToxoDB database version 28 (http://www.toxodb.org) using the

TopHat2 v2.1.0 algorithm (Kim et al., 2013). Picard Tools (http://picard.sourceforge.net) was used to eliminate low quality reads. High quality reads were selected, assembled and identified via Bayesian interference through the algorithm proposed by Cufflinks v2.2.1 (Trapnell et al., 2010). Gene quantification was carried out using htseq_count 0.6.1p1 (Anders et al., 2015). For isoform quantification and differential expression, the Cufflinks method (Trapnell et al., 2010) was used.

2.5. Differential expression determination and functional analyses

The statistical software R (http://www.r-project.org) was used to determine the correlation between samples of the same condition prior to their acceptance as biological replicates by considering the whole transcriptome normalized by the size of the library.

Differential expression between sample groups was studied using the algorithm proposed by DESeq2 (Anders and Huber, 2010), with a binomial negative distribution for determination of the statistical significance (Love et al., 2014). Genes and isoforms were considered differentially expressed (DE) when they presented a Fold Change (FC) ≥ 2 and a false discovery rate (FDR) – adjusted (Benjamini and Hochberg, 1995) p-value (p adj) ≤ 0.05.

For functional analyses of *N. caninum* genes, an orthology analysis was carried out using the *T. gondii* database (http://toxodb.org/toxo/, ToxoDB release 42) due to the more complete annotation of the *T. gondii* genome.

2.6. Transcriptome validation via RT-qPCR

Transcriptome validation analysis was carried out as previously described with minimal modification (García-Sánchez et al., submitted). Briefly, three additional biological replicates were collected and prepared as described for RNA-seq analysis. cDNA was obtained from extracted RNA using a master mix SuperScript VILO cDNA Synthesis Kit (Invitrogen, UK). The expression levels of selected genes of interest were measured via quantitative real-time PCR (qPCR) using four serial dilutions (1:20, 1:80, 1:320 and 1:1280) of each sample and normalized to those of the housekeeping genes NcTUBα (NCLIV_058890) and NcSAG1 (NCLIV_033230). Primers used to amplify the target genes are listed in **Supplementary Table 1**. Reactions were performed in a 7500 Fast Real-Time PCR System (Applied Biosystems, USA) using Power SYBR PCR Master Mix (Applied Biosystems). Relative gene expression was calculated using the 2-ΔΔCt method (Livak and Schmittgen, 2001) and by comparing the expression of Nc-Spain1H *versus* Nc-Spain7.

2.7. Data availability statement

All data analyzed in this study are included in this published article. Raw data have been deposited in the NCBI Sequence Read Archive under the identifier PRJNA552526.
Data are available for review at the following address:

https://dataview.ncbi.nlm.nih.gov/object/reviewer=kt4dnoctuuqej3rc24mfhe4vqq

3. RESULTS AND DISCUSSION

3.1. Sequencing and mapping data obtained from RNA-seq analysis

In total, three biological replicates from boMØs inoculated with Nc-Spain1H and three from boMØs inoculated with Nc-Spain7 were sequenced individually via RNA-seq. Over 50 million

reads were obtained for each sample. Between 6 and 16% of reads were mapped against the *N. caninum* genome (ToxoDB release 28). The lack of degradation of the starting biological material and the absence of significant deviations in the sequencing processes was verified by data quality controls based on duplication studies and G+C content. Distribution analysis of normalized data showed a correct distribution of biological replicates. No outliers were identified. **Table 1** shows the results obtained by sample in the sequencing process: number of reads generated, mapped reads against the *N. caninum* genome and splice reads (related to the capability of the system to detect isoforms and splicing events). A low percentage of mapped reads against the parasite observed was expected because the majority of RNA from the samples would belong to the bovine host cell. Nevertheless, 6,672 parasite genes were detected (RPKM >1 in at least 1 sample), indicating representation of the parasite transcriptome. Of these, 6,484 genes were identified using the *N. caninum* Liverpool strain genome from ToxoDB database, and 188 predicted genes were not identified. These were named with an identification number preceded by "XLOC" (**Supplementary Table 2**). Thus, this study, together with other *N. caninum* high throughput experimental analyses, could be used to reveal previously undiscovered genes and to improve annotation of the reference genome, the only available to date (Saha et al., 2002). Among the total *N. caninum* genes identified, 474 genes (7.31%) were DE between Nc-Spain1H and Nc-Spain7 isolates: 265 with higher expression in Nc-Spain7 and 209 with higher expression in Nc-Spain1H (**Supplementary Table 2**). Additionally, of the total genes identified and categorized as DE between isolates, 16 were exclusively expressed in Nc-Spain7, and 8 were exclusively expressed in Nc-Spain1H. Among the XLOC genes, 31 were DE, 16 were overexpressed in Nc-Spain1H, and 19 were overexpressed in Nc-Spain7. Three of these were exclusively expressed in the low virulence isolate and 1 in the high virulence isolate. Genes exclusively expressed by certain isolates should be taken into account because they may be related to the observed biological variability between isolates. Thus, a further study of these genes as putative virulence factors should be considered in future research. RNA-seq results were validated by RT-qPCR for 7 genes DE between Nc-Spain7 and Nc-Spain1H (**Figure 1**).

It is noteworthy that the number of DEGs detected in our study is markedly higher than that reported in the transcriptomic analysis of trophoblast cells infected with Nc-Spain7 and Nc-Spain1H isolates at 12 hpi (Horcajo et al., 2017). In that study, 176 genes were found to be DE with FC $\geq$ 2 and p adj $\leq$ 0.05; 28 were highly expressed in Nc-Spain7, and 148 were highly expressed in Nc-Spain1H. We found that 25 genes were DE with a similar fold change between isolates in both boMØs and trophoblast cells (**Table 2**). However, comparison of both studies also revealed that the gene expression profile of the isolates strongly differed depending on

TABLE 1 | Mapped and paired reads by sample against *N. caninum* genome.

Sample[1]	Total reads	Mapped reads	Mapped reads (%)	High quality reads	High quality reads (%)	Splice reads	Splice reads (%)
1	45726510	5750052	12.57	4067318	8.89	465001	1.02
2	49810014	3120428	6.26	2160028	4.34	245772	0.49
3	46709092	3987977	8.54	2949996	6.32	340289	0.73
4	50818888	6302701	12.4	4260546	8.38	525535	1.03
5	59129224	4957694	8.38	3321220	5.62	404784	0.68
6	48795612	7718581	15.82	5774492	11.83	724179	1.48

[1]Samples 1-3 correspond to Nc-Spain1H- infected boMØs; samples 4-6 correspond to Nc-Spain7-infected boMØs.

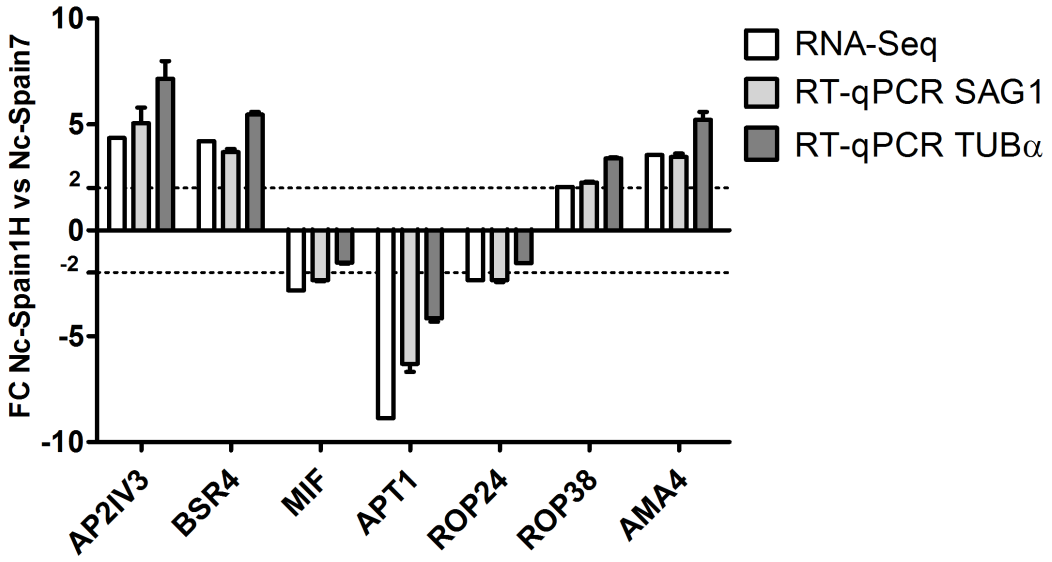

FIGURE 1 | Validation of RNA-seq analyses via RT-qPCR. Bar graphs show Fold Change (FC) in *N. caninum* gene expression in Nc-Spain1H *versus* Nc-Spain7; SAG1 and TUBα served as housekeeping genes.

the infected host cell. This behavior has also been reported in *T. gondii* and has been associated with the high ability of the parasite to adapt to different niches (Swierzy et al., 2017). Because trophoblasts and macrophages are important targets for the parasite in the bovine host, the genes that may be inherent to the isolate phenotype independent of the host cell might be related to the differences in pathogenesis reported for both isolates (Rojo-Montejo et al., 2009; Regidor-Cerrillo et al., 2014), specifically with differences in proliferation or immune response modulation between the isolates described in both cell lines (Jiménez-Pelayo et al., 2017, 2019; García-Sánchez et al., 2019). Thus, they should be considered for functional validation in future studies.

A further analysis of the 474 DEGs between the isolates was undertaken. Orthological analysis with the *T. gondii* database revealed that 26-29% of the DEGs between Nc-Spain7 and Nc-Spain1H were annotated as hypothetical proteins. The remaining genes were functionally classified and are listed in Supplementary **Table 3**. The most representative subsets are presented in **Figures 2** and **3**, where a very different expression pattern is shown for the two isolates.

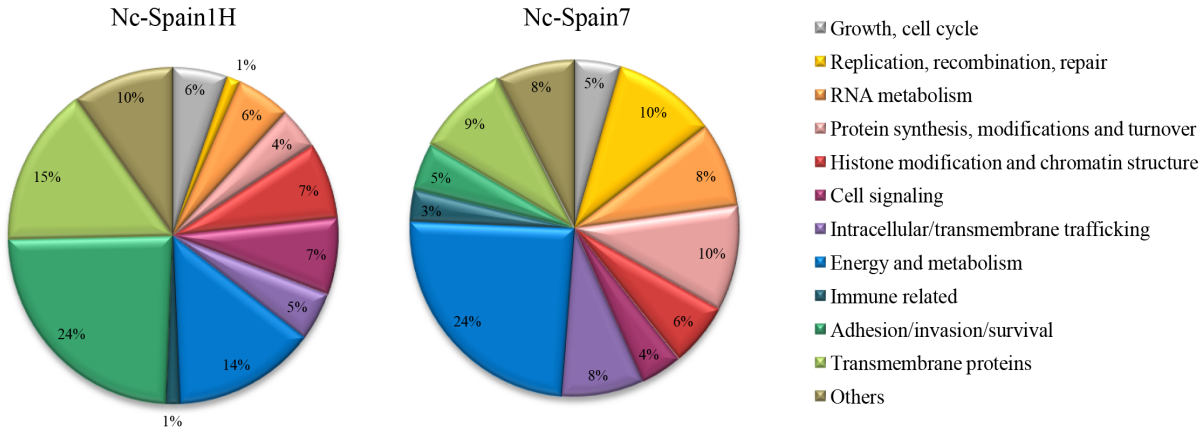

FIGURE 2 | Functional classification of *N. caninum* genes differentially expressed between isolates. Pie charts showing the percentage of genes for each functional category relative to the total overexpressed genes for each isolate.

Table 2. DEG in the comparison Nc-Spain1H versus Nc-Spain7 in infected bovine macrophages and trophoblast cells

Nc gene id	*Nc* description	*Tg* gene id	*Tg* description	FC[1]	padj[1]	FC[2]	padj[2]
NCLIV_046430	Putative protein kinase	TGME49_226540	Protein kinase	2.48	9.2E-27	7.66	7.34E-03
NCLIV_019730	Hypothetical protein	TGME49_280420	HEAT repeat-containing protein	8.54	4.57E-133	16.16	1.45E-02
NCLIV_044060	Hypothetical protein	TGME49_305590	ABC transporter transmembrane region domain-containing protein	2.56	3.77E-35	3.61	4.50E-04
NCLIV_052500	Hypothetical protein	TGME49_215590	Flavoprotein subunit of succinate dehydrogenase	2.42	2.54E-06	3.56	3.17E-02
NCLIV_005970	Putative oocyst wall protein	TGME49_222940	Hypothetical protein	2.31	6.51E-23	5.29	4.23E-03
NCLIV_056890	Hypothetical protein	-		2.36	8.25E-10	3.34	4.50E-04
NCLIV_038440	Hypothetical protein	TGVEG_279350	Putative transmembrane protein	8.48	7.49E-101	9.63	4.50E-04
NCLIV_036640	Hypothetical protein	TGME49_269950	Hypothetical protein	5.39	1.12E-122	10.55	4.50E-04
NCLIV_038280	Hypothetical protein	TGME49_200450	Hypothetical protein	4.75	8.43E-97	8.56	4.50E-04
NCLIV_037980	Hypothetical protein	TGME49_268220	Hypothetical protein	3.63	7.48E-44	2.79	4.50E-04
NCLIV_069090	Hypothetical protein	-		3.02	6.81E-03	4.07	5.56E-03
NCLIV_049520	Hypothetical protein	TGME49_234380	Hypothetical protein	2.78	7.30E-04	5.64	4.50E-04
NCLIV_033310	Hypothetical protein	-		2.50	2.40E-34	6.36	4.50E-04
NCLIV_013400	Hypothetical protein	TGRUB_213445A	Hypothetical protein	2.00	1.69E-21	2.19	4.50E-04
NCLIV_065390	Bifunctional dihydrofolate reductase-thymidylate synthase, related	TGME49_249180	Bifunctional dihydrofolate reductase-thymidylate synthase	-2.72	4.67E-17	-2.04	2.51E-02
NCLIV_065280	Proliferating cell nuclear antigen, related	TGME49_247460	Proliferating cell nuclear antigen PCNA1	-3.14	1.04E-23	-2.81	4.22E-02
NCLIV_006510	Putative TCP-1/cpn60 family chaperonin	TGME49_297500	T-complex protein 1 eta subunit	-2.31	1.50E-12	-2.30	2,27E-02
NCLIV_025530	Putative TPR domain-containing protein	TGME49_262100	Tetratricopeptide repeat-containing protein	-2.70	3.42E-20	-2.28	4.57E-02
NCLIV_062520	3-ketoacyl-(Acyl-carrier-protein) reductase, related	TGME49_217740	3-ketoacyl-(acyl-carrier-protein) reductase	-9.03	9.13E-27	-5.02	3.27E-02
NCLIV_063860	Putative thioredoxin	TGME49_247350	Thioredoxin domain-containing protein	-2.52	1.78E-25	-2.11	4.50E-04
NCLIV_014020	Peroxiredoxin-2E-1, related	TGME49_286630	Redoxin domain-containing protein	-6.06	2.83E-33	-3.18	3.56E-02
NCLIV_007770	Putative Rhoptry kinase family protein, truncated (incomplete catalytic triad)	TGME49_253330	Rhoptry kinase family protein, truncated (incomplete catalytic triad)	-4.75	4.63E-104	-2.40	4.50E-04
NCLIV_068850	Unspecified product	TGME49_252360[3]	Rhoptry kinase family protein ROP24 (incomplete catalytic triad)	-2.47	1.63E-35	-2.79	4.50E-04
NCLIV_052780	Putative penicillin amidase domain-containing protein	TGME49_275320	Penicillin amidase	-2.87	1.07E-31	-2.53	4.50E-04
NCLIV_047150	Hypothetical protein	TGME49_225560	Hypothetical protein	-4.16	2.96E-74	-2.35	4.50E-04

[1]Corresponds to infected bovine macrophages samples.
[2]Corresponds to infected trophoblast cells (F3 cell line) samples.
[3]No synthenic

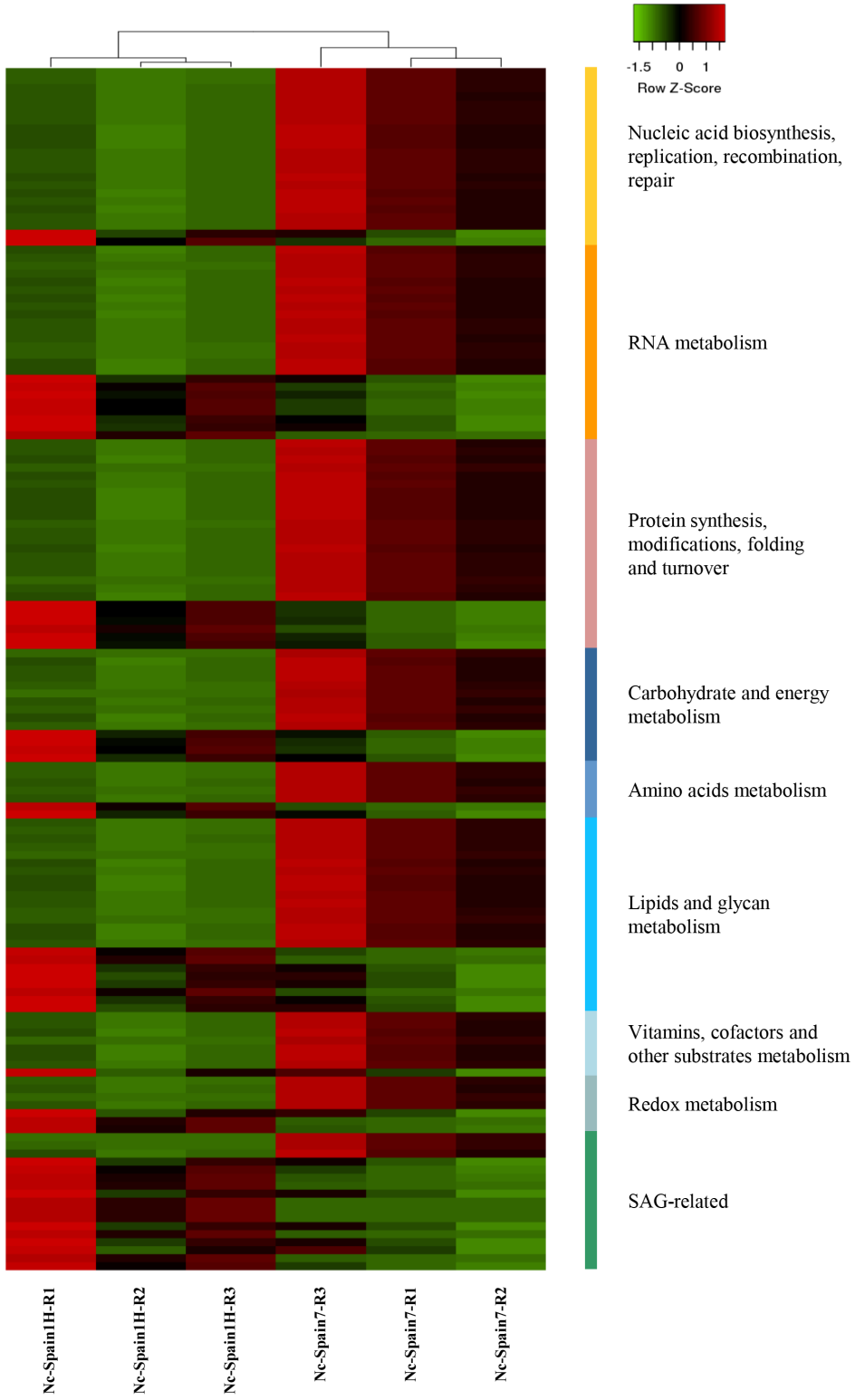

FIGURE 3 | Clustering of *N. caninum* genes differentially expressed between isolates. Heatmap showing a selection of *N. caninum* DEGs with Z-scores (row) based on expression data of three replicates (R1-R3) of boMØs challenged for 8 h with Nc-Spain1H and Nc-Spain7 tachyzoites. The heatmap was generated using Heatmapper (http://www2.heatmapper.ca). The genes are grouped according to functional categories and were clustered using the Pearson computing distance method.

3.2. Host cell adhesion-related SRS and MIC genes were highly expressed in Nc-Spain1H and genes related to gliding motility were highly expressed in Nc-Spain7

Adhesion of *N. caninum* to the host cell prior to invasion initially occurs through a low-affinity and reversible interaction mediated by the tachyzoite surface antigen molecules. This is followed by establishment of a more stable adhesion that requires secretion of proteins from micronemes (Hemphill et al., 2006). A total of 14 surface antigen (SAG)-related sequences were overexpressed in Nc-Spain1H, and only 3 were overexpressed in Nc-Spain7. In addition, 2 microneme proteins, MIC12 (NCLIV_069310) and MIC14 (NCLIV_061910), showed higher expression in Nc-Spain1H but none showed higher expression in Nc-Spain7. Other proteins that could also be related to parasite-host cell adhesion are those containing epidermal grow factor (EGF) and thrombospondin (TSP) domains (Hemphill et al., 2006; Hemphill et al., 2013), among which 3 genes (NCLIV_036660, NCLIV_011000 and NCLIV_001350) were overexpressed in Nc-Spain1H, and only 1 gene (NCLIV_003470) was overexpressed in Nc-Spain7. NCLIV_001350 corresponds to the orthologous apical membrane antigen 4 (AMA4) of *T. gondii*. TgAMA4 has been described as not only being involved in attachment but also in internalization of the parasite through interaction with the rhoptry neck protein RON2L1. In fact, RON2L1 (NCLIV_001400) is also overexpressed in Nc-Spain1H and is necessary to maintain the moving junction structural integrity required for tachyzoite entry (Lamarque et al., 2014).

The higher expression of genes associated with adhesion in Nc-Spain1H is striking, because *in vitro* studies with different cell lines have shown that Nc-Spain1H has a lower invasion rate than Nc-Spain7 (Jiménez-Pelayo et al., 2017; Regidor-Cerrillo et al., 2011), including boMØs (García-Sánchez et al., 2019). However, a similar result was obtained in a transcriptomic analysis of these isolates in bovine trophoblast cells (Horcajo et al., 2017), in which 9 SAG-related sequences and 22 proteins from micronemes were found to be overexpressed in Nc-Spain1H, and none were overexpressed in Nc-Spain7. In further support of our results, a proteome analysis of Nc-Spain7 and Nc-Spain1H cultured in MARC-145 cells revealed that surface antigen and microneme protein abundance differed between isolates throughout the tachyzoite lytic cycle (Horcajo et al., 2018). It is worth noting that the adhesion function of SRS and MIC proteins has been determined by homology with *T. gondii*, but to the best of our knowledge, this function has only been demonstrated in *N. caninum* for SAG1, SRS2, MIC1-4 and 17 (Hemphill et al., 2006; Sohn et al., 2011), none of which were differentially expressed between our isolates. In addition, mechanisms other than adhesion are involved in invasion and may be enhanced in Nc-Spain7. With regard to this connection, previous studies in trophoblast cell lines (Jiménez-Pelayo et al., 2017; Horcajo et al., 2017), have associated the higher invasion capacity of Nc-Spain7 with enhanced expression of gliding-associated proteins by the isolate in the trophoblast cell line. For Nc-Spain7, enhanced expression of two glideosome genes has been reported: the microtubule-associated protein SPM1 (NCLIV_024420), which colocalizes with the subpellicular microtubules and whose deletion decreases tachyzoite fitness in *T. gondii* (Tran et al., 2012); and a putative actin-like family protein (ALP, NCLIV_037160). Although ALPs may be implicated in actin-based gliding motility, vesicle transport and transcriptional regulation through chromatin remodeling are other functions attributable to these proteins (Gordon and Sibley, 2005).

Apart from their putative relationship with adhesion to the host cell, SRS proteins have been recognized as the primary surface antigens and may determine the immunogenic potential

of the isolates (Lekutis et al., 2001). In this connection, SRS genes are overexpressed in Nc-Spain1H and may be related to its capacity to induce a higher proinflammatory response by boMØs infected *in vitro* than Nc-Spain7 (García-Sánchez et al., 2019). A study of these antigen determinants differentially expressed between Nc-Spain7 and Nc-Spain1H (**Supplementary Table 3**) may help to determine why Nc-Spain1H seems to be more efficiently detected by the host immune system (García-Sánchez et al., 2019; Jiménez-Pelayo et al., 2017).

3.3. Rhoptry proteins were differentially expressed between the isolates

Once *N. caninum* attachment to the host cell is achieved, rhoptries are released to form the moving junction, which is a structure that facilitates parasite entry and formation of the parasitophorous vacuole. Then, dense granules secrete proteins to modify the parasitophorous vacuole, enabling intracellular survival of the parasite. These organelles also inject proteins into the cytosol of the host cell to modulate their functions, ensuring success of the infection (Sohn et al., 2011).

For Nc-Spain7, genes encoding for two predicted rhoptry proteins were highly expressed: a predicted member of the rhoptry-kinase-like family (ROPKL) subfamily BPK1 (NCLIV_007770), and a member of the rhoptry kinase family ROP20 (NCLIV_068850), specific for *N. caninum* and orthologous but not syntenic to *T. gondii* ROP24. Higher NCLIV_007770 expression was also observed for Nc-Spain7 in the comparative transcriptomic analysis of infected bovine trophoblast cells (Horcajo et al., 2017). However, of special interest is NCLIV_068850, whose enhanced expression in Nc-Spain7 has been demonstrated to be maintained for tachyzoite cell cycle progression regardless of the host cell (Horcajo et al., 2017, 2018).

Regarding Nc-Spain1H, in addition to RON2L1, mentioned above, higher expression was observed for the predicted rhoptry kinase subfamily gene ROP30 (NCLIV_001950), an ortholog to *T. gondii* ROP4/ROP7, and two predicted lineage-specific rhoptry kinases of the subfamily ROPK-Eten1 (NCLIV_017420 and NCLIV_068890), which are orthologs to the *T. gondii* gene locus ROP19/ROP28/ROP38 (Kemp et al., 2013). Peixoto et al. (2010) pointed to ROP38 and ROP4/ROP7 as likely to be particularly important in the biology of *T. gondii*, considering that ROP38, which is highly expressed by low virulence *T. gondii* strains and during tachyzoite to bradyzoite conversion, down-modulates genes associated with MAPK signaling in the host cell and regulation of apoptosis and proliferation (Peixoto et al., 2010). It has also been shown that knockout of ROP38 leads to increased invasion and proliferation of *T. gondii,* and infection of mice with ROP38-deficient parasites resulted in lower levels of IL-18 and IL-1β production, which was related to a decrease in *T. gondii* profilin expression relative to wild-type parasites (Xu et al., 2018). In addition, ROP38 is among the most deeply regulated genes in the genome of the parasite, and evidence of evolutionary selection at the species and population level has been reported (Khan et al., 2009; Peixoto et al., 2010). Its ancestor gene was independently triplicated in *N. caninum* and *T. gondii.* Notably, expanded genes have been linked to virulence, immune evasion or host range in *T. gondii* and other pathogens, such as *Plasmodium* spp. (Adomako-Ankomah et al., 2014). ROP4/ROP7, which are among the most highly expressed genes in the genome of *T. gondii*, may be functionally relevant based on studies showing that expression levels are important for virulence (Saeij et al., 2007; Peixoto et al., 2010).

Interestingly, no dense granule or other rhoptry-encoding genes recognized as virulence factors in *T. gondii* or *N. caninum* were found to be DE between Nc-Spain7 and Nc-Spain1H isolates. It is important to emphasize that characterization of *N. caninum* ROP and GRA proteins is limited, and host regulation in many cases does not correlate with the respective *T. gondii* orthologs. Such is the case with NcROP16, which in *N. caninum* activates STAT3, thereby promoting host

cell apoptosis and enhancing the pathogenicity of the parasites (Jensen et al., 2011; Ma et al., 2017a), whereas TgROP16 secreted by type I and III strains activates STAT6 in MØs, leading to alternative activation of these cells (Jensen et al., 2011). More importantly, *T. gondii* and *N. caninum* virulence factors have been identified in mice, and it has been demonstrated that virulence can be host-dependent (Sánchez-Sánchez et al., 2018b), likely due to the marked differences in the immune system observed between species that may determine the host-pathogen interplay.

3.4. Bradyzoite-related genes showed higher expression in Nc-Spain1H

Bradyzoites represent the quiescent stage of the parasite, triggered by stress caused by the host immune response (Hemphill et al., 2006). The transcriptomic analysis of *N. caninum* isolates in boMØs revealed a higher expression of two *N. caninum* bradyzoite-specific genes in the Nc-Spain1H isolate: the surface proteins SAG4 (NCLIV_019580) and BSR4 (NCLIV_010030) (Fernández-García et al., 2006; Risco-Castillo et al., 2007; Horcajo et al., 2017, 2018). In addition, our results showed differential expression of other genes that have been shown to be related to the tachyzoite-to-bradyzoite conversion in *T. gondii*, such as AP2 transcription factors (Huang et al., 2017). Nc-Spain1H showed overexpression of two AP2 factors known to be up-regulated during bradyzoite development in *T. gondii:* AP2IV-3 (NCLIV_010930), whose deletion in *T. gondii* results in a lower capacity to form tissue cysts (Hong et al., 2017); and AP2X-10 (NCLIV_052260), which is highly expressed by low virulence *T. gondii* isolates in murine MØs (Melo et al., 2013). In contrast, Nc-Spain7 showed enhanced expression of two transcription factors related to the tachyzoite stage: AP2XII-2 (NCLIV_062490) and AP2IV-4 (NCLIV_011080) (Radke et al., 2018; Huang et al., 2017). AP2IV-4 is necessary for suppression of bradyzoite surface antigens and cyst wall proteins in the tachyzoite stage and is exclusively expressed in the tachyzoite division cycle (Radke et al., 2018). Previous results from a murine *T. gondii* infection model determined that tachyzoites lacking this gene expressed bradyzoite antigens at the wrong time, stimulating a strong immune response by monocytes. This response successfully eliminated the parasite, preventing tissue cyst formation in mouse brain (Radke et al., 2018). Thus, it would be interesting to assess the implication of AP2IV-4 in the observed differential response induced by Nc-Spain1H and Nc-Spain7 in boMØs and in their improved capacity to evade the innate immune response (García-Sánchez et al., submitted).

Other genes overexpressed in the Nc-Spain1H isolate and with higher expression during bradyzoite development reported in *T. gondii* encode for H2A histone proteins (NCLIV_025910), which are implicated in transcription regulation and DNA repair and whose enhanced expression is likely associated with DNA damage resulting from oxidative stress (Dalmasso et al., 2009), and a cAMP-dependent protein kinase (PKA, NCLIV_004220), which is involved in cell cycle regulation and stress response (Wei et al., 2013; Pittman et al., 2014). Overexpression of bradyzoite-specific genes by Nc-Spain1H has been previously described and related to a prebradyzoite stage in which the parasite cell cycle shifts towards slower growth (Horcajo et al., 2018). Finally, two putative oocyst wall proteins (NCLIV_003900 and NCLIV_005970) exhibited higher expression in Nc-Spain1H.

3.5. Higher expression of genes involved in parasite growth was found for the virulent isolate Nc-Spain7

Increased expression of genes involved in DNA replication, RNA metabolism, protein synthesis, cell division and energy production was observed in Nc-Spain7, which is consistent with the active parasite replication and higher growth rate of Nc-Spain7 shown *in vitro* in different studies (Regidor-Cerrillo et al., 2011 ; Jiménez-Pelayo et al., 2017; García-Sánchez et al., 2019).

3.5.1 Nucleic acid biosynthesis, replication, recombination, and repair

Higher expression of four genes related to purine and pyrimidine biosynthesis and salvage were observed in Nc-Spain7. We also found enhanced expression of DNA polymerases, origin recognition complexes, DNA replication licensing factors, a DNA topoisomerase, and several other genes encoding proteins associated with DNA replication (Supplementary Table S3), such as orthologs to the two putative proliferating cell nuclear antigens of *T. gondii*, PCNA1 (NCLIV_065280) and PCNA2 (NCLIV_010140). PCNA1, likely the major replisomal PCNA in *T. gondii* (Guerini et al., 2005), is one of the 11 genes up-regulated in Nc-Spain7 during infection of both boMØs and trophoblast cells (Horcajo et al., 2017).

3.5.2 Histone modification, chromatin structure and microtubule dynamics

Enhanced expression of genes related to chromatin assembly and chromosome condensation was also shown for Nc-Spain7. This may reflect the need of proliferating tachyzoites to maintain active chromatin organization dynamics to accompany DNA replication (Parthun, 2007). The putative HU protein (NCLIV_045430) is a histone-like protein with fundamental roles in transcription, replication initiation, and DNA repair. In *T. gondii*, this protein localizes to the apicoplast and is required for genome maintenance and inheritance (Reiff et al., 2012). Because the apicoplast is unique to apicomplexan parasites and is not found in the host, proteins associated with this organelle are considered good target candidates for pathogen-specific drugs (Reiff et al., 2012).

Interestingly, six genes encoding dynein heavy chains and one encoding a dynein intermediate chain were found to be overexpressed in Nc-Spain1H. Dyneins are microtubule-associated proteins that function as motors for several processes, such as axoneme beating, organelle transport, spindle function, and centrosome assembly (Morrissette, 2015). *Neospora caninum* dyneins have been poorly studied. To the best of our knowledge, only the cytoplasmic dynein LC8 light chain 2 has been characterized and has been found to be related to virulence through regulation of host immunity (Cao et al., 2019). Future research is necessary to unravel the specific functions of the dynein proteins up-regulated in the low virulence isolate.

3.5.3 RNA metabolism, protein synthesis and turnover

Thirty-six genes related to RNA metabolism and protein synthesis, modification, folding and turnover were also highly expressed in the high virulence isolate (**Supplementary Table 3**) *versus* 14 in the low virulence isolate. Among these genes, we identified two RNA pseudouridine synthases (NCLIV_020280 and NCLIV_048340). Pseudouridine synthases catalyze the conversion of the RNA base uridine to pseudouridine. Although the role of pseudouridylation of RNA has been poorly studied, pseudouridylation seems to confer an important selective advantage in a natural biological context. It is known that mutation of pseudouridine synthases in *Escherichia coli* and *Saccharomyces cerevisiae* results in a slow-growth phenotype, and a *T. gondii* pseudouridine synthase has been discovered to be important in tachyzoite-to-bradyzoite differentiation (Charette and Gray, 2000; Anderson et al., 2009).

Nc-Spain7 showed enhanced expression of six genes related to the ubiquitin-proteasome system, three of them encoding proteasome beta subunits (NCLIV_048880, NCLIV_057270 and NCLIV_061460), one ortholog to the *T. gondii* NEDD8-activating enzyme E1 catalytic subunit (NCLIV_040320), one putative SUMO activating enzyme (NCLIV_011590), and cullin-associated NEDD8-dissociated protein 1 (NCLIV_052060). Proteasomes play essential roles in

parasite biological processes, such as cell differentiation, cell cycle progression, proliferation, and encystation and have been suggested as virulence factors (Munoz et al., 2015). The proteasome system also seems to be an attractive drug target because inhibitors of this protein complex have been shown to diminish infectivity and block intracellular growth and replication of *T. gondii in vitro* (Paugam et al., 2002; Shaw et al., 2000), and differences between the proteasomes of mammals and parasites have been observed (Munoz et al., 2015).

3.5.4. Carbohydrate, amino acid and fatty acid metabolism

A great number of genes related to *N. caninum* metabolism, primarily involved in carbohydrate, amino acid and fatty acid metabolism, exhibited higher expression in the Nc-Spain7 isolate. Similar results were obtained by (Horcajo et al., 2017), through transcriptomic analysis of both isolates in trophoblast cells, where it was hypothesized that more energy is consumed by an isolate with a higher growth rate, and thus, a more activate metabolism may be present in Nc-Spain7 than in Nc-Spain1H.

With respect to carbohydrate metabolism, we found higher expression of ten genes involved in obtaining energy via glycolysis, pyruvate metabolism and starch and galactose metabolism pathways in Nc-Spain7. Regarding lipid metabolism, eight genes of the apicoplast-localized FAS II system were highly expressed in this isolate *versus* only one in the Nc-Spain1H isolate. In *T. gondii, de novo* fatty acid synthesis via FAS II is essential for parasite growth and virulence (Mazumdar et al., 2006), and because this pathway is parasite-specific, its components represent key targets for the development of selective drugs (Coppens, 2013; Wu et al., 2018). One of these targets may be the apicoplast triosephosphate translocator APT1, whose ortholog in *N. caninum* was highly expressed in the high virulence isolate in this and previous studies (Horcajo et al., 2018). TgAPT1 is not only required for the FASII pathway, but it also delivers carbon for another anabolic process in the apicoplast, the DOXP pathway. In addition, it has a role in indirectly supplying the apicoplast with ATP and redox equivalents (Brooks et al., 2010).

Another interesting gene related to fatty acid metabolism that was highly expressed by Nc-Spain7 is a putative patatin-like phospholipase (PLP, NCLIV_033980). PLPs are found in many pathogens and have been associated with host-cell interactions and immune evasion. Multiple PLPs are conserved across the subphylum Apicomplexa, suggesting a critical role for these enzymes in parasites, and several *T. gondii* PLPs are currently under investigation for their potential importance in parasite virulence (Wilson and Knoll, 2018). Prominent among them is TgPL1, which protects tachyzoites from nitric oxide-related degradation in activated MØs (Tobin Magle et al., 2014).

3.6. Genes involved in redox homeostasis were differentially expressed between isolates

Four genes highly expressed by Nc-Spain7 were identified as belonging to the redox metabolism pathway: an *N. caninum* ortholog (NCLIV_055730) to *T. gondii* apicoplast-associated thioredoxin Atx1 (NCLIV_055730), glutaredoxin (NCLIV_045930), thioredoxin (NCLIV_063860) and peroxiredoxin (NCLIV_014020). In addition, these two last enzymes are also highly expressed in the high virulence isolate Nc-Spain7 according to a previous transcriptomic analysis of bovine trophoblast cells (Horcajo et al., 2017).

TgATrx1 is a redox-regulated enzyme essential for the parasite. It is involved in endoplasmic reticulum-to-apicoplast trafficking and contributes to apicoplast biogenesis. Due to its

importance in parasite biology, the potential of apicoplast thioredoxins as drug targets has been suggested (Biddau et al., 2018). Antioxidant enzymes permit apicomplexan parasites to address oxidative levels inside the host cells and seem especially important in regard to intracellular survival in MØs, which use reactive oxygen species to kill pathogens (Bosch et al., 2015). Thus, their enhanced expression may confer an advantage to the high virulence isolate. In fact, higher parasite survival rates accompanied by lower intracellular ROS levels in boMØs infected by this isolate have been described previously (García-Sánchez et al., 2019).

3.7. Immune response modulation-related genes were found to be differentially expressed in Nc-Spain1H and Nc-Spain7

Interestingly, a dichotomy was found in the gene expression profiles of Nc-Spain 7 and Nc-Spain1H regarding potential immunomodulation functions. Genes potentially implicated in induction were found to be up-regulated in Nc-Spain1H, whereas genes involved in evasion of immune responses were found to be up-regulated in Nc-Spain7.
In addition to SRS genes, overexpressed in Nc-Spain1H as mentioned above, higher expression of a gene encoding a putative tryptophan-rich protein belonging to the Pv-fam-a family (NCLIV_004020) was shown for the low virulence isolate. This family of immunogenic proteins has been characterized in malaria human and rodent parasites and been proposed as candidate antigens for potential vaccines (Wang et al., 2015).

Enhanced expression of proteophosphoglycans (PPGs) PPG3 (NCLIV_005160), PPG4 (NCLIV_020320) and PPG5 (NCLIV_065610) was found in Nc-Spain7. These surface-coating molecules have been associated with immune evasion in *Leishmania* spp due to their ability to modulate MØ function during early infection by inhibiting TNF-α production. The ability of secreted PPGs to induce complement activation has been related to prevention of the opsonization of the parasite, and may contribute to the lesion development and pathology caused by *Leishmania mexicana*. In addition, the possibility of *Leishmania major* PPGs involvement *in* suppression of IL-12 production by dendritic cells has been also suggested (Peters et al., 1999; Depledge et al., 2009; Favila et al., 2015).

Glycosylphosphatidylinositols (GPIs) of *N. caninum* have recently been demonstrated to be secreted in supernatant and likely recognized by TLR2 and TLR4, are able to modulate APC immune responses. Interestingly, host-cell modulation seems to differ depending on the host origin of APCs. *Neospora caninum* GPIs have been shown to induce production of the proinflammatory cytokines TNF-α, IL-1β and IL-12 in murine macrophages and dendritic cells. However, bovine PBMCs showed reduced levels of IL-12p40 and MHC II in response to GPIs (Débare et al., 2019). In the present study, three genes involved in the GPI biosynthetic pathway (orthologs to *T. gondii* mannosyltransferase (NCLIV_004260), N-acetylglucosaminyl phosphatidylinositol deacetylase (NCLIV_028260) and a PGAP1 family protein (NCLIV_054430)) were highly expressed by Nc-Spain7.

Nc-Spain7 also showed up-regulation of *N. caninum* macrophage migration inhibitory factor (MIF, NCLIV_042400). MIF homologues have been reported in several protozoan parasites, including *T. gondii*, *Plasmodium* spp, *Eimeria* spp and *Leishmania* spp and have been suggested to play a role in immune evasion (Qu et al., 2013; Sommerville et al., 2013).

In addition, the virulent isolate expressed higher levels of two genes that may be involved in dissemination and transmission: a putative cyclophilin (NCLIV_015405) and a calreticulin

family member (NCLIV_054410). *Neospora caninum* molecules from the cyclophilin family have been shown to work as chemokine-like proteins by inducing chemoattraction of immune cells, which may consequently enhance their invasion by the parasites (Mineo et al., 2010). Because we have previously shown the ability of *N. caninum* to survive in boMØs and induce a hypermigratory phenotype in these cells upon infection (García-Sánchez et al., 2019), the higher expression of cyclophilin by Nc-Spain7 may potentially be related to the increased dissemination of this isolate found *in vivo* (Collantes-Fernández et al., 2012). Calreticulin is an endoplasmic reticule-resident chaperone involved in protein folding. In trypanosomatids, it seems to help in establishment of infection by modulating the host complement system (Ramakrishnan and Docampo, 2018). In addition, alteration of the function of this chaperone in *Leishmania donovani* results in a lower survival rate in MØs, and interestingly, *Trypanosoma cruzi* calreticulin likely facilitates placental infection by interacting with the maternal classical complement component C1, which would bridge it with the fetal calreticulin in placental tissues (Castillo et al., 2013).

The roles of these proteins in *N. caninum* pathogenesis, particularly with regard to differences in the proinflammatory response induced by the isolates during infection *in vitro* (García-Sánchez et al., 2019) and transmission found *in vivo* (Rojo-Montejo et al., 2009a; Regidor-Cerrillo et al., 2014), require further investigation.

4. CONCLUDING REMARKS

Intraspecific variations in the biological behavior of *N. caninum* isolates have been widely described and associated with differences in virulence. In previous studies, we demonstrated that Nc-Spain7 and Nc-Spain1H isolates, which exhibit marked differences in virulence, show different abilities to invade, survive and proliferate in boMØs and modulate the cell response in different manners. The Nc-Spain1H isolate, despite showing a lower proliferation and survival rate, induces higher expression of genes involved in pathogen recognition, chemotaxis and proinflammatory and regulatory cytokine release, which may result in key differences in the immune responses generated by the host against the isolates. Here, we describe that these differences are connected with specific gene expression profiles in the tachyzoite stage. Specifically, bradyzoite stage-related genes and genes encoding for surface antigens were among the primary up-regulated genes in the Nc-Spain1H isolate, whereas Nc-Spain7 showed enhanced expression of genes involved in parasite growth and survival in activated MØs.

Further studies are necessary to determine the virulence factor potential of the proteins identified to be differentially expressed between the isolates and determine whether these proteins may be implicated in parasite fitness and immune response modulation.

SUPPLEMENTARY FILES

SUPPLEMENTARY TABLE 1 | Sequences of primers used for transcriptomic validation by RT-qPCR

Target	Ortholog TgME49	Sequences (5' to 3')	Product size (bp)	References
NCLIV_042400	TGME49_290040	CCGACCCGTGTGCGTACATT	132	This study
NcMIF	TgMIF	TGGTGTAGATGCGGTTTTTGGA		
NCLIV_026210	TGME49_261070	GTCATCATGGCGTCAGTCAC	154	This study
Hypothetical protein	TgAPT1	TGTTCGCAGACGACAGATTC		
NCLIV_017420	TGME49_242110	AGTGAGTCTATTCGACGACGA	169	This study
Unspecified product	TgROP38	AGCCACCTGCGTTCGCTGTCT		
NCLIV_010930	TGME49_318610	AGAACAAGCGGACAACTTGGT	202	This study
Unspecified product	TgAP2IV-3	GAAGTCGTCGAGATCCACTTC		
NCLIV_001350	TGME49_294330	ACGGTAACCAGCATTTCCAG	195	This study
Putative EGF-like domain containing protein	TgAMA4	TTCTTCTGCGTCTTCCTCGT		
NCLIV_068850	TGME49_252360	GGCGAACCTTCATAAGCAAC	139	Horcajo et al., 2018
Unspecified product	TgROP24[a]	AAGTAAATCGGGGGAGCAAC		
NCLIV_010030	TGME49_320230	CCATGAAGGACTCCAGAATCG	101	Risco-Castillo et al., 2007
NcBSR4	TgSRS15C	TCGCTGGAAACGCACATTTA		
NCLIV_058890	TGME49_316400	GGTAACGCCTGCTGGGAG	166	Alaeddine et al., 2013
NcTUBα	TgTUBA1	GCTCCAAATCCAAGAAGACGCA		
NCLIV_033230	TGME49_233460	CGGTGTCGCAATGTGCTCTT	150	Fernández-García et al., 2006
SRS domain containing protein	TgSAG1	ACGGTCGTCCCAGAACAAAC		

[a]No syntenic

SUPPLEMENTARY TABLE 2 | *Neospora caninum* differentially expressed genes in the comparison Nc-Spain1H-infected macrophages *versus* Nc-Spain7-infected macrophages. Genes were considered as differentially expressed when presented a FoldChange (FC) ≥ 2 and with a false discovery rate (FDR)-adjusted p-value (p adj) ≤ 0.05.

Gene id	Gene description	FC	padj	Nc-Spain7			Nc-Spain1H		
XLOC_000093		-372,85	1,20E-31	55,45	44,14	75,35	0,00	0,00	0,00
NCLIV_052460	Hypothetical protein	-210,27	9,60E-73	143,44	114,18	194,94	0,44	0,24	0,32
XLOC_000021		-54,97	0,00E+00	6170,99	4912,26	8386,37	92,85	49,93	67,43
NCLIV_014580	Hypothetical protein, related	-49,71	6,17E-05	7,26	5,78	9,87	0,00	0,00	0,00
NCLIV_004432	SRS domain-containing protein	-37,12	7,00E-04	5,39	4,29	7,32	0,00	0,00	0,00
XLOC_000077		-24,96	2,83E-64	176,22	140,28	239,48	5,73	3,08	4,16
NCLIV_019790	Cation-transporting ATPase, related	-21,41	6,50E-28	71,48	56,90	97,14	2,65	1,42	1,92
NCLIV_007170	Conserved hypothetical protein	-18,02	3,10E-02	2,54	2,02	3,45	0,00	0,00	0,00
NCLIV_007740	Hypothetical protein	-17,92	3,18E-02	2,52	2,01	3,43	0,00	0,00	0,00
NCLIV_005160	Putative ppg3	-15,87	4,77E-02	2,22	1,76	3,01	0,00	0,00	0,00
NCLIV_007360	Conserved hypothetical protein	-15,84	4,78E-02	2,21	1,76	3,01	0,00	0,00	0,00
NCLIV_023620	SRS domain-containing protein	-15,22	1,60E-07	18,45	14,69	25,08	0,89	0,48	0,64
XLOC_000053		-12,90	9,79E-143	789,49	628,45	1072,92	50,57	27,19	36,72
XLOC_000180		-10,40	4,50E-07	18,04	14,36	24,52	1,32	0,71	0,96
NCLIV_062060	Hypothetical protein	-9,73	3,46E-03	6,50	5,18	8,84	0,44	0,24	0,32
NCLIV_067320	Conserved hypothetical protein	-9,49	3,34E-03	6,33	5,04	8,61	0,44	0,24	0,32
NCLIV_026210	Hypothetical protein	-8,87	3,73E-18	53,19	42,34	72,28	4,85	2,61	3,53
NCLIV_005420	Phosphoglycerate kinase, related	-7,95	7,01E-13	39,24	31,24	53,33	3,98	2,14	2,89
NCLIV_014630	Novel protein similar to quinoid dihydropteridine reductase (QDPR, zgc:112405), related	-7,90	5,11E-04	9,48	7,55	12,89	0,89	0,48	0,64
NCLIV_023430	Putative WD domain, G-beta repeat-containing protein	-7,42	3,41E-06	16,83	13,39	22,87	1,77	0,95	1,29
NCLIV_034590	Conserved hypothetical protein	-7,13	2,20E-02	4,72	3,76	6,41	0,44	0,24	0,32
NCLIV_042840	Hypothetical protein	-6,37	3,89E-03	7,60	6,05	10,33	0,88	0,48	0,64
NCLIV_040810	Conserved hypothetical protein	-6,25	4,21E-02	4,11	3,27	5,59	0,44	0,24	0,32
NCLIV_023350	Conserved hypothetical protein	-6,19	4,88E-17	60,06	47,81	81,62	7,94	4,27	5,76
NCLIV_028530	Putative phospholipid-transporting P-type ATPase	-6,14	5,79E-24	92,59	73,70	125,83	12,39	6,66	9,00
NCLIV_014020	Peroxiredoxin-2E-1, related	-6,06	2,83E-33	133,44	106,22	181,35	18,13	9,75	13,17
NCLIV_062520	3-ketoacyl-(Acyl-carrier-protein) reductase, related	-6,03	9,13E-27	107,28	85,40	145,80	14,62	7,86	10,62
NCLIV_025780	Conserved hypothetical protein	-5,90	1,13E-03	10,15	8,08	13,79	1,32	0,71	0,96
NCLIV_058960	Conserved hypothetical protein	-5,85	2,90E-21	81,80	65,11	111,16	11,48	6,17	8,34
NCLIV_031330	Conserved hypothetical protein	-5,78	1,86E-08	31,70	25,23	43,08	4,44	2,39	3,22
XLOC_007067		-5,63	3,52E-04	12,75	10,15	17,33	1,77	0,95	1,29
NCLIV_024260	Conserved hypothetical protein	-5,62	2,84E-04	12,66	10,08	17,21	1,76	0,95	1,28
NCLIV_010830	Putative UDP-N-acetyl-D-galactosamine:polypeptide N-acetylgalactosaminyltransferase T3	-5,43	2,43E-12	46,90	37,34	63,74	7,05	3,79	5,12
NCLIV_030570	Hypothetical protein	-5,31	3,84E-08	28,91	23,01	39,29	4,41	2,37	3,20
NCLIV_028260	Hypothetical protein	-5,13	4,63E-07	25,37	20,19	34,48	3,99	2,15	2,90
NCLIV_065930	Conserved hypothetical protein	-5,12	4,88E-03	8,79	7,00	11,95	1,32	0,71	0,96
NCLIV_005670	Conserved hypothetical protein	-5,11	3,03E-14	57,99	46,16	78,81	9,29	5,00	6,75
NCLIV_007770	Putative Rhoptry kinase family protein, truncated (incomplete catalytic triad)	-4,75	4,63E-104	1630,19	1297,67	2215,42	284,13	152,78	206,34
NCLIV_069650	Phenylalanine-4-hydroxylase, related	-4,71	3,95E-02	5,57	4,43	7,57	0,88	0,47	0,64
NCLIV_052110	Conserved hypothetical protein	-4,69	4,11E-06	23,03	18,33	31,30	3,97	2,13	2,88
XLOC_007283		-4,64	2,50E-03	10,46	8,32	14,21	1,77	0,95	1,28
NCLIV_053480	Large protein with signal peptide. cysteine-rich,threonine-rich, possible mucin, related	-4,53	4,27E-02	5,36	4,27	7,28	0,88	0,48	0,64
NCLIV_058660	Conserved hypothetical protein	-4,53	1,27E-03	12,53	9,98	17,03	2,20	1,18	1,60
NCLIV_004340	Hypothetical protein	-4,42	5,10E-17	83,10	66,15	112,94	15,47	8,32	11,23
NCLIV_038170	Hypoxanthine phosphoribosyltransferase, related	-4,39	1,91E-11	57,06	45,42	77,55	10,66	5,73	7,74
NCLIV_061740	Hydrolase, alpha/beta fold family, related	-4,31	5,47E-04	14,25	11,34	19,36	2,64	1,42	1,92
NCLIV_016780	Conserved hypothetical protein	-4,27	8,93E-04	14,11	11,23	19,17	2,64	1,42	1,92
NCLIV_020280	YDL036Cp-like protein, related	-4,25	6,55E-03	9,54	7,59	12,96	1,77	0,95	1,28
NCLIV_069870	Hypothetical protein, conserved	-4,20	9,68E-05	18,40	14,65	25,01	3,54	1,90	2,57
NCLIV_047150	Conserved hypothetical protein	-4,16	2,96E-74	1203,85	958,29	1636,03	239,51	128,79	173,94

NCLIV_002110	Putative TPR domain-containing protein	-4,16	1,26E-04	20,49	16,31	27,84	3,99	2,14	2,90
NCLIV_045930	Putative glutaredoxin	-4,10	1,05E-03	13,61	10,84	18,50	2,65	1,43	1,93
NCLIV_053100	Conserved hypothetical protein	-4,06	1,65E-04	17,81	14,18	24,21	3,54	1,90	2,57
NCLIV_0245	NAD binding domain of 6-phosphogluconate dehydrogenase	-4,04	4,79E-06	26,25	20,90	35,67	5,29	2,84	3,84
NCLIV_032950	Putative deoxyuridine 5'-triphosphate nucleotidohydrolase	-4,04	3,35E-41	331,34	263,75	450,28	67,86	36,49	49,28
NCLIV_066970	Putative enoyl-acyl carrier reductase	-4,03	5,19E-25	135,83	108,13	184,60	27,83	14,97	20,21
NCLIV_007960	Conserved hypothetical protein	-4,02	9,88E-07	32,63	25,97	44,34	6,63	3,56	4,81
XLOC_007284		-3,95	5,19E-03	11,03	8,78	14,99	2,22	1,19	1,61
NCLIV_004260	Hypothetical protein	-3,93	6,19E-09	42,30	33,67	57,48	8,82	4,74	6,41
NCLIV_033590	Conserved hypothetical protein	-3,92	1,89E-03	12,97	10,33	17,63	2,65	1,43	1,92
NCLIV_053980	Conserved hypothetical protein	-3,92	6,91E-06	29,72	23,66	40,40	6,19	3,33	4,50
XLOC_007504		-3,83	1,55E-02	8,56	6,81	11,63	1,76	0,95	1,28
NCLIV_032060	Putative peptidase family T4	-3,82	7,19E-07	32,86	26,16	44,66	7,03	3,78	5,11
NCLIV_047210	Conserved hypothetical protein	-3,78	3,78E-08	40,91	32,56	55,60	8,87	4,77	6,44
NCLIV_009520	Conserved hypothetical protein	-3,77	3,36E-05	24,63	19,61	33,47	5,33	2,86	3,87
NCLIV_034300	Conserved hypothetical protein	-3,61	1,89E-04	19,66	15,65	26,71	4,42	2,38	3,21
NCLIV_010760	Hypothetical protein	-3,57	6,58E-15	95,83	76,28	130,23	22,11	11,89	16,06
XLOC_000128		-3,57	3,97E-16	95,37	75,92	129,61	22,02	11,84	15,99
NCLIV_062940	Putative pyruvate dehydrogenase	-3,53	6,61E-14	88,36	70,34	120,08	20,64	11,10	14,99
NCLIV_030730	Putative acetyltransferase domain-containing protein	-3,49	1,05E-08	48,82	38,86	66,35	11,51	6,19	8,36
NCLIV_012460	Lysyl-tRNA synthetase, related	-3,48	1,19E-11	69,31	55,17	94,19	16,38	8,81	11,90
NCLIV_000330	Conserved hypothetical protein	-3,44	5,98E-06	29,79	23,71	40,48	7,08	3,81	5,14
XLOC_007693		-3,39	3,61E-02	7,61	6,06	10,34	1,77	0,95	1,29
NCLIV_015650	Hypothetical protein	-3,39	7,07E-05	23,81	18,96	32,36	5,73	3,08	4,16
NCLIV_044360	Conserved hypothetical protein	-3,38	1,99E-05	27,47	21,87	37,33	6,64	3,57	4,82
NCLIV_037160	Putative actin-like family protein	-3,37	7,17E-05	23,76	18,91	32,29	5,75	3,09	4,17
NCLIV_055500	Conserved hypothetical protein	-3,33	2,25E-06	35,87	28,55	48,74	8,83	4,75	6,41
NCLIV_017800	Hypothetical protein	-3,33	2,15E-02	9,22	7,34	12,53	2,21	1,19	1,61
NCLIV_037170	Conserved hypothetical protein	-3,31	5,25E-04	23,27	18,52	31,62	5,74	3,09	4,17
NCLIV_045430	Putative DNA-binding protein HU	-3,27	4,54E-20	140,09	111,51	190,38	35,36	19,01	25,68
NCLIV_055220	Putative CAMP-dependent protein kinase regulatory subunit	-3,26	4,94E-02	7,31	5,82	9,93	1,77	0,95	1,29
NCLIV_066620	Conserved hypothetical protein	-3,22	1,10E-05	33,02	26,29	44,88	8,41	4,52	6,11
NCLIV_000530	3-oxoacyl-(Acyl-carrier-protein) synthase II,related	-3,21	1,27E-17	127,55	101,54	173,34	32,79	17,63	23,81
NCLIV_055730	Hypothetical protein	-3,20	4,96E-13	103,92	82,72	141,23	26,78	14,40	19,45
NCLIV_055510	Conserved hypothetical protein	-3,20	1,29E-03	17,41	13,86	23,67	4,42	2,38	3,21
NCLIV_064560	Hypothetical protein	-3,19	4,28E-03	13,96	11,11	18,97	3,54	1,90	2,57
NCLIV_044150	Conserved hypothetical protein	-3,18	3,85E-04	22,35	17,79	30,37	5,73	3,08	4,16
NCLIV_065280	Proliferating cell nuclear antigen, related	-3,14	1,04E-23	205,19	163,34	278,86	53,99	29,03	39,21
NCLIV_008230	Delta-aminolevulinic acid dehydratase, related	-3,12	2,90E-10	72,19	57,47	98,11	19,07	10,25	13,85
NCLIV_016930	Hypothetical protein	-3,11	3,79E-03	15,29	12,17	20,78	3,99	2,14	2,89
NCLIV_024790	Conserved hypothetical protein	-3,11	6,47E-03	13,59	10,81	18,46	3,54	1,90	2,57
NCLIV_051570	Conserved hypothetical protein	-3,09	2,08E-03	16,76	13,34	22,78	4,40	2,37	3,20
NCLIV_045700	Putative transmembrane amino acid transporter domain-containing protein	-3,07	7,25E-04	19,94	15,88	27,10	5,30	2,85	3,85
NCLIV_000900	Conserved hypothetical protein	-3,06	3,92E-06	37,97	30,22	51,60	10,19	5,48	7,40
NCLIV_012560	Putative SNF7 family domain-containing protein	-3,05	1,34E-02	11,74	9,34	15,95	3,10	1,67	2,25
NCLIV_010140	Putative proliferating cell nuclear antigen	-3,05	1,90E-09	63,68	50,69	86,54	17,20	9,25	12,49
NCLIV_014720	Conserved hypothetical protein	-3,05	1,12E-08	55,72	44,35	75,72	15,06	8,10	10,94
XLOC_000200		-3,04	4,79E-06	35,83	28,52	48,69	9,68	5,20	7,03
XLOC_000137		-3,02	5,39E-14	103,57	82,44	140,75	28,28	15,21	20,54
NCLIV_0155	Alpha/beta hydrolase fold domain containing protein	-3,00	1,26E-09	81,05	64,52	110,15	22,31	12,00	16,20
NCLIV_036050	Conserved hypothetical protein	-2,98	6,93E-07	43,46	34,59	59,06	11,98	6,44	8,70
NCLIV_053630	Putative zinc finger (CCCH type) protein	-2,97	9,14E-17	145,44	115,77	197,65	40,51	21,78	29,42
NCLIV_053090	Conserved hypothetical protein	-2,95	1,62E-03	19,20	15,28	26,09	5,31	2,85	3,85
NCLIV_015430	Hypothetical protein	-2,94	2,50E-16	132,82	105,73	180,51	37,32	20,07	27,10
NCLIV_001900	Putative histidyl-tRNAsynthetase	-2,92	4,69E-37	598,90	476,74	813,90	169,78	91,29	123,30
NCLIV_012540	Hypothetical protein	-2,91	1,24E-04	28,40	22,60	38,59	7,99	4,30	5,80
NCLIV_0153	Longevity-assurance (LAG1) domain-containing protein	-2,89	1,38E-05	35,66	28,39	48,47	10,16	5,46	7,38
NCLIV_041450	cDNA FLJ39191 fis, clone OCBBF2004669, highly similar to Homo sapiens ATPase type 13A4, related	-2,88	7,86E-09	69,36	55,21	94,25	19,87	10,68	14,43

NCLIV_052780	Putative penicillin amidase domain-containing protein	-2,87	1,07E-31	472,45	376,08	642,06	136,14	73,21	98,87
NCLIV_058920	Hypothetical protein	-2,86	1,15E-04	30,70	24,44	41,72	8,81	4,74	6,40
NCLIV_048340	Putative pseudouridylate synthase 1	-2,86	1,45E-06	46,18	36,76	62,75	13,30	7,15	9,66
NCLIV_042400	Macrophage migration inhibitory factor, related	-2,84	1,08E-10	85,39	67,97	116,04	24,84	13,36	18,04
NCLIV_008220	Putative M16 family peptidase	-2,84	6,34E-06	47,14	37,52	64,06	13,69	7,36	9,94
NCLIV_003550	Hypothetical protein	-2,83	3,25E-05	34,92	27,80	47,46	10,15	5,46	7,37
NCLIV_053050	Putative indole-3-glycerol phosphate synthase domain containing protein	-2,83	3,89E-09	67,97	54,10	92,37	19,83	10,66	14,40
NCLIV_052060	Cullin-associated NEDD8-dissociated protein 1,related	-2,77	6,75E-05	31,32	24,93	42,57	9,27	4,98	6,73
NCLIV_062490	Unspecified product	-2,77	1,23E-09	80,00	63,68	108,71	23,84	12,82	17,31
NCLIV_015080	Conserved hypothetical protein	-2,76	2,75E-03	24,34	19,38	33,08	7,22	3,88	5,24
NCLIV_060910	Putative DNA replication licensing factor	-2,74	2,70E-13	129,52	103,10	176,02	39,01	20,98	28,33
NCLIV_065610	Proteophosphoglycan 5, related	-2,74	1,36E-09	84,10	66,95	114,30	25,32	13,61	18,39
NCLIV_011590	Hypothetical protein	-2,74	4,43E-05	33,80	26,91	45,93	10,14	5,45	7,37
NCLIV_065390	Bifunctional dihydrofolate reductase-thymidylate synthase, related	-2,72	4,67E-17	161,63	128,66	219,66	49,08	26,39	35,64
NCLIV_068350	Conserved hypothetical protein	-2,72	1,12E-02	14,81	11,79	20,12	4,43	2,38	3,22
NCLIV_023470	Ribonuclease, related	-2,71	2,27E-05	36,38	28,96	49,44	11,05	5,94	8,02
NCLIV_025530	Putative TPR domain-containing protein	-2,70	3,42E-20	215,73	171,72	293,17	65,97	35,47	47,91
NCLIV_033420	Hypothetical protein	-2,70	1,27E-04	30,51	24,29	41,47	9,28	4,99	6,74
NCLIV_056970	Conserved hypothetical protein	-2,70	2,98E-06	46,51	37,02	63,20	14,18	7,63	10,30
NCLIV_012730	Os10g0412100 protein, related	-2,68	2,75E-02	11,67	9,29	15,87	3,53	1,90	2,56
NCLIV_0319	3-oxoacyl-(acyl-carrier-protein) synthase III family protein	-2,68	9,75E-07	52,12	41,49	70,83	16,01	8,61	11,63
NCLIV_055940	Putative TPR domain-containing protein	-2,68	3,63E-07	56,12	44,67	76,27	17,25	9,28	12,53
NCLIV_023120	Chorismate synthase, related	-2,67	1,65E-11	107,54	85,61	146,15	33,24	17,87	24,14
NCLIV_035870	Putative glycerol-3-phosphate acyltransferase	-2,67	1,18E-06	49,94	39,75	67,87	15,44	8,30	11,21
NCLIV_026360	Conserved hypothetical protein	-2,64	2,71E-06	46,63	37,12	63,36	14,54	7,82	10,56
NCLIV_015150	Conserved hypothetical protein	-2,63	1,57E-07	67,37	53,63	91,56	21,11	11,35	15,33
NCLIV_049750	Putative replication factor c subunit	-2,63	6,15E-07	69,67	55,46	94,69	21,86	11,75	15,88
NCLIV_025810	Conserved hypothetical protein	-2,63	1,08E-04	35,40	28,18	48,11	11,07	5,95	8,04
NCLIV_008810	Conserved hypothetical protein	-2,62	8,60E-05	36,59	29,12	49,72	11,48	6,17	8,34
NCLIV_010790	Putative Aurora kinase(incomplete catalytic triad)	-2,62	1,92E-06	54,62	43,48	74,22	17,20	9,25	12,49
NCLIV_003470	Putative thrombospondin type 1 domain-containing protein	-2,62	2,18E-07	60,09	47,83	81,66	18,94	10,18	13,75
NCLIV_025100	Hypothetical protein	-2,61	3,41E-02	11,37	9,05	15,46	3,53	1,90	2,56
NCLIV_058270	Conserved hypothetical protein	-2,61	3,67E-06	47,74	38,00	64,88	15,07	8,10	10,94
NCLIV_015770	Conserved hypothetical protein	-2,61	1,36E-04	32,33	25,73	43,93	10,20	5,48	7,41
NCLIV_005700	Conserved hypothetical protein	-2,59	6,73E-05	37,53	29,87	51,00	11,94	6,42	8,67
NCLIV_059870	onserved hypothetical protein	-2,57	7,77E-04	26,23	20,88	35,65	8,39	4,51	6,09
NCLIV_051700	Conserved hypothetical protein	-2,56	5,09E-07	69,79	55,55	94,84	22,47	12,08	16,32
NCLIV_052470	Hypothetical protein	-2,56	2,97E-04	31,49	25,07	42,80	10,12	5,44	7,35
NCLIV_038450	Conserved hypothetical protein	-2,55	3,54E-05	42,69	33,98	58,02	13,78	7,41	10,01
NCLIV_021700	C hypothetical protein	-2,55	3,66E-04	34,12	27,16	46,37	11,03	5,93	8,01
NCLIV_063860	Putative thioredoxin	-2,52	1,78E-25	570,21	453,90	774,91	187,10	100,61	135,88
NCLIV_032420	Conserved hypothetical protein	-2,52	2,25E-05	44,46	35,39	60,42	14,55	7,83	10,57
NCLIV_045290	cDNA FLJ30053 fis, clone ADRGL1000144, highly similar to StAR-related lipid transfer protein 7, related	-2,51	2,37E-09	87,67	69,79	119,15	28,80	15,49	20,91
NCLIV_009830	Conserved hypothetical protein	-2,51	1,68E-06	55,28	44,00	75,12	18,19	9,78	13,21
XLOC_000201		-2,51	5,20E-05	42,96	34,20	58,38	14,13	7,60	10,26
NCLIV_034340	Hypothetical protein	-2,50	9,44E-03	17,52	13,95	23,81	5,74	3,09	4,17
NCLIV_012905	Unspecified product	-2,49	4,55E-04	36,29	28,89	49,32	11,98	6,44	8,70
NCLIV_032890	T10O22.7, related	-2,49	2,60E-04	32,01	25,48	43,50	10,57	5,68	7,67
NCLIV_016250	Putative cytidine deaminase	-2,49	4,79E-06	53,38	42,49	72,54	17,68	9,51	12,84
NCLIV_010990	Conserved hypothetical protein	-2,49	4,49E-02	12,07	9,61	16,40	3,94	2,12	2,86
NCLIV_006110	Conserved hypothetical protein	-2,49	1,31E-06	57,11	45,46	77,61	18,94	10,18	13,76
NCLIV_004820	Phospho-2-dehydro-3-deoxyheptonate aldolase,related	-2,48	2,28E-10	101,38	80,70	137,78	33,74	18,14	24,50
NCLIV_0253	GTP-binding conserved hypothetical domain-containing protein	-2,48	7,90E-04	27,95	22,25	37,99	9,26	4,98	6,73
NCLIV_068850	Unspecified product	-2,47	1,63E-35	3484,03	2773,38	4734,80	1166,69	627,35	847,27
NCLIV_063790	Hypothetical protein	-2,47	8,49E-05	39,66	31,57	53,90	13,22	7,11	9,60
NCLIV_018380	Putative dihydrodipicolinate reductase	-2,46	4,91E-05	39,61	31,53	53,83	13,24	7,12	9,61
NCLIV_046950	UDP-glucose 4-epimerase, related	-2,46	1,80E-07	72,03	57,33	97,88	24,18	13,00	17,56

NCLIV_046530	Putative reticulon domain-containing protein	-2,44	3,29E-14	165,38	131,65	224,76	55,95	30,09	40,63
NCLIV_033270	Hypothetical protein	-2,44	2,02E-07	78,96	62,85	107,30	26,69	14,35	19,38
NCLIV_064730	Hypothetical protein	-2,44	9,10E-03	18,37	14,63	24,97	6,16	3,31	4,48
NCLIV_018180	Putative Ras family domain-containing protein	-2,43	6,64E-05	39,01	31,05	53,02	13,23	7,12	9,61
NCLIV_009420	Putative pyruvate kinase	-2,43	1,18E-02	18,31	14,58	24,89	6,18	3,32	4,49
NCLIV_044550	Conserved hypothetical protein	-2,42	5,52E-03	23,17	18,45	31,49	7,87	4,23	5,71
NCLIV_029610	Putative prefoldin subunit 3	-2,41	1,05E-04	42,80	34,07	58,17	14,61	7,85	10,61
NCLIV_057630	Putative dolichyl pyrophosphate Glc1Man9GlcNAc2 alpha-1,3-glucosyltransferase	-2,41	1,25E-06	63,38	50,45	86,13	21,67	11,65	15,74
NCLIV_068360	Putative toprim domain-containing protein	-2,40	1,38E-05	47,57	37,87	64,65	16,34	8,79	11,87
NCLIV_014740	Unspecified product	-2,39	1,91E-02	15,54	12,37	21,11	5,30	2,85	3,85
NCLIV_011620	Conserved hypothetical protein	-2,39	1,73E-02	16,83	13,40	22,87	5,76	3,10	4,18
NCLIV_005790	Conserved hypothetical protein	-2,39	2,64E-03	25,60	20,38	34,80	8,81	4,74	6,40
NCLIV_056840	Putative regulator of chromosome condensation domain-containing protein	-2,37	9,43E-04	30,41	24,20	41,32	10,57	5,68	7,68
NCLIV_010800	Conserved hypothetical protein	-2,36	1,13E-03	29,29	23,31	39,80	10,19	5,48	7,40
NCLIV_034920	Hypothetical protein	-2,35	4,94E-04	35,28	28,09	47,95	12,38	6,66	8,99
NCLIV_006700	Structural maintenance of chromosome 2, related	-2,35	1,20E-03	29,06	23,14	39,50	10,19	5,48	7,40
NCLIV_012270	Putative calmodulin	-2,34	1,15E-03	31,39	24,99	42,66	11,06	5,95	8,03
NCLIV_063770	Hypothetical protein	-2,32	6,11E-09	97,70	77,77	132,78	34,78	18,70	25,26
NCLIV_062840	Putative origin recognition complex subunit 2	-2,32	1,83E-03	28,66	22,81	38,95	10,15	5,46	7,37
NCLIV_006510	Putative TCP-1/cpn60 family chaperonin	-2,32	1,50E-12	158,34	126,05	215,19	56,53	30,40	41,05
NCLIV_042120	Conserved hypothetical protein	-2,31	2,38E-04	40,60	32,32	55,17	14,47	7,78	10,51
NCLIV_027700	SRS domain-containing protein	-2,31	1,82E-10	114,96	91,51	156,24	41,10	22,10	29,85
NCLIV_020320	Proteophosphoglycan ppg4, related	-2,31	8,55E-03	21,21	16,89	28,83	7,53	4,05	5,47
NCLIV_024480	Conserved hypothetical protein	-2,31	1,85E-03	29,71	23,65	40,37	10,58	5,69	7,68
NCLIV_018960	Conserved hypothetical protein	-2,31	1,90E-02	17,36	13,82	23,59	6,15	3,31	4,47
NCLIV_005130	Conserved hypothetical protein	-2,31	8,24E-03	22,51	17,92	30,60	8,00	4,30	5,81
NCLIV_015810	Putative retinitis pigmentosa GTPase regulator	-2,30	4,49E-02	13,72	10,92	18,64	4,86	2,61	3,53
NCLIV_023770	Hypothetical protein	-2,30	1,12E-03	34,78	27,68	47,26	12,46	6,70	9,05
NCLIV_063160	Conserved hypothetical protein	-2,29	3,39E-11	146,48	116,60	199,06	52,86	28,42	38,39
NCLIV_018460	Conserved hypothetical protein	-2,29	3,82E-04	38,31	30,49	52,06	13,79	7,41	10,01
NCLIV_050400	Hypothetical protein	-2,29	1,60E-07	98,58	78,48	133,98	35,64	19,17	25,88
NCLIV_023990	Acyl carrier protein, related	-2,29	5,73E-13	202,18	160,94	274,77	73,19	39,36	53,15
NCLIV_005950	Putative trafficking protein particle complex protein	-2,28	3,11E-04	36,78	29,28	49,99	13,27	7,14	9,64
NCLIV_006330	Hypothetical protein	-2,27	8,62E-04	35,58	28,32	48,35	12,90	6,94	9,37
NCLIV_032430	Conserved hypothetical protein	-2,27	9,48E-18	407,60	324,46	553,93	148,83	80,03	108,08
NCLIV_051000	Ethylene-inducible protein hever, related	-2,26	4,65E-02	14,52	11,56	19,73	5,24	2,82	3,81
NCLIV_060300	cDNA, FLJ96396, highly similar to Homo sapiens ERO1-like beta (S. cerevisiae) (ERO1LB), mRNA, related	-2,26	2,20E-11	140,74	112,03	191,26	51,50	27,69	37,40
NCLIV_056010	Conserved hypothetical protein	-2,25	3,02E-02	15,85	12,62	21,54	5,76	3,10	4,18
NCLIV_029560	Conserved hypothetical protein	-2,25	1,75E-03	34,00	27,07	46,21	12,43	6,69	9,03
NCLIV_057480	Hypothetical protein	-2,25	1,54E-03	30,09	23,95	40,89	11,01	5,92	8,00
NCLIV_037190	Putative glyceraldehyde-3-phosphate dehydrogenase	-2,25	1,68E-17	340,87	271,34	463,25	125,50	67,48	91,14
NCLIV_025050	SPRY domain-containing protein, related	-2,24	1,14E-02	21,76	17,32	29,57	7,96	4,28	5,78
NCLIV_042850	Pyridoxal phosphate-dependent acyltransferase, related	-2,24	9,65E-08	89,66	71,37	121,85	33,07	17,78	24,02
NCLIV_053010	Conserved hypothetical protein	-2,23	4,64E-07	91,77	73,05	124,72	33,98	18,27	24,68
NCLIV_015405	Putative cyclophilin	-2,23	3,14E-06	71,96	57,28	97,79	26,63	14,32	19,34
NCLIV_007290	Putative protein kinase	-2,23	1,55E-09	121,62	96,81	165,28	45,09	24,25	32,74
NCLIV_007340	Conserved hypothetical protein	-2,23	2,35E-03	34,80	27,70	47,29	12,86	6,92	9,34
NCLIV_028690	Multisite-specific tRNA m(5)C methyltransferase, related	-2,22	1,19E-02	22,90	18,23	31,12	8,47	4,55	6,15
NCLIV_017360	Hypothetical protein	-2,22	4,04E-03	28,75	22,89	39,07	10,67	5,74	7,75
NCLIV_054680	Conserved hypothetical protein	-2,21	4,19E-04	41,26	32,85	56,08	15,38	8,27	11,17
NCLIV_023230	Conserved hypothetical protein	-2,21	9,33E-13	176,31	140,35	239,61	66,00	35,49	47,93
NCLIV_005330	At4g25910 protein, related	-2,21	4,11E-04	39,11	31,13	53,15	14,60	7,85	10,60
NCLIV_026390	Putative centrin	-2,21	5,75E-04	42,01	33,44	57,09	15,69	8,44	11,39
NCLIV_035250	GK18150, related	-2,21	9,49E-06	61,51	48,97	83,60	23,02	12,38	16,72

NCLIV_035450	Hypothetical protein	-2,21	3,46E-04	39,06	31,10	53,09	14,60	7,85	10,60
NCLIV_010530	Conserved hypothetical protein	-2,19	5,08E-05	51,67	41,13	70,21	19,49	10,48	14,15
NCLIV_046780	Conserved hypothetical protein	-2,18	3,42E-06	74,48	59,29	101,22	28,19	15,16	20,47
NCLIV_010420	Conserved hypothetical protein	-2,18	1,36E-02	21,23	16,90	28,85	7,99	4,30	5,80
XLOC_007662		-2,18	2,36E-02	18,85	15,00	25,61	7,09	3,81	5,15
NCLIV_031540	Putative chromosome condensation protein	-2,18	6,28E-09	114,42	91,08	155,50	43,47	23,37	31,57
NCLIV_015100	Conserved hypothetical protein	-2,17	1,24E-04	48,95	38,97	66,53	18,61	10,01	13,52
NCLIV_009390	Putative Cleft lip and palate transmembrane protein 1	-2,17	8,04E-09	111,30	88,60	151,25	42,42	22,81	30,80
NCLIV_002980	Putative 5-formyltetrahydrofolate cyclo-ligase domain-containing protein	-2,17	2,21E-02	19,83	15,78	26,95	7,50	4,03	5,45
NCLIV_039650	Genome sequencing data, contig C317, related	-2,17	1,85E-02	19,86	15,81	26,98	7,51	4,04	5,46
NCLIV_037850	Conserved hypothetical protein	-2,17	2,39E-02	21,08	16,78	28,65	7,99	4,30	5,81
NCLIV_039850	Hypothetical protein	-2,16	9,53E-08	93,76	74,63	127,42	35,89	19,30	26,06
NCLIV_057620	Conserved hypothetical protein	-2,16	3,85E-04	40,52	32,26	55,07	15,49	8,33	11,25
NCLIV_019620	Conserved hypothetical protein	-2,15	4,27E-02	17,45	13,89	23,71	6,64	3,57	4,82
NCLIV_054410	Calr protein, related	-2,15	1,97E-04	50,02	39,82	67,98	19,24	10,35	13,97
NCLIV_044720	Conserved hypothetical protein	-2,15	8,64E-03	24,17	19,24	32,85	9,27	4,98	6,73
NCLIV_048150	Conserved hypothetical protein	-2,14	1,98E-04	47,05	37,45	63,94	18,10	9,73	13,14
NCLIV_032510	FAD binding domain containing protein, related	-2,14	3,41E-04	45,78	36,44	62,22	17,62	9,48	12,80
NCLIV_059570	Conserved hypothetical protein	-2,14	3,50E-02	17,27	13,75	23,47	6,61	3,55	4,80
XLOC_000199		-2,13	1,53E-06	87,96	70,02	119,54	34,18	18,38	24,82
NCLIV_056530	Conserved hypothetical protein	-2,12	6,99E-03	28,39	22,60	38,58	11,00	5,91	7,99
NCLIV_025060	Conserved hypothetical protein	-2,12	1,20E-02	23,99	19,09	32,60	9,29	4,99	6,75
NCLIV_038630	Conserved hypothetical protein	-2,12	4,79E-06	75,87	60,39	103,10	29,58	15,91	21,48
NCLIV_058040	Conserved hypothetical protein	-2,12	9,12E-05	53,28	42,41	72,41	20,78	11,18	15,09
NCLIV_048560	Conserved hypothetical protein	-2,10	5,55E-05	58,27	46,39	79,19	22,95	12,34	16,67
NCLIV_003190	Putative mitochondrial carrier domain-containing protein	-2,10	2,45E-08	110,81	88,21	150,59	43,73	23,51	31,75
NCLIV_029370	Conserved hypothetical protein	-2,09	8,00E-03	26,90	21,42	36,56	10,58	5,69	7,68
NCLIV_044100	Conserved hypothetical protein	-2,09	1,38E-04	58,54	46,60	79,56	23,10	12,42	16,78
NCLIV_001000	Conserved hypothetical protein	-2,09	6,30E-03	28,04	22,32	38,11	11,06	5,95	8,03
NCLIV_061460	Family T1, proteasome beta subunit, threonine peptidase, related	-2,09	1,34E-10	174,29	138,74	236,86	69,11	37,16	50,19
NCLIV_050450	Conserved hypothetical protein	-2,09	1,25E-03	41,78	33,26	56,79	16,52	8,88	12,00
NCLIV_065150	Putative sybindin-like family domain-containing protein	-2,09	5,42E-08	114,90	91,47	156,16	45,57	24,51	33,10
NCLIV_061380	Hypothetical protein	-2,08	1,67E-04	59,21	47,13	80,47	23,50	12,64	17,07
NCLIV_015250	Hypothetical protein	-2,08	1,20E-03	36,80	29,30	50,02	14,59	7,84	10,59
NCLIV_053850	Conserved hypothetical protein	-2,08	2,41E-04	51,00	40,60	69,31	20,27	10,90	14,72
NCLIV_018660	Conserved hypothetical protein	-2,07	5,90E-03	29,98	23,86	40,74	11,92	6,41	8,66
NCLIV_005800	Unspecified product	-2,07	3,34E-03	31,07	24,74	42,23	12,37	6,65	8,98
NCLIV_031690	Oligosaccharyl transferase-like protein, related	-2,06	1,54E-08	128,89	102,60	175,16	51,66	27,78	37,52
NCLIV_016000	Conserved hypothetical protein	-2,06	1,04E-03	40,94	32,59	55,63	16,38	8,81	11,89
NCLIV_010380	DNA polymerase, related	-2,06	1,05E-07	118,10	94,01	160,50	47,47	25,52	34,47
NCLIV_005740	Conserved hypothetical protein	-2,06	8,17E-07	91,31	72,69	124,09	36,70	19,73	26,65
NCLIV_063710	Conserved hypothetical protein	-2,05	3,25E-06	85,18	67,81	115,76	34,34	18,46	24,94
NCLIV_057270	Hypothetical protein	-2,05	2,48E-04	58,03	46,19	78,86	23,38	12,57	16,98
NCLIV_046425	Unspecified product	-2,05	5,55E-05	66,56	52,98	90,46	26,86	14,44	19,51
NCLIV_040320	Putative ubiquitin-activating enzyme	-2,04	1,25E-03	40,42	32,18	54,93	16,31	8,77	11,85
NCLIV_006990	Conserved hypothetical protein	-2,04	3,63E-04	53,21	42,36	72,32	21,58	11,61	15,67
NCLIV_013120	Putative activator 1 36 kDa	-2,04	6,85E-04	44,80	35,66	60,89	18,16	9,77	13,19
NCLIV_024420	Hypothetical protein	-2,03	1,55E-13	310,90	247,49	422,52	126,56	68,05	91,91
NCLIV_014390	Hypothetical protein	-2,03	4,29E-05	81,79	65,11	111,16	33,27	17,89	24,16
NCLIV_056670	Conserved hypothetical protein	-2,03	4,79E-16	423,30	336,95	575,26	172,79	92,91	125,48
NCLIV_068490	Conserved hypothetical protein	-2,03	4,21E-02	17,44	13,88	23,70	7,06	3,80	5,13
NCLIV_011080	Unspecified product	-2,03	1,14E-06	94,72	75,40	128,72	38,67	20,79	28,08
NCLIV_059560	Putative DNA replication licensing factor	-2,02	3,18E-09	153,92	122,53	209,18	62,94	33,85	45,71
NCLIV_045950	Conserved hypothetical protein	-2,02	3,20E-03	40,14	31,95	54,55	16,42	8,83	11,92
NCLIV_013900	Conserved hypothetical protein	-2,01	1,62E-02	23,74	18,90	32,26	9,70	5,22	7,05
NCLIV_053750	Smc ABC ATpase, related	-2,01	2,35E-04	51,63	41,10	70,17	21,18	11,39	15,38
NCLIV_054430	Conserved hypothetical protein	-2,01	2,44E-04	53,86	42,87	73,19	22,12	11,90	16,07
NCLIV_033980	Conserved hypothetical protein	-2,01	6,90E-04	48,19	38,36	65,48	19,81	10,65	14,39
NCLIV_062650	Putative DNA polymerase alpha catalytic subunit	-2,01	2,47E-06	100,15	79,72	136,11	41,27	22,19	29,97
NCLIV_048050	Conserved hypothetical protein	-2,00	7,90E-04	48,72	38,78	66,21	20,06	10,79	14,57

NCLIV_048880	Proteasome subunit beta type-7, related	-2,00	1,97E-10	182,37	145,17	247,85	75,31	40,50	54,69
NCLIV_009750	Conserved hypothetical protein	-2,00	4,81E-02	19,40	15,44	26,36	7,97	4,28	5,78
NCLIV_013400	Conserved hypothetical protein	2,00	1,69E-21	522,38	415,83	709,91	865,47	465,38	628,51
NCLIV_068890	Unspecified product	2,00	4,19E-15	228,98	182,27	311,18	380,28	204,49	276,17
NCLIV_001070	Histone H2B, related	2,01	2,07E-07	58,70	46,73	79,78	97,64	52,50	70,91
NCLIV_040930	Putative NEK kinase	2,01	3,92E-15	266,32	212,00	361,93	442,71	238,05	321,50
NCLIV_068872	SRS domain-containing protein	2,02	3,41E-07	49,97	39,78	67,91	83,74	45,03	60,81
NCLIV_049520	Conserved hypothetical protein	2,02	4,58E-27	2616,01	2082,41	3555,16	4383,64	2357,16	3183,46
NCLIV_000440	Molybdopterin biosynthesis protein, related	2,04	1,37E-06	47,54	37,84	64,61	80,43	43,25	58,41
NCLIV_017420	Unspecified product	2,04	6,10E-06	38,88	30,95	52,83	65,92	35,44	47,87
NCLIV_020800	Cyclic nucleotide-binding domain containing protein	2,05	7,82E-05	27,45	21,85	37,31	46,74	25,13	33,94
NCLIV_034710	Conserved hypothetical protein	2,06	1,35E-02	10,75	8,55	14,60	18,49	9,94	13,43
NCLIV_056890	Hypothetical protein	2,07	8,89E-36	4840,06	3852,81	6577,63	8289,76	4457,55	6020,14
NCLIV_020210	Conserved hypothetical protein	2,07	9,51E-05	24,42	19,44	33,19	41,96	22,56	30,47
NCLIV_015630	Conserved hypothetical protein	2,08	4,08E-04	21,15	16,84	28,74	36,55	19,65	26,54
NCLIV_030330	Putative cAMP-specific phosphodiesterase	2,08	1,52E-02	10,16	8,08	13,80	17,67	9,50	12,83
NCLIV_064920	Conserved hypothetical protein	2,14	2,84E-02	7,92	6,30	10,76	14,14	7,61	10,27
NCLIV_004580	Hypothetical protein	2,14	3,95E-14	114,30	90,99	155,33	202,44	108,86	147,02
NCLIV_069030	Hypothetical protein	2,14	2,71E-05	31,33	24,94	42,58	55,78	29,99	40,51
NCLIV_007660	Hypothetical protein	2,15	1,56E-02	8,86	7,06	12,05	15,93	8,57	11,57
NCLIV_065220	Putative ABC transporter	2,16	1,37E-06	33,65	26,78	45,73	60,41	32,48	43,87
NCLIV_012440	Conserved hypothetical protein	2,16	3,38E-11	68,49	54,52	93,08	122,82	66,04	89,20
NCLIV_032400	Hypothetical protein	2,17	3,40E-06	30,52	24,30	41,48	55,08	29,62	40,00
NCLIV_045640	Conserved hypothetical protein	2,18	2,35E-12	87,49	69,64	118,90	157,76	84,83	114,57
NCLIV_003900	Putative oocyst wall protein COWP	2,18	2,08E-04	19,30	15,37	26,23	34,96	18,80	25,39
NCLIV_036660	Conserved hypothetical protein	2,19	6,38E-05	20,59	16,39	27,99	37,54	20,19	27,26
NCLIV_011000	Fibrillin 1, related	2,20	1,80E-02	7,93	6,31	10,77	14,56	7,83	10,58
NCLIV_001950	Unspecified product	2,22	4,86E-07	41,44	32,98	56,31	76,28	41,02	55,40
NCLIV_053410	Putative peroxisome biogenesis factor 1	2,23	1,77E-03	13,49	10,74	18,33	25,01	13,45	18,16
NCLIV_000210	Hypothetical protein	2,23	1,20E-02	8,52	6,78	11,58	15,89	8,54	11,54
NCLIV_013310	Hypothetical protein	2,23	3,34E-03	11,43	9,10	15,53	21,30	11,45	15,47
NCLIV_012520	Putative 3'5'-cyclic nucleotide phosphodiesterase	2,27	8,14E-08	41,63	33,14	56,57	78,28	42,09	56,85
NCLIV_067410	Conserved hypothetical protein	2,28	7,97E-03	8,83	7,03	12,00	16,83	9,05	12,22
XLOC_000078		2,30	5,78E-46	2237,99	1781,50	3041,42	4255,77	2288,40	3090,59
NCLIV_026900	Conserved hypothetical protein	2,31	8,56E-03	8,23	6,55	11,19	15,89	8,54	11,54
NCLIV_012450	Conserved hypothetical protein	2,31	2,35E-12	60,16	47,89	81,76	115,29	61,99	83,72
NCLIV_005970	Putative oocyst wall protein	2,31	6,51E-23	207,37	165,07	281,82	397,10	213,53	288,38
XLOC_007591		2,32	2,21E-02	6,36	5,06	8,64	12,36	6,65	8,98
NCLIV_064170	Conserved hypothetical protein	2,33	1,25E-06	29,89	23,79	40,62	57,73	31,05	41,93
XLOC_007417		2,34	8,73E-03	8,18	6,51	11,11	15,99	8,60	11,61
NCLIV_0269	GDA1/CD39 (nucleoside phosphatase) family domain containing protein	2,34	1,70E-05	19,30	15,36	26,22	37,59	20,21	27,30
NCLIV_066090	Putative leucine rich repeat protein	2,34	2,30E-02	6,35	5,05	8,63	12,49	6,71	9,07
NCLIV_049380	Conserved hypothetical protein	2,36	3,74E-03	9,17	7,30	12,46	18,05	9,71	13,11
NCLIV_057140	Conserved hypothetical protein	2,36	8,25E-10	41,22	32,81	56,01	80,77	43,43	58,65
NCLIV_058520	Conserved hypothetical protein	2,36	1,14E-04	16,93	13,47	23,00	33,29	17,90	24,18
NCLIV_057150	Hypothetical protein	2,36	5,69E-03	8,53	6,79	11,59	16,87	9,07	12,25
NCLIV_052740	SRS domain-containing protein	2,37	1,54E-02	6,67	5,31	9,07	13,25	7,12	9,62
NCLIV_034381	SRS domain-containing protein	2,37	1,75E-02	6,69	5,33	9,09	13,33	7,17	9,68
NCLIV_049510	SRS domain-containing protein	2,38	1,66E-04	16,28	12,96	22,12	32,28	17,36	23,44
NCLIV_044250	Conserved hypothetical protein	2,40	2,68E-14	74,28	59,13	100,95	147,91	79,53	107,41
NCLIV_053260	Putative platelet binding protein GspB	2,42	2,54E-06	22,39	17,82	30,42	45,06	24,23	32,73
NCLIV_002220	SRS domain-containing protein	2,43	1,75E-02	6,02	4,80	8,19	12,28	6,60	8,92
NCLIV_044760	Conserved hypothetical protein	2,44	2,28E-02	5,38	4,28	7,31	11,05	5,94	8,02
XLOC_000204		2,46	7,44E-05	15,46	12,31	21,01	31,63	17,01	22,97
NCLIV_024520	Hypothetical protein	2,46	6,19E-03	7,28	5,79	9,89	15,00	8,07	10,89
NCLIV_026560	Cell wall surface anchor family protein, related	2,47	2,35E-03	8,55	6,81	11,62	17,67	9,50	12,83
NCLIV_046430	Putative protein kinase	2,48	9,20E-27	260,90	207,68	354,56	536,24	288,35	389,43
NCLIV_028730	Putative peroxisomal-type ATPase	2,49	2,27E-02	5,07	4,04	6,89	10,62	5,71	7,72
NCLIV_069020	ATP-dependent RNA helicase, putative	2,49	3,93E-08	28,30	22,53	38,46	58,57	31,49	42,54
NCLIV_050890	Putative KR domain domain-containing protein	2,50	1,96E-04	12,31	9,80	16,72	25,62	13,77	18,60
NCLIV_033310	Hypothetical protein	2,50	2,40E-34	572,86	456,01	778,52	1184,36	636,85	860,10
NCLIV_067170	Conserved hypothetical protein	2,50	7,75E-09	37,08	29,52	50,39	76,99	41,40	55,91
NCLIV_000800	Hypothetical protein	2,50	6,04E-08	28,02	22,31	38,08	58,27	31,33	42,31

NCLIV_001225	Unspecified product	2,52	2,20E-07	23,39	18,62	31,78	48,98	26,34	35,57
NCLIV_020010	Putative F5/8 type C domain-containing protein	2,52	3,31E-07	23,26	18,52	31,61	48,83	26,26	35,46
NCLIV_049360	Conserved hypothetical protein	2,53	4,58E-05	15,20	12,10	20,66	32,07	17,24	23,29
NCLIV_019900	Hypothetical protein	2,53	8,89E-04	11,27	8,97	15,31	23,82	12,81	17,30
NCLIV_006430	Conserved hypothetical protein	2,55	1,64E-06	21,38	17,02	29,06	45,27	24,34	32,87
NCLIV_044060	Hypothetical protein	2,56	3,77E-35	335,16	266,80	455,49	710,20	381,89	515,76
NCLIV_000990	Conserved hypothetical protein	2,58	6,47E-03	6,32	5,03	8,58	13,69	7,36	9,94
NCLIV_037530	Conserved hypothetical protein	2,60	2,66E-03	7,27	5,79	9,88	15,89	8,54	11,54
NCLIV_036370	Conserved hypothetical protein	2,62	3,27E-02	4,50	3,58	6,12	9,98	5,36	7,25
NCLIV_002700	Conserved hypothetical protein	2,64	1,54E-02	4,75	3,78	6,46	10,58	5,69	7,69
NCLIV_013240	Conserved hypothetical protein	2,65	1,46E-08	25,87	20,59	35,16	56,96	30,63	41,37
NCLIV_025910	Histone H2A, related	2,67	4,07E-02	3,77	3,00	5,12	8,53	4,59	6,19
NCLIV_069090	Hypothetical protein	2,67	2,50E-21	106,76	84,99	145,09	236,15	126,98	171,50
NCLIV_059220	Conserved hypothetical protein	2,69	2,60E-17	57,64	45,89	78,34	128,61	69,15	93,39
NCLIV_065960	Dynein heavy chain 1, axonemal, related	2,73	3,29E-13	37,82	30,10	51,39	85,84	46,16	62,34
NCLIV_002790	Conserved hypothetical protein	2,74	2,24E-05	12,63	10,05	17,16	28,90	15,54	20,99
NCLIV_067100	Cysteine synthase, related	2,75	4,66E-09	24,02	19,12	32,64	54,88	29,51	39,85
NCLIV_022740	Putative enoyl-CoA hydratase/isomerase family protein	2,76	4,71E-04	8,22	6,55	11,18	19,01	10,22	13,81
NCLIV_016090	Conserved hypothetical protein	2,77	3,46E-03	6,30	5,02	8,57	14,65	7,88	10,64
NCLIV_006930	Hypothetical protein	2,77	4,34E-02	3,16	2,51	4,29	7,46	4,01	5,42
NCLIV_049930	Conserved hypothetical protein	2,78	7,30E-04	7,59	6,04	10,31	17,69	9,51	12,85
NCLIV_019610	Hypothetical protein	2,79	1,59E-24	87,36	69,54	118,72	202,20	108,73	146,84
NCLIV_000780	Carboxyvinyl-carboxyphosphonate phosphorylmutase protein, related	2,84	7,56E-13	34,68	27,61	47,13	81,92	44,05	59,49
XLOC_007376		2,85	5,55E-03	5,08	4,05	6,91	12,25	6,59	8,90
NCLIV_027990	Putative WD domain, G-beta repeat-containing protein	2,85	2,57E-03	5,70	4,54	7,75	13,72	7,38	9,96
NCLIV_014810	Putative Patched family domain containing protein	2,88	5,02E-03	5,10	4,06	6,93	12,42	6,68	9,02
NCLIV_047410	Hypothetical protein	2,89	4,28E-03	5,06	4,02	6,87	12,35	6,64	8,97
NCLIV_059080	Conserved hypothetical protein	2,92	3,76E-07	17,28	13,75	23,48	42,04	22,61	30,53
NCLIV_035550	GH22156, related	2,92	9,37E-03	4,11	3,27	5,59	10,19	5,48	7,40
NCLIV_060290	Conserved hypothetical protein	2,95	3,16E-04	7,28	5,79	9,89	18,05	9,70	13,11
NCLIV_069530	Hypothetical protein	3,02	6,81E-03	4,13	3,29	5,61	10,58	5,69	7,69
NCLIV_043290	Conserved hypothetical protein	3,04	3,83E-02	2,53	2,01	3,44	6,61	3,56	4,80
NCLIV_057880	Hypothetical protein	3,04	4,00E-02	2,55	2,03	3,46	6,67	3,59	4,85
XLOC_000109		3,08	1,87E-22	76,13	60,60	103,46	194,75	104,72	141,43
XLOC_000138		3,09	7,49E-11	21,20	16,88	28,82	54,54	29,33	39,61
NCLIV_004020	Tryptophan-rich antigen (Pv-fam-a), related	3,09	9,01E-03	3,81	3,03	5,18	10,01	5,39	7,27
NCLIV_068600	Conserved hypothetical protein	3,10	1,72E-06	11,41	9,09	15,51	29,54	15,89	21,46
NCLIV_008245	Hypothetical protein	3,12	6,00E-25	59,16	47,09	80,40	153,14	82,35	111,21
NCLIV_052260	Unspecified product	3,15	1,00E-02	3,47	2,76	4,72	9,32	5,01	6,77
NCLIV_011720	Hypothetical protein	3,16	9,84E-07	11,41	9,08	15,51	30,12	16,20	21,88
NCLIV_037300	Conserved hypothetical protein	3,21	2,50E-03	4,42	3,52	6,01	12,04	6,47	8,74
NCLIV_036180	Hypothetical protein	3,28	1,39E-02	2,84	2,26	3,86	7,99	4,29	5,80
NCLIV_001400	Unspecified product	3,28	6,58E-41	135,33	107,73	183,91	368,07	197,92	267,30
NCLIV_022830	Conserved hypothetical protein	3,28	2,35E-03	4,12	3,28	5,59	11,47	6,17	8,33
NCLIV_003880	Conserved hypothetical protein	3,39	4,10E-02	1,91	1,52	2,59	5,66	3,04	4,11
NCLIV_026330	Conserved hypothetical protein	3,44	3,98E-13	22,21	17,68	30,18	63,66	34,23	46,23
XLOC_000107		3,46	5,91E-31	59,71	47,53	81,14	171,60	92,27	124,62
NCLIV_063000	Coiled-coil protein, related	3,47	4,17E-20	38,11	30,34	51,79	109,76	59,02	79,71
NCLIV_014420	Conserved hypothetical protein	3,47	3,45E-05	6,35	5,05	8,62	18,56	9,98	13,48
NCLIV_017220	Hypothetical protein	3,48	3,98E-05	6,33	5,04	8,61	18,55	9,98	13,47
NCLIV_050200	GF18580, related	3,50	6,20E-12	17,71	14,10	24,07	51,61	27,75	37,48
NCLIV_052500	Hypothetical protein	3,52	7,46E-45	110,61	88,05	150,33	323,01	173,69	234,58
NCLIV_059880	Conserved hypothetical protein	3,54	8,22E-06	6,98	5,55	9,48	20,78	11,17	15,09
NCLIV_001350	Putative EGF-like domain-containing protein	3,55	2,04E-03	3,49	2,78	4,75	10,58	5,69	7,69
NCLIV_029430	Conserved hypothetical protein	3,58	3,24E-03	3,17	2,52	4,31	9,72	5,23	7,06
NCLIV_021800	Hypothetical protein	3,59	2,40E-16	23,47	18,68	31,89	70,06	37,67	50,88
NCLIV_037560	Conserved hypothetical protein	3,63	8,04E-03	2,55	2,03	3,46	7,99	4,30	5,80
NCLIV_054260	Hypothetical protein	3,63	6,11E-09	11,08	8,82	15,06	33,67	18,10	24,45
NCLIV_037980	Conserved hypothetical protein	3,63	7,48E-44	99,38	79,11	135,05	299,47	161,03	217,48
NCLIV_051320	Conserved hypothetical protein	3,65	1,27E-02	2,23	1,77	3,03	7,07	3,80	5,13
NCLIV_018840	Conserved hypothetical protein	3,69	2,58E-28	44,14	35,14	59,99	135,13	72,66	98,13
NCLIV_041840	Conserved hypothetical protein	3,69	1,64E-16	24,92	19,84	33,86	76,42	41,09	55,50
NCLIV_001410	Conserved hypothetical protein	3,70	2,79E-15	20,32	16,17	27,61	62,60	33,66	45,46

NCLIV_064130	Conserved hypothetical protein	3,70	3,27E-08	10,10	8,04	13,73	31,33	16,85	22,76
NCLIV_059130	Hypothetical protein	3,71	2,16E-46	100,30	79,84	136,31	308,88	166,09	224,31
NCLIV_035930	Hypothetical protein	3,73	1,89E-02	1,90	1,51	2,58	6,21	3,34	4,51
NCLIV_000920	Putative tRNA(guanine-N(7)-)-methyltransferase	3,78	4,82E-29	44,40	35,34	60,34	139,20	74,85	101,09
NCLIV_011760	Hypothetical protein	3,79	1,48E-40	84,60	67,35	114,97	265,88	142,97	193,08
NCLIV_017690	Conserved hypothetical protein	3,80	1,25E-37	60,03	47,79	81,58	189,50	101,90	137,61
NCLIV_004220	Unspecified product	3,81	4,37E-05	5,08	4,04	6,90	16,38	8,81	11,89
NCLIV_001470	Putative rhodanese-like domain containing protein	3,84	1,24E-21	32,10	25,55	43,63	102,45	55,09	74,40
NCLIV_002710	Conserved hypothetical protein	3,87	4,63E-02	1,27	1,01	1,72	4,43	2,38	3,22
NCLIV_041540	Putative adenylyl cyclase	3,88	3,97E-16	22,82	18,16	31,01	73,68	39,62	53,51
NCLIV_059230	Hypothetical protein	3,96	1,19E-02	1,90	1,52	2,59	6,60	3,55	4,79
NCLIV_000080	Conserved hypothetical protein	3,98	3,83E-12	13,96	11,11	18,97	46,35	24,93	33,66
NCLIV_038021	Unspecified product	3,98	3,57E-07	6,98	5,56	9,49	23,38	12,57	16,98
NCLIV_033570	Putative protein kinase (incomplete catalytic triad)	4,02	9,10E-04	3,17	2,53	4,31	10,95	5,89	7,95
NCLIV_064070	Conserved hypothetical protein	4,08	2,46E-39	52,24	41,59	71,00	176,89	95,11	128,46
NCLIV_037830	Putative RNA recognition motif-containing protein	4,10	2,24E-34	43,29	34,46	58,84	147,26	79,19	106,94
NCLIV_069520	Hypothetical protein	4,13	6,27E-12	12,90	10,27	17,53	44,50	23,93	32,32
NCLIV_010030	Bradyzoite surface protein BSR4	4,20	8,59E-05	4,41	3,51	5,99	15,71	8,45	11,41
NCLIV_028010	Putative cAMP-specific phosphodiesterase	4,25	2,37E-08	7,30	5,81	9,92	26,07	14,02	18,93
XLOC_000092		4,29	1,06E-33	50,61	40,29	68,78	180,27	96,93	130,91
NCLIV_062190	GK22245, related	4,35	1,20E-06	5,39	4,29	7,32	19,81	10,65	14,39
NCLIV_010930	Unspecified product	4,35	4,81E-47	57,76	45,98	78,50	208,47	112,10	151,39
NCLIV_018110	Hypothetical protein	4,37	3,27E-29	35,15	27,98	47,77	127,56	68,59	92,63
XLOC_007424		4,39	8,98E-03	1,59	1,26	2,16	6,19	3,33	4,49
NCLIV_048010	Putative regulator of chromosome condensation domain-containing protein	4,39	3,37E-08	6,99	5,57	9,50	25,84	13,90	18,77
NCLIV_004471	SRS domain-containing protein	4,40	1,35E-16	17,66	14,06	24,01	64,81	34,85	47,07
XLOC_007468		4,40	1,06E-02	1,58	1,26	2,15	6,19	3,33	4,50
NCLIV_027630	Conserved hypothetical protein	4,41	1,25E-15	15,51	12,35	21,08	57,06	30,68	41,44
NCLIV_010741	Hypothetical protein	4,49	1,98E-09	8,49	6,76	11,54	32,03	17,22	23,26
NCLIV_023530	Conserved hypothetical protein	4,60	1,27E-03	2,22	1,77	3,02	8,91	4,79	6,47
NCLIV_001340	Putative oxysterol-binding protein domain-containing protein	4,62	2,52E-06	4,70	3,74	6,39	18,43	9,91	13,38
NCLIV_021160	Conserved hypothetical protein	4,64	1,37E-02	1,27	1,01	1,72	5,31	2,85	3,86
NCLIV_062990	Hypothetical protein	4,69	1,02E-08	6,35	5,05	8,63	25,12	13,51	18,24
NCLIV_034170	Hypothetical protein	4,70	1,28E-36	34,13	27,17	46,39	133,17	71,61	96,71
NCLIV_038280	Conserved hypothetical protein	4,75	8,43E-97	379,42	302,03	515,63	1492,91	802,77	1084,17
NCLIV_041620	Conserved hypothetical protein	4,84	2,49E-08	5,73	4,56	7,79	23,44	12,60	17,02
NCLIV_068430	Hypothetical protein	4,94	4,83E-05	4,51	3,59	6,13	18,95	10,19	13,76
NCLIV_039840	Conserved hypothetical protein	5,02	2,65E-03	1,58	1,26	2,15	7,07	3,80	5,13
NCLIV_036640	Conserved hypothetical protein	5,39	1,12E-122	297,20	236,58	403,90	1327,53	713,84	964,07
NCLIV_043550	Glycerol-3-phosphate dehydrogenase, related	5,40	6,04E-09	5,36	4,27	7,29	24,51	13,18	17,80
NCLIV_056990	Proteophosphoglycan 5, related	5,46	1,23E-38	28,61	22,78	38,89	129,90	69,85	94,33
NCLIV_013590	Conserved hypothetical protein	5,51	1,08E-02	0,95	0,76	1,29	4,89	2,63	3,55
NCLIV_010160	Conserved hypothetical protein	5,64	2,97E-02	0,63	0,50	0,86	3,53	1,90	2,56
NCLIV_031720	Conserved hypothetical protein	5,64	2,97E-02	0,64	0,51	0,86	3,54	1,91	2,57
NCLIV_004630	Putative threonine synthase	5,77	8,51E-31	21,41	17,04	29,09	102,91	55,34	74,74
NCLIV_064160	Conserved hypothetical protein	5,83	6,62E-10	5,08	4,04	6,90	25,11	13,50	18,24
NCLIV_013250	GK19899, related	5,87	2,79E-124	238,18	189,60	323,69	1157,96	622,65	840,92
NCLIV_061910	Hypothetical protein	5,88	1,77E-30	18,70	14,88	25,41	91,68	49,30	66,58
NCLIV_041630	Conserved hypothetical protein	5,89	2,44E-45	29,29	23,31	39,80	143,40	77,11	104,14
NCLIV_010040	SRS domain-containing protein	5,96	5,49E-03	0,95	0,76	1,29	5,30	2,85	3,85
NCLIV_067480	Putative UDP-N-acetyl-D-galactosamine:polypeptide N-acetylgalactosaminyltransferase T5	6,04	7,10E-05	1,90	1,51	2,58	10,14	5,45	7,36
XLOC_007074		6,52	4,92E-04	1,27	1,01	1,72	7,52	4,04	5,46
NCLIV_056000	Hypothetical protein	6,83	2,22E-08	3,17	2,52	4,31	18,65	10,03	13,55
NCLIV_000380	Potential mitochondrial membrane protein,related	6,95	1,40E-03	0,95	0,76	1,29	6,20	3,34	4,51
NCLIV_026260	GA26239, related	7,08	7,50E-49	28,09	22,36	38,18	165,48	88,98	120,17
NCLIV_002460	Conserved hypothetical protein	7,17	3,89E-02	0,32	0,25	0,43	2,64	1,42	1,92
NCLIV_049630	SRS domain-containing protein	7,18	3,88E-02	0,32	0,25	0,43	2,64	1,42	1,92
NCLIV_007690	Putative oxidoreductase	7,20	3,83E-02	0,32	0,25	0,43	2,65	1,43	1,92

NCLIV_022940	Putative AT hook motif-containing protein	7,22	3,83E-02	0,32	0,25	0,43	2,66	1,43	1,93
NCLIV_017300	Putative 3', 5'-cyclic nucleotide phosphodiesterase	7,50	5,87E-45	19,77	15,74	26,87	123,61	66,47	89,77
NCLIV_027380	Putative 2OG-Fe(II) oxygenase family oxidoreductase	7,83	4,60E-83	42,49	33,83	57,75	276,27	148,56	200,63
NCLIV_034180	Conserved hypothetical protein	7,91	5,42E-07	1,90	1,51	2,58	13,28	7,14	9,64
NCLIV_066170	Hypothetical protein	8,02	4,27E-40	18,59	14,80	25,26	124,25	66,81	90,23
NCLIV_058060	SRS domain-containing protein	8,36	1,64E-03	0,63	0,51	0,86	5,30	2,85	3,85
NCLIV_021240	Zinc finger (C3HC4 type) / FHA domain-containing protein	8,38	5,08E-26	11,47	9,13	15,59	80,59	43,33	58,52
NCLIV_038440	Conserved hypothetical protein	8,48	7,49E-101	60,86	48,45	82,71	428,40	230,36	311,11
NCLIV_019730	Conserved hypothetical protein	8,54	4,57E-133	146,94	116,97	199,70	1040,52	559,50	755,64
NCLIV_067570	Unspecified product	9,29	4,28E-05	0,95	0,76	1,30	8,38	4,50	6,08
NCLIV_021430	Hypothetical protein	9,32	1,47E-07	1,58	1,26	2,15	13,25	7,13	9,62
NCLIV_046880	Conserved hypothetical protein	9,48	8,13E-03	0,32	0,25	0,43	3,54	1,90	2,57
NCLIV_016200	Conserved hypothetical protein	9,71	3,63E-04	0,63	0,50	0,86	6,18	3,32	4,48
NCLIV_062130	Conserved hypothetical protein	10,66	3,67E-03	0,32	0,25	0,43	3,99	2,14	2,89
NCLIV_002730	Conserved hypothetical protein	10,70	3,75E-03	0,32	0,25	0,43	4,00	2,15	2,91
NCLIV_069310	Unspecified product	10,98	1,91E-85	21,85	17,39	29,69	199,82	107,45	145,11
NCLIV_062170	Conserved hypothetical protein	11,41	2,45E-20	3,79	3,02	5,15	37,10	19,95	26,94
NCLIV_002740	Related to CG16984 PROTEIN, related	11,66	4,43E-06	0,95	0,76	1,29	10,51	5,65	7,63
XLOC_007282		11,81	1,64E-03	0,32	0,25	0,43	4,43	2,38	3,22
NCLIV_070090	Hypothetical protein, conserved	11,83	9,71E-39	8,26	6,58	11,23	82,31	44,26	59,78
NCLIV_0280	Axonemal inner arm I1 intermediate chain dynein IC138	11,93	7,95E-10	1,59	1,26	2,16	17,02	9,15	12,36
NCLIV_046230	Putative cGMP-inhibited 3',5'-cyclic phosphodiesterase	12,00	6,14E-92	23,42	18,64	31,82	234,11	125,89	170,01
NCLIV_061840	Hypothetical protein	12,78	2,16E-29	4,75	3,78	6,46	51,75	27,83	37,58
NCLIV_019580	SRS domain-containing protein	14,10	7,18E-41	6,03	4,80	8,20	72,06	38,75	52,33
NCLIV_040620	Conserved hypothetical protein	15,28	2,52E-02	0,00	0,00	0,00	1,76	0,95	1,28
NCLIV_019260	Hypothetical protein	15,30	2,52E-02	0,00	0,00	0,00	1,77	0,95	1,28
NCLIV_043430	SRS domain-containing protein	15,35	2,50E-02	0,00	0,00	0,00	1,77	0,95	1,29
NCLIV_060170	Hypothetical protein	15,36	2,50E-02	0,00	0,00	0,00	1,77	0,95	1,29
NCLIV_031800	Hypothetical protein	15,42	2,47E-02	0,00	0,00	0,00	1,78	0,96	1,29
XLOC_000143		17,10	8,27E-08	0,63	0,51	0,86	10,98	5,90	7,97
NCLIV_048760	Conserved hypothetical protein	17,22	2,03E-148	29,43	23,43	40,00	421,67	226,74	306,23
NCLIV_033540	Conserved hypothetical protein	17,99	4,29E-174	32,38	25,78	44,01	484,66	260,61	351,97
NCLIV_006950	Conserved hypothetical protein	23,98	6,55E-15	0,95	0,76	1,29	21,76	11,70	15,80
NCLIV_044990	Putative high-affinity cGMP-specific 3',5'-cyclic phosphodiesterase 9A	25,15	1,22E-93	7,61	6,06	10,34	161,45	86,81	117,25
NCLIV_047940	SRS domain-containing protein	25,92	1,75E-03	0,00	0,00	0,00	3,08	1,66	2,24
NCLIV_010680	Conserved hypothetical protein	34,54	1,37E-10	0,32	0,25	0,43	13,21	7,11	9,60
NCLIV_043730	Hypothetical protein	35,89	5,22E-155	9,51	7,57	12,93	286,98	154,31	208,41
NCLIV_023940	Conserved hypothetical protein	43,13	2,69E-277	23,06	18,36	31,34	828,89	445,71	601,95
XLOC_000176		60,79	4,20E-07	0,00	0,00	0,00	7,39	3,97	5,36
NCLIV_038490	Conserved hypothetical protein	62,51	2,70E-07	0,00	0,00	0,00	7,59	4,08	5,52
NCLIV_015120	Hypothetical protein	62,92	1,35E-152	5,70	4,53	7,74	304,39	163,68	221,05
NCLIV_038930	SRS domain-containing protein	211,83	1,04E-23	0,00	0,00	0,00	26,03	14,00	18,91

SUPPLEMENTARY TABLE 3 | Functional classification of *N. caninum* genes differentially expressed between the low virulent isolate Nc-Spain1H and the high virulent isolate Nc-Spain7 in bovine macrophages. Negative FC values correspond to genes up-regulated in Nc-Spain7 and positive values to genes up-regulated in Nc-Spain1H.

	Nc gene id	*Nc* gene description	FC	padj	*Tg* gene id	*Tg* gene description	Function	References
	Growth, cell cycle							
Nc-Spain7	NCLIV_061380	hypothetical protein	-2,08	1,67E-04	TGME49_219100	cyclin-dependent kinase regulatory subunit protein	Cell cycle regulation	Nigg, 1995
	NCLIV_012540	hypothetical protein	-2,91	1,24E-04	TGME49_220440	cyclin-dependent kinase regulatory subunit protein		
	NCLIV_029370	conserved hypothetical protein	-2,09	8,00E-03	TGME49_255430	Rad9 protein	Cell cycle checkpoint protein required for cell cycle arrest and DNA damage repair	Clarke and Giménez-Abián, 2000
	NCLIV_021700	conserved hypothetical protein	-2,55	3,66E-04	TGVEG_203260	Rad17 cell cycle checkpoint protein		
	NCLIV_044150	conserved hypothetical protein	-3,18	3,85E-04	TGVEG_206390	Hus1-like protein	DNA damage checkpoint	ToxoDB (GO:0000077)
	NCLIV_001000	conserved hypothetical protein	-2,09	6,30E-03	TGME49_294250	WD domain, G-beta repeat-containing protein	Implicated in a wide range of functions from signal transduction and transcription regulation to apoptosis and control of cell cycle	Stirnimann et al., 2010
	NCLIV_023430	putative WD domain, G-beta repeat-containing protein	-7,42	3,41E-06	TGME49_281480	WD domain, G-beta repeat-containing protein		
	NCLIV_0253	GTP-binding conserved hypothetical domain-containing protein	-2,48	7,90E-04	TGME49_262510	GTP-binding protein engB, putative	Cell division control	Leipe et al., 2002
	NCLIV_038630	conserved hypothetical protein	-2,12	4,79E-06	TGME49_267550	leucine-rich repeat protein LRR1	May play a role in the regulation of the *T. gondii* cell cycle through the modulation of phosphatase activity	Daher et al., 2007
Nc-Spain1H	NCLIV_027990	putative WD domain, G-beta repeat-containing protein	2,85	2,57E-03	TGME49_258530	flagellar associated protein	Implicated in a wide range of functions from signal transduction and transcription regulation to apoptosis and control of cell cycle	Stirnimann et al., 2010
	NCLIV_062990	hypothetical protein	4,08	2,46E-39	TGME49_245752	WD domain, G-beta repeat-containing protein		
	NCLIV_063000	Coiled-coil protein, related	3,70	3,27E-08	TGME49_245752	WD domain, G-beta repeat-containing protein		
	NCLIV_006430	conserved hypothetical protein	2,55	1,64E-06	TGVEG_297390	putative WD domain, G-beta repeat protein		
	NCLIV_034180	conserved hypothetical protein	7,91	5,42E-07	TGVEG_273472	tumor suppressor mitostatin	Role in guarding the fidelity of mitosis, enabling the optimal activation of the spindle checkpoint	Lauriola, 2017
	NCLIV_049930	conserved hypothetical protein	2,50	1,96E-04	TGME49_235515	MORN repeat-containing protein	Apicoplast segregation and daughter cell budding	Lorestani et al., 2010
	NCLIV_061840	hypothetical protein	12,78	2,16E-29	TGME49_218400	NEK kinase	Kinase family first identified as essential for division in Aspergilus nidulans. Its members have been identified as cell cycle regulators in eukaryotes	Gubbels et al., 2008
	NCLIV_040930	putative NEK kinase	2,01	3,92E-15	TGME49_288440	NEK kinase		

Nucleic acid biosynthesis, replication, recombination, repair								
Nc-Spain7	NCLIV_038170	Hypoxanthine phosphoribosyltransferase, related	-4,39	1,91E-11	TGME49_200320	hypoxanthine-xanthine-guanine phosphoribosyl transferase HXGPRT	Purine metabolism (salvage)	Shanmugasundram et al., 2013
	NCLIV_032950	putative deoxyuridine 5'-triphosphate nucleotidohydrolase	-4,04	3,35E-41	TGME49_233140	deoxyuridine 5'-triphosphate nucleotidohydrolase, putative	Pyrimidine metabolism (biosynthesis and salvage)	Shanmugasundram et al., 2013
	NCLIV_065390	Bifunctional dihydrofolate reductase-thymidylate synthase, related	-2,72	4,67E-17	TGME49_249180	bifunctional dihydrofolate reductase-thymidylate synthase	Folate biosynthesis, Pyrimidine metabolism (biosynthesis and salvage)	Shanmugasundram et al., 2013
	NCLIV_016250	putative cytidine deaminase	-2,49	4,79E-06	TGME49_239630	cytidine and deoxycytidylate deaminase zinc-binding region domain-containing protein	Pyrimidine metabolism (biosynthesis and salvage)	Shanmugasundram et al., 2013
	NCLIV_010140	putative proliferating cell nuclear antigen	-3,05	1,90E-09	TGME49_320110	proliferating cell nuclear antigen PCNA2	DNA replication, chromatin remodelling, DNA repair, sister-chromatid cohesion and cell cycle control	Strzalka and Ziemienowicz, 2010
	NCLIV_065280	Proliferating cell nuclear antigen, related	-3,14	1,04E-23	TGME49_247460	proliferating cell nuclear antigen PCNA1		
	NCLIV_033420	hypothetical protein	-2,70	1,27E-04	TGME49_233820	DNA polymerase epsilon subunit B protein	DNA replication	ToxoDB (GO:0006260)
	NCLIV_010380	DNA polymerase, related	-2,06	1,05E-07	TGME49_319860	DNA polymerase family B protein		
	NCLIV_062650	putative DNA polymerase alpha catalytic subunit	-2,01	2,47E-06	TGME49_217910	DNA polymerase (pol2) superfamily protein		
	NCLIV_013120	putative activator 1 36 kDa	-2,04	6,85E-04	TGME49_213000	replication factor C, subunit 5, putative		
	NCLIV_049750	putative replication factor c subunit	-2,63	6,15E-07	TGME49_235170	ATPase, AAA family protein	DNA replication and repair	ToxoDB (GO:0006260; GO:0006281)
	NCLIV_023470	Ribonuclease, related	-2,71	2,27E-05	TGME49_281510	ribonuclease H1 large subunit, putative	DNA replication and repair	Cerritelli and Crouch, 2009
	NCLIV_025810	conserved hypothetical protein	-2,63	1,08E-04	TGME49_261670	ribonuclease H1/H2 small subunit protein	DNA replication and repair	Cerritelli and Crouch, 2009
	NCLIV_062840	putative origin recognition complex subunit 2	-2,32	1,83E-03	TGME49_245570	origin recognition complex subunit 2 protein	DNA replication	Chesnokov, 2007
	NCLIV_060910	putative DNA replication licensing factor	-2,74	2,70E-13	TGME49_219700	DNA replication licensing factor MCM4, putative	DNA replication	Das et al., 2014
	NCLIV_059560	putative DNA replication licensing factor	-2,02	3,18E-09	TGME49_216730	MCM2/3/5 family protein		
	NCLIV_068360	putative toprim domain-containing protein	-2,40	1,38E-05	TGME49_277530	DNA topoisomerase domain-containing protein	DNA replication and transcription	Wang, 2002
	NCLIV_050400	hypothetical protein	-2,29	1,60E-07	TGME49_236080	replication factor-a protein 1 (rpa1) subfamily protein	DNA replication, repair, and recombination	Broderick et al., 2009
	NCLIV_032890	T10O22.7, related	-2,49	2,60E-04	TGME49_233090	XPG N-terminal domain-containing protein	DNA repair	Fenoy et al., 2016
	NCLIV_052470	hypothetical protein	-2,56	2,97E-04	TGVEG_215550	defects in morphology 1 precursor	Single-stranded DNA 5'-3' exodeoxyribonuclease activity	ToxoDB (GO:0045145)
Nc-Spain1H	NCLIV_0269	GDA1/CD39 (nucleoside phosphatase) family domain containing protein	2,34	1,70E-05	TGME49_259960	Nucleoside-diphosphatase	Purine metabolism (salvage)	Shanmugasundram et al., 2013
	NCLIV_041540	putative adenylyl cyclase	3,88	3,97E-16	TGME49_289170	adenylate and guanylate cyclase catalytic domain-containing protein	Purine metabolism (salvage)	Shanmugasundram et al., 2013

RNA metabolism								
Nc-Spain7	NCLIV_017360	hypothetical protein	-2,22	4,04E-03	TGME49_242055	DEAD/DEAH box helicase domain-containing protein	Associated with most aspects of RNA processing, from transcriptional regulation to mRNA decay	Cherry and Ananvoranich, 2014
	NCLIV_053630	putative zinc finger (CCCH type) protein	-2,97	9,14E-17	TGME49_309200	zinc finger (CCCH type) motif-containing protein	CCCH type zinc finger proteins are RNA binding proteins with regulatory functions in mRNA metabolism	Kramer et al., 2010
	NCLIV_020280	YDL036Cp-like protein, related	-4,25	6,55E-03	TGME49_205410	RNA pseudouridine synthase superfamily protein	Catalyzes the conversion of the RNA base uridine to pseudouridine. Mutation of single pseudouridine synthases in Escherichia coli and Saccharomyces cerevisiae results in slow-growing phenotypes	Anderson et al., 2009
	NCLIV_048340	putative pseudouridylate synthase 1	-2,86	1,45E-06	TGME49_224210	hypothetical protein		
	NCLIV_018660	conserved hypothetical protein	-2,07	5,90E-03	TGVEG_244050	PPR repeat protein	PPR proteins are sequence-specific RNA-binding proteins involved in several aspects of RNA metabolism	InterPro (IPR002885)
	NCLIV_009830	conserved hypothetical protein	-2,51	1,68E-06	TGVEG_320440A	XRN 5'-3' exonuclease amine-terminal protein	5'-3'-exoribonucleases are enzymes that degrade RNA by removing terminal nucleotides from the 5' endprocesses	InterPro (IPR027073)
	NCLIV_011080	unspecified product	-2,03	1,14E-06	TGME49_318470	AP2 domain transcription factor AP2IV-4	Cell cycle-regulated factor with peak expression in the tachyzoite S/M phase that also suppresses bradyzoite gene expression	Huang et al., 2017
	NCLIV_012905	unspecified product	-2,49	4,55E-04	TGME49_292010	transcription initiation factor IIB	Transcription factor involved in the formation of the RNA polymerase II preinitiation complex	Deng and Roberts, 2006
	NCLIV_058040	conserved hypothetical protein	-2,12	9,12E-05	TGME49_315300	transcription factor IIB, putative		
	NCLIV_062490	unspecified product	-2,77	1,23E-09	TGME49_217700	AP2 domain transcription factor AP2XII-2	Transcription factor associated with tachyzoite stage	Radke et al., 2018
	NCLIV_008810	conserved hypothetical protein	-2,62	8,60E-05	TGME49_254520	mediator complex subunit MED11	The multisubunit Mediator (MED) complex bridges DNA-bound transcriptional regulators to the RNA polymerase II initiation machinery	Bourbon, 2008
	NCLIV_044550	conserved hypothetical protein	-2,42	5,52E-03	TGME49_306320	Myb family DNA-binding domain-containing protein	Transcriptional transactivators. Myb domain proteins control stage conversion and cell fate in a broad range of systems	Ehrenkaufer et al., 2009
	NCLIV_069870	hypothetical protein, conserved	-4,20	9,68E-05	TGME49_301000	methyltransferase	Methylation of protein lysine and arginine residues. Crucial roles in gene transcription	Copeland et al., 2009
	NCLIV_030730	putative acetyltransferase domain-containing protein	-3,49	1,05E-08	TGME49_230060	acetyltransferase, GNAT family protein	Histone-modifying proteins involved in regulating gene expression	Vanagas et al., 2013
	NCLIV_032430	conserved hypothetical protein	-2,27	9,48E-18	TGME49_232440	Brf1p family coiled coil protein	Component of the RNA polymerase III transcription factor TFIIIB	InterPro (IPR029529)
	NCLIV_045950	conserved hypothetical protein	-2,02	3,20E-03	TGVEG_227080	phosphorylated CTD-interacting factor 1 (PCIF1)	WW domain-containing protein that interacts with phosphorylated RNA polymerase II carboxy-terminal domain. PCIF1 may regulate negatively gene expression by RNA polymerase II	InterPro (IPR039881)

RNA metabolism (continuation)

Nc-Spain1H	NCLIV_000800	hypothetical protein	2,50	6,04E-08	TGME49_293830	methyltransferase domain-containing protein	Methylation of protein lysine and arginine residues. Crucial roles in gene transcription	Copeland et al., 2009
	NCLIV_010930	unspecified product	4,35	4,81E-47	TGME49_318610	AP2 domain transcription factor AP2IV-3	Stress-induced transcription factor. Activator of bradyzoite gene expression	Huang et al., 2017
	NCLIV_052260	unspecified product	2,37	1,54E-02	TGME49_215340	AP2 domain transcription factor AP2X-10	Transcription factor that is known to be upregulated during bradyzoite development	Melo et al., 2013
	NCLIV_037830	putative RNA recognition motif-containing protein	4,10	2,24E-34	TGME49_268380	RNA recognition motif-containing protein	One of the most common domains of RNA binding proteins (RBP). Proteins containing this domain are involved in the RNA cycle. RBPs are essential for the fast gene expression remodeling that occurs during cell differentiation or the stress response	Alves and Goldenberg, 2016
	NCLIV_059230	hypothetical protein	15,36	2,50E-02	TGME49_217182	RNA-dependent RNA polymerase RDP	RNA-directed 5'-3' RNA polymerase activity	ToxoDB (GO:0003968)
	NCLIV_059220	conserved hypothetical protein	3,54	8,22E-06	TGP89_217182B	RNA-dependent RNA polymerase RDP		
	NCLIV_069020	ATP-dependent RNA helicase, putative	2,67	2,50E-21	TGME49_223440	DEAD/DEAH box helicase domain-containing protein	Associated with most aspects of RNA processing, from transcriptional regulation to mRNA decay	Cherry and Ananvoranich, 2014
	NCLIV_046880	conserved hypothetical protein	9,48	8,13E-03	TGP89_225950	putative zinc finger, CCCH type domain protein	CCCH type zinc finger proteins are RNA binding proteins with regulatory functions in mRNA metabolism	Kramer et al., 2010

	Protein synthesis, modifications, folding and turnover							
Nc-Spain7	NCLIV_014740	unspecified product	-2,39	1,91E-02	TGME49_285530	ribosomal protein RPL35	Ribosomal protein	
	NCLIV_001900	putative histidyl-tRNAsynthetase	-2,92	4,69E-37	TGME49_295050	tRNA ligase class II core domain (G, H, P, S and T) domain-containing protein	Synthesis of histidyl-transfer RNA, essential for the incorporation of histidine into proteins	Freist et al., 1999
	NCLIV_028690	Multisite-specific tRNA m(5)C methyltransferase, related	-2,22	1,19E-02	TGME49_255250	tRNA (cytosine(34)-C(5))-methyltransferase, putative	The primary role of tRNA modifications is the regulation of protein synthesis	Hori, 2014
	NCLIV_010830	putative UDP-N-acetyl-D-galactosamine:polypeptide N-acetylgalactosaminyltransferase T3	-5,43	2,43E-12	TGME49_318730	glycosyl transferase	Mucin-type O-glycosylation	(Stwora-Wojczyk et al., 2004)
	NCLIV_006510	putative TCP-1/cpn60 family chaperonin	-2,32	1,50E-12	TGME49_297500	T-complex protein 1 eta subunit	Protein folding	ToxoDB (GO:0006457)
	NCLIV_029610	putative prefoldin subunit 3	-2,41	1,05E-04	TGME49_257490	prefoldin subunit	Protein folding	InterPro (IPR016655)
	NCLIV_060300	cDNA, FLJ96396, highly similar to Homo sapiens ERO1-like beta (S. cerevisiae) (ERO1LB), mRNA, related	-2,26	2,20E-11	TGME49_300380	endoplasmic reticulum oxidoreductin, putative	Protein folding	(Hague et al., 2012)
	NCLIV_048880	Proteasome subunit beta type-7, related	-2,00	1,97E-10	TGME49_223590	proteasome subunit	Proteasomes are large complexes with crucial roles in many cellular pathways by degrading proteins in the nucleus and cytosol to enforce quality control and regulate many basic cellular processes	(Muñoz et al., 2015)
	NCLIV_057270	hypothetical protein	-2,05	2,48E-04	TGME49_314090	proteasome beta subunit		
	NCLIV_061460	Family T1, proteasome beta subunit, threonine peptidase, related	-2,09	1,34E-10	TGME49_218920	proteasome subunit beta type, putative		
	NCLIV_002110	putative TPR domain-containing protein	-4,16	1,26E-04	TGME49_295730	tetratricopeptide repeat-containing protein	It mediates protein-protein interactions and the assembly of protein complexes. Proteins containing TPRs are involved in a wide range of biological processes, such as cell cycle regulation, transcriptional control, and protein transport and folding.	InterPro (IPR013026)
	NCLIV_025530	putative TPR domain-containing protein	-2,70	3,42E-20	TGME49_262100	tetratricopeptide repeat-containing protein		
	NCLIV_055940	putative TPR domain-containing protein	-2,68	3,63E-07	TGME49_312380	tetratricopeptide repeat-containing protein		
	NCLIV_040320	putative ubiquitin-activating enzyme	-2,04	1,25E-03	TGME49_264880	NEDD8-activating enzyme E1 catalytic subunit	Ubiquitin-like protein. NEDD8 appears to play an essential role in cell cycle control in actively proliferating cells.	Ponts et al., 2008
	NCLIV_052060	Cullin-associated NEDD8-dissociated protein 1,related	-2,77	6,75E-05	TGME49_215040	HEAT repeat-containing protein		
	NCLIV_011590	hypothetical protein	-2,74	4,43E-05	TGVEG_211390	putative SUMO activating enzyme	Ubiquitin-like protein. Reversible modification by SUMO is generally associated with nuclear transport, subnuclear targeting and genome stability.	Ponts et al., 2008
	NCLIV_008220	putative M16 family peptidase	-2,84	6,34E-06	TGME49_253890	peptidase M16 inactive domain-containing protein	Metallopeptidase (Mitochondrial processing peptidase)	Escotte Binet et al., 2018
	NCLIV_024260	conserved hypothetical protein	-5,62	2,84E-04	TGVEG_263690	DIE2/alg10 family protein	dolichol-linked oligosaccharide biosynthetic process	ToxoDB (GO:0006488)
	NCLIV_051570	conserved hypothetical protein	-3,09	2,08E-03	TGME49_214330	DnaJ domain-containing protein	DnaJ/Hsp40 (heat shock protein 40) proteins are important for protein translation, folding, unfolding, translocation, and degradation, mainly by stimulating the ATPase activity of Hsp70s chaperones	Qiu et al., 2006
	NCLIV_005800	unspecified product	-2,07	3,34E-03	TGVEG_222410	lipase maturation factor	Lipase maturation in the ER.	InterPro (IPR009613)

Protein synthesis, modifications, folding and turnover (continuation)

Nc-Spain1H	NCLIV_000920	putative tRNA(guanine-N(7)-)-methyltransferase	3,78	4,82E-29	TGME49_294180	tRNA -methyltransferase family protein	The primary role of tRNA modifications is the regulation of protein synthesis	Hori, 2014
	NCLIV_011760	hypothetical protein	3,79	1,48E-40	TGME49_211230	eukaryotic initiation factor-2B, alpha subunit, putative	Regulation of translation iniciation. Mediates Responses to ER and cytosolic stresses in *T. gondii*	Narasimhan et al., 2008
	NCLIV_054260	hypothetical protein	2,07	8,89E-36	TGME49_310160	argonaute AGO	RNA induced gene silencing	Riyahi et al., 2006
	NCLIV_067480	putative UDP-N-acetyl-D-galactosamine:polypeptide N-acetylgalactosaminyltransferase T5	4,94	4,83E-05	TGME49_259530[1]	GalNac	Mucin-type O-glycosylation	(Stwora-Wojczyk et al., 2004)
	NCLIV_036180	hypothetical protein	3,28	1,39E-02	TGME49_270580	HECT-domain (ubiquitin-transferase) domain-containing protein	Ubiquitin-protein transferase activity	InterPro (IPR000569)
					TGME49_270595	UBA/TS-N domain-containing protein		
	NCLIV_068600	conserved hypothetical protein	2,00	4,19E-15	TGME49_276960	tetratricopeptide repeat-containing protein	It mediates protein-protein interactions and the assembly of protein complexes. Proteins containing TPRs are involved in a wide range of biological processes, such as cell cycle regulation, transcriptional control, and protein transport and folding.	InterPro (IPR013026)

Histone modification, chromatin structure and microtubule dynamics								
Nc-Spain7	NCLIV_010790	putative Aurora kinase(incomplete catalytic triad)	-2,62	1,92E-06	TGME49_318770	aurora kinase(incomplete catalytic triad)	Serine/threonine protein kinases that regulate key events associated with chromatin condensation, centrosome and spindle function and cytokinesis	Berry et al., 2016
	NCLIV_000330	conserved hypothetical protein	-3,44	5,98E-06	TGME49_293380	histone lysine acetyltransferase HAT1	Histone acetylation	Parthun, 2007
	NCLIV_006700	structural maintenance of chromosome 2, related	-2,35	1,20E-03	-		Responsible for the large-scale organizational dynamics of chromatin, including chromosome condensation	Lyer et al., 2008
	NCLIV_031540	putative chromosome condensation protein	-2,18	6,28E-09	TGME49_231170	RecF/RecN/SMC N terminal domain-containing protein		
	NCLIV_053750	Smc ABC ATpase, related	-2,01	2,35E-04	TGME49_309400	RecF/RecN/SMC N terminal domain-containing protein		
	NCLIV_003550	hypothetical protein	-2,83	3,25E-05	TGME49_209140	anti-silencing protein, ASF1 family protein	Highly conserved chaperone of histones H3/H4 that assembles or disassembles chromatin during replication, transcription and repair	English et al., 2006
	NCLIV_045430	putative DNA-binding protein HU	-3,27	4,54E-20	TGME49_227970	histone family DNA-binding protein	Histone-like protein with fundamental roles in transcription, replication initiation, and DNA repair. In *T. gondii* this protein localizes to the apicoplast	Reiff et al., 2012
	NCLIV_063770	hypothetical protein	-2,32	6,11E-09	TGME49_247250	RbAp46	Histone chaperone that play key roles in establishing and maintaining chromatin structure.	Murzina et al., 2008
	NCLIV_025100	hypothetical protein	-2,61	3,41E-02	TGME49_262760	poly(ADP-ribose) glycohydrolase	Histone ADP-ribosylation	Dixon et al., 2010
	NCLIV_056840	putative regulator of chromosome condensation domain-containing protein	-2,37	9,43E-04	TGME49_313570	regulator of chromosome condensation (RCC1) repeat-containing protein	Essential nuclear protein that functions as a guanine exchange factor (GEF) for the GTPase Ran to control several cellular processes including nuclear transport	Frankel and Knoll, 2008
	NCLIV_026390	putative centrin	-2,21	5,75E-04	TGME49_260670	centrin, putative	Key roles in cell division, including centrosome duplication	Morrissette, 2015
	NCLIV_025060	conserved hypothetical protein	-2,12	1,20E-02	TGME49_262825	peptidase family c50 protein	Chromatid separation during mitosis	Mottram et al., 2003

Histone modification, chromatin structure and microtubule dynamics (continuation)

Nc-Spain1H	NCLIV_022940	putative AT hook motif-containing protein	7,22	3,83E-02	TGME49_201820	hypothetical protein	Chromatin remodeling factor by modulating H3 acetylation and methylation	Matsubayashi et al., 2016
	NCLIV_025910	Histone H2A, related	2,67	4,07E-02	TGME49_261250	histone H2A1	Histone protein involved in the structure of chromatin. Probably associated with oxidant DNA damage stress. Higher expression during bradyzoite development reported in *T. gondii*	Dalmasso et al., 2009
					TGME49_261580	histone H2AX		
	NCLIV_001070	histone H2B, related	2,01	2,07E-07	TGME49_305160	histone H2Ba		
	NCLIV_048010	putative regulator of chromosome condensation domain-containing protein	4,39	3,37E-08	TGME49_266040	regulator of chromosome condensation (RCC1) repeat-containing protein	Essential nuclear protein that functions as a guanine exchange factor (GEF) for the GTPase Ran to control several cellular processes including nuclear transport	Frankel and Knoll, 2008
	NCLIV_022830	conserved hypothetical protein	3,28	2,35E-03	TGVEG_202030	poly(ADP-ribose) polymerase catalytic domain protein	Family of enzymes which catalyze the poly(ADP-ribosyl)ation of a limited number of proteins involved in chromatin structure, DNA metabolism and DNA repair	InterPro (IPR012317)
	NCLIV_021800	hypothetical protein	3,59	2,40E-16	TGME49_203135	dynein heavy chain family protein	Microtubule-associated proteins. Function as motors either to power axoneme beating or in organelle transport, spindle function, and centrosome assembly in the cytoplasm	Morrisette, 2015
	NCLIV_026260	GA26239, related	7,08	7,50E-49	TGME49_261022	dynein heavy chain family protein		
	NCLIV_034170	hypothetical protein	4,70	1,28E-36	TGME49_243482	dynein heavy chain, putative		
					TGME49_273478	dynein heavy chain, n-terminal region 2 protein		
	NCLIV_050200	GF18580, related	3,65	1,27E-02	TGME49_235920	dynein, axonemal, heavy chain 2 family protein		
	NCLIV_0280	axonemal inner arm I1 intermediate chain dynein IC138	11,93	7,95E-10	TGME49_258520	WD domain, G-beta repeat-containing protein		
	NCLIV_065960	Dynein heavy chain 1, axonemal, related	8,02	4,27E-40	TGME49_249840	dynein heavy chain 2, putative		

	Cell signaling							
Nc-Spain7	NCLIV_007290	putative protein kinase	-2,23	1,55E-09	TGME49_275610	protein kinase, other	Responsible for protein phosphorylation. Protein kinases (PKs) play crucial roles in the proliferation, differentiation, and pathogenesis of *T. gondii*	Wei et al., 2013
	NCLIV_012270	putative calmodulin	-2,34	1,15E-03	TGME49_220140	EF hand domain-containing protein	Calcium-binding messenger protein. Calcium plays a critical role in several parasite-specific functions including host cell invasion and egress	Krishna et al., 2015
	NCLIV_0153	longevity-assurance (LAG1) domain-containing protein	-2,89	1,38E-05	TGME49_283702	FATC domain-containing protein	Lag1p and its homologues likely play a role in ceramide signaling, which affects proliferation, resistance to stress and apoptosis	Jazwinski and Conzelmann, 2002
	NCLIV_058920	hypothetical protein	-2,86	1,15E-04	TGME49_316450	longevity-assurance protein (LAG1) domain-containing protein		
	NCLIV_018180	putative Ras family domain-containing protein	-2,43	6,64E-05	TGME49_243450	Ras-related protein Rab2BV, putative	Small GTPase mediated signal transduction	ToxoDB (GO:0007264)
	NCLIV_055220	putative CAMP-dependent protein kinase regulatory subunit	-3,26	4,94E-02	TGME49_311300	cyclic nucleotide-binding domain-containing protein	Protein phosphorylation. Involved in tachyzoite replication	Wei et al., 2013
	NCLIV_056970	conserved hypothetical protein	-2,70	2,98E-06	TGME49_313690	Sel1 repeat-containing protein	Involved in the degradation of proteins from the endoplasmatic reticulum. Putative role in signal transduction	Mittl and Schneider-Brachert, 2007
	NCLIV_046425	unspecified product	-2,05	5,55E-05	TGME49_226550	TBC domain containing protein	Regulation of GTP-ase activity	ToxoDB (GO:0043087)
Nc-Spain1H	NCLIV_046430	putative protein kinase	2,48	9,20E-27	TGME49_226540	protein kinase	Crucial roles in the proliferation, differentiation, and pathogenesis of *T. gondii*	Wei et al., 2013
	NCLIV_033570	putative protein kinase (incomplete catalytic triad)	4,02	9,10E-04	TGME49_274170	protein kinase (incomplete catalytic triad)		
	NCLIV_004220	unspecified product	3,81	4,37E-05	TGME49_209985	cAMP-dependent protein kinase	*T. gondii* cAMP-dependent protein kinase (PKA) is involved in cell cycle regulation or functions involved in growth, stress response and tachyzoite to bradyzoite conversion	Wei et al., 2013
	NCLIV_046230	putative cGMP-inhibited 3',5'-cyclic phosphodiesterase	12,00	6,14E-92	TGP89_226755B	3'5'-cyclic nucleotide phosphodiesterase domain-containing protein	The cyclic nucleotide phosphodiesterases (PDE) degrade the phosphodiester bond in cAMP and cGMP molecules. Important for signal transduction, likely play an essential role in the regulation of invasion and egress	InterPro (IPR002073); Howard et al., 2015
	NCLIV_012520		2,27	8,14E-08	TGME49_220420			
	NCLIV_017300		7,50	5,87E-45	TGME49_241880			
	NCLIV_028010		4,25	2,37E-08	TGME49_258508			
	NCLIV_030330		2,08	1,52E-02	TGME49_229405			
	NCLIV_044990	putative high-affinity cGMP-specific 3',5'-cyclic phosphodiesterase 9A	25,15	1,22E-93	TGME49_228500	3'5'-cyclic nucleotide phosphodiesterase domain-containing protein		
	NCLIV_020800	cyclic nucleotide-binding domain containing protein	2,05	7,82E-05	TGME49_204440	cyclic nucleotide-binding domain-containing protein	Bind cyclic nucleotides (cAMP or cGMP). cAMP- and cGMP-dependent protein kinases (cAPK and cGPK) contain two tandem copies of the cyclic nucleotide-binding domain	InterPro (IPR000595)
	NCLIV_002740	related to CG16984 protein, related	11,66	4,43E-06	TGME49_207790	enkurin, putative	Mitochondrial calcium-signaling protein	Gray and Gubbels, 2015

	Intracellular/transmembrane trafficking							
Nc-Spain7	NCLIV_055730	hypothetical protein	-3,20	4,96E-13	TGME49_312110	apicoplast-associated thioredoxin family protein Atrx1	Involved in the control of protein trafficking to the apicoplast	Biddau et al., 2018
	NCLIV_014390	hypothetical protein	-2,03	4,29E-05	TGVEG_286050	Tic22-like family protein	Chaperone Required for Protein Import into the Apicoplast	Glaser et al., 2012
	NCLIV_059570	conserved hypothetical protein	-2,14	3,50E-02	TGME49_216710	transporter, major facilitator family protein	Transmembrane transport. MFS proteins selectively transport diverse substrates across membranes	ToxoDB (GO_0055085); Yan, 2013
	NCLIV_006330	hypothetical protein	-2,27	8,62E-04	TGME49_297245	transporter, major facilitator family protein		
	NCLIV_003190	putative mitochondrial carrier domain-containing protein	-2,10	2,45E-08	TGME49_208560	carrier superfamily protein	Transport of a variety of metabolites, nucleotides and coenzymes across the inner membrane of mitochondria	Palmieri and Pierri., 2010
	NCLIV_064730	hypothetical protein	-2,44	9,10E-03	TGRUB_248550C	SPX domain-containing protein	Domain found in the amino terminus of proteins involved in the regulation of phosphate transport. Many proteins containing SPX domains seem to to be involved in G-protein associated signal transduction	InterPro (IPR004331)
	NCLIV_065150	putative sybindin-like family domain-containing protein	-2,09	5,42E-08	TGME49_247648	Sybindin family protein	vesicle-mediated transport (TRAPP complex)	ToxoDB (GO:0016192; GO:0030008)
	NCLIV_045700	putative transmembrane amino acid transporter domain-containing protein	-3,07	7,25E-04	TGME49_227430; TGME49_227570; TGME49_227580	transmembrane amino acid transporter protein	amino acid transmembrane transport	Rajendran et al., 2017
	NCLIV_005950	putative trafficking protein particle complex protein	-2,28	3,11E-04	TGME49_222920	mbp-1 interacting protein-2a family protein	Endoplasmic reticulum to Golgi vesicle-mediated transport	ToxoDB (GO:0006888)
	NCLIV_057620	conserved hypothetical protein	-2,16	3,85E-04	TGME49_314720	Sedlin, N-terminal region protein, putative	Endoplasmic reticulum to Golgi vesicle-mediated transport	ToxoDB (GO:0006888)
	NCLIV_038450	conserved hypothetical protein	-2,55	3,54E-05	TGVEG_279340	VMA21-like domain protein	Vacuolar proton-transporting V-type ATPase complex assembly	ToxoDB (GO:0070072)
	NCLIV_012560	putative SNF7 family domain-containing protein	-3,05	1,34E-02	TGME49_220460	SNF7 family protein	Vacuolar transport	ToxoDB (GO:0007034)
	NCLIV_019790	Cation-transporting ATPase, related	-21,41	6,50E-28	TGME49_304450	cation-transporting ATPase	Membrane-bound enzyme complexes/ion transporters that use hydrolysis of ATP for the transport of protons across membranes	InterPro (IPR004014)
	NCLIV_028530	putative phospholipid-transporting P-type ATPase	-6,14	5,79E-24	TGME49_257720	proton ATPase, putative	Catalyzes the translocation of phospholipids across membranes	InterPro (IPR026871)
	NCLIV_041450	cDNA FLJ39191 fis, clone OCBBF2004669, highly similar to Homo sapiens ATPase type 13A4 (ATP13A4), mRNA,related	-2,88	7,86E-09	TGME49_289070	E1-E2 ATPase subfamily protein	Catalizes the transport across membranes of different compounds, including ions and phospholipids	InterPro (IPR001757)
	NCLIV_046530	putative reticulon domain-containing protein	-2,44	3,29E-14	TGME49_226430	reticulon protein	Reticulons mainly localize to the endoplasmic reticulum. They influence endoplasmic reticulum-Golgi trafficking, vesicle formation and membrane morphogenesis	Yang and Strittmatter, 2007

Intracellular/transmembrane trafficking (continuation)								
Nc-Spain1H	NCLIV_002790	conserved hypothetical protein	2,74	2,24E-05	TGME49_207865	GCC2 and GCC3 domain-containing protein	Regulates vesicular transport between the endosomes and the Golgi	InterPro (IPR032023)
	NCLIV_008245	hypothetical protein	3,12	6,00E-25	TGME49_253930	GCC2 and GCC3 domain-containing protein		
	NCLIV_019610	hypothetical protein	2,79	1,59E-24	TGME49_280540	HEAT repeat-containing protein	Arrays of HEAT repeats consists of 3 to 36 units forming a rod-like helical structure which appear to function as protein-protein interaction surfaces. Many HEAT repeat-containing proteins are involved in intracellular transport	InterPro (IPR000357)
	NCLIV_019730	conserved hypothetical protein	8,54	4,57E-133	TGME49_280420	HEAT repeat-containing protein		
	NCLIV_038021	unspecified product	3,98	3,57E-07	TGME49_268020	transporter, major facilitator family protein	Transmembrane transport. MFS proteins selectively transport diverse substrates across membranes	Yan et al., 2013
	NCLIV_044060	hypothetical protein	2,56	3,77E-35	TGME49_305590	ABC transporter transmembrane region domain-containing protein	Transmembrane transport	Sauvage et al., 2006
	NCLIV_065220	putative ABC transporter	2,34	2,30E-02	TGME49_247540	ATP-binding cassette G family transporter ABCG107	It has been suggested a role for *T. gondii* ABCG107 in lipid movement inside the parasitophorous vacuole	Ehreman et al., 2010

	Energy and metabolism							
	Carbohydrate and energy metabolism							
Nc-Spain7	NCLIV_005420	phosphoglycerate kinase, related	-7,95	7,01E-13	TGME49_222020	phosphoglycerate kinase PGKII	Glycolysis	Shanmugasundram et al., 2013
	NCLIV_037190	putative glyceraldehyde-3-phosphate dehydrogenase	-2,25	1,68E-17	TGME49_269190	glyceraldehyde-3-phosphate dehydrogenase GAPDH2		
	NCLIV_033270	hypothetical protein	-2,44	2,02E-07	TGME49_233500	triose-phosphate isomerase TPI-II		
	NCLIV_009420	putative pyruvate kinase	-2,43	1,18E-02	TGME49_299070	pyruvate kinase PyKII	Pyruvate metabolism	Shanmugasundram et al., 2013
	NCLIV_062940	putative pyruvate dehydrogenase	-3,53	6,61E-14	TGME49_245670	pyruvate dehydrogenase complex subunit PDH-E1Alpha	Pyruvate metabolism, thiamine salvage	Shanmugasundram et al., 2013
	NCLIV_014580[3]	Hypothetical protein, related	-49,71	6,17E-05	TGME49_208420[1]	Sodium:neurotransmitter symporter family protein	Glutamine Utilization and GABA Shunt	Shanmugasundram et al., 2013
	NCLIV_046950	UDP-glucose 4-epimerase, related	-2,46	1,80E-07	TGME49_225880	UDP-glucose 4-epimerase	Starch and galactose metabolism	Shanmugasundram et al., 2013
	NCLIV_030570	hypothetical protein	-5,31	3,84E-08	TGME49_229780	GHMP kinase, N-terminal domain-containing protein		
	NCLIV_054680	conserved hypothetical protein	-2,21	4,19E-04	TGME49_310620	starch binding domain-containing protein	Starch metabolism	Uboldi et al., 2015
	NCLIV_010760	hypothetical protein	-3,57	6,58E-15	TGVEG_319308	putative adenylate kinase	Energy homeostasis	InterPro (IPR033690)
Nc-Spain1H	NCLIV_000780	Carboxyvinyl-carboxyphosphonate phosphorylmutase protein, related	2,84	7,56E-13	TGME49_293810	carboxyvinyl-carboxyphosphonate phosphorylmutase	2-Methylcitrate cycle	Shanmugasundram et al., 2013
	NCLIV_052500	hypothetical protein	2,42	2,54E-06	TGME49_215590	flavoprotein subunit of succinate dehydrogenase	Tricarboxylic acid (TCA) cycle, electron transport chain	Shanmugasundram et al., 2013
	NCLIV_035930	hypothetical protein	3,73	1,89E-02	TGME49_270850	glycosyl hydrolase family 17		
	NCLIV_002700	conserved hypothetical protein	2,64	1,54E-02	TGVEG_207750	glycosyltransferase family 17 protein	Glycosyltransferases catalyse the transfer of a sugar moiety from an activated sugar donor onto saccharide or non-saccharide acceptors	Coutinho et al., 2003
	Aminoacids metabolism							
Nc-Spain7	NCLIV_0245	NAD binding domain of 6-phosphogluconate dehydrogenase	-4,04	4,79E-06	TGME49_263430	3-hydroxyisobutyrate dehydrogenase	Leucine, isoleucine and valine metabolism	Shanmugasundram et al., 2013
	NCLIV_012460	Lysyl-tRNA synthetase, related	-3,48	1,19E-11	TGME49_220340	hypothetical protein	Lysine biosynthesis	Shanmugasundram et al., 2013
					TGME49_220350	tRNA ligases class II (D, K and N) domain-containing protein	Lysine degradation	Shanmugasundram et al., 2013
	NCLIV_018380	putative dihydrodipicolinate reductase	-2,46	4,91E-05	TGME49_243680	dihydrodipicolinate reductase	Lysine biosynthesis	Shanmugasundram et al., 2013
	NCLIV_069650[3]	Phenylalanine-4-hydroxylase, related	-4,71	3,95E-02	-		Phenylalanine and tyrosine metabolism	Shanmugasundram et al., 2013
	NCLIV_053050	putative indole-3-glycerol phosphate synthase domain containing protein	-2,83	3,89E-09	TGME49_207180	indole-3-glycerol phosphate synthase domain-containing protein	Tryptophan metabolism	InterPro (IPR013798)
Nc-Spain1H	NCLIV_004630	putative threonine synthase	5,77	8,51E-31	TGME49_220840	threonine synthase	Threonine metabolism	Shanmugasundram et al., 2013
	NCLIV_067100	Cysteine synthase, related	2,28	7,97E-03	TGME49_278910	O-acetylserine (thiol) lyase 2, putative	Glycine, serine and cysteine metabolism	Shanmugasundram et al., 2013

	Lipids and Glycan metabolism							
Nc-Spain7	NCLIV_000530	3-oxoacyl-(Acyl-carrier-protein) synthase II,related	-3,21	1,27E-17	TGME49_293590	3-oxoacyl-acyl-carrier protein synthase I/II, putative	Fatty acid biosynthesis in the apicoplast (FAS II system)	Shanmugasundram et al., 2013
	NCLIV_066970	putative enoyl-acyl carrier reductase	-4,03	5,19E-25	TGME49_251930	enoyl-acyl carrier reductase ENR		
	NCLIV_0319	3-oxoacyl-(acyl-carrier-protein) synthase III family protein	-2,68	9,75E-07	TGME49_231890	beta-ketoacyl-acyl carrier protein synthase III, putative		
	NCLIV_004340	hypothetical protein	-4,42	5,10E-17	TGME49_321570	beta-hydroxyacyl-acyl carrier protein dehydratase (FABZ)		
	NCLIV_062520	3-ketoacyl-(Acyl-carrier-protein) reductase, related	-6,03	9,13E-27	TGME49_217740	3-ketoacyl-(acyl-carrier-protein) reductase		
	NCLIV_023990	Acyl carrier protein, related	-2,29	5,73E-13	TGME49_264080	acyl carrier protein ACP	Fatty acid biosynthesis in the apicoplast (FAS II system); Pantothenate and CoA biosynthesis	Shanmugasundram et al., 2013
	NCLIV_035870	putative glycerol-3-phosphate acyltransferase	-2,67	1,18E-06	TGME49_270910	acyltransferase domain-containing protein	Fatty acid biosynthesis in the apicoplast (FAS II system); Recycling of phospholipids; Phosphatidylethanolamine and phosphatidylserine metabolism	Shanmugasundram et al., 2013
	NCLIV_035250	GK18150, related	-2,21	9,49E-06	TGME49_271888	3-ketoacyl-CoA reductase, putative	Fatty acid elongation via elongase pathway of ER	Shanmugasundram et al., 2013
	NCLIV_015250	hypothetical protein	-2,08	1,20E-03	TGME49_256830	SacI domain-containing protein	Inositol phosphate metabolism	Shanmugasundram et al., 2013
	NCLIV_045290	cDNA FLJ30053 fis, clone ADRGL1000144, highly similar to StAR-related lipid transfer protein 7, related	-2,51	2,37E-09	TGVEG_228130	START domain protein	START domain-containing proteins (START proteins) play important functions in eukaryotic cells, including the redistribution of phospholipids to subcellular compartments and delivering sterols to the mitochondrion for steroid synthesis	Hill et al., 2016
	NCLIV_057630	putative dolichyl pyrophosphate Glc1Man9GlcNAc2 alpha-1,3-glucosyltransferase	-2,41	1,25E-06	TGME49_314730	ALG6, ALG8 glycosyltransferase family protein	N-Glycan biosynthesis	Shanmugasundram et al., 2013
	NCLIV_004260	hypothetical protein	-3,93	6,19E-09	TGME49_321660	mannosyltransferase, putative	Glycosylphosphatidylinositol (GPI) anchor biosynthesis; N-Glycan biosynthesis	Shanmugasundram et al., 2013
	NCLIV_028260	hypothetical protein	-5,13	4,63E-07	TGME49_258110	N-acetylglucosaminyl phosphatidylinositol deacetylase	Glycosylphosphatidylinositol (GPI) anchor biosynthesis	Shanmugasundram et al., 2013
	NCLIV_054430	conserved hypothetical protein	-2,01	2,44E-04	TGME49_310350	PGAP1 family protein	GPI anchor metabolic process	ToxoDB (GO:0006505)
	NCLIV_033980	conserved hypothetical protein	-2,01	6,90E-04	TGME49_273730	phospholipase, patatin family protein	Lipid metabolism and immune regulation during host infection	Wilson et al., 2017
	NCLIV_016930	hypothetical protein	-3,11	3,79E-03	TGME49_240770	cytochrome b5 family heme/steroid binding domain-containing protein	Fatty acid biosynthetic process; oxidation-reduction process	ToxoDB (GO:0006633; GO:0055114)

	Lipids and Glycan metabolism (continuation)							
Nc-Spain1H	NCLIV_001340	putative oxysterol-binding protein domain-containing protein	4,62	2,52E-06	TGME49_294320	Oxysterol-binding protein	Lipid trafficking and metabolism	Zeng and Zhu., 2006
	NCLIV_021430	hypothetical protein	9,32	1,47E-07	TGME49_203580	NAD-binding domain 4 domain-containing protein	Fatty acid elongation via elongase pathway of ER	Shanmugasundram et al., 2013
	NCLIV_050890	putative KR domain domain-containing protein	3,15	1,00E-02	TGME49_236980	AMP-binding enzyme domain-containing protein	Fatty acid elongation in the cytosol (FAS I system)	Shanmugasundram et al., 2013
	NCLIV_013310	hypothetical protein	2,23	3,34E-03	TGME49_213340	GMC oxidoreductase	Phosphatidylcholine metabolism	Shanmugasundram et al., 2013
	NCLIV_057150	hypothetical protein	8,36	1,64E-03	TGME49_313950	GMC oxidoreductase		
	NCLIV_064160	conserved hypothetical protein	2,14	2,84E-02	TGVEG_248170	peroxisomal membrane anchor	Peroxisome biosynthesis and integrity. Peroxisomes are organelles involved in fatty acid degradation and cellular detoxification.	Moog et al., 2017
	NCLIV_028730	putative peroxisomal-type ATPase	2,49	2,27E-02	TGME49_255210	ATPase, AAA family protein		
	NCLIV_053410	putative peroxisome biogenesis factor 1	6,83	2,22E-08	TGME49_308960	ATPase, AAA family protein		
					TGME49_236990	beta-ketoacyl synthase, N-terminal domain-containing protein	Fatty acid elongation in the cytosol (FAS I system)	Shanmugasundram et al., 2013
	Vitamins, cofactors and other substrates metabolism							
Nc-Spain7	NCLIV_023120	Chorismate synthase, related	-2,67	1,65E-11	TGME49_201380	chorismate synthase, putative	Shikimate biosynthesis	Shanmugasundram et al., 2013
	NCLIV_004820	phospho-2-dehydro-3-deoxyheptonate aldolase,related	-2,48	2,28E-10	TGVEG_221250	phospho-2-dehydro-3-deoxyheptonate aldolase	Shikimate biosynthesis; Ubiquinone metabolism	InterPro (IPR006268)
	NCLIV_002980	putative 5-formyltetrahydrofolate cyclo-ligase domain-containing protein	-2,17	2,21E-02	TGME49_208090	5-formyltetrahydrofolate cyclo-ligase	Folate metabolism	Ulland et al., 2013
	NCLIV_014630[3]	Novel protein similar to quinoid dihydropteridine reductase, related	-7,90	5,11E-04	TGME49_285750	6,7-dihydropteridine reductase	Folate biosynthesis	Shanmugasundram et al., 2013
	NCLIV_051000	Ethylene-inducible protein hever, related	-2,26	4,65E-02	TGME49_237140	ethylene inducible protein, putative	Pyridoxal phosphate (Vitamin B6) metabolism	Shanmugasundram et al., 2013
	NCLIV_032510	FAD binding domain containing protein, related	-2,14	3,41E-04	TGME49_232540	FAD binding domain-containing protein	Ubiquinone metabolism	Shanmugasundram et al., 2013
	NCLIV_008230	delta-aminolevulinic acid dehydratase, related	-3,12	2,90E-10	TGME49_253900	parasite porphobilinogen synthase PBGS	Porphyrin metabolism	Shanmugasundram et al., 2013
Nc-Spain1H	NCLIV_000440	Molybdopterin biosynthesis protein, related	2,04	1,37E-06	TGME49_293480	MoeA N-terminal region (domain I and II) domain-containing protein	Folate biosynthesis	Shanmugasundram et al., 2013
	Redox metabolism							
Nc-Spain7	NCLIV_045930	putative glutaredoxin	-4,10	1,05E-03	TGVEG_227100	putative glutaredoxin	Redox metabolism	Shanmugasundram et al., 2013
	NCLIV_063860	putative thioredoxin	-2,52	1,78E-25	TGME49_247350	thioredoxin domain-containing protein		
	NCLIV_014020	Peroxiredoxin-2E-1, related	-6,06	2,83E-33	TGME49_286630	redoxin domain-containing protein		
	NCLIV_015430	hypothetical protein	-2,94	2,50E-16	TGME49_238040	protein disulfide-isomerase domain-containing protein	Redox homeostasis	ToxoDB
Nc-Spain1H	NCLIV_007660	hypothetical protein	2,15	1,56E-02	TGP89_253120A	mandelonitrile lyase, putative	Oxidation-reduction process	ToxoDB (GO:0055114)
	NCLIV_007690	putative oxidoreductase	7,20	3,83E-02	TGME49_253150	hypothetical protein		
	NCLIV_027380	putative 2OG-Fe(II) oxygenase family oxidoreductase	7,83	4,60E-83	TGME49_259150	hypothetical protein	Oxidation-reduction process	InterPro (I7MKU4)

	Others							
Nc-Spain7	NCLIV_026210	hypothetical protein	-8,87	3,73E-18	TGME49_261070	apicoplast triosephosphate translocator APT1	Pyruvate metabolism, Isoprenoids metabolism, Fatty acid biosynthesis in the apicoplast (FAS II system)	Shanmugasundram et al., 2013, Brooks et al., 2010
	NCLIV_042840[3]	hypothetical protein	-6,37	3,89E-03	TGME49_290970	8-amino-7-oxononanoate synthase	Sphingomyelin and ceramide metabolism, Pyridoxal phosphate (Vitamin B6) metabolism	Shanmugasundram et al., 2013
					TGME49_290980	glycine C-acetyltransferase, putative		
	NCLIV_042850	pyridoxal phosphate-dependent acyltransferase, related	-2,24	9,65E-08	TGME49_290970	8-amino-7-oxononanoate synthase		
					TGME49_290980	glycine C-acetyltransferase, putative		
	NCLIV_039650	genome sequencing data, contig C317, related	-2,17	1,85E-02	TGME49_265860	hydrolase, carbon-nitrogen family protein	Nitrogen compound metabolic process	InterPro (IPR003010)
	NCLIV_031690	Oligosaccharyl transferase-like protein, related	-2,06	1,54E-08	TGME49_231430	oligosaccharyl transferase stt3 protein, putative	Aminosugars metabolism; N-Glycan biosynthesis	Shanmugasundram et al., 2013
	NCLIV_006990	conserved hypothetical protein	-2,04	3,63E-04	TGVEG_276155	AMP-binding enzyme	The family of enzymes includes long chain fatty acid Co-A ligase, acetyl-CoA synthetase and various other closely-related synthetases	InterPro (IPR020459)
Nc-Spain1H	NCLIV_022740	putative enoyl-CoA hydratase/isomerase family protein	2,76	4,71E-04	TGME49_202140	enoyl-CoA hydratase/isomerase family protein	Leucine, isoleucine and valine metabolism; Fatty acid recycling and degradation	Shanmugasundram et al., 2013
	NCLIV_043550	glycerol-3-phosphate dehydrogenase, related	5,40	6,04E-09	TGME49_210260	NAD-dependent glycerol-3-phosphate dehydrogenase	Fatty acid biosynthesis in the apicoplast (FAS II system); Glycolysis; Electron transport chain	Shanmugasundram et al., 2013
	NCLIV_001470	putative rhodanese-like domain containing protein	3,84	1,24E-21	TGME49_294570	rhodanese family domain-containing protein	Cyanide detoxification; Sulfur and selenium metabolism; Biosynthesis of prosthetic groups in iron-sulfur proteins	Cipollone et al, 2007
	Immune related							
Nc-Spain7	NCLIV_005160[3]	putative ppg3	-15,87	4,77E-02	TGVEG_221630	putative ppg3	Cellular surface coat molecules	Favila et al., 2015
	NCLIV_020320	Proteophosphoglycan ppg4, related	-2,31	8,55E-03	TGVEG_205370	putative proteophosphoglycan protein ppg4		
	NCLIV_065610	Proteophosphoglycan 5, related	-2,74	1,36E-09	TGVEG_249440	putative proteophosphoglycan 5, related protein		
	NCLIV_015405	putative cyclophilin	-2,23	3,14E-06	TGME49_238000	peptidyl-prolyl isomerase	*N. caninum* antigen related with interferon production and CC-chemokine receptor 5-dependent cell migration	Mineo et al., 2010
	NCLIV_054410	Calr protein, related	-2,15	1,97E-04	TGME49_310320	calreticulin family protein	Protein folding. Putative role in immune evasion	ToxoDB (GO:0006457); Castillo et al., 2014
	NCLIV_042400	macrophage migration inhibitory factor, related	-2,84	1,08E-10	TGME49_290040	macrophage migration inhibitory factor, putative	Immunomodulatory activity and parasite dissemination	Sommerville et al., 2013
Nc-Spain1H	NCLIV_004020	tryptophan-rich antigen (Pv-fam-a), related	3,09	9,01E-03	TGVEG_209755	putative tryptophan-rich antigen, related protein	Candidate antigens for potential vaccines in Plasmodium vivax	Wang et al., 2015
	NCLIV_056990	Proteophosphoglycan 5, related	2,36	5,69E-03	TGVEG_313725	proteophosphoglycan 5, related	Cellular surface coat molecules	Favila et al., 2015

Adhesion/invasion/survival								
Cell adhesion and invasion								
Nc-Spain7	NCLIV_004432[3]	srs domain-containing protein	-37,12	7,00E-04	TGME49_321470	SAG-related sequence SRS12D	Surface antigen	Piraine et al., 2015
					TGME49_321490	SAG-related sequence SRS12A		
	NCLIV_023620[3]	SRS domain-containing protein	-15,22	1,60E-07	TGME49_281930	SAG-related sequence SRS39		
	NCLIV_027700	SRS domain-containing protein	-2,31	1,82E-10	TGME49_258810	SAG-related sequence SRS27B		
	NCLIV_056530	conserved hypothetical protein	-2,12	6,99E-03	TGME49_313200	LRR-containing protein	Proteins containing LRRs include tyrosine kinase receptors, cell adhesion molecules, extracellular matrix binding glycoproteins and virulence factors.	InterPro (IPR001611)
	NCLIV_003470	putative thrombospondin type 1 domain-containing protein	-2,62	2,18E-07	TGME49_209060	thrombospondin type 1 domain-containing protein	Genes containing TSP1 domains have been identified in several genera of apicomplexans, including thrombospondin-related adhesive proteins (TRAPs)key molecules of glideosome.	Boucher and Bosch, 2015
	NCLIV_024420	hypothetical protein	-2,03	1,55E-13	TGME49_263520	microtubule associated protein SPM1	Stabilizes Subpellicular Microtubules in *T. gondii.* Loss of SPM1 decreases parasite fitness	Tran et al., 2012
	NCLIV_037160	putative actin-like family protein	-3,37	7,17E-05	TGME49_269240	actin-like family protein	May be implicated in actin-based gliding motility	Boucher and Bosch, 2015; Gordon and Sibley, 2005
Nc-Spain1H	NCLIV_002220	srs domain-containing protein	2,43	1,75E-02	TGME49_295600	SAG-related sequence SRS10	Surface antigen	Piraine et al., 2015
	NCLIV_004471	srs domain-containing protein	4,40	1,35E-16	TGME49_321470	SAG-related sequence SRS12D		
					TGME49_321490	SAG-related sequence SRS12A		
	NCLIV_010040	srs domain-containing protein	5,96	5,49E-03	TGVEG_320230	SAG-related sequence SRS15C		
	NCLIV_058060	SRS domain-containing protein	2,92	3,76E-07	TGME49_315320	SAG-related sequence SRS52A		
	NCLIV_034381	SRS domain-containing protein	2,37	1,75E-02	TGME49_273110	SAG-related sequence SRS30D		
					TGME49_273120	SAG-related sequence SRS30C		
	NCLIV_038930[2]	srs domain-containing protein	211,83	1,04E-23	TGME49_267130	SAG-related sequence SRS38A		
					TGME49_267140	SAG-related sequence SRS38B		
					TGME49_267150	SAG-related sequence SRS38C		
					TGME49_267160	SAG-related sequence SRS38D		
	NCLIV_043430[2]	srs domain-containing protein	15,35	2,50E-02	TGVEG_440320	SAG-related sequence SRS36C		
	NCLIV_047940[2]	SRS domain-containing protein	25,92	1,75E-03	TGME49_224790	SAG-related sequence SRS40A		
	NCLIV_049510	SRS domain-containing protein	7,18	3,88E-02	TGME49_234370	SAG-related sequence SRS42		
	NCLIV_049630	SRS domain-containing protein	3,50	6,20E-12	TGME49_234930	SAG-related sequence SRS43		
	NCLIV_052740	SRS domain-containing protein	2,23	1,77E-03	-			
	NCLIV_068872	SRS domain-containing protein	2,49	3,93E-08	-			

Adhesion and invasion (continuation)								
Nc-Spain1H	NCLIV_019580	SRS domain-containing protein	14,10	7,18E-41	TGME49_280570	SAG-related sequence SRS35A	Bradyzoite-specific surface protein (SAG4)	Fernández-García et al., 2006
	NCLIV_010030	Bradyzoite surface protein BSR4	4,20	8,59E-05	TGME49_320230	SAG-related sequence SRS15C	Bradyzoite-specific surface protein	Risco-Castillo et al., 2007
	NCLIV_020010	putative F5/8 type C domain-containing protein	2,52	3,31E-07	TGME49_205658	F5/8 type C domain-containing protein	Cell adhesion	ToxoDB (GO:0007155)
					TGME49_205662	LCCL domain-containing protein		
	NCLIV_011720	hypothetical protein	3,16	9,84E-07	TGME49_211270	sushi domain (scr repeat) domain-containing protein	Cell diferentiation; Domain found in many complement and adhesion proteins	ToxoDB (GO:0030154); Lamarque et al., 2012
	NCLIV_026560	Cell wall surface anchor family protein, related	2,47	2,35E-03	TGME49_260480	leucine rich repeat-containing protein	Proteins containing LRRs include tyrosine kinase receptors, cell adhesion molecules, extracellular matrix binding glycoproteins and virulence factors	InterPro (IPR001611)
	NCLIV_066090	putative leucine rich repeat protein	2,75	4,66E-09	TGME49_249980	leucine rich repeat-containing protein		
	NCLIV_036660	conserved hypothetical protein	2,19	6,38E-05	TGME49_269930	calcium binding egf domain-containing protein	Several parasite proteins containing EGF or TSR-like domains have adhesive properties. Hypothetical proteins containing these domains are likely involved in invasion. EGF-containing MICs activate Akt signaling via EGF receptors to avoid autophagic killing of the parasite by the host cell	Huynh et al., 2014
	NCLIV_011000	fibrillin 1, related	2,20	1,80E-02	TGME49_318540	calcium binding egf domain-containing protein		
	NCLIV_001350	putative EGF-like domain-containing protein	3,55	2,04E-03	TGME49_294330	EGF family domain-containing protein	Apical membrane antigen (AMA) 4	Lamarque et al., 2014
	NCLIV_038490[2]	conserved hypothetical protein	62,51	2,70E-07	TGME49_267875	NBP2b protein, putative	Cell binding	Meyer et al., 2010; Boucher et al., 2015
	NCLIV_024520	hypothetical protein	2,46	6,19E-03	TGME49_263410	scavenger receptor cysteine-rich domain-containing protein	Domain found in cell-surface and secreted proteins. They likely mediate protein-protein interactions and ligand binding	(IPR001190)
	NCLIV_053260	putative platelet binding protein GspB	3,63	6,11E-09	TGME49_306890	hypothetical protein		
	NCLIV_064920	conserved hypothetical protein	2,73	3,29E-13	TGME49_248780	SRR1 protein		
	NCLIV_069310	unspecified product	10,98	1,91E-85	TGME49_267680	microneme protein MIC12	Microneme protein	Piraine et al., 2015
	NCLIV_061910	hypothetical protein	4,69	1,02E-08	TGME49_218310	microneme protein MIC14		
	NCLIV_020210	conserved hypothetical protein	2,07	9,51E-05	TGME49_205480	IMC subcompartment protein ISP4	Protein of the inner membrane complex (IMC), used by apicomplexan parasites to facilitate host cell invasion and replication.	Fung et al., 2012

	Rhoptry proteins							
Nc-Spain7	NCLIV_007770	putative Rhoptry kinase family protein, truncated (incomplete catalytic triad)	-4,75	4,63E-104	TGME49_253330	Rhoptry kinase family protein, truncated (incomplete catalytic triad)	Rhoptry protein	Piraine et al., 2015
	NCLIV_068850	unspecified product	-2,47	1,63E-35	TGME49_252360[1]	rhoptry kinase family protein ROP24 (incomplete catalytic triad)		
Nc-Spain1H	NCLIV_001400	unspecified product	3,28	6,58E-41	TGME49_294400	hypotetical protein	Rhoptry protein RON2L1. RON2L1 interacts in a selective and exclusive manner with AMA4 to assist invasion in *T. gondii*	Lamarque et al., 2014
	NCLIV_068890	unspecified product	2,14	2,71E-05	TGVEG_442710	rhoptry kinase family protein	Rhoptry protein	Piraine et al., 2015
	NCLIV_017420	unspecified product	2,04	6,10E-06	TGME49_242110	rhoptry kinase family protein ROP38		
					TGME49_242118	myosin-light-chain kinase		
					TGME49_242230	rhoptry kinase family protein ROP29		
					TGME49_242240	rhoptry kinase family protein ROP19A		
					TGME49_242250	rhoptry kinase family protein ROP19B		
	NCLIV_001950	unspecified product	2,22	4,86E-07	TGME49_295105	rhoptry protein, putative		
					TGME49_295110	rhoptry protein ROP7		
					TGME49_295125	rhoptry protein ROP4		
	Parasite survival							
Nc-Spain1H	NCLIV_062190	GK22245, related	3,47	4,17E-20	TGME49_217430	protease inhibitor PI1	Protection of parasites from proteolytic damage in the gut, suppression of proteolytic activity during parasite replication, and counteraction of host proteases of the innate immune system	Pszenny et al., 2012
					TGME49_246130	serpin (serine proteinase inhibitor) superfamily protein		
	NCLIV_056890	hypothetical protein	2,36	8,25E-10	-		NcPI-S. Serine-protease inhibitor	Morris et al., 2004
	NCLIV_003900	putative oocyst wall protein COWP	2,18	2,08E-04	TGME49_209610	oocyst wall protein OWP2	Cyst wall protein	Sullivan and Jeffers, 2012
	NCLIV_005970	putative oocyst wall protein	2,31	6,51E-23	TGME49_222940	hypothetical protein		

	Transmembrane proteins					
Nc-Spain7	NCLIV_000900	conserved hypothetical protein	-3,06	3,92E-06	TGVEG_294050	
	NCLIV_005700	conserved hypothetical protein	-2,59	6,73E-05	TGVEG_222300	
	NCLIV_005740	conserved hypothetical protein	-2,06	8,17E-07	TGMAS_222350B	
	NCLIV_005790	conserved hypothetical protein	-2,39	2,64E-03	TGVEG_222400	
	NCLIV_007170[3]	conserved hypothetical protein	-18,02	3,10E-02	TGVEG_275760	
	NCLIV_007740[3]	hypothetical protein	-17,92	3,18E-02	TGVEG_253300	
	NCLIV_010530	conserved hypothetical protein	-2,19	5,08E-05	TGVEG_319630	
	NCLIV_010990	conserved hypothetical protein	-2,49	4,49E-02	TGVEG_318550	
	NCLIV_016780	conserved hypothetical protein	-4,27	8,93E-04	TGVEG_240580	putative transmembrane protein
	NCLIV_024790	conserved hypothetical protein	-3,11	6,47E-03	TGVEG_263120	
	NCLIV_044100	conserved hypothetical protein	-2,09	1,38E-04	TGVEG_206320	
	NCLIV_047210	conserved hypothetical protein	-3,78	3,78E-08	TGVEG_225500	
	NCLIV_048050	conserved hypothetical protein	-2,00	7,90E-04	TGVEG_266090	
	NCLIV_048150	conserved hypothetical protein	-2,14	1,98E-04	TGVEG_224570	
	NCLIV_056010	conserved hypothetical protein	-2,25	3,02E-02	TGVEG_312470	
	NCLIV_063790	hypothetical protein	-2,47	8,49E-05	TGVEG_247280	
	NCLIV_066620	conserved hypothetical protein	-3,22	1,10E-05	TGVEG_251520	
	NCLIV_009390	putative Cleft lip and palate transmembrane protein 1	-2,17	8,04E-09	TGME49_299110	cleft lip and palate transmembrane protein 1 (clptm1) protein
Nc-Spain1H	NCLIV_000990	conserved hypothetical protein	2,58	6,47E-03	TGVEG_294240	
	NCLIV_012450	conserved hypothetical protein	2,31	2,35E-12	TGVEG_220330	
	NCLIV_013240	conserved hypothetical protein	2,65	1,46E-08	TGVEG_213240	
	NCLIV_014420	conserved hypothetical protein	3,47	3,45E-05	TGVEG_286010	
	NCLIV_018840	conserved hypothetical protein	3,69	2,58E-28	TGVEG_244260	
	NCLIV_019260[2]	hypothetical protein	15,30	2,52E-02	TGVEG_244715	
	NCLIV_021160	conserved hypothetical protein	4,64	1,37E-02	TGVEG_203930	
	NCLIV_023530	conserved hypothetical protein	4,60	1,27E-03	TGVEG_281590	
	NCLIV_027630	conserved hypothetical protein	4,41	1,25E-15	TGVEG_258840	
	NCLIV_038440	conserved hypothetical protein	8,48	7,49E-101	TGVEG_279350	
	NCLIV_039840	conserved hypothetical protein	5,02	2,65E-03	TGVEG_265430	
	NCLIV_043290	conserved hypothetical protein	3,04	3,83E-02	TGVEG_291910	putative transmembrane protein
	NCLIV_062130	conserved hypothetical protein	10,66	3,67E-03	TGVEG_217370	
	NCLIV_062170	conserved hypothetical protein	11,41	2,45E-20	TGVEG_217410	
	NCLIV_049360	conserved hypothetical protein	2,53	4,58E-05	TGVEG_211860	
	NCLIV_051320	conserved hypothetical protein	3,52	7,46E-45	TGVEG_237585	
	NCLIV_059880	conserved hypothetical protein	2,95	3,16E-04	TGVEG_216335	
	NCLIV_064070	conserved hypothetical protein	5,83	6,62E-10	TGVEG_247970	
	NCLIV_002730	conserved hypothetical protein	10,70	5,56E-04	TGVEG_207780	
	NCLIV_064130	conserved hypothetical protein	2,33	1,25E-06	TGVEG_248140	
	NCLIV_069520	hypothetical protein	4,13	1,51E-13	TGRUB_213460	
	NCLIV_069530	hypothetical protein	3,02	1,11E-03	TGRUB_213460	
	NCLIV_003880	conserved hypothetical protein	3,39	4,10E-02	TGVEG_209590	

	Others							
Nc-Spain7	NCLIV_005130	conserved hypothetical protein	-2,31	8,24E-03	TGVEG_221600	oligomerisation domain protein		
	NCLIV_052780	putative penicillin amidase domain-containing protein	-2,87	1,07E-31	TGME49_275320	penicillin amidase		
	NCLIV_025050	SPRY domain-containing protein	-2,24	1,14E-02	TGME49_262850	hypothetical protein	Unknown	InterPro (IPR003877)
	NCLIV_016000	conserved hypothetical protein	-2,06	1,04E-03	TGVEG_239340	GTP1/Obg protein	GTP-binding protein. Uncertain function, but it has been shown to be important in development and normal cell metabolism	InterPro (IPR036726)
	NCLIV_032060	putative peptidase family T4	-3,82	7,19E-07	TGME49_232060	hypothetical protein	Peptidase	
	NCLIV_018460	conserved hypothetical protein	-2,29	3,82E-04	TGVEG_243760	TLC domain protein	Protein domain with at least 5 transmembrane alpha-helices. Proteins containing this domain may possess diverse functions such as lipid trafficking, sensing or metabolism.	InterPro (IPR006634)
	NCLIV_019620	conserved hypothetical protein	-2,15	4,27E-02	TGVEG_280530	DTW domain protein	Unknown	InterPro (IPR005636)
	NCLIV_005330	at4g25910 protein, related	-2,21	4,11E-04	TGME49_221922	NifU family domain-containing protein	Iron-sulfur cluster assembly	ToxoDB (GO:0016226)
	NCLIV_0155	alpha/beta hydrolase fold domain containing protein	-3,00	1,26E-09	TGME49_238200	alpha/beta hydrolase fold domain-containing protein	Hydrolytic enzymes of widely differing catalytic function	InterPro (IPR029058)
	NCLIV_053980	conserved hypothetical protein	-3,92	6,91E-06	TGVEG_309860	alpha/beta hydrolase family protein		
	NCLIV_053480[3]	Large protein with signal peptide. cysteine-rich,threonine-rich, possible mucin, related	-4,53	4,27E-02	TGME49_309030	hypothetical protein	Unknown	
	NCLIV_061740	Hydrolase, alpha/beta fold family, related	-4,31	5,47E-04	TGME49_218540	peptidase S15, putative	Proteolytic enzime	InterPro (IPR008252)
	NCLIV_015810	putative retinitis pigmentosa GTPase regulator	-2,30	4,49E-02	TGME49_238980	hypothetical protein	Unknown	
	NCLIV_012730	Os10g0412100 protein, related	-2,68	2,75E-02	TGME49_301216	endonuclease/exonuclease/phosphatase family protein	It includes magnesium dependent endonucleases and phosphatases involved in intracellular signalling, AP endonuclease proteins, DNase I proteins, Synaptojanin an inositol-1,4,5-trisphosphate phosphatase and Sphingomyelinase	InterPro (IPR005135)
	NCLIV_052110	conserved hypothetical protein	-4,69	4,11E-06	TGME49_215100	PP-loop family protein	The PP-loop motif appears to be a modified version of the P-loop of nucleotide binding domain involved in phosphate binding	InterPro (IPR012122)

	Others (continuation)							
Nc-Spain1H	NCLIV_012440	conserved hypothetical protein	2,16	3,38E-11	TGME49_220320	BSD domain-containing protein	Unknown function. Domain present in basal transcription factors, synapse-associated proteins and several hypothetical proteins.	InterPro (IPR005607)
	NCLIV_014810	putative Patched family domain containing protein	2,88	5,02E-03	TGME49_285470	patched family protein	Integral component of membrane. Hedgehog receptor activity	Toxo DB (GO:0016021; GO:0008158)
	NCLIV_021240	zinc finger (C3HC4 type) / FHA domain-containing protein	8,38	5,08E-26	TGME49_203830	FHA domain-containing protein	FHA domains are protein-protein interaction domains specific for phosphoproteins, found in signalling molecules. FHA-containing proteins act in maintaining cell-cycle checkpoints, DNA repair and transcriptional regulation	InterPro (IPR008984)
	NCLIV_056000	hypothetical protein	5,46	1,23E-38	TGME49_312460	zinc finger, MYND-type containing 12 family protein		
	NCLIV_067570	unspecified product	3,10	1,72E-06	TGME49_278320	Toxoplasma gondii family A protein	Unknown	
	NCLIV_006930	hypothetical protein	2,77	4,34E-02	TGME49_200480[1]	Toxoplasma gondii family B protein	Unknown	
	NCLIV_060290	conserved hypothetical protein	4,35	1,20E-06				
	NCLIV_040620[2]	conserved hypothetical protein	15,28	2,52E-02	TGVAND_287960	putative toxoplasma gondii family D protein	Unknown	
	NCLIV_000380	potential mitochondrial membrane protein,related	6,95	1,40E-03	TGME49_293425	hypothetical protein	Mitochondrial membane protein	
	NCLIV_010741	hypothetical protein	4,49	1,98E-09	TGARI_356120	putative kelch repeat protein	Unknown	
	NCLIV_016090	conserved hypothetical protein	2,77	3,46E-03	TGARI_239475A	putative flagellar protein	Unknown	
	NCLIV_044250	conserved hypothetical protein	2,40	2,68E-14	TGRUB_206550	putative hydrocephalus-inducing-like protein	Unknown	
	NCLIV_004580	hypothetical protein	2,14	3,95E-14	TGME49_321340	membrane protein, putative	Membrane protein	
	NCLIV_013250	GK19899, related	5,87	2,79E-124	TGRUB_213255	hypothetical protein	Unknown	
	NCLIV_035550	GH22156, related	2,92	9,37E-03	TGME49_271315	hypothetical protein	Unknown	

Nc, *Neospora caninum*; Tg, *Toxoplasma gondii*; FC, Fold change in the comparison Nc-Spain1H *versus* Nc-Spain7; P adj, p-value adjusted by FDR. Genes were considered differentially expressed when presented a FC ≥ 1.5 and p adj ≤ 0.05.

[1]No synthenic

[2]Exclusively expressed by Nc-Spain1H

[3]Exclusively expressed by Nc-Spain7

VI

GENERAL DISCUSSION
DISCUSIÓN GENERAL

Bovine neosporosis is one of the most important causes of abortion in cattle worldwide. *Neospora caninum*, the causal agent of the disease, is transplacentally transmitted very efficiently (Dubey et al., 2007). Abortion is the main clinical manifestations of bovine neosporosis. Fetuses may die in utero and be reabsorbed, autolyzed, mummified, stillborn, or born alive with clinical signs. However, most calves from infected dams born clinically healthy but congenitally infected (Almeria and López-Gatius, 2013). A major factor in determining to the outcome of infection is the virulence of the infecting isolate (Dubey et al., 2006). However, little is known about the influence of the biological diversity of *N. caninum* in the clinical presentation and immune responses in bovine neosporosis (Regidor-Cerrillo et al., 2014). Moreover, specific *N. caninum* virulence factors in cattle have not yet been determined and the mechanisms used by the parasite to modulate bovine host cells of the innate immune system during early infection are largely unknown, supporting the need for new research.

In vitro studies involving *N. caninum* infection of murine and human APCs (macrophages and DCs) suggest that the parasite may modulate the cell ROS production, cytokine secretion and lymphocyte activation (Strohbusch et al., 2009; Dion et al., 2011; Mota el al., 2016; He et al., 2017; Silva et al., 2017; Boucher et al., 2018). However, because mice and humans are not natural hosts for *N. caninum*, these results may not necessarily reflect the dynamic of the parasite interaction with immune system cells in cattle. Thus, the ability of the parasite to initiate innate immune responses should be determined in bovine APCs.

The host-cell regulatory events associated with the parasite intracellular development were investigated in bovine macrophages, selected because they mediate innate immune responses against infection. Macrophages are able to recognize pathogens by means of PRRs, activating signaling pathways which lead to phagocytosis, antigen presentation, and release of cytokines and chemokines, which in turn recruit and activate other immune cells enhancing the initial response. By presenting antigen to naive T cells, they are also the link with the adaptive response, directing Th1 or Th2 responses (Hume, 2008). Bovine macrophages used in all the experiments were obtained from monocytes isolated from peripheral blood cultured in the presence of GM-CSF. These cells displayed morphological features characteristic of macrophages regarding size, shape, adherence, cytoplasmic granularity and expression of surface molecules, and their functionality was broadly demonstrated, being an adequate model for the study of *N. caninum* interaction with the innate immune system.

As a first approach, *N. caninum*-infected cells were characterized phenotypically. Then, the transcriptional profile was investigated to determine the molecular basis implicated in the parasite-host cell crosstalk. With the aim to differentiate the active modulation of host cell functions by live tachyzoites upon infection *versus* the response induced by phagocytosis of the parasite, macrophages inoculated with heat-inactivated tachyzoites were included in all the experiments. Once determined the processes related with parasite manipulation of the host cell environment, these were further investigated by means of comparison of macrophage responses induced by the infection with high and low virulence isolates, to identify *N. caninum* isolate-specific virulence traits. In all the experiments, macrophages were infected with two isolates showing marked differences in virulence *in vitro* and *in vivo* (Rojo-Montejo et al., 2009a, 2009b; Regidor-Cerrillo et al., 2011; Dellarupe et al., 2014a, 2014b; Jiménez-Pelayo 2017, 2019a, 2019b Jiménez-Pelayo et al., submitted), the high virulence isolate Nc-Spain7 and the low virulence isolate Nc-Spain1H. The effects of macrophage infection by *N. caninum* are first discussed, followed by the results obtained from the comparison between both isolates.
The ability of *N. caninum* tachyzoites to infect, survive, and replicate in bovine macrophages was studied. Both isolates were internalized into the cells with a higher efficiency than previously

described for other cell lines (Rojo-Montejo et al., 2009a; Regidor-Cerrillo et al., 2011; Jiménez-Pelayo et al., 2017), which may be due to the phagocytic capacity of macrophages. It would enable tachyzoites to enter the cell by two complementary routes: macrophage phagocytosis and parasite active invasion. These studies demonstrated that both processes were in fact involved, and the percentages of internalization attributable to active invasion were highly similar to those determined in other cell lines (Regidor-Cerrillo et al., 2011; Jiménez-Pelayo et al., 2017). These results contrast with the reported in a recent study in human macrophages, where it was described that *N. caninum* internalization probably occurred only by active invasion (Boucher et al., 2018).

Mechanism of entry may determine not only the fate of the parasite but also the immune response generated by the cell (Butcher and Denkers, 2002). Killing and degradation would be expected for tachyzoites internalized via phagocytosis, leading to antigen processing and presentation in the context of molecules of the major histocompatibility complex (Mantegazza et al., 2012). On the other hand, active invasion may facilitate the parasite survival and intracellular growth in the parasitophorous vacuoles. Moreover, phagosome maturation can be altered in response to effectors generated by the infecting pathogen or by innate signaling pathways initiated by the enclosed particles (Mantegazza et al., 2012). In support to this, absence of lysosome activity in macrophages containing parasites in replication was observed. This phenotype was coincident with the gene expression inhibition of the lysosome-related pathway by live infection (but not by heat-inactivated tachyzoites), with down-regulation of genes related to the maturation of the phagosome to a phagolysosome containing a robust antimicrobial environment Uribe-Querol and Rosales, 2017). Thus combined, the results of phenotypic and transcriptional studies suggest that impairing phagolysosome maturation is a mechanism used by *N. caninum* to survive and proliferate into phagocytic cells. The ability of *N. caninum* to circumvent degradation and thus antigen processing and presentation was also evidenced by a decrease in MHC class II expression by flow cytometry and by the downregulation of the major MHC class II transactivator CIITA by live parasites. The mechanism of CIITA expression inhibition seems to be also used by *T. gondii* to limit MHC II expression in neural APCs to evade $CD4^+$-mediated immune responses (Luder et al., 2003). A reduction in MHC Class II has also been observed in *T. gondii*-infected murine macrophages (Luder et al., 1998; Leroux et al., 2015), which has been indicated to be an important strategy for parasite survival by interfering the antigen presentation pathway. Because up-regulation of MHC class II on *N. caninum* murine macrophages has been associated with host survival (Nishikawa et al., 2001), a similar strategy may be attributed. *Neospora caninum* infection also modulated cell surface proteins CD1b, and CD86, whose expression was observed diminished in infected cells at 4 hpi. Lower CD1b expression has been correlated with a reduced specific T-lymphocyte proliferation (Balboa et al., 2010). A reduced expression of CD86, co-stimulatory signal for activation of lymphocytes (Saubaste et al., 1996), has also been observed in *Leishmania*-infected macrophages (Denkers and Butcher, 2005) and in murine peritoneal macrophages inoculated with *N. caninum* (Dion et al., 2011). These data could indicate that *N. caninum* would reduce antigen presentation and T-cell activation to escape from host immune response, which may explain the impaired IFN-γ production at the early stages of infection observed for lymphocytes in co-culture with macrophages inoculated with both isolates.

Differences in mechanism of entry between live and heat-inactivated tachyzoites may be also determinant for parasite recognition by PRRs of the host cell, which would lead to the activation of signaling cascades that stimulate host defenses (Jungi et al., 2011; Moretti and Blander, 2014; Kim et al., 2016). The intracellular TLR3 and NLRs related to inflammasome formation (Kim et al., 2016) NAIP, NOD2, and NLRC4 were only over-expressed in cells infected with live tachyzoites of both isolates. The importance of TLR3 in *N. caninum* recognition has been

previously described in murine macrophages, triggering the production of pro-inflammatory cytokines (Beiting et al., 2014; Miranda et al., 2019). Amongst NLR, NOD2 activation in *N. caninum* infected mice has been related to an exacerbation of the inflammatory response, which would contribute to initial parasite control, but may cause tissue damage during acute neosporosis (Davoli-Ferreira et al., 2016).

Upon pathogen-associated molecular patterns (PAMP) engagement, PRRs trigger intracellular signaling cascades ultimately culminating in the expression of a variety of proinflammatory molecules (Mogensen, 2009). The results obtained in the transcriptomic analysis of bovine macrophages indicate that NF-ĸB is the main signaling pathway involved in the immune response against *N. caninum* in its host. Activation of NF-ĸB signaling pathway polarized the macrophage response towards a predominantly M1 (pro-inflammatory) phenotype. The pro-inflammatory response observed in *N. caninum* infected macrophages was characterized by the expression of cytokines IL-12p40, IL-1β, IL-6, TNF-α and of NOS2 (iNOS).

An enhanced expression of NLR related to NF-ĸB negative regulation NLRC3 and NLRP12 (Cui et al., 2010; Tuncer et al., 2014; Kim et al., 2016) was also observed by live infection. It points towards a modulation with the aim to avoid pathologic consequences due to a persistent activation of NF-ĸB (Jha and Pan-Yun Ting, 2015).

Enrichment analysis of differentially expressed genes in infected cells also showed an impact of *N. caninum* on the host cell metabolism. Parasites manipulate host metabolism to obtain energy and nutrients that it needs to survive (Xu et al., 2010). Besides, there are evidences of a role for metabolic processes in controlling immunological effector functions such as cytokine production (Diskin and Palsson-Mc-Dermott, 2018). Interestingly, fatty acid synthesis and fatty acid degradation have been related macrophages polarization. M1 macrophages, have been shown to drive fatty acid synthesis, whereas the inhibition of inflammatory signals required for the differentiation of M2 macrophages involves fatty acid degradation (Remmerie and Scott, 2018). In this study, downregulation of fatty acid degradation together with upregulation of fatty acid synthesis was observed, that may reflect M1 polarization.

The lytic cycle of *N. caninum* is a tightly regulated process. After invasion, the parasite develops a parasitophorous vacuole and replicates within. Parasite proliferation will determine the number of tachyzoites that disseminate intraorganically during the acute phase of infection, after egress occurs (Pastor et al., 2016). Study of parasite proliferation showed a lower *N. caninum* replication efficacy in bovine macrophages than in other cell lines previously assayed (Regidor-Cerrillo et al., 2011; Jiménez-Pelayo et al., 2017), which may be due to the impact of other mechanisms used by macrophages for killing intracellular pathogens, such as ROS production and apoptosis. However, these mechanisms were not able to eliminate the infection, as our results suggest that *N. caninum* is able at least partially to inhibit these processes, ensuring to complete their lytic cycle. At early infection (1 hpi), intracellular ROS levels were reduced in macrophages infected with both isolates in relation to those inoculated with heat-inactivated tachyzoites. Mechanisms of modulation of intracellular ROS by intracellular pathogens include interference of NADPH complex assembly, scavenging of ROS produced by NADPH oxidase and interference of mitochondrion-based ROS production during infection (Spooner and Yilmaz, 2011). The use of this latter mechanism by *N. caninum* is supported by the observed down-modulation in macrophages inoculated with live tachyzoites of NLRX1 receptor, located in the mitochondria and involved in ROS production.

Regarding apoptosis modulation, the transcriptome profile of infected macrophages showed upregulation and downregulation both for genes annotated as pro-apoptotic and for those annotated as anti-apoptotic. This behavior has been widely described in *T. gondii* and many other intracellular protozoan parasites (Schaumburg et al., 2006). On the one hand, stress signals promoted by the parasite during infection may lead to a pro-apoptotic response by the host cell as an innate defense mechanism. On the other, these obligate intracellular parasites need to hijack apoptosis-regulating cascades to suppress or delay cell death to favor parasite multiplication. Our results indicate that *N. caninum* counteract stress-induced cell death by inducing the expression of certain anti-apoptotic BCL-2 genes, inhibitors of apoptosis (IAPs) and FLIP (also named CFLAR) among others. It would lead to a lower release of cytochrome c from mitochondria into the cytosol and to a direct interference with caspase processing and function, as it has been previously described for other protozoan parasites including *T. gondii* (Schaumburg et al., 2006; Besteiro, 2015).

Another phenotypic trait that may be related to parasite virulence is the capacity to modulate the migratory properties of immune cells, which may facilitate parasite dissemination, transmission, or establishment of chronic infections in the host. The induction of a hypermigratory phenotype has been previously described in human and murine APCs upon *T. gondii* infection. This phenotype characterizes by hypermotility, enhanced transmigration, abrogation of extracellular matrix degradation and induction of marked cytoskeletal changes shortly after infection, inducing an ameboid migratory activation of the infected cell (Lambert et al., 2006; Fuks et al., 2012; Weidner et al., 2013; Kanatani et al., 2015; Ólafson et al., 2018).

In the present work, the induction of hypermigration by *N. caninum* in bovine macrophages was demonstrated for the first time. In line with the reported for APCs infection by *T. gondii*, dissolution of podosomes was observed in *N. caninum*-infected bovine macrophages. Podosomes are essential cytoskeletetal structures linked to adhesion, cell signaling, matrix degradation, and therefore migration. Podosomes dissolution upon *N. caninum* infection would imply fundamental mechanistic changes regarding how the parasitized cells interact with the surrounding environment and migrate. More specifically, integrin-mediated adhesion and signaling and metalloproteinase activity is focalized and regulated in podosomes (Ólafsson et al., 2018, 2019).

The induction of hypermigration of leukocytes upon parasite infection has been related with a higher dissemination for *T. gondii* and *N. caninum* in mice (Lambert et al., 2006; Collantes-Fernández et al., 2012). The results of these studies, consistent with the existence of a conserved mechanism between *N. caninum* and *T. gondii* for migratory activation of infected leukocytes, motivates further studies to address a putative utilization of APCs infection as Trojan horse mechanism for *N. caninum* systemic dissemination in the cow. It has been recently described that *T. gondii* hijacks DCs GABAergic signaling and voltage-dependent calcium channel signaling for Trojan horse-mediated dissemination (Bhandage and Barragan, 2019). How *N. caninum* molecularly orchestrates the migratory activation of parasitized cells and the identification of implicated parasite and host it cell-mediated signaling, requires further investigation.
In summary, *N. caninum* is able to actively invade and complete its lytic cycle in bovine macrophages, by avoiding phagolysosome maturation, diminishing intracellular ROS levels and ensuring host-cell survival by interfering with apoptosis-related pathways. *Neospora caninum* infection polarized the cell response towards a predominantly M1 phenotype, with the activation of NF-kB signaling as the main pathway involved in the pro-inflammatory response generated. Additionally, the parasite is able to exploit the migratory properties of these innate immune cells, which may be a strategy used by *N. caninum* to disseminate and transmit.

Although these mechanisms of induction and evasion of immune responses seem to be common for Nc-Spain7 and Nc-Spain1H, important differences in parasite-host cell interaction were found between isolates. Higher invasion, survival and proliferation rates were observed for the high virulent isolate, which also induced lower production of ROS by the macrophages and of IFN-γ by lymphocytes. On the other hand, a higher pro-inflammatory immune response was shown by macrophages infected with the low virulence isolate.

Nc-Spain7 showed a higher active invasion rate than Nc-Spain1H in bovine macrophages, as previously described for other cell types assayed (Regidor-Cerrillo et al., 2011; Jiménez-Pelayo et al., 2017). With regard to this, previous studies have associated the higher invasion capacity of Nc-Spain7 in bovine trophoblast cells (Horcajo et al., 2017) with enhanced expression of gliding-associated proteins by the parasite. In agreement with that work, the transcriptome profile in bovine macrophages also showed an enhanced expression of genes related with the glideosome for the high virulent isolate.

The higher active invasion of Nc-Spain7 tachyzoites may determine their higher ability to survive in the cell. Thus, a higher proportion of tachyzoites would scape phagolysosome degradation, diminishing antigen presentation. This fact, together with a lower induction of IL-12 expression by the host cell shown for this isolate, may at least partially explain the impairment of IFN-γ response by lymphocytes co-cultured with Nc-Spain7-infected macrophages.

Our results also suggest that higher intracellular survival of Nc-Spain7 may also be related with a higher capacity of this isolate to keep a cellular redox balance and detoxify ROS by expressing higher levels of antioxidant enzimes such as glutaredoxin, peroxiredoxin and an ortholog to *T. gondii* apicoplast-associated thioredoxin Atx1. TgATrx1 is a redox-regulated enzyme essential for the parasite. It is involved in endoplasmic reticulum-to-apicoplast trafficking and contributes to apicoplast biogenesis. Due to its importance in parasite biology, it has been suggested the potential of apicoplast thioredoxins as drug targets (Biddau et al., 2018). Because antioxidant enzymes allow apicomplexan parasites to address oxidative levels inside the host cells, these seem especially important in regard to intracellular survival in macrophages, which use ROS to kill pathogens (Bosch et al., 2015). Thus, their enhanced expression may confer an advantage to the high virulence isolate and would explain why despite both isolates were able to reduce ROS levels at early infection, only the high virulent isolate maintained this downregulation over time.

In addition to higher invasion and survival, a more efficient proliferation was shown for Nc-Spain7, which suggest the success of the high virulent isolate in establishing a replicative niche in bovine macrophages. The higher proliferation of Nc-Spain7 correlated with an enhanced expression of genes involved in parasite growth. More specifically in nucleic acid biosynthesis, DNA replication, RNA metabolism, protein synthesis, cell division and energy production. On the contrary, higher expression of bradyzoite specific genes were observed in Nc-Spain1H, including surface proteins SAG4 and BSR4 (Fernández-García et al., 2006; Risco-Castillo et al., 2007), AP2 transcription factors and oocyst wall proteins among others. Overexpression of bradyzoite-specific genes by Nc-Spain1H has been previously described and related to a pre-bradyzoite stage in which the parasite cell cycle shifts towards slower growth (Horcajo et al., 2018). This results may at least partially explain the lower proliferation observed for Nc-Spain1H than in Nc-Spain7 in bovine macrophages and all the other cell lines assayed (Regidor-Cerrillo et al., 2011; Jiménez-Pelayo et al., 2017).

Despite the higher invasion and proliferation shown by Nc-Spain7 in bovine macrophages, a higher impact in the host cell was observed with Nc-Spain1H infection. It can be highlighted the upregulation of genes associated with NLR signaling pathway, chemokine signaling pathway and cytokine-cytokine receptor interaction. Amongst NLR, NLRP3 was shown to be upregulated only in macrophages infected with Nc-Spain1H. Involvement of this receptor in the acute host immune response to *N. caninum* has been suggested, by limiting parasite growth via the Th1 response and IFN-γ induction in infected mice (Wang et al., 2018). The upregulation of NLRP3 in Nc-Spain1H-infected cells is consistent with the lower parasite survival of this isolate in macrophages. Expression levels of up-regulated genes from the NF-κB signaling pathway were also higher for macrophages infected with the low virulence isolate, which may explain their higher expression of pro-inflammatory cytokines. In *T. gondii*, differences in the activation of this pathway have shown between parasite types, with type II strains inducing a higher NF-κB activation than type I and III strains, which affects cytokine expression and virulence (Rosowski et al., 2011). This results support those obtained in the phenotypic analysis, where a stronger cellular stimulation induced by Nc-Spain1H was shown, that may activate a more efficient immune response that leads to the control of Nc-Spain1H infection. However the higher induction of pro-inflammatory responses by the low virulence isolate Nc-Spain1H seems to be highly regulated, as higher expression of the regulatory cytokine IL-10 was also observed in cells infected with this isolate. In addition, the Th1 and Th2 differentiation pathway was exclusively enriched for Nc-Spain1H infection. Although it is accepted that in order to confer protection without causing pathology, immunity against neosporosis requires a mixed Th1 and Th2 response (Almería et al., 2017), the adequate balance between both remains to be defined. In our results, genes involved in induction of Th1 responses and those involved in the macrophage polarization towards an M2 phenotype and in the differentiation of Th2 cells were both upregulated in Nc-Spain1H-infected macrophages.

Our results are in agreement with those obtained from an experimental infection of pregnant heifers by Nc-Spain7 and Nc-Spain1H, regarding outcome of infection and local immune responses in the placenta (Jiménez-Pelayo et al., 2019b). In that work is reported that Nc-Spain7 seems not to be detected by PRRs in the placenta at early infection, whose later activation and subsequent exacerbated Th1 response is likely a consequence of lesion development due to parasite proliferation. On the contrary, Nc-Spain1H induced upregulation of PRRs, cytokines, and chemokines genes maintaining a modulation characterized by a balance of Th1/Th2. The authors conclude that rapid immune responses together with a minor proliferation ability of the low virulence isolate may be the causes of the low parasite burden found in placental and fetal tissues of animals infected with this isolate.

Regarding gene expression profiles of Nc-Spain7 and Nc-Spain1H in bovine macrophages, these showed a dichotomy regarding potential immunomodulation functions. Whereas genes implicated in induction of immune responses were found up-regulated in the low virulence isolate, genes potentially involved in evasion of immune responses were found to be up-regulated in Nc-Spain7.

A higher expression of SRS proteins, recognized as the primary surface antigens which may determine the immunogenic potential of the isolates (Lekutis et al., 2001), where found for Nc-Spain1H. Specific SRS proteins identified in the present work differentially expressed between isolates may be useful in future studies focused on vaccine development. For Nc-Spain7, surface-coating molecules associated with immune evasion in *Leishmania spp* (Peters et al., 1997; Depledge et al., 2009; Favila et al., 2015) and glycosylphosphatidylinositols (GPIs), which secreted in the supernatant of *N. caninum* cultures seem to be able to modulate APC immune responses (Débare et al., 2019), were shown highly expressed.

Additionally, differences in the expression of genes potentially involved in parasite dissemination and transmission were found between isolates. The virulent isolate expressed higher levels of a putative cyclophilin and a calreticulin family member. *Neospora caninum* molecules from the cyclophilin family have been shown to work as chemokine-like proteins by inducing chemoattraction of immune cells, which may enhance their invasion by the parasites (Mineo et al., 2010). Because the ability of *N. caninum* to survive in bovine macrophages and induce a hypermigratory phenotype in these cells upon infection has been demonstrated, the higher expression of cyclophilin by Nc-Spain7 may potentially be related to the increased dissemination of this isolate found *in vivo* (Collantes-Fernández et al., 2012; Jiménez-Pelayo et al., 2019b). On the other hand, calreticulin has been demonstrated to be important in trypanosomatids by helping in the establishment of infection by modulating the host complement system (Ramakrishnan and Docampo, 2018) and likely facilitating placental infection by interacting with the maternal classical complement component C1, which would bridge it with the fetal calreticulin in placental tissues (Castillo et al., 2013). The roles of these proteins in *N. caninum* pathogenesis, particularly with regard to differences in the proinflammatory response induced by the isolates during infection *in vitro* and transmission found *in vivo* (Rojo-Montejo et al., 2009b; Regidor-Cerrillo et al., 2014; Jiménez-Pelayo et al., 2019a, 2019b), require further investigation.

In summary, the results of the present Doctoral Thesis indicate that *N. caninum* possess mechanism of evasion of innate immune responses mediated by macrophages, which enables their intracellular survival. These include the reduction of ROS intracellular levels and the impairment of phagolysosome maturation. In addition, the high virulence isolate Nc-Spain7 exhibits a higher ability to evade the host innate immune response via a long time maintenance of reduced ROS levels and a reduction in the expression of pro-inflamatory cytokines including IL-12 and IFN-γ, essential for restraining *N. caninum* proliferation (Hemphill et al., 2006). Higher expression of surface-coating molecules associated with immune evasion may be responsible of the lower recognition of the high virulence isolate by the host's immune response. The consequence would be lower control of parasite survival, which together with its higher proliferation may be associated with the higher virulence and pathology found in vivo. On the other hand, Nc-Spain1H elicits a strong Th1 response likely due to its higher expression of surface antigens (which would reduce the parasite load in host cells) and that would be counterbalanced by a higher expression of regulatory cytokines (such as IL-10), minimizing pathology. This strategy may suggest a better adaptation of the low virulence isolate Nc-Spain1H to be transmitted without causing clinical disease, keeping a delicate balance between suppression and induction of the host immune response to ensure hosting survival and chronic infection.

VII

CONCLUSIONS

CONCLUSIONES

OBJECTIVE I | *In vitro* phenotypic characterization of bovine monocyte-derived macrophages infected with *Neospora caninum* isolates of high and low virulence

First. Bovine peripheral blood monocytes cultured *in vitro* in the presence of GM-CSF present morphological and functional features characteristic of macrophages and they are an adequate model for the study of *N. caninum* interactions with the innate immune system of its natural host.

Second. *Neospora caninum* is able to actively invade bovine macrophages, survive and complete its intracellular lytic cycle, stablishing a replicative niche. However, a lower parasite proliferation rate is recorded with regards to other cell types previously assayed, suggesting a partial capacity of the macrophage to restrain the infection.

Third. Infection of bovine macrophages with viable *N. caninum* tachyzoites represses phagolysosome degradation and reduces intracellular ROS levels at the early stages of infection. Moreover, infected macrophages show an altered antigen presentation mechanism characterized by a lower expression of MHC Class II, CD86 and CD1b. These altered mechanisms could be related to parasite strategies of immune response evasion that may lead to an inability to eliminate the infection by the host.

Fourth. Different host-parasite interaction patterns are observed in bovine macrophages infected with high and low virulence isolates of *N. caninum*, which indicates that both isolates may modulate the immune response in a different manner and may be related with differences in pathogenesis observed *in vivo*.

Fifth. The highly virulent isolate Nc-Spain7 shows higher active invasion rates and proliferation than the low-virulence isolate Nc-Spain1H in bovine macrophages, in agreement with the results obtained in other target cells, which is one of the bases of their differences in virulence.

Sixth. Nc-Spain1H elicits a pro-inflammatory response characterized by elevated IL-12 expression levels and IFN-γ secretion by lymphocytes, which might lead to a better control of this isolate by the immune response, and that is counterbalanced by a high expression of the regulatory cytokine IL-10. This strategy suggests a better adaptation of the low virulence isolate Nc-Spain1H to be transmitted without causing clinical disease, maintaining a delicate balance between suppression and induction of the host immune response, to ensure pregnancy maintenance and fetal chronic infection.

Seventh. Nc-Spain7 exhibits a higher ability to evade the host innate immune response mediated by macrophages, via a long time maintenance of reduced ROS levels and a decrease in the expression of pro-inflammatory cytokines IL-12 and IFN-γ, essential for restraining *N. caninum* proliferation. The inability of the macrophages to mount a protective response against Nc-Spain7 infection together with the high prolificacy of this isolate may explain its higher virulence observed *in vivo*.

Eighth. *Neospora caninum* induces a hypermigratory phenotype in bovine macrophages characterized by hypermotility, enhanced transmigration, abrogated extracellular matrix degradation and rapid cytoskeletal remodeling indicating that bovine macrophages may serve as a vehicle for *N. caninum* systemic dissemination.

Ninth. Induction of migration of parasitized antigen presenting cells are conserved features for *T. gondii* and *N. caninum*, as it was shown with macrophages or dendritic cells from bovine, murine and human origin. It also advocates for the utilization of a Trojan horse mechanism for systemic dissemination as an evolutionary conserved strategy by these two coccidian parasites.

Tenth. Nc-Spain7 induces a higher motility in bovine macrophages, which could suggest a superior capacity to induce migration of these cells. As result, Nc-Spain7 would have a higher ability to disseminate and to rapidly cross cellular barriers, leading to higher parasite tissue burdens, and to reach the central nervous system and the developing fetus.

OBJECTIVE II | Transcriptome modulation of bovine monocyte-derived macrophages by *Neospora caninum* isolates of different virulence

First. Transcriptome analysis has been demonstrated to be a suitable approach for studying *N. caninum* host-parasite interactions in innate immune response target cells.

Second. Gene expression profile after bovine macrophages infection by *N. caninum* shows a metabolic and immune M1 inflammatory phenotype needed for the control of infection. TLRs (TLR2, TLR3 and TLR9) and NLRs (NAIP, NOD2 and NLRC4) seem to be implicated in *N. caninum* recognition and macrophages activation.

Third. *Neospora caninum* activates NF-ƙB in bovine macrophages upon infection, which seems to be the main signaling pathway involved in the response against the parasite and in the upregulation of proinflammatory cytokines TNF-γ, IL-12, IL-1β and IL-6.

Fourth. Apoptosis and degradation by lysosomes are processes repressed by *N. caninum* infection, which may guarantee its survival in bovine macrophages.

Fifth. Nc-Spain1H induces higher expression of genes involved in pathogen recognition, a higher activation NF-ƙB signaling pathway, and an enhanced expression of chemokines and proinflammatory and regulatory cytokines. These findings support the results obtained in the phenotypic analysis. The induction of an early protective response to infection by Nc-Spain1H would contribute to explain the limited infection of placental tissues with no transmission to the fetus observed during early infection with this isolate in a pregnant bovine model.

Sixth. Nc-Spain7 induces a lower immune response by bovine macrophages upon infection. Mechanisms of evasion by Nc-Spain7 support the higher transmission of this isolate to the fetus causing abortion.

Seventh. A dichotomy regarding parasite development and potential immunomodulatory functions was proven in the gene expression profiles of Nc-Spain7 and Nc-Spain1H. Bradyzoite stage-related genes and genes encoding for surface antigens are among the primary up-regulated genes in the Nc-Spain1H isolate, whereas Nc-Spain7 shows an enhanced expression of genes involved in parasite growth, redox homeostasis and immune evasion in activated macrophages.

Eighth. Divergence in gene expression profiling between Nc-Spain7 and Nc-Spain1H correlates with the differences observed between these isolates concerning both *in vitro* proliferation and intracellular survival and macrophage responses.

OBJETIVO I | Caracterización fenotípica *in vitro* de macrófagos bovinos derivados de monocitos infectados con aislados de alta y baja virulencia de *Neospora caninum*.

Primera. Los monocitos bovinos de sangre periférica cultivados *in vitro* en presencia de GM-CSF presentan características morfológicas y funcionales propias de macrófagos y son un modelo adecuado para el estudio de la interacción entre *N. caninum* y el sistema inmunitario innato de su hospedador natural.

Segunda. *Neospora caninum* es capaz de invadir activamente los macrófagos bovinos, sobrevivir y completar su ciclo lítico intracelular estableciendo un nicho de replicación. Sin embargo, presenta una menor tasa de proliferación en relación con otras células estudiadas previamente, lo que sugiere una capacidad parcial del macrófago para limitar la infección.

Tercera. La infección de los macrófagos bovinos con taquizoítos vivos de *N. caninum* reprime la degradación en el fagolisosoma y reduce los niveles intracelulares de ROS en la fase temprana de la infección. Además, los macrófagos infectados muestran una presentación de antígeno modificada caracterizada por una menor expresión de CMH de clase II, CD86 y CD1b. Estos resultados se relacionan con estrategias del parásito para la evasión de la respuesta inmunitaria que pueden conducir a una incapacidad del hospedador de eliminar la infección.

Cuarta. Se observan diferentes patrones de infección en macrófagos bovinos infectados con aislados de alta y baja virulencia de *N. caninum*, lo que indica que ambos aislados podrían modular la respuesta inmunitaria de manera diferente, hecho que podría estar relacionado con las diferencias en virulencia observadas *in vivo*.

Quinta. El aislado de alta virulencia Nc-Spain7 muestra mayores tasas de invasión activa que el aislado de baja virulencia Nc-Spain1H en macrófagos bovinos, en consonancia con los resultados obtenidos en otras células diana, siendo ésta una de las bases de sus diferencias en virulencia.

Sexta. Nc-Spain1H induce una respuesta proinflamatoria caracterizada por elevados niveles de expresión de IL-12 y secreción de IFN-γ por linfocitos, que podría conducir a un mejor control de este aislado por la respuesta inmunitaria, compensado además por una mayor expresión de la citoquina reguladora IL-10. Esta estrategia sugiere una mejor adaptación del aislado de baja virulencia Nc-Spain1H para ser transmitido sin causar lesiones, manteniendo un delicado balance entre inducción y supresión de la respuesta inmunitaria, para asegurar la supervivencia del hospedador y una infección crónica.

Séptima. Nc-Spain7 exhibe una mayor habilidad para evadir la respuesta inmunitaria del hospedador mediada por macrófagos, mediante el mantenimiento a lo largo del tiempo de niveles intracelulares de ROS reducidos y de una disminución en la expresión de citoquinas proinflamatorias IL-12 e IFN-γ, esenciales para limitar la proliferación del parásito. La incapacidad de los macrófagos para generar una respuesta protectora frente a la infección por Nc-Spain7, junto con la elevada prolificidad de este aislado, podría explicar su mayor virulencia *in vivo*.

Octava. *Neospora caninum* induce un fenotipo hipermigratorio en macrófagos bovinos caracterizado por hipermotilidad, aumento en la transmigración, reducción de la degradación de la matriz extracelular y una rápida remodelación del citoesqueleto, indicando que los macrófagos bovinos podrían servir de vehículo para la diseminación sistémica de *N. caninum*.

Novena. La capacidad de modular la migración de células presentadoras de antígeno mediante la infección es una característica conservada entre *T. gondii* y *N. caninum*, como se ha visto para macrófagos o células dendríticas de origen bovino, murino o humano. También aboga por la utilización del mecanismo "Caballo de Troya" para la diseminación sistémica, como una estrategia evolutiva conservada para estos dos parásitos coccidios.

Décima. Nc-Spain7 induce una mayor motilidad en macrófagos bovinos, lo que podría sugerir una capacidad superior de inducir la migración de estas células. Como resultado, Nc-Spain7 podría tener una mayor capacidad para diseminarse y rápidamente cruzar barreras celulares, conduciendo a mayores cargas parasitarias en tejidos y a alcanzar el Sistema Nervioso Central y el feto en desarrollo.

OBJETIVO II | Estudio transcriptómico de la modulación de macrófagos bovinos derivados de monocitos por aislados de *Neospora caninum* de distinta virulencia

Primera. El análisis transcriptómico ha demostrado ser una herramienta apropiada para el estudio de la interacción de *N. caninum* y células de la respuesta inmunitaria innata de su hospedador.

Segunda. El perfil de expresión génica tras la infección de los macrófagos por *N. caninum* muestra un fenotipo metabólico e inmunitario inflamatorio M1, necesario para el control de la infección. Los receptores de tipo TLR (TLR2, TLR3 y TLR9) y de tipo NLR (NAIP, NOD2 y NLRC4), parecen estar implicados en el reconocimiento de *N. caninum* y en la activación de los macrófagos bovinos.

Tercera. La infección por *N. caninum* activa la ruta NF-ƙB en macrófagos bovinos que parece ser la principal ruta de señalización celular involucrada en la respuesta inmunitaria frente al parásito por su hospedador natural y la responsable de la sobreexpresión de citoquinas proinflamatorias TNF-γ, IL-12, IL-1β e IL-6 tras la infección.

Cuarta. La apoptosis y la degradación por lisosomas son procesos reprimidos por la infección por *N. caninum*, que podrían garantizar su supervivencia en macrófagos bovinos.

Quinta. Nc-Spain1H induce una mayor expresión de genes involucrados en el reconocimiento de patógenos, una mayor activación de la ruta de señalización NF-ƙB y un aumento en la expresión de quimioquinas y citoquinas proinflamatorias y reguladoras, que apoyan los resultados obtenidos en el análisis fenotípico. La inducción de una respuesta protectora a la infección por Nc-Spain1H podría explicar que este aislado presente una infección limitada de los tejidos placentarios sin transmisión al feto durante la fase temprana de la infección en un modelo bovino gestante.

Sexta. Nc-Spain7 induce una menor respuesta de los macrófagos bovinos a la infección. La utilización de mecanismos de evasión por el aislado de alta virulencia Nc-Spain7 apoya la mayor transmisión de este aislado al feto causando aborto.

Séptima. Los perfiles de expresión de Nc-Spain7 y Nc-Spain1H mostraron una dicotomía en relación al desarrollo del parásito y a potenciales funciones inmunomoduladoras. Entre los genes sobreexpresados en el aislado Nc-Spain1H destacan los relacionados con la fase de bradizoíto y los que codifican para antígenos de superficie. Por el contrario, el aislado Nc-Spain7 muestra un aumento en la expresión de genes relacionados con el crecimiento, la homeostasis redox y la evasión de la respuesta inmunitaria en macrófagos activados.

Octava. Los diferentes perfiles de expresión génica entre Nc-Spain7 y Nc-Spain1H guardan relación con las diferencias observadas *in vitro* entre estos aislados en proliferación y supervivencia intracelular, y en la inducción de la respuesta inducida en el macrófago bovino.

VIII REFERENCES
BIBLIOGRAFÍA

Abe, C., Tanaka, S., Nishimura, M., Ihara, F., Xuan, X., and Nishikawa, Y. (2015). Role of the chemokine receptor CCR5-dependent host defense system in *Neospora caninum* infections. *Parasite.Vector.* 8, 5.

Abe, C., Tanaka, S., Ihara, F., and Nishikawa, Y. (2014). Macrophage depletion prior to *Neospora caninum* infection results in severe neosporosis in mice. *Clin.Vaccine Immunol.* 21, 1185-8.

Adomako-Ankomah, Y., Wier, G. M., Borges, A. L., Wand, H. E., and Boyle, J. P. (2014). Differential locus expansion distinguishes Toxoplasmatinae species and closely related strains of *Toxoplasma gondii*. *MBio* 5, e01003-13.

Aguado-Martínez, A., Ortega-Mora, L. M., Álvarez-García, G., Rodríguez-Marco, S., Risco-Castillo, V., Marugán-Hernández, V., et al. (2009). Stage-specific expression of Nc SAG4 as a marker of chronic *Neospora caninum* infection in a mouse model. *Parasitology* 136, 757-64.

Ahmed, N.H. (2014). Cultivation of parasites. *Trop.Parasitol.* 4, 80-9.

Al Riyahi, A., Al-Anouti, F., Al-Rayes, M., and Ananvoranich, S. (2006). Single argonaute protein from *Toxoplasma gondii* is involved in the double-stranded RNA induced gene silencing. *Int.J.Parasitol.* 36, 1003-14.

Alaeddine, F., Hemphill, A., Debache, K., and Guionaud, C. (2013). Molecular cloning and characterization of NcROP2Fam-1, a member of the ROP2 family of rhoptry proteins in *Neospora caninum* that is targeted by antibodies neutralizing host cell invasion in vitro. *Parasitology* 140, 1033-50.

Almeria, S., Serrano-Pérez, B., Darwich, L., Mur-Novales, R., Garcia-Ispierto, I., Cabezón, O., et al. (2016a). Cytokine gene expression in aborting and non-aborting dams and in their foetuses after experimental infection with *Neospora caninum* at 110 days of gestation. *Vet.Parasitol.* 227, 138-42.

Almería, S., López-Gatius, F. (2015). Markers related to the diagnosis and to the risk of abortion in bovine neosporosis. *Res.Vet.Sci.* 100, 169-75.

Almeria, S., Serrano-Pérez, B., Darwich, L., Araujo, R., Lopez-Gatius, F., Dubey, J., et al. (2014). Maternal and fetal immune response patterns in heifers experimentally infected with *Neospora caninum* in the second trimester of pregnancy–A descriptive study. *Vet.Parasitol.* 204, 146-52.

Almería, S., Serrano-Perez, B., Darwich, L., Domingo, M., Mur-Novales, R., Regidor-Cerrillo, J., et al. (2016b). Foetal death in naive heifers inoculated with *Neospora caninum* isolate Nc-Spain7 at 110 days of pregnancy. *Exp. Parasitol.* 168, 62-9.

Almería, S., Araujo, R., Tuo, W., López-Gatius, F., Dubey, J. P., and Gasbarre, L. C. (2010). Fetal death in cows experimentally infected with *Neospora caninum* at 110 days of gestation. *Vet.Parasitol.* 45, 10.

Almería, S., De Marez, T., Dawson, H., Araujo, R., Dubey, J. P., and Gasbarre, L. C. (2003). Cytokine gene expression in dams and foetuses after experimental *Neospora caninum* infection of heifers at 110 days of gestation. *Parasite Immunol.* 25, 383-92.

Almería, S.,López-Gatius, F. (2013). Bovine neosporosis: Clinical and practical aspects. *Res.Vet.Sci.* 95, 303-9.

Almería, S, Serrano-Pérez, B, and López-Gatius, F. (2017) Immune response in bovine neosporosis: Protection or contribution to the pathogenesis of abortion. *Microb. Pathog.* 109.

Álvarez-García, G., Pitarch, A., Zaballos, A., Fernández-García, A., Gil, C., Gómez-Bautista, M., et al. (2007). The NcGRA7 gene encodes the immunodominant 17 kDa antigen of *Neospora caninum*. *Parasitology* 134, 41-50.

Alves, L.R.,Goldenberg, S. (2016). RNA-binding proteins related to stress response and differentiation in protozoa. *World J.Biol.Chem.* 7, 78-87.

Anders, S.,Huber, W. (2010). Differential expression analysis for sequence count data. *Genome Biol.* 11, R106.

Anders, S., Pyl, P. T., and Huber, W. (2015). HTSeq—a Python framework to work with high-throughput sequencing data. *Bioinformatics* 31, 166-9.

Anderson, M.Z., Brewer, J., Singh, U., and Boothroyd, J. C. (2009). A pseudouridine synthase homologue is critical to cellular differentiation in *Toxoplasma gondii*. *Eukaryot.Cell.* 8, 398-409.

Andrianarivo, A.G., Anderson, M. L., Rowe, J. D., Gardner, I. A., Reynolds, J. P., Choromanski, L., et al. (2005). Immune responses during pregnancy in heifers naturally infected with *Neospora caninum* with and without immunization. *Parasitol.Res.* 96, 24-31.

Arrizabalaga, G., Ruiz, F., Moreno, S., and Boothroyd, J. C. (2004). Ionophore-resistant mutant of *Toxoplasma gondii* reveals involvement of a sodium/hydrogen exchanger in calcium regulation. *J.Cell Biol.* 165, 653-62.

Atkinson, R., Harper, P. A., Ryce, C., Morrison, D. A., and Ellis, J. T. (1999). Comparison of the biological characteristics of two isolates of *Neospora caninum*. *Parasitology* 118 (Pt 4), 363-70.

Bacigalupe, D., Basso, W., Caspe, S. G., More, G., Lischinsky, L., Gos, M. L., et al. (2013). *Neospora caninum* NC-6 Argentina induces fetopathy in both serologically positive and negative experimentally inoculated pregnant dams. *Parasitol.Res.* 112, 2585-92.

Balboa, L., Romero, M. M., Yokobori, N., Schierloh, P., Geffner, L., Basile, J. I., et al. (2010). *Mycobacterium tuberculosis* impairs dendritic cell response by altering CD1b, DC-SIGN and MR profile. *Immunol.Cell Biol.* 88, 716-26.

Barber, J.S., Holmdahl, O. J., Owen, M. R., Guy, F., Uggla, A., and Trees, A. J. (1995). Characterization of the first European isolate of *Neospora caninum*. *Parasitology* 111, 563-8.

Barr, B.C., Rowe, J. D., Sverlow, K. W., BonDurant, R. H., Ardans, A. A., Oliver, M. N., et al. (1994). Experimental reproduction of bovine fetal *Neospora infection* and death with a bovine *Neospora* isolate. *J.Vet.Diag.Invest.* 6, 207-15.

Barragan, A., Sibley, L. D. (2002). Transepithelial migration of *Toxoplasma gondii* is linked to parasite motility and virulence. *J.Exp.Med.* 195, 1625-33.

Bartels, C.J., van, S. G., Veldhuisen, J. P., van, d. B., Wouda, W., and Dijkstra, T. (2006). Effect of *Neospora caninum*-serostatus on culling, reproductive performance and milk production in Dutch dairy herds with and without a history of *Neospora caninum*-associated abortion epidemics. *Prev.Vet.Med.* 77, 186-98.

Bartley PM, M., Wright SE, M., Maley SW, D., Macaldowie CN, D., Nath, M. D., Hamilton CM, D., et al. (2012). Maternal and foetal immune responses of cattle following an experimental challenge with *Neospora caninum* at day 70 of gestation. *Vet.Res.* 43, 38.

Bartley, P.M., Katzer, F., Rocchi, M. S., Maley, S. W., Benavides, J., Nath, M., et al. (2013). Development of maternal and foetal immune responses in cattle following experimental challenge with *Neospora caninum* at day 210 of gestation. *Vet.Res.* 44, 91.

Basso, W., Schares, S., Barwald, A., Herrmann, D. C., Conraths, F. J., Pantchev, N., et al. (2009). Molecular comparison of *Neospora caninum* oocyst isolates from naturally infected dogs with cell culture-derived tachyzoites of the same isolates using nested polymerase chain reaction to amplify microsatellite markers. *Vet.Parasitol.* 160, 43-50.

Basso, W., Schares, S., Minke, L., Barwald, A., Maksimov, A., Peters, M., et al. (2010). Microsatellite typing and avidity analysis suggest a common source of infection in herds with epidemic *Neospora caninum*-associated bovine abortion. *Vet.Parasitol.* 173, 24-31. doi:10.1016/j.vetpar.2010.06.009.

Basso, W., Venturini, L., Venturini, M. C., Hill, D. E., Kwok, O. C., Shen, S. K., et al. (2001). First isolation of *Neospora caninum* from the feces of a naturally infected dog. *J.Parasitol.* 87, 612-8.

Baszler, T.V., Long, M. T., McElwain, T. F., and Mathison, B. A. (1999). Interferon-gamma and interleukin-12 mediate protection to acute *Neospora caninum* infection in BALB/c mice. *Int.J.Parasitol.* 29, 1635-46.

Beck, H, Blake, D, Dardé, M, Felger, I, Pedraza-Díaz, S, Regidor-Cerrillo, J, et al. (2009). Molecular approaches to diversity of populations of apicomplexan parasites. *Int.Journ.Parasit.* 39:2. doi:10.1016/j.ijpara.2008.10.001.

Becker, I., Salaiza, N., Aguirre, M., Delgado, J., Carrillo-Carrasco, N., Kobeh, L. G., et al. (2003). *Leishmania* lipophosphoglycan (LPG) activates NK cells through toll-like receptor-2. *Mol.Biochem.Parasitol.* 130, 65-74.

Beiting, D.P., Peixoto, L., Akopyants, N. S., Beverley, S. M., Wherry, E. J., Christian, D. A., et al. (2014). Differential induction of TLR3-dependent innate immune signaling by closely related parasite species. *PloS one* 9, e88398.

Benavides, J., Collantes-Fernandez, E., Ferre, I., Perez, V., Campero, C., Mota, R., et al. (2014). Experimental ruminant models for bovine neosporosis: what is known and what is needed. *Parasitology* 141, 1471-88.

Benavides, J., Katzer, F., Maley, S. W., Bartley, P. M., Canton, G., Palarea-Albaladejo, J., et al. (2012). High rate of transplacental infection and transmission of *Neospora caninum* following experimental challenge of cattle at day 210 of gestation. *Vet.Res.* 43, 83.

Benjamini, Y.,Hochberg, Y. (1995). Controlling the false discovery rate: a practical and powerful approach to multiple testing. *J.R.Stat.Soc. B (Methodological)* 57, 289-300.

Berry, L., Chen, C., Reininger, L., Carvalho, T. G., El Hajj, H., Morlon-Guyot, J., et al. (2016). The conserved apicomplexan Aurora kinase TgArk3 is involved in endodyogeny, duplication rate and parasite virulence. *Cell. Microbiol.* 18, 1106-20.

Besteiro, S. (2015). *Toxoplasma* control of host apoptosis: the art of not biting too hard the hand that feeds you. *Microb.Cell.* 2, 178-81.

Bhandage, A. K., Kanatani, S., & Barragan, A. (2019). *Toxoplasma*-Induced Hypermigration of Primary Cortical Microglia Implicates GABAergic Signaling. *Front.Cell.Infect.Microb*. 9, 73.

Biddau, M., Bouchut, A., Major, J., Saveria, T., Tottey, J., Oka, O., et al. (2018). Two essential Thioredoxins mediate apicoplast biogenesis, protein import, and gene expression in *Toxoplasma gondii*. *PLoS pathogens* 14, e1006836.

Bortoluci, K.R.,Medzhitov, R. (2010). Control of infection by pyroptosis and autophagy: role of TLR and NLR. *Cell. Mol.Life Sci.* 67, 1643-51.

Bosch, S.S., Kronenberger, T., Meissner, K. A., Zimbres, F. M., Stegehake, D., Izui, N. M., et al. (2015). Oxidative stress control by apicomplexan parasites. *Biomed.Res.Int.* 2015, 351289.

Boucher, E., Marin, M., Holani, R., Young-Speirs, M., Moore, D., and Cobo, E. (2018). Characteristic pro-inflammatory cytokines and host defence cathelicidin peptide produced by human monocyte-derived macrophages infected with *Neospora caninum*. *Parasitology* 145, 871-84.

Boucher, L.E., Bosch, J. (2015). The apicomplexan glideosome and adhesins - Structures and function. *J.Struct.Biol.* 190, 93-114.

Bourbon, H. (2008). Comparative genomics supports a deep evolutionary origin for the large, four-module transcriptional mediator complex. *Nucleic Acids Res.* 36, 3993-4008.

Boysen, P., Klevar, S., Olsen, I., and Storset, A. K. (2006). The protozoan *Neospora caninum* directly triggers bovine NK cells to produce gamma interferon and to kill infected fibroblasts. *Infect.Immun.* 74, 953-60.

Brasil, T.R., Freire-de-Lima, C. G., Morrot, A., and Vetö Arnholdt, A. C. (2017). Host-*Toxoplasma gondii* coadaptation leads to fine tuning of the immune response. *Front.Immunol.* 8, 1080.

Broderick, S, Rehmet, K, Concannon, C, and Nasheuer, H. (2001). Eukaryotic single-stranded DNA binding proteins: central factors in genome stability. *Subcell.Biochem*. 50:143-63.

Brooks, C.F., Johnsen, H., van Dooren, G. G., Muthalagi, M., Lin, S. S., Bohne, W., et al. (2010). The *Toxoplasma* apicoplast phosphate translocator links cytosolic and apicoplast metabolism and is essential for parasite survival. *Cell.Host Microbe* 7, 62-73.

Butcher, B.A., Denkers, E. Y. (2002). Mechanism of entry determines the ability of *Toxoplasma gondii* to inhibit macrophage proinflammatory cytokine production. *Infect.Immun.* 70, 5216-24.

Bystry, R.S., Aluvihare, V., Welch, K. A., Kallikourdis, M., and Betz, A. G. (2001). B cells and professional APCs recruit regulatory T cells via CCL4. *Nat.Immunol.* 2, 1126-32.

Calarco, L., Barratt, J., and Ellis, J. (2018). Genome wide identification of mutational hotspots in the apicomplexan parasite *Neospora caninum* and the implications for virulence. *Genome Biol.Evol.* 10, 2417-31.

Calero-Bernal, R., Horcajo, P., Hernandez, M., Ortega-Mora, L. M., and Fuentes, I. (2019). Absence of *Neospora caninum* DNA in Human Clinical Samples, Spain. *Emerg.Infect.Dis.* 25, 1226-7.

Cao, L., Fetterer, R., Qu, G., Zhang, X., and Tuo, W. (2019). *Neospora caninum* cytoplasmic dynein LC8 light chain 2 (NcDYNLL2) is differentially produced by pathogenically distinct isolates and regulates the host immune response. *Parasitology* 146, 588-95.

Carl, J.W.,Bai, X. F. (2008). IL27: its roles in the induction and inhibition of inflammation. *Int.J.Clin.Exp.Pathol.* 1, 117-23.

Caspe, S.G., Moore, D. P., Leunda, M. R., Cano, D. B., Lischinsky, L., Regidor-Cerrillo, J., et al. (2012). The *Neospora caninum*-Spain 7 isolate induces placental damage, fetal death and abortion in cattle when inoculated in early gestation. *Vet.Parasitol.* 189, 171-81.

Castillo, C., Ramírez, G., Valck, C., Aguilar, L., Maldonado, I., Rosas, C., et al. (2013). The interaction of classical complement component C1 with parasite and host calreticulin mediates *Trypanosoma cruzi* infection of human placenta. *PLoS Negl.Trop.Dis.* 7, e2376.

Cerritelli, S.M.,Crouch, R. J. (2009). Ribonuclease H: the enzymes in eukaryotes. *The FEBS journal* 276, 1494-505.

Chandramohanadas, R., Davis, P. H., Beiting, D. P., Harbut, M. B., Darling, C., Velmourougane, G., et al. (2009). Apicomplexan parasites co-opt host calpains to facilitate their escape from infected cells. *Science* 324, 794-7.

Charette, M.,Gray, M. W. (2000). Pseudouridine in RNA: what, where, how, and why. *IUBMB Life* 49, 341-51.

Cherry, A.A., Ananvoranich, S. (2014). Characterization of a homolog of DEAD-box RNA helicases in *Toxoplasma gondii* as a marker of cytoplasmic mRNP stress granules. *Gene* 543, 34-44.

Chesnokov, I.N. (2007). Multiple functions of the origin recognition complex. *Int.Rev.Cytol.* 256, 69-109.

Chu, J.Q., Shi, G., Fan, Y. M., Choi, I. W., Cha, G. H., Zhou, Y., et al. (2016). Production of IL-1beta and Inflammasome with Up-Regulated Expressions of NOD-Like Receptor Related Genes in *Toxoplasma gondii*-Infected THP-1 Macrophages. *Korean J.Parasitol.* 54, 711-7.

Cipollone, R., Ascenzi, P., and Visca, P. (2007). Common themes and variations in the rhodanese superfamily. *IUBMB Life* 59, 51-9.

Clarke, D.J.,Giménez-Abián, J. F. (2000). Checkpoints controlling mitosis. *Bioessays* 22, 351-63.

Clay, G.M., Sutterwala, F. S., and Wilson, M. E. (2014). NLR proteins and parasitic disease. *Immunol.Res.* 59, 142-52.

Collantes-Fernández, E., Arnaiz-Seco, I., Burgos, B. M., Rodríguez-Bertos, A., Aduriz, G., Fernández-García, A., et al. (2006). Comparison of *Neospora caninum* distribution, parasite loads and lesions between epidemic and endemic bovine abortion cases. *Vet.Parasitol.* 142, 187-91.

Collantes-Fernández, E., Arrighi, R. B., Álvarez-García, G., Weidner, J. M., Regidor-Cerrillo, J., Boothroyd, J. C., et al. (2012). Infected dendritic cells facilitate systemic dissemination and transplacental passage of the obligate intracellular parasite *Neospora caninum* in mice. *PLoS One* 7, e32123.

Collantes-Fernández, E., Rodríguez-Bertos, A., Arnaiz-Seco, I., Moreno, B., Aduriz, G., and Ortega-Mora, L. M. (2006). Influence of the stage of pregnancy on *Neospora caninum* distribution, parasite loads and lesions in aborted bovine foetuses. *Theriogenology* 65, 629-41.

Collantes-Fernández, E., Zaballos, A., Álvarez-García, G., and Ortega-Mora, L. M. (2002). Quantitative detection of *Neospora caninum* in bovine aborted fetuses and experimentally infected mice by real-time PCR. *J.Clin.Microbiol.* 40, 1194-8.

Conrad, P.A., Sverlow, K., Anderson, M., Rowe, J., BonDurant, R., Tuter, G., et al. (1993). Detection of serum antibody responses in cattle with natural or experimental *Neospora* infections. *J.Vet.Diagn.Invest.* 5, 572-8.

Copeland, R.A., Solomon, M. E., and Richon, V. M. (2009). Protein methyltransferases as a target class for drug discovery. *Nat.Rev.Drug Discov.* 8:724-32.

Coppens, I. (2013). Targeting lipid biosynthesis and salvage in apicomplexan parasites for improved chemotherapies. *Nat.Rev.Microbiol.* 11: 823.

Courret, N., Darche, S., Sonigo, P., Milon, G., Buzoni-Gatel, D., and Tardieux, I. (2006). CD11c- and CD11b-expressing mouse leukocytes transport single *Toxoplasma gondii* tachyzoites to the brain. *Blood* 107, 309-16.

Coutinho, P.M., Deleury, E., Davies, G. J., and Henrissat, B. (2003). An evolving hierarchical family classification for glycosyltransferases. *J.Mol.Biol.* 328, 307-17.

Cui, J., Zhu, L., Xia, X., Wang, H. Y., Legras, X., Hong, J., et al. (2010). NLRC5 negatively regulates the NF-κB and type I interferon signaling pathways. *Cell* 141, 483-96.

Cuteri, V., Nisoli, L., Preziuso, S., Attili, A., Guerra, C., Lulla, D., et al. (2005). Application of a new therapeutic protocol against *Neospora caninum*-induced abortion in cattle: a field study. *J.Anim.Vet.Adv.* 4, 510-4.

Daher, W., Oria, G., Fauquenoy, S., Cailliau, K., Browaeys, E., Tomavo, S., et al. (2007). A *Toxoplasma gondii* leucine-rich repeat protein binds phosphatase type 1 protein and negatively regulates its activity. *Eukaryot.Cell.* 6, 1606-17.

Dalmasso, M.C., Onyango, D. O., Naguleswaran, A., Sullivan Jr, W. J., and Angel, S. O. (2009). *Toxoplasma* H2A variants reveal novel insights into nucleosome composition and functions for this histone family. *J.Mol.Biol.* 392, 33-47.

Darwich, L., Li, Y., Serrano-Pérez, B., Mur-Novales, R., Garcia-Ispierto, I., Cabezón, O., et al. (2016). Maternal and foetal cytokine production in dams naturally and experimentally infected with *Neospora caninum* on gestation day 110. *Res.Vet.Sci.* 107, 55-61.

Das, M., Singh, S., Pradhan, S., and Narayan, G. (2014). MCM Paradox: Abundance of Eukaryotic Replicative Helicases and Genomic Integrity. *Mol.Biol.Int.* 2014, 574850. doi:10.1155/2014/574850.

Davoli-Ferreira, M., Fonseca, D. M., Mota, C. M., Dias, M. S., Lima-Junior, D. S., da Silva, M. V., et al. (2016). Nucleotide-binding oligomerization domain-containing protein 2 prompts potent inflammatory stimuli during *Neospora caninum* infection. *Sci.Rep.* 6, 29289.

De Marez, T., Liddell, S., Dubey, J. P., Jenkins, M. C., and Gasbarre, L. (1999). Oral infection of calves with *Neospora caninum* oocysts from dogs: humoral and cellular immune responses. *Int.J.Parasitol.* 29, 1647-57.

de Yaniz, M.G., Moore, D. P., Odeon, A. C., Cano, A., Cano, D. B., Leunda, M. R., et al. (2007). Humoral immune response in pregnant heifers inoculated with *Neospora caninum* tachyzoites by conjunctival route. *Vet.Parasitol.* 148, 213-8.

Débare, H., Schmidt, J., Moiré, N., Ducournau, C., Paguay, Y. D. A., Schwarz, R. T., et al. (2019). *In vitro* cellular responses to *Neospora caninum* glycosylphosphatidylinositols depend on the host origin of antigen presenting cells. *Cytokine* 119, 119-28.

Dellarupe, A., Regidor-Cerrillo, J., Jimenez-Ruiz, E., Schares, G., Unzaga, J. M., Venturini, M. C., et al. (2014b). Clinical outcome and vertical transmission variability among canine *Neospora caninum* isolates in a pregnant mouse model of infection. *Parasitology* 141, 356-66..

Dellarupe, A., Regidor-Cerrillo, J., Jimenez-Ruiz, E., Schares, G., Unzaga, J. M., Venturini, M. C., et al. (2014a). Comparison of host cell invasion and proliferation among *Neospora caninum* isolates obtained from oocysts and from clinical cases of naturally infected dogs. *Exp.Parasitol.* 145, 22-8.

Deng, W.,Roberts, S. G. (2006). Core promoter elements recognized by transcription factor IIB. *Biochem.Soc.Trans.* 34, 1051-3.

Denkers, E.Y.,Butcher, B. A. (2005). Sabotage and exploitation in macrophages parasitized by intracellular protozoans. *Trends Parasitol.* 21, 35-41.

Depledge, D.P., Evans, K. J., Ivens, A. C., Aziz, N., Maroof, A., Kaye, P. M., et al. (2009). Comparative expression profiling of *Leishmania*: modulation in gene expression between species and in different host genetic backgrounds. *PLoS Negl.Trop.Dis.* 3, e476.

Dion, S., Germon, S., Guiton, R., Ducournau, C., and Dimier-Poisson, I. (2011). Functional activation of T cells by dendritic cells and macrophages exposed to the intracellular parasite *Neospora caninum*. *Int.J.Parasitol.* 41, 685-95.

Diskin, C.,Palsson-McDermott, E. M. (2018). Metabolic modulation in macrophage effector function. *Front.Immunol.* 9, 270.

Dixon, S.E., Stilger, K. L., Elias, E. V., Naguleswaran, A., and Sullivan Jr, W. J. (2010). A decade of epigenetic research in *Toxoplasma gondii*. *Mol.Biochem.Parasitol.* 173, 1-9.

Donahoe, S.L., Lindsay, S. A., Krockenberger, M., Phalen, D., and Slapeta, J. (2015). A review of neosporosis and pathologic findings of *Neospora caninum* infection in wildlife. *Int.J.Parasitol.Parasites Wildl.* 4, 216-38.

Du, J., An, R., Chen, L., Shen, Y., Chen, Y., Cheng, L., et al. (2014). *Toxoplasma gondii* virulence factor ROP18 inhibits the host NF-kappaB pathway by promoting p65 degradation. *J.Biol.Chem.* 289, 12578-92.

Dubey, J, Hemphill, A, Calero-Bernal, R, and Schares, G. *Neosporosis in animals* CRC Press (2017).

Dubey, J.,Schares, G. (2011). Neosporosis in animals—the last five years. *Vet.Parasitol.* 180, 90-108.

Dubey, J.P., Buxton, D., and Wouda, W. (2006). Pathogenesis of bovine neosporosis. *J.Comp.Pathol.* 134, 267-89.

Dubey, J.P., Carpenter, J. L., Speer, C. A., Topper, M. J., and Uggla, A. (1988). Newly recognized fatal protozoan disease of dogs. *J.Am.Vet.Med.Assoc.* 192, 1269-85.

Dubey, J.P.,Schares, G. (2006). Diagnosis of bovine neosporosis. *Vet.Parasitol.* 140, 1-34.

Dubey, J.P., Schares, G., and Ortega-Mora, L. M. (2007). Epidemiology and control of neosporosis and *Neospora caninum*. *Clin.Microbiol.Rev.* 20, 323-67.

Ehrenkaufer, G.M., Hackney, J. A., and Singh, U. (2009). A developmentally regulated Myb domain protein regulates expression of a subset of stage□specific genes in *Entamoeba histolytica*. *Cell.Microbiol.* 11, 898-910.

Ehrenman, K., Sehgal, A., Lige, B., Stedman, T. T., Joiner, K. A., and Coppens, I. (2010). Novel roles for ATP□binding cassette G transporters in lipid redistribution in *Toxoplasma*. *Mol.Microbiol.* 76, 1232-49.

Eiras, C., Arnaiz, I., Álvarez-García, G., Ortega-Mora, L. M., Sanjuanl, M. L., Yus, E., et al. (2011). *Neospora caninum* seroprevalence in dairy and beef cattle from the northwest region of Spain, Galicia. *Prev.Vet.Med.* 98, 128-32.

English, C.M., Adkins, M. W., Carson, J. J., Churchill, M. E., and Tyler, J. K. (2006). Structural basis for the histone chaperone activity of Asf1. *Cell* 127, 495-508.

Escotte-Binet, S., Huguenin, A., Aubert, D., Martin, A. P., Kaltenbach, M., Florent, I., et al. (2018). Metallopeptidases of *Toxoplasma gondii*: in silico identification and gene expression. *Parasite* 25, 26.

Favila, M.A., Geraci, N. S., Jayakumar, A., Hickerson, S., Mostrom, J., Turco, S. J., et al. (2015). Differential impact of LPG-and PG-deficient *Leishmania major* mutants on the immune response of human dendritic cells. *PLoS Negl.Trop.Dis.* 9, e0004238.

Feng, X., Zhang, N., and Tuo, W. (2010). *Neospora caninum* tachyzoite- and antigen-stimulated cytokine production by bone marrow-derived dendritic cells and spleen cells of naive BALB/c mice. *J.Parasitol.* 96, 717-23.

Fenoy, I.M., Bogado, S. S., Contreras, S. M., Gottifredi, V., and Angel, S. O. (2016). The knowns unknowns: exploring the homologous recombination repair pathway in *Toxoplasma gondii*. *Front.Microb.* 7, 627.

Fereig, R.M., Shimoda, N., Abdelbaky, H. H., Kuroda, Y., and Nishikawa, Y. (2019). *Neospora* GRA6 possesses immune-stimulating activity and confers efficient protection against *Neospora caninum* infection in mice. *Vet. Parasitol.* 267, 61-8.

Fernández-García, A., Risco-Castillo, V., Zaballos, A., Álvarez-García, G., and Ortega-Mora, L. M. (2006). Identification and molecular cloning of the *Neospora caninum* SAG4 gene specifically expressed at bradyzoite stage. *Mol. Biochem.Parasitol.* 146, 89-97.

Ferre, I., Serrano-Martínez, E., Martínez, A., Osoro, K., Mateos-Sanz, A., Del-Pozo, I., et al. (2008). Effects of re-infection with *Neospora caninum* in bulls on parasite detection in semen and blood and immunological responses. *Theriogenology* 69, 905-11.

Flynn, R.J.,Marshall, E. S. (2011). Parasite limiting macrophages promote IL-17 secretion in naive bovine CD4 T-cells during *Neospora caninum* infection. *Vet.Immunol.Immunopathol.* 144, 423-9.

Frankel, M.B.,Knoll, L. J. (2008). Functional analysis of key nuclear trafficking components reveals an atypical Ran network required for parasite pathogenesis. *Mol.Microbiol.* 70, 410-20.

Freist, W., Verhey, J. F., Ruhlmann, A., Gauss, D. H., and Arnez, J. G. (1999). Histidyl-tRNA synthetase. *Biol.Chem.* 380, 623-46.

French, N.P., Clancy, D., Davison, H. C., and Trees, A. J. (1999). Mathematical models of *Neospora caninum* infection in dairy cattle: transmission and options for control. *Int.J.Parasitol.* 29, 1691-704.

Frey, C.F., Regidor-Cerrillo, J., Marreros, N., García-Lunar, P., Gutiérrez-Expósito, D., Schares, G., et al. (2016). *Besnoitia besnoiti* lytic cycle in vitro and differences in invasion and intracellular proliferation among isolates. *Parasit.Vectors.* 9, 1.

Fuks, J.M., Arrighi, R. B., Weidner, J. M., Mendu, S. K., Jin, Z., Wallin, R. P., et al. (2012). GABAergic signaling is linked to a hypermigratory phenotype in dendritic cells infected by *Toxoplasma gondii*. *PLoS Pathog.* 8, e1003051.

Fung, C., Beck, J. R., Robertson, S. D., Gubbels, M., and Bradley, P. J. (2012). *Toxoplasma* ISP4 is a central IMC sub-compartment protein whose localization depends on palmitoylation but not myristoylation. *Mol.Biochem. Parasitol.* 184, 99-108.

García-Sánchez, M., Jiménez-Pelayo, L., Horcajo, P., Regidor-Cerrillo, J., Ólafsson, E. B., Bhandage, A. K., et al. (2019). Differential responses of bovine monocyte-derived macrophages to infection by *Neospora caninum* isolates of high and low virulence. *Front.Immunol.* 10, 915.

Garrison, E., Treeck, M., Ehret, E., Butz, H., Garbuz, T., Oswald, B. P., et al. (2012). A forward genetic screen reveals that calcium-dependent protein kinase 3 regulates egress in *Toxoplasma*. *PLoS Pathog.* 8, e1003049.

Gibney, E.H., Kipar, A., Rosbottom, A., Guy, C. S., Smith, R. F., Hetzel, U., et al. (2008). The extent of parasite-associated necrosis in the placenta and foetal tissues of cattle following *Neospora caninum* infection in early and late gestation correlates with foetal death. *Int.J.Parasitol.* 38, 579-88.

Glaser, S., van Dooren, G. G., Agrawal, S., Brooks, C. F., McFadden, G. I., Striepen, B., et al. (2012). Tic22 is an essential chaperone required for protein import into the apicoplast. *J.Biol.Chem.* 287, 39505-12.

Gondim, L.F., Laski, P., Gao, L., and McAllister, M. M. (2004). Variation of the internal transcribed spacer 1 sequence within individual strains and among different strains of *Neospora caninum* . *J.Parasitol.* 90, 119-22.

Gondim, L.F., Pinheiro, A. M., Santos, P. O., Jesus, E. E., Ribeiro, M. B., Fernandes, H. S., et al. (2001). Isolation of *Neospora caninum* from the brain of a naturally infected dog, and production of encysted bradyzoites in gerbils. *Vet.Parasitol.* 101, 1-7.

Gondim, L.F.P., Gao, L., and McAllister, M. M. (2002). Improved production of *Neospora caninum* oocysts, cyclical oral transmission between dogs and cattle, and *in vitro* isolation from oocysts. *J.Parasitol.* 88, 1159-63.

Gonzalez-Warleta, M., Castro-Hermida, J. A., Carro-Corral, C., Cortizo-Mella, J., and Mezo, M. (2007). Epidemiology of neosporosis in dairy cattle in Galicia (NW Spain). *Parasitol.Res.* 102, 243-249.

Goodswen, S., Kennedy, P., and Ellis, J. T. (2012). A review of the infection, genetics, and evolution of *Neospora caninum*: from the past to the present. *Infect.Genet.Evol.* 13, 133-150.

Gordon, J.L.,Sibley, L. D. (2005). Comparative genome analysis reveals a conserved family of actin-like proteins in apicomplexan parasites. *BMC Genomics* 6, 179.

Grohmann, U., Mondanelli, G., Belladonna, M. L., Orabona, C., Pallotta, M. T., Iacono, A., et al. (2017). Amino-acid sensing and degrading pathways in immune regulation. *Cytokine Growth Factor Rev.* 35, 37-45.

Gubbels, M., Lehmann, M., Muthalagi, M., Jerome, M. E., Brooks, C. F., Szatanek, T., et al. (2008). Forward genetic analysis of the apicomplexan cell division cycle in *Toxoplasma gondii*. *PLoS Pathog.* 4, e36.

Guerini, M.N., Behnke, M. S., and White, M. W. (2005). Biochemical and genetic analysis of the distinct proliferating cell nuclear antigens of *Toxoplasma gondii*. *Mol.Biochem.Parasitol.* 142, 56-65.

Guido, S., Katzer, F., Nanjiani, I., Milne, E., and Innes, E. A. (2016). Serology-based diagnostics for the control of bovine neosporosis. *Trends Parasitol.* 32, 131-43.

Gurung, P.,Kanneganti, T. (2016). Immune responses against protozoan parasites: a focus on the emerging role of Nod-like receptors. *Cell.Mol.Life Sci.* 73, 3035-51.

Guy, C.S., Williams, D. J. L., Kelly, D. F., McGarry, J. W., Guy, F., Bjorkman, C., et al. (2001). *Neospora caninum* in persistently infected, pregnant cows: spontaneous transplacental infection is associated with an acute increase in maternal antibody. *Vet.Rec.* 149, 443-9.

Haque, S.J., Majumdar, T., and Barik, S. (2012). Redox-assisted protein folding systems in eukaryotic parasites. *Antioxid.Redox Signal.* 17, 674-83.

Hasler, B., Regula, G., Stark, K. D., Sager, H., Gottstein, B., and Reist, M. (2006). Financial analysis of various strategies for the control of *Neospora caninum* in dairy cattle in Switzerland. *Prev.Vet.Med.* 77, 230-53.

Hay, W.H., Shell, L. G., Lindsay, D. S., and Dubey, J. P. (1990). Diagnosis and treatment of *Neospora caninum* infection in a dog. *J.Am.Vet.Med.Assoc.* 197, 87-9.

He, X., Gong, P., Wei, Z., Liu, W., Wang, W., Li, J., et al. (2017). Peroxisome proliferator-activated receptor-γ-mediated polarization of macrophages in *Neospora caninum* infection. *Exp.Parasitol.* 178, 37-44.

Heaslip, A.T., Leung, J. M., Carey, K. L., Catti, F., Warshaw, D. M., Westwood, N. J., et al. (2010). A small-molecule inhibitor of T. gondii motility induces the posttranslational modification of myosin light chain-1 and inhibits myosin motor activity. *PLoS Pathog.* 6, e1000720..

Heaslip, A.T., Nishi, M., Stein, B., and Hu, K. (2011). The motility of a human parasite, *Toxoplasma gondii,* is regulated by a novel lysine methyltransferase. *PLoS Pathog.* 7, e1002201.

Hecker, Y.P., Coceres, V., Wilkowsky, S. E., Jaramillo Ortiz, J. M., Morrell, E. L., Verna, A. E., et al. (2014). A *Neospora caninum* vaccine using recombinant proteins fails to prevent foetal infection in pregnant cattle after experimental intravenous challenge. *Vet.Immunol.Immunopathol.* 162, 142-53.

Hecker, Y.P., Moore, D. P., Quattrocchi, V., Regidor-Cerrillo, J., Verna, A., Leunda, M. R., et al. (2013). Immune response and protection provided by live tachyzoites and native antigens from the NC-6 Argentina strain of *Neospora caninum* in pregnant heifers. *Vet.Parasitol.* 197, 436-46.

Hehl, A.B., Basso, W. U., Lippuner, C., Ramakrishnan, C., Okoniewski, M., Walker, R. A., et al. (2015). Asexual expansion of *Toxoplasma gondii* merozoites is distinct from tachyzoites and entails expression of non-overlapping gene families to attach, invade, and replicate within feline enterocytes. *BMC Genomics* 16, 66,015-1225-x.

Hemphill, A., Aguado-Martínez, A., Müller, J. (2015). Approaches for the vaccination and treatment of *Neospora caninum* infections in mice and ruminant models. *Parasitology*, 1-15.

Hemphill, A., Debache, K., Monney, T., Schorer, M., Guionaud, C., Alaeddine, F., et al. (2013). Proteins mediating the *Neospora caninum*-host cell interaction as targets for vaccination. *Front.Biosci.(Elite Ed)* 5, 23-36.

Hemphill, A., Gottstein, B., and Kaufmann, H. (1996). Adhesion and invasion of bovine endothelial cells by *Neospora caninum*. *Parasitology* 112 (Pt 2), 183-97.

Hemphill, A., Vonlaufen, N., and Naguleswaran, A. (2006). Cellular and immunological basis of the host-parasite relationship during infection with *Neospora caninum* . *Parasitology* 133, 261-78.

Hill, R.J., Ringel, A., Knuepfer, E., Moon, R. W., Blackman, M. J., and van Ooij, C. (2016). Regulation and Essentiality of the StAR-related Lipid Transfer (START) Domain-containing Phospholipid Transfer Protein PFA0210c in Malaria Parasites. *J.Biol.Chem.* 291, 24280-92.

Ho, H., Cheng, M., and Chiu, D. T. (2007). Glucose-6-phosphate dehydrogenase – from oxidative stress to cellular functions and degenerative diseases. *Redox Report* 12, 109-18.

Hong, D.P., Radke, J. B., and White, M. W. (2017). Opposing transcriptional mechanisms regulate *Toxoplasma* development. *mSphere* 2, 10.1128/mSphere.00347,16.

Horcajo, P., Xia, D., Randle, N., Collantes-Fernández, E., Wastling, J., Ortega-Mora, L., et al. (2018). Integrative transcriptome and proteome analyses define marked differences between *Neospora caninum* isolates throughout the tachyzoite lytic cycle. *J.Proteomics* 180, 108-19.

Horcajo, P., Regidor-Cerrillo, J., Aguado-Martínez, A., Hemphill, A., and Ortega-Mora, L. M. (2016). Vaccines for bovine neosporosis: current status and key aspects for development. *Parasite Immunol.* 38, 709-23.

Horcajo, P., Jimenez-Pelayo, L., Garcia-Sanchez, M., Regidor-Cerrillo, J., Collantes-Fernandez, E., Rozas, D., et al. (2017). Transcriptome modulation of bovine trophoblast cells *in vitro* by *Neospora caninum*. *Int.J.Parasitol.* 47, 791-9.

Hori, H. (2014). Methylated nucleosides in tRNA and tRNA methyltransferases. *Front.Genet.* 5, 144.

Howard, B.L., Harvey, K. L., Stewart, R. J., Azevedo, M. F., Crabb, B. S., Jennings, I. G., et al. (2015). Identification of potent phosphodiesterase inhibitors that demonstrate cyclic nucleotide-dependent functions in apicomplexan parasites. *ACS Chem.Biol.* 10, 1145-54.

Huang, D.W., Sherman, B. T., and Lempicki, R. A. (2009). Systematic and integrative analysis of large gene lists using DAVID bioinformatics resources. *Nat.Protoc.* 4, 44.

Huang, S., Holmes, M. J., Radke, J. B., Hong, D. P., Liu, T. K., White, M. W., et al. (2017). *Toxoplasma gondii* AP2IX-4 regulates gene expression during bradyzoite development. *mSphere* 2, 10.1128/mSphere.00054,17.

Hume, D.A. (2008). Macrophages as APC and the dendritic cell myth. *J.Immunol.* 181, 5829-35.

Huynh, M.H., Boulanger, M. J., and Carruthers, V. B. (2014). A conserved apicomplexan microneme protein contributes to *Toxoplasma gondii* invasion and virulence. *Infect.Immun.* 82, 4358-68.

Innes, E.A.,Mattsson, J. G. (2007). *Neospora caninum* emerges from the shadow of *Toxoplasma gondii*. *Trends Parasitol.* 23, 43-4.

Innes, E.A., Wright, S., Bartley, P., Maley, S., Macaldowie, C., Esteban-Redondo, I., et al. (2005). The host-parasite relationship in bovine neosporosis. *Vet.Immunol.Immunopathol.* 108, 29-36.

Innes, E.A., Wright, S. E., Maley, S., Rae, A., Schock, A., Kirvar, E., et al. (2001). Protection against vertical transmission in bovine neosporosis. *Int.J.Parasitol.* 31, 1523-34.

Iyer, L.M., Anantharaman, V., Wolf, M. Y., and Aravind, L. (2008). Comparative genomics of transcription factors and chromatin proteins in parasitic protists and other eukaryotes. *Int.J.Parasitol.* 38, 1-31.

Jazwinski, S.M.,Conzelmann, A. (2002). LAG1 puts the focus on ceramide signaling. *Int.J.Biochem.Cell Biol.* 34, 1491-5.

Jensen, K.D., Wang, Y., Wojno, E. D. T., Shastri, A. J., Hu, K., Cornel, L., et al. (2011). *Toxoplasma* polymorphic effectors determine macrophage polarization and intestinal inflammation. *Cell Host Mibrobe.* 9, 472-83.

Jensen, K., Gallagher, I. J., Johnston, N., Welsh, M., Skuce, R., Williams, J. L., et al. (2018). Variation in the early host-pathogen Interaction of bovine macrophages with divergent *Mycobacterium bovis* strains in the United Kingdom. *Infect.Immun.* 86, 10.1128/IAI.00385,17.

Jesus, L.B., Santos, A. B., Jesus, E. E. V., Santos, R. G. D., Grangeiro, M. S., Bispo-da-Silva, A., et al. (2019). IDO, COX and iNOS have an important role in the proliferation of *Neospora caninum* in neuron/glia co-cultures. *Vet. Parasitol.* 266, 96-102.

Jewett, T.J.,Sibley, L. D. (2003). Aldolase forms a bridge between cell surface adhesins and the actin cytoskeleton in apicomplexan parasites. *Mol.Cell* 11, 885-94.

Jha, S.,Pan-Yun Ting, J. (2015). Holding the inflammatory system in check: NLRs keep it cool. *F1000Prime Rep.* 7, 15,15.

Jiménez-Pelayo, L., García-Sánchez, M., Regidor-Cerrillo, J., Horcajo, P., Collantes-Fernández, E., Gómez-Bautista, M., et al. (2019a). Immune response profile of caruncular and trophoblast cell lines infected by high- (Nc-Spain7) and low virulente (Nc-Spain1H) isolates of *Neospora caninum*. *Parasit.Vectors*. 12,218.

Jiménez-Pelayo (2019b) Interacciones entre aislados de alta y baja virulencia de *Neospora caninum* y la placenta bovina. Doctoral Thesis.

Jiménez-Pelayo, L., García-Sánchez, M., Regidor-Cerrillo, J., Horcajo, P., Collantes-Fernández, E., Gómez-Bautista, M., et al. (2017). Differential susceptibility of bovine caruncular and trophoblast cell lines to infection with high and low virulence isolates of *Neospora caninum*. *Parasit.Vectors* 10, 463.

Jimenez-Ruiz, E., Alvarez-Garcia, G., Aguado-Martinez, A., and Ortega-Mora, L. M. (2013). Mice congenitally infected with low-to-moderate virulence *Neospora caninum* isolates exhibited clinical reactivation during the mating period without transmission to the next generation. *Exp.Parasitol.* 134, 244-8.

Jin, X., Gong, P., Zhang, X., Li, G., Zhu, T., Zhang, M., et al. (2017). Activation of ERK signaling via TLR11 induces IL-12p40 production in peritoneal macrophages challenged by *Neospora caninum*. *Front.Microb.* 8, 1393.

Jinno, A.,Park, P. W. (2015). Role of glycosaminoglycans in infectious disease. *Methods Mol.Biol.* 1229, 567-85.

Journel C., Chatagnon G., Martin D., Richard A., Tainturier D. Proceedings of the XXII World Buiatrics Congress; Hannover, Germany. 2002.

Jung, C., Lee, C. Y., and Grigg, M. E. (2004). The SRS superfamily of *Toxoplasma* surface proteins. *Int.J.Parasitol.* 34, 285-96.

Jungi, T.W., Farhat, K., Burgener, I. A., and Werling, D. (2011). Toll-like receptors in domestic animals. *Cell Tissue Res.* 343, 107-20.

Kafsack, B.F., Pena, J. D., Coppens, I., Ravindran, S., Boothroyd, J. C., and Carruthers, V. B. (2009). Rapid membrane disruption by a perforin-like protein facilitates parasite exit from host cells. *Science* 323, 530-3.

Kanatani, S., Fuks, J. M., Olafsson, E. B., Westermark, L., Chambers, B., Varas-Godoy, M., et al. (2017). Voltage-dependent calcium channel signaling mediates GABAA receptor-induced migratory activation of dendritic cells infected by *Toxoplasma gondii*. *PLoS Pathog.*

Kanatani, S., Uhlén, P., and Barragan, A. (2015). Infection by *Toxoplasma gondii* induces amoeboid-like migration of dendritic cells in a three-dimensional collagen matrix. *PloS one* 10, e0139104.

Kapellos, T.S.,Iqbal, A. J. (2016). Epigenetic control of macrophage polarisation and soluble mediator gene expression during inflammation. *Mediators Inflamm.* 2016.

Kemp, L.E., Yamamoto, M., and Soldati-Favre, D. (2013). Subversion of host cellular functions by the apicomplexan parasites. *FEMS Microbiol.Rev.* 37, 607-31..

Khan, A., Taylor, S., Ajioka, J. W., Rosenthal, B. M., and Sibley, L. D. (2009). Selection at a single locus leads to widespread expansion of *Toxoplasma gondii* lineages that are virulent in mice. *PLoS Genetics* 5, e1000404.

Khan, A., Fujita, A. W., Randle, M., Quinones, K., Shen, A., Oler, N., et al. (2015). Selective sweep of an inbred population of the protozoan pathogen *Neospora caninum*. *Apicomplexa in farm animals* 30th June-3rd July, Edinburgh (UK) (oral communication).

Khan, I.A., Thomas, S. Y., Moretto, M. M., Lee, F. S., Islam, S. A., Combe, C., et al. (2006). CCR5 is essential for NK cell trafficking and host survival following *Toxoplasma gondii* infection. *PLoS Pathog.* 2, e49.

Kim, Y.K., Shin, J., and Nahm, M. H. (2016). NOD-like receptors in infection, immunity, and diseases. *Yonsei Med.J.* 57, 5-14.

Klevar, S., Kulberg, S., Boysen, P., Storset, A. K., Moldal, T., Bjorkman, C., et al. (2007). Natural killer cells act as early responders in an experimental infection with *Neospora caninum* in calves. *Int.J.Parasitol.* 37, 329-39.

Kramer, S., Kimblin, N. C., and Carrington, M. (2010). Genome-wide in silico screen for CCCH-type zinc finger proteins of *Trypanosoma brucei*, *Trypanosoma cruzi* and *Leishmania major*. *BMC Genomics* 11, 283.

Krishna, R., Xia, D., Sanderson, S., Shanmugasundram, A., Vermont, S., Bernal, A., et al. (2015). A large-scale proteogenomics study of apicomplexan pathogens-*Toxoplasma gondii* and *Neospora caninum*. *Proteomics* 15, 2618-28.

Kritzner, S., Sager, H., Blum, J., Krebber, R., Greif, G., and Gottstein, B. (2002). An explorative study to assess the efficacy of Toltrazuril-sulfone (Ponazuril) in calves experimentally infected with *Neospora caninum*. *Ann.Clin. Microbiol.Antimicrob.* 1, 4.

Lamarque, M.H., Papoin, J., Finizio, A., Lentini, G., Pfaff, A. W., Candolfi, E., et al. (2012). Identification of a new rhoptry neck complex RON9/RON10 in the Apicomplexa parasite *Toxoplasma gondii*. *PLoS One* 7, e32457.

Lamarque, M.H., Roques, M., Kong-Hap, M., Tonkin, M. L., Rugarabamu, G., Marq, J., et al. (2014). Plasticity and redundancy among AMA–RON pairs ensure host cell entry of *Toxoplasma* parasites. *Nat.Commun.* 5, 4098.

Lambert, H.,Barragan, A. (2010). Modelling parasite dissemination: host cell subversion and immune evasion by *Toxoplasma gondii*. *Cell.Microbiol.* 12, 292-300.

Lambert, H., Dellacasa-Lindberg, I., and Barragan, A. (2011). Migratory responses of leukocytes infected with *Toxoplasma gondii*. *Microb.Infect.* 13, 96-102.

Lambert, H., Hitziger, N., Dellacasa, I., Svensson, M., and Barragan, A. (2006). Induction of dendritic cell migration upon *Toxoplasma gondii* infection potentiates parasite dissemination. *Cell.Microbiol.* 8, 1611-23.

Lauriola, A. (2017). Ruolo di Mitostatin nel mantenimento della stabilità genomica e suo coinvolgimento nella trasformazione cellulare. Doctoral Thesis.

Lavine, M.D.,Arrizabalaga, G. (2008). Exit from host cells by the pathogenic parasite *Toxoplasma gondii* does not require motility. *Eukaryot.Cell.* 7, 131-40.

Lee, E.G., Kim, J. H., Shin, Y. S., Shin, G. W., Kim, Y. R., Palaksha, K. J., et al. (2005). Application of proteomics for comparison of proteome of *Neospora caninum* and *Toxoplasma gondii* tachyzoites. *J Chromatogr.B Analyt.Technol.Biomed.Life Sci.* 815, 305-14.

Lee, E.G., Kim, J. H., Shin, Y. S., Shin, G. W., Suh, M. D., Kim, D. Y., et al. (2003). Establishment of a two-dimensional electrophoresis map for *Neospora caninum* tachyzoites by proteomics. *Proteomics* 3, 2339-50.

Leipe, D.D., Wolf, Y. I., Koonin, E. V., and Aravind, L. (2002). Classification and evolution of P-loop GTPases and related ATPases. *J.Mol.Biol.* 317, 41-72.

Lekutis, C., Ferguson, D. J., Grigg, M. E., Camps, M., and Boothroyd, J. C. (2001). Surface antigens of *Toxoplasma gondii*: variations on a theme. *Int.J.Parasitol.* 31, 1285-92.

Leroux, L., Dasanayake, D., Rommereim, L. M., Fox, B. A., Bzik, D. J., Jardim, A., et al. (2015). Secreted *Toxoplasma gondii* molecules interfere with expression of MHC-II in interferon gamma-activated macrophages. *Int.J.Parasitol.* 45, 319-32.

Li, S., Gong, P., Zhang, N., Li, X., Tai, L., Wang, X., et al. (2019). 14-3-3 protein of Neospora caninum modulates host cell innate immunity through the activation of MAPK and NF-kB pathways. *Front.Microbiol.* 10, 37.

Li, S., Gong, P., Tai, L., Li, X., Wang, X., Zhao, C., et al. (2018). Extracellular Vesicles Secreted by Neospora caninum Are Recognized by Toll-Like Receptor 2 and Modulate Host Cell Innate Immunity Through the MAPK Signaling Pathway. *Front.Immunol.* 9, 1633.

Lima, T.S.,Lodoen, M. B. (2019). Mechanisms of Human Innate Immune Evasion by *Toxoplasma gondii*. *Front.Cell. Infect.Microbiol.*9.

Lindsay, D.S., Rippey, N. S., Toivio-Kinnucan, M. A., and Blagburn, B. L. (1995). Ultrastructural effects of diclazuril against *Toxoplasma gondii* and investigation of a diclazuril-resistant mutant. *J.Parasitol.*, 459-66.

Lindsay, D.S., Dubey, J. P., and Duncan, R. B. (1999). Confirmation that the dog is a definitive host for *Neospora caninum*. *Vet.Parasitol.* 82, 327-33.

Linge, H.M., Collin, M., Nordenfelt, P., Morgelin, M., Malmsten, M., and Egesten, A. (2008). The human CXC chemokine granulocyte chemotactic protein 2 (GCP-2)/CXCL6 possesses membrane-disrupting properties and is antibacterial. *Antimicrob.Agents Chemother.* 52, 2599-607.

Liu, T., Zhang, L., Joo, D., and Sun, S. (2017). NF-κB signaling in inflammation. *Signal Transduct.Target.Ther.* 2, 17023.

Livak, K.J.,Schmittgen, T. D. (2001). Analysis of relative gene expression data using real-time quantitative PCR and the 2(-Delta Delta C(T)) Method. *Methods* 25, 402-8.

Lobato, J., Silva, D. A., Mineo, T. W., Amaral, J. D., Segundo, G. R., Costa-Cruz, J. M., et al. (2006). Detection of immunoglobulin G antibodies to *Neospora caninum* in humans: high seropositivity rates in patients who are infected by human immunodeficiency virus or have neurological disorders. *Clin.Vaccine Immunol.* 13, 84-9.

Lopez-Gatius, F., Lopez-Bejar, M., Murugavel, K., Pabon, M., Ferrer, D., and Almeria, S. (2004). *Neospora*-associated abortion episode over a 1-year period in a dairy herd in north-east Spain. *J.Vet.Med.B Infect.Dis.Vet.Public Health* 51, 348-52.

Lorestani, A., Sheiner, L., Yang, K., Robertson, S. D., Sahoo, N., Brooks, C. F., et al. (2010). A *Toxoplasma* MORN1 null mutant undergoes repeated divisions but is defective in basal assembly, apicoplast division and cytokinesis. *PloS one* 5, e12302.

Lourido, S., Tang, K., and Sibley, L. D. (2012). Distinct signalling pathways control *Toxoplasma* egress and host-cell invasion. *EMBO J.* 31, 4524-34.

Love, M.I., Huber, W., and Anders, S. (2014). Moderated estimation of fold change and dispersion for RNA-seq data with DESeq2. *Genome Biol.* 15, 550.

Lüder, C.G., Lang, C., Giraldo-Velasquez, M., Algner, M., Gerdes, J., and Gross, U. (2003). *Toxoplasma gondii* inhibits MHC class II expression in neural antigen-presenting cells by down-regulating the class II transactivator CIITA. *J.Neuroimmunol.* 134, 12-24.

Luder, C.G., Lang, T., Beuerle, B., and Gross, U. (1998). Down-regulation of MHC class II molecules and inability to up-regulate class I molecules in murine macrophages after infection with *Toxoplasma gondii*. *Clin.Exp.Immunol.* 112, 308-16.

Lunden, A., Marks, J., Maley, S. W., and Innes, E. A. (1998). Cellular immune responses in cattle experimentally infected with *Neospora caninum*. *Parasite Immunol.* 20, 519-26.

Luo, W.,Brouwer, C. (2013). Pathview: an R/Bioconductor package for pathway-based data integration and visualization. *Bioinformatics* 29, 1830-1.

Ma, L., Liu, G., Liu, J., Li, M., Zhang, H., Tang, D., et al. (2017a). *Neospora caninum* ROP16 play an important role in the pathogenicity by phosphorylating host cell STAT3. *Vet.Parasitol.* 243, 135-47.

Ma, L., Liu, J., Li, M., Fu, Y., Zhang, X., and Liu, Q. (2017b). Rhoptry protein 5 (ROP5) Is a Key Virulence Factor in *Neospora caninum*. *Front.Microbiol.* 8, 370.

Ma, X., Yan, W., Zheng, H., Du, Q., Zhang, L., Ban, Y., et al. (2015). Regulation of IL-10 and IL-12 production and function in macrophages and dendritic cells. *F1000Res* 4, 10.12688/f1000research.7010.1. eCollection 2015.

Macaldowie, C., Maley, S. W., Wright, S., Bartley, P., Esteban-Redondo, I., Buxton, D., et al. (2004). Placental pathology associated with fetal death in cattle inoculated with *Neospora caninum* by two different routes in early pregnancy. *J.Comp.Pathol.* 131, 142-56.

Maley, S.W., Buxton, D., Macaldowie, C. N., Anderson, I. E., Wright, S. E., Bartley, P. M., et al. (2006). Characterization of the immune response in the placenta of cattle experimentally Infected with *Neospora caninum* in early gestation. *J.Comp.Pathol.* 135, 130-41.

Maley, S.W., Buxton, D., Rae, A. G., Wright, S. E., Schock, A., Bartley, P. M., et al. (2003). The pathogenesis of neosporosis in pregnant cattle: inoculation at mid-gestation. *J.Comp.Pathol.* 129, 186-95.

Maley, S.W., Buxton, D., Thomson, K. M., Schriefer, C. E., and Innes, E. A. (2001). Serological analysis of calves experimentally infected with *Neospora caninum*: a 1-year study. *Vet.Parasitol.* 96, 1-9.

Mantegazza, A. R., Guttentag, S. H., El-Benna, J., Sasai, M., Iwasaki, A. et al. (2012). Adaptor protein-3 in dendritic cells facilitates phagosomal toll-like receptor signaling and antigen presentation to CD4(+) T cells. Immunity, 36(5), 782–794.

Marin, M.S., Hecker, Y. P., Quintana, S., Pérez, S., Leunda, M. R., Cantón, G., et al. (2017). Toll-like receptors 3, 7 and 8 are upregulated in the placental caruncle and fetal spleen of *Neospora caninum* experimentally infected cattle. *Vet.Parasitol.* 236, 58-61.

Marks, J., Lunden, A., Harkins, D., and Innes, E. (1998). Identification of *Neospora* antigens recognized by CD4+ T cells and immune sera from experimentally infected cattle. *Parasite Immunol.* 20, 303-9.

Marsh, A.E., Barr, B. C., Madigan, J., Lakritz, J., Nordhausen, R., and Conrad, P. A. (1996). Neosporosis as a cause of equine protozoal myeloencephalitis. *J.Am.Vet.Med.Assoc.* 209, 1907-13.

Marsh, A.E., Barr, B. C., Packham, A. E., and Conrad, P. A. (1998). Description of a new *Neospora* species (Protozoa: Apicomplexa: *Sarcocystidae*). *J.Parasitol.* 84, 983-91.

Marsh, A.E., Barr, B. C., Sverlow, K., Ho, M., Dubey, J. P., and Conrad, P. A. (1995). Sequence analysis and comparison of ribosomal DNA from bovine *Neospora* to similar coccidial parasites. *J.Parasitol.* 81, 530-5.

Martinez, F.O.,Gordon, S. (2014). The M1 and M2 paradigm of macrophage activation: time for reassessment. *F1000Prime Rep.* 6, 13,13.

Martinez, P., Denys, A., Delos, M., Sikora, A. S., Carpentier, M., Julien, S., et al. (2015). Macrophage polarization alters the expression and sulfation pattern of glycosaminoglycans. *Glycobiology* 25, 502-13.

Marugán-Hernández, V., Álvarez-García, G., Risco-Castillo, V., Regidor-Cerrillo, J., and Ortega-Mora, L. M. (2010). Identification of *Neospora caninum* proteins regulated during the differentiation process from tachyzoite to bradyzoite stage by DIGE. *Proteomics* 10, 1740-50.

Matsubayashi, M., Kawahara, F., Hatta, T., Yamagishi, J., Miyoshi, T., Sasai, K., et al. (2016). Transcriptional profiles of virulent and precocious strains of *Eimeria tenella* at sporozoite stage; novel biological insight into attenuated asexual development. *Infect.Genet.Evol.* 40, 54-62.

Matsuzaki, G.,Umemura, M. (2007). Interleukin-17 as an effector molecule of innate and acquired immunity against infections. *Microbiol.Immunol.* 51, 1139-47.

Matta, S.K., Patten, K., Wang, Q., Kim, B. H., MacMicking, J. D., and Sibley, L. D. (2018). NADPH oxidase and guanylate binding protein 5 restrict survival of avirulent type III strains of *Toxoplasma gondii* in naive macrophages. *MBio* 9, 10.1128/mBio.01393-18.

Mazumdar, J., H Wilson, E., Masek, K., A Hunter, C., and Striepen, B. (2006). Apicoplast fatty acid synthesis is essential for organelle biogenesis and parasite survival in *Toxoplasma gondii*. *Proc.Natl.Acad.Sci.U.S.A.* 103, 13192-7.

McCoy, J.M., Whitehead, L., van Dooren, G. G., and Tonkin, C. J. (2012). TgCDPK3 regulates calcium-dependent egress of Toxoplasma gondii from host cells. *PLoS Pathog.* 8,

Melo, M.B., Jensen, K. D., and Saeij, J. P. (2011). *Toxoplasma gondii* effectors are master regulators of the inflammatory response. *Trends Parasitol.* 27, 487-95.

Melo, M.B., Nguyen, Q. P., Cordeiro, C., Hassan, M. A., Yang, N., McKell, R., et al. (2013). Transcriptional analysis of murine macrophages infected with different *Toxoplasma* strains identifies novel regulation of host signaling pathways. *PLoS Pathog.* 9, e1003779.

Meyer, E.V., Semenya, A. A., Okenu, D. M., Dluzewski, A. R., Bannister, L. H., Barnwell, J. W., et al. (2009). The reticulocyte binding-like proteins of *P. knowlesi* locate to the micronemes of merozoites and define two new members of this invasion ligand family. *Mol.Biochem.Parasitol.* 165, 111-21.

Miller, C.M., Quinn, H. E., Windsor, P. A., and Ellis, J. T. (2002). Characterisation of the first Australian isolate of *Neospora caninum* from cattle. *Aust.Vet.J.* 80, 620-5.

Millholland, M.G., Mishra, S., Dupont, C. D., Love, M. S., Patel, B., Shilling, D., et al. (2013). A host GPCR signaling network required for the cytolysis of infected cells facilitates release of apicomplexan parasites. *Cell.Host Microbe* 13, 15-28.

Mineo, T.W., Benevides, L., Silva, N. M., and Silva, J. S. (2009). Myeloid differentiation factor 88 is required for resistance to *Neospora caninum* infection. *Vet.Res.* 40, 1-12.

Mineo, T.W., Oliveira, C. J., Gutierrez, F. R., and Silva, J. S. (2010). Recognition by toll-like receptor 2 induces antigen-presenting cell activation and Th1 programming during infection by *Neospora caninum*. *Immunol.Cell Biol.* doi:10.1038/icb.2010.52.

Mineo, T.W., Oliveira, C. J., Silva, D. A., Oliveira, L. L., Abatepaulo, A. R., Ribeiro, D. P., et al. (2010). Neospora caninum excreted/secreted antigens trigger CC-chemokine receptor 5-dependent cell migration. *Int.J.Parasitol.*

Minns, L.A., Menard, L. C., Foureau, D. M., Darche, S., Ronet, C., Mielcarz, D. W., et al. (2006). TLR9 is required for the gut-associated lymphoid tissue response following oral infection of *Toxoplasma gondii*. *J.Immunol.* 176, 7589-97.

Miranda, V.D.S., Franca, F. B. F., da Costa, M. S., Silva, V. R. S., Mota, C. M., Barros, P. D. S. C., et al. (2019). Toll-Like Receptor 3-TRIF Pathway Activation by *Neospora caninum* RNA Enhances Infection Control in Mice. *Infect. Immun.* 87, 10.1128/IAI.00739,18.

Mittl, P.R.,Schneider-Brachert, W. (2007). Sel1-like repeat proteins in signal transduction. *Cell.Signal.* 19, 20-31.

Mogensen, T.H. (2009). Pathogen recognition and inflammatory signaling in innate immune defenses. *Clin.Microbiol. Rev.* 22, 240,73.

Moog, D., Przyborski, J. M., and Maier, U. G. (2017). Genomic and proteomic evidence for the presence of a peroxisome in the apicomplexan parasite *Toxoplasma gondii* and other Coccidia. *Genome Biol.Evol.* 9, 3108-21.

Moradin, N.,Descoteaux, A. (2012). *Leishmania* promastigotes: building a safe niche within macrophages. *Front.Cell. Infect.Microbiol.* 2, 121.

Moretti, J.,Blander, J. M. (2014). Insights into phagocytosis-coupled activation of pattern recognition receptors and inflammasomes. *Curr.Opin.Immunol.* 26, 100-10.

Morris, M.T., Cheng, W. C., Zhou, X. W., Brydges, S. D., and Carruthers, V. B. (2004). *Neospora caninum* expresses an unusual single-domain Kazal protease inhibitor that is discharged into the parasitophorous vacuole. *Int.J.Parasitol.* 34, 693-701.

Morrissette, N. (2015). Targeting *Toxoplasma* tubules: tubulin, microtubules, and associated proteins in a human pathogen. *Eukaryot.Cell.* 14, 2-12.

Mota, C.M., Oliveira, A., Davoli-Ferreira, M., Silva, M. V., Santiago, F. M., Nadipuram, S. M., et al. (2016). *Neospora caninum* activates p38 MAPK as an evasion mechanism against innate immunity. *Front.Microbiol.* 7, 1456.

Mottram, J.C., Helms, M. J., Coombs, G. H., and Sajid, M. (2003). Clan CD cysteine peptidases of parasitic protozoa. *Trends Parasitol.* 19, 182-7.

Muller, J.,Hemphill, A. (2012). *In vitro* culture systems for the study of apicomplexan parasites in farm animals. *Int.J.Parasitol.* 43, 115-124.

Munoz, C., San Francisco, J., Gutierrez, B., and Gonzalez, J. (2015). Role of the ubiquitin-proteasome systems in the biology and virulence of protozoan parasites. *Biomed.Res.Int.* 2015, 141526.

Muraille, E., Leo, O., and Moser, M. (2014). TH1/TH2 paradigm extended: macrophage polarization as an unappreciated pathogen-driven escape mechanism?. *Front.Immunol.* 5, 603.

Murzina, N.V., Pei, X., Zhang, W., Sparkes, M., Vicente-Garcia, J., Pratap, J. V., et al. (2008). Structural basis for the recognition of histone H4 by the histone-chaperone RbAp46. *Structure* 16, 1077-85.

Naguleswaran, A., Alaeddine, F., Guionaud, C., Vonlaufen, N., Sonda, S., Jenoe, P., et al. (2005). *Neospora caninum* protein disulfide isomerase is involved in tachyzoite-host cell interaction. *Int.J.Parasitol.* 35, 1459-72.

Nalpas, N.C., Magee, D. A., Conlon, K. M., Browne, J. A., Healy, C., McLoughlin, K. E., et al. (2015). RNA sequencing provides exquisite insight into the manipulation of the alveolar macrophage by tubercle bacilli. *Scientific reports* 5, 13629.

Narasimhan, J., Joyce, B. R., Naguleswaran, A., Smith, A. T., Livingston, M. R., Dixon, S. E., et al. (2008). Translation regulation by eukaryotic initiation factor-2 kinases in the development of latent cysts in *Toxoplasma gondii*. *J.Biol.Chem.* 283, 16591-601.

Nigg, E.A. (1995). Cyclin-dependent protein kinases: key regulators of the eukaryotic cell cycle. *Bioessays* 17, 471-80.

Nishikawa, Y., Shimoda, N., Fereig, R. M., Moritaka, T., Umeda, K., Nishimura, M., et al. (2018). *Neospora caninum* dense granule protein 7 regulates the pathogenesis of neosporosis by modulating host immune response. *Appl. Environ.Microbiol.* 84, 10.1128/AEM.01350,18.

Nishikawa, Y., Tragoolpua, K., Inoue, N., Makala, L., Nagasawa, H., Otsuka, H., et al. (2001). In the absence of endogenous gamma interferon, mice acutely infected with *Neospora caninum* succumb to a lethal immune response characterized by inactivation of peritoneal macrophages. *Clin.Diagn.Lab.Immunol.* 8, 811-6.

Nishikawa, Y., Zhang, H., Ibrahim, H. M., Yamada, K., Nagasawa, H., and Xuan, X. (2010). Roles of CD122+ cells in resistance against *Neospora caninum* infection in a murine model. *J.Vet.Med.Sci.* 72, 1275-82.

Nishikawa, Y., Zhang, H., Ikehara, Y., Kojima, N., Xuan, X., and Yokoyama, N. (2009). Immunization with oligomannose-coated liposome-entrapped dense granule protein 7 protects dams and offspring from *Neospora caninum* infection in mice. *Clin.Vaccine Immunol.* 16, 792-7.

Nogareda, C., López-Gatius, F., Santolaria, P., García-Ispierto, I., Bech-Sabat, G., Pabón, M., et al. (2007). Dynamics of anti-*Neospora caninum* antibodies during gestation in chronically infected dairy cows. *Vet.Parasitol.* 148, 193-9.

Ólafsson, E.B., Varas-Godoy, M., and Barragan, A. (2018). *Toxoplasma gondii* infection shifts dendritic cells into an amoeboid rapid migration mode encompassing podosome dissolution, secretion of TIMP-1, and reduced proteolysis of extracellular matrix. *Cell.Microbiol.* 20, e12808.

Ólafsson, E.B., Ross, E. C., Varas-Godoy, M., and Barragan, A. (2019). TIMP-1 promotes hypermigration of *Toxoplasma*-infected primary dendritic cells via CD63–ITGB1–FAK signaling. *J.Cell.Sci.* 132, jcs225193.

Ortega-Mora, L.M., Calero-Bernal, R., Regidor-Cerrillo, J., 2019. Chapter 32 Neosporosis. In Manual práctico de enfermedades infectocontagiosas en rumiantes. García-Bocanegra, I., 2019. 289-300. ISBN: 978-84-9113-353-7.

Ortega-Mora, L.M., Fernández-García, A., and Gómez-Bautista, M. (2006). Diagnosis of bovine neosporosis: Recent advances and perspectives. *Acta Parasitol.* 51, 1-14.

Osoro, K., Ortega-Mora, L. M., Martínez, A., Serrano-Martínez, E., and Ferre, I. (2008). Natural breeding with bulls experimentally infected with *Neospora caninum* failed to induce seroconversion in dams. *Theriogenology*. 71, 639-642.

Ouologuem, D.T.,Roos, D. S. (2014). Dynamics of the *Toxoplasma gondii* inner membrane complex. *J.Cell.Sci.* 127, 3320-30.

Palmieri, F.,Pierri, C. L. (2010). Mitochondrial metabolite transport. *Essays Biochem.* 47, 37-52.

Parthun, M. (2007). Hat1: the emerging cellular roles of a type B histone acetyltransferase. *Oncogene* 26, 5319.

Pastor-Fernandez, I., Regidor-Cerrillo, J., Alvarez-Garcia, G., Marugan-Hernandez, V., Garcia-Lunar, P., Hemphill, A., et al. (2016). The tandemly repeated NTPase (NTPDase) from *Neospora caninum* is a canonical dense granule protein whose RNA expression, protein secretion and phosphorylation coincides with the tachyzoite egress. *Parasit.Vectors.* 9.

Paugam, A., Creuzet, C., Dupouy-Camet, J., and Roisin, M. (2002). *In vitro* effects of gliotoxin, a natural proteasome inhibitor, on the infectivity and proteolytic activity of *Toxoplasma gondii*. *Parasitol.Res.* 88, 785-7.

Pedraza-Díaz, S., Marugán-Hernández, V., Collantes-Fernández, E., Regidor-Cerrillo, J., Rojo-Montejo, S., Gómez-Bautista, M., et al. (2009). Microsatellite markers for the molecular characterization of *Neospora caninum*: application to clinical samples. *Vet.Parasitol.* 166, 38-46.

Peixoto, L., Chen, F., Harb, O. S., Davis, P. H., Beiting, D. P., Brownback, C. S., et al. (2010). Integrative genomic approaches highlight a family of parasite-specific kinases that regulate host responses. *Cell.Host Microbe* 8, 208-18.

Pepper, M., Dzierszinski, F., Wilson, E., Tait, E., Fang, Q., Yarovinsky, F., et al. (2008). Plasmacytoid dendritic cells are activated by *Toxoplasma gondii* to present antigen and produce cytokines. *J.Immunol.* 180, 6229-36.

Pereira García-Melo, D., Regidor-Cerrillo, J., Collantes-Fernández, E., Aguado-Martínez, A., Del Pozo, I., Minguijon, E., et al. (2010). Pathogenic characterization in mice of *Neospora caninum* isolates obtained from asymptomatic calves. *Parasitology*, 1-12.

Pereira-Bueno, J., Quintanilla-Gozalo, A., Pérez-Pérez, V., Espi-Felgueroso, A., Álvarez, G.,G., Collantes-Fernández, E., et al. (2003). Evaluation by different diagnostic techniques of bovine abortion associated with *Neospora caninum* in Spain. *Vet.Parasitol.* 111, 143-52.

Pérez-Zaballos, F.J., Ortega-Mora, L. M., Álvarez-García, G., Collantes-Fernández, E., Navarro-Lozano, V., García-Villada, L., et al. (2005). Adaptation of *Neospora caninum* isolates to cell-culture changes: an argument in favor of its clonal population structure. *J.Parasitol.* 91, 507-10.

Peters, C., Kawakami, M., Kaul, M., Ilg, T., Overath, P., and Aebischer, T. (1997). Secreted proteophosphoglycan of *Leishmania mexicana* amastigotes activates complement by triggering the mannan binding lectin pathway. *Eur.J.Immunol.* 27, 2666-72.

Piraine REA, Silva RAE, Junior AGDS, Cunha RC, Leite FPL. (2015). The Potential of *Neospora caninum* Immunogens against Neosporosis. 6: 298. doi:2157-7560.1000298. *J Vaccines Vaccin* 6, 298.

Pittman, K.J., Aliota, M. T., and Knoll, L. J. (2014). Dual transcriptional profiling of mice and *Toxoplasma gondii* during acute and chronic infection. *BMC Genomics* 15, 806,2164-15-806.

Ponts, N., Yang, J., Chung, D. D., Prudhomme, J., Girke, T., Horrocks, P., et al. (2008). Deciphering the ubiquitin-mediated pathway in apicomplexan parasites: a potential strategy to interfere with parasite virulence. *PloS one* 3, e2386.

Pszenny, V., Davis, P. H., Zhou, X. W., Hunter, C. A., Carruthers, V. B., and Roos, D. S. (2012). Targeted disruption of *Toxoplasma gondii* serine protease inhibitor 1 increases bradyzoite cyst formation in vitro and parasite tissue burden in mice. *Infect.Immun.* 80, 1156-65.

Qiu, X., Shao, Y., Miao, S., and Wang, L. (2006). The diversity of the DnaJ/Hsp40 family, the crucial partners for Hsp70 chaperones. *Cell.Mol.Life Sci. CMLS* 63, 2560-70.

Qu, G., Fetterer, R., Jenkins, M., Leng, L., Shen, Z., Murphy, C., et al. (2013). Characterization of *Neospora caninum* macrophage migration inhibitory factor. *Exp.Parasitol.* 135, 246-56.

Quinn, H.E., Ellis, J. T., and Smith, N. C. (2002). *Neospora caninum*: a cause of immune-mediated failure of pregnancy?. *Trends Parasitol.* 18, 391-4.

Quintanilla-Gozalo, A., Pereira-Bueno, J., Seijas-Carballedo, A., Costas, E., and Ortega Mora, L. M. (2000). Observational studies in *Neospora caninum* infected dairy cattle: relationship infection-abortion and gestational antibody fluctuations. In: Hemphill A, Gottstein B. A European perspective on *Neospora caninum. Int.J.Parasitol.* 30, 877-924.

Radke, J.B., Worth, D., Hong, D., Huang, S., Sullivan Jr, W. J., Wilson, E. H., et al. (2018). Transcriptional repression by ApiAP2 factors is central to chronic toxoplasmosis. *PLoS Pathog.* 14, e1007035.

Rajendran, E., Hapuarachchi, S. V., Miller, C. M., Fairweather, S. J., Cai, Y., Smith, N. C., et al. (2017). Cationic amino acid transporters play key roles in the survival and transmission of apicomplexan parasites. *Nat.Commun.* 8, 14455.

Ramakrishnan, S.,Docampo, R. (2018). Membrane proteins in trypanosomatids involved in Ca2 homeostasis and signaling. *Genes* 9, 304.

Regidor-Cerrillo, J., Alvarez-Garcia, G., Pastor-Fernandez, I., Marugan-Hernandez, V., Gomez-Bautista, M., and Ortega-Mora, L. M. (2012). Proteome expression changes among virulent and attenuated *Neospora caninum* isolates. *J.Proteomics* 75, 2306-18.

Regidor-Cerrillo, J., Arranz-Solis, D., Benavides, J., Gomez-Bautista, M., Castro-Hermida, J. A., Mezo, M., et al. (2014). *Neospora caninum* infection during early pregnancy in cattle: how the isolate influences infection dynamics, clinical outcome and peripheral and local immune responses. *Vet.Res.* 45, 10,9716-45-10.

Regidor-Cerrillo, J., Diez-Fuertes, F., Garcia-Culebras, A., Moore, D. P., Gonzalez-Warleta, M., Cuevas, C., et al. (2013). Genetic diversity and geographic population structure of bovine *Neospora caninum* determined by microsatellite genotyping analysis. *PLoS One* 8, e72678.

Regidor-Cerrillo, J., Garcia-Lunar, P., Pastor-Fernandez, I., Alvarez-Garcia, G., Collantes-Fernandez, E., Gomez-Bautista, M., et al. (2015). *Neospora caninum* tachyzoite immunome study reveals differences among three biologically different isolates. *Vet.Parasitol.* 212, 92-9.

Regidor-Cerrillo, J., Gómez-Bautista, M., Del Pozo, I., Jiménez-Ruiz, E., Aduriz, G., and Ortega-Mora, L. M. (2010). Influence of *Neospora caninum* intra-specific variability in the outcome of infection in a pregnant BALB/c mouse model. *Vet.Res.* 41, 52.

Regidor-Cerrillo, J., Gómez-Bautista, M., Pereira-Bueno, J., Adúriz, G., Navarro-Lozano, V., Risco-Castillo, V., et al. (2008). Isolation and genetic characterization of *Neospora caninum* from asymptomatic calves in Spain. *Parasitology* 135, 1651-9.

Regidor-Cerrillo, J., Gomez-Bautista, M., Sodupe, I., Aduriz, G., Alvarez-Garcia, G., Del Pozo, I., et al. (2011). In vitro invasion efficiency and intracellular proliferation rate comprise virulence-related phenotypic traits of *Neospora caninum*. *Vet.Res.* 42, 41.

Regidor-Cerrillo, J., Pedraza-Díaz, S., Gómez-Bautista, M., and Ortega-Mora, L. M. (2006). Multilocus microsatellite analysis reveals extensive genetic diversity in *Neospora caninum*. *J.Parasitol.* 92, 517-24.

Reichel, M.P.,Ellis, J. T. (2009). *Neospora caninum*--how close are we to development of an efficacious vaccine that prevents abortion in cattle?. *Int.J.Parasitol.* 39, 1173-87.

Reichel, M.P., Moore, D. P., Hemphill, A., Ortega-Mora, L. M., Dubey, J. P., and Ellis, J. T. (2015). A live vaccine against *Neospora caninum* abortions in cattle. *Vaccine* 33, 1299-301.

Reichel, M.P., Alejandra Ayanegui-Alcérreca, M., Gondim, L. F. P., and Ellis, J. T. (2013). What is the global economic impact of *Neospora caninum* in cattle – The billion dollar question. *Int.J.Parasitol.* 43, 133-42.

Reid, A.J. (2015). Large, rapidly evolving gene families are at the forefront of host-parasite interactions in Apicomplexa. *Parasitology* 142 Suppl 1, S57-70.

Reiff, S.B., Vaishnava, S., and Striepen, B. (2012). The HU protein is important for apicoplast genome maintenance and inheritance in *Toxoplasma gondii*. *Eukaryot.Cell.* 11, 905-15.

Remmerie, A.,Scott, C. L. (2018). Macrophages and lipid metabolism. *Cell.Immunol.* 330, 27-42.

Risco-Castillo, V., Fernández-García, A., and Ortega-Mora, L. M. (2004). Comparative analysis of stress agents in a simplified in vitro system of *Neospora caninum* bradyzoite production. *J.Parasitol.* 90, 466-70.

Risco-Castillo, V., Fernández-García, A., Zaballos, A., Aguado-Martínez, A., Hemphill, A., Rodríguez-Bertos, A., et al. (2007). Molecular characterisation of BSR4, a novel bradyzoite-specific gene from *Neospora caninum* . *Int.J.Parasitol.* 37, 887-96.

Risco-Castillo, V., Marugán-Hernández, V., Fernadez-García, A., Aguado-Martínez, A., Jiménez-Ruiz, E., Rodriguez-Marco, S., et al. (2011). Identification of a gene cluster for cell-surface genes of the SRS superfamily in *Neospora caninum* and characterization of the novel SRS9 gene. *Parasitology*, 1-11.

Roiko, M.S.,Carruthers, V. B. (2013). Functional dissection of *Toxoplasma gondii* perforin-like protein 1 reveals a dual domain mode of membrane binding for cytolysis and parasite egress. *J.Biol.Chem.* 288, 8712-25.

Rojo-Montejo, S., Collantes-Fernández, E., Regidor-Cerrillo, J., Álvarez-García, G., Marugan-Hernández, V., Pedraza-Díaz, S., et al. (2009a). Isolation and characterization of a bovine isolate of *Neospora caninum* with low virulence. *Vet.Parasitol.* 159, 7-16.

Rojo-Montejo, S., Collantes-Fernández, E., Blanco-Murcia, J., Rodríguez-Bertos, A., Risco-Castillo, V., and Ortega-Mora, L. M. (2009b). Experimental infection with a low virulence isolate of *Neospora caninum* at 70 days gestation in cattle did not result in foetopathy. *Vet.Res.* 40, 49.

Rojo-Montejo, S., Collantes-Fernandez, E., Perez-Zaballos, F., Rodriguez-Marcos, S., Blanco-Murcia, J., Rodriguez-Bertos, A., et al. (2013). Effect of vaccination of cattle with the low virulence Nc-Spain 1H isolate of *Neospora caninum* against a heterologous challenge in early and mid-gestation. Vet.Res. 44, 106,9716-44-106.

Romero, J.J., Pérez, E., and Frankena, K. (2004). Effect of a killed whole *Neospora caninum* tachyzoite vaccine on the crude abortion rate of Costa Rican dairy cows under field conditions. *Vet.Parasitol.* 123, 149-59.

Rosbottom, A., Guy, C. S., Gibney, E. H., Smith, R. F., Valarcher, J. F., Taylor, G., et al. (2007). Peripheral immune responses in pregnant cattle following *Neospora caninum* infection. *Parasite Immunol.* 29, 219-28.

Rosowski, E.E., Lu, D., Julien, L., Rodda, L., Gaiser, R. A., Jensen, K. D., et al. (2011). Strain-specific activation of the NF-kappaB pathway by GRA15, a novel *Toxoplasma gondii* dense granule protein. *J.Exp.Med.* 208, 195-212.

Ruttkay-Nedecky, B., Nejdl, L., Gumulec, J., Zitka, O., Masarik, M., Eckschlager, T., et al. (2013). The role of metallothionein in oxidative stress. *Int.J.Mol.Sci.* 14, 6044-66.

Saeij, J.P., Coller, S., Boyle, J. P., Jerome, M. E., White, M. W., and Boothroyd, J. C. (2007). *Toxoplasma* co-opts host gene expression by injection of a polymorphic kinase homologue. *Nature* 445, 324-7.

Saha, S., Sparks, A. B., Rago, C., Akmaev, V., Wang, C. J., Vogelstein, B., et al. (2002). Using the transcriptome to annotate the genome. *Nat.Biotechnol.* 20, 508.

Sánchez-Sánchez, R., Ferre, I., Regidor-Cerrillo, J., Gutiérrez-Expósito, D., Ferrer, L. M., Arteche-Villasol, N., et al. (2018b). Virulence in mice of a *Toxoplasma gondii* type II isolate does not correlate with the outcome of experimental infection in pregnant sheep. *Front.Cell.Infect.Microbiol.* 8.

Sánchez-Sánchez, R., Vazquez, P., Ferre, I., and Ortega-Mora, L. M. (2018). Treatment of toxoplasmosis and neosporosis in farm ruminants: state of knowledge and future trends. *Curr.Top.Med.Chem.* 18, 1304-1323.

Sauvage, V., Millot, J., Aubert, D., Visneux, V., Marle-Plistat, M., Pinon, J., et al. (2006). Identification and expression analysis of ABC protein-encoding genes in *Toxoplasma gondii*: *Toxoplasma gondii* ATP-binding cassette superfamily. *Mol.Biochem.Parasitol.* 147, 177-92.

Schares, G., Pantchev, N., Barutzki, D., Heydorn, A. O., Bauer, C., and Conraths, F. J. (2005). Oocysts of *Neospora caninum*, *Hammondia heydorni*, *Toxoplasma gondii* and *Hammondia hammondi* in faeces collected from dogs in Germany. *Int.J.Parasitol.* 35, 1525-37.

Schock, A., Innes, E. A., Yamane, I., Latham, S. M., and Wastling, J. M. (2001). Genetic and biological diversity among isolates of *Neospora caninum*. *Parasitology* 123, 13-23.

Serrano-Martínez, E., Ferre, I., Martínez, A., Osoro, K., Mateos-Sanz, A., Del-Pozo, I., et al. (2007). Experimental neosporosis in bulls: Parasite detection in semen and blood and specific antibody and interferon-gamma responses. *Theriogenology* 67, 1175-84.

Shanmugam, D., Wu, B., Ramirez, U., Jaffe, E. K., and Roos, D. S. (2010). Plastid-associated porphobilinogen synthase from *Toxoplasma gondii*: kinetic and structural properties validate therapeutic potential. *J.Biol.Chem.* 285, 22122-31.

Shanmugasundram, A., Gonzalez-Galarza, F. F., Wastling, J. M., Vasieva, O., and Jones, A. R. (2012). Library of apicomplexan metabolic pathways: a manually curated database for metabolic pathways of apicomplexan parasites. *Nucleic Acids Res.*

Sharma, P., Guy, C. S., Haque, M., Coffey, T. J., Egan, S. A., and Flynn, R. J. (2018). Bovine neonatal monocytes display phenotypic differences compared with adults after challenge with an infectious abortifacient agent. *Front. Immunol.* 9, 3011.

Shaw, M., He, C., Roos, D., and Tilney, L. (2000). Proteasome inhibitors block intracellular growth and replication of *Toxoplasma gondii*. *Parasitology* 121, 35-47.

Sheiner, L., Vaidya, A. B., and McFadden, G. I. (2013). The metabolic roles of the endosymbiotic organelles of *Toxoplasma* and *Plasmodium spp.* *Curr.Opin.Microbiol.* 16, 452-8.

Shin, Y.S., Lee, E. G., and Jung, T. S. (2005). Exploration of immunoblot profiles of *Neospora caninum* probed with different bovine immunoglobulin classes. *J Vet Sci.* 6, 157-60.

Shin, Y.S., Shin, G. W., Kim, Y. R., Lee, E. Y., Yang, H. H., Palaksha, K. J., et al. (2005). Comparison of proteome and antigenic proteome between two *Neospora caninum* isolates. *Vet.Parasitol.* 134, 41-52.

Shrestha, S.P., Tomita, T., Weiss, L. M., and Orlofsky, A. (2006). Proliferation of *Toxoplasma gondii* in inflammatory macrophages in vivo is associated with diminished oxygen radical production in the host cell. *Int.J.Parasitol.* 36, 433-41.

Silva, M.V.d., Ferreira França, F. B., Mota, C. M., Macedo Júnior, Arlindo Gomes de, Ramos, E. L. P., Santiago, F. M., et al. (2017). Dectin-1 compromises innate responses and host resistance against *Neospora caninum* infection. *Front.Immunol.* 8, 245.

Sohn, E.J., Paape, M. J., Connor, E. E., Bannerman, D. D., Fetterer, R. H., and Peters, R. R. (2007). Bacterial lipopolysaccharide stimulates bovine neutrophil production of TNF-alpha, IL-1beta, IL-12 and IFN-gamma. *Vet.Res.* 38, 809-18.

Sohn, C.S., Cheng, T. T., Drummond, M. L., Peng, E. D., Vermont, S. J., Xia, D., et al. (2011). Identification of novel proteins in *Neospora caninum* using an organelle purification and monoclonal antibody approach. *PLoS One* 6, e18383.

Sommerville, C., Richardson, J. M., Williams, R. A., Mottram, J. C., Roberts, C. W., Alexander, J., et al. (2013). Biochemical and immunological characterization of *Toxoplasma gondii* macrophage migration inhibitory factor. *J.Biol.Chem.* 288, 12733-41.

Souza, C.D. (2015). Blocking the mitogen activated protein kinase-p38 pathway is associated with increase expression of nitric oxide synthase and higher production of nitric oxide by bovine macrophages infected with *Mycobacterium avium* subsp *paratuberculosis*. *Vet.Immunol.Immunopathol.* 164, 1-9.

Sowrirajan, B., Saito, Y., Poudyal, D., Chen, Q., Sui, H., DeRavin, S. S., et al. (2017). Interleukin-27 enhances the potential of reactive oxygen species generation from monocyte-derived macrophages and dendritic cells by Induction of p47(phox). *Sci.Rep.* 7, 43441.

Speer, C.A., Dubey, J. P., McAllister, M. M., and Blixt, J. A. (1999). Comparative ultrastructure of tachyzoites, bradyzoites, and tissue cysts of *Neospora caninum* and *Toxoplasma gondii*. *Int.J.Parasitol.* 29, 1509-19.

Spooner, R.,Yilmaz, Ö. (2011). The role of reactive-oxygen-species in microbial persistence and inflammation. *Int.J.Mol.Sci.* 12, 334-52.

Sreekumar, C., Hill, D. E., Miska, K. B., Rosenthal, B. M., Vianna, M. C., Venturini, L., et al. (2004). *Hammondia heydorni*: evidence of genetic diversity among isolates from dogs. *Exp.Parasitol.* 107, 65-71.

Stafford, J.L., Neumann, N. F., and Belosevic, M. (2002). Macrophage-mediated innate host defense against protozoan parasites. *Crit.Rev.Microbiol.* 28, 187-248.

Staska, L.M., McGuire, T. C., Davies, C. J., Lewin, H. A., and Baszler, T. V. (2003). *Neospora caninum*-infected cattle develop parasite-specific CD4+ cytotoxic T lymphocytes. *Infect.Immun.* 71, 3272-9.

Stirnimann, C.U., Petsalaki, E., Russell, R. B., and Müller, C. W. (2010). WD40 proteins propel cellular networks. *Trends Biochem.Sci.* 35, 565-74.

Strohbusch, M., Muller, N., Hemphill, A., Margos, M., Grandgirard, D., Leib, S., et al. (2009). *Neospora caninum* and bone marrow-derived dendritic cells: parasite survival, proliferation, and induction of cytokine expression. *Parasite Immunol.* 31, 366-72.

Strzalka, W.,Ziemienowicz, A. (2010). Proliferating cell nuclear antigen (PCNA): a key factor in DNA replication and cell cycle regulation. *Annals of botany* 107, 1127-40.

Stwora-Wojczyk, M.M., Dzierszinski, F., Roos, D. S., Spitalnik, S. L., and Wojczyk, B. S. (2004). Functional characterization of a novel *Toxoplasma gondii* glycosyltransferase: UDP-N-acetyl-D-galactosamine: polypeptide N-acetylgalactosaminyltransferase-T3. *Arch.Biochem.Biophys.* 426, 231-40.

Suarez, C., Bishop, R., Alzan, H., Poole, W., and Cooke, B. (2017). Advances in the application of genetic manipulation methods to apicomplexan parasites. *Int.J.Parasitol.* 47, 701-10.

Subauste, C.S., de Waal Malefyt, R., and Fuh, F. (1998). Role of CD80 (B7.1) and CD86 (B7.2) in the immune response to an intracellular pathogen. *J.Immunol.* 160, 1831-40.

Sullivan Jr, W.J.,Jeffers, V. (2012). Mechanisms of *Toxoplasma gondii* persistence and latency. *FEMS Microbiol.Rev.* 36, 717-33.

Supek, F., Bosnjak, M., Skunca, N., and Smuc, T. (2011). REVIGO summarizes and visualizes long lists of gene ontology terms. *PLoS One* 6, e21800.

Swierzy, I.J., Händel, U., Kaever, A., Jarek, M., Scharfe, M., Schlüter, D., et al. (2017). Divergent co-transcriptomes of different host cells infected with *Toxoplasma gondii* reveal cell type-specific host-parasite interactions. *Scientific reports* 7, 7229.

Tanaka, T., Nagasawa, H., Fujisaki, K., Suzuki, N., and Mikami, T. (2000). Growth-inhibitory effects of interferon-gamma on *Neospora caninum* in murine macrophages by a nitric oxide mechanism. *Parasitol.Res.* 86, 768-71.

Tattoli, I., Carneiro, L. A., Jéhanno, M., Magalhaes, J. G., Shu, Y., Philpott, D. J., et al. (2008). NLRX1 is a mitochondrial NOD-like receptor that amplifies NF-κB and JNK pathways by inducing reactive oxygen species production. *EMBO Rep.* 9, 293-300.

Taubert, A., Krull, M., Zahner, H., and Hermosilla, C. (2006). *Toxoplasma gondii* and *Neospora caninum* infections of bovine endothelial cells induce endothelial adhesion molecule gene transcription and subsequent PMN adhesion. *Vet.Immunol.Immunopathol.* 112, 272-83.

Taylor, S., Barragan, A., Su, C., Fux, B., Fentress, S. J., Tang, K., et al. (2006). A secreted serine-threonine kinase determines virulence in the eukaryotic pathogen *Toxoplasma gondii. Science* 314, 1776-80.

Teixeira, L., Botelho, A. S., Mesquita, S. D., Correia, A., Cerca, F., Costa, R., et al. (2010). Plasmacytoid and conventional dendritic cells are early producers of IL-12 in *Neospora caninum*-infected mice. *Immunol.Cell Biol.* 88, 79-86.

Tenter, A.M., Barta, J. R., Beveridge, I., Duszynski, D. W., Mehlhorn, H., Morrison, D. A., et al. (2002). The conceptual basis for a new classification of the coccidia. *Int.J.Parasitol.* 32, 595-616.

Tindemans, I., Peeters, M. J. W., and Hendriks, R. W. (2017). Notch Signaling in T Helper Cell Subsets: Instructor or Unbiased Amplifier?. *Front.Immunol.* 8, 419.

Tobin Magle, C., Pittman, K. J., Moser, L. A., Boldon, K. M., and Knoll, L. J. (2014). A *Toxoplasma* patatin-like protein changes localization and alters the cytokine response during toxoplasmic encephalitis. *Infect.Immun.* 82, 618-25.

Tran, J.Q., Li, C., Chyan, A., Chung, L., and Morrissette, N. S. (2012). SPM1 stabilizes subpellicular microtubules in *Toxoplasma gondii. Eukaryot.Cell.* 11, 206-16.

Trapnell, C., Williams, B. A., Pertea, G., Mortazavi, A., Kwan, G., van Baren, M. J., et al. (2010). Transcript assembly and quantification by RNA-Seq reveals unannotated transcripts and isoform switching during cell differentiation. *Nat.Biotechnol.* 28, 511-5.

Tuncer, S., Fiorillo, M. T., and Sorrentino, R. (2014). The multifaceted nature of NLRP12. *J.Leukoc.Biol.* 96, 991-1000.

Uboldi, A.D., McCoy, J. M., Blume, M., Gerlic, M., Ferguson, D. J., Dagley, L. F., et al. (2015). Regulation of starch stores by a Ca 2 -dependent protein kinase is essential for viable cyst development in *Toxoplasma gondii. Cell Host Microb.* 18, 670-81.

Ulland, T.K., Janowski, A. M., Buchan, B. W., Faron, M., Cassel, S. L., Jones, B. D., et al. (2013). *Francisella tularensis* live vaccine strain folate metabolism and pseudouridine synthase gene mutants modulate macrophage caspase-1 activation. *Infect.Immun.* 81, 201-8.

Uribe-Querol, E.,Rosales, C. (2017). Control of phagocytosis by microbial pathogens. *Front.Immunol.* 8, 1368.

Vanagas, L., Jeffers, V., Bogado, S. S., Dalmasso, M. C., Sullivan Jr, W. J., and Angel, S. O. (2012). *Toxoplasma* histone acetylation remodelers as novel drug targets. *Expert Rev. Anti Infect. Ther.* 10, 1189-201.

Vanleeuwen, J.A., Greenwood, S., Clark, F., Acorn, A., Markham, F., McCarron, J., et al. (2011). Monensin use against *Neospora caninum* challenge in dairy cattle. *Vet.Parasitol.* 175, 372-6.

Villagra-Blanco, R., Silva, L. M., Muñoz-Caro, T., Yang, Z., Li, J., Gärtner, U., et al. (2017). Bovine polymorphonuclear neutrophils cast neutrophil extracellular traps against the abortive parasite *Neospora caninum*. *Front.Immunol.* 8, 606.

von Blumröder, D., Schares, G., Norton, R., Williams, D. J., Esteban-Redondo, I., Wright, S., et al. (2004). Comparison and standardisation of serological methods for the diagnosis of *Neospora caninum* infection in bovines. *Vet. Parasitol.* 120, 11-22.

Wang, J.C. (2002). Cellular roles of DNA topoisomerases: a molecular perspective. *Nat.Rev.Mol.Cell Biol.* 3, 430.

Wang, X., Gong, P., Zhang, N., Li, L., Chen, S., Jia, L., et al. (2019). Inflammasome activation restrains the intracellular *Neospora caninum* proliferation in bovine macrophages. *Vet.Parasitol.* 268, 16-20.

Wang, X., Gong, P., Zhang, X., Li, S., Lu, X., Zhao, C., et al. (2018). NLRP3 inflammasome participates in host response to *Neospora caninum* infection. *Front.Immunol.* 9, 1791.

Wang, X., Gong, P., Zhang, X., Wang, J., Tai, L., Wang, X., et al. (2017). NLRP3 inflammasome activation in murine macrophages caused by *Neospora caninum* infection. *Parasit.Vectors.* 10, 266.

Wang, B., Lu, F., Cheng, Y., Chen, J. H., Jeon, H. Y., Ha, K. S., et al. (2015). Immunoprofiling of the tryptophan-rich antigen family in *Plasmodium vivax*. *Infect.Immun.* 83, 3083-95. doi:10.1128/IAI.03067-14 [doi].

Weber, F.H., Jackson, J. A., Sobecki, B., Choromanski, L., Olsen, M., Meinert, T., et al. (2013). On the efficacy and safety of vaccination with live tachyzoites of *Neospora caninum* for prevention of *Neospora*-associated fetal loss in cattle. *Clin.Vaccine Immunol.* 20, 99-105.

Wei, F., Wang, W., and Liu, Q. (2013). Protein kinases of *Toxoplasma gondii*: functions and drug targets. *Parasitol. Res.* 112, 2121-9.

Wei, Z., Wang, Y., Zhang, X., Wang, X., Gong, P., Li, J., et al. (2018). Bovine macrophage-derived extracellular traps act as early effectors against the abortive parasite *Neospora caninum*. *Vet.Parasitol.* 258, 1-7.

Weidner, J.M., Kanatani, S., Hernández-Castañeda, M. A., Fuks, J. M., Rethi, B., Wallin, R. P., et al. (2013). Rapid cytoskeleton remodelling in dendritic cells following invasion by *Toxoplasma gondii* coincides with the onset of a hypermigratory phenotype. *Cell.Microbiol.* 15, 1735-52.

Weiss, L.M., Ma, Y. F., Halonen, S., McAllister, M. M., and Zhang, Y. W. (1999). The in vitro development of *Neospora caninum* bradyzoites. *Int.J.Parasitol.* 29, 1713-23.

Werling, D., Hope, J. C., Howard, C. J., and Jungi, T. W. (2004). Differential production of cytokines, reactive oxygen and nitrogen by bovine macrophages and dendritic cells stimulated with Toll-like receptor agonists. *Immunology* 111, 41-52.

Werling, D.,Jungi, T. W. (2003). TOLL-like receptors linking innate and adaptive immune response. *Vet.Immunol. Immunopathol.* 91, 1-12.

Weston, J.F., Heuer, C., and Williamson, N. B. (2012). Efficacy of a *Neospora caninum* killed tachyzoite vaccine in preventing abortion and vertical transmission in dairy cattle. *Prev.Vet.Med.* 103, 136-44.

Weston, J.F., Williamson, N. B., and Pomroy, W. E. (2005). Associations between pregnancy outcome and serological response to *Neospora caninum* among a group of dairy heifers. *N.Z.Vet.J.* 53, 142-8.

Williams, D.J., Guy, C. S., McGarry, J. W., Guy, F., Tasker, L., Smith, R. F., et al. (2000). *Neospora caninum*-associated abortion in cattle: the time of experimentally-induced parasitaemia during gestation determines foetal survival. *Parasitology* 121 (Pt 4), 347-58.

Williams, D.J., Guy, C. S., Smith, R. F., Ellis, J., Bjorkman, C., Reichel, M. P., et al. (2007). Immunization of cattle with live tachyzoites of *Neospora caninum* confers protection against fetal death. *Infect.Immun.* 75, 1343-8.

Williams, D.J., Guy, C. S., Smith, R. F., Guy, F., McGarry, J. W., McKay, J. S., et al. (2003). First demonstration of protective immunity against foetopathy in cattle with latent *Neospora caninum* infection. *Int.J.Parasitol.* 33, 1059-65.

Wilson, S.K.,Knoll, L. J. (2018). Patatin-like phospholipases in microbial infections with emerging roles in fatty acid metabolism and immune regulation by Apicomplexa. *Mol.Microbiol.* 107, 34-46.

Wouda, W., Moen, A. R., Visser, I. J., and van Knapen, F. (1997). Bovine fetal neosporosis: a comparison of epizootic and sporadic abortion cases and different age classes with regard to lesion severity and immunohistochemical identification of organisms in brain, heart, and liver. *J.Vet.Diagn.Invest.* 9, 180-5.

Wu, L., Wu, L., Tang, C., Wang, J., Jin, X., Jiang, X., et al. (2018). Induction of FAS II Metabolic Disorders to Cause Delayed Death of *Toxoplasma gondii*. *J.Nanosci.Nanotechnol.* 18, 8155-9.

Xu, Y., Wang, X., Liu, J., Fu, Y., Xu, J., and Liu, Q. (2018). *Toxoplasma gondii* rhoptry protein38 (TgROP38) affects parasite invasion, egress, and induces IL-18 secretion during early infection. *Acta Biochim.Biophys.* 50, 766-75.

Xu, T., Ping, J., Yu, Y., Yu, F., Yu, Y., Hao, P., et al. (2010). Revealing parasite influence in metabolic pathways in Apicomplexa infected patients. *BMC Bioinformatics* 11 Suppl 11, S13,2105-11-S11-S13.

Yan, N. (2013). Structural advances for the major facilitator superfamily (MFS) transporters. *Trends Biochem.Sci.* 38, 151-9.

Yang, Y.S.,Strittmatter, S. M. (2007). The reticulons: a family of proteins with diverse functions. *Genome Biol.* 8, 234.

Zeng, B.,Zhu, G. (2006). Two distinct oxysterol binding protein-related proteins in the parasitic protist *Cryptosporidium parvum* (Apicomplexa). *Biochem.Biophys.Res.Commun.* 346, 591-9.

Zhang, L.,Wang, C. (2014). Inflammatory response of macrophages in infection. *Hepatobiliary Pancreat.Dis.Int.* 13, 138-52.

Zhang, X., Tang, N., Hadden, T. J., and Rishi, A. K. (2011). Akt, FoxO and regulation of apoptosis. *Biochim.Biophys. Acta* 1813, 1978-86.

Zhong, Y.,Yi, C. (2016). MicroRNA-720 suppresses M2 macrophage polarization by targeting GATA3. *Biosci.Rep.* 36, 10.1042/BSR20160105.

Znalesniak, E., Fu, T., Salm, F., Händel, U., and Hoffmann, W. (2017). Transcriptional responses in the murine spleen after *Toxoplasma gondii* infection: Inflammasome and mucus-associated genes. *Int.J.Mol.Sci.* 18, 1245.